



HAL
open science

Modèles d'infection de la plaie du pied chez le diabétique : approche in vitro et in vivo de la formation de biofilms de bactéries pathogènes seules ou en association

Cassandra Pouget

► To cite this version:

Cassandra Pouget. Modèles d'infection de la plaie du pied chez le diabétique : approche in vitro et in vivo de la formation de biofilms de bactéries pathogènes seules ou en association. Médecine humaine et pathologie. Université Montpellier, 2021. Français. NNT : 2021MONTT053 . tel-03558260

HAL Id: tel-03558260

<https://theses.hal.science/tel-03558260v1>

Submitted on 4 Feb 2022

HAL is a multi-disciplinary open access archive for the deposit and dissemination of scientific research documents, whether they are published or not. The documents may come from teaching and research institutions in France or abroad, or from public or private research centers.

L'archive ouverte pluridisciplinaire **HAL**, est destinée au dépôt et à la diffusion de documents scientifiques de niveau recherche, publiés ou non, émanant des établissements d'enseignement et de recherche français ou étrangers, des laboratoires publics ou privés.

THÈSE POUR OBTENIR LE GRADE DE DOCTEUR DE L'UNIVERSITÉ DE MONTPELLIER

En Microbiologie

École doctorale 168 : Science Chimiques et Biologiques pour la Santé

Unité de recherche Inserm U1047 : Virulence Bactérienne & Infections Chroniques

**Modèles d'infections de la plaie du pied chez le patient
diabétique :**

**Approches *in vitro* de la formation de biofilm de
bactéries pathogènes seules ou en association**

Présentée par Cassandra POUGET

Le 30 Novembre 2021

Sous la direction du Pr Jean-Philippe LAVIGNE & du Pr Albert SOTTO

Devant le jury composé de

Pr Christiane FORESTIER, Professeur des Universités, Université Clermont Auvergne

Pr David BOUTOILLE, Professeur des Universités-Praticien Hospitalier, Université de Nantes

Dr Virginie MOLLE, Directrice de Recherche, Université de Montpellier

Pr Ariane SULTAN, Professeur des Universités-Praticien Hospitalier, Université de Montpellier

Dr Damien SEYER, Maître de Conférence, Université de Cergy Pontoise

Pr Albert SOTTO, Professeur des Universités-Praticien Hospitalier, Université de Montpellier

Rapporteur

Rapporteur

Examineur

Examineur

Examineur

Co-directeur de thèse



**UNIVERSITÉ
DE MONTPELLIER**

REMERCIEMENTS

Au Professeur Christiane Forestier et au Professeur David Boutoille, rapporteurs

Je tenais vivement à vous exprimer mes profonds remerciements pour avoir pris le temps de lire et de juger mon travail. Je suis honorée de pouvoir bénéficier de votre expertise qui valorisent ce projet.

Au Docteur Damien Seyer, examinateur

Je vous remercie d'avoir accepté de faire partie de mon jury de thèse.

Au Professeur Ariane Sultan, examinateur

Merci d'avoir accordé de votre temps et de votre expertise pour évaluer mon travail de thèse.

Au Docteur Virginie Molle, présidente du jury

Merci du fond du cœur Virginie pour ta gentillesse, ta disponibilité et ton « smile » légendaire. Je suis honorée que tu puisses faire partie de mon jury de thèse. Et ouiii ... c'est que le début pour la Dream Team.

Au Professeur Jean Philippe Lavigne, mon super directeur de thèse

Certainement un des remerciements les plus compliqué à écrire pour la simple et bonne raison que je ne pourrais pas assez te remercier pour tout ce que tu as fait pour moi. Merci pour ta confiance tout au long de ces années et pour tous tes conseils et tes remarques constructives. Je te remercie pour ta patience, tes encouragements mais aussi ces valeurs que tu m'as transmise de rigueur et précision. C'est pour moi un grand plaisir que de travailler avec toi et j'espère que notre collaboration s'épanouira encore de longs moments.

Au Professeur Albert Sotto, mon sensationnel co-directeur de thèse (oui oui, je ne veux pas de jalousie)

Merci Albert d'avoir permis la réalisation de cette thèse. Même si nos échanges ont été plutôt rares, la faute entre autres à ce fameux virus, je garderai en mémoire ton travail et ton soutien pour me motiver dans cette aventure ... et aussi ton sens de l'humour mémorable.

Au Docteur Catherine Dunyach-Remy, ma tout aussi géniale presque directrice de thèse

Catherine, merci de m'avoir encadrée, orientée, aidée et conseillée. Je te remercie également d'avoir partagé avec moi tes connaissances et ton expérience si bien professionnelle que personnelle de ce long chemin qu'est la thèse. Merci pour ta confiance et ton écoute dans les moments difficiles. Sans ton soutien et tes conseils je ne serai pas à ce stade de ma carrière et je n'aurai certainement pas pu m'épanouir autant dans ce travail de thèse.

Signé ta petite espionne (smiley badass un peu James Bond sur les bords...).

A monsieur le PDG Thierry Bernardi

Merci d'avoir pu me donner ma chance pour réaliser cette thèse avec vous et de m'avoir si bien accueilli au sein de votre entreprise. J'espère que l'aventure BioFilm

ne s'arrêtera pas là et que nos folles aventures seront au moins aussi productives que ce travail. Oh et j'allais oublier ... merci aussi de nous faire tous un peu voyager avec vous au travers des photos sur le groupe WhatsApp.

A Christian Provot et Jason Tasse

Je tenais à vous remercier pour votre soutien et votre gentillesse à tous les deux durant ces trois longues années. Christian, merci pour tout ce que tu as fait pour moi mais surtout pour ses nombreux appels quand j'étais en plein doute, pour ces échanges lors de l'écriture du TERRIBLE brevet, pour la visite à Clermont et j'en passe... J'espère que tu t'épanouiras dans ton nouveau chemin, tu le mérites. Jason, je te remercie pour tous tes conseils et ton expérience récente de la thèse, qui, à mainte reprise m'a été plus qu'utile (oui oui j'ai certainement lu ta thèse plus de fois que tes examinateurs...). Je serais très heureuse de pouvoir continuer notre collaboration.

A Stéphanie Badel-Berchoux et toute l'équipe de BioFilm Control et BioFilm

Pharma ; Arnaud Clément, Laurine Gastal, Elodie Lebouvier, Lauriane Saulnier, Marie Aubertin, Rémi Laurent, Elodie Olivares, Aurélie Comby et Jérôme Groelly. La situation sanitaire a quelque peu chamboulé nos plans et je n'ai pas eu beaucoup l'occasion de venir partager mon travail avec vous sur Clermont. Merci tout de même pour votre accueil lors de ma première venue en attendant de vous rendre visite à l'avenir.

Au Docteur David O'Callaghan, directeur du laboratoire U1047

Merci David de m'avoir accueilli dans ton laboratoire il y a de ça ... way to much time. Completely lost in the timeline, I suppose it's one side effect of the writing process... Well, thanks a lot for everything you do for us to make our completely crazy experiments possible. Thanks for the support, the advices, the help and last but not least to your (not always) funny super jokes in a (not always) super timing. Finally, thanks for my English; it was scary as hell to say a single word when I arrived and the minute after I realize that I am writing those acknowledgments in English...

Au Docteur Annette Vergunst et au Docteur Anne Keriél

Je vous remercie pour votre aide, vos précieux conseils, votre patience et votre disponibilité. Merci également pour ses moments de cohésion d'équipe qui vous sont chers et qui ont réellement fait du bien pendant cette période particulière. D'ailleurs, il serait temps pour vous de remettre mon titre de meilleur pâtissier de l'U1047 en jeu, je dis ça je ne dis rien ...

A tous les membres de l'unité U1047, **Christine Carrio, Alex, Ludo, Fanny, Théo**. A mes co-thésards, ceux qui ont déjà fini cette aventure extraordinaire : ma **Yara**, qu'est-ce qu'on a pu rire dans ce bureau. **Elia**, gracias para el mejooooooor consejo de todos los tiempos : Inhaaaaaale solutioooooones, exhhaaaale problemaaaaaas. Besos a Olivia. A ceux encore dans cette aventure et qui sont sortis de la phase de lune de miel avec leur thèse (courage d'ailleurs vous verrez ça s'arrange à la fin ... ou pas ^^). **Johan, Benjamin**, merci pour nos discussions sérieuses mais aussi celles sans queue ni tête quelque fois, merci pour tes conseils, merci pour tes blagues (les bonnes comme les archiiii nuelles) et merci pour tes mots gentils quand

le moral n'était pas au max du max. **Sonia**, well well well, on y est... un grand MERCI d'abord pour avoir eu la folle idée de faire ta thèse sur Brucella (WTF) et d'avoir choisi ce labo. Plus qu'une collègue tu es devenue mon amie. Merci pour ses brainstormings et tous tes conseils toujours très pertinents sur des sujets scientifiques mais aussi dans la vie en général. Merci d'avoir été là pour moi quand j'étais graaaave dans le creux de la vague et de toujours vouloir me protéger (tu veux que j'aïlle la voir mwaaaa, j'y vaiiiiis ?!, s'il faut on lui crève les pneus rien à faire !!!). Merci pour ces soirées à boire du vin, celles à faire du shopping, celles à regarder des vidéos YouTubetuto make-up, celles à partager des liens Amazon pour acheter des trucs complètement inutiles (ps : plus j'écris ses remerciements plus je me dis que si quelqu'un d'autre que toi les regarde il va croire qu'on n'a rien foutu de nos thèses mdrrrr). A nos road trips (d'ailleurs on part quand chez toi ? je veux voir la neige moi), et à notre belle collaboration qui va voir le jour prochainement, merci pour tout. **Juju**, je te remercie pour ton soutien sans faille et pour tous ces repas du midi où on aura beaucoup rigolé. Merci aussi pour nous embarquer avec Sonia dans tes histoires et d'avoir une confiance aveugle en nous (tkt juju toujours là pour twoaaa). Enfin merci à **Flavia** pour ta patience, ton écoute, ton sourire, ta gentillesse et ta compréhension.

A tous les membres de notre super équipe clinique **Alix Pantel, Jérôme Ory, Robin Stephan, Agathe Boudet** pour m'avoir guidé lors de nos présentations du vendredi après-midi.

Andréa, ma super stagiaire, qui a fait un vrai travail de pro et qui m'a vraiment bien avancé pour les manips à un moment où j'en avais suuuuper marre de rentrer dans ce labo terriiiiible ^^ . Merci aussi pour nos bavardages pas toujours scientifiques on ne va pas mentir, merci pour ta bonne humeur, ta joie de vivre et ta gentillesse. Merci aussi d'avoir fait la pompom girl quelque fois, j'hésite d'ailleurs à t'acheter un costume pour ton anniversaire avec écrit « team super cassou » devant. Sérieusement j'espère avoir pu te transmettre un petit peu de ma passion pour la recherche même si c'est un domaine exigeant. Je te souhaite vraiment le meilleur et de t'épanouir pour la suite.

A mes amis, un grand merci à vous tous. **Sonia** (et ouiiii bien sûr que je te remets dans cette partie, trop hâte de voir où nos aventures vont encore nous mener. D'ailleurs ça fait bien longtemps qu'on n'a pas manger des nuggets à 5h du mat en regardant un film de fille...**Julien** (Aka Aquaman, sans les muscles, sorry mais la précision était OBLIGATOIRE), **Ludo** (mon binôme du P2 for ever & ever qui est devenu plus que ça) et sa folie famille, **Marine et Ambre. Thomas** (le S), **Thibaut** (A tous nos vocaux de 389 minutes), **Mélanie** (que de chemin parcouru depuis l'époque de l'école d'ingé dans la chambre dark vador...) & **Antonin. Anaïs** (ma cousine d'amour).

A ma famille, qui, avec cette question récurrente et bien angoissante « quand est-ce que tu la soutiens ENFIN cette thèse ? » m'a permis de ne jamais dévier de mon objectif final.

A ma belle-famille, et en particulier à Cricri, Queen Coco, tatie Guillaume et Daniel pour leur accueil et leur gentillesse.

A mes parents, mes plus grands fans, pour tous vos efforts, votre soutien, vos sacrifices, votre confiance pour mes études (ce n'était pas évident mais vous pouvez souffler c'est ENFIN fini) et mon bonheur, merci. Merci de m'avoir inculqué des valeurs si importantes qui ne font qu'aujourd'hui jamais rien n'est impossible. A ma sœur, **Coleen** pour m'avoir tenu compagnie lors de ces nombreux allers-retours à la fac (oui on sait très bien que si t'avais pas eu besoin de moi, tu ne les aurais pas fait lol) et aussi, ça n'a rien à voir, mais pour accepter de me coiffer même quand t'en a pas envie et même si je perds 80% de mes cheveux à chaque fois vu ta douceur légendaire...

A **Nicolas**, merci pour tous ces moments, les bons comme les un peu plus compliqués, partagés durant ces années. Merci pour ton soutien indéfectible et ton enthousiasme quelque fois même exagéré à l'égard de mes travaux de recherche (elles sont fluoooooooo c'est diiiiiiiiiingue) mais aussi dans nos projets en général. Je suis certaine que la vie nous réserve encore des aventures de fou et j'ai hâte de vivre tout ça avec toi.

Je remercie en dernier lieu le dispositif de Conventions Industrielles de Formation par la Recherche (CIFRE) mis en œuvre par l'Association Nationale de la Recherche et de la Technologie (ANRT) pour les aides financières à ce projet.

L'imagination est plus importante que la connaissance. Car la connaissance est limitée, alors que l'imagination embrasse l'univers tout entier

Albert Einstein

TABLE DES MATIÈRES

LISTE DES ABBRÉVIATIONS	11
RÉSUMÉ	13
I. GÉNÉRALITÉS	15
1. Plaies chroniques	17
A. Définition	17
B. Classification	17
C. Complications	17
D. Environnement des plaies chroniques	18
2. Cas particulier de l'infection du Pied Diabétique	20
A. Diabète sucré	20
B. Définition	21
C. Physiopathologie	21
a. Facteurs liés à l'hôte	21
b. Facteurs bactériens	22
D. Écologie microbienne	23
3. Biofilm	25
A. Définition	25
B. Formation du biofilm	26
a. Adhésion	27
b. Maturation	28
c. Dispersion	29
C. Composition des biofilms	29
a. Polysaccharides	29
b. Protéines	31
c. ADN extracellulaire	34
D. Infections du pied diabétique & Biofilm	35
<u>Travail n°1: Biofilms in Diabetic Foot Ulcers</u>	37
4. Méthodes d'études du biofilm	55

5. Stratégies thérapeutiques dans la prise en charge des plaies chroniques	58
<u>Travail n°2:</u> <i>Alternative approaches for the management of DFI</i>	61
PROBLEMATIQUE GÉNÉRALE	79
II. MISE EN PLACE D'UN NOUVEL OUTIL <i>IN VITRO</i> POUR L'ÉTUDE DES PLAIES CHRONIQUES : LE MILIEU PLAIE	83
<u>Travail n°3:</u> <i>Adaptation of S. aureus in a medium mimicking DFI</i>	85
<u>Travail n°4:</u> <i>A wound-like media to study bacterial cooperation and biofilm in CW</i>	113
III. MISE EN PLACE D'UN SYSTÈME DE FORMATION DE BIOFILM EN FLUX	137
<u>Travail n°5:</u> <i>New in vitro technology to evaluate biofilm and antibiotic activity</i>	139
<u>Travail n°6:</u> <i>Evaluation of Bioflux 200 to characterize biofilm organization and the effect of antibiotics in an environment mimicking CW</i>	159
DISCUSSION & PERSPECTIVES	199
REFERENCES BIBLIOGRAPHIQUES	218
ANNEXES	239
<u>Annexe 1:</u> Brevet de propriété intellectuelle - Milieu Plaie	239
<u>Annexe 2:</u> Publication associée - Success of <i>E. coli</i> O25b:H4 Sequence type 131 Clade C Associated with a decrease in Virulence	241
<u>Annexe 3:</u> Publication associée – <i>S. aureus</i> toxins: An update on their pathogenic properties and potential treatments	263
<u>Annexe 4:</u> Publication associée - Biofilm formation in MRSA isolated in Cystic Fibrosis patients in absence and presence of antibiotics	285
<u>Annexe 5:</u> Tableau récapitulatif des communications	301

LISTE DES ABBRÉVIATIONS

Termes généraux

ADN : Acide désoxyribonucléique
ADNe : Acide désoxyribonucléique extracellulaire
AHL : Acyl-homosérines lactones
BGN : Bacilles à Gram négatif
BMR : Bactéries multi résistantes
EPS : Extracellular polymeric substance
FEP : Functionally equivalent pathogroups
IPD : Infection du pied diabétique
MSCRAMM : Microbial surface components recognizing adhesive matrix molecules
OMS : Organisation mondiale de la santé
P. aeruginosa : *Pseudomonas aeruginosa*
PSM : Phenol-soluble modulin
QS : Quorum-sensing
S. aureus : *Staphylococcus aureus*
SARM : *Staphylococcus aureus* résistant à la méthicilline
SERAM : Secretable expanded repertoire adhesive molecules

Gènes & protéines

agrA : Accessory gene regulator A
atlA : Autolysine
clf : Clumping factor
cna : Collagen adhesin
crc : Catabolite repression protein
fnbPA : Fibronectin-binding protein A
gyrB : DNA Gyrase subunit B
hlaA : Hemolysine α A
Isd : Protéine à motif NEAT
lasI : Contrôle la synthèse de l'acyl-homoserine-lactone synthase
pel : Contrôle la synthèse de l'exopolysaccharide pel
pqsH : Pseudomonas quinolone system subunit H
psl : Contrôle la synthèse de l'exopolysaccharide psl
rhII : Contrôle la synthèse de l'acyl-homoserine-lactone synthase
sarA : Contrôle la synthèse du facteur de transcription sarA
spaA : *S. aureus* protein A

RÉSUMÉ

Les plaies chroniques sont un réel problème de santé publique. L'une des principales complications est l'évolution fréquente vers l'infection avec un risque sous-jacent d'amputation. La difficulté de prise en charge repose notamment sur la présence d'un biofilm polymicrobien au niveau du lit de la plaie. L'objectif de cette thèse était de promouvoir l'amélioration de l'état de l'art relatif à la compréhension de ce phénomène physiopathologique important mais également de développer de nouvelles approches concernant le traitement thérapeutique des plaies chroniques pour réduire les risques d'infections morbides. Ce travail de doctorat a permis : i) de parfaire les outils diagnostiques de par la création d'un nouveau modèle *in vitro* mimant l'environnement dans lequel les bactéries évoluent au niveau des plaies chroniques ; ii) d'étudier le comportement (virulence, fitness, génomique, morphologie, formation de biofilm précoce, expression de gènes clés pour la formation de biofilm) de souches de références et de souches cliniques de *Staphylococcus aureus* (SA) et *Pseudomonas aeruginosa* (PA). Ces souches, isolées au sein d'une même plaie, étaient exposées de façon courte ou prolongée, à un milieu classique ou mimant l'environnement chronique d'une plaie. Les résultats ont montré qu'une exposition dans des conditions environnementales stressantes réduisaient la virulence et le fitness des souches au profit d'un comportement plus tourné vers la formation de biofilm ; iii) de démontrer l'impact de la présence de plusieurs bactéries au sein d'un environnement. Ce travail a particulièrement mis en évidence la baisse de pathogénicité et l'évolution de l'expression de certains gènes impliqués dans le biofilm de souche de SA en présence de PA. Enfin ce travail s'est concentré sur iv) la mise au point d'une technique de formation de biofilm dynamique et d'imagerie confocale permettant la visualisation d'un biofilm polymicrobien en trois dimensions et l'évaluation de molécules antimicrobiennes sur chaque espèce bactérienne composant le biofilm polymicrobien après un débridement mécanique automatisé. La combinaison de notre nouveau milieu « plaie chronique » et du système de formation en flux et visualisation en 3D du biofilm polymicrobien représente des outils puissants pour améliorer la compréhension des interactions régissant les biofilms mais aussi pour évaluer l'efficacité de molécules candidates dans la prise en charge des plaies chroniques.

Mots clés : Plaies chroniques, infections, biofilms, coopération bactérienne

ABSTRACT

Chronic wounds are a real public health problem. One of the main complications is the recurrent progress towards infection with an underlying risk of amputation. The difficulty of management lies in the presence of a polymicrobial biofilm at the wound bed. The objective of this thesis was to promote the development of the state-of-the-art of this important pathophysiology phenomenon of biofilm but also to promote new approaches for therapeutic treatment of chronic wounds to reduce risk of morbid infections. This doctoral work enabled: i) to perfect diagnostic tools by creating a new *in vitro* model mimicking the environment in which bacteria evolve at the level of chronic wounds; ii) to study behavior (virulence, fitness, genomics, morphology, early biofilm formation, expression of key genes for biofilm formation) of reference strains and clinical strains of *Staphylococcus aureus* (SA) and *Pseudomonas aeruginosa* (PA) isolated on a patient wound, based on short or long-term exposure to a conventional or a chronic wound like environment. The results showed that exposure under stressful environmental conditions reduced the virulence and fitness of the strains in favor of a biofilm-oriented behavior; iii) demonstrate the impact of multiple bacteria in an environment. This work has particularly highlighted the decrease of the pathogenicity and the evolution of the expression of some genes involved in the biofilm of SA strain when in contact with PA strain. iv) the development of a dynamic biofilm formation and confocal imaging technique allowing the visualization of a three-dimensional polymicrobial biofilm and the evaluation of antimicrobial molecules on each bacterial species composing the biofilm polymicrobial after an automatized mechanical debridement. The combination of our new chronic wound-like medium and the microfluidic biofilm formation and 3D visualization system of the polymicrobial biofilm represents powerful tools to improve the understanding of the interactions governing biofilms but also to evaluate the effectiveness of candidate molecules in chronic wounds management.

Key words: Chronic wounds, infections, biofilms, bacterial cooperation

PARTIE I.

GÉNÉRALITÉS

1. Plaies chroniques

A. Définition

Une plaie est définie comme un défaut ou une rupture de la peau résultant en une perturbation de la structure anatomique naturelle ¹. Elle peut s'étendre à d'autres tissus tels que les tissus sous-cutanés, les muscles, les tendons, les nerfs, les vaisseaux et les os ². En se basant sur le délai de cicatrisation, une plaie est classée aiguë ou chronique. Le terme **plaie chronique** désigne les plaies dont le délai de cicatrisation est prolongé. La plaie est considérée comme chronique après **4 à 6 semaines** d'évolution sans tendance à la cicatrisation malgré un traitement local approprié ³.

B. Classification

Il existe 4 types de plaies chroniques décrites en clinique :

- **Les escarres** : ce sont des lésions cutanées d'origine ischémique liées à une compression excessive et prolongée sur les tissus mous ⁴.
- **Les ulcères** : ce sont des plaies fréquentes situées principalement au niveau de la jambe. L'ulcère de jambe est majoritairement dû à une cause vasculaire : **veineuse** ou **artérielle** voire mixte ⁵.
- **Les plaies du pied diabétique** ⁶.

C. Complications

La problématique majeure des plaies chroniques est la **complication infectieuse**. L'infection peut être localisée aux tissus sous cutanés ou à la structure osseuse la plus proche mais elle peut, dans certains cas plus graves, être généralisée entraînant une bactériémie ou un sepsis ⁷. La mortalité des suites de ces infections systémiques est estimée entre 10 et 50 % des cas faisant de l'infection des plaies un défi considérable en termes de soins de santé ⁸. La prise en charge des plaies

chroniques est compliquée puisqu'elle nécessite non seulement de détecter la présence de bactéries dans la plaie mais surtout de distinguer la contamination de la colonisation par les souches du microbiote cutané, appelant une vigilance de l'état de la plaie, au processus d'infection, impliquant l'intervention par le clinicien ⁹. Or, il n'existe à ce jour aucun moyen formel de faire la distinction entre colonisation et infection. On estime aujourd'hui en France que 2 millions de personnes souffrent chaque année de plaies chroniques nécessitant entre 147 et 271 jours en moyenne pour cicatriser incluant un séjour hospitalier d'au moins 2 mois. Chaque année, on recense 51 000 décès des suites des complications infectieuses liées aux plaies chroniques ¹⁰. Ces dernières donnent, des infections des plaies chroniques, un réel problème de santé publique de par leurs répercussions dramatiques sur la vie des patients mais également d'un point de vue socio-économique ¹¹.

D. Environnement des plaies chroniques

Pour améliorer la prise en charge thérapeutique des infections des plaies chroniques, il est indispensable de mieux connaître l'environnement cellulaire, microbiologique et inflammatoire dans lequel évoluent les bactéries. Il existe des paramètres intrinsèques aux plaies chroniques.

Ainsi, il est depuis longtemps admis qu'une plaie présente un exsudat dont la fonction principale est de prévenir la dessiccation qui conduirait à un retard de cicatrisation. Une plaie chronique contient donc des protéases dont le rôle est de préparer le lit de la plaie et de dégrader les composants de la matrice extracellulaire (collagène et l'élastine) afin de préparer le processus de réépithélisation de la plaie ¹². Elle contient également plusieurs éléments dont : sodium, potassium, chlorure, urée, créatinine (concentrations sérique), bicarbonate, **cytokines** (Interleukines, TNF- β , Interféron- α), **leucocytes**, polynucléaires neutrophiles, débris de cellules (kératinocytes), lysozyme, **protéines** (Métallo-protéinases matricielles) ¹².

Les facteurs extrinsèques quant à eux sont de nature environnementale. Ces paramètres physiques extrinsèques tels que la concentration en oxygène, l'hygrométrie, la température ou encore le pH sont intimement liés et interdépendants.

La cicatrisation requiert des besoins en oxygène afin de permettre l'intégration des cytokines au processus ainsi qu'une différenciation cellulaire intensive grâce la production d'ATP par l'intermédiaire de la phosphorylation oxydative dans les mitochondries. L'oxygène est aussi un effecteur au stress oxydatif des neutrophiles. Ainsi, l'oxygène joue un rôle central dans le processus de cicatrisation et le taux relevé au lit de la plaie varie en fonction de l'étiologie ¹³.

La température cutanée dépend de phénomènes physiologiques comme le flux sanguin ou l'état métabolique ainsi que de facteurs environnementaux tels que la température ambiante, l'humidité ou la zone anatomique concernée. Elle est, en général, plus basse que la température corporelle. Des études ont démontré que la température idéale permettant une cicatrisation optimale semble se situer aux alentours de 36°C. Elle ne doit, dans tous les cas, pas descendre en dessous de 32°C, la normothermie et l'hyperthermie devant être préférées à une hypothermie, clairement péjorative ¹⁴.

Une particularité notable des plaies chroniques repose sur le **pH** présent à la surface de la peau qui reste alcalin tout le long du processus de chronicité. L'acidification de la peau étant signe de re-épithélisation et de cicatrisation, les plaies chroniques ont un pH décrits constant aux alentours de 8 ^{15,16}.

D'autre part, il est également connu que les infections de plaies chroniques sont polymicrobiennes ⁸. Les conditions stringentes présentes au niveau des plaies chroniques combiné au polymicrobisme influencent également sur un autre paramètre très important dans la physiopathologie : **les interactions** bactériennes. Les coopérations ou inhibitions entre différentes espèces bactériennes semblent modifier le comportement (virulence, croissance, formation de biofilm...) des souches. Les différentes espèces bactériennes ne sont pas organisées de manière aléatoire mais regroupées dans des structures qui leur confèrent un avantage sélectif pour leurs coopérations. Parmi ces structures particulières source d'interactions on notera le biofilm. La présence de biofilm polymicrobien au niveau des plaies chroniques est fréquente et sa conséquence majeure est un retard de cicatrisation de la plaie ³. La formation de ce biofilm multi-espèce ainsi que les coopérations qui s'y jouent dépendent de l'environnement dans lequel évoluent les bactéries.

Les plaies chroniques constituent donc des environnements particuliers qui, pour être étudiées ou pour évaluer l'effet de molécules thérapeutiques nécessitent l'obtention de modèles *in vitro* mimant ces plaies. Il n'existe cependant pas à l'heure actuelle de modèle de référence représentatif pour l'étude des plaies chroniques.

2. Cas particulier de l'infection du pied diabétique

A. Diabète sucré

Le diabète sucré, *diabetes mellitus*, est une affection chronique métabolique caractérisée par une déficience sécrétoire et/ou une anomalie de l'action de l'insuline générant une hyperglycémie chronique pathologique ¹⁷.

En 2019, le diabète affectait plus de **463 millions de personnes** dans le monde ¹⁸. Le diabète sucré est considéré comme la 1^{er} pandémie de maladie non-contagieuse¹⁹.

L'hyperglycémie chronique associée aux anomalies métaboliques induites par le diabète sucré entraînent des complications cliniques à long terme responsables d'une mortalité importante. Aussi, l'espérance de vie d'un patient diabétique est réduite d'environ 5 ans à partir de 50 ans par rapport à une personne non diabétique ²⁰. Environ 80 % des patients présentant un diabète sucré, risquent, au cours de leur vie, de développer une complication chronique liée au diabète sucré, c'est pourquoi le dépistage et le traitement de ces complications constituent un réel enjeu dans la prise en charge thérapeutique ²¹.

On différencie communément 3 sous-groupes de complications relatives au diabète sucré :

- Les complications micro-angiopathiques : résultent en l'altération des petits vaisseaux par infiltration de glycoprotéines. Les conséquences sont particulièrement sévères sur les vaisseaux de la rétine, du système nerveux et des reins ²² ;

- Les complications macro-angiopathiques : l'atteinte des gros vaisseaux (athérosclérose) est dû à un rétrécissement des artères secondaire à un dépôt de plaque d'athérome. Les artères les plus touchées dans le cadre de la macro-angiopathie diabétique sont celles du cœur, des jambes et du cou ²² ;
- Enfin **l'infection du pied diabétique** ²².

B. Définition

Le pied diabétique regroupe les infections et ulcérations des tissus profonds du pied chez le patient diagnostiqué avec un diabète sucré ²³. L'origine et l'apparition des plaies aux pieds chez les patients diabétiques sont multifactorielles. Trois facteurs associés sont incriminés dans le développement des ulcères du pied diabétique (UPD) : la neuropathie diabétique, l'artériopathie et la présence d'infection(s) ²⁴.

Il a été démontré qu'au cours de leur vie, 15% des patients diabétiques déclencheront des UPD ²⁵. Entre 50% et 80% de ces ulcères deviendront infectés et la propagation de l'infection aux tissus mous et aux structures osseuses augmente considérablement le risque d'amputation du membre inférieur ^{26,27}.

L'infection du pied diabétique (IPD) est ainsi un réel **problème de santé publique** de par sa fréquence et la gravité de cette complication, avec un taux d'amputation et de morbidité extrêmement élevé, mais aussi de par ses conséquences socio-économiques.

C. Physiopathologie

Les facteurs de risques de survenue d'une infection secondaire à l'apparition d'une plaie du pied sont multiples. On peut les diviser en 2 grands groupes, les facteurs liés à l'hôte et ceux liés aux bactéries responsables de l'infection :

a. Facteurs liés à l'hôte

- La neuropathie : la polyneuropathie distale sensitive, motrice et autonome, est responsable d'une hyposensibilité au niveau de la

plaie du pied. L'indolence rend le diagnostic plus difficile et retarde la prise en charge thérapeutique ²⁸.

- L'artériopathie des membres inférieurs : la présence d'une ischémie ou d'une artériopathie est le résultat d'une maladie microvasculaire, effet direct de l'hyperglycémie chronique. La présence d'une artériopathie, en cas d'ulcération de plaie, complique la prise en charge, aggrave le pronostic par un apport artériel insuffisant et augmente la propagation de l'infection ²⁹.
- L'immunopathie : l'hyperglycémie chronique engendre des défaillances des mécanismes de défense immunitaire (immunité innée et humorale) avec notamment une altération des polynucléaires neutrophiles, une diminution de la phagocytose ou encore un chimiotactisme réduit favorisant la survenue de l'infection ³⁰.
- La susceptibilité génétique & les facteurs métaboliques : certains facteurs génétiques et métaboliques tels que la diminution de l'acuité visuelle, le surpoids, la présence d'une mycose du pied, une protéinurie ou encore une rétinopathie sont décrits dans la littérature comme facteurs de risques ³¹.
- L'anatomie du pied : le pied a une anatomie particulière, cloisonnée en plusieurs loges inter-communicantes, expliquant la dissémination rapide du processus infectieux ²⁴.

b. Facteurs bactériens

- Virulence bactérienne : le pouvoir pathogène des bactéries est important dans la prise en charge thérapeutique des IPD ³².
- Résistance ou tolérance : de la même manière que la virulence bactérienne, la résistance (mécanisme irréversible) ou la tolérance

(mécanisme réversible) aux antibiotiques des bactéries participent à la difficulté de prise en charge thérapeutique. Il est reporté une augmentation du nombre de bactéries multi résistantes (BMR) aux antibiotiques dans les UPD, notamment le *Staphylococcus aureus* résistant à la méthicilline (SARM) retardant la cicatrisation et compliquant la prise en charge ³².

- Formation de biofilm : les bactéries existent sous 2 types, planctoniques c'est-à-dire sous forme de cellules libres, ou sessiles, attachées à un support biotique ou non, formant une communauté polymicrobienne où les interactions intra et inter espèces sont privilégiées. On recense la présence de biofilm polymicrobien dans 60 à 80 % des plaies chroniques ^{33, 34}. La conséquence clinique de ce biofilm est un retard de cicatrisation et une chronicisation de l'infection ³⁵.

Le diagnostic d'infection du pied diabétique est basé sur la clinique, toutefois la difficulté majeure pour le clinicien est de faire la distinction entre l'infection, processus pathologique, de la colonisation bactérienne, processus physiologique. Il existe en effet un équilibre fragile entre la colonisation de la plaie par le microbiote cutané ou par des bactéries environnementales de façon transitoire, ne nécessitant pas d'intervention clinique, de l'infection de la plaie par des micro-organismes pathogènes conduisant à un retard de cicatrisation ³⁶. A ce jour, les cliniciens ne disposent que de peu d'outils pour les aider dans la différenciation de ces deux états orientant la prise en charge thérapeutique des patients.

D. Écologie microbienne

Les études sur les communautés microbiennes associées aux plaies du pied chez le diabétique ne cessent d'augmenter ces dernières années. Il apparait en effet que la composition du microbiote de la plaie aurait une incidence sur la cicatrisation ou le risque d'amputation chez les patients ⁸.

Dans une récente étude, les chercheurs ont recueilli des données à partir du microbiome d'UPD chez plus de 100 patients. Les prélèvements ont été réalisés avant et après débridement ainsi que sur un suivi à long terme de 26 semaines à raison d'un prélèvement tous les 15 jours. Le suivi, en parallèle de l'évolution de l'infection et de l'état de la plaie, a permis de rendre compte que le potentiel de virulence de chaque espèce mais surtout l'association bactérienne jouent un rôle dans la cicatrisation de la plaie ³⁷.

De manière descriptive, les bactéries les plus fréquemment isolées sont les cocci à **Gram positif** dont les *Staphylococcus aureus* (35% des souches isolées) et à moindre mesure les streptocoques β -hémolytiques (13%) et les entérocoques (7%) ³⁸. La bactérie *S. aureus*, isolée dans la majorité des plaies, est connue pour son potentiel de résistance aux antibiotiques. Si, au niveau de l'espèce, la présence de *S. aureus* ne permet pas de prédire l'évolution de la plaie, les chercheurs ont découvert que la présence de certaines souches particulières (présence de facteurs de virulence, gènes de résistance aux antibiotiques) coïncidait avec des plaies dont la cicatrisation était très difficile ^{39, 40}.

En ce qui concerne les bactéries à **Gram négatif**, la plupart sont des entérobactéries (*Escherichia coli*, *Proteus mirabilis*, *Klebsiella* spp. - 29%). Des souches de *Pseudomonas aeruginosa* (8%) sont également isolées ⁴⁰. Cette bactérie est fréquemment isolée dans les cas d'ostéites ou d'infection des tissus mous et en cas d'hospitalisation prolongée ⁴¹. Son potentiel pathogène est aujourd'hui discuté mais il semblerait que ce soit l'association avec d'autres espèces bactériennes qui lui confère une pathogénicité ⁴².

Des **bactéries anaérobies** sont aussi isolées dans 4% des IPD après mise en culture dans les milieux classiquement utilisés. La métagénomique mais également la culturomique démontrent que ce chiffre est sous-estimé. L'importance de ces souches et notamment leur présence dans les plaies profondes ont été décrites ⁴³. L'étude a mis en évidence la présence de Gram positif de la classe des Clostridiales (*Anaerococcus*, *Fingoldia* et *Peptoniphilus*) ainsi que d'autres anaérobies stricts tels *Porphyromonas* et *Prevotella*. Une seconde étude récemment publiée a pu identifier le même type de communauté tout en soulignant que ces anaérobies strictes et

facultatifs sont en une sous-représentation dans les plaies chroniques associées aux maladies auto-immunes ⁴⁴.

Les interactions bactériennes influençant la survenue de la cicatrisation, il est important de prendre en considération l'ensemble de la communauté bactérienne présente sur la plaie et non pas une espèce isolée ⁴⁵. Les scientifiques s'intéressent donc à comprendre les mécanismes qui régissent ces interactions bactériennes et comment elles adviennent. Un des écosystèmes favorisant la survenue des coopérations ou des inhibitions entre espèces bactériennes est le biofilm.

3. Biofilm

A. Définition

Un biofilm est une **communauté de micro-organismes** adhérente à une surface et enrobée dans une matrice d'exopolysaccharides protectrice et adhésive que ces microbes secrètent ⁴⁶. Les bactéries sont des êtres unicellulaires qui peuvent évoluer dans leur environnement de manière isolée et libre dans un milieu liquide. Ces bactéries sont alors dites sous forme planctonique. L'autre alternative de mode de vie des bactéries est celui en biofilm. Le comportement dit alors **sessile** est prédominant chez les organismes unicellulaires ⁴⁷. Les premières descriptions de biofilms bactériens sont anciennes (1683 ⁴⁸) mais il faudra attendre la fin du 20^{ème} siècle et la découverte en 1980 de John William Costerton pour considérer les bactéries et leur comportement sous forme sessile en santé humaine ⁴⁹.

Les biofilms se développent dans divers milieux et peuvent adhérer sur pléthore de surfaces naturelles ou artificielles posant ainsi des problèmes industriels mais également en matière de santé publique. En effet, les biofilms sont recensés dans nombres de **maladies infectieuses** et peuvent être à l'origine de maladies nosocomiales. Près de 65% des infections nosocomiales seraient induites ou persisteraient en raison de la présence de biofilm bactérien, on parle de 80% dans le cas des infections bactériennes chroniques ⁵⁰. Les principales infections associées aux biofilms sont dues soit à la présence de biofilms sur des dispositifs médicaux (cathéters, prothèses, sondes urinaires et valves cardiaques) ⁵¹⁻⁵³ soit à des affections chroniques avec présence de biofilm directement sur les tissus (infections

ostéoarticulaires, mucoviscidose, endocardite infectieuse, infections urinaires, plaies chroniques infectées, pathologies dentaires) ⁵⁴⁻⁵⁶.

Les biofilms ont un rôle majeur dans la faculté des bactéries à coloniser des environnements variés et résister à une multitude d'agressions externes notamment par la protection que leur confère la matrice d'exopolysaccharides de l'action du système immunitaire et des antibiotiques ⁵⁷. Enfin, l'organisation communautaire décrite dans les biofilms permet aux bactéries de coopérer et d'interagir entre elles rendant la prise en charge thérapeutique encore plus complexe ⁵⁷.

B. Formation du biofilm

Le passage d'un mode de vie à l'autre est un processus dynamique et complexe. Le mécanisme de formation d'un biofilm passe par 5 étapes (**Figure 1**). Les premières phases sont relatives à l'adhésion des bactéries planctoniques à la surface, réversible dans un premier temps puis irréversible. Ces phases sont suivies d'étapes de maturation où les micro-organismes poursuivent leur développement en formant des micro-colonies et produisent leur matrice extracellulaire protectrice. Enfin, certains micro-organismes peuvent se détacher du biofilm mature sous l'effet de facteurs environnementaux. C'est l'étape finale de dispersion.

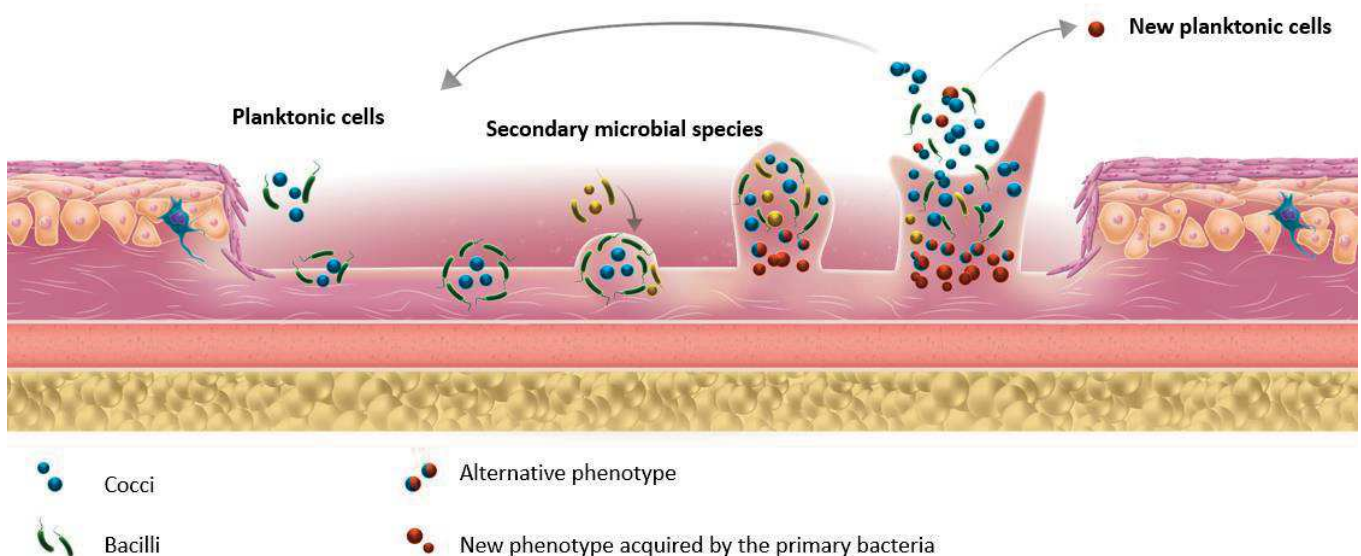


Figure 1 : Représentation des différentes étapes de formation de biofilm.

Source : Pouget *et al*, 2020, Microorganisms ⁵⁸

a. Adhésion

L'adhésion bactérienne initiale est une **adhésion réversible** à un support qui peut être biotique (peaux, muqueuses, poumons, tissus, yeux, gencives ...) ou abiotique (dispositifs et implants médicaux, roches, surfaces en plastique, aluminium ...). Cette adhésion fait intervenir des liaisons faibles de type électrostatiques et des forces de Van der Waals entre les bactéries et le support. Il existe des facteurs influençant cette liaison entre bactéries et support, tels que les forces hydrodynamiques qui régissent le matériel mais également qui s'exercent sur la membrane bactérienne, les propriétés physico-chimique du support, des bactéries et du milieu (pH, force ionique, température) ⁵⁹. L'adhésion réversible est aussi influencée par l'état des bactéries et les produits qu'elles sécrètent. Aussi, il a été démontré que chez *S. aureus* les acides téichoïques ou l'ADN extracellulaire (ADNe) interviennent dans le processus d'attachement aux surfaces ^{60, 61}. Sur les dispositifs médicaux implantés, il a été reporté chez *S. aureus* l'implication de protéines bactériennes de surface capables de se lier aux protéines de la matrice extracellulaire de l'hôte qui recouvrent ces dispositifs. Les microbial surface components recognizing adhesive matrix molecules (MSCRAMM) regroupent des protéines d'adhésion jouant un rôle dans l'infection et l'échappement au système immunitaire ⁶².

Chez *S. aureus*, il existe une vingtaine de MSCRAMMs décrits dont les principaux sont le clumping factor A et B (ClfA et ClfB) ⁶³, les fibronectin-binding proteins A et B (FnbpA et FnbpB) ⁶⁴ et la collagen adhesin (Cna) ⁶⁵. Ces protéines se lient respectivement au fibrinogène, à la fibronectine et au collagène de la matrice extracellulaire. Chez *P. aeruginosa*, pas de MSCRAMMs mais d'autres éléments ont été décrits comme participant au mécanisme primaire d'adhésion. Les principales molécules sont des polysaccharides dont l'alginate, Pel et Psl qui permettent la liaison de la matrice extracellulaire au support ⁶⁶.

L'adhésion des bactéries déclenche ensuite des modifications physiologiques qui induisent une **adhésion irréversible** à la surface ⁶⁷. Les bactéries se redistribuent ensuite le long de la surface et vont former des micro-colonies.

b. Maturation

La maturation du biofilm se poursuit avec la multiplication bactérienne et la production de l'**extracellular polymeric substance** (EPS), leur matrice protectrice⁶⁸. La formation initiale de cette EPS concourt à l'organisation de micro-colonies sous forme de structure en champignons en 3 dimensions. Ces structures en 3 dimensions sont séparées par des canaux permettant la mise en place d'un gradient de diffusion d'oxygène et de nutriments. La concentration décroît depuis la surface vers la base du biofilm où les nutriments sont plus rares et où les déchets du métabolisme bactérien s'accumulent. Ces canaux ne desservent pas toutes les régions du biofilm de la même manière créant ainsi des microenvironnements très hétérogènes au sein du biofilm⁶⁹. Ces **micro-colonies** se développent ensuite au sein de l'EPS et des micro-organismes secondaires viennent s'intégrer au biofilm préexistant formant ainsi un écosystème microbien hétérogène⁵².

La formation de ces microniches environnementales conduit donc à l'émergence de sous-populations physiologiquement distinctes, en particulier vis-à-vis de la tolérance aux antibiotiques. La matrice extracellulaire pourrait en effet constituer une barrière de diffusion aux antibiotiques permettant une adaptation progressive de la physiologie des bactéries exposées au stress antibiotique.

Enfin, la présence fréquente de microorganismes d'espèces différentes au sein d'un même biofilm constitue un niveau supplémentaire d'hétérogénéité biologique. En effet, la proximité et les contacts entre bactéries du biofilm facilitent la communication et les échanges conduisant à des mécanismes de **coopération bactérienne**, mais peuvent également induire des phénomènes de compétition⁷⁰. Les bactéries communiquent et adaptent leurs comportements en fonction de la concentration extracellulaire de petites molécules diffusibles telles que les acyl-homosérines lactones (AHL), les quinolones, les furanosyles chez les bactéries à Gram négatif ou de peptides à courtes chaînes chez les bactéries à Gram positif⁷¹. Ces molécules se fixent généralement à des récepteurs spécifiques et permettent l'activation d'un régulateur conduisant alors à une réponse phénotypique collective lorsqu'un seuil de molécules diffusibles est dépassé, c'est ce qu'on appelle le quorum-sensing (QS)⁷². De nombreuses interactions ont été décrites au cours desquelles une bactérie peut utiliser des nutriments produits par des bactéries voisines, conduisant à une

complémentarité métabolique. À l'opposé de ces phénomènes coopératifs, les bactéries composant un biofilm peuvent entrer en compétition via la production de molécules inhibant la croissance ou l'installation dans le biofilm ou encore la compétition pour des nutriments. Aussi, la proximité physique des bactéries favorise le transfert horizontal de matériel génétique par conjugaison ou transformation permettant l'acquisition de gènes de résistance aux antibiotiques ⁷³.

c. Dispersion

Enfin la dernière étape de la formation du biofilm est caractérisée par un **détachement** d'une partie des bactéries sessiles qui vont envahir de nouvelles surfaces ou initier un nouveau biofilm. Dans un biofilm mature, un équilibre s'établit entre la croissance bactérienne et la dispersion des bactéries sessiles ⁷⁴. C'est un processus physiologique contrôlé ⁷⁵. La dispersion est divisée en 2 processus : **l'érosion**, processus passif, qui est défini par le détachement continu de bactéries individuelles ou de partie de biofilm et **la desquamation** qui est un processus actif consistant en la perte massive de grandes parties de biofilm. Ce processus facilite la dissémination des infections ⁷⁶.

Chez *S. aureus* la dispersion des biofilms bactériens est globalement médiée par des peptides amphiphiles aux propriétés surfactantes appelés PSM (phenol-soluble moduline) ⁷⁷. Chez *P. aeruginosa*, les systèmes BdlA (Biofilm dispersion locus A), NicD (nutrient-induced cyclase D), DipA (dispersion-induced phosphodiesterase A), RbdA et GcbA sont impliqués dans le processus de desquamation ⁷⁸⁻⁸⁰.

C. Composition des biofilms

Les biofilms sont majoritairement constitués de 3 composés, à savoir les polysaccharides, les protéines et l'ADNe.

a. Polysaccharides

Les polysaccharides sont les constituants majoritaires de l'EPS ⁸¹.

Ceux des bactéries à Gram négatif sont de nature neutre ou polyanionique. Leur caractère anionique est renforcé par la présence de dérivés de l'acide uronique permettant la chélation des cations divalents tels que le calcium ou le magnésium ⁸². Cette chélation permet indirectement d'augmenter les forces d'adhésion des biofilms matures par réticulation des polymères. L'alginate, Pel et Psl sont des polysaccharides produits par *P. aeruginosa*. Ils jouent un rôle essentiel dans l'établissement et la stabilisation des biofilms ⁶⁶.

Le phénotype mucoïde très caractéristique de la majorité des souches de *P. aeruginosa* est dû à la surproduction de **l'alginate**, facteur de virulence polysaccharidique capsulaire conférant à la souche un avantage sélectif ⁸³. L'alginate est un polymère acétylé de poids moléculaire élevé composé de monomères non répétitifs d'acides L-gluronique et de D-mannuronique ⁸⁴. La surproduction de ce polysaccharide entraîne des changements architecturaux importants dans le biofilm se traduisant particulièrement par une augmentation de la résistance aux antibiotiques. Sa production dépend de l'opéron *mucA* ⁸⁵.

Des études ont démontré sur des souches non-mucoïdes la possibilité de former un biofilm dense suggérant qu'un ou plusieurs autres polysaccharides indépendants de l'alginate pouvaient être essentiels dans le développement de biofilm chez *P. aeruginosa* ⁶⁹. Un premier locus polysaccharidique a ainsi été découvert et désigné ***psl*** (polysaccharide synthesis locus) (**Figure 2**). Ce locus est un opéron comportant 15 gènes impliqués dans la machinerie de synthèse de Psl, essentiel à la formation de biofilm. L'inactivation du groupe de gène *psl* conduit à un défaut de formation de biofilm et notamment d'adhésion surface-bactéries. Plus tard, d'autres études ont montré que Psl fonctionnerait également comme un échafaudage indispensable à la tenue des bactéries dans l'EPS ⁶⁹. Psl est un polysaccharide riche en mannose et en galactose ⁸⁶.

Enfin, lors des recherches sur l'implication d'autres polysaccharides permettant l'établissement du biofilm chez *P. aeruginosa*, les chercheurs ont découvert un second locus, appelé ***pel***. Ce locus comporte 7 gènes induisant le maintien de la structure en biofilm ⁸⁷ (**Figure 2**). Les analyses ont permis de mettre en évidence que *pel* code un polysaccharide riche en glucose (structure complète non résolue à ce jour).

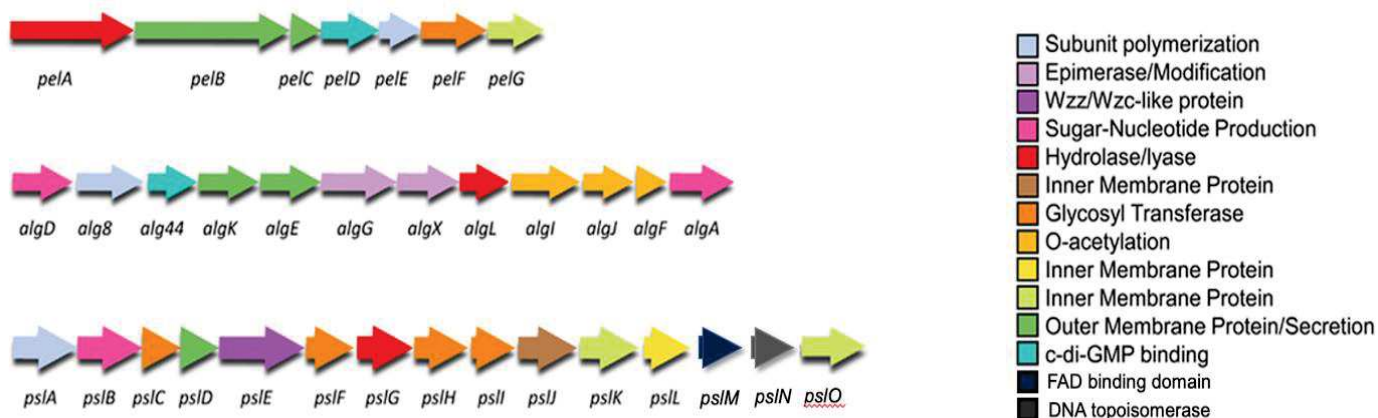


Figure 2 : Représentation des opérons impliqués dans la formation du biofilm chez *Pseudomonas aeruginosa*

Adapté depuis Franklin *et al.* ⁸⁸

Chez les bactéries à Gram positif dont *S. aureus*, le polysaccharide majoritaire est le **PIA** ⁸⁹. Initialement nommé PNAG pour Poly-N-acetyl-Glucosamine. C'est un polymère acétylé composé de monomère de glucopyranose qui possède une charge positive ⁹⁰. Sa synthèse est sous le contrôle de l'opéron *ica* ⁹¹.

b. Protéines

Les protéines bactériennes sont capables d'assurer plusieurs rôles de la formation à la dissémination du biofilm. On différenciera deux types de protéines bactériennes ; les protéines sécrétées et les bactéries ancrées à la surface bactérienne.

Pour ce qui est des **protéines sécrétées** chez les bactéries à Gram positif et en particulier chez *S. aureus*, les principales protéines clés sont les *secretable expanded repertoire adhesive molecules* ⁹², ou SERAM, parmi lesquelles on retrouve les protéines Eap et Emp. Ces protéines sont connues pour leurs liaisons multiples avec les protéines de la matrice extracellulaire et jouent un rôle dans le cycle de vie du biofilm facilitant la libération d'agrégats depuis la structure initiale ⁹³. L'autre protéine clé est la β -toxine. Elle permet la formation d'un réseau architectural de nucléoprotéines via sa capacité à se lier à l'ADNe ⁹⁴. Enfin, l' α -toxine, codée par

l'opéron *hla* joue un rôle dans la phase précoce d'attachement du biofilm en établissant des contacts cellules-cellules permettant la formation des micro-colonies en forme de champignon ⁹⁵. Chez les bacilles à Gram négatif dont *P. aeruginosa*, on sait que la protéine Crc (catabolite repression protein) réprime le métabolisme des hydrates de carbones en présence d'intermédiaires du cycle de Krebs (pyruvate et succinate) et intervient dans une voie de signalisation contrôlant la formation du biofilm ⁹⁶. GacA, le régulateur de réponse du couple GacA/GacS, un système à deux composants, influe également sur la capacité de la souche à former du biofilm. *Pseudomonas aeruginosa* est également capable de sécréter des protéines (élastases, protéases) qui détruisent l'intégrité des tissus de l'hôte en dégradant les protéines de la matrice extracellulaire telles que l'élastine ou le collagène ⁹⁷. Enfin, d'autres protéines sécrétées correspondant à des toxines, telle que la pyocyanine ⁹⁸, ont été décrites.

En ce qui concerne les **protéines ancrées** à la membrane bactérienne des staphylocoques, elles peuvent être classées en 4 groupes : les MSCRAMMs, précédemment décrites ⁶², les protéines comportant un motif NEAT (NEAr iron Transporter), la protéine A (SpaA) et les protéines de la famille du motif G5-E répété. Les protéines comportant un motif NEAT comprennent les protéines LsdA, LsdB et LsdC responsables de la liaison au fibrinogène et à la fibronectine ⁹⁹. La protéine A (SpaA) de la famille « three-helical bundle » est capable de se lier au immunoglobulines G via leur région Fc ¹⁰⁰. Enfin, les protéines de la famille du motif G5-E répété comprennent la protéine SasG qui est impliquée dans les processus d'adhésion aux cellules épithéliales endommagées ¹⁰¹. Chez *P. aeruginosa*, les mécanismes influençant la formation du biofilm sont majoritairement sous le contrôle de facteurs de mobilité et d'adhérence que sont le flagelle, les pili de type IV ou encore les *fimbriae*. La présence et le fonctionnement du flagelle sont importants pour l'attachement initial des bactéries planctoniques au support ⁵². Les pili de type IV sont des structures fibrillaires présentes au pôle des bactéries à Gram négatif dont *P. aeruginosa*. Ils sont impliqués dans un phénomène de « twitching » permettant des mouvements à l'interface de surfaces solides indispensables à la formation des micro-colonies ¹⁰². Enfin, un autre appendice de surface a été décrit chez *P. aeruginosa*, les *fimbriae*, essentiels à la formation de biofilm surtout dans les phases précoces ¹⁰³.

Le biofilm est une structure hautement complexe dont la mise en place nécessite une grande diversité d'acteurs moléculaires. Chez les Gram positif et en particulier chez *S. aureus*, de l'étape primaire d'adhésion à la maturation, une régulation est indispensable pour que la succession d'expression génique permette le passage d'une étape à l'autre (**Figure 3**). La synthèse des PIA est par exemple fortement régulée. La répression de *icaR* induit une augmentation de l'expression des gènes *icaABCD* responsable de la synthèse des PIA ¹⁰⁴. La maturation du biofilm de *S. aureus* est également contrôlé par le système Agr assurant la régulation du quorum-sensing. La croissance et de détachement du biofilm ont été reliées à ce régulateur clé par l'analyse de l'expression d'*agr* chez des bactéries sessiles ¹⁰⁵ ou par addition de l'inducteur du système Agr directement dans le milieu de croissance ¹⁰⁶. Agr régule l'expression d'un grand nombre de molécules et en particulier, réprime l'expression des adhésines. La synthèse des PSM est également connue pour être régulée par Agr ¹⁰⁷. AgrA se fixe directement sur le promoteur de l'opéron *psm* pour permettre leur transcription. Ainsi, le système Agr limiterait l'installation du biofilm en induisant sa dissémination et au contraire permettrait la synthèse des facteurs de virulence tel hla ⁹³. Le facteur de transcription SarA est également impliqué dans la régulation de la formation du biofilm en modulant l'expression de plusieurs gènes comme *bap* et *mgrA* qu'il induit ^{108,109}. SarA est démontré comme ayant un rôle inverse de Agr en permettant la formation du biofilm et en réprimant sa dissémination (**Figure 3**).

CidABC/LrgAB ¹¹². Chez *P. aeruginosa*, les mécanismes sont moins décrits mais il semblerait que l'autolyse résultant en la libération de l'ADNe est contrôlée par CdpR ¹¹³. Une autre partie de l'ADNe circulant isolé dans l'EPS est aussi due aux bactéries, qui sous le contrôle de signaux du quorum sensing, libèrent des copies de leur ADN dans le milieu ¹¹⁴.

Le rôle de l'ADNe est multiple. L'ADNe, chargé négativement, s'accumule autour des bactéries et les protège contre l'activité de composés cationiques bactéricides tels que les peptides antimicrobiens ou certains antibiotiques ¹¹⁵. Le second rôle important de l'ADNe est un rôle structural. La polarité de l'ADNe influence les propriétés membranaires des bactéries agissant comme un réseau ou échafaudage structurant les bactéries du biofilm ¹¹⁶. Il permet également des échanges de gènes au sein du biofilm et peut servir de source de nutriments dans des conditions oligotrophiques ¹¹⁷. Enfin, l'ADNe pourrait avoir un rôle dans l'affaiblissement de la réponse inflammatoire de l'hôte par une interaction et une activation du TLR9 ¹¹⁸.

D. Infection du pied diabétique et biofilms

A partir des années 2010, de nombreuses études de recherche clinique ont vu le jour démontrant l'impact du biofilm dans les IPD. En 2011, Neut *et al* montrent au travers de 2 études la présence d'un écosystème microbien, le biofilm, au niveau d'ulcères de plaie non cicatrisants ¹¹⁹. S'en est alors suivi de nombreuses recherches qui ont permis de mieux définir l'incidence et la composition des biofilms des UPD.

La principale caractéristique des ulcères du pied diabétique est qu'ils sont associés à un polymicrobisme qui influence l'intensité du processus physiopathologique ⁸. L'intercommunication et les coopérations entre micro-organismes au sein du biofilm sont complexes et n'ont été au cœur des recherches que récemment. Les chercheurs travaillent aujourd'hui à caractériser et documenter le plus possible les interactions qui régissent les biofilms polymicrobiens afin de mieux comprendre la physiopathologie de ces infections ¹²⁰. L'interaction la plus décrite des IPD est celle entre *P. aeruginosa* et *S. aureus*, bien que ces deux bactéries ne soient pas isolées à la même localité du lit de la plaie, *P. aeruginosa* étant plus en profondeur

^{121, 122}. Les premières études de cette interaction rendaient compte d'une **concurrence** entre les deux espèces bactériennes comme en témoigne la concurrence pour l'ion ferrique ^{123, 124} ou l'action de certains antibiotiques ¹²⁵. *Pseudomonas aeruginosa* peut ainsi simultanément inhiber la croissance de *S. aureus* et acquérir une résistance aux aminoglycosides ^{126, 127}.

Aujourd'hui de plus en plus d'études rapportent des mécanismes de **coopération** entre les deux bactéries. De nombreuses substances produites chez *P. aeruginosa* peuvent jouer un rôle protecteur sur *S. aureus* (exemple de l'alginate). La coopération synergique entre *P. aeruginosa* et *S. aureus* a été rapportée. Cette coopération permet, en outre, la sécrétion de facteurs de virulence (cyanide d'hydrogène, exoenzyme S, exotoxine A et pyocyanine pour *P. aeruginosa* et hémolysine A et leucocidine de Panton-Valentine pour *S. aureus*), la capacité à former un biofilm plus rapidement et/ou plus dense et enfin, l'apparition de mécanisme de tolérance à certains antibiotiques ¹²⁸⁻¹³⁴.

D'autres coopérations entre micro-organismes ont largement été décrites dans les IPD ⁵⁸. En effet, de nombreux articles ont étudié le microbiote des IPD rendant compte de la complexité des associations de micro-organismes provenant de différentes niches colonisant la plaie. Particulièrement dans les IPD, cette communauté microbienne est organisée en différents « pathogroupes » ou **FEP** pour **fonctionnel équivalent pathogroups** ¹³⁵. Lors de la maturation du biofilm, des espèces secondaires aux colonisateurs initiaux viennent intégrer le biofilm préexistant ce qui donne lieu à des biofilms hétérogènes. Les micro-organismes à l'intérieur de ces biofilms ne sont pas organisés de manière aléatoire mais de façon à ce que les bactéries puissent tirer profit au mieux de l'environnement dans lequel elles s'établissent. On retrouve alors des profils d'interaction bactéries-bactéries préférentiels. Les FEP permettent les relations symbiotiques et synergiques de groupe de bactéries, le partage de nutriment (catabolisme ou anabolisme) et accentuent la résistance aux antibiotiques ¹³⁶. La présence de certaines FEP aux premiers stades de l'infection est associée à des biofilms pathologiques retardant la cicatrisation et favorisant la chronicisation de l'infection par le fait que certaines espèces, considérées comme non pathogènes ou incapables de maintenir la chronicisation de l'infection à elles seules, pourraient coexister symbiotiquement dans un biofilm pathogène.

Travail n°1 : Revue de la littérature

Biofilms in Diabetic Foot Ulcers: Significance and Clinical Relevance

Cassandra Pouget, Catherine Dunyach-Remy, Alix Pantel, Sophie Schuldiner, Albert Sotto and Jean-Philippe Lavigne

Accepté dans Microorganisms le 11 Octobre 2020

Résumé travail n°1 :

Comme décrit précédemment, les infections de plaies au niveau du pied sont des complications fréquentes et potentiellement préjudiciables sur la vie du patient diabétique. L'infection touche un pied ulcéré sur deux et conduit fréquemment à une amputation, augmentant la morbidité à moyen terme et les coûts de santé.

Dans la première partie de ce travail bibliographique, le but est d'identifier et de définir la **physiopathologie des plaies du pied** chez le patient diabétique ainsi que de décrire les nombreux critères intervenant dans la gravité de l'infection. Ce travail se focalise notamment sur un des critères en particulier : celui de la capacité des micro-organismes présents au niveau du lit de la plaie à former du biofilm.

La seconde partie de cette revue se concentre sur la formation de **biofilms bactériens** dans les ulcères de pied diabétique et des facteurs influençant cette formation. Dans cette partie, une liste non-exhaustive des descriptions de biofilms présents dans des modèles animaux et humains d'UPD a été réalisée permettant de comprendre l'évolution des connaissances sur les micro-organismes infectants les plaies du pied diabétique. Les différents modèles ont permis notamment la découverte d'une des particularités des biofilms de plaies chroniques, à savoir la formation de biofilm polymicrobien. Ce biofilm pluri-espèces est une étape importante dans la physiopathologie des ulcères de pied diabétique.

Enfin, les biofilms décrits au niveau des plaies chroniques ont d'importantes **conséquences cliniques** dont les principales sont le développement de résistances aux antibiotiques, de retarder la cicatrisation et d'induire la chronicisation de la plaie.

Review

Biofilms in Diabetic Foot Ulcers: Significance and Clinical Relevance

Cassandra Pouget ¹, Catherine Dunyach-Remy ², Alix Pantel ², Sophie Schuldiner ³,
Albert Sotto ⁴ and Jean-Philippe Lavigne ^{2,*} 

- ¹ Virulence Bactérienne et Maladies Infectieuses, INSERM U1047, Université de Montpellier, 30908 Nîmes, France; cassandra.pouget@gmail.com
- ² Virulence Bactérienne et Maladies Infectieuses, INSERM U1047, Université de Montpellier, Service de Microbiologie et Hygiène Hospitalière, Clinique du Pied Gard Occitanie, CHU Nîmes, 30029 Nîmes, France; catherine.remy@chu-nimes.fr (C.D.-R.); alix.pantel@chu-nimes.fr (A.P.)
- ³ Virulence Bactérienne et Maladies Infectieuses, INSERM U1047, Université de Montpellier, Service des Maladies Métaboliques et Endocriniennes, Clinique du Pied Gard Occitanie, CHU Nîmes, 30240 Le Grau du Roi, France; sophie.schuldiner@chu-nimes.fr
- ⁴ Virulence Bactérienne et Maladies Infectieuses, INSERM, Université de Montpellier, Service des Maladies Infectieuses et Tropicales, Clinique du Pied Gard Occitanie, CHU Nîmes, 30029 Nîmes, France; albert.sotto@chu-nimes.fr
- * Correspondence: jean.philippe.lavigne@chu-nimes.fr; Tel.: +33-466-683-202; Fax: +33-466-684-254

Received: 8 September 2020; Accepted: 11 October 2020; Published: 14 October 2020



Abstract: Foot infections are the main disabling complication in patients with diabetes *mellitus*. These infections can lead to lower-limb amputation, increasing mortality and decreasing the quality of life. Biofilm formation is an important pathophysiology step in diabetic foot ulcers (DFU)—it plays a main role in the disease progression and chronicity of the lesion, the development of antibiotic resistance, and makes wound healing difficult to treat. The main problem is the difficulty in distinguishing between infection and colonization in DFU. The bacteria present in DFU are organized into functionally equivalent pathogroups that allow for close interactions between the bacteria within the biofilm. Consequently, some bacterial species that alone would be considered non-pathogenic, or incapable of maintaining a chronic infection, could co-aggregate symbiotically in a pathogenic biofilm and act synergistically to cause a chronic infection. In this review, we discuss current knowledge on biofilm formation, its presence in DFU, how the diabetic environment affects biofilm formation and its regulation, and the clinical implications.

Keywords: biofilm; commensal bacteria; diabetic foot infection; diabetic foot ulcer; pathogenic bacteria; pathogroups

1. Introduction

People suffering from diabetes *mellitus* have a 15–25% lifetime incidence of developing a diabetic foot ulcer (DFU) [1]. Infection is the most common, severe, and costly complication of diabetes *mellitus* [2], with high risk of mortality and morbidity due to lower limb amputation [3]. Wound infection, faulty wound healing, and ischemia are the most common precursors to diabetes-related amputations. Indeed, 80% of lower-limb amputations in diabetic patients are preceded by biofilm infected foot ulceration [4,5]. Infected wounds result in an increased risk of death within 18 months [6]. The host–microorganism interface plays a major role in DFU development. In DFU, bacteria are classically organized into functionally equivalent pathogroups (FEP), where pathogenic and commensal bacteria co-aggregate symbiotically in a pathogenic biofilm to maintain a chronic infection [7].

This polymicrobial biofilm has been observed both in pre-clinical studies using animal models and in clinical research on DFU. It represents the main cause of delayed healing.

2. Pathophysiology of Diabetic Foot Ulcers

2.1. Main Host-Related Factors

The triopathy induced by diabetes *mellitus* plays a role in the origin and chronicity of the DFU.

- **Diabetic immunopathy:** Diabetic patients have an altered function of polymorphonuclear cells and impaired phagocytosis, chemotaxis, and bactericidal activity (related to both non oxidative and oxidative mechanisms), which are more evident in the presence of high hyperglycemia [8]. A study on diabetic mice showed that persistent hyperglycemia had a deleterious effect on the innate immunity and could lead to skin and soft tissue infections by *Staphylococcus aureus* [9].
- **Diabetic neuropathy:** Neuropathy by C-fiber and autonomic nerve fiber dysfunction is a common and frequent complication of diabetes *mellitus*. An evolution of the deregulation of glycemic balance is the inhibition of nociception and the perception of pain, a process called loss of protective sensation [10]. Thus, patients may not initially notice small wounds in the legs and feet, and may fail to prevent infection. Studies have observed a reduction in foot skin innervation and the expression of neurogenic factors in DFU, correlated with low inflammatory cell accumulation and therefore in the chronicity of DFU. This contributes to enhancing susceptibility to infection of diabetic neuropathic foot ulcers [11].
- **Diabetic angiopathy:** Peripheral arterial disease (PAD) and microangiopathy are the main risk factors for DFU. The decrease in the oxygenation of tissues by thickening the capillary basement membrane is a hallmark of diabetic angiopathy [12]. Disease of arteries in the lower limb is a well-known risk factor for DFU. Indeed, studies have shown that PAD presents a 5.5-fold increased risk for DFU [13]. The ischemia caused by the angiopathy also enhances the severity of the infection as a result of a poor delivery of oxygen and nutrients in the infected wound and because of poor antibiotic tissue penetration [14].

Finally, the anatomical characteristics of the foot, with its division into compartments, participates in the pathophysiology by increasing the severity of the infectious process by promoting the spread of infection and aggravating tissue damage.

2.2. DFU Microbiota

The host–microbiota interface is often the key point in the development of wound infections. Defining the diabetic foot microbiota implies the possibility of distinguishing it from skin microbiota associated with other clinical statuses. Compared with the feet of non-diabetic men, those of diabetic men had decreased populations of *Staphylococcus* spp., increased populations of *S. aureus*, and increased bacterial diversity [15]. When compared with contralateral healthy skin, the DFU microbiota harbored less bacterial diversity with greater levels of opportunistic pathogens [16]. However, neither patient demographics nor wound type influenced the bacterial composition of the chronic wound microbiome [17]. Different studies have described this DFU microbiota [17–25]. Although they have produced interesting results and confirmed that the microbiota is a highly dynamic microbial community that maintains a relationship with the host, understanding the complex competitive or synergistic interaction between commensal and pathogenic microorganisms is necessary as it could play an important role in the severity and evolution of the wound.

2.3. Disturbances in the Host–Microorganism Interplay

- **Bacterial virulence:** The virulence of pathogens is a key element in the pathophysiology of DFU. The ability of a bacterium to be virulent is key to the precarious balance between colonization and infection [26]. Bacterial virulence has been characterized using DNA microarray-based

genotyping, multiplex polymerase chain reaction (PCR), and in vivo assays [26,27]. Among the large panel of virulence factors, bacterial proteases (serine-, cysteine-, and metallo-proteases), produced by a wide range of pathogenic bacteria, could play a major role in the pathogenesis of wound healing [28]. However, these wounds, and especially DFU, are highly polymicrobial, and bacterial interactions should also be studied in order to better understand the mechanisms of infection and the role of each of the pathogens involved in DFU.

- **Biofilm organization:** In a 2008 study assessing wound tissue biopsies using electron microscopy, James et al. suggested that 60% of chronic wounds present biofilms versus 6% for acute wounds [29]. In the following sections of this review, we focus on the formation of biofilms, evidence of biofilms in DFU, influence of the diabetic environment, and finally the clinical implications of biofilms in DFU.

3. Overview of Biofilms in DFU

3.1. Biofilm Formation in DFU and Tools for Detection

In the environment, microorganisms can exist in two main states, namely: planktonic and sessile. In the planktonic state, bacteria move freely in their environment. In the sessile state, microorganisms are attached either to solid surfaces (e.g., urinary catheter or prosthesis), or more frequently, to each other, constituting multicellular aggregates that can lead to biofilm formation. Biofilm formation is a multistep process (for review, see Percival et al., 2015 [30]; Figure 1) whereby heterogeneous communities of microorganisms (bacteria and/or fungi) [30] are embedded into a self-produced matrix of extracellular polymeric substance (EPS). EPS contains proteins, glycoproteins, and polysaccharides and confers the ability to adhere to biotic or abiotic surfaces [31]. Clinically, biopsy tissues are the most reliable samples for revealing biofilms in deep tissues. However, the use of swabs to collect biofilm samples from the wound surface is considered an improper technic because of contamination from the skin microbiota, the difficulty in detaching the biofilm from the host epithelium, and the growth of anaerobes in the deep tissues. If a moderate to severe soft tissue infection is suspected and a wound is present, a tissue sample from the base of the debrided wound should be examined. Biofilms in tissue samples are commonly quantified through microscopy. Techniques such as confocal laser scanning microscopy and scanning electron microscopy or fluorescence in situ hybridization (FISH) are the most appropriate for revealing biofilms in biopsies [32].

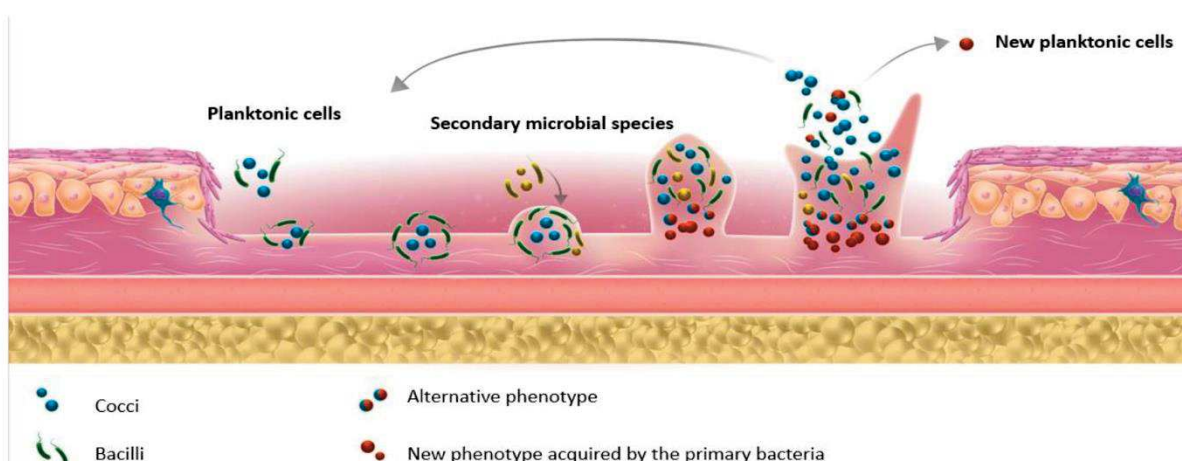


Figure 1. Different bacterial steps of biofilm formation.

Some important features of chronic wounds, and notably DFU, could be noted as follows:

- Cells included in the biofilm can develop an intracellular communication mechanism called quorum sensing (QS) [33], which controls bacterial pathogenicity and biofilm formation. The bacterial density influences the biofilm production [34].
- Microbial cells within a biofilm can detach and disseminate in the wound environment. The behavior of the released bacteria may differ from that of the pioneering colonizing bacteria because of adaptation within the biofilm [30,35].
- The concept of FEP was proposed by Dowd et al. after observing that different bacterial species can collaborate and interact with each other. FEPs are responsible for the chronicity of infection and for the maintenance of the pathogenic biofilm [7].

3.2. Biofilm Studies in Animal Models of DFU

Several studies have described the presence of biofilms in animal wounds since the early 2000s, and experimental diabetic models were developed in 2010 (Table 1). Pioneering groups in this field have shown that in db/db mice (a model of diabetic dyslipidemia), *Pseudomonas aeruginosa* or *S. aureus* biofilms delayed wound healing, and that the diabetic condition slowed down healing and increased the biofilm thickness [36,37]. Hsu et al. also reported that high glucose levels encourage the formation of vancomycin-resistant *S. aureus* biofilms [38]. Other studies have shown that the host response and neutrophil oxidative burst activity were decreased in the wound, and that oxidative stress and reactive oxygen species promoted biofilm appearance [39,40]. James et al. suggested that biofilms in wounds induced oxygen-limiting conditions (and thus stress) by the following two mechanisms: (i) bacterial metabolic activities and (ii) oxygen-deprivation by the host defenses [41]. These findings were recently confirmed by Hunt et al., who showed delayed healing in diabetic mice concomitantly with increased pus production [42]. They also suggested that in db/db mice, the deleterious impact of *P. aeruginosa* on wound healing cannot be explained solely by its ability to form biofilms, and that the type-3 secretion system virulence structure was also involved in the wound damage caused by this pathogen [43] (Table 1).

Table 1. Examples of biofilm studies in animal models of diabetes.

Animal Model	Strain Used	Findings	Reference
db/db mice	<i>P. aeruginosa</i> (PAO1)	Biofilm evidence after a 6-mm punch biopsy wound on the dorsal skin	[36]
db/db mice	<i>P. aeruginosa</i> (PAO1)	Biofilm delays wound healing	[37]
TallyHo mice (Type 2 diabetes mellitus)	<i>P. aeruginosa</i>	Biofilm decreases TLR 2, TLR 4, IL-1 α , and TNF- α expression and neutrophil oxidative burst activity	[39]
BALB/c mice with injection of STZ	Vancomycin-resistant <i>S. aureus</i>	Correlation between glucose concentration and biofilm formation	[38]
db/db mice	Wound microbiome	Oxidative stress and ROS favor biofilm formation and establish a chronic wound	[40]
db/db mice	<i>P. aeruginosa</i>	Bacteria in biofilm induce oxygen stress by producing metabolites and recruiting defense cells that reduce oxygen	[41]
Mice with injection of STZ	<i>P. aeruginosa</i>	Biofilm increases wound depth, mortality rate, and pus production	[42]
db/db mice	<i>P. aeruginosa</i>	<i>P. aeruginosa</i> infection is independent of its ability to form biofilm and primarily depends on T3SS	[43]

db/db mice—diabetic mice; TLR—toll-like receptor; IL—interleukin; TNF—tumor necrosis factor; ROS—reactive oxygen species; STZ—streptozocin (a pancreatic β -cell toxin); T3SS—type-3 secretion system.

3.3. Biofilm Studies in Human Clinical DFU

Many clinical studies emerged in the 2010s demonstrating the impact of biofilms in chronic wounds (Table 2). In 2011, Neut et al. published two case studies of diabetic patients with non-healing ulcers. Using the confocal laser scanning microscope technique, they showed evidence of biofilms in diabetic wounds [44]. Subsequently, several studies have shown the presence and the impact of biofilms in clinical DFU. Malik et al. showed that on 162 diabetic foot infections (DFI), biofilms were present in 67.9% of the cases [45]. Other studies supported this and, in particular, the implication of *S. aureus* within the biofilms [46,47]. Oates et al. confirmed the importance of biofilms, using 26 human samples after debridement, employing FISH and scanning electron microscopy [48]. Recent research has shown that, during infection, in particular at the wound level, a single bacteria species is not responsible for biofilm formation [49]. Instead, microbes represent a complex polymicrobial biofilm community communicating with each other [50]. Interactions between microbes are complex and play an important role in the pathogenesis of the infection. These interactions range from competition for nutrients to evolving cooperative mechanisms that support their mutual growth in a specific environment [51]. Proximity and contact between bacteria in the biofilm promote communication and exchanges. To adapt their behavior, bacteria communicate through diffusible molecules like homoserines lactones or quinolones for Gram-negative bacteria, whereas Gram-positive cocci use short peptides [52]. Moreover, this proximity contributes to horizontal gene transfer, providing tolerance to antimicrobial agents and enhancing survival. Mottola et al. studied 53 staphylococci clinical isolates from DFU [53]. They discovered that biofilms cells were 10 to 1000 more tolerant to antibiotics than planktonic cells. In their work, of the 10 antibiotics tested, only gentamicin and ceftaroline were able to eradicate the biofilms. It has been reported that bacterial biofilms are also highly resistant to ultraviolet and heavy metals [54]. In addition to bacteria, fungi, especially *Candida*, are present in DFU biofilm-associated wound samples [55].

Table 2. Examples of biofilm studies in clinical human DFU.

Model	N° of Patients	Biofilm Visualization	Findings	Reference
DFU	2	CLSM	Evidence of biofilms	[44]
DFU	162	Microtiter plate assay	Biofilms in 67.9% of infected DFUs	[45]
DFU	26	FISH and ESEM	Observation of the formed biofilms and their bacterial constitution	[48]
DFU	357	Crystal violet	Observation of the formed biofilms	[46]
DFU	100	Congo Red dye, tissue culture plates, and crystal violet staining	Biofilm formation in 46.3% of isolates, predominantly by <i>S. aureus</i> (38.8% of isolates) and MDR bacteria (46.3%)	[47]
DFU	49	Calgary biofilm pin lid device with resazurin and PCR of genes associated with biofilm formation	Biofilms are resistant to antibiotics at concentrations 10–1000 times higher than those required to kill planktonic cells	[53]
DFU	155	Microtiter plate assay and ELISA, XTT formazan, and SEM	Presence and importance of non- <i>Candida albicans</i> species in biofilms	[55]
DFU	95	Microtiter plate assay and FISH	Polymicrobial biofilms are thicker	[56]

DFU—diabetic foot ulcer; CLSM—confocal laser scanning microscopy; ELISA—enzyme-linked immunosorbent assay; ESEM—environmental scanning electron microscopy; FISH—fluorescent in situ hybridization; MDR—multidrug resistant; PIA—polysaccharide intercellular adhesin; SEM—scanning electron microscopy; XTT—2H-tetrazolium-5-carboxanilide.

3.4. Factors Influencing Biofilm Formation in DFU

DFUs are mainly colonized by commensal bacteria. Numerous papers have analyzed the DFU microbiome, showing that the wounds contain commensal microorganisms from different niches [57,58]. All of these studies highlight the high bacterial complexity of wounds. This complexity is one of the major characteristics of DFU, and the lack of knowledge regarding the interactions of these microorganisms in the wound renders these infections as being complicated to manage [59]. The microorganisms appear to be organized as multi-layered communities surrounded by a self-produced protective extracellular matrix, and are organized into different FEPs [7]. Biofilm formation is a multistep process, including random settlement of early bacterial colonizers, with increased competition among species and niche differentiation, resulting in highly heterogeneous biofilms [30]. The biofilms detected in patients with foot ulcers may be responsible for the delayed healing of these chronic wounds [18]. Moreover, the presence of some bacterial communities in the initial stages of the wounds has been associated with delayed healing [24].

Several microbial and host factors specific to DFU may interfere in the development and feature of the biofilms:

- High bacterial diversity [7,15,60,61], including opportunistic pathogens [16] and anaerobic bacteria [57,62].
- Increased *S. aureus* population [15], particularly in neuropathic DFUs [61]. However, their microbiota present a similar level of richness (number of different species in the wound community), abundance, and diversity compared to other chronic wounds [63], suggesting that the microbiota is not influenced by the wound type.
- The wound depth with a more diverse and complex microbiota in the deep part of the wound [64] where pathogenic, particularly anaerobic, bacteria are sheltered.
- Environmental factors (e.g., demographic characteristics, personal hygiene, geographical location of the patient, high glycemic level, and previous exposure to antimicrobial therapy) [65].
- Patient immune status that modifies the role of low-virulence bacteria (e.g., *Staphylococcus* sp. and corynebacteria) towards a higher pathogenicity [66], and where excessive secretion of pro-inflammatory cytokines, pH, temperature, or antimicrobial treatment (topic or systemic administration) [67] can increase tissue destruction [68].
- DFU duration is positively correlated with the ecological diversity of the bacteria present in the wounds, species richness, and relative abundance of *Proteobacteria*. It is also negatively correlated with the relative abundance of staphylococci [69].
- Local tissue hypoxemia is often observed as a result of obstructive arteriopathy. This hypoxic environment influences bacterial diversity, with a higher prevalence of proteobacteria and strict anaerobic bacteria in deeper ulcers [61,68].
- The development of a “unique microbiota” in each DFU (new or recurrent) [17].

3.5. Bacterial Organization Inside DFU

The main characteristic of DFU is the polymicrobial content that modulates bacterial virulence. Within DFU, microorganisms form a complex polymicrobial biofilm community and intercommunicate [7]. As described above, bacterial interactions play an important role in pathogenesis, competing and cooperating in order to support their mutual growth in a specific environment [51] via interactions through diffusible molecules [52].

The most studied bacterial interaction in DFU is the cooperation between *S. aureus* and *P. aeruginosa*, despite the location of *P. aeruginosa* being deeper in the wound bed than *S. aureus* [70]. Many substances produced by *P. aeruginosa* may play a protective role for *S. aureus* [17,70–74]. In a rat model of orthopedic wounds, even a low presence of both *P. aeruginosa* and *S. aureus* increased their infection rates in the wound [75]. A similar synergistic cooperation between *P. aeruginosa* and *S. aureus* also increased their tolerance to antibiotics, ability to form biofilms, and the secretion of virulence factors (hydrogen

cyanide, exoenzyme S, exotoxin A, and pyocyanin for *P. aeruginosa*, and Panton-Valentine leukocidin and α hemolysin for *S. aureus*) [76]. These interactions can also be competitive, as exemplified by the competition for iron or the one-way growth inhibition of *S. aureus* [37,77]. Indeed, *P. aeruginosa* can simultaneously suppress *S. aureus* growth and enhance its resistance to aminoglycosides [71].

Other bacterial interactions have also been described. For instance, the combined inoculation of different pathogenic bacteria (*Escherichia coli*, *Bacteroides fragilis*, and *Clostridium perfringens*) increased the mortality rate in type-2 diabetic mice compared with those receiving inoculation of single strains [78]. Competition between commensal and pathogenic bacteria has been observed during cutaneous colonization [79]. In contrast, *Helcococcus kunzii* (a commensal Gram-positive coccus) and *S. aureus* cooperation led to a decrease of *S. aureus* virulence in *Caenorhabditis elegans* [80]. *S. aureus* shifts toward commensalism in response to *Corynebacterium* sp. [81]. Moreover, *S. epidermidis*, a commensal bacterium, produces a serine protease (Esp) that inhibits *S. aureus* biofilm formation [56,82]. Finally, the co-culture of *Fusobacterium nucleatum* (ATCC 25586) with *Prevotella intermedia/Prevotella nigrescens* promotes biofilm formation compared with single cultures [83].

Another pertinent aspect of polymicrobial biofilms in DFU is their ability to adapt under various circumstances via enhanced metabolic cooperation and gene regulation between sessile cells. Biofilm diversity promotes its survival by creating a thicker biofilm, resulting in more severe infections. In this context, Mottola et al. reported that the biofilms formed by *P. aeruginosa* and *Enterococcus faecalis* and *Acinetobacter baumannii*, and *S. aureus* resulted in a thicker biofilm than the bacteria alone, which were difficult to eradicate [84]. Furthermore, these microbial communities are heterogeneous. Interestingly, fungi can also form biofilms. Both yeasts and filamentous fungi can adhere to biotic and abiotic surfaces, and form highly organized communities that are resistant to antimicrobials and environmental conditions. Many fungi have been correlated with biofilm formation, however, *Candida* biofilms remain the most widely studied. The biofilms formed by yeast and filamentous fungi present differences, and studies of polymicrobial communities have become increasingly important. Interactions have been observed between bacterial and fungal species in chronic wounds [55]. Infections that are thought to involve polymicrobial biofilms are most frequently associated with the abiotic surfaces of indwelling medical devices. In a review written by Lynch and Robertson [85], they highlighted the indwelling medical devices commonly associated with biofilm formation. In all of the devices tested, the principal pathogen responsible for the biofilms was a bacterium, however in 70% of cases, fungi was found as a secondary species. Among fungal pathogens, *Candida albicans*, a commensal mucosal organism and opportunistic pathogen of the immunocompromised, was most commonly associated with biofilms. Numerous studies have described co-infections of fungi and bacteria in different diseases. For example, cystic fibrosis lungs are a major site of polymicrobial infection, with bacteria such as *P. aeruginosa*, *S. aureus*, *Burkholderia cepacia*, *A. baumannii*, and *Haemophilus influenzae* mixed with *C. albicans*, *A. fumigatus*, and *Scedosporium* sp. [86]. In a DFI context, Kalan et al. showed that the presence of fungal communities in the polymicrobial biofilms of chronic wounds is associated with a poor prognosis and delayed healing [87]. Further studies are needed in order to fully elaborate on the role of each microorganism in the polymicrobial biofilms of DFU.

4. Clinical Impact of Biofilms in DFU

As biofilms are implicated in 60 to 80% of chronic wounds [29,88], the clinical impact of biofilms is particularly relevant. For clinicians, the main difficulty is in distinguishing between infecting and colonizing bacteria. Misidentification can lead to inappropriate antibiotic prescriptions that may contribute to the emergence of multidrug resistant (MDR) bacteria, a major DFU health issue [30].

4.1. Antibiotics Resistance

Sessile cells involved in biofilm formation display different characteristics compared with non-biofilm-associated cells (i.e., planktonic cells) [89]. In particular, sessile cells show a higher tolerance towards antimicrobial agents, one of the main causes of treatment failure [90,91]. Antimicrobial agent

tolerance arises by several mechanisms, namely: (i) inability of drugs to penetrate through the polymeric matrix; (ii) the lack of intracellular accumulation of antibiotics due to impermeability (e.g., excessive production of glucans by *P. aeruginosa*) or active efflux (e.g., increased expression of efflux pump genes in Gram-negative bacilli); (iii) the presence of sessile bacteria, whereby cells are metabolically inactive and thus tolerate the antibiotic action better; and (iv) the importance of horizontal gene transfer between bacteria for the diffusion of resistant traits [92,93]. Biofilms increase the opportunity of gene transfer of virulence factors and antibiotic-resistant genes to susceptible bacterial species. The rate of mutation occurring in biofilms is markedly higher compared with planktonic cells [94]. In addition, (v) stress response to hostile environmental conditions (e.g., leading to an overexpression of antimicrobial agent-destroying enzymes) can result in an altered microenvironment inside the biofilm matrix (pH and oxygen content) and may contribute to enhanced degradation of antimicrobial agents in the biofilm matrix [95]. Finally, the hypoxic environment present in DFU also modulates the tolerance of bacteria to some antibiotics. For instance, the in vitro bactericidal effect of vancomycin on *S. aureus* isolates is lower in anaerobic conditions [96].

4.2. Host Immune Response

Pioneering colonizing bacteria released from the biofilm can adapt to their environment and form a new biofilm. To our knowledge, the only study conducted in this field focused on *Klebsiella pneumoniae* [35]. In addition, EPS is a mechanical barrier to antimicrobials, as well as to immune system cells [97]. Bacteria within biofilms evade the host's natural defenses and are resistant to the host immune defense by different mechanisms, including the following: (i) limited penetration of leukocytes and their products into the biofilm [98]; (ii) global response regulators and quorum sensing, which protect the biofilm bacteria [99]; (iii) decreased phagocytic capacity of host cells against biofilm bacteria [100]; (iv) genetic switches that increase the resistance of biofilm bacteria [101]; and (v) suppression of the leukocyte effector function, including softening the magnitude of the respiratory burst [102]. Indeed, stimulation of the immune system without effectively eradicating the infection causes collateral damage to surrounding tissue and causes chronic inflammation [103]. This persistent chronic inflammation, added to the diabetic immune context, leads to the production of auto-inflammatory cytokines that aggravate the wound and slow the healing process.

5. Therapeutic Perspectives

Biofilms have a crucial role in DFU and DFIs and contribute to delayed healing. They are especially difficult to treat using classical antibiotics because of EPS, which prevents diffusion into the biofilm. They also support gene transfer, the selection of strains with beneficial characteristics, and the development of new bacterial characteristics. This difficulty in treating DFU/DFI could be enhanced in the context of the diabetic environment.

Biofilms encountered in chronic wounds, such as DFU, are highly polymicrobial, which can enhance bacterial interactions. Bacterial cooperation is key to understanding the formation and regulation of biofilms at a wound level, but also for highlighting new therapeutic targets. The available approaches against biofilms are quite limited, and new prevention, diagnosis, and treatment methods are crucially needed, particularly because of the extent of the MDR bacteria in this pathology.

Targeting biofilm formation could be an interesting strategy to prevent or at least reduce this problem. Classically, clinicians reduce the bacteria load (constituting commensal and pathogen species) resulting from the biofilm organization and FEP. The best method involves physical removal, also called debridement, of the infected tissue in order to improve healing [104,105]. It is often performed using surgical instruments or by irrigation [105], and is the initial and essential stage in the management of infected wounds. This strategy is still the preferred method used to prepare the wound bed and to promote moist wound healing, but it might not completely remove the biofilms immediately. Therefore, it must be repeated at regular intervals [104]. The results obtained with ultrasound debridement could represent a promising approach [106]. Other approaches could be

proposed with the aim to inhibit bacterial adhesion or biofilm metabolism, such as (i) blocking bacterial adhesins (using ions chelators such as ethylenediaminetetraacetic acid (EDTA) and citrate, the most promising compounds of this class [107]), (ii) inhibiting the adhesion structure biogenesis (e.g., plant-derived natural compounds [108]), (iii) modulating QS (e.g., furanone [109], savarine [110], or deferiprone [111]), and (iv) enhancing bacterial dispersion (such as the α -amylase enzyme [112], 2-aminoimidazole [113], or Cis-2-decenoic acid [114]). Physical inhibition could also represent an interesting method, such as photodynamic therapy-induced pathogen cell death by killing sessile bacteria [115].

Some antimicrobial strategies as alternatives to antibiotics have also been developed, such as phagotherapy [116,117], nanotechnologies [118], antimicrobial peptides (AMP) [119–121], or agent mimicking AMPs [122], as well as natural compounds (such as honey [123]). These approaches have an interesting potential, but further studies are required to really understand the mechanism of action of each of these solutions and to improve their role in DFI management.

Researchers are now aware of and consider the polymicrobial characteristics of DFI and biofilms. Further studies on bacterial interactions are required in order to really understand the pathophysiology and to help with the development of new therapeutic tools that will target polymicrobial biofilms. This needs to be done through the development of (i) validated, consistent, and robust animal wound models reproducing the clinical situation and biofilm constitution; (ii) *ex vivo* and *in vivo* imaging technologies to visualize bacterial biofilms and to confirm their eradication; and (iii) “omics” tools to detect biofilm formation at the bedside and to evaluate the best course of action for the debridement.

6. Conclusions

Biofilms have a crucial role in DFIs and contribute to delayed healing. These wounds are characterized by a complex microbiome and a polymicrobial organization, especially within the biofilm. Even if most experimental biofilm studies provide descriptive and interesting information, they are derived from *in vitro* studies or non-adapted *in vivo* models. The development of processes and methodologies to study biofilms is needed. This represents the next step to validating new antibiofilm molecules with a promising therapeutic potential.

Author Contributions: Conceptualization, C.P., A.S., and J.-P.L.; validation, C.D.-R., A.S., and J.-P.L.; formal analysis, C.P. and A.P.; investigation, C.P. and S.S.; writing—original draft preparation, C.P. and J.-P.L.; writing—review and editing, C.D.-R., A.P., S.S., and A.S.; supervision, A.S. and J.-P.L. All of the authors have read and agreed to the published version of the manuscript. All authors have read and agreed to the published version of the manuscript.

Funding: Cassandra Pouget’s PhD is supported by a CIFRE grant (Biofilm Pharma).

Acknowledgments: We thank Sarah Kabani for her editing assistance. We thank the Nîmes University hospital for its structural, human, and financial support through the award obtained by our team during the internal call for tenders “Thématiques phares”. The authors belong to the FHU InCh (Federation Hospitalo Universitaire Infections Chroniques, Aviesan).

Conflicts of Interest: The authors declare no conflict of interest.

References

1. Armstrong, D.G.; Boulton, A.J.M.; Bus, S.A. Diabetic foot ulcers and their recurrence. *N. Engl. J. Med.* **2017**, *376*, 2367–2375. [[CrossRef](#)]
2. Prompers, L.; Schaper, N.; Apelqvist, J.; Edmonds, M.; Jude, E.; Mauricio, D.; Uccioli, L.; Urbancic, V.; Bakker, K.; Holstein, P.; et al. Prediction of outcome in individuals with diabetic foot ulcers: Focus on the differences between individuals with and without peripheral arterial disease. The EURODIALE Study. *Diabetologia* **2008**, *51*, 747–755. [[CrossRef](#)] [[PubMed](#)]
3. Bakker, K.; Apelqvist, J.; Lipsky, B.A.; Van Netten, J.J.; International Working Group on the Diabetic Foot. The 2015 IWGDF guidance documents on prevention and management of foot problems in diabetes: Development of an evidence-based global consensus. *Diabetes Metab. Res. Rev.* **2016**, *32*, 2–6. [[CrossRef](#)] [[PubMed](#)]

4. Palumbo, P.J.; Melton, L.J.I. *Diabetes in America: Diabetes Data Compiled 1984*; Peripheral vascular disease and diabetes; Government Printing Office: Washington, DC, USA, 1985.
5. Adler, A.I.; Boyko, E.J.; Ahroni, J.H.; Smith, D.G. Lower-extremity amputation in diabetes. The independent effects of peripheral vascular disease, sensory neuropathy, and foot ulcers. *Diabetes Care* **1999**, *22*, 1029–1035. [[CrossRef](#)] [[PubMed](#)]
6. Ndosu, M.; Wright-Hughes, A.; Brown, S.; Backhouse, M.; Lipsky, B.A.; Bhogal, M.; Reynolds, C.; Vowden, P.; Jude, E.B.; Nixon, J.; et al. Prognosis of the infected diabetic foot ulcer: A 12-month prospective observational study. *Diabet. Med.* **2018**, *35*, 78–88. [[CrossRef](#)] [[PubMed](#)]
7. Dowd, S.E.; Wolcott, R.D.; Sun, Y.; McKeehan, T.; Smith, E.; Rhoads, D. Polymicrobial nature of chronic diabetic foot ulcer biofilm infections determined using bacterial tag encoded FLX amplicon pyrosequencing (bTEFAP). *PLoS ONE* **2008**, *3*, e3326. [[CrossRef](#)] [[PubMed](#)]
8. Lecube, A.; Pachón, G.; Petriz, J.; Hernández, C.; Simó, R. Phagocytic activity is impaired in type 2 diabetes mellitus and increases after metabolic improvement. *PLoS ONE* **2011**, *6*, e23366. [[CrossRef](#)]
9. Park, S.; Rich, J.; Hanses, F.; Lee, J.C. Defects in innate immunity predispose C57BL/6J-Leprdb/Leprdb mice to infection by *Staphylococcus aureus*. *Infect. Immun.* **2009**, *77*, 1008–1014. [[CrossRef](#)]
10. Yagihashi, S.; Mizukami, H.; Sugimoto, K. Mechanism of diabetic neuropathy: Where are we now and where to go? *J. Diabetes Investig.* **2011**, *2*, 18–32. [[CrossRef](#)]
11. Galkowska, H.; Olszewski, W.L.; Wojewodzka, U.; Rosinski, G.; Karnafel, W. Neurogenic factors in the impaired healing of diabetic foot ulcers. *J. Surg. Res.* **2006**, *134*, 252–258. [[CrossRef](#)]
12. Chawla, A.; Chawla, R.; Jaggi, S. Microvascular and macrovascular complications in diabetes mellitus: Distinct or continuum? *Indian J. Endocrinol. Metab.* **2016**, *20*, 546–551. [[CrossRef](#)] [[PubMed](#)]
13. Peters, E.J.; Lipsky, B.A.; Berendt, A.R.; Embil, J.M.; Lavery, L.A.; Senneville, E.; Urbančič-Rovan, V.; Bakker, K.; Jeffcoate, W.J. A systematic review of the effectiveness of interventions in the management of infection in the diabetic foot. *Diabetes Metab. Res. Rev.* **2012**, *28*, 142–162. [[CrossRef](#)] [[PubMed](#)]
14. Raymakers, J.T.; Houben, A.J.; van der Heyden, J.J.; Tordoir, J.H.; Kitslaar, P.J.; Schaper, N.C. The effect of diabetes and severe ischaemia on the penetration of ceftazidime into tissues of the limb. *Diabet. Med.* **2001**, *18*, 229–234. [[CrossRef](#)] [[PubMed](#)]
15. Redel, H.; Gao, Z.; Li, H.; Alekseyenko, A.V.; Zhou, Y.; Perez-Perez, G.I.; Weinstock, G.; Sodergren, E.; Blaser, M.J. Quantitation and composition of cutaneous microbiota in diabetic and nondiabetic men. *J. Infect. Dis.* **2013**, *207*, 1105–1114. [[CrossRef](#)] [[PubMed](#)]
16. Gontcharova, V.; Youn, E.; Sun, Y.; Wolcott, R.D.; Dowd, S.E. A comparison of bacterial composition in diabetic ulcers and contralateral intact skin. *Open Microbiol. J.* **2010**, *4*, 8–19. [[CrossRef](#)] [[PubMed](#)]
17. Jneid, J.; Lavigne, J.P.; La Scola, B.; Cassir, N. The diabetic foot microbiota: A review. *Hum. Microbiome J.* **2017**, *5*, 1–6. [[CrossRef](#)]
18. Pereira, S.G.; Moura, J.; Carvalho, E.; Empadinhas, N. Microbiota of Chronic Diabetic Wounds: Ecology, Impact, and Potential for Innovative Treatment Strategies. *Front. Microbiol.* **2017**, *8*, 1791. [[CrossRef](#)]
19. Gardiner, M.; Vicaretti, M.; Sparks, J.; Bansal, S.; Bush, S.; Liu, M.; Darling, A.; Harry, E.; Burke, C.M. A longitudinal study of the diabetic skin and wound microbiome. *PeerJ* **2017**, *5*, e3543. [[CrossRef](#)]
20. Malone, M.; Johani, K.; Jensen, S.O.; Gosbell, I.B.; Dickson, H.G.; Hu, H.; Vickery, K. Next Generation DNA Sequencing of Tissues from Infected Diabetic Foot Ulcers. *EBioMedicine* **2017**, *21*, 142–149. [[CrossRef](#)]
21. MacDonald, A.; Brodell, J.D.; Daiss, J.L.; Schwarz, E.M.; Oh, I. Evidence of differential microbiomes in healing versus non-healing diabetic foot ulcers prior to and following foot salvage therapy. *J. Orthop. Res.* **2019**, *37*, 1596–1603. [[CrossRef](#)]
22. Verbanic, S.; Shen, Y.; Lee, J.; Deacon, J.M.; Chen, I.A. Microbial predictors of healing and short-term effect of debridement on the microbiome of chronic wounds. *NPJ Biofilms Microbiomes* **2020**, *6*, 21. [[CrossRef](#)] [[PubMed](#)]
23. Sloan, T.J.; Turton, J.C.; Tyson, J.; Musgrove, A.; Fleming, V.M.; Lister, M.M.; Loose, M.W.; Sockett, R.E.; Diggle, M.; Game, F.L.; et al. Examining diabetic heel ulcers through an ecological lens: Microbial community dynamics associated with healing and infection. *J. Med. Microbiol.* **2019**, *68*, 230–240. [[CrossRef](#)] [[PubMed](#)]
24. Loesche, M.; Gardner, S.E.; Kalan, L.; Horwinski, J.; Zheng, Q.; Hodgkinson, B.P.; Tyldsley, A.S.; Franciscus, C.L.; Hillis, S.I.; Mehta, S.; et al. Temporal Stability in Chronic Wound Microbiota is Associated with Poor Healing. *J. Investig. Dermatol.* **2017**, *137*, 237–244. [[CrossRef](#)] [[PubMed](#)]

25. Kalan, L.R.; Meisel, J.S.; Loesche, M.A.; Horwinski, J.; Soaita, I.; Chen, X.; Uberoi, A.; Gardner, S.E.; Grice, E.A. Strain- and Species- Level Variation in the Microbiome of Diabetic Wounds Is Associated with Clinical Outcomes and Therapeutic Efficacy. *Cell Host Microbe* **2019**, *25*, 641–655. [[CrossRef](#)] [[PubMed](#)]
26. Spichler, A.; Hurwitz, B.L.; Armstrong, D.G.; Lipsky, B.A. Microbiology of diabetic foot infections: From Louis Pasteur to ‘crime scene investigation’. *BMC Med.* **2015**, *13*, 2. [[CrossRef](#)] [[PubMed](#)]
27. Lavigne, J.P.; Sotto, A.; Dunyach-Remy, C.; Lipsky, B.A. New molecular techniques to study the skin microbiota of diabetic foot ulcers. *Adv. Wound Care* **2015**, *4*, 38–49. [[CrossRef](#)] [[PubMed](#)]
28. McCarty, S.M.; Cochrane, C.A.; Clegg, P.D.; Percival, S.L. The Role of Endogenous and Exogenous Enzymes in Chronic Wounds: A Focus on the Implications of Aberrant Levels of Both Host and Bacterial Proteases in Wound Healing. *Wound Repair Regen.* **2012**, *20*, 125–136. [[CrossRef](#)]
29. James, G.A.; Swogger, E.; Wolcott, R.; Pulcini, E.D.; Secor, P.; Sestrich, J.; Costerton, J.W.; Stewart, P.S. Biofilms in chronic wounds. *Wound Repair Regen.* **2008**, *16*, 37–44. [[CrossRef](#)]
30. Percival, S.L.; McCarty, S.M.; Lipsky, B. Biofilms and Wounds: An Overview of the Evidence. *Adv. Wound Care* **2015**, *4*, 373–381. [[CrossRef](#)]
31. Bjarnsholt, T. The role of bacterial biofilms in chronic infections. *APMIS* **2013**, *121*, 1–58. [[CrossRef](#)]
32. Høiby, N.; Bjarnsholt, T.; Moser, C.; Bassi, G.L.; Coenye, T.; Donelli, G.; Hall-Stoodley, L.; Holá, V.; Imbert, C.; Kirketerp-Møller, K.; et al. ESCMID guideline for the diagnosis and treatment of biofilm infections 2014. *Clin. Microbiol. Infect.* **2015**, *21*, S1–S25. [[CrossRef](#)] [[PubMed](#)]
33. Solano, C.; Echeverz, M.; Lasa, I. Biofilm dispersion and quorum sensing. *Curr. Opin. Microbiol.* **2014**, *18*, 96–104. [[CrossRef](#)] [[PubMed](#)]
34. Asfour, H. Anti-quorum sensing natural compounds. *J. Microsc. Ultrastruct.* **2018**, *6*, 1. [[CrossRef](#)] [[PubMed](#)]
35. Guilhen, C.; Forestier, C.; Balestrino, D. Biofilm dispersal: Multiple elaborate strategies for dissemination of bacteria with unique properties. *Mol. Microbiol.* **2017**, *105*, 188–210. [[CrossRef](#)]
36. Zhao, G.; Usui, M.L.; Underwood, R.A.; Singh, P.K.; James, G.A.; Stewart, P.S.; Fleckman, P.; Olerud, J.E. Time course study of delayed wound healing in a biofilm challenged diabetic mouse model. *Wound Repair Regen.* **2012**, *20*, 342–352. [[CrossRef](#)]
37. Nguyen, A.T.; Oglesby-Sherrouse, A.G. Interactions between *Pseudomonas aeruginosa* and *Staphylococcus aureus* during co-cultivations and polymicrobial infections. *Appl. Microbiol. Biotechnol.* **2016**, *100*, 6141–6148. [[CrossRef](#)]
38. Hsu, C.Y.; Shu, J.C.; Lin, M.H.; Chong, K.Y.; Chen, C.C.; Wen, S.M.; Hsieh, Y.T.; Lia, W.T. High Glucose concentration promotes vancomycin-enhanced biofilm formation of vancomycin-non-susceptible *Staphylococcus aureus* in diabetic mice. *PLoS ONE* **2015**, *10*, e0134852. [[CrossRef](#)]
39. Nouvong, A.; Ambrus, A.M.; Zhang, E.R.; Hultman, L.; Coller, H.A. Reactive oxygen species and bacterial biofilms in diabetic wound healing. *Physiol. Genom.* **2016**, *48*, 889–896. [[CrossRef](#)]
40. Dhall, S.; Do, D.C.; Garcia, M.; Kim, J.; Mirebrahim, S.H.; Lyubovitsky, J.; Lonardi, S.; Nothnagel, E.A.; Schiller, N.; Martins-Green, M. Generating and reversing chronic wounds in diabetic mice by manipulating wound redox parameters. *J. Diabetes Res.* **2014**, *2014*, 1–18. [[CrossRef](#)]
41. James, G.A.; Ge Zhao, A.; Usui, M.; Underwood, R.A.; Nguyen, H.; Beyenal, H.; Pulcini, E.D.; Agostino Hunt, A.; Bernstein, H.C.; Fleckman, P.; et al. Microsensor and transcriptomic signatures of oxygen depletion in biofilms associated with chronic wounds. *Wound Repair Regen.* **2016**, *24*, 373–383. [[CrossRef](#)]
42. Agostinho Hunt, A.M.; Gibson, J.A.; Larrivee, C.L.; O’Reilly, S.; Navitskaya, S.; Needle, D.B.; Abramowitch, R.B.; Busik, J.V.; Waters, C.M. A bioluminescent *Pseudomonas aeruginosa* wound model reveals increased mortality of type 1 diabetic mice to biofilm infection. *J. Wound Care* **2017**, *26*, S24–S33. [[PubMed](#)]
43. Goldufsky, J.; Wood, S.J.; Jayaraman, V.; Majdobe, O.; Chen, L.; Qin, S.; Zhang, C.; DiPietro, L.A.; Shafikhani, S.H. *Pseudomonas aeruginosa* uses T3SS to inhibit diabetic wound healing. *Wound Repair Regen.* **2015**, *23*, 557–564. [[CrossRef](#)] [[PubMed](#)]
44. Neut, D.; Tijdens-Creusen, E.J.; Bulstra, S.K.; van der Mei, H.C.; Busscher, H.J. Biofilms in chronic diabetic foot ulcers—A study of 2 cases. *Acta Orthop.* **2011**, *82*, 383–385. [[CrossRef](#)]
45. Malik, A.; Mohammad, Z.; Ahmad, J. The diabetic foot infections: Biofilms and antimicrobial resistance. *Diabetes Metab. Syndr.* **2013**, *7*, 101–107. [[CrossRef](#)] [[PubMed](#)]

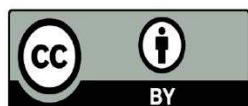
46. Murali, T.S.; Kavitha, S.; Spoorthi, J.; Bhat, D.V.; Prasat, A.S.B.; Upton, Z.; Ramachandra, L.; Acharya, R.V.; Satyamoorthy, K. Characteristics of microbial drug resistance and its correlates in chronic diabetic foot ulcer infections. *J. Med. Microbiol.* **2014**, *63*, 1377–1385. [[CrossRef](#)]
47. Banu, A.; Noorul Hassan, M.M.; Rajkumar, J.; Srinivasa, S. Spectrum of bacteria associated with diabetic foot ulcer and biofilm formation: A prospective study. *Australas. Med. J.* **2015**, *8*, 280–285. [[CrossRef](#)]
48. Oates, A.; Bowling, F.L.; Boulton, A.J.; Bowler, P.G.; Metcalf, D.G.; McBain, A.J. The visualization of biofilms in chronic diabetic foot wounds using routine diagnostic microscopy methods. *J. Diabetes Res.* **2014**, *2014*, 153586. [[CrossRef](#)]
49. Zhao, G.; Usui, M.L.; Lippman, S.I.; James, G.A.; Stewart, P.S.; Fleckman, P.; Olerud, J.E. Biofilms and Inflammation in Chronic Wounds. *Adv. Wound Care* **2013**, *2*, 389–399. [[CrossRef](#)]
50. Peters, B.M.; Jabra-Rizk, M.A.; O'May, G.A.; Costerton, J.W.; Shirtliff, M.E. Polymicrobial interactions: Impact on pathogenesis and human disease. *Clin. Microbiol. Rev.* **2012**, *25*, 193–213. [[CrossRef](#)]
51. Hibbing, M.E.; Fuqua, C.; Parsek, M.R.; Peterson, S.B. Bacterial competition: Surviving and thriving in the microbial jungle. *Nat. Rev. Microbiol.* **2010**, *8*, 15–25. [[CrossRef](#)]
52. Rutherford, S.T.; Bassler, B.L. Bacterial quorum sensing: Its role in virulence and possibilities for its control. *Cold Spring Harb. Perspect. Med.* **2012**, *2*, a012427. [[CrossRef](#)] [[PubMed](#)]
53. Mottola, C.; Semedo-Lemsaddek, T.; Mendes, J.J.; Melo-Cristino, J.; Tavares, L.; Cavaco-Silva, P.; Oliveira, M. Molecular typing, virulence traits and antimicrobial resistance of diabetic foot staphylococci. *J. Biomed. Sci* **2016**, *23*, 33. [[CrossRef](#)] [[PubMed](#)]
54. Yin, W.; Wang, Y.; Liu, L.; He, J. Biofilms: The microbial “protective clothing” in extreme environments. *Int. J. Mol. Sci.* **2019**, *20*, 3423. [[CrossRef](#)]
55. Kumar, D.; Banerjee, T.; Chakravarty, J.; Singh, S.K.; Dwivedi, A.; Tilak, R. Identification, antifungal resistance profile, in vitro biofilm formation and ultrastructural characteristics of *Candida* species isolated from diabetic foot patients in Northern India. *Indian J. Med. Microbiol.* **2016**, *34*, 308–314. [[PubMed](#)]
56. Sugimoto, S.; Iwamoto, T.; Takada, K.; Okuda, K.I.; Tajima, A.; Iwase, T.; Mizunoe, Y. *Staphylococcus epidermidis* Esp degrades specific proteins associated with *Staphylococcus aureus* biofilm formation and host-pathogen interaction. *J. Bacteriol.* **2013**, *195*, 1645–1655. [[CrossRef](#)] [[PubMed](#)]
57. Wolcott, R.D.; Hanson, J.D.; Rees, E.J.; Koenig, L.D.; Philips, C.D.; Wolcott, R.A.; Cox, S.B.; White, J.S. Analysis of the chronic wound microbiota of 2,963 patients by 16S rDNA pyrosequencing. *Wound Repair Regen.* **2016**, *24*, 163–174. [[CrossRef](#)] [[PubMed](#)]
58. Jneid, J.; Cassir, N.; Schuldiner, S.; Jourdan, N.; Sotto, A.; Lavigne, J.P.; La Scola, B. Exploring the microbiota of diabetic foot infections with culturomics. *Front. Cell Infect. Microbiol.* **2018**, *8*, 282. [[CrossRef](#)] [[PubMed](#)]
59. Bowler, P.G.; Duerden, B.I.; Armstrong, D.G. Wound Microbiology and Associated Approaches to Wound Management. *Clin. Microbiol. Rev.* **2001**, *14*, 244–269. [[CrossRef](#)]
60. Oates, A.; Bowling, F.L.; Boulton, A.J.M.; McBain, A.J. Molecular and culture-based assessment of the microbial diversity of diabetic chronic foot wounds and contralateral skin sites. *J. Clin. Microbiol.* **2012**, *50*, 2263–2271. [[CrossRef](#)]
61. Gardner, S.E.; Hillis, S.L.; Heilmann, K.; Segre, J.A.; Grice, E.A. The neuropathic diabetic foot ulcer microbiome is associated with clinical factors. *Diabetes* **2013**, *62*, 923–930. [[CrossRef](#)]
62. Percival, S.L.; Malone, M.; Mayer, D.; Salisbury, A.M.; Schultz, G. Role of anaerobes in polymicrobial communities and biofilms complicating diabetic foot ulcers. *Int. Wound J.* **2018**, *15*, 776–782. [[CrossRef](#)] [[PubMed](#)]
63. Johnson, T.R.; Gómez, B.I.; McIntyre, M.K.; Dubick, M.A.; Christy, R.J.; Nicholson, S.E.; Burmeister, D.M. The Cutaneous Microbiome and Wounds: New Molecular Targets to Promote Wound Healing. *Int. J. Mol. Sci.* **2018**, *19*, 2699. [[CrossRef](#)] [[PubMed](#)]
64. Lipsky, B.A.; Richard, J.L.; Lavigne, J.P. Diabetic foot ulcer microbiome: One small step for molecular microbiology... One giant leap for understanding diabetic foot ulcers? *Diabetes* **2013**, *62*, 679–681. [[CrossRef](#)] [[PubMed](#)]
65. Percival, S.L.; Thomas, J.G.; Williams, D.W. Biofilms and bacterial imbalances in chronic wounds: Anti-Koch. *Int. Wound J.* **2010**, *7*, 169–175. [[CrossRef](#)] [[PubMed](#)]
66. Smith, K.; Collier, A.; Townsend, E.M.; O'Donnell, L.E.; Bal, A.M.; Butcher, J.; MacKay, W.G.; Ramage, G.; Williams, C. One step closer to understanding the role of bacteria in diabetic foot ulcers: Characterising the microbiome of ulcers. *BMC Microbiol.* **2016**, *16*, 54. [[CrossRef](#)]

67. Rahim, K.; Saleha, S.; Zhu, X.; Huo, L.; Basit, A.; Franco, O.L. Bacterial contribution in chronicity of wounds. *Microb. Ecol.* **2017**, *73*, 710–721. [[CrossRef](#)]
68. Patel, S.; Srivastava, S.; Singh, M.R.; Singh, D. Mechanistic insight into diabetic wounds: Pathogenesis, molecular targets and treatment strategies to pace wound healing. *Biomed. Pharm.* **2019**, *112*, 108615. [[CrossRef](#)]
69. Cogen, A.L.; Nizet, V.; Gallo, R.L. Skin microbiota: A source of disease or defence? *Br. J. Dermatol.* **2008**, *158*, 442–455. [[CrossRef](#)]
70. Fazli, M.; Bjarnsholt, T.; Kirketerp-Møller, K.; Jørgensen, B.; Andersen, A.S.; Kroghfelt, K.A.; Givskov, M.; Tolker-Nielsen, T. Nonrandom distribution of *Pseudomonas aeruginosa* and *Staphylococcus aureus* in chronic wounds. *J. Clin. Microbiol.* **2009**, *47*, 4084–4089. [[CrossRef](#)]
71. Hoffman, L.R.; Deziel, E.; D'Argenio, D.A.; Lépine, F.; Emerson, J.; McNamara, S.; Gibson, R.L.; Ramsey, B.W.; Miller, S.I. Selection for *Staphylococcus aureus* small-colony variants due to growth in the presence of *Pseudomonas aeruginosa*. *Proc. Natl. Acad. Sci. USA* **2006**, *103*, 19890–19895. [[CrossRef](#)]
72. Chan, K.G.; Liu, Y.C.; Chang, C.Y. Inhibiting N-acyl-homoserine lactone synthesis and quenching *Pseudomonas* quinolone quorum sensing to attenuate virulence. *Front. Microbiol.* **2015**, *6*, 1173. [[CrossRef](#)] [[PubMed](#)]
73. Schurr, M.J. *Pseudomonas aeruginosa* alginate benefits *Staphylococcus aureus*? *J. Bacteriol.* **2020**, *202*. [[CrossRef](#)] [[PubMed](#)]
74. Price, C.E.; Brown, D.G.; Limoli, D.H.; Phelan, V.V.; O'Toole, G.A. Exogenous alginate protects *Staphylococcus aureus* from killing by *Pseudomonas aeruginosa*. *J. Bacteriol.* **2020**, *202*. [[CrossRef](#)] [[PubMed](#)]
75. Hendricks, K.J.; Burd, T.A.; Anglen, J.O.; Simpson, A.W.; Christensen, G.D.; Gainor, B.J. Synergy between *Staphylococcus aureus* and *Pseudomonas aeruginosa* in a rat model of complex orthopaedic wounds. *J. Bone Joint Surg.* **2001**, *83*, 855–861. [[CrossRef](#)] [[PubMed](#)]
76. Hotterbeekx, A.; Kumar-Singh, S.; Goossens, H.; Malhotra-Kumar, S. In vivo and in vitro interactions between *Pseudomonas aeruginosa* and *Staphylococcus* spp. *Front. Cell Infect. Microbiol.* **2017**, *7*, 106. [[CrossRef](#)] [[PubMed](#)]
77. DeLeon, S.; Clinton, A.; Fowler, H.; Everett, J.; Horswill, A.R.; Rumbaugh, K.P. Synergistic interactions of *Pseudomonas aeruginosa* and *Staphylococcus aureus* in an in vitro wound model. *Infect. Immun.* **2014**, *82*, 4718–4728. [[CrossRef](#)]
78. Mastropaolo, M.D.; Evans, N.P.; Byrnes, M.K.; Stevens, A.M.; Robertson, J.L.; Melville, S.B. Synergy in polymicrobial infections in a mouse model of Type 2 diabetes. *Infect. Immun.* **2005**, *73*, 6055–6063. [[CrossRef](#)]
79. Nair, N.; Biswas, R.; Gotz, F.; Biswas, L. Impact of *Staphylococcus aureus* on pathogenesis in polymicrobial infections. *Infect. Immun.* **2014**, *82*, 2162–2169. [[CrossRef](#)]
80. Ngba Essebe, C.; Visvikis, O.; Fines-Guyon, M.; Vergne, A.; Cattoir, V.; Lecoustumier, A.; Lemichez, E.; Sotto, A.; Lavigne, J.P.; Dunyach-Remy, C. Decrease of *Staphylococcus aureus* virulence by *Helicococcus kunzii* in a *Caenorhabditis elegans* model. *Front. Cell Infect. Microbiol.* **2017**, *7*, 77. [[CrossRef](#)]
81. Ramsey, M.W.; Freire, M.O.; Gabriłska, R.A.; Rumbaugh, K.P.; Lemon, K.P. *Staphylococcus aureus* shifts toward commensalism in response to *Corynebacterium* species. *Front. Microbiol.* **2016**, *7*, 1230. [[CrossRef](#)]
82. Vandecandelaere, I.; Depuydt, P.; Nelis, H.J.; Coenye, T. Protease production by *Staphylococcus epidermidis* and its effect on *Staphylococcus aureus* biofilms. *Pathog. Dis.* **2014**, *70*, 321–331. [[CrossRef](#)] [[PubMed](#)]
83. Okuda, T.; Kokubu, E.; Kawana, T.; Saito, A.; Okuda, K.; Ishihara, K. Synergy in biofilm formation between *Fusobacterium nucleatum* and *Prevotella* species. *Anaerobe* **2012**, *18*, 110–116. [[CrossRef](#)] [[PubMed](#)]
84. Mottola, C.; Mendes, J.J.; Cristino, J.M.; Cavasco-Silva, P.; Tavares, L.; Oliveira, M. Polymicrobial biofilms by diabetic foot clinical isolates. *Folia Microbiol.* **2016**, *61*, 35–43. [[CrossRef](#)] [[PubMed](#)]
85. Lynch, A.S.; Robertson, G.T. Bacterial and fungal biofilm infections. *Annu. Rev. Med.* **2008**, *59*, 415–428. [[CrossRef](#)]
86. Costa-Orlandi, C.B.; Sardi, J.C.O.; Pitangui, N.S.; de Oliveira, H.C.; Scorzoni, L.; Galeane, M.C.; Medina-Alarcón, K.P.; Melo, W.C.M.A.; Marcelino, M.Y.; Braz, J.D.; et al. Fungal Biofilms and Polymicrobial Diseases. *J. Fungi* **2017**, *3*, 22. [[CrossRef](#)]
87. Kalan, L.; Loesche, M.; Hodkinson, B.P.; Heilmann, K.; Ruthel, G.; Gardner, S.E.; Grice, E.A. Redefining the chronic-wound microbiome: Fungal communities are prevalent, dynamic, and associated with delayed healing. *mBio* **2016**, *7*. [[CrossRef](#)]

88. Malone, M.; Bjarnsholt, T.; McBain, A.J.; James, G.A.; Stoodley, P.; Leaper, D.; Tachi, M.; Schultz, G.; Swanson, T.; Wolcott, R.D. The prevalence of biofilms in chronic wounds: A systematic review and meta-analysis of published data. *J. Wound Care* **2017**, *26*, 20–25. [[CrossRef](#)]
89. Donlan, R.M.; Costerton, J.W. Biofilms: Survival mechanisms of clinically relevant microorganisms. *Clin. Microbiol. Rev.* **2002**, *15*, 167–193. [[CrossRef](#)]
90. Hall-Stoodley, L.; Costerton, J.W.; Stoodley, P. Bacterial biofilms: From the natural environment to infectious diseases. *Nat. Rev. Microbiol.* **2004**, *2*, 95–108. [[CrossRef](#)]
91. Mah, T.F.; O'Toole, G.A. Mechanisms of biofilm resistance to antimicrobial agents. *Trends Microbiol.* **2001**, *9*, 34–39. [[CrossRef](#)]
92. Alav, I.; Sutton, J.M.; Rahman, K.M. Role of bacterial efflux pumps in biofilm formation. *J. Antimicrob. Chemother.* **2018**, *73*, 2003–2020. [[CrossRef](#)] [[PubMed](#)]
93. Ghigo, J.M. Natural conjugative plasmids induce bacterial biofilm development. *Nature* **2001**, *412*, 442–445. [[CrossRef](#)] [[PubMed](#)]
94. Berlanga, M.; Guerrero, R. Living together in biofilms: The microbial cell factory and its biotechnological implications. *Microb. Cell Fact.* **2016**, *15*, 165. [[CrossRef](#)] [[PubMed](#)]
95. Gebreyohannes, G.; Nyerere, C.; Bii, C.; Sbhatu, D.B. Challenges of intervention, treatment, and antibiotic resistance of biofilm-forming microorganism. *Heliyon* **2019**, *5*, e02192. [[CrossRef](#)] [[PubMed](#)]
96. Suller, M.T.E.; Lloyd, D. The antibacterial activity of vancomycin towards *Staphylococcus aureus* under aerobic and anaerobic conditions. *J. Appl. Microbiol.* **2002**, *92*, 866–872. [[CrossRef](#)]
97. González, J.F.; Hahn, M.M.; Gunn, J.S. Chronic biofilm-based infections: Skewing of the immune response. *Pathog. Dis.* **2018**, *76*, fty023. [[CrossRef](#)]
98. Jefferson, K.K. What drives bacteria to produce a biofilm? *FEMS Microbiol. Lett.* **2004**, *236*, 163–173. [[CrossRef](#)]
99. Castillo-Juárez, I.; Maeda, T.; Mandujano-Tinoco, E.A.; Tomás, M.; Pérez-Eretza, B.; García-Contreras, S.J.; Wood, T.K.; García-Contreras, R. Role of quorum sensing in bacterial infections. *World J. Clin. Cases* **2015**, *3*, 575–598. [[CrossRef](#)]
100. Hirschfeld, J. Dynamic interactions of neutrophils and biofilms. *J. Oral Microbiol.* **2014**, *6*, 26102. [[CrossRef](#)]
101. Wolska, K.I.; Grudniak, A.M.; Rudnicka, Z.; Markowska, K. Genetic control of bacterial biofilms. *J. Appl. Genet.* **2016**, *57*, 225–238. [[CrossRef](#)]
102. Moser, C.; Pedersen, H.T.; Lerche, C.J.; Kolpen, M.; Line, L.; Thomsen, K.; Høiby, N.; Jensen, P.O. Biofilms and host response—Helpful or harmful. *APMIS* **2017**, *125*, 320–338. [[CrossRef](#)] [[PubMed](#)]
103. Clinton, A.; Carter, T. Chronic Wound Biofilms: Pathogenesis and Potential Therapies. *Lab. Med.* **2015**, *46*, 277–284. [[CrossRef](#)] [[PubMed](#)]
104. Lipsky, B.A.; Senneville, E.; Abbas, Z.G.; Aragón-Sánchez, J.; Diggle, M.; Embil, J.M.; Kono, S.; Lavery, L.A.; Malone, M.; van Asten, S.A.; et al. Guideline on the diagnostic and treatment of foot infection in persons with diabetes (IWGDF 2019 update). *Diabetes Metab. Res. Rev.* **2020**, *36*, e3280. [[CrossRef](#)] [[PubMed](#)]
105. Wolcott, R.D.; Kennedy, J.P.; Dowd, S.E. Regular debridement is the main tool for maintaining a healthy wound bed in most chronic wounds. *J. Wound Care* **2009**, *18*, 54–56. [[CrossRef](#)]
106. Lázaro-Martínez, J.L.; Alvaro-Afonso, F.J.; Garcia-Alvarez, Y.; Molines-Barroso, R.J.; García-Morales, E.; Sevillano-Fernández, D. Ultrasound-assisted debridement of neuroischaemic diabetic foot ulcers, clinical and microbiological effects: A case series. *J. Wound Care* **2018**, *27*, 278–286. [[CrossRef](#)] [[PubMed](#)]
107. Raad, I.I.; Fang, X.; Keutgen, X.M.; Jiang, Y.; Sherertz, R.; Hachem, R. The role of chelators in preventing biofilm formation and catheter-related bloodstream infections. *Curr. Opin. Infect. Dis.* **2008**, *21*, 385–392. [[CrossRef](#)] [[PubMed](#)]
108. Cui, H.; Li, W.; Li, C.; Vittayapadung, S.; Lin, L. Liposome containing cinnamon oil with antibacterial activity against methicillin-resistant *Staphylococcus aureus* biofilm. *Biofouling* **2016**, *32*, 215–225. [[CrossRef](#)]
109. Kim, S.G.; Yoon, Y.H.; Choi, J.W.; Rha, K.S.; Park, Y.H. Effect of furanone on experimentally induced *Pseudomonas aeruginosa* biofilm formation: In vitro study. *Int. J. Pediatr. Otorhinolaryngol.* **2012**, *76*, 1575–1578. [[CrossRef](#)]
110. Sully, E.K.; Malachowa, N.; Elmore, B.O.; Alexander, S.M.; Femling, J.K.; Gray, B.M.; DeLeo, F.R.; Otto, M.; Cheung, A.L.; Edwards, B.S.; et al. Selective chemical inhibition of *agr* quorum sensing in *Staphylococcus aureus* promotes host defense with minimal impact on resistance. *PLoS Pathog.* **2014**, *10*, e1004174. [[CrossRef](#)]

111. Coraça-Huber, D.C.; Dichtl, S.; Steixner, S.; Nogler, M.; Weiss, G. Iron chelation destabilizes bacterial biofilms and potentiates the antimicrobial activity of antibiotics against coagulase-negative Staphylococci. *Pathog. Dis.* **2018**, *76*, fty052. [[CrossRef](#)]
112. Kalpana, B.J.; Aarthy, S.; Pandian, S.K. Antibiofilm activity of α -amylase from *Bacillus subtilis* S8–18 against biofilm forming human bacterial pathogens. *Appl. Biochem. Biotechnol.* **2012**, *167*, 1778–1794. [[CrossRef](#)] [[PubMed](#)]
113. Rogers, S.A.; Huigens, R.W., III; Cavanagh, J.; Melander, C. Synergistic effects between conventional antibiotics and 2-aminoimidazole-derived antibiofilm agents. *Antimicrob. Agents Chemother.* **2010**, *54*, 2112–2118. [[CrossRef](#)]
114. Chung, P.Y.; Toh, Y.S. Anti-biofilm agents: Recent breakthrough against multi-drug resistant *Staphylococcus aureus*. *Pathog. Dis.* **2014**, *70*, 231–239. [[CrossRef](#)] [[PubMed](#)]
115. Tardivo, J.P.; Adami, F.; Correa, J.A.; Pinhal, M.A.S.; Baptista, M.S. A clinical trial testing the efficacy of PDT in preventing amputation in diabetic patients. *Photodiagnosis Photodyn. Ther.* **2014**, *11*, 342–350. [[CrossRef](#)] [[PubMed](#)]
116. Taha, O.A.; Connerton, P.L.; Connerton, I.F.; El-Shibiny, A. Bacteriophage ZCKP1: A potential treatment for *Klebsiella pneumoniae* isolated from diabetic foot patients. *Front. Microbiol.* **2018**, *9*, 2127. [[CrossRef](#)] [[PubMed](#)]
117. Fish, R.; Kutter, E.; Bryan, D.; Wheat, G.; Kuhl, S. Resolving digital staphylococcal osteomyelitis using bacteriophage—A case report. *Antibiotics* **2018**, *7*, 87. [[CrossRef](#)] [[PubMed](#)]
118. Ahmadi, M.; Adibhesami, M. The effect of silver nanoparticles on wounds contaminated with *Pseudomonas aeruginosa* in mice: An experimental study. *Iran. J. Pharm. Res.* **2017**, *16*, 661–669.
119. Thombare, N.; Jha, U.; Mishra, S.; Siddiqui, M.Z. Guar gum as a promising starting material for diverse applications: A review. *Int. J. Biol. Macromol.* **2016**, *88*, 361–372. [[CrossRef](#)]
120. Cirioni, O.; Giacometti, A.; Ghiselli, R.; Kamysz, W.; Orlando, F.; Mocchegiani, F.; Silvestri, C.; Licci, A.; Chiodi, L.; Lukasiak, J.; et al. Citropin 1.1-treated central venous catheters improve the efficacy of hydrophobic antibiotics in the treatment of experimental staphylococcal catheter-related infection. *Peptides* **2006**, *27*, 1210–1216. [[CrossRef](#)]
121. Dutta, P.; Das, S. Mammalian antimicrobial peptides: Promising therapeutic targets against infection and chronic inflammation. *Curr. Top. Med. Chem.* **2016**, *16*, 99–129. [[CrossRef](#)]
122. Bilyayeva, O.O.; Neshta, V.V.; Golub, A.A.; Sams-Dodd, F. Comparative clinical study of the wound healing effects of a novel micropore particle technology: Effects on wounds, venous leg ulcers, and diabetic foot ulcers. *Wounds* **2017**, *29*, 1–9. [[PubMed](#)]
123. Minden-Bjirkenmajer, B.; Bowlin, G. Honey-based templates in wound healing and tissue engineering. *Bioengineering* **2018**, *5*, 46. [[CrossRef](#)] [[PubMed](#)]

Publisher’s Note: MDPI stays neutral with regard to jurisdictional claims in published maps and institutional affiliations.



© 2020 by the authors. Licensee MDPI, Basel, Switzerland. This article is an open access article distributed under the terms and conditions of the Creative Commons Attribution (CC BY) license (<http://creativecommons.org/licenses/by/4.0/>).

4. Méthodes d'étude du biofilm

Il existe différentes méthodes d'étude du biofilm.

Les techniques de visualisation de biofilm reposent principalement sur l'utilisation de colorants. La culture sur Rouge Congo Agar permet la détection des souches productrices de biofilm. Une fois ensemencées sur ce milieu, les souches exprimant le PIA donnent des colonies noires contre des colonies rouges pour les souches PIA négatives ¹³⁷. Cette technique présente des limites pour l'identification des souches au phénotype variable. La méthode en tube permet l'évaluation qualitative de la présence de biofilm. Après culture en milieu liquide dans un tube microbiologique, les tubes sont lavés au PBS puis séchés avant coloration au cristal violet. La formation de biofilm est considérée comme positive lorsqu'un film visible recouvre les parois et le bas du tube ¹³⁸. Ces techniques, même si elles renseignent l'aspect qualitatif à la production de biofilm, ne permettent pas de rendre compte de la biomasse bactérienne présente à l'intérieur de l'EPS.

La plus répandue des techniques permettant la quantification du biofilm est la formation de biofilm **en microplaque**. C'est la méthode la plus simple à mettre en œuvre et la moins coûteuse. Son principe repose sur la formation du biofilm dans une plaque 96 puits et sur la quantification des bactéries sessiles par coloration puis lecture d'absorbance, ou par dénombrement ¹³⁹. Parmi les méthodes les plus utilisées on notera les techniques de comptages direct qui après désagrégation des bactéries du biofilm par sonication ¹⁴⁰ ou agitation avec des billes de verre ¹⁴¹ permettent l'ensemencement sur milieu gélosé afin de quantifier le nombre de micro-organismes viables cultivables dans l'échantillon. Le test de coloration au Cristal Violet permet aussi la quantification de la densité bactérienne présente dans le biofilm. Le cristal violet est un colorant basique qui se lit sur les bactéries et les exopolysaccharides dans la matrice extracellulaire du biofilm. Après coloration de la biomasse bactérienne, la lecture de l'absorbance à 540 nm permet une quantification relative des microorganismes présents dans l'échantillon ¹⁴². Le modèle Calgary ¹⁴³, système adapté, permettant la détermination de la concentration minimale éradiquant le biofilm fait partie des techniques les plus répandue à ce jour. L'une des limites majeures de toutes ces méthodes destructrices repose sur les nombreux rinçages à effectuer avant

quantification afin d'éliminer les bactéries planctoniques non adhérentes. Dans ce contexte, des techniques alternatives n'utilisant pas de colorant ont été développées permettant, entre autres, de mesurer la formation de biofilm, via l'utilisation de microbilles para électromagnétiques ¹⁴⁴ (**Figure 4**). Cette méthode renseigne via le phénomène d'adhésion bactérienne, la capacité d'une souche à former un biofilm. Toutefois, une critique émise de la technique d'agrégation des billes para électromagnétiques est qu'elle ne permet pas la visualisation ou la quantification à proprement dit d'un biofilm mature. Enfin tous les micro-organismes vivants contiennent de l'Adénosine TriPhosphate qui peut être extrait et dosée à l'aide de l'enzyme Firefly-luciférase. La quantité de lumière produite par cette réaction enzymatique peut être ensuite mesurée et est directement liée à la quantité d'ATP, et par extrapolation, au nombre de cellules microbienne présente dans l'échantillon ¹⁴⁵. Cependant l'usage de cette technique peut être influencée par la présence de métaux ou d'acides présents dans les milieux de culture bactérien. Ces composés interfèrent avec la réaction et peuvent fausser les analyses. De plus cette méthode nécessite un prétraitement des cellules aux diméthylsulfoxyde, composé toxique.

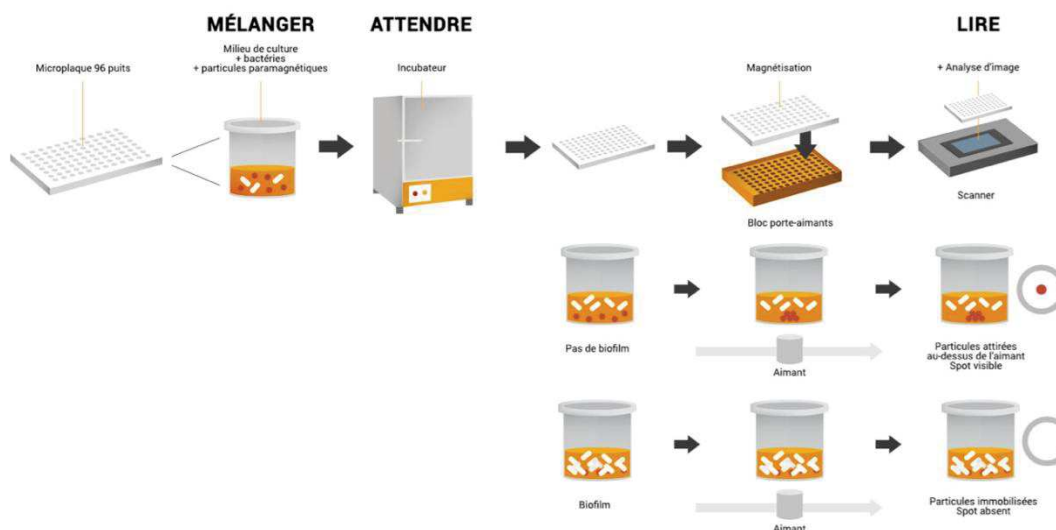


Figure 4 : Principe du suivi de la formation de biofilm grâce à des billes para électromagnétiques (BRT®)

Source : Biofilmcontrol.com

Tous les modèles décrits précédemment ne permettent pas de prendre en compte les forces de flux qui s'exercent lors de la formation d'un biofilm *in vivo*. Aussi, des **modèles en flux** ont été développés pour renouveler le milieu de culture, mimant le flux sanguin et l'acheminement des nutriments et de l'oxygène ¹⁴⁶. Dans un premier temps des modèles de cuves à flux continu (dits « flow cell ») ont été développés. Les flow cell permettent la formation d'un biofilm à l'interface solide-liquide en présence d'une force de cisaillement et d'un apport continu d'éléments nutritifs. Ce système reproduit assez bien les conditions auxquelles sont exposés les bactéries dans leur environnement naturel. De plus, il permet de visualiser facilement le biofilm sous un microscope inversé classique ou confocal ¹⁴⁷. Toutefois, l'inconvénient notable de la technique réside dans le fait qu'elle est très laborieuse à mettre en place au laboratoire. L'absence d'automatisation ainsi que l'impossibilité à lancer un grand nombre d'expérience en même temps sont également des points négatifs de la technique. Plus récemment, des systèmes de **micro fluidique** ont été développés et adaptés à l'étude des biofilms permettant la formation de biofilm dans des canaux de micro fluidiques reliant des puits d'une microplaque 24 ou 48 puits ¹⁴⁸ (**Figure 5**). Les avantages de cette technique résident, en plus du renouvellement de milieu, dans la possibilité de positionner un microscope sous la chambre de formation du biofilm permettant la visualisation en temps réel des différentes étapes du cycle de vie en biofilm ainsi que le criblage haut débit de différentes conditions expérimentales.

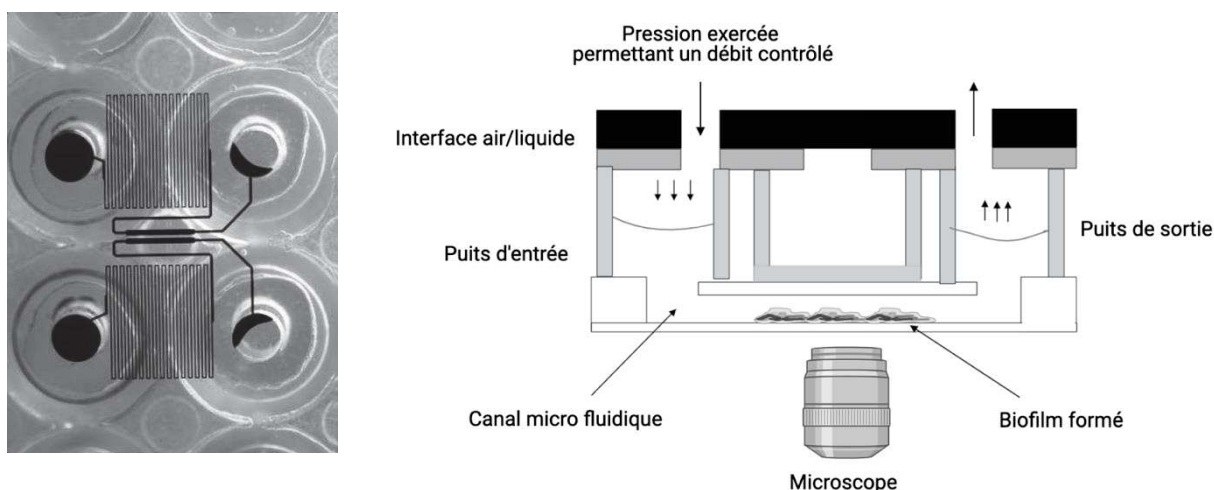


Figure 5 : Principe des techniques de micro fluidique

Source : Fluxion.com

Plusieurs **méthodes de microscopie** permettent de visualiser les biofilms. La microscopie optique permet la visualisation, après coloration ou non des biofilms ¹⁴⁹. La microscopie à fluorescence est très utilisée et permet via l'utilisation de marqueurs ou de sondes fluorescentes, la visualisation de composés spécifiques du biofilm ¹⁵⁰. L'utilisation notamment du marqueur Live/Dead composé du SYTO 9 (marqueur vert se fixant sur toutes les cellules) en combinaison avec l'iodure de propidium (se fixant uniquement sur les cellules endommagées ou mortes) permet l'étude de la viabilité bactérienne et la quantification de la biomasse avant et après traitement du biofilm bactérien ¹⁵¹. La microscopie confocale permet d'apporter une information supplémentaire par rapport à l'épifluorescence en générant une image en 3D par empilement des stacks. On notera aussi l'utilisation de la microscopie électronique à balayage et de la microscopie à force atomique pour l'étude poussée des structures en biofilm ¹⁵².

Enfin, l'utilisation de **modèles *in vivo*** est essentielle puisqu'ils apportent des informations complémentaires et nécessaires à la recherche de nouvelles molécules thérapeutiques visant le biofilm. Cependant ces modèles restent aujourd'hui très difficiles à mettre en place car complexes, coûteux et relevant des questions éthiques. On notera le développement de modèles sur *Caenorhabditis elegans* (*C. elegans*) ¹⁵³ ou sur Zebrafish, *Danio rerio* ¹⁵⁴ pour l'appréhension des études du biofilm.

5. Stratégies thérapeutiques dans la prise en charge des plaies chroniques

Les traitements généraux associés aux plaies chroniques reposent sur des **traitements locaux** impliquant :

- Des soins de la plaie qui permettent l'élimination des tissus nécrotiques et de l'exsudat comprenant le lavage et le débridement de la plaie ¹⁵⁵. Le débridement consiste à retirer les tissus fibrineux, nécrotiques, dévitalisés et/ou infectés, les corps étrangers, les débris ou les fragments d'os présent au niveau de la plaie ¹⁵⁶. Il existe plusieurs types de débridement : mécanique, autolytique,

enzymatique et enfin chirurgical ¹⁵⁷. Le débridement chirurgical est la méthode habituellement la plus utilisée. L'objectif de cette étape dans la prise en charge de la plaie chronique est le contrôle de la charge bactérienne qui permet de faciliter la cicatrisation. Il permet en effet la stimulation de la plaie pour la convertir en plaie aiguë en redémarrant par le saignement, la phase initiale du processus de cicatrisation. Le débridement fait partie du protocole standard de soins d'une plaie profonde en association avec la décharge ¹⁵⁸.

- L'application de pansements qui préparent efficacement le lit de la plaie à la cicatrisation dirigée ¹⁵⁹.
- Dans certains cas, l'utilisation de la thérapie par pression négative est recommandée. La dépression absorbe l'excès d'exsudat en maintenant des conditions humides, elle réduit la contamination bactérienne et stimule la microcirculation en périphérie de la plaie ¹⁶⁰.
- Enfin, la solution chirurgicale peut être également envisagée. Elle permet de fournir à la plaie les éléments de cicatrisation nécessaire dont font partie les facteurs de croissance, les cellules épidermiques ou encore des cellules matricielles ¹⁶¹.

Le **traitement systémique** repose lui sur l'utilisation d'une antibiothérapie adaptée en fonction des bactéries identifiées au niveau de la plaie et de leur profil de sensibilité aux antibiotiques. La durée du traitement se base sur l'évolution clinique ¹⁶². Toutefois, compte tenu de la complexité microbiologique présente sur la plaie (présence de biofilm, interactions bactériennes, augmentation du pourcentage de BMR isolées...) le choix pour le clinicien de l'antibiothérapie la plus adaptée est difficile. Le mauvais usage des antibiotiques que ce soit par un usage abusif ou par un mauvais choix d'antibiotique à prescrire, accélère le phénomène de résistance des micro-organismes aux antibiotiques ¹⁶³. La sensibilité aux antibiotiques par rapport aux bactéries planctoniques est différente chez leurs homologues sessiles ^{164,165}. En fait, les bactéries d'un biofilm peuvent être de 10 à 1000 fois plus résistantes aux agents antimicrobiens ¹⁶⁶. Ce mécanisme de **tolérance** peut être liée à l'EPS secrétée par les bactéries sessiles qui constitue une barrière physique empêchant la pénétration des antibiotiques. Les charges électrostatiques à la surface de la matrice polymérique

peuvent aussi lier certains agents antimicrobiens ¹⁶⁷. Le métabolisme des bactéries au sein d'un biofilm joue également un rôle très important. Étant donné la faible concentration de certains nutriments et le gradient en oxygène présent, certaines cellules du biofilm sont inactives métaboliquement et peuvent même être sous forme dormante ; ces cellules bactériennes dormantes sont d'ailleurs probablement responsables d'une grande partie de la tolérance associée aux biofilms ¹⁶⁸. De plus, la proximité des bactéries au sein du biofilm favorise le transfert horizontal de gènes et ainsi l'augmentation des **résistances** aux antibiotiques ¹⁶⁹. Également, les taux de mutation survenant dans les biofilms sont nettement plus élevés que celui rencontrés chez les cellules planctoniques. De plus, la réponse au stress à des conditions environnementales hostiles peut entraîner une modification du microenvironnement à l'intérieur du biofilm (pH et teneur en oxygène) et peut contribuer à une dégradation accrue des antimicrobiens ¹⁷⁰.

Aussi, les biofilms sont polymicrobiens, la sensibilité aux antibiotiques est souvent hétérogène ; certaines espèces étant sensibles à l'antibiotique donné et pas les autres.

Cette sélection de clones bactériens résistants est aujourd'hui un problème dans la prise en charge des plaies chroniques puisqu'on estime que plus de 10% des bactéries isolées sur des infections de plaies chroniques sont des BMR ¹⁷¹. Le mésusage des antibiotiques engendre des conséquences dramatiques tant sur l'inefficacité de répondre au besoin de soin du patient que sur l'aggravation de l'infection.

Il est, en outre, absolument nécessaire à l'heure actuelle de développer de nouvelles approches alternatives pour aider le clinicien dans la prise en charge des plaies chroniques. La recherche de ces nouvelles stratégies devra prendre en compte les micro-organismes isolés au niveau de la plaie mais également l'environnement dans lequel ils évoluent.

Travail n°2 : Revue de la littérature

Alternative approaches for the management of Diabetic Foot Infections

Cassandra Pouget, Catherine Dunyach-Remy, Alix Pantel, Sophie Schuldiner,
Albert Sotto and Jean-Philippe Lavigne

Accepté dans Frontiers in Microbiology le 7 Septembre 2021

Résumé travail n°2 :

Cette revue de la littérature a comme but de s'intéresser à la **prise en charge** actuelle des UPD mais surtout d'énoncer de **potentielles nouvelles solutions de gestion** de ces infections comme, par exemple, **les solutions antibiofilms**. Ces stratégies novatrices pourraient, en effet, compléter les méthodes thérapeutiques classiques afin d'améliorer le traitement et la cicatrisation des plaies du pied diabétique.

Dans une première partie de la revue, nous discutons des étapes sur lesquelles repose la **prise en charge classique des UPD** et des améliorations possibles. L'utilisation des antibiotiques sur les UPD infectées est aujourd'hui l'un des seuls moyens de combattre les micro-organismes causant l'infection. L'antibiothérapie est dans un premier cas empirique puis le traitement définitif repose sur les résultats de la culture microbiologique. Toutefois, il semblerait que 74% des UPD ne réagissent pas aux agents topiques et systémiques. L'efficacité des antimicrobiens topiques est limitée notamment par l'EPS protégeant les bactéries sessiles. Une des pistes d'amélioration réside dans l'utilisation de systèmes d'administration pouvant apporter des concentrations élevées d'antibiotiques au sein du biofilm (véhicules biodégradables tels que les billes de sulfate de calcium ou polymères naturels ou les éponges de collagène).

Dans la partie suivante, nous nous concentrons sur d'autres approches pouvant être utilisées pour **inhiber la formation du biofilm**. La plupart des solutions qui sont décrites dans cette partie cible différentes étapes de la formation du biofilm et permettent soit de i) bloquer les adhérences bactériennes (chélateurs ioniques, propolis, miel, composés dérivés de plantes) ; ii) d'inhiber le métabolisme du biofilm (en ciblant le QS ou la synthèse des polysaccharides, c-di-GMP) ou iii) d'améliorer la dispersion bactérienne (composés anti-EPS, nanoparticules, phages).

Enfin, dans la dernière partie nous abordons des **approches alternatives** pouvant être adaptées à la prise en charge thérapeutique des UPD. Dans cette partie nous décrivons des méthodes physiques moins usuelles telles que l'utilisation de probiotiques, l'électrostimulation ou les thérapies au plasma. Nous décrivons

également la possibilité d'utiliser de nouveaux agents antimicrobiens (peptides antimicrobiens, cadexomer iodine, guanylated polymethacrylates, métabolites produits par les bactéries elles-mêmes ¹⁷²) et le potentiel thérapeutique de nouveaux types de pansements (next generation antibiofilm carboxymethylcellulose, gel à base de surfactant, biomatériaux favorisant la régénération de la peau) ou de greffes (allogreffe de membrane amniotique, substituts de peau, greffes de kératinocytes ou de cellules souches).

Les biofilms jouant un rôle crucial dans les UPD, la recherche doit maintenant prendre en compte cet écosystème dans les plaies chroniques afin d'identifier de nouvelles alternatives thérapeutiques et d'améliorer la gestion des plaies chroniques. Certaines alternatives présentées dans cette revue sont des stratégies intéressantes et montrent des résultats prometteurs. Tous ces composés pourraient être une solution contre les BMR et le biofilm présent dans les UPD. Cependant, des études complémentaires sont nécessaires pour comprendre les mécanismes sous-jacents à l'action de chacun de ces potentiels candidats médicaments.



Alternative Approaches for the Management of Diabetic Foot Ulcers

Cassandra Pouget¹, Catherine Dunyach-Remy², Alix Pantel², Adeline Boutet-Dubois², Sophie Schuldiner³, Albert Sotto⁴, Jean-Philippe Lavigne^{2*} and Paul Loubet⁴

¹ Virulence Bactérienne et Infections Chroniques, INSERM U1047, Université de Montpellier, Nîmes, France, ² Virulence Bactérienne et Infections Chroniques, INSERM U1047, Université de Montpellier, Service de Microbiologie et Hygiène Hospitalière, Clinique du Pied Gard Occitanie, CHU Nîmes, Nîmes, France, ³ Virulence Bactérienne et Infections Chroniques, INSERM U1047, Université de Montpellier, Service des Maladies Métaboliques et Endocriniennes, Clinique du Pied Gard Occitanie, CHU Nîmes, Le Grau-du-Roi, France, ⁴ Virulence Bactérienne et Infections Chroniques, INSERM U1047, Université de Montpellier, Service des Maladies Infectieuses et Tropicales, Clinique du Pied Gard Occitanie, CHU Nîmes, Nîmes, France

OPEN ACCESS

Edited by:

Giovanna Batoni,
University of Pisa, Italy

Reviewed by:

Xingwu Ran,
Sichuan University, China
Derek Fleming,
Mayo Clinic, United States

*Correspondence:

Jean-Philippe Lavigne
jean.philippe.lavigne@chu-nimes.fr

Specialty section:

This article was submitted to
Infectious Agents and Disease,
a section of the journal
Frontiers in Microbiology

Received: 26 July 2021

Accepted: 07 September 2021

Published: 05 October 2021

Citation:

Pouget C, Dunyach-Remy C,
Pantel A, Boutet-Dubois A,
Schuldiner S, Sotto A, Lavigne J-P
and Loubet P (2021) Alternative
Approaches for the Management
of Diabetic Foot Ulcers.
Front. Microbiol. 12:747618.
doi: 10.3389/fmicb.2021.747618

Diabetic foot ulcers (DFU) represent a growing public health problem. The emergence of multidrug-resistant (MDR) bacteria is a complication due to the difficulties in distinguishing between infection and colonization in DFU. Another problem lies in biofilm formation on the skin surface of DFU. Biofilm is an important pathophysiology step in DFU and may contribute to healing delays. Both MDR bacteria and biofilm producing microorganism create hostile conditions to antibiotic action that lead to chronicity of the wound, followed by infection and, in the worst scenario, lower limb amputation. In this context, alternative approaches to antibiotics for the management of DFU would be very welcome. In this review, we discuss current knowledge on biofilm in DFU and we focus on some new alternative solutions for the management of these wounds, such as antibiofilm approaches that could prevent the establishment of microbial biofilms and wound chronicity. These innovative therapeutic strategies could replace or complement the classical strategy for the management of DFU to improve the healing process.

Keywords: alternative therapeutic approaches, biofilm, chronic wound, diabetic foot, antibiofilm

INTRODUCTION

Diabetic foot ulcers (DFU) have a lifetime prevalence of 15–25% (Armstrong et al., 2017). Infection is the most common, severe and costly (Prompers et al., 2008) DFU complication with high risk of mortality and morbidity associated with lower limb amputation (Bakker et al., 2016). The diagnosis of diabetic foot infection (DFI) is often difficult, leading to the inappropriate use of antibiotics. The bacterial organization in DFU and the involvement of multidrug-resistant (MDR) bacteria require new antimicrobial solutions. This review discusses the role of the biofilm in DFU and alternative approaches to classical treatment that could improve DFU management.

Abbreviations: AMP, antimicrobial peptide; c-di-GMP, cyclic diguanylate; C2DA, *cis*-2-decenoic acid; DFI, diabetic foot infection; DFP, deferiprone; DFU, diabetic foot ulcer; DNA, deoxyribonucleic acid; DMSO, dimethyl sulfoxide; EDTA, ethylene diamine tetra-acetic; EGTA, egtazic acid; EPS, extracellular polymeric substance; FE, functionally equivalent pathogroups; MDR, multidrug resistance; MRSA, methicillin-resistant *Staphylococcus aureus*; MSC, mesenchymal stem cells; NGAD, next generation antibiofilm carboxymethyl cellulose silver containing wound dressing; QS, quorum sensing.

Clinical and Translational Relevance

Sixty to 80% of chronic wounds harbor bacterial structures in a biofilm (James et al., 2008; Malone et al., 2017a). For the clinician, the main difficulty is to distinguish between infecting and colonizing bacteria. Misclassification can lead to inappropriate antibiotic prescriptions that contribute to promoting the emergence of MDR bacteria, a major DFU health issue (Caravaggi et al., 2013). Better understanding of the bacterial organization of biofilms in chronic wounds would allow development of tailored antimicrobial strategies and improving wound healing. In this context, a large majority of current fundamental studies on DFUs focuses on bacterial cooperation and the impact of local microenvironment on microorganisms. Thus, the host-microorganism interface plays a major role in DFI development. In DFU, bacteria are classically organized in functionally equivalent pathogroups (FEP) where pathogenic and commensal bacteria co-aggregate symbiotically in a pathogenic biofilm to maintain a chronic infection (Dowd et al., 2008). Polymicrobial biofilms have been observed both in pre-clinical studies using animal models and in clinical research on DFU. They represent the main cause of healing delay. Recently, some approaches have targeted biofilm formation with the aim of controlling infections (Snyder et al., 2017). Better understanding of the host-bacterial interactions is essential to develop new therapeutic solutions that take into account the biofilm to limit the diffusion of MDR bacteria.

Diabetic Foot Ulcers and Biofilms

Biofilm formation is a multistep process (see for review Percival et al., 2015) whereby heterogeneous communities of microorganisms (bacteria and/or fungi) are embedded into an extracellular polymeric substance (EPS) matrix that contains proteins, deoxyribonucleic acid (DNA), glycoproteins and polysaccharides, and confers the ability to adhere to biotic or abiotic surfaces (Bjarnsholt, 2013). In DFU, the biofilm architectural structure differs among patients due to the variability of the involved bacterial genera and species. Conversely, the multistep formation process is similar. Biofilm formation is a major mechanism of adaptation that protects bacteria from antibiotics, due to several characteristics (Singh et al., 2017). Biofilm structure provides a protective layer against antimicrobial compounds. Wounds biofilms are polymicrobial, formed by complex and order combinations of microorganisms. Hence, compounds produced by different bacterial strains might impair the contact between the bacterial cell wall and the antibiotic by changing the composition of the EPS. Finally, the production of degradative enzymes by different pathogens can act in synergy against antibiotics. These biofilm aspects are responsible for a reduced diffusion of the antibiotic within the biofilm matrix leading to an inefficient activity of the antibiotic treatment (Sharma et al., 2019). In addition to this feature, the ability to form a biofilm is an effective strategy to enhance survival and persistence of microorganisms by increasing their antimicrobial resistance. The antimicrobial resistance in organisms producing biofilms acts by delayed penetration of the antimicrobial agents through the biofilm matrix, altered growth

rate of biofilm organisms, and other physiological changes due to the biofilm mode of growth (Donlan and Costerton, 2002).

CLASSICAL STRATEGIES IN THE MANAGEMENT OF DIABETIC FOOT ULCERS

The management of patients with a DFU is a multidisciplinary approach that includes all relevant specialties (i.e., nursing, orthopedics, plastic surgery, vascular surgery, nutrition, infectious diseases, microbiology, and endocrinology departments) (Cahn et al., 2014). To aid the clinician during the management of DFUs, classification of stage and severity of the wound must be established (Lipsky et al., 2020). The classical care for the control and treatment of DFUs is centered on perfusion, pressure moderation, control of the infection, control of the glycaemic balance, foot discharge and debridement (Wu et al., 2007) (Table 1).

Debridement of the Wound

Debridement consists in the removal of necrotic, devitalized and/or infected tissue from a wound, leaving healthy tissue preserved. Surgical debridement is the usual method used. The objective is to control the bacterial load, which, in combination with antimicrobial treatment, allows early closure of the wound and surrounding tissues to promote normal healing by removing infected tissues, biofilms, and senescent cells. Debridement allows the reepithelialization of soft-tissue by eradication of (early or established) infection and reduction of bioburden, the improvement of local blood flow, and the revitalization of the wound bed. When it was performed correctly, it optimizes the diabetic wound healing.

Negative Pressure Wound Therapy

Associated with debridement, negative pressure wound therapy is an airtight open-pore placed onto the wound and covered by an airtight dressing. Then, the wound is connected to a vacuum source and a negative pressure is generated. The negative pressure at the wound site reduces the size of the wound through contraction; it continuously cleans the wound by removing small debris through suction and reduces levels of proteases through wound fluid removal (Apelqvist et al., 2017). The efficiency of this therapy has been confirmed and it represents an effective measure of promoting wound healing, although the evidence is low (Liu et al., 2018).

Antimicrobial Therapy for Infected Diabetic Foot Ulcers

Antibiotics are not used to manage colonized DFU (Lipsky et al., 2020). Their use concerned the different stages of DFI. Antibiotics are mainly empirical in the first instance, in accordance with the causative pathogen and the severity of the infection. The definitive antibiotic treatment is changed according to the microbiological culture and the response of the

TABLE 1 | *In vitro* and *in vivo* effects of the main alternative approaches studied.

	<i>In vitro</i> effects	<i>In vivo</i> effects	References
Debridement			
Negative pressure therapy	–	Enhance wound closure	Apelqvist et al., 2017; Liu et al., 2018
Antimicrobial agents			
Calcium sulfate beads with antibiotics	Decreased viability of MRSA strains	No clinical evaluation	Price et al., 2016
Nanoparticles	Silver nanoparticles affect <i>P. aeruginosa</i> biofilm formation	No clinical evaluation	Beyth et al., 2015; Ahmadi and Acibhesami, 2017; Hamdan et al., 2017; Mihai et al., 2018
Oxyclozanide	Enhances aminoglycoside and tetracycline killing in <i>S. aureus</i> biofilms	No clinical evaluation	Maiden et al., 2019
Guanylated polymethacrylates	Effective killing of <i>C. albicans</i> and <i>S. aureus</i> in polymicrobial biofilms	Untested in human DFU	Qu et al., 2016
Guar gum-associated nisin	Reduction of biofilm formation by <i>S. aureus</i> isolates from patients	Evaluation with strains isolated from DFU	Cirioni et al., 2006; Dutta and Das, 2016; Santos et al., 2016; Thombare et al., 2016
Acapsil	–	Shorter hospital stay and faster wound healing	Bilyayeva et al., 2017
Antiseptics			
Cadexomer iodine	–	Reduction (1 log10) of microbial load and biofilm in DFU (11/17 patients)	Schwartz et al., 2013; Malone et al., 2017b
Nutraceuticals			
Cranberry	Inhibition of pilus synthesis and prevention of biofilm formation	Decrease of <i>Escherichia coli</i> , <i>S. aureus</i> adhesion	LaPlante et al., 2012
Tannic acid	Inhibition of <i>S. aureus</i> biofilm formation by peptidoglycan cleavage	Acceleration of cutaneous wound healing in rat model	Payne et al., 2013; Orłowski et al., 2018; Chen et al., 2019
Tea-tree oil and Cinnamon oil	Effect on MRSA biofilm	Reduction of the quantity of colonized MRSA and promotion of healing of chronic wounds in a clinical trial	Kwieciński et al., 2009; Lee et al., 2014; Cui et al., 2016; Seyed Ahmadi et al., 2019
Ellagic acid	Limits <i>S. aureus</i> biofilm formation and enhances antibiotic susceptibility	No clinical evaluation	Quave et al., 2012
Propolis and honey	Anti-inflammatory and anti-bacterial properties	Reduction of bacterial load of chronic wounds in combination with antibiotics	Henshaw et al., 2014; Jull et al., 2015; Martinotti and Ranzato, 2015; Minden-Birkenmaier and Bowlin, 2018; McLoone et al., 2020
Probiotics	<i>Lactobacilli</i> antibiofilm activity	Acceleration of wound healing in mice	Vuotto et al., 2014; Vägesjö et al., 2018
Phage therapy			
	Reduction of biofilm formation and infection by <i>P. aeruginosa</i> , <i>S. aureus</i> , and <i>A. baumannii</i>	Reduction of bacterial load and wound closure in diabetic mouse wound infections	Mendes et al., 2014; Fish et al., 2018; Hill et al., 2018; Morozova et al., 2018; Taha et al., 2018; Albac et al., 2020; Kifelew et al., 2020
Action on wound healing			
Photodynamic therapy	–	Increase of reepithelization	Tardivo et al., 2014
Hyperbaric oxygen therapy	–	Improvement of short-term healing	Kranke et al., 2015
Non-thermal plasma	–	Acceleration of wound healing in animal models of ulcers	Chatraie et al., 2018; Cooley et al., 2020
Electrostimulation	Enhanced wound closure time	Evaluation with dressings	Barki et al., 2019
Alternatives for inhibition of adhesion and biofilm			
Inhibition of initial bacterial adhesion			
EDTA and citrate	Prevention of biofilm formation and degradation of pre-existing biofilm (via Mg ²⁺ , Ca ²⁺ , and iron chelators)	Prevention of infection in a rabbit catheter model (with minocycline)	Raad et al., 2008
Aryl rhodanines	Inhibition of biofilm formation by <i>S. aureus</i> and other Gram-positive bacteria by targeting early stage of adhesion	No clinical evaluation	Opperman et al., 2009
Interaction with biofilm metabolism by QS stimulus modulation			
Furanone	Inhibition of biofilm formation and expression of <i>P. aeruginosa</i> virulence factors	Decrease of <i>P. aeruginosa</i> virulence	Kim et al., 2012; García-Contreras et al., 2013
Sodium ascorbate	Modulation of QS signal in <i>P. aeruginosa</i>	No clinical evaluation	EI-Mowafy et al., 2014

(Continued)

TABLE 1 | (Continued)

	<i>In vitro</i> effects	<i>In vivo</i> effects	References
Savarin	Inhibition of <i>S. aureus</i> biofilm formation (by targeting <i>agr</i>)	No clinical evaluation	Sully et al., 2014
Azithromycin	Inhibition of biofilm formation and expression of <i>P. aeruginosa</i> virulence factors	Improvement of clinical signs in patients with CF and <i>P. aeruginosa</i> infections	Bala et al., 2011
RNAlI inhibiting peptide	Reduction of <i>S. aureus</i> virulence	Healing improvement in a chronic wound mouse model	Giacometti et al., 2003
c-di-GMP	Reduction of biofilm formation in <i>P. aeruginosa</i> and <i>A. baumannii</i>	No clinical evaluation	Romling et al., 2013; Lieberman et al., 2014; Wu et al., 2015
Exo-polysaccharides	Reduction of biofilm formation (<i>P. aeruginosa</i>) by targeting virulence factors + PAO1 and <i>S. epidermidis</i> in co-culture	No clinical evaluation	Pihl et al., 2010; Jiang et al., 2011; Rendueles et al., 2013; Limoli et al., 2015
1,018-peptide and derivatives	Disruption of <i>P. aeruginosa</i> and <i>B. cenocepacia</i> mature biofilms	No clinical evaluation	Willcox et al., 2008; de la Fuente-Núñez et al., 2012, 2014
Deferiprone	Activity against coagulase-negative staphylococci	No clinical evaluation	Coraça-Huber et al., 2018
Enzymes enhancing bacterial dispersion			
α -amylase	Disruption of biofilm formed by <i>S. aureus</i>	No clinical evaluation	Kalpna et al., 2012
α -amylase and cellulase	Disruption of biofilm	<i>In vivo</i> disruption but the dispersal can cause systemic infection	Fleming et al., 2017
DNase, dispersin B	Eradication of single and multi-species biofilms	No clinical evaluation	Chen and Lee, 2018; Sharma and Pagedar Singh, 2018
2-aminoimidazole	Disruption of biofilms formed by <i>S. aureus</i>	No clinical evaluation	Rogers et al., 2010
Lysostaphin	Eradication of <i>P. aeruginosa</i> biofilms	Effective treatment for biofilm disruption on jugular vein catheters in mice	Kokai-Kun et al., 2009
C2DA	Dispersion of <i>S. aureus</i> , Action on MRSA biofilm	No clinical evaluation	Jennings et al., 2012
Next-generation dressings and grafts			
NGAD NGAD + mesenchymal stem cells	Removal of biofilms by <i>S. aureus</i> and antibiotic-resistant <i>P. aeruginosa</i>	Evaluation with clinical strains	Parsons et al., 2016; Pérez-Díaz et al., 2018; Tarusha et al., 2018
Electrospun nanofibers	Prevent biofilm formation and enhance fibroblast development	No clinical evaluation	Ramalingam et al., 2019
Surfactant based gel	–	Reduced bacteria development and biofilm infection	Yang et al., 2017; Percival et al., 2018
Dehydrated amniotic membranes	Faster wound healing in patients with severe comorbidities	Lower extremity wounds	Lullove, 2017
Sucrose octasulfate	–	Significant increase of wound closure rate	Edmonds et al., 2018
Skin substitutes	–	Fish skin offers natural anti-inflammatory properties and promotes growth of new skin. Other wounds and patients with burns	See clinicaltrials.gov NCT01348581
<i>Arenicola marina</i>	This new dressing delivers oxygen to the wound bed, enhancing healing and cell proliferation	No evaluation clinical	Le Pape et al., 2018
Epigel®	This new bioactive hydrogel hydrates the wound bed	No clinical evaluation	See www.epinovabiotech.com
Keratinocyte treatment, Skin grafts (epithelial or fetal cells). Stem cells. Collagen I matrix. Human placental tissues.	–	Improve closure time	Kanji and Das, 2017; Lo et al., 2019; Lintzeris et al., 2018; Mao et al., 2018; Momeni et al., 2019; Hassanshahi et al., 2019; Hwang et al., 2019; Oropallo, 2019
3D-printed scaffolds	–	Shorter healing time	Pushparaj and Ranganathan, 2017; Sun et al., 2018

EDTA, ethylene diamine tetra-acetic; EGTA, egtazic acid; MRSA, methicillin-resistant *Staphylococcus aureus*; QS, quorum sensing; CF, cystic fibrosis; C2DA, cis-2-decenoic acid; DFI, diabetic foot infection; DFU, diabetic foot ulcer; NGAD, next-generation carboxymethylcellulose silver-containing wound dressing.

empirical treatment (Kwon and Armstrong, 2018). Its duration will depend on the severity of the infection. However, Walker et al. (2015) reported that 74% of DFUs did not respond to topical and systemic agents. Recently, Johani et al. (2018) confirmed

this observation. Uçkay et al. (2018) could not demonstrate a beneficial effect of topical therapy using gentamicin-sponges in 88 DFUs. Similar conclusions were drawn for vancomycin powder, although infections were more superficial in patients

treated with vancomycin than in controls (untreated) (Wukich et al., 2015). A recent Cochrane review on this topic indicated that randomized controlled data on the effectiveness and safety of topical antimicrobial for DFI are limited (Dumville et al., 2017).

As bacteria in biofilms display 100 to 1,000-fold higher tolerance to antibiotics, new solutions to deliver antibiotics at high concentration into the biofilm have been developed. Delivery systems could be used to administer high concentrations of antibiotics to the wound with limited side effects. Biodegradable vehicles, such as calcium sulfate beads, display a good elution profile and seem to be compatible with many antibiotics. Natural polymers, such as collagen sponges, are another emerging delivery system, although data are still limited for DFU (Markakis et al., 2018). For instance, calcium sulfate beads are mineral elements that are naturally absorbed into biofilms and then slowly dissolve to release antibiotics. Price et al. (2016) showed *in vitro* that calcium sulfate beads loaded with gentamicin or tobramycin eradicated *Pseudomonas aeruginosa* biofilms in DFU, and also reduced the viability of MRSA strains. The main problem of this approach is the potential risk of bacterial resistance selection. Randomized trials are required to confirm the efficacy of these approaches.

Recently, Maiden et al. (2019) showed that the ionophore oxyclozanide can enhance aminoglycoside and tetracycline killing activity in *P. aeruginosa* biofilms by reducing the bacterial cell membrane potential and increasing antibiotic accumulation within the biofilm. Currently, this compound is mainly used in veterinary medicine for parasitic infections, but this finding suggests that in combination with aminoglycosides, oxyclozanide could represent a new antibiofilm agent for chronic wound treatment.

ALTERNATIVE APPROACHES IN THE MANAGEMENT OF DIABETIC FOOT ULCERS

In addition to conventional approaches, new alternative solutions have emerged in recent years, targeting the bacterial organization and notably the biofilm formation of DFU (Table 1).

Antimicrobial Peptides and Related Drugs

Santos et al. (2016) reported that nisin, a bacteriocin against Gram-positive bacteria, was active against some Gram-negative bacteria. Nisin promotes the disintegration of the bacterial cell membrane lipid bilayer by electrostatic interactions. Its use in DFU requires an effective delivery system. An *in vitro* study showed that guar gum-associated nisin reduced biofilm formation by 23 *S. aureus* strains isolated from DFU, including MDR strains (Thombare et al., 2016). Similarly, citropin is active against *P. aeruginosa* and *S. aureus* without major toxicity in animal models (Cirioni et al., 2006). However, Dutta and Das (2016) highlighted the limitations of antimicrobial peptides (AMPs), especially in terms of production costs, bioavailability, and difficult clinical translation.

Guanylated polymethacrylates are a new class of antimicrobial agents that structurally mimics AMPs and efficiently kills both fungi and bacteria in polymicrobial biofilms (*Candida albicans* and *S. aureus*) (Qu et al., 2016). A study on 266 patients with venous leg ulcers and DFU showed that, compared with gentaxane and iodine/dimethyl sulfoxide (DMSO), Acapsil® (Willingsford Healthcare), a powder based on a micropore particle technology, accelerated wound healing and reduced hospitalization length (Bilyayeva et al., 2017).

Nanotechnologies

Nanotechnology-based therapies open the door to new therapeutic solutions for chronic wounds (Hamdan et al., 2017). Nanoparticles made of iron, silver, zinc, or titanium showed antibacterial activity (disruption of the bacterial membrane) (Beyth et al., 2015), and due to their high bioavailability, they can penetrate into mature biofilms and target sessile bacteria. Therefore, these materials could be used to target both surface bacteria and biofilm-organized bacteria in deeper tissues. A recent study showed that the combination of silver nanoparticles and tetracycline reduced the bacterial load and promoted healing in wounds inoculated with *P. aeruginosa* in mice (Ahmadi and Adibhesami, 2017). A recent review has summarized nanotechnology-based wound healing approaches and their benefits (Mihai et al., 2018).

Antiseptics

Topical antiseptics are antimicrobial agents that inhibit or reduce the number of microorganisms. Unlike antibiotics, antiseptics have multiple targets and a broader spectrum of activity including bacteria, fungi, viruses, or protozoa. They have commonly been used on wounds to prevent or treat infection; however, antiseptic fluid irrigation have received little scientific study and their efficiency remain questioned (Lipsky et al., 2020). Indeed, wound cleansers may affect normal human cells and may be antimitotic affecting normal tissue repair. Repeated and excessive treatment of wounds with antiseptics without proper indications may have negative outcomes or promote a microenvironment similar to those found in chronic wounds. With the discovery of polymicrobial biofilms and the emergence of bacteria tolerant to antiseptics, their effectiveness is even more questionable (Sheldon, 2005; Ortega Morente et al., 2013; Stewart, 2015). Following these observations, international guidelines suggest that antiseptics are not appropriate in the management of DFU (Lipsky et al., 2020).

However, some recent studies present interesting results. Products, such as Octenilin® (Schülke & Mayr GmbH), iodine-based solutions, polyhexamethylene biguanide or silver-impregnated dressings, are good *in vitro* candidates (Kucisec-Tepes, 2016; Pavlik et al., 2019) to reduce biofilms, but their effectiveness against polymicrobial and complex biofilms remains to be demonstrated (Khan and Naqvi, 2006). Similarly, chlorhexidine action is clearly limited on multi-species biofilms (Touzel et al., 2016). Townsend et al. (2016) developed a new *in vitro* inter-kingdom wound biofilm model on hydrogel-based cellulose to test the efficacy of common topical antiseptics. They treated biofilms composed of *C. albicans*, *P. aeruginosa*, and

S. aureus with chlorhexidine or povidone iodine, and found that the structure of polymicrobial biofilms was only slightly affected compared with that of monomicrobial biofilms. They also showed that topical antiseptics were less efficient against polymicrobial biofilms.

Cadexomer iodine is a topical antimicrobial agent that could be used to deliver iodine into wounds. Iodine can penetrate the pathogen cell wall and disrupt proteins, as well as the nucleic acid structure and synthesis. Cadexomer iodine can be encapsulated within small polysaccharide beads that, in the presence of the wound exudate, start to swell and release iodine into the wound. *In vivo* studies have demonstrated that cadexomer iodine significantly reduced biofilm and microbial load in DFU (Schwartz et al., 2013; Malone et al., 2017b).

Nutraceuticals

Nutraceuticals are pharmaceutical alternatives that include all foods or food products which provide medical benefits and can be delivered under medical form. These products could present health benefits, and several plant-derived natural compounds could prove clinically beneficial.

A study has reported that cranberry extracts inhibited biofilm production of Gram-positive bacteria (LaPlante et al., 2012). Polyphenolic compounds, such as tannic acid (Orlowski et al., 2018; Chen et al., 2019 in a rats model) and tea-tree oil (Lee et al., 2014 in a clinical trial), also inhibited biofilm formation by *S. aureus*, including methicillin-resistant *S. aureus* (MRSA) (Kwieciński et al., 2009), by cleaving peptidoglycan (Payne et al., 2013). An active compound found in cinnamon oil has also been shown to prevent MRSA biofilm formation *in vitro* (Cui et al., 2016), and also in a mice model of wound infection (Seyed Ahmadi et al., 2019). Finally, ellagic acid derivatives also limited *S. aureus* biofilm formation and enhanced its susceptibility to some antibiotics (Quave et al., 2012). All these compounds must be clinically evaluated in chronic wounds.

The natural anti-inflammatory and antimicrobial properties of propolis produced by honeybees are well known. Its regenerative properties and low cost explain the increased interest in propolis for promoting chronic wound healing (Henshaw et al., 2014; Martinotti and Ranzato, 2015). To our knowledge, propolis alone has not been used in DFU, but a recent review summarized the effect of propolis with a combination of several antibiotics in skin problems including wounds (McLoone et al., 2020).

Honey has been used for a long time to treat wounds with no real proof of its efficiency. A study demonstrated that in animals, honey has a clear antibacterial effect, but no anti-inflammatory activity (Jull et al., 2015). Recently, Minden-Birkenmaier and Bowlin (2018) reviewed the effects of different types of honey on wound closure and antibiofilm activity. They also discussed the advantages of honey in the field of tissue engineering and biomaterials (Cryogels, Electrospun templates, and Hydrogels).

Within a biofilm, intra- and inter-species interactions and cooperation can be observed at the different stages of its formation. Another approach could be to harness the bacterial competition to modify the dispersion or modification of the growing matrix. Probiotic bacteria, such as Lactobacilli, could have antibiofilm activities and be good candidates for

wound treatment (Vuotto et al., 2014; Vågesjö et al., 2018 in *in vivo* model).

Phage Therapy

There is renewed interest in bacteriophages to fight bacteria. In this treatment, viruses infect a specific bacterium and reproduce inside it. Several areas must be investigated to evaluate the potential of bacteriophages in the therapeutic arsenal (Knezevic et al., 2021). Indeed, the success of phage therapy is highly dependent on the efficiency and safety of phage preparations, which raises manufacturing and formulation challenges. The production of phages must comply with the strict regulations that are usually applied for pharmaceutical products to ensure the high-quality standards appropriate for their intended. This needs a production with a controlled and reproducible process. One of the requirements is to avoid phages encoding for lysogeny, virulence factors or antibiotic resistance. The presence of impurities such as endotoxins in phage preparations should also be avoided or be below a threshold. The presence/absence of neutralizing antibodies binding against phages must be known. The development of “phagogram” (in parallel to antibiogram) could be also an important way for the routine use of phage therapy. However, this could represent another approach for the treatment of infected wounds with minimal effects on the host microbiome (Hill et al., 2018; Morozova et al., 2018). Mendes et al. (2014) tested an *in vitro* cocktail of bacteriophages targeting *S. aureus*, *P. aeruginosa*, and *Acinetobacter baumannii* on both planktonic cells and biofilm-associated cells, and found that it reduced biofilm formation and infection. Other case reports have described encouraging results in patients with diabetic foot and chronic wounds (Fish et al., 2018; Taha et al., 2018).

To date, one of the main limitations is that the evaluation of phage efficiency has been performed using mainly *in vitro* studies and a single species in a biofilm. However, biofilms in DFU are multi-species, impacting the spatial organization and the interaction with phages. The specific outcome of phage infection in a multi-species biofilm seems to strongly depend on the bacterial species composing the biofilm (e.g., whether they establish synergist or antagonist interactions). The complexity of phage-biofilm interactions is increased by evidence of biofilm formation induced by exposure to certain phages (Lacqua et al., 2006; Tan et al., 2015; Henriksen et al., 2019). Overall, even if the potential of phages to control the complex biofilm observed in DFU is proved, the complexity and diversity of phage-biofilm interactions could limit broad conclusions and need more research to claim that phage therapy becomes a real solution in the DFU situation.

Therapeutic Solutions on Wound Healing

Photodynamic therapy could be an interesting approach to aid wound healing. In this therapeutic procedure, pathogen cell death is induced upon exposure to light to generate oxygen species by activation of a photosensitizing agent. This agent is non-toxic in the dark, but after illumination, it becomes a very efficient antimicrobial agent. This method is used mainly in oncology, but it could also be employed to manage chronic wounds notably by its ability to prevent amputation in diabetic patients with

DFU. Indeed, a clinical study showed that all non-treated patients ($n = 16$) underwent amputation, compared to only one patient in the group that received photodynamic therapy ($n = 18$) (Tardivo et al., 2014).

Another technology uses non-thermal plasma. Here, plasma is a partially ionized medium composed of many elements, such as charged particles (electrons and ions), neutral and excited atoms, UV photons and radicals. A recent study in rats showed that this technology could be used on pressure ulcers to accelerate wound healing (Chatraie et al., 2018). Additional investigations are needed to determine its value in humans, but recent results using an *in vivo* mouse model of type 2 diabetes showed promotion of bacterial killing of *P. aeruginosa* and wound disinfection without metabolic complication (Cooley et al., 2020).

Application of electrical stimulation has also been investigated in wound repair and regeneration. Wireless electroceutical dressings were recently tested in a porcine chronic wound polymicrobial biofilm infection model with *P. aeruginosa* (PAO1) and *A. baumannii* (19606) (Barki et al., 2019). The data suggested that the dressing disrupted wound biofilm aggregates and accelerated wound closure by restoring skin barrier function. The dressing changed expression of *P. aeruginosa* quorum sensing *mvfR* (*pqsR*), *rhlR*, and *lasR* genes and silencing of E-cadherin (a protein required for skin barrier function). Finally, this study highlighted the rescue effect against biofilm-induced persistent inflammation by decreased cytokines production.

Finally, hyperbaric oxygen therapy had been used for several years in the management of DFU. It consists in inhalation of pure oxygen after entering a special compression chamber. The treatment aims to increase the oxygen supply to the wound. However, the value of this therapy is controversial and its effect seems more due to the foot discharge than the oxygen itself. In a Cochrane review, the authors concluded that the therapy improved short-term but not long-term healing in patients with DFUs (Kranke et al., 2015).

Alternatives in the Inhibition of Bacterial Adhesion and Biofilm

Inhibition of Initial Bacterial Adhesion

Bacterial growth requires the presence of metals (particularly, calcium, iron, and magnesium). Ionic chelators could be used to limit bacterial growth and initial adhesion. Ethylene diamine tetra-acetic (EDTA) and citrate are the most promising compounds of this class (Raad et al., 2008). However, the efficiency of these chelators is dependent on the bacterial strains. For instance, Abraham et al. (2012) observed that the anti-biofilm effect varied among *S. aureus* isolates. Aryl rhodanines also can inhibit the early stages of biofilm development by preventing the attachment on the surface of *S. aureus* and other Gram-positive bacteria, but not of Gram-negative bacteria (Opperman et al., 2009).

Inhibiting Biofilm Metabolism

Quorum Sensing (QS) is important for the transition from antimicrobial-sensitive planktonic cells to antimicrobial-resistant cell aggregates in a biofilm. In the absence of QS signal, biofilm formation is inhibited. Many researchers have evaluated

compounds to modulate QS, such as furanone that inhibited, among others, *P. aeruginosa* biofilms (Kim et al., 2012), sodium ascorbate that modulated the QS signal in *P. aeruginosa* (El-Mowafy et al., 2014), savarin (a *S. aureus* virulence inhibitor) (Sully et al., 2014), and azithromycin in *P. aeruginosa* (Bala et al., 2011). Moreover, RNA III inhibiting peptide reduced *S. aureus* and *Staphylococcus epidermidis* virulence and improved healing in rats (Giacometti et al., 2003). These approaches are efficient only on a restricted number of bacterial species, and due to their potential toxicity, they have a limited use. Moreover, it has been reported that some bacteria isolated from clinical samples have become resistant to some QS modulators (García-Contreras et al., 2013), suggesting the emergence of multi-QS inhibitor resistant bacteria (Koul et al., 2016).

Another approach uses the cyclic diguanylate inhibition. Cyclic diguanylate (c-di-GMP) is a second messenger that controls many cellular functions, including biofilm formation. Various stress factors, such as starvation, reduced c-di-GMP level, leading to biofilm dispersal (Romling et al., 2013). This study also found that dispersed cells were more virulent compared with the first planktonic cells that induced the biofilm and with biofilm sessile cells. Moreover, small molecules, such as LP 3134, LP 3145, LP 4010, and LP 1062, inhibited a key enzyme that mediated c-di-GMP synthesis and consequently also biofilm formation in *P. aeruginosa* and *A. baumannii* (Wu et al., 2015). Unfortunately, these molecules seem to be toxic to eukaryotic cells. Finally, ebselen inhibited c-di-GMP and displayed good results on *P. aeruginosa* biofilms (Lieberman et al., 2014).

The biofilm matrix mainly contains proteins, extracellular DNA and polysaccharides. Polysaccharides are important for the early stage of biofilm formation and can protect cells during biofilm maturation. They also provide the basal biofilm structure that allows the bacterial community stratification. A recent study demonstrated that the exo-polysaccharide EPS273, obtained from a marine bacterium, reduced biofilm formation in *P. aeruginosa* by targeting virulence factors (Jiang et al., 2011). Other antibiofilm polysaccharides have been discovered, for instance Psl and Pel from *P. aeruginosa* PAO1 that decreased *S. epidermidis* biofilm formation in a co-culture biofilm *in vivo* model (Pihl et al., 2010). Other non-bacterial polysaccharides from animals, plants and algae have also shown antibiofilm activity (Rendueles et al., 2013).

In stress conditions, bacteria synthesize alarmones (guanosine tetraphosphate and guanosine pentaphosphate) called (p)ppGpp (Willcox et al., 2008). The antibiofilm peptide 1,018 inhibited their accumulation upon nutritional stress and prevented biofilm formation. Moreover, at low concentration, it eradicated biofilm-associated bacteria and disrupted mature biofilms. This peptide and its derivatives HE4 and HE10 were similarly effective against *P. aeruginosa* and *Burkholderia cenocepacia* biofilms (de la Fuente-Núñez et al., 2014). In addition, peptide 1,037 reduced biofilms formed by other bacteria (the Gram-negative pathogens *P. aeruginosa* and *B. cenocepacia*, and the Gram-positive *Listeria monocytogenes*) (de la Fuente-Núñez et al., 2012).

Finally, a recent study showed that the iron chelator deferiprone (DFP) affected bacterial biofilm formation and had synergistic effects (antibacterial activity) with some antibiotic

compounds against coagulase-negative staphylococci. The potential of DFP is clearly based on its potentiation of the antibiotics action, leading to a significant biofilm reduction (Coraça-Huber et al., 2018).

Promoting Bacterial Dispersion

One promising therapeutic approach consists in targeting the EPS matrix with dispersing agents in combination with antibiotics. For instance, the α -amylase (Kalpana et al., 2012; Fleming et al., 2017) enzyme, which is produced by marine bacteria, can disrupt polysaccharide bonds. It is now used as a dispersing agent to target the polysaccharide bonds of the EPS matrix, leading to biofilm degradation *in vitro*. Other enzymes (deoxyribonuclease I, the hydrolases dispersin B and DNase) also showed EPS matrix-degrading properties (Fleming et al., 2017; Chen and Lee, 2018; Sharma and Pagedar Singh, 2018).

Some synthetic agents have been developed, such as 2-aminoimidazole for *S. aureus* biofilms (Rogers et al., 2010) and synthetic lysostaphin, an effective treatment for established biofilm infections on implanted jugular vein catheters in mice (Kokai-Kun et al., 2009).

In addition, the enzymes proteinase K and trypsin can eradicate biofilms from a variety of staphylococcal strains on inert surfaces. However, their efficacy for the elimination of established biofilms is not well known *in vivo*, thus limiting their therapeutic potential. Moreover, this strategy might lead to the release of bacteria from the biofilm into the blood circulation that could induce a strong inflammatory response or a systemic acute infection.

Cis-2-Decenoic acid (C2DA) is a fatty acid chemical messenger produced by *P. aeruginosa* that induces the dispersion of biofilms with *S. aureus* and other Gram-positive and Gram-negative bacteria (Davies and Marques, 2009). C2DA controls the initiation of biofilm formation and the dispersion of mature biofilms. C2DA can inhibit MRSA biofilm formation/growth, but cannot eradicate them (Jennings et al., 2012).

New Generation of Dressing and Grafts

Parsons et al. (2016) developed a next-generation antibiofilm carboxymethylcellulose silver-containing wound dressing (NGAD). This hydrofiber dressing was designed to disperse the wound biofilm and to enhance ionic silver antimicrobial action. The authors showed that NGAD was more efficient (biofilm disruption and removal) than other commercial dressings in a large panel of clinical isolates, including *S. aureus* and antibiotic-resistant *P. aeruginosa*. Another *in vitro* study conducted on a novel wound-dressing material based on a matrix of the polysaccharides alginate, hyaluronic acid and Chitlac-silver nanoparticles concluded that hyaluronic acid was able to stimulate the wound healing simultaneously to the silver particles allowing efficient antibacterial activity against biofilms (Tarusha et al., 2018). Pérez-Díaz et al. (2018) combined these nanoparticles with mesenchymal stem cells (MSC) that can improve wound healing due to their ability to differentiate and release growth factors. In addition to the MSC and nanoparticles, they used radiosterilized pig skin as a matrix to deliver MSC into wound beds. *In vitro* data suggested a decrease of bacterial

growth and biofilm formation. Finally, Ramalingam et al. (2019) conducted a study presenting the utility of electrospun nanofiber containing a natural extract (*Gymnema sylvestris*) that prevented biofilm formation, inhibited both Gram-positive and Gram-negative bacteria, and enhanced human dermal fibroblasts development in an *in vitro* model.

A surfactant-based wound gel dressing described in a porcine skin explant infected with *P. aeruginosa* (PAO1) biofilm showed encouraging results. Dressing the wound with this gel reduced bacteria development and biofilm infection (Yang et al., 2017). More recently, Percival et al. (2018) highlighted the effects of a non-ionic surfactant, the Pluronic F127 used in combination with melatonin and chitosan in a wound dressing. The microspheres of Pluronic F127 enhanced chitosan properties allowing antimicrobial and antibiofilm activity against *S. aureus* (Percival et al., 2018).

A dehydrated amniotic membrane allograft was used in 22 patients with lower extremity wounds (Lullove, 2017). At week 12 after application of the human amniotic membrane, DFU were completely healed.

A randomized double-blind clinical trial showed that sucrose octasulfate significantly improves wound closure in neuroischemic DFU after 20 weeks of treatment (Edmonds et al., 2018).

Skin substitutes could be another therapeutic solution in wound healing. The Food and Drug Administration recently approved a treatment for wound care involving fish skin after a clinical trial to determine its effectiveness on burns and different wound types. Fish skin contains omega-3 fatty acids that have natural anti-inflammatory properties and can accelerate healing. An ongoing clinical trial is evaluating an extracellular matrix that binds to the cells around the wound and promotes the growth of new skin (see clinicaltrials.gov/NCT01348581).

Arenicola marina is a technology based on the finding that lack of oxygen in chronic wounds hampers healing and cell proliferation (Le Pape et al., 2018). HEMHealing® (Hemarine) provides oxygenation to the wound by including M101 hemoglobin in the dressing matrix. M101 hemoglobin is an oxygen carrier that belongs to the extra-cellular hemoglobin family and is found in the *Arenicola marina* marine worm. This hemoglobin can naturally fix oxygen from the external environment and then gradually release it in the hypoxic medium to restart the healing process. In a wound context, it could restart cell proliferation and decrease wound budding.

Skin works as an extracellular matrix that binds to the cells around the wound and promotes the growth of new skin. Epigel® (Epinova Biotech) is an innovative patch based on a highly hydrophilic, biocompatible and bioactive hydrogel scaffold that supports wound bed hydration, thus reducing healing time. Clinical trials must be done to evaluate the value of Epigel® as wound dressing.

Hwang et al. (2019) evaluated allogeneic keratinocyte grafts (weekly grafts for up to 12 weeks) in 71 patients with intractable DFUs. They reported wound healing in 78.8% of patients: 64.7% with complete healing within an average of 6.1 weeks, and 14.1% with partial healing and an average 35.5% reduction of the initial size at the end of the follow up. This treatment seems effective for

chronic and difficult-to-treat DFUs. In line with other studies [in fetal cells (Momeni et al., 2019) or epithelial cells (Lo et al., 2019)] in other wound types, this study showed the benefit of skin grafts that could represent the future management of chronic wounds. Indeed, progenitor stem cells present in these grafts can accelerate wound repair and tissue regeneration, and consequently decrease the risk of wound infection. A significant number of stem cell therapies for cutaneous wounds are currently under development (Kanji and Das, 2017).

Chronic wounds are inflammatory processes that result in the increase of proteolytic enzymes and degradation of the extracellular matrix. Two studies investigated the impact of providing a biocompatible scaffold to support the healing. They used a purified Type I collagen matrix containing polyhexamethylene biguanide on patients ($n = 8$ and $n = 41$) suffering from DFU. Their results suggested that the collagen matrix improved both wound closure and the wound bed condition (Lintzeris et al., 2018; Oropallo, 2019). Finally, a study investigated the effect of human placental tissues against *P. aeruginosa* and *S. aureus* biofilm (Mao et al., 2018). It highlighted the fact that both human cryopreserved viable amniotic membrane and cryopreserved viable umbilical tissue had antibacterial activity against multiple bacterial pathogens and demonstrated that these tissues released factors that inhibited biofilm formation of *P. aeruginosa* and *S. aureus* in an *ex vivo* porcine model. Recently, use of adipose-derived stem cell improved wound healing by promoting angiogenesis and/or vascularization, modulating immune response, and inducing epithelialization in the wound (Hassanshahi et al., 2019).

The effectiveness of 3D-printed scaffolds in chronic wounds has not yet been proven, but this seems to be a promising strategy. Sun et al. (2018) reported that 3D-printed scaffold membrane alone ($n = 1$ patient), and 3D-printed scaffold powder mixed with platelet-rich fibrinogen ($n = 2$) reduced healing time in patients with pressure ulcer and/or DFU (Sun et al., 2018). Another group developed a 3D-printed scaffold that included a drug delivery system based on the body temperature (Pushparaj and Ranganathan, 2017). Although this device has not been tested *in vivo* yet, it is the first step toward the use of 3D-printed

scaffolds that incorporate the delivery of drugs (antibiotics or antibiofilm molecules) to shorten healing time and decrease the risks of infection and complication.

CONCLUSION

The severity of DFU and the difficulty in treating it has prompted researchers to take a closer look at these infections and the associated issues. Biofilms play a crucial role in DFUs and contribute to delay healing. Research now must take into account the biofilm bacterial organization in these chronic wounds in order to identify novel alternative therapeutic candidates to improve DFU management. As we described above, alternative strategies such as bacteriophages, probiotics, AMPs or antibiofilms are exciting strategies and show promising results. All these compounds could provide solutions against MDR bacteria. However, additional studies are required to understand the biofilm bacterial organization in DFU, and also the mechanisms behind each of the candidates to improve the wound healing management and thus offer new therapeutic solution for the management of DFU.

AUTHOR CONTRIBUTIONS

CP, PL, J-PL, and AS wrote the manuscript. CD-R, AP, AB-D, and SS critically reviewed the manuscript. All authors contributed to the article and approved the submitted version.

ACKNOWLEDGMENTS

AP, CD-R, AS, PL, and J-PL belong to the FHU INCh (Federation Hospitalo Universitaire Infections Chroniques, Aviesan). We thank the Nîmes University Hospital for its structural, human and financial support through the award obtained by our team during the internal call for tenders “Thématiques phares”. We thank Sarah Kabani for her editing assistance.

REFERENCES

- Abraham, N. M., Lamlerthton, S., Fowler, V. G., and Jefferson, K. K. (2012). Chelating agents exert distinct effects on biofilm formation in *Staphylococcus aureus* depending on strain background: role for clumping factor B. *J. Med. Microbiol.* 61, 1062–1070. doi: 10.1099/jmm.0.040758-0
- Ahmadi, M., and Adibhesami, M. (2017). The effect of silver nanoparticles on wounds contaminated with *Pseudomonas aeruginosa* in mice: an experimental study. *Iran. J. Pharm. Res.* 16, 661–669.
- Albac, S., Medina, M., Labrousse, D., Hayez, D., Bonnot, D., Anzala, N., et al. (2020). Efficacy of bacteriophages in a *Staphylococcus aureus* nondiabetic or diabetic foot infection murine model. *Antimicrob. Agents Chemother.* 64, e01870–19. doi: 10.1128/AAC.01870-19
- Apelqvist, J., Willy, C., Fagerdahl, A. M., Fracalvieri, M., Malmsjö, M., Piagesi, A., et al. (2017). Negative pressure wound therapy - overview, challenges and perspectives. *J. Wound Care.* 26:3. doi: 10.12968/jowc.2017.26.Sup3.S1
- Armstrong, D. G., Boulton, A. J. M., and Bus, S. A. (2017). Diabetic Foot Ulcers and Their Recurrence. *N. Engl. J. Med.* 376, 2367–2375. doi: 10.1056/NEJMra1615439
- Bakker, K., Apelqvist, J., Lipsky, B. A., Van Netten, J. J., and International Working Group on the Diabetic Foot. (2016). The 2015 IWGDF guidance documents on prevention and management of foot problems in diabetes: development of an evidence-based global consensus. *Diabetes Metab. Res. Rev.* 32, 2–6. doi: 10.1002/dmrr.2694
- Bala, A., Kumar, R., and Harjai, K. (2011). Inhibition of quorum sensing in *Pseudomonas aeruginosa* by azithromycin and its effectiveness in urinary tract infections. *J. Med. Microbiol.* 60, 300–306. doi: 10.1099/jmm.0.025387-0
- Barki, K. G., Das, A., Dixith, S., Ghatak, P. D., Mathew-Steiner, S., Schwab, E., et al. (2019). Electric Field Based Dressing Disrupts Mixed-Species Bacterial Biofilm Infection and Restores Functional Wound Healing. *Ann. Surg.* 269, 756–766. doi: 10.1097/SLA.0000000000002504
- Beyth, N., Hourri-Haddad, Y., Domb, A., Khan, W., and Hazan, R. (2015). Alternative antimicrobial approach: nano-antimicrobial materials. *Evid. Based Complement. Alternat. Med.* 2015:246012. doi: 10.1155/2015/246012
- Bilyayeva, O. O., Neshita, V. V., Golub, A. A., and Sams-Dodd, F. (2017). Comparative clinical study of the wound healing effects of a novel micropore particle technology: effects on wounds, venous leg ulcers, and diabetic foot ulcers. *Wounds* 29, 1–9.

- Bjarnsholt, T. (2013). The role of bacterial biofilms in chronic infections. *APMIS* 136, 1–51. doi: 10.1111/apm.12099
- Cahn, A., Elishuv, O., and Olshtain-Pops, K. (2014). Establishing a multidisciplinary diabetic foot team in a large tertiary hospital: a workshop. *Diabetes Metab. Res. Rev.* 30, 350–353. doi: 10.1002/dmrr.2527
- Caravaggi, C., Sganzeroli, A., Galenda, P., Bassetti, M., Ferraresi, R., and Gabrielli, L. (2013). The management of the infected diabetic foot. *Curr. Diabetes Rev.* 9, 7–24.
- Chatraie, M., Torkaman, G., Khani, M., Salehi, H., and Shokri, B. (2018). In vivo study of non-invasive effects of non-thermal plasma in pressure ulcer treatment. *Sci. Rep.* 8:5621. doi: 10.1038/s41598-018-24049-z
- Chen, K. J., and Lee, C. K. (2018). Twofold enhanced dispersin B activity by N-terminal fusion to silver-binding peptide for biofilm eradication. *Int. J. Biol. Macromol.* 118, 419–426. doi: 10.1016/j.ijbiomac.2018.06.066
- Chen, Y., Tian, L., Yang, F., Tong, W., Jia, R., Zou, Y., et al. (2019). Tannic Acid Accelerates Cutaneous Wound Healing in Rats Via Activation of the ERK 1/2 Signaling Pathways. *Adv Wound Care* 8, 341–354. doi: 10.1089/wound.2018.0853
- Cirioni, O., Giacometti, A., Ghiselli, R., Kamysz, W., Orlando, F., Mocchegiani, F., et al. (2006). Citropin 1.1-treated central venous catheters improve the efficacy of hydrophobic antibiotics in the treatment of experimental staphylococcal catheter-related infection. *Peptides* 27, 1210–1216. doi: 10.1016/j.peptides.2005.10.007
- Cooley, C. R., McLain, J. M., Dupuy, S. D., Eder, A. E., Wintenberg, M., Kelly-Wintenberg, K., et al. (2020). Indirect, Non-Thermal Atmospheric Plasma Promotes Bacterial Killing in vitro and Wound Disinfection in vivo Using Monogenic and Polygenic Models of Type 2 Diabetes (Without Adverse Metabolic Complications). *Shock* 54, 681–687. doi: 10.1097/SHK.0000000000001583
- Coraçá-Huber, D. C., Dichtl, S., Steixner, S., Nogler, M., and Weiss, G. (2018). Iron chelation destabilizes bacterial biofilms and potentiates the antimicrobial activity of antibiotics against coagulase-negative Staphylococci. *Pathog. Dis.* 76. doi: 10.1093/femspd/fty052
- Cui, H., Li, W., Li, C., Vittayapadung, S., and Lin, L. (2016). Liposome containing cinnamon oil with antibacterial activity against methicillin-resistant *Staphylococcus aureus* biofilm. *Biofouling* 32, 215–225. doi: 10.1080/08927014.2015.1134516
- Davies, D. G., and Marques, C. N. (2009). A fatty acid messenger is responsible for inducing dispersion in microbial biofilms. *J. Bacteriol.* 191, 1393–1403. doi: 10.1128/JB.01214-08
- de la Fuente-Núñez, C., Korolik, V., Bains, M., Nguyen, U., Breidenstein, E. B. M., Horsman, S., et al. (2012). Inhibition of bacterial biofilm formation and swarming motility by a small synthetic cationic peptide. *Antimicrob. Agents Chemother.* 56, 2696–2704. doi: 10.1128/AAC.00064-12
- de la Fuente-Núñez, C., Mansour, S., Wang, Z., Jiang, L., Breidenstein, E. B. M., Elliott, M., et al. (2014). Anti-biofilm and immunomodulatory activities of peptides that inhibit biofilms formed by pathogens isolated from cystic fibrosis patients. *Antibiotics* 3, 509–526. doi: 10.3390/antibiotics3040509
- Donlan, R. M., and Costerton, J. W. (2002). Biofilms: survival mechanisms of clinically relevant microorganisms. *Clin. Microbiol. Rev.* 15, 167–193. doi: 10.1128/cmr.15.2.167-193.2002
- Dowd, S. E., Wolcott, R. D., Sun, Y., McKeenan, T., Smith, E., and Rhoads, D. (2008). Polymicrobial nature of chronic diabetic foot ulcer biofilm infections determined using bacterial tag encoded FLX amplicon pyrosequencing (bTEFAP). *PLoS One* 3:e3326. doi: 10.1371/journal.pone.0003326
- Dumville, J. C., Lipsky, B. A., Hoey, C., Cruciani, M., Fison, M., and Xia, J. (2017). Topical antimicrobial agents for treating foot ulcers in people with diabetes. *Cochrane Database Syst. Rev.* 6:CD011038. doi: 10.1002/14651858.CD011038.pub2
- Dutta, P., and Das, S. (2016). Mammalian antimicrobial peptides: promising therapeutic targets against infection and chronic inflammation. *Curr. Top. Med. Chem.* 16, 99–129. doi: 10.2174/1568026615666150703121819
- Edmonds, M., Lázaro-Martínez, J. L., Alfayate-García, J. M., Martini, J., Petit, J. M., Rayman, G., et al. (2018). Sucrose octasulfate dressing versus control dressing in patients with neuroischaemic diabetic foot ulcers (Explorer): an international, multicentre, double-blind, randomised, controlled trial. *Lancet Diabetes Endocrinol.* 6, 186–196. doi: 10.1016/S2213-8587(17)30438-2
- El-Mowafy, S. A., Shaaban, M. I., and Abd El Galil, K. H. (2014). Sodium ascorbate as a quorum sensing inhibitor of *Pseudomonas aeruginosa*. *J. Appl. Microbiol.* 117, 1388–1399. doi: 10.1111/jam.12631
- Fish, R., Kutter, E., Bryan, D., Wheat, G., and Kuhl, S. (2018). Resolving digital staphylococcal osteomyelitis using bacteriophage—A case report. *Antibiotics* 7:87. doi: 10.3390/antibiotics7040087
- Fleming, D., Chahin, L., and Rumbaugh, K. (2017). Glycoside hydrolases degrade polymicrobial bacterial biofilms in wounds. *Antimicrob. Agents Chemother.* 61, e01998–16. doi: 10.1128/AAC.01998-16
- García-Contreras, R., Martínez-Vázquez, M., Velázquez Guadarrama, N., Villegas Pañeda, A. G., Hashimoto, T., Maeda, T., et al. (2013). Resistance to the quorum-quenching compounds brominated furanone C-30 and 5-fluorouracil in *Pseudomonas aeruginosa* clinical isolates. *Pathog. Dis.* 68, 8–11. doi: 10.1111/2049-632X.12039
- Giacometti, A., Cirioni, O., Gov, Y., Ghiselli, R., Del Prete, M. S., Mocchegiani, F., et al. (2003). RNA III inhibiting peptide inhibits in vivo biofilm formation by drug-resistant *Staphylococcus aureus*. *Antimicrob. Agents Chemother.* 47, 1979–1983. doi: 10.1128/AAC.47.6.1979-1983.2003
- Hamdan, S., Pastar, I., Drakulich, S., Dikici, E., Tomic-Canic, M., Deo, S., et al. (2017). Nanotechnology-driven therapeutic interventions in wound healing: potential uses and applications. *ACS Cent. Sci.* 3, 163–175. doi: 10.1021/acscentsci.6b00371
- Hassanshahi, A., Hassanshahi, M., Khabbazi, S., Hosseini-Khah, Z., Peymanfar, Y., Ghalamkari, S., et al. (2019). Adipose-derived stem cells for wound healing. *J. Cell Physiol.* 234, 7903–7914. doi: 10.1002/jcp.27922
- Henriksen, K., Rørbo, N., Rybtke, M. L., Martinet, M. G., Tolker-Nielsen, T., Høiby, N., et al. (2019). *P. aeruginosa* flow-cell biofilms are enhanced by repeated phage treatments but can be eradicated by phage-ciprofloxacin combination. *Pathog. Dis.* 77:ftz011. doi: 10.1093/femspd/ftz011
- Henshaw, F. R., Bolton, T., Nube, V., Hood, A., Veidhoen, D., Pfrunder, L., et al. (2014). Topical application of the bee hive protectant propolis is well tolerated and improves human diabetic foot ulcer healing in a prospective feasibility study. *J. Diabetes Complications* 28, 850–857. doi: 10.1016/j.jdiacomp.2014.07.012
- Hill, C., Mills, S., and Ross, R. P. (2018). Phages & antibiotic resistance: are the most abundant entities on earth ready for a comeback? *Future Microbiol.* 13, 711–726. doi: 10.2217/fmb-2017-0261
- Hwang, Y. G., Lee, J. W., Park, K. H., and Han, S. H. (2019). Allogeneic keratinocyte for intractable chronic diabetic foot ulcers: a prospective observational study. *Int. Wound J.* 16, 486–491. doi: 10.1111/iwj.13061
- James, G. A., Swogger, E., Wolcott, R., Pulcini, Secor, P., Sestrich, J., et al. (eds) (2008). Biofilms in chronic wounds. *Wound Repair. Regen.* 16, 37–44. doi: 10.1111/j.1524-475X.2007.00321.x
- Jennings, J. A., Courtney, H. S., and Haggard, W. O. (2012). Cis-2-decenoic acid inhibits *S. aureus* growth and biofilm in vitro: a pilot study. *Clin. Orthop. Relat. Res.* 470, 2663–2670. doi: 10.1007/s11999-012-2388-2
- Jiang, P., Li, J., Han, F., Duan, G., Lu, X., Gu, Y., et al. (2011). Antibiofilm activity of an exopolysaccharide from marine bacterium *Vibrio* sp. QY101. *PLoS One* 6:e18514. doi: 10.1371/journal.pone.0018514
- Johani, K., Malone, M., Jensen, S. O., Dickson, H. G., Gosbell, I. B., Hu, H., et al. (2018). Evaluation of short exposure times of antimicrobial wound solutions against microbial biofilms: from in vitro to in vivo. *J. Antimicrob. Chemother.* 73, 494–502. doi: 10.1093/jac/dkx391
- Jull, A. B., Cullum, N., Dumville, J. C., Westby, M. J., Deshpande, S., and Walker, N. (2015). Honey as a topical treatment for wounds. *Cochrane Database Syst. Rev.* 3:CD005083. doi: 10.1002/14651858.CD005083.pub4
- Kalpana, B. J., Aarthy, S., and Pandian, S. K. (2012). Antibiofilm activity of α -amylase from *Bacillus subtilis* S8-18 against biofilm forming human bacterial pathogens. *Appl. Biochem. Biotechnol.* 167, 1778–1794. doi: 10.1007/s12010-011-9526-2
- Kanji, S., and Das, H. (2017). Advances of stem cell therapeutics in cutaneous wound healing and regeneration. *Mediators Inflamm.* 2017:5217967. doi: 10.1155/2017/5217967
- Khan, M. N., and Naqvi, A. H. (2006). Antiseptics, iodine, povidone iodine and traumatic wound cleansing. *J. Tissue Viability* 16, 6–10. doi: 10.1016/s0965-206x(06)64002-3
- Kifelew, L. G., Warner, M. S., Morales, S., Vaughan, L., Woodman, R., Fitridge, R., et al. (2020). Efficacy of phage cocktail AB-SA01 therapy in diabetic mouse

- wound infections caused by multidrug-resistant *Staphylococcus aureus*. *BMC Microbiol.* 20:204. doi: 10.1186/s12866-020-01891-8
- Kim, S. G., Yoon, Y. H., Choi, J. W., Rha, K. S., and Park, Y. H. (2012). Effect of furanone on experimentally induced *Pseudomonas aeruginosa* biofilm formation: in vitro study. *Int. J. Pediatr. Otorhinolaryngol.* 76, 1575–1578. doi: 10.1016/j.ijporl.2012.07.015
- Knezevic, P., Hoyle, N. S., Matsuzaki, S., and Gorski, A. (2021). Advances in phage therapy: present challenges and future perspectives. *Front. Microbiol.* 12:701898. doi: 10.3389/fmicb.2021.701898
- Kokai-Kun, J. F., Chanturiya, T., and Mond, J. J. (2009). Lysostaphin eradicates established *Staphylococcus aureus* biofilms in jugular vein catheterized mice. *J. Antimicrob. Chemother.* 64, 94–100. doi: 10.1093/jac/dkp145
- Koul, S., Prakash, J., Mishra, A., and Kalia, V. C. (2016). Potential Emergence of Multi-quorum Sensing Inhibitor Resistant (MQSIR) Bacteria. *Indian J. Microbiol.* 56, 1–18. doi: 10.1007/s12088-015-0558-0
- Kranke, P., Bennett, M. H., Martyn-St James, M., Schnabel, A., Debus, S. E., and Weibel, S. (2015). Hyperbaric oxygen therapy for chronic wounds. *Cochrane Database Syst. Rev.* 2015:CD004123. doi: 10.1002/14651858.CD004123.pub4
- Kucisec-Tepes, N. (2016). [The role of antiseptics and strategy of biofilm removal in chronic wound]. *Acta Med. Croat.* 70, 33–42.
- Kwieciński, J., Eick, S., and Wójcik, K. (2009). Effects of tea tree (*Melaleuca alternifolia*) oil on *Staphylococcus aureus* in biofilms and stationary growth phase. *Int. J. Antimicrob. Agents* 33, 343–347. doi: 10.1016/j.ijantimicag.2008.08.028
- Kwon, K. T., and Armstrong, D. G. (2018). Microbiology and Antimicrobial Therapy for Diabetic Foot Infections. *Infect. Chemother.* 50, 11–20. doi: 10.3947/ic.2018.50.1.11
- Lacqua, A., Wanner, O., Colangelo, T., Martinotti, M. G., and Landini, P. (2006). Emergence of biofilm-forming subpopulations upon exposure of *Escherichia coli* to environmental bacteriophages. *Appl. Environ. Microbiol.* 72, 956–959. doi: 10.1128/AEM.72.1.956-959.2006
- LaPlante, K. L., Sarkisian, S. A., Woodmansee, S., Rowley, D. C., and Seeram, N. P. (2012). Effects of cranberry extracts on growth and biofilm production of *Escherichia coli* and *Staphylococcus* species. *Phyther. Res.* 26, 1371–1374. doi: 10.1002/ptr.4592
- Le Pape, F., Richard, G., Porchet, E., Sourice, S., Dubrana, F., Férec, C., et al. (2018). Adhesion, proliferation and osteogenic differentiation of human MSCs cultured under perfusion with a marine oxygen carrier on an allogenic bone substitute. *Artif. Cells Nanomed. Biotechnol.* 46, 95–107. doi: 10.1080/21691401.2017.1365724
- Lee, R. L. P., Leung, P. H. M., and Wong, T. K. S. (2014). A randomized controlled trial of topical tea tree preparation for MRSA colonized wounds. *Int. J. Nursing Sci.* 1, 7–14. doi: 10.1016/j.ijnss.2014.01.001
- Lieberman, O. J., Orr, M. W., Wang, Y., and Lee, V. T. (2014). High-Throughput screening using the differential radial capillary action of ligand assay identifies Ebselen as an inhibitor of diguanylate cyclases. *ACS Chem. Biol.* 9, 183–192. doi: 10.1021/cb400485k
- Limoli, D. H., Jones, C. J., and Wozniak, D. J. (2015). Bacterial extracellular polysaccharides in biofilm formation and function. *Microbiol. Spectr.* 3, 10.1128/microbiolspec.MB-0011-2014. doi: 10.1128/microbiolspec.MB-0011-2014
- Lintzeris, D., Vernon, K., Percise, H., Strickland, A., Yarrow, K., White, A., et al. (2018). Effect of a New Purified Collagen Matrix With Polyhexamethylene Biguanide on Recalcitrant Wounds of Various Etiologies: a Case Series. *Wounds* 30, 72–78.
- Lipsky, B. A., Senneville, E., Abbas, Z. G., Aragón-Sánchez, J., Diggle, M., Embil, J. M., et al. (2020). Guidelines on the diagnosis and treatment of foot infection in persons with diabetes (IWGDF 2019 update). *Diabetes Metab. Res. Rev.* 36:e3280. doi: 10.1002/dmrr.3280
- Liu, Z., Dumville, J. C., Hinchliffe, R. J., Cullum, N., Game, F., Stubbs, N., et al. (2018). Negative pressure wound therapy for treating foot wounds in people with diabetes mellitus. *Cochrane Database Syst. Rev.* 10:CD010318. doi: 10.1002/14651858.CD010318.pub3
- Lo, C. H., Akbarzadeh, S., McLean, C., Ives, A., Paul, E., Brown, W. A., et al. (2019). Wound healing after cultured epithelial autografting in patients with massive burn injury: a cohort study. *J. Plast. Reconstr. Aesthet. Surg.* 72, 427–437. doi: 10.1016/j.jbjs.2018.11.003
- Lullove, E. J. (2017). Use of a dehydrated amniotic membrane allograft in the treatment of lower extremity wounds: a retrospective cohort study. *Wounds* 29, 346–351.
- Maiden, M. M., Zachos, M. P., and Waters, C. M. (2019). The ionophore oxyclozanide enhances tobramycin killing of *Pseudomonas aeruginosa* biofilms by permeabilizing cells and depolarizing the membrane potential. *J. Antimicrob. Chemother.* 74, 894–906. doi: 10.1093/jac/dky545
- Malone, M., Bjarnsholt, T., McBain, A. J., James, G. A., Stoodley, P., Leaper, D., et al. (2017a). The prevalence of biofilms in chronic wounds: a systematic review and meta-analysis of published data. *J. Wound Care* 26, 20–25. doi: 10.12968/jowc.2017.26.1.20
- Malone, M., Johani, K., Jensen, S. O., Gosbell, I. B., Dickson, H. G., McLennan, S., et al. (2017b). Effect of cadexomer iodine on the microbial load and diversity of chronic non-healing diabetic foot ulcers complicated by biofilm in vivo. *J. Antimicrob. Chemother.* 72, 2093–2101. doi: 10.1093/jac/dkx099
- Mao, Y., Sharma-Varma, A., Hoffman, T., Dhall, S., Danikovitch, A., Kohn, J., et al. (2018). The Effect of Cryopreserved Human Placental Tissues on Biofilm Formation of Wound-Associated Pathogens. *J. Funct. Biomater.* 9:3. doi: 10.3390/jfb9010003
- Markakis, K., Faris, A. R., Sharaf, H., Faris, B., Rees, S., and Bowling, F. L. (2018). Local antibiotic delivery systems: current and future applications for diabetic foot infections. *Int. J. Low Extrem. Wounds* 17, 14–21. doi: 10.1177/1534734618757532
- Martinotti, S., and Ranzato, E. (2015). Propolis: a new frontier for wound healing? *Burns Trauma* 3, 9. doi: 10.1186/s41038-015-0010-z
- McLoone, P., Tabys, D., and Fyfe, L. (2020). Honey Combination Therapies for Skin and Wound Infections: a Systematic Review of the Literature. *Clin. Cosmet. Investig. Dermatol.* 13, 875–888. doi: 10.2147/CCID.S282143
- Mendes, J. J., Leandro, C., Mottola, C., Barbosa, R., Silva, F. A., Oliveira, M., et al. (2014). In vitro design of a novel lytic bacteriophage cocktail with therapeutic potential against organisms causing diabetic foot infections. *J. Med. Microbiol.* 63, 1055–1065. doi: 10.1099/jmm.0.071753-0
- Mihai, M. M., Preda, M., Lungu, J., Gestal, M. C., Popa, M. I., and Holban, A. M. (2018). Nanocoatings for Chronic wound repair modulation of microbial colonization and biofilm formation. *Int. J. Mol. Sci.* 19:1179. doi: 10.3390/ijms19041179
- Minden-Birkenmaier, B., and Bowlin, G. (2018). Honey-based templates in Wound healing and tissue engineering. *Bioengineering* 5:46. doi: 10.3390/bioengineering5020046
- Momeni, M., Fallah, N., Bajouri, A., Bagheri, T., Orouji, Z., Pahlevanpour, P., et al. (2019). A randomized, double-blind, phase I clinical trial of fetal cell-based skin substitutes on healing of donor sites in burn patients. *Burns* 45, 914–922. doi: 10.1016/j.burns.2018.10.016
- Morozova, V. V., Vlassov, V. V., and Tikunova, N. V. (2018). Applications of bacteriophages in the treatment of localized infections in humans. *Front. Microbiol.* 9:1696. doi: 10.3389/fmicb.2018.01696
- Opperman, T. J., Kwasny, S. M., Williams, J. D., Khan, A. R., Peet, N. P., Moir, D. T., et al. (2009). Aryl rhodanines specifically inhibit staphylococcal and enterococcal biofilm formation. *Antimicrob. Agents Chemother.* 53, 4357–4367. doi: 10.1128/AAC.00077-09
- Orlowski, P., Zmigrodzka, M., Tomaszewska, E., Ranzoszek-Soliwoda, K., Czupryn, M., Antos-Bielska, M., et al. (2018). Tannic acid-modified silver nanoparticles for wound healing: the importance of size. *Int. J. Nanomed.* 13, 991–1007. doi: 10.2147/IJN.S154797
- Oropallo, A. R. (2019). Use of Native Type I Collagen Matrix Plus Polyhexamethylene Biguanide for Chronic Wound Treatment. *Plast. Reconstr. Surg. Glob. Open* 7:e2047. doi: 10.1097/GOX.0000000000002047
- Ortega Morente, E., Fernández-Fuentes, M. A., Grande Burgos, M. J., Abriouel, H., Pérez Pulido, R., and Gálvez, A. (2013). Biocide tolerance in bacteria. *Int. J. Food Microbiol.* 162, 13–25. doi: 10.1016/j.ijfoodmicro.2012.12.028
- Parsons, D., Meredith, K., Rowlands, V. J., Short, D., Metcalf, D. G., and Bowler, P. G. (2016). Enhanced performance and mode of action of a novel antibiofilm hydrofiber® wound dressing. *Biomed. Res. Int.* 2016:7616471. doi: 10.1155/2016/7616471
- Pavlik, V., Sojka, M., Mazúrová, M., and Velebný, V. (2019). Dual role of iodine, silver, chlorhexidine and octenidine as antimicrobial and antiprotease agents. *PLoS One* 14:e0211055. doi: 10.1371/journal.pone.0211055

- Payne, D. E., Martin, N. R., Parzych, K. R., Rickard, A. H., Underwood, A., and Boles, B. R. (2013). Tannic acid inhibits *Staphylococcus aureus* surface colonization in an IsaA-dependent manner. *Infect. Immun.* 81, 496–504. doi: 10.1128/IAI.00877-12
- Percival, S. L., Chen, R., Mayer, D., and Salisbury, A. M. (2018). Mode of action of poloxamer-based surfactants in wound care and efficacy on biofilms. *Int. Wound J.* 15, 749–755. doi: 10.1111/iwj.12922
- Percival, S. L., McCarty, S. M., and Lipsky, B. (2015). Biofilms and Wounds: an Overview of the Evidence. *Adv. Wound Care* 4, 373–381. doi: 10.1089/wound.2014.0557
- Pérez-Díaz, M. A., Silva-Bermudez, P., Jiménez-López, B., Martínez-López, V., Melgarejo-Ramire, Y., Brena-Molina, A., et al. (2018). Silver-pig skin nanocomposites and mesenchymal stem cells: suitable antibiofilm cellular dressings for wound healing. *J. Nanobiotechnol.* 16:2. doi: 10.1186/s12951-017-0331-0
- Pihl, M., Davies, J. R., Chávez de Paz, L. E., and Svensäter, G. (2010). Differential effects of *Pseudomonas aeruginosa* on biofilm formation by different strains of *Staphylococcus epidermidis*. *FEMS Immunol. Med. Microbiol.* 59, 439–446. doi: 10.1111/j.1574-695X.2010.00697.x
- Price, B. L., Lovering, A. M., Bowling, F. L., and Dobson, C. B. (2016). Development of a novel collagen wound model to simulate the activity and distribution of antimicrobials in soft tissue during diabetic foot infection. *Antimicrob. Agents Chemother.* 60, 6880–6889. doi: 10.1128/AAC.01064-16
- Prompers, L., Schaper, N., Apelqvist, J., Edmonds, M., Jude, E., Mauricio, D., et al. (2008). Prediction of outcome in individuals with diabetic foot ulcers: focus on the differences between individuals with and without peripheral arterial disease. *Eurodiab. Study. Diabetol.* 51, 747–755. doi: 10.1007/s00125-008-0940-0
- Pushparaj, M., and Ranganathan, R. (2017). Application of 3D printing in electro-induced drug delivery based on wound temperature. *Int. Res. J. Pharm.* 8, 179–183. doi: 10.7897/2230-8407.0811238
- Qu, Y., Locock, K., Verma-Gaur, J., Hay, I. D., Meagher, L., and Traven, A. (2016). Searching for new strategies against polymicrobial biofilm infections: guanlylated polymethacrylates kill mixed fungal/bacterial biofilms. *J. Antimicrob. Chemother.* 71, 413–421. doi: 10.1093/jac/dkv334
- Quave, C. L., Estévez-Carmona, M., Compadre, C. M., Hobby, G., Hendrickson, H., Beenken, K. E., et al. (2012). Ellagic acid derivatives from *Rubus ulmifolius* inhibit *Staphylococcus aureus* biofilm formation and improve response to antibiotics. *PLoS One* 7:e28737. doi: 10.1371/journal.pone.0028737
- Raad, I. I., Fang, X., Keutgen, X. M., Jiang, Y., Sherertz, R., and Hachem, R. (2008). The role of chelators in preventing biofilm formation and catheter-related bloodstream infections. *Curr. Opin. Infect. Dis.* 21, 385–392. doi: 10.1097/QCO.0b013e32830634d8
- Ramalingam, R., Dhand, C., Leung, C. M., Ong, S. T., Annamalai, S. K., Kamruddin, M., et al. (2019). Antimicrobial properties and biocompatibility of electrospun poly-ε-caprolactone fibrous mats containing *Gymnema sylvestre* leaf extract. *Mater. Sci. Eng. C Mater. Biol. Appl.* 98, 503–514. doi: 10.1016/j.msc.2018.12.135
- Rendueles, O., Kaplan, J. B., and Ghigo, J. M. (2013). Antibiofilm polysaccharides. *Environ. Microbiol.* 15, 334–346. doi: 10.1111/j.1462-2920.2012.02810.x
- Rogers, S. A., Huigens, R. W. III, Cavanagh, J., and Melander, C. (2010). Synergistic effects between conventional antibiotics and 2-aminoimidazole-derived antibiofilm agents. *Antimicrob. Agents Chemother.* 54, 2112–2118. doi: 10.1128/AAC.01418-09
- Romling, U., Galperin, M. Y., and Gomelsky, M. (2013). Cyclic di-GMP: the first 25 years of a universal bacterial second messenger. *Microbiol. Mol. Biol. Rev.* 77, 1–52. doi: 10.1128/MMBR.00043-12
- Santos, R., Gomes, D., Macedo, H., Barros, D., Tibéro, C., Veiga, A. S., et al. (2016). Guar gum as a new antimicrobial peptide delivery system against diabetic foot ulcers *Staphylococcus aureus* isolates. *J. Med. Microbiol.* 65, 1092–1099. doi: 10.1099/jmm.0.000329
- Schwartz, J. A., Lantis, J. C. II, Gendics, C., Fuller, A. M., Payne, W., and Ochs, D. (2013). A prospective, non comparative, multicenter study to investigate the effect of cadexomer iodine on bioburden load and other wound characteristics in diabetic foot ulcers. *Int. Wound J.* 10, 193–199. doi: 10.1111/j.1742-481X.2012.01109.x
- Seyed Ahmadi, S. G., Farahpour, M. R., and Hamishehkar, H. (2019). Topical application of Cinnamon verum essential oil accelerates infected wound healing process by increasing tissue antioxidant capacity and keratin biosynthesis. *Kaohsiung J. Med. Sci.* 35, 686–694. doi: 10.1002/kjm2.12120
- Sharma, D., Misba, L., and Khan, A. U. (2019). Antibiotics versus biofilm: an emerging battleground in microbial communities. *Antimicrob. Resist. Infect. Control.* 8:76. doi: 10.1186/s13756-019-0533-3
- Sharma, K., and Pagedar Singh, A. (2018). Antibiofilm effect of DNase against single and mixed species biofilm. *Foods* 7:E42. doi: 10.3390/foods7030042
- Sheldon, A. T. (2005). Antiseptic “Resistance”: real or perceived threat? *Clin. Infect. Dis.* 40, 1650–1656. doi: 10.1086/430063
- Singh, S., Singh, S. K., Chowdhury, I., and Singh, R. (2017). Understanding the Mechanism of Bacterial Biofilms Resistance to Antimicrobial Agents. *Open Microbiol. J.* 11, 53–62. doi: 10.2174/1874285801711010053
- Snyder, R. J., Bohn, G., Hanft, J., Harkless, L., Kim, P., Lavery, L., et al. (2017). Wound Biofilm: current Perspectives and Strategies on Biofilm Disruption and Treatments. *Wounds* 29, S1–S17.
- Stewart, P. S. (2015). Antimicrobial tolerance in biofilms. *Microbiol. Spectr.* 3, 10.1128/microbiolspec.MB-0010-2014. doi: 10.1128/microbiolspec.MB-0010-2014
- Sully, E. K., Malachowa, N., Elmore, B. O., Alexander, S. M., Femling, J. K., Gray, B. M., et al. (2014). Selective chemical inhibition of *agr* quorum sensing in *Staphylococcus aureus* promotes host defense with minimal impact on resistance. *PLoS Pathog.* 10:e1004174. doi: 10.1371/journal.ppat.1004174
- Sun, H., Lv, H., Qiu, F., Sun, D., Gao, Y., Chen, N., et al. (2018). Clinical application of a 3D-printed scaffold in chronic wound treatment: a case series. *J. Wound Care* 27, 262–271. doi: 10.12968/jowc.2018.27.5.262
- Taha, O. A., Connerton, P. L., Connerton, I. F., and El-Shibiny, A. (2018). Bacteriophage ZCKP1: a potential treatment for *Klebsiella pneumoniae* isolated from diabetic foot patients. *Front. Microbiol.* 9:2127. doi: 10.3389/fmicb.2018.02127
- Tan, D., Dahl, A., and Middelboe, M. (2015). Vibriophages Differentially Influence Biofilm Formation by *Vibrio anguillarum* Strains. *Appl. Environ. Microbiol.* 81, 4489–4497. doi: 10.1128/AEM.00518-15
- Tardivo, J. P., Adami, F., Correa, J. A., Pinhal, M. A., and Baptista, M. S. (2014). A clinical trial testing the efficacy of PDT in preventing amputation in diabetic patients. *Photodiagnosis Photodyn. Ther.* 11, 342–350. doi: 10.1016/j.pdpdt.2014.04.007
- Tarusha, L., Paoletti, S., Travan, A., and Marsich, E. (2018). Alginate membranes loaded with hyaluronic acid and silver nanoparticles to foster tissue healing and to control bacterial contamination of non-healing wounds. *J. Mater. Sci. Mater. Med.* 29:22. doi: 10.1007/s10856-018-6027-7
- Thombare, N., Jha, U., Mishra, S., and Siddiqui, M. Z. (2016). Guar gum as a promising starting material for diverse applications: a review. *Int. J. Biol. Macromol.* 88, 361–372. doi: 10.1016/j.ijbiomac.2016.04.001
- Touzel, R. E., Sutton, J. M., and Wand, M. E. (2016). Establishment of a multi-species biofilm model to evaluate chlorhexidine efficacy. *J. Hosp. Infect.* 92, 154–160. doi: 10.1016/j.jhin.2015.09.013
- Townsend, E. M., Sherry, L., Rajendran, R., Hansom, D., Butcher, J., MacKay, W. G., et al. (2016). Development and characterisation of a novel three-dimensional inter-kingdom wound biofilm model. *Biofouling* 32, 1259–1270. doi: 10.1080/08927014.2016.1252337
- Uçkay, I., Kressmann, B., Malacarne, S., Tournanova, A., Jaafar, J., Lew, D., et al. (2018). A randomized, controlled study to investigate the efficacy and safety of a topical gentamicin-collagen sponge in combination with systemic antibiotic therapy in diabetic patients with a moderate or severe foot ulcer infection. *BMC Infect. Dis.* 18:361. doi: 10.1186/s12879-018-3253-z
- Vågesjö, E., Öhnstedt, E., Mortier, A., Lofton, H., Huss, F., Proost, P., et al. (2018). Accelerated wound healing in mice by on-site production and delivery of CXCL12 by transformed lactic acid bacteria. *Proc. Natl. Acad. Sci. U. S. A.* 115, 1895–1900. doi: 10.1073/pnas.1716580115
- Vuotto, C., Longo, F., and Donelli, G. (2014). Probiotics to counteract biofilm-associated infections: promising and conflicting data. *Int. J. Oral Sci.* 6, 189–194. doi: 10.1038/ijos.2014.52
- Walker, M., Metcalf, D., Parsons, D., and Bowler, P. (2015). A real-life clinical evaluation of a next-generation antimicrobial dressing on acute and chronic wounds. *J. Wound Care* 24, 11–22. doi: 10.12968/jowc.2015.24.1.11

- Willcox, M. D. P., Hume, E. B. H., Aliwarga, Y., Kumar, N., and Cole, N. (2008). A novel cationic-peptide coating for the prevention of microbial colonization on contact lenses. *J. Appl. Microbiol.* 105, 1817–1825. doi: 10.1111/j.1365-2672.2008.03942.x
- Wolcott, R. D., Kennedy, J. P., and Dowd, S. E. (2009). Regular debridement is the main tool for maintaining a healthy wound bed in most chronic wounds. *J. Wound Care* 18, 54–56.
- Wu, H., Moser, C., Wang, H. Z., Høiby, N., and Song, Z. J. (2015). Strategies for combating bacterial biofilm infections. *Int. J. Oral Sci.* 7, 1–7. doi: 10.1038/ijos.2014.65
- Wu, S. C., Driver, V. R., Wrobel, J. S., and Armstrong, D. G. (2007). Foot ulcers in the diabetic patient, prevention and treatment. *Vasc. Health Risk Manag.* 3, 65–76.
- Wukich, D. K., Dikis, J. W., Monaco, S. J., Strannigan, K., Suder, N. C., and Rosario, B. L. (2015). Topically applied vancomycin powder reduces the rate of surgical site infection in diabetic patients undergoing foot and ankle surgery. *Foot Ankle Int.* 36, 1017–1024. doi: 10.1177/1071100715586567
- Yang, Q., Larose, C., Della Porta, A. C., Schultz, G. S., and Gibson, D. J. (2017). A surfactant-based wound dressing can reduce bacterial biofilms in a porcine skin explant model. *Int. Wound J.* 14, 408–413. doi: 10.1111/iwj.12619
- Conflict of Interest:** CP is the recipient of a grant from Biofilm Control (Bourse CIFRE).
- The remaining authors declare that the research was conducted in the absence of any commercial or financial relationships that could be construed as a potential conflict of interest.
- Publisher's Note:** All claims expressed in this article are solely those of the authors and do not necessarily represent those of their affiliated organizations, or those of the publisher, the editors and the reviewers. Any product that may be evaluated in this article, or claim that may be made by its manufacturer, is not guaranteed or endorsed by the publisher.

Copyright © 2021 Pouget, Dunyach-Remy, Pantel, Boutet-Dubois, Schuldiner, Sotto, Lavigne and Loubet. This is an open-access article distributed under the terms of the Creative Commons Attribution License (CC BY). The use, distribution or reproduction in other forums is permitted, provided the original author(s) and the copyright owner(s) are credited and that the original publication in this journal is cited, in accordance with accepted academic practice. No use, distribution or reproduction is permitted which does not comply with these terms.

PROBLÉMATIQUE GÉNÉRALE

Une plaie chronique est définie comme une plaie dont le délai de cicatrisation est allongé. La plaie est considérée comme chronique après 4 à 6 semaines d'évolution non favorable selon son étiologie. L'un des enjeux majeurs dans la prise en charge de ces plaies repose dans la distinction précoce de l'**infection** sous-jacente. Toutefois, les plaies chroniques étant colonisées naturellement par des bactéries, le diagnostic clinique est rendu difficile. Il existe en effet un contraste faible entre la colonisation et le processus d'infection. Il est nécessaire de tenir compte de l'interface **homme-microbe** qui est souvent la zone clé dans le développement d'infections des plaies. A cette interface, le nombre d'espèces microbiennes pathogènes est souvent très faible par rapport aux nombreuses bactéries commensales. Mieux définir le microbiote cutané est essentiel pour comprendre les interactions hôte-bactérie qui conduisent aux infections et aux problèmes de cicatrisation. Des études réalisées chez des patients diabétiques présentant des plaies du pied ont ainsi mis en évidence que des coopérations entre les bactéries présentes au sein d'une même communauté influençaient la chronicité de la plaie ^{163, 23}.

Les **conséquences cliniques** du biofilm sont importantes surtout en ce qui concerne les mécanismes de tolérance et de résistance aux antibiotiques qui participent à la sévérité, la chronicité et les récurrences des plaies chroniques.

Actuellement, en ce qui concerne les plaies chroniques, la question fondamentale est de savoir s'il y a des biofilms 'protecteurs' (tourné vers la colonisation) et d'autres qui sont responsables d'infection. Une des hypothèses les plus usuelles pour répondre à cette question est la supposition **des communautés bactériennes**. Elle considère que le biofilm est composé d'une seule « unité fonctionnelle pathogène » sans tenir compte singulièrement des espèces bactériennes qui la compose. Ce concept de **pathogroupes** (ou FEP, functionally equivalent pathogroups) a été proposé par Dowd et *al.* ¹³⁵. Suivant cette hypothèse, certaines espèces bactériennes considérées comme non pathogènes seules ou n'étant pas capables de maintenir une infection chronique, peuvent s'organiser dans un **biofilm pathologique** et participaient à la chronicité de la plaie. Des données préliminaires de ce concept ont été publiées montrant l'existence de différents pathogroupes au sein des plaies chroniques. Une analyse quantitative de la distance séparant les bactéries agrégées à la surface de la plaie a montré que *P. aeruginosa* est retrouvé plus en

profondeur par rapport à *S. aureus* et que ces deux bactéries ne sont jamais co-agrégées¹³¹.

Ces observations démontrent qu'au niveau des plaies chroniques, les bactéries ont une organisation influençant leur comportement et leur virulence (polymicrobisme, biofilm, FEP ...). De plus, l'environnement dans lequel se trouvent les bactéries semble jouer un rôle prépondérant dans la pathogénicité de ces dernières. Toutefois plusieurs questions restent en suspens : - Quelles relations existe-t-il entre les bactéries et leur environnement ? - Quelles relations existe-t-il entre les bactéries pathogènes ? - Quelles relations existe-t-il entre bactéries commensales et pathogènes ? - Comment le biofilm pathologique est organisé ? - Peut-on éviter ce biofilm pathologique ?

Aussi, une meilleure compréhension des biofilms polymicrobiens observés dans les plaies chroniques est nécessaire pour améliorer la prise en charge thérapeutique. Cette compréhension passe notamment par la nécessité de développer de **nouveaux outils ou modèles *in vitro*** pouvant mimer l'environnement des plaies chroniques afin d'évaluer l'effet de **molécules thérapeutiques**. Les objectifs de cette thèse étaient donc :

- La création d'un **nouveau modèle *in vitro*** dont la composition permettait de mimer l'environnement stressant observé au niveau du lit de la plaie chronique,
- D'étudier l'effet à court terme (24h) ou dans le cadre d'une exposition dite chronique (6 semaines) de cet environnement stressant sur plusieurs **caractéristiques bactériennes** (virulence, génomique, fitness, formation de biofilm précoce et mature, expression de gènes impliqués dans la formation et la régulation du biofilm),
- D'étudier **l'interaction** entre des espèces fréquemment co-isolées sur les plaies chroniques. Le but était de renseigner l'impact de la coopération entre *S. aureus* et *P. aeruginosa* sur leur capacité à former du biofilm et leur potentiel de virulence notamment,
- De mettre au point une technique permettant **la formation et la visualisation en temps réel du biofilm de façon dynamique** avec

un contrôle des paramètres extérieurs (température, vitesse d'écoulement ...) dans des conditions proches de ce que l'on observe chez le patient. Un sous objectif de cette partie de la thèse était de pouvoir tester l'efficacité de molécules antibiofilms sur un biofilm polymicrobien en situation semblable à ce qui peut être réalisé en clinique.

PARTIE II.

MISE EN PLACE D'UN NOUVEL OUTIL *IN VITRO* POUR L'ÉTUDE DES PLAIES CHRONIQUES : LE MILIEU PLAIE

Travail n°3 : Article Scientifique

Adaptation of *Staphylococcus aureus* in a Medium Mimicking a Diabetic Foot Environment

Cassandra Pouget, Claude-Alexandre Gustave, Christelle Ngba-Essebe,
Frédéric Laurent, Emmanuel Lemichez, Anne Tristan, Albert Sotto, Catherine
Dunyach-Remy and Jean-Philippe Lavigne

Accepté dans Toxins le 18 Mars 2021

Résumé travail n°3 :

Les plaies chroniques sont des plaies ouvertes faisant suite à une altération tissulaire sans tendance à la cicatrisation au-delà de 4 à 6 semaines. Elles sont liées de façon constante à des pathologies sous-jacentes dont les plus fréquentes sont le diabète sucré et les vasculopathies.

Le diabète sucré concerne en France près de 3 millions de personnes. La fréquence des lésions des pieds est élevée dans la population diabétique, bien supérieure à celle dans la population générale. Globalement, on estime que 15 à 25% des patients diabétiques présenteront au cours de leur vie une ulcération des membres inférieurs. Le diabète sucré est caractérisé par une hyperglycémie entraînant de nombreuses complications telles que l'ischémie, l'artériopathie et la neuropathie à l'origine de l'ulcération du pied diabétique. Ces conditions défavorables ajoutée à la prescription d'antibiotique permettant de contrôler l'infection de ces plaies, font du pied diabétique un environnement particulier. La bactérie la plus fréquemment isolée dans le cas des infections du pied diabétique (IPD) est la bactérie à Gram positif ***S. aureus***. Notre objectif dans cette étude était donc d'évaluer le comportement de *S. aureus* dans un modèle *in vitro* mimant les conditions stressantes observées dans l'IPD.



Dans un premier temps, nous avons développé un modèle *in vitro* modulable permettant de se rapprocher des conditions environnementales observées dans le pied diabétique. Ce milieu a permis la culture pendant **24 heures** (court terme) ou **16 semaines** (long terme) de souches cliniques de *S. aureus* dans différents environnements stressants : ajout de glucose (**hyperglycémie**), ajout de concentrations subinhibitrices d'**antibiotiques** couramment utilisés dans le traitement des IPD (linézolide et vancomycine) ou encore en condition **anaérobie**. Une fois l'adaptation des souches réalisée dans le milieu, nous avons évalué par qRT-PCR l'expression de gènes codant pour les principaux **facteurs de virulence** de *S. aureus* (*lukF/lukS-PV*, *edinB*, *edinC*, *hla*, *spa*, *eap*, *fnbpA*) ainsi que le régulateur global *agr*. Les études sur le potentiel de pathogénicité ont été complétées par des tests sur modèle *C. elegans*. Des **études phénotypiques** et des expériences sur le potentiel de **formation de biofilm** ont également été menées.

Après 16 semaines de culture, les études phénotypiques ont mis en évidence la présence de small colony variants (SCVs). Ce changement phénotypique est caractéristique chez *S. aureus* en cas d'infection chronique permettant ainsi la validation de notre modèle de culture. Une **baisse significative de la virulence** des souches de *S. aureus* grâce au modèle *C. elegans* a été démontrée. Les études transcriptomiques ont confirmé la diminution d'expression des gènes de virulence (*lukF/lukS-PV*, *edinB* et *edinC*) après une culture prolongée dans des concentrations élevées de glucose, en anaérobiose et en présence d'antibiotique. De manière intéressante, la capacité à former du **biofilm** ainsi que l'expression de **gènes d'adhésion** (*fnbpA*) été augmentée en présence de glucose et de vancomycine.

Le développement d'un modèle d'étude d'infection chronique a montré qu'après plusieurs semaines d'adaptation à des conditions stressantes, on observait une baisse du potentiel de pathogénicité de *S. aureus* en présence de fortes concentrations de glucose, en anaérobiose et en présence de concentrations subinhibitrices d'antibiotiques. Cette étude a permis de confirmer l'impact de l'environnement sur l'adaptation de *S. aureus* aux conditions de stress prolongé.

Article

Adaptation of *Staphylococcus aureus* in a Medium Mimicking a Diabetic Foot Environment

Cassandra Pouget ¹, Claude-Alexandre Gustave ² , Christelle Ngba-Essebe ¹, Frédéric Laurent ^{2,3}, Emmanuel Lemichez ⁴, Anne Tristan ^{2,3}, Albert Sotto ⁵ , Catherine Dunyach-Rémy ⁶  and Jean-Philippe Lavigne ^{6,*} 

- ¹ Virulence Bactérienne et Infections Chroniques, INSERM U1047, Université de Montpellier, 30908 Nîmes, France; cassandra.pouget@gmail.com (C.P.); ngbachristelle@yahoo.fr (C.N.-E.)
- ² Centre International de Recherche en Infectiologie, Inserm U1111, CNRS UMR5308, ENS Lyon, Université Claude Bernard Lyon 1, 69365 Lyon, France; claude-alexandre.gustave@outlook.fr (C.-A.G.); frederic.laurent@univ-lyon.fr (F.L.); anne.tristan@chu-lyon.fr (A.T.)
- ³ Laboratoire de Bactériologie, Institut des Agents Infectieux, Centre National de Référence des Staphylocoques, Hôpital de la Croix-Rousse, Hospices Civils de Lyon, 69365 Lyon, France
- ⁴ Unité des Toxines Bactériennes, UMR CNRS 2001, Institut Pasteur, 75015 Paris, France; emmanuel.lemichez@pasteur.fr
- ⁵ Virulence Bactérienne et Infections Chroniques, INSERM U1047, Université de Montpellier, Department of Infectious and Tropical Diseases, CHU Nîmes, Univ Montpellier, 30908 Nîmes, France; albert.sotto@chu-nimes.fr
- ⁶ Virulence Bactérienne et Infections Chroniques, INSERM U1047, Université de Montpellier, Department of Microbiology and Hospital Hygiene, CHU Nîmes, Univ Montpellier, 30908 Nîmes, France; catherine.remy@chu-nimes.fr
- * Correspondence: jean.philippe.lavigne@chu-nimes.fr; Tel.: +33-466-68-32-02; Fax: +33-466-68-42-54



Citation: Pouget, C.; Gustave, C.-A.; Ngba-Essebe, C.; Laurent, F.; Lemichez, E.; Tristan, A.; Sotto, A.; Dunyach-Rémy, C.; Lavigne, J.-P. Adaptation of *Staphylococcus aureus* in a Medium Mimicking a Diabetic Foot Environment. *Toxins* **2021**, *13*, 230. <https://doi.org/10.3390/toxins13030230>

Received: 8 February 2021

Accepted: 18 March 2021

Published: 22 March 2021

Publisher's Note: MDPI stays neutral with regard to jurisdictional claims in published maps and institutional affiliations.



Copyright: © 2021 by the authors. Licensee MDPI, Basel, Switzerland. This article is an open access article distributed under the terms and conditions of the Creative Commons Attribution (CC BY) license (<https://creativecommons.org/licenses/by/4.0/>).

Abstract: *Staphylococcus aureus* is the most prevalent pathogen isolated from diabetic foot infections (DFIs). The purpose of this study was to evaluate its behavior in an in vitro model mimicking the conditions encountered in DFI. Four clinical *S. aureus* strains were cultivated for 16 weeks in a specific environment based on the wound-like medium biofilm model. The adaptation of isolates was evaluated as follows: by *Caenorhabditis elegans* model (to evaluate virulence); by quantitative Reverse Transcription-Polymerase Chain Reaction (qRT-PCR) (to evaluate expression of the main virulence genes); and by Biofilm Ring test[®] (to assess the biofilm formation). After 16 weeks, the four *S. aureus* had adapted their metabolism, with the development of small colony variants and the loss of β -hemolysin expression. The in vivo nematode model suggested a decrease of virulence, confirmed by qRT-PCRs, showing a significant decrease of expression of the main staphylococcal virulence genes tested, notably the toxin-encoding genes. An increased expression of genes involved in adhesion and biofilm was noted. Our data based on an in vitro model confirm the impact of environment on the adaptation switch of *S. aureus* to prolonged stress environmental conditions. These results contribute to explore and characterize the virulence of *S. aureus* in chronic wounds.

Keywords: adaptation; biofilm; diabetic foot infection; EDIN; in vitro model; nematode; Pantón-Valentin leukocidin; *Staphylococcus aureus*; virulence

Key Contribution: This paper highlights the impact of environmental conditions on *Staphylococcus aureus* in an in vitro model mimicking the conditions encountered in diabetic foot infections, a genomic and transcriptomic adaptation of *S. aureus* that could drive the escape to the host immune response and foster chronicity of the wound.

1. Introduction

Diabetes *mellitus* is a public health problem representing a major cause of mortality and morbidity worldwide [1]. This disease affects 442 million adults in the world

and represents the seventh leading cause of death (Global report on diabetes: Executive Summary. Available online: <https://www.who.int/health-topics/diabetes/publications&publication=who-nmh-nvi-16.3> (accessed on 14 March 2021)). One of the most serious complications of diabetes *mellitus* is foot ulceration due to the triopathy associating ischemia, neuropathy, and arteriopathy [2–4]. It is a source of major suffering and financial costs for the patient, but also for the health care professionals and facilities and society. Infection in diabetic foot ulcer (DFU) is particularly frequent and, untreated, ultimately results in lower-limb amputation [5]. Diabetic foot infection (DFI) is estimated to be the most common cause of diabetes-related admission in hospitals. Outcomes in patients presenting with a DFI are poor with a high mortality following this complication (around 15% in the following year) [1,5]. DFIs are polymicrobial and *Staphylococcus aureus* is the most frequent pathogen isolated [6,7]. This Gram-positive coccus is a leading cause of a wide range of diseases, from skin and soft tissue infections (SSTIs) (e.g., impetigo, carbuncles) to life-threatening bacteremia, toxic shock syndrome, endocarditis, and osteomyelitis [6,8]. However, the mechanisms of *S. aureus* pathogenicity and switch from colonization to infection in DFI remain unclear.

S. aureus deploys an arsenal of virulence factors to colonize, invade, and destroy tissues and host immune cells [9,10]. These virulence factors include adhesins (called microbial surface components recognizing adhesive matrix molecules (MSCRAMMs), such as fibronectin binding proteins (FnBPs), that bind to different host proteins and are important for tissular colonization [11,12]. The protein A (SpA) promotes immune evasion and protects against host-mediated clearance [10]. *S. aureus* also secretes toxins (e.g., the pore-forming cytotoxin alpha-hemolysin (Hla), which can lead to tissue necrosis. In addition, the superantigens can induce an unregulated polyclonal activation of lymphocyte T cells, leading to a cytokine storm. The regulation of these virulence factors is complex and extensive, but virulence is very closely regulated in *S. aureus*, notably owing to the *agr* gene. This bacterium can also secrete specific toxins such as the Pantone–Valentine Leukocidin (PVL), which is a pore-forming toxin [6,13], or the exoenzymes EDINs (EDIN-A, -B, and -C), which inactivate the small GTPase RhoA to promote bacterial dissemination [14,15]. These cytolytic toxins can damage membranes of host cells, leading to cell lysis [16]. Finally, to adapt to the environmental conditions, *S. aureus* is able to survive in a metabolically inactive state while preserving the integrity of the host cell by forming small-colony variants (SCVs). SCVs differ metabolically and phenotypically to ordinary *S. aureus* isolates [17].

During DFI, *S. aureus* has been shown to activate its virulence factors to invade the tissue [18]. However, this infection is chronic and complex, with a different clinical presentation to SSTIs, notably with the mitigated impact of toxinogenic strains [6]. Indeed, *S. aureus* is exposed to various stress conditions in DFU: elevated glucose concentration, decreased temperature, decreased tissue oxygenation, and presence of antibiotics for several weeks [19]. Previous studies have analyzed the impact of antibiotics or glucose on the virulence of *S. aureus* strains during short-term [20–24] or long-term exposure [25–27] in a stress environment. These lifestyles involve forming quasi-dormant sub-populations and the presence of persister cells and SCVs [28]. Under prolonged nutrient limitation, the downregulation or loss of *agr* has been reported and seems to play a crucial role [17,28].

The purpose of this study was to evaluate the impact of an in vitro model mimicking the conditions encountered in DFU on the adaptation/switch in the virulence profile of *S. aureus*. This manuscript used the Lubbock wound pathogenic biofilm model [29] firstly adapted by De Leon et al. [30]. This model contains physiological concentrations of blood components, notably utilizing a chopped-meat-based medium supplemented with heparinized plasma and red blood cells. This medium was formulated to represent the conditions of human wounds and better simulate the nutrient environment in the chronic ulcer. In this study, the media formulation was modified by the addition of 10% glucose (allowing a concentration above 150 mg/dL, the limit that defined an uncontrolled diabetes) and two antibiotics at sub-inhibitory concentrations (a condition frequently observed in this pathology due to arteriopathy). The antibiotics used correspond to two

of the main molecules used in DFI: vancomycin, a glycopeptide that inhibits cell wall synthesis by binding to the D-Ala-D-Ala terminal of the growing peptide chain during cell wall synthesis; and linezolid, an oxazolidinone that disrupts bacterial growth by inhibiting the initiation process of protein synthesis by binding to a site on the bacterial 23S ribosomal RNA of the 50S subunit. Thus, *S. aureus* virulence was evaluated in this in vitro wound-like medium (WLM) that mimics a diabetic environment.

2. Results

2.1. Phenotypic Effects on *S. aureus* after a Prolonged Culture in a Medium Mimicking a DFI Environment

Firstly, we investigated the impact of the WLM supplemented with 10% glucose and/or vancomycin and linezolid tested at 0.5× minimum inhibitory concentration (MIC) on three virulent *S. aureus* strains (NSA739, NSA1077, and NSA7475) isolated from DFI and one colonizing strain (NSA1385) (Table 1). First, the presence/absence of β-hemolysis on blood agar plates and the emergence of SCVs were determined.

Table 1. *S. aureus* strains used in the study.

Strains	Characteristics	References
NSA739	<i>S. aureus</i> strain isolated from DFI (Grade 3), PVL-, <i>edin</i> -, <i>agr2</i> , ST8	[31]
NSA1385	<i>S. aureus</i> strain isolated from colonized DFI (Grade 1), PVL-, <i>edin</i> -, <i>agr1</i> , ST8	[31]
NSA1077	<i>S. aureus</i> strain isolated from DFI (Grade 3), PVL+, <i>edinB</i> +, <i>agr1</i> , ST152	[32]
NSA7475	<i>S. aureus</i> strain isolated from DFI (Grade 3), PVL-, <i>edinB</i> +, <i>agr1</i> , ST25	[32]

DFI, diabetic foot infection; DFI, diabetic foot ulcer; PVL, Pantone–Valentine Leukocidin; ST, sequence type.

2.1.1. Addition of 10% Glucose

The WLM had no impact on the phenotype of the *S. aureus* strains tested after 24 h incubation, with or without the addition of glucose (Supplementary Materials Table S1). However, after 16 weeks in WLM alone, all the bacteria displayed mostly β-hemolytic activity (98–99%), with low level SCV (1–2%) (Table 2). The addition of 10% glucose significantly modified the phenotype of the virulent strains with a clear loss of β-hemolytic production (particularly for NSA739 and NSA1077) and a high level of SCVs compared with the medium without glucose ($p < 0.01$). Interestingly, the colonizing NSA1385 was not significantly affected under any of the conditions tested (Table 2).

Table 2. Phenotypical modifications of *S. aureus* cultivated in an in vitro wound-like medium (WLM) mimicking the conditions encountered in chronic wounds and with the addition of other stress parameters (high glucose concentration, addition of antibiotics) for 16 weeks. Bold results are statistically significant ($p < 0.01$) compared with WLM alone.

Strains	In Vitro WLM Alone		WLM + 10% Glucose		WLM + Vancomycin		WLM + Linezolid		WLM + 10% Glucose + Vancomycin		WLM + 10% Glucose + Linezolid	
	β-hemol ¹	SCV ²	β-hemol	SCV	β-hemol	SCV	β-hemol	SCV	β-hemol	SCV	β-hemol	SCV
NSA739	99% ± 2	2% ± 2	12% ± 5	22% ± 2	93% ± 5	2% ± 2	28% ± 4	5% ± 2	5% ± 2	30% ± 7	13% ± 6	18% ± 7
NSA1077	98% ± 3	2% ± 2	5% ± 5	11% ± 2	91% ± 7	2% ± 3	55% ± 5	20% ± 5	8% ± 4	18% ± 5	10% ± 10	10% ± 5
NSA7475	98% ± 2	1% ± 2	65% ± 3	24% ± 2	88% ± 7	4% ± 2	48% ± 2	15% ± 4	50% ± 5	15% ± 3	37% ± 8	17% ± 8
NSA1385	99% ± 2	0% ± 2	93% ± 7	4% ± 2	100% ± 2	0% ± 2	75% ± 5	7% ± 2	94% ± 2	2% ± 2	91% ± 5	3% ± 3

¹ β-hemolysis. ² SCV, small colony variant. % corresponds to a mean of counts (±standard deviation) performed on three independent experiments on an average of 200 colonies.

2.1.2. Addition of Antibiotics

The addition of sub-MICs of vancomycin (0.5× MIC) and linezolid (0.5× MIC) in WLM supplemented with 10% glucose produced the same observations with a significant modification of the phenotype of the virulent strains (Table 2): a loss of β-hemolytic

production (50–95%) and a high level of SCVs (10–30%) compared with WLM alone ($p < 0.01$). These modifications did not affect the colonizing strain NSA1385.

To clearly evaluate the effect of antibiotics, vancomycin and linezolid were tested alone in WLM. Interestingly, in sub-MIC of vancomycin alone, the modifications of *S. aureus* phenotype were variable, with a significant effect only on the β -hemolytic activity on NSA1077 and NSA7475 ($p < 0.01$). No statistical effect was noted for the level of SCV. The addition of linezolid alone significantly altered the β -hemolytic activity of all four tested strains ($p < 0.01$).

2.2. Effect of a Prolonged Culture in a Medium Mimicking DFU Environment on *S. aureus* Virulence

2.2.1. Addition of 10% Glucose

In the *C. elegans* model, all *S. aureus* strains killed the nematodes more rapidly than the avirulent *E. coli* OP50 strain used as nutrient for the nematodes ($p < 0.001$) (Table 3). The LT50 was similar for the three virulent strains (NSA739, NSA1077, and NSA7475), but significantly shorter ($p < 0.001$) for the colonizing strain (NSA1385) (1.7 to 2.3 days \pm 0.3 vs. 4.3 \pm 0.3, respectively; Table 3). The differences in virulence were not due to differences in the survival and proliferation of strains within the nematode intestine, as the intestine colonization by the strains was not significantly different (Supplementary Materials Table S2).

Table 3. 50% lethal time (in days) of *Caenorhabditis elegans* infected by different *S. aureus* cultivated in an in vitro wound-like medium (WLM) mimicking the conditions encountered in chronic wounds and with the addition of stress factors (high glucose concentration, sub-minimum inhibitory concentration (MIC) of antibiotics). The results are representative of at least four independent trials for each strain.

Strains	Length of Preculture	Without Pre-Culture in WLM	WLM Alone	WLM + 10% Glucose	WLM + Vancomycin	WLM + Linezolid	WLM + 10% Glucose + Vancomycin	WLM + 10% Glucose + Linezolid
NSA739 24 h	24 h	1.7 \pm 0.3	3.5 \pm 0.2	3.5 \pm 0.3	3.4 \pm 0.2	3.8 \pm 0.3	3.9 \pm 0.2	5.00 \pm 0.4
NSA739 16-week	16 weeks	NA	3.9 \pm 0.2	4.9 \pm 0.2	3.2 \pm 0.3	4.9 \pm 0.2	5.0 \pm 0.2	4.9 \pm 0.2
NSA1077 24 h	24 h	2.2 \pm 0.2	3.9 \pm 0.2	4.2 \pm 0.3	4.1 \pm 0.1	4.3 \pm 0.2	4.4 \pm 0.1	4.9 \pm 0.2
NSA1077 16-week	16 weeks	NA	4.4 \pm 0.1	5.4 \pm 0.4	3.7 \pm 0.2	5.4 \pm 0.4	5.5 \pm 0.3	5.5 \pm 0.4
NSA7475 24 h	24 h	2.3 \pm 0.3	3.8 \pm 0.2	3.9 \pm 0.3	3.7 \pm 0.2	3.5 \pm 0.2	3.8 \pm 0.2	5.2 \pm 0.4
NSA7475 16-week	16 weeks	NA	4.3 \pm 0.3	5.3 \pm 0.4	3.5 \pm 0.2	4.7 \pm 0.3	5.4 \pm 0.4	5.0 \pm 0.2
1385 24 h	24 h	4.3 \pm 0.3	4.8 \pm 0.3	4.6 \pm 0.3	4.3 \pm 0.4	5.1 \pm 0.2	4.8 \pm 0.3	4.4 \pm 0.2
1385 16-week	16 weeks	NA	5.0 \pm 0.4	5.2 \pm 0.2	5.1 \pm 0.2	5.1 \pm 0.3	4.9 \pm 0.3	4.9 \pm 0.2
OP50 (Control strain)	-	7.7 \pm 0.2	NA	NA	NA	NA	NA	NA

In bold, $p < 0.01$ after a pairwise comparison between LT50s (strain in WLM alone vs. others) using a log rank test. NA, not applicable.

Infecting *S. aureus* strains pre-cultivated for 24 h in WLM showed significantly decreased virulence compared with the same strains without pre-culture (1.7–2.3 days \pm 0.3 vs. 3.5–3.9 \pm 0.2, respectively; $p < 0.001$, Table 3). No impact was noted on virulence when these strains were pre-cultivated for 16 weeks (3.5–3.9 \pm 0.2 vs. 3.9–4.4 \pm 0.2, respectively; $p =$ not significant (NS), Table 3). Interestingly, no significant difference of LT50 was noted for the colonizing strain, irrespective of the length of pre-culture (24 h vs. 16 weeks), although an increased nematode lifespan was noted: 4.3 days \pm 0.3, without pre-culture; 4.8 \pm 0.3, with a 24 h pre-culture; and 5.0 \pm 0.4, with a 16-week pre-culture ($p =$ NS) (Table 3).

When the infecting *S. aureus* strains were pre-cultivated in WLM supplemented with 10% glucose, their virulence was similar to that observed after pre-culture in WLM alone (3.5–3.9 \pm 0.2 vs. 3.5–4.2 \pm 0.3, respectively; $p =$ NS, Table 3). In contrast, the virulence of the three infecting strains was significantly decreased after a 16-week pre-culture in the glucose supplemented medium compared with medium alone (4.9–5.4 \pm 0.4 vs. 3.9–4.4 \pm 0.3, respectively; $p < 0.001$, Table 3).

As previously observed, no significant modification of lifespan of the *C. elegans* was observed in the colonizing strain NSA1385 after a short or a long pre-culture in the WLM

with or without glucose (24 h: 4.8 ± 0.3 vs. 4.6 ± 0.3 and 16-week: 5.0 ± 0.4 vs. 5.2 ± 0.2 , respectively; $p = \text{NS}$, Table 3).

2.2.2. Addition of Antibiotics

The addition of vancomycin to the WLM had no effect on the lifespan of nematodes in the presence of *S. aureus*. No significant difference of LT50 of nematodes fed with the different strains was observed when these strains were pre-cultivated for 24 h or 16 weeks in medium plus antibiotic ($p = \text{NS}$) (Table 3). However, a trend for increased virulence could be noted for the three infecting *S. aureus* strains pre-cultivated with vancomycin versus without pre-culture (LT50: $3.2\text{--}3.7$ days ± 0.4 vs. $3.9\text{--}4.4 \pm 0.3$, respectively; $p = \text{NS}$, Table 3).

The addition of linezolid also had no significant impact on the virulence of the infecting *S. aureus* pre-cultivated in supplemented WLM for 24 h compared with a pre-culture in WLM medium alone ($3.5\text{--}4.3 \pm 0.3$ vs. $3.5\text{--}3.9 \pm 0.2$, respectively; $p = \text{NS}$, Table 3). Interestingly, during a long period of pre-culture (16 weeks), a significant increase of the lifespan of the *C. elegans* was observed in two of the three virulent *S. aureus* strains (NSA739 and NSA1077) ($4.9\text{--}5.4 \pm 0.4$ vs. $3.9\text{--}4.4 \pm 0.2$, respectively; $p < 0.001$, Table 3). No significant modification of lifespan of the *C. elegans* was observed in the colonizing strain NSA1385 after a short or long pre-culture in the WLM with or without addition of antibiotics (24 h: 4.8 ± 0.3 vs. 5.1 ± 0.2 and 16-week: 5.0 ± 0.4 vs. 5.1 ± 0.3 , respectively; $p = \text{NS}$, Table 3).

The addition of vancomycin to WLM supplemented with 10% glucose showed the same observation as pre-cultivation without antibiotic. A significant decrease of *S. aureus* virulence was shown for the isolates pre-incubated for 16 weeks ($5.0\text{--}5.5 \pm 0.4$ vs. $3.9\text{--}4.4 \pm 0.3$, respectively; $p < 0.001$, Table 3), suggesting a role of glucose alone in this effect.

While the same observation was noted for the long exposure of two of the three isolates (NSA739 and NSA1077) in WLM medium supplemented with 10% glucose and linezolid ($4.9\text{--}5.5 \pm 0.4$ vs. $3.9\text{--}4.4 \pm 0.2$, respectively; $p < 0.001$, Table 3), a clear impact of linezolid was also observed after a short exposure (24 h) of the three infecting *S. aureus* to this medium ($4.9\text{--}5.2 \pm 0.4$ vs. $3.5\text{--}3.9 \pm 0.2$, respectively; $p < 0.001$, Table 3), suggesting an effect of linezolid on *S. aureus* virulence in the WLM supplemented with glucose.

Finally, no impact of the addition of antibiotics and glucose to WLM medium was noted for the colonizing strain NSA1385 (Table 3).

2.3. Effect of a Prolonged Culture in a Medium Mimicking DFU Environment on Kinetics of *S. aureus* Biofilm Formation

The Biofilm Ring test[®] was performed to evaluate the effect of WLM with or without the addition of 10% glucose and antibiotics on the capacity of *S. aureus* to form biofilm.

2.3.1. Addition of 10% Glucose

The pre-cultivation of *S. aureus* in WLM supplemented with glucose had no significant effect on biofilm formation for all the studied strains after a short exposure (24 h) (Supplementary Materials Table S3).

After a long exposure (16 weeks) of the infecting strains with the WLM supplemented with 10% glucose, all the strains had impeded potential to form biofilm (Figure 1).

For NSA739 and NSA7475, biofilm was completely formed after 5 h of incubation (BFI = 1.5 ± 0.2). When the strain was pre-cultivated in WLM + 10% glucose, we observed a trend of faster formation of biofilm (at 2 and 3 h), but no impact on the biofilm formation at the end-point (5 h).

For NSA1077, the strain pre-cultivated with glucose showed a significantly faster biofilm formation than the strain pre-cultivated in WLM alone at 2, 3, and 4 h, with the beads immobilized after 4 h (BFI = 1.6 ± 0.2) ($p < 0.001$).

For the colonizing strain NSA1385, the addition of glucose had no impact on the kinetics of biofilm formation: the BFI values were similar between all conditions tested.

2.3.2. Addition of Antibiotics

As observed with glucose supplementation, pre-cultivation of *S. aureus* in WLM plus antibiotics (with or without 10% glucose) had no effect on biofilm formation for all the studied strains after a short exposure (24 h) (Supplementary Materials Table S3).

For the three infecting strains NSA739, NSA1077, and NS7475, the kinetics of biofilm formation were slowed in the presence of sub-MIC of vancomycin alone, with a biofilm not constituted after 5 h ($p < 0.0001$) (Figure 1). Interestingly, although the addition of sub-MICs of linezolid had no effect on the biofilm formation of NSA7475 or NSA1077, pre-cultivation of these strains in WLM plus antibiotics and 10% glucose had a significant effect, with the beads immobilized at 3 h ($p < 0.001$).

Antibiotic pressure had no significant impact on the kinetics of biofilm formation for the colonizing strain NSA1385 (Figure 1).

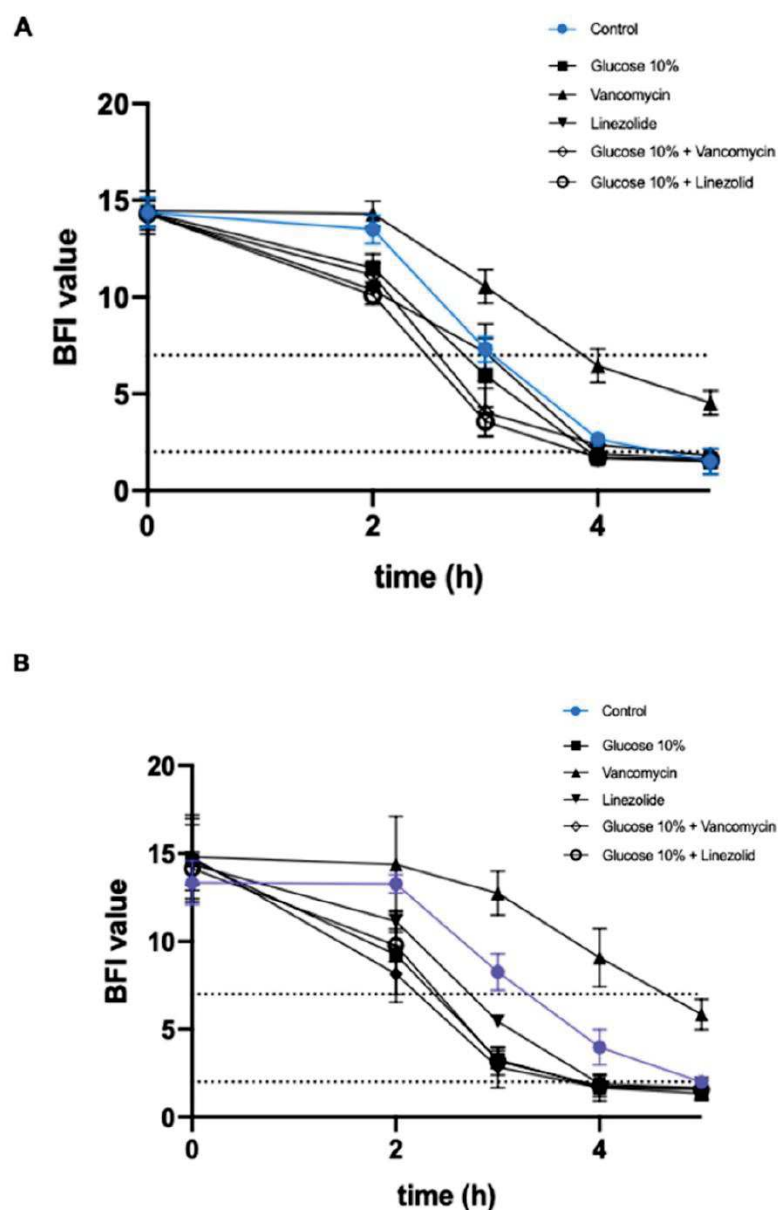


Figure 1. Cont.

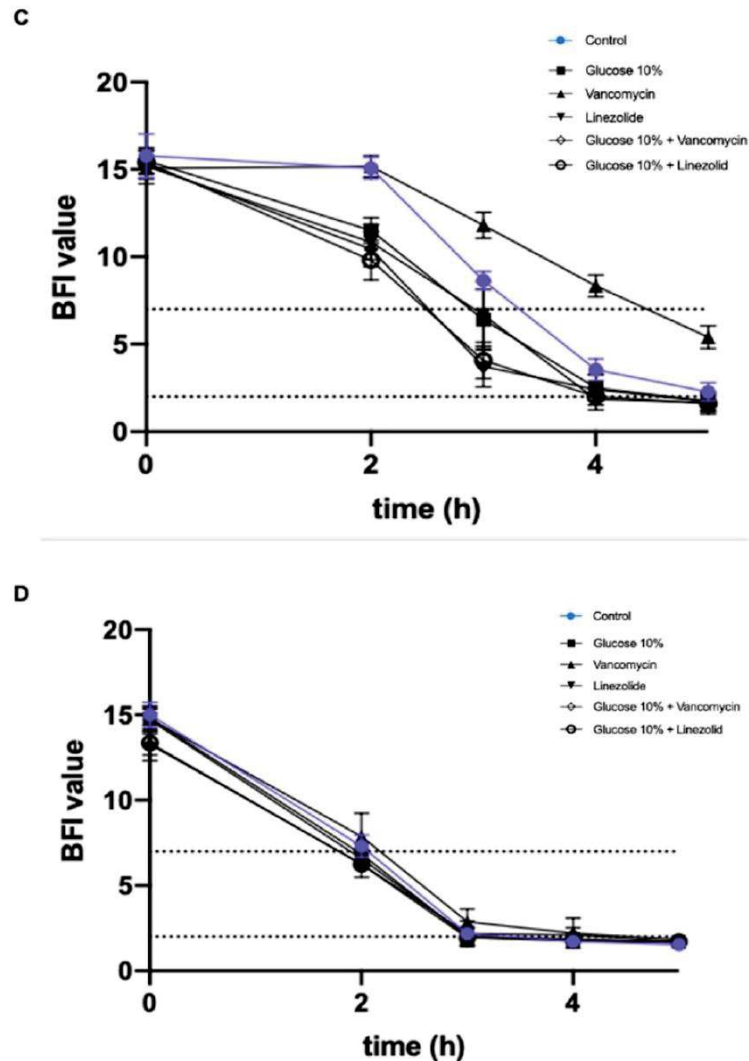


Figure 1. Effects of a pre-culture in a wound-like medium (WLM) and 10% glucose combined with sub-minimum inhibitory concentration (MIC) of vancomycin ($0.5 \times \text{MIC}$) and linezolid ($0.5 \times \text{MIC}$) on *S. aureus* biofilm formation after 16 weeks of culture. The kinetics of the early phase of biofilm formation were determined on (A) NSA739; (B) NSA1077; (C) NSA7475; and (D) NSA1385 by the BioFilm ring test[®] (BioFilm Control, France). The control corresponds to the evaluation of biofilm formation of strains in Brain Heart Infusion (BHI) medium alone. Dotted horizontal lines: >7 , no biofilm; <2 , fixed biofilm. Means \pm standard errors of the mean of biofilm indexes (BFIs) for at least three independent replicates are presented. Statistical differences between the different culture conditions at each time were obtained using two-way analysis of variance (ANOVA), followed by Dunnett's multiple-comparison test.

2.4. Effect of a Prolonged Culture in a Medium Mimicking DFU Environment on *S. aureus* Genes' Expression

To assess the impact of WLM on bacteria at the genetic level, the expression levels of some important genes involved in *S. aureus* virulence were measured. Their log relative transcription levels are shown in Supplementary Materials Table S4 for all the strains and Figures 2 and 3 for NSA1077 and NSA739, respectively.

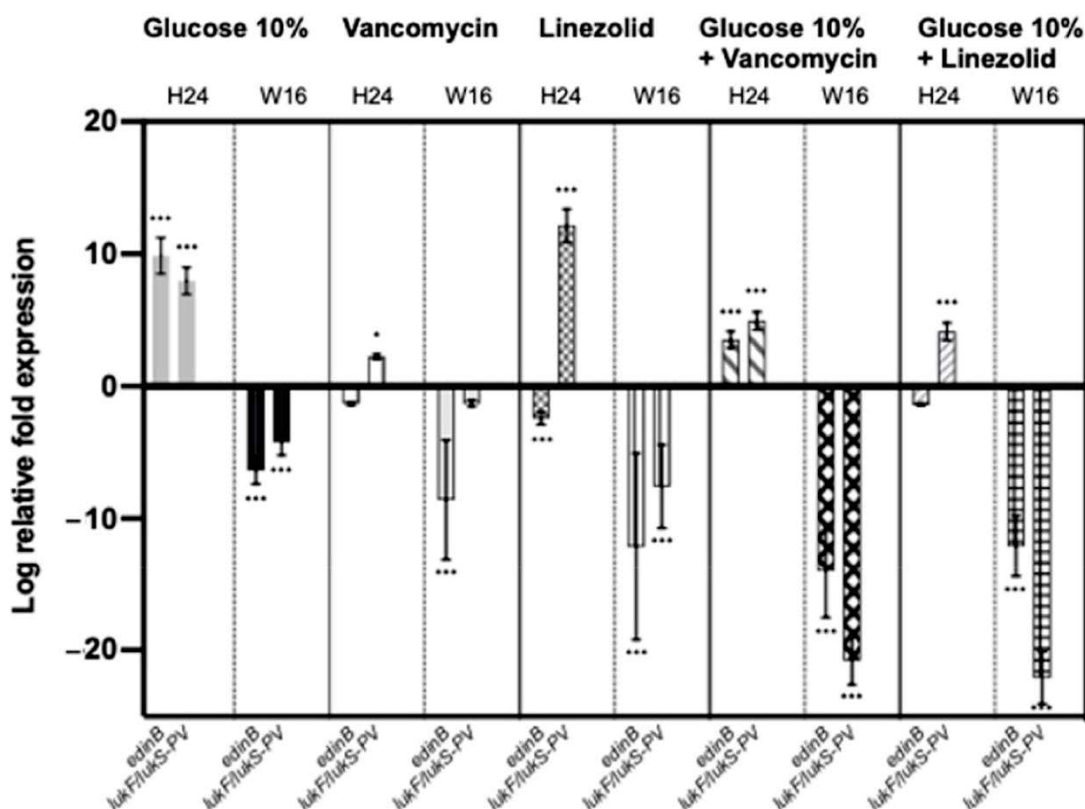


Figure 2. Relative mRNA expression levels of toxinogenic genes of *S. aureus* NSA1077 strain cultivated in WLM supplemented with 10% glucose, vancomycin ($0.5 \times \text{MIC}$), linezolid ($0.5 \times \text{MIC}$), 10% glucose + vancomycin ($0.5 \times \text{MIC}$), and 10% glucose + linezolid ($0.5 \times \text{MIC}$) after 24 h (H24) and 16 weeks (W16). The log-transformed averages of relative fold changes of NSA1077 in different environmental media compared with NSA1077 in Luria-Bertani (LB) medium for 24 h and 16 weeks are presented. The error bars represent the standard deviations from the three independent RNA preparations. Significant differences from the NSA1077 in LB medium for 24 h and 16 weeks using Dunnett's test are indicated. *, $p < 0.01$; ***, $p < 0.001$.

Globally, the expression of studied genes was not significantly affected in strains pre-cultivated in WLM alone (Supplementary Materials Table S4).

2.4.1. Addition of 10% Glucose

After 24 h of exposure to WLM and 10% glucose, *spa* gene, which encodes protein A (a major colonizing factor), was significantly decreased in all the infecting *S. aureus* strains ($p < 0.05$ to $p < 0.001$) (Supplementary Materials Table S4). Moreover, the two toxinogenic *pvl* and *edn-B* genes were significantly upregulated ($p < 0.001$) in the two strains harboring these genes: NSA1077 (Figure 2) and NSA7475 (Supplementary Materials Table S4).

No modification in the expression of any tested gene was noted in the colonizing strain NSA1385 (Supplementary Materials Table S4).

The same trend was observed after a long exposure of the infecting strains in WLM supplemented with 10% glucose: *hla*, which encodes the α -hemolysin (another major virulence factor); *sea*, which encodes the staphylococcal enterotoxins (exotoxins with pyrogenicity, superantigenicity, and capacity to enhance lethality of endotoxin); and the global regulator of the staphylococcal virulence, *agr* genes, were significantly down-regulated ($p < 0.001$) (Supplementary Materials Table S4, Figure 3). Moreover, the expressions of the toxinogenic PVL- and EDIN-encoding genes were also significantly decreased ($p < 0.001$) (Supplementary Materials Table S4, Figure 2). In contrast, *spa* and *fnbA* genes were signifi-

cantly over-produced when *S. aureus* strains were pre-cultivated in WLM supplemented with 10% glucose ($p < 0.001$) (Supplementary Materials Table S4, Figure 3).

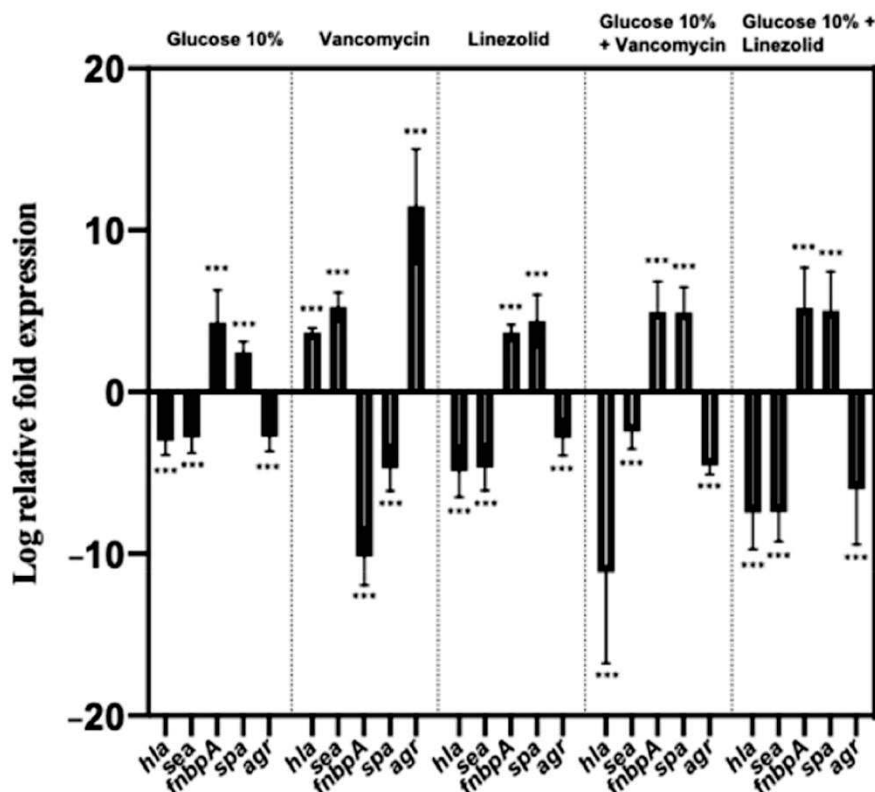


Figure 3. Relative mRNA expression levels of virulence genes and a regulator gene of *S. aureus* NSA739 strain cultivated in WLM supplemented with 10% glucose, vancomycin ($0.5 \times \text{MIC}$), linezolid ($0.5 \times \text{MIC}$), 10% glucose + vancomycin ($0.5 \times \text{MIC}$), and 10% glucose + linezolid ($0.5 \times \text{MIC}$) after a long exposure (16 weeks). The log-transformed averages of relative fold changes of NSA739 in different environmental media compared with NSA739 in LB medium are presented. The error bars represent the standard deviations from the three independent RNA preparations. Significant differences from the NSA739 in LB medium using Dunnett's test are indicated. ***, $p < 0.001$.

The expression of the studied genes was not modified in any conditions of pre-cultivation for the colonizing strain NSA1385 (Supplementary Materials Table S4).

2.4.2. Addition of Antibiotics

With sub-MIC of vancomycin: Short pre-cultivation of the infecting *S. aureus* strains in WLM plus vancomycin (24 h) did not significantly modify the expression of the virulence genes tested (Supplementary Materials Table S4).

After a long exposure of the infecting strains with the WLM + sub-MIC of vancomycin, *hla*, *sea*, and *agr* genes were significantly up-regulated ($p < 0.001$). In contrast, the expression of *fnbpA* and *spa* genes was significantly decreased ($p < 0.001$) (Supplementary Materials Table S4, Figure 3). Interestingly, although *pvl* gene was not affected by this pre-cultivation, the toxinogenic *edinB* gene was significantly under-expressed ($p < 0.001$) (Supplementary Materials Table S4, Figure 2).

No significant modification in the expression of any studied gene was observed for any pre-cultivating conditions of the colonizing strain NSA1385 (Supplementary Materials Table S4).

With sub-MIC of vancomycin + 10% glucose: The infecting *S. aureus* strains pre-cultivated for 24 h presented a significant increase of *fnbpA*, *spa*, *pvl*, and *edinB* expression ($p < 0.001$) (Supplementary Materials Table S4). Moreover, a decrease of the expression of *hla* gene was noted for NSA1077 ($p < 0.05$).

Contrary to the results with WLM plus vancomycin alone, *hla*, *sea*, and *agr* genes were significantly down-regulated after a long exposure of the infecting strains in WLM + glucose + vancomycin ($p < 0.001$) (Supplementary Materials Table S4, Figure 3). Moreover, the expression of *fnbpA* and *spa* genes was significantly increased ($p < 0.001$) (Supplementary Materials Table S4, Figure 3). Finally, the PVL- and EDIN-encoding genes were significantly under-expressed ($p < 0.001$) (Supplementary Materials Table S4, Figure 2).

After a long exposure of the colonizing strain NSA1385 to the medium, an increased expression of *fnbpA* gene ($p < 0.001$) and a decrease of *hla* gene ($p < 0.05$) (Supplementary Materials Table S4) were observed.

With sub-MIC of linezolid: After a 24 h exposure of the infecting strains in the WLM + linezolid, *hla*, *sea*, and *spa* genes were significantly down-regulated (with the exception of *spa* gene in NSA739) ($p < 0.05$ to $p < 0.001$). In contrast, the expression of *fnbpA* gene was notably increased in NSA739 ($p < 0.001$) (Supplementary Materials Table S2). Interestingly, while PVL-encoding genes were over-produced in this condition, the toxinogenic *edinB* genes were significantly under-expressed ($p < 0.001$) (Supplementary Materials Table S4).

After a 16-week exposure of the infecting strains to WLM + linezolid, *hla*, *sea*, and *agr* genes were significantly down-regulated ($p < 0.001$) (Supplementary Materials Table S4, Figure 3). In contrast, the expressions of *fnbpA* and *spa* genes were significantly increased ($p < 0.001$) (Supplementary Materials Table S4, Figure 3). All the toxinogenic-encoding genes were significantly under-expressed ($p < 0.001$) (Supplementary Materials Table S4, Figure 2).

No significant modification of the expression of the studied genes was observed in any conditions of pre-cultivation for the colonizing strain NSA1385 (Supplementary Materials Table S4).

With sub-MIC of linezolid + 10% glucose: The addition of glucose replicated the results observed with linezolid alone. Two infecting *S. aureus* strains (NSA739 and NSA1077) pre-cultivated in this condition for 24 h presented a significant decrease of *hla* and *sea* genes' expression ($p < 0.05$), and the infecting strain NSA7475 showed a decrease of *spa* gene ($p < 0.001$) (Supplementary Materials Table S4). Moreover, an increase of the expression of *fnbpA* gene was noted for NSA739 ($p < 0.001$). The PVL-encoding gene was over-expressed in this condition ($p < 0.001$). The only difference concerned the toxinogenic *edinB* gene, which was not significantly modified (Supplementary Materials Table S4).

These different observations were replicated after a long exposure, with a significant decrease of expression of *hla*, *sea*, and *agr* genes ($p < 0.001$) and a significant over-expression of *fnbpA* and *spa* genes ($p < 0.001$) (Supplementary Materials Table S4, Figure 3). The PVL- and EDIN-encoding genes were significantly under-expressed in this condition ($p < 0.001$) (Supplementary Materials Table S4, Figure 2).

Finally, the colonizing strain NSA1385 was significantly affected after a long exposure, with a decrease of *hla* gene expression ($p < 0.05$) and an increase of *fnbpA* gene expression ($p < 0.001$) (Supplementary Materials Table S4).

3. Discussion

The host–microbiota interface is often the key point in the development of wound infections. Various studies have described the DFU microbiota to determine the role of microorganisms [33]. Although they have produced interesting results and confirmed that the microbiota is a highly dynamic microbial community that maintains a relationship with the host, better understanding of the complex competitive or synergistic interaction between commensal and/or pathogenic microorganisms is necessary as it could affect the severity and progression of the wound [7]. The virulence capacity of a bacterium has a direct impact on the equilibrium between colonization and infection [34]. However, in

chronic wounds, bacteria can adapt their virulence, such as forming a polymicrobial biofilm community [35]. These biofilms may be responsible for the delayed healing of these chronic wounds [36]. Bacterial interactions play an important role in pathogenesis, competing and cooperating in order to support their mutual growth in a specific environment [37]. However, it seems that the behavior of bacteria can also be greatly influenced by the environmental conditions [24]. Here, we evaluated the role of a high glucose concentration and sub-MICs of two antibiotics in a WLM mimicking the conditions encountered in DFU on a series of clinical bacterial strains isolated from this clinical situation. To study bacterial virulence, most studies have previously used in vitro planktonic cultures on rich media or in vivo diabetes animal models (e.g., db/db mice), but without the ability to create genuine wound chronicity [7]. The WLM represents a convenient and reliable model to study bacteria in a relevant environment [29,30].

Using the WLM, we observed that this environment clearly impacts bacterial behavior, and its virulence. Firstly, we observed that a long exposure of *S. aureus* in the medium significantly decreased the bacterial virulence in a *C. elegans* model (Table 3). Moreover, the addition of 10% glucose (a condition similar to that encountered in DFU) more drastically affected the behavior of the infecting bacteria (Table 4): the strains significantly decreased their virulence in the nematodes model (Table 3), in parallel with dramatic under-expression of the virulent genes (and decreased β -hemolytic activity) and an over-expression of genes involved in adhesion and colonization (Figure 3, Supplementary Materials Supplementary Materials Table S4), as observed by Kalan et al. [38]. The bacterial stress induced by the glucose accelerated biofilm formation (Figure 1) and significantly increased SCV phenotypes (Table 2). These observations support previous clinical studies demonstrating that biofilms were implicated in 60 to 80% of chronic wounds versus 6% for acute wounds [39,40]. Bacteria within biofilms evade the host's natural defenses and are resistant to the host immune defense. Stimulation of the immune system without effectively eradicating the infection causes collateral damage to surrounding tissue and causes chronic inflammation [41]. This persistent chronic inflammation, exacerbated by the diabetic immune context, leads to the production of auto-inflammatory cytokines that aggravate the wound and slow the healing process. The influence of glucose on bacterial virulence has been studied by Regassa et al. [42]. They noted that glucose inhibited the expression of *agr* gene in *S. aureus*. The effect on this regulator gene directly reduced the virulence expression, as observed in our study. Moreover, the influence of glucose on the poly-*N*-acetylglucosamine synthesis, the most common components of biofilm in *S. aureus*, has been previously described [43–45]. Glucose stimulates the *gbaAB* operon that regulates biofilm formation through activating the expression of the *ica* operon in *S. aureus*. GbaA is modulated by inducing compounds and facilitates *S. aureus* to adapt to stress via aggregation of biofilm formation [46], as we found here. Interestingly, the response of neutrophils towards *S. aureus* also varies depending on the available glucose. *S. aureus*-mediated NET (neutrophil extracellular trap) release (a process used by neutrophils to kill or trap pathogens) is impaired at a high glucose concentration [47], notably due to an ejection of NET by vesicles outside neutrophils [48]. NET diffusion contributes to extensive tissue damage in the host and could participate in wound chronicity.

Antistaphylococcal regimens must be taken into account in the influence on bacterial virulence, as previously determined [24]. In our study, we observed that vancomycin and linezolid acted differentially on *S. aureus* virulence. This could be explained by the impact of these antibiotics on the expression of regulation of several virulence genes, possibly affecting the expression of the *agr* system. Previous in vitro studies have shown a decreased level of virulence expression upon treatment with ribosomally active antibiotics [24]. Here, the same trend was noted when the bacteria were pre-cultivated in WLM plus linezolid for 24 h. This effect was amplified after a long exposure (16 weeks) to the WLM, especially when combined with a high glucose concentration and sub-MIC of the antibiotic (Figures 2 and 3), applying stress involving a rapid biofilm formation and consistent with the development of a hyper-adhesive phenotype, as previously observed [49]. Studies have shown

that linezolid was a potent inhibitor of *hla* and *sea* genes' expression in a concentration-dependent manner owing to a positive regulation of *agr* gene [24]. Our results confirmed that these three genes were clearly affected in the same manner by the environmental condition encountered in DFI, while these genes were significantly over-expressed in the presence of sub-MICs of linezolid alone or in combination with glucose (Table 4). The effect of linezolid on *agr* expression is of importance. The link between the dysfunction of this major virulence regulatory system in *S. aureus* and chronic infections has been described [50]. As we noted in our study, this gene plays a crucial role in the evolution to persister cells' formation and SCVs under antibiotic pressure [50]. The negative impact of linezolid on hemolytic activity has also been noted [51]. Moreover, sub-MICs of linezolid induced a decrease in *spa* expression [21,52]. Although this trend was observed in all the studied strains after a short exposure (24 h) (Supplementary Materials Table S4), the opposite results were observed after a long exposure in the WLM plus linezolid alone or in combination with glucose, suggesting that *S. aureus* clearly modified its virulence in this environment.

Table 4. Overview of effect of glucose and sub-MIC antibiotic concentrations on *S. aureus* virulence expression from an in vitro wound-like medium (WLM) mimicking the conditions encountered in chronic wounds.

	Effect on Expression of Virulence Factor ¹			
	PVL	EDIN	Alpha-Hemolysin	Protein A
Short exposure in WLM added to				
Glucose	↑↑	↑↑	-	↓
Vancomycin	-	-	-	-
Linezolid	↑↑	↓	↓	↓
Long exposure in WLM added to				
Glucose	↓	↓	↓	↑
Vancomycin	-	↓↓	↑	↓
Linezolid	↓↓	↓↓	↓	↑

¹ ↑, significant increase; ↑↑, >8-fold significant increase; ↓, significant decrease; ↓↓, >8-fold significant decrease; -, no significant effect.

The influence of vancomycin on bacterial virulence was totally different compared with linezolid exposure. This antibiotic had limited effects on *S. aureus* virulence after a short exposure, as previously published [24]. In *C. elegans*, no significant modification of bacterial virulence could be noted (Table 3). As seen above, the impact of antibiotics on *agr* expression is crucial. Vancomycin increased the expression of this regulator influencing the virulence by acting on the expression of several virulence genes and by limiting the colonizing behaviour of the bacteria. This trend was confirmed by a huge impact of vancomycin to β -hemolytic activity and the low presence of SCVs even after prolonged exposure in the WLM. Vancomycin-induced upregulation of enterotoxin expression has previously been described during the first 8 h in an in vitro hollow-fiber infection model, followed by a downregulation [53]. Our study confirmed this result. Moreover, previous studies indicated that the effects of vancomycin on *spa* expression were variable [24]. We confirmed that this antibiotic had no relevant impact when used in sub-MIC after a short exposure. In contrast, a significant decrease of *spa* expression was found after a long exposure in the WLM (Table 4).

Finally, the addition of glucose and antistaphylococcal antibiotics demonstrated the main influence of glucose on the bacterial virulence. If the association of glucose plus linezolid impacted more negatively the expressions of *S. aureus* virulence genes, the combination of glucose and vancomycin was clearly influenced by glucose, while a reversed effect of vancomycin alone on genes' expression level was observed. This is probably due to preferentially interaction between glucose and regulatory genes of *S. aureus* virulence. Further investigations must be developed to confirm this trend.

The PVL is the most studied bi-component leukotoxin produced by *S. aureus* [6]. This toxin confers cytotoxicity on neutrophils and monocytes-macrophages, leading to a

high virulence [54]. The PVL-positive strains are responsible for SSTIs, severe necrotizing pneumonia, and aggressive bone and joint infections [55–57]. In DFI, the role of PVL in the pathogenicity of *S. aureus* is not clearly established. Firstly, the PVL-producing strains are rarely isolated from this pathology [6]. Its prevalence varies between countries: France (~3%), Algeria, and The Netherlands (~14%) [6]. Classically, the different PVL clones are equally distributed among the various DFI grades. The majority of Grade 1 ulcers where PVL-positive strains were isolated had a rapid clinical amelioration [31]. Moreover, no strains harboring *pvl* gene have been isolated from diabetic foot osteomyelitis (DFOM) [58]. In this study, we explored the impact of environmental conditions on the expression of this gene. We observed that NSA1077 presented a significant decrease of the *pvl* expression after a long exposure in the WLM plus glucose, linezolid, and glucose + linezolid and glucose + vancomycin (Table 4). The antitoxin effect of sub-MICs of linezolid has been previously published [24]. This antibiotic induced concentration-dependent decreases in *pvl* expression and PVL production. Surprisingly, the *pvl* expression was strongly increased after a short exposure to linezolid, in contrast to previous publications. One hypothesis could be the role of the medium used in this study. Interestingly, we observed the same effect when the bacteria were exposed to glucose + linezolid, although to a lesser degree (Figure 2). Sub-MICs of vancomycin have no relevant impact on *pvl* expression [24]. Despite confirming this trend in our study after 24 h exposure to this antibiotic, we observed a significant effect when vancomycin was combined with 10% glucose, with an increase of *pvl* expression after 24 h and a strong decrease of expression after 16 weeks. We suggest that the observed effect was mainly due to glucose.

The same trend was also observed for EDIN toxins. These proteins are members of a group of major bacterial virulence factors targeting host Rho GTPases [59]. Recent findings suggest that EDIN toxins might favor bacterial dissemination in tissues by a hematogenous route, through the induction of large transcellular tunnels in endothelial cells named macroapertures [60–62]. In addition, Munro et al. showed that EDIN toxins promote the formation of infection foci in a mouse model of bacteremia [63]. Previous studies on the prevalence of *edin* genes in DFI showed that these genes are rarely isolated in this pathology [64]. EDIN might collaborate with the arsenal of *S. aureus* virulence factors to confer a higher potential for systemic infection [60]. However, bacteremia is a rare complication in DFI [5], possibly because of the impact of environment, as we observed in this work. Altogether, our study corroborates that *S. aureus* can adapt to different environments and infection phases; this adaptation is modulated by tight transcriptional and (post)translational regulation of its virulence factors.

4. Conclusions

DFI is a complex environment where multiple bacterial species coexist. The interface between host and bacteria directly affects the healing of the wound. In these chronic ulcers, the virulence of bacteria is influenced by their intrinsic virulence profile and virulent factor equipment, but also by the environmental conditions and the phenotypic switch that these environmental stresses induce. Here, we showed that toxinogenic and non-toxinogenic *S. aureus* decreased their virulence in a WLM mimicking the conditions encountered in chronic wounds or/and required to establish chronic wounds. Our observations deserve to be placed in perspective with the clinical situation and epidemiological data where toxinogenic strains are absent from DFI or DFOM, suggesting that these strains have no clear virulence in this context. Subsequent studies are required to understand how bacteria could adapt their virulence in chronic conditions and to correlate these in vitro data using clinical strains. Such studies are pivotal for better ways to manage of DFU and could help in defining new therapeutics.

5. Materials and Methods

5.1. Bacterial Strains and Growth Conditions

All bacterial strains used in this study are listed in Table 1.

NSA739, 1077, and 7475 are infecting strains isolated from deep DFI. The strain 1077 was PVL+ and EDIN-B+; the strain 7475 was EDIN-B+. NSA1385 was a colonizing strain isolated from an uninfected ulcer, and NSA739 was isolated from DFI.

The avirulent *Escherichia coli* OP50 was used as a food source and a control for the nematode assays.

We used the in vitro WLM adapted from De Leon et al. that mimics the conditions encountered in the wound [30]. Briefly, the WLM contained 45% Bolton broth, 50% bovine plasma, and 5% laked horse red blood cells. A 1 mL volume of WLM was placed in a 14.5 cm by 1.8 cm glass tube, inoculated with approximately 10^4 to 10^5 CFU of *S. aureus*. The strains were grown in different conditions described in Figure 1. Thus, bacteria were grown at 37 °C with shaking at 220 rpm in WLM supplemented with 10% glucose and/or sub-inhibitory concentration of antibiotics (sub-MICs, 0.5× MIC linezolid and vancomycin). Every day, the optical density was adjusted to OD 0.1. Cultures were maintained for 16 weeks (Figure 1).

The vancomycin and linezolid MICs were determined for each strain by the microdilution method in Mueller–Hinton (MH) as recommended by the European Committee for Antimicrobial Susceptibility Testing (EUCAST) [65]. The impact of sub-MIC exposure for 16 weeks on MICs of the different *S. aureus* strains was evaluated each week. No significant difference could be noted (less than threefold dilution). However, the concentration of antibiotics used in the prolonged cultures was always adapted to these MICs.

Then, 100 µL samples of culture were plated on Columbia agar supplemented with 5% fresh sheep blood (bioMérieux, Marcy l’Étoile, France) at 37 °C each week to assess the loss of beta-hemolysin in each condition.

5.2. Nematode Killing Assay

The *C. elegans* infection assay was performed as previously described using the Fer-15 mutant line, which has a temperature sensitive fertility defect [66]. Fer-15 was provided by the Caenorhabditis Genetics Center, which is funded by the NIH National Center for Research Resources (NCRR). To synchronize the growth of nematodes, eggs were collected using the hypochlorite method. Overnight cultures of *E. coli* strains in nematode growth medium (NGM) were harvested, centrifuged, washed once, and suspended in phosphate buffered saline solution (PBS) at pH 7.0 at a concentration of 10^5 CFU/mL. NGM agar plates were inoculated with 10 µL of bacterial suspension in different conditions (without pre-incubation in WLM, after pre-incubation in WLM alone or with 10% glucose, sub-MICs of vancomycin or linezolid) and incubated at 37 °C for 8–10 h. Plates were brought back to room temperature and seeded with L4 stage *C. elegans* (≈30 per plate). Plates were then incubated at 25 °C and scored each day for live nematode under a stereomicroscope (Leica MS5). A nematode was considered dead when it no longer responded to touch. *C. elegans* that died from being trapped by the wall of the plate were excluded from the analysis.

At least three replicates repeated twice were performed for each selected strain. Lethal time 50% (LT50) corresponded to time (in days) required to kill 50% of the nematodes. The definition of virulence is limited to a narrow definition of virulence and the direct impact of *S. aureus* on the mortality of the worms. Three replicates were performed for each condition.

5.3. Feeding Behavior Assays

For occupancy assays, each bacterial strain was cultured overnight at 25 °C in LB media, spotted as a circular lawn on NGM plates, and dried at room temperature for 20 min. Approximately 30 L4 animals were placed in the center of the bacteria lawn. The number of nematodes inside or outside each lawn was counted after 16 h, as previously described [66]. The results were described in percent occupancy corresponding to the number of *C. elegans*

in the bacterial lawn/the total number of nematodes. The experiments were performed in triplicate.

The number of bacteria within the *C. elegans* digestive tract was obtained as previously described [67]. Briefly, nematodes were picked at 72 h, and the surface bacteria were removed by washing the nematodes twice in M9 medium containing 25 µg/mL gentamicin. The *C. elegans* were then mechanically disrupted in M9 medium containing 1% Triton X-100 [56]. Serial dilutions of the sample were then plated on LB-agar and the colonies were counted after 24 h. Three replicates were performed for each strain.

5.4. Biofilm Formation

To evaluate the biofilm formation, we used the Biofilm ring Test[®] (BioFilm Control[®], Saint Beauzire, France) following the manufacturer recommendations [68]. Briefly, standardized bacterial cultures were incubated at 37 °C in 96-well microtiter plates in the presence of magnetic beads. At set time-points, the plates were placed onto a magnetic block and put in the reader. The images of each well before and after magnetic attraction were analyzed with the BioFilm Control software, which gives a biofilm index (BFI). A high BFI value (>7) corresponds to high mobility of the beads under magnetic action (no biofilm), while a low value (<2) corresponds to full immobilization of the beads due to the sessile cells. Three experiments with two repeats were performed per strain and per incubation time.

All the experiments were performed in BHI medium (=control) as recommended by the manufacturer. To study the impact of different conditions tested on biofilm formation, the strains were pre-cultured for 24 h or 16 weeks in WLM with or without 10% glucose and sub-MICs of vancomycin or linezolid. The experiments were done in BHI (the WLM was not adapted to the technology).

5.5. qRT-PCR Assays

Virulence genes' expressions of *S. aureus* were quantified under different stress conditions after 24 h and 16 weeks. The virulence and regulator genes tested were adhesins (*fimbA*, *spa*), toxins (*hla*, *pvl*, *sea*, *edinB*), and the global regulator *agr* (Supplementary Materials Table S5).

Briefly, overnight *S. aureus* cultures obtained in different media were diluted to an OD₆₀₀ of 0.1 in MH broth and cultured again until an OD₆₀₀ of 0.7 was reached. The OD at 600 nm was then adjusted to 0.75 in Tris buffer (10 mM). A 1.5 mL aliquot of OD-adjusted and washed bacterial suspension was centrifuged at 10,000 × g for 10 min, and the pellets were treated with lysostaphin (Sigma) at a final concentration of 200 µg/mL. Total RNA from bacteria pellets was extracted as described by the manufacturer using Qiagen RNeasy Mini kit (Qiagen, Courtaboeuf, France) during exponential stages. RNA was treated with the RNase-Free DNase Set (Qiagen, Courtaboeuf, France). Purity and concentration were determined using the NanoDrop[™] 2000 spectrophotometer (Fisher Scientific, Pittsburgh, PA, USA). cDNA was synthesized from 1 µg of total RNA for each sample, using the iScript[™] Select cDNA Synthesis Kit (Bio-Rad) with random primers according to the manufacturer's instructions.

Real-time PCR assays were performed in a LightCycler[®] 480 device using the LightCycler FastStart DNA Master^{PLUS} SYBRGreen I kit (Roche, Meylan, France) with 100 ng of cDNA and 10 pmol of target primers (Supplementary Materials Table S5) [18,69–74]. The specificity of the PCR products was tested by melting point analysis. Amplifications were performed in triplicate from three different RNA preparations. The $2^{-\Delta\Delta CT}$ method was used to analyze transcriptional changes in target genes using *gyrB* as the housekeeping control gene (Supplementary Materials Table S5). Error bars indicate the standard deviation (SD) of three independent experiments. Cycle threshold (*Ct*) values of the different target genes were compared with the *Ct*-values of the house-keeping gene (*gyrB*). The normalized relative expressions of the studied genes were obtained for each strain following the equation: $2^{-\Delta\Delta Ct}$ ($\Delta\Delta Ct = (Ct_{\text{gene}} - Ct_{\text{gyrB}})_{\text{studied strain in different conditions}} -$

$(Ct_{\text{gene}} - Ct_{\text{gyrB}})_{\text{studied strain in LB medium}}$) [75]. The results obtained for each gene were log-transformed to obtain a fold change difference between strains and conditions used.

5.6. Statistical Analysis

Statistics and graphs were prepared using the software package (GraphPad Prism 8.0, GraphPad Software, San Diego, CA, USA).

The comparison between the behavior of *S. aureus* in the in vitro medium alone versus in different conditions was assessed using one-way analysis of variance (ANOVA) followed by Dunnett's multiple comparisons test.

For the nematode killing assays, differences in survival rates between the different strains were tested by a log-rank (Mantel-cox) test for statistical significance.

Log-transformed data were used for qRT-PCR. The effects of the different additions to the WLM medium on the expression of selected genes and a regulator of *S. aureus* were assessed using one-way analysis of variance (ANOVA), followed by Dunnett's multiple comparisons test.

The kinetics of biofilm formation were compared by two-way ANOVA, followed by Dunnett's multiple comparison test.

A $p < 0.05$ was considered to reflect a statistically significant difference.

Supplementary Materials: The following are available online at <https://www.mdpi.com/2072-6651/13/3/230/s1>, Table S1: Phenotypical modifications of *S. aureus* cultivated in an in vitro wound-like medium (WLM) mimicking the conditions encountered in chronic wounds and with the addition of high glucose concentration and antibiotics during 24 h. Table S2: Evaluation of feeding behavior by measuring bacterial content of *C. elegans* and pathogen avoidance of *S. aureus* cultivated in an in vitro wound-like medium (WLM) mimicking the conditions encountered in chronic wounds and with the addition of high glucose concentration and antibiotics during 16 weeks. Table S3: Effects of a preculture in a WLM and glucose 10% associated or not to sub-MICs of vancomycin ($0.5 \times \text{MIC}$) and linezolid ($0.5 \times \text{MIC}$) on *S. aureus* biofilm formation after 24 h of culture. The kinetics of the early phase of biofilm formation were determined on (a) NSA739; (b) NSA1077; (c) NSA7475; and (d) NSA1385 by the BioFilm ring test® (BioFilm Control, France). The results represent the mean of BFI for at least three independent replicates. Table S4: Relative mRNA expression levels of virulence genes of four *S. aureus* strains cultivated in a WLM added with glucose 10%, vancomycin ($0.5 \times \text{MIC}$), linezolid ($0.5 \times \text{MIC}$), glucose 10% + vancomycin ($0.5 \times \text{MIC}$), and glucose 10% + linezolid ($0.5 \times \text{MIC}$) after 24 h (H24) and 16 weeks (W16). Table S5: Primers used in the study.

Author Contributions: Conceptualization, C.P., A.S., F.L., E.L., C.D.-R. and J.-P.L.; methodology, C.D.-R. and J.-P.L.; validation, F.L. and A.T.; formal analysis, C.P., C.-A.G. and C.N.-E.; investigation, C.P., C.-A.G. and C.N.-E.; writing—original draft preparation, C.P. and J.-P.L.; writing—review and editing, C.-A.G., C.N.-E., F.L., E.L., A.T., A.S. and C.D.-R.; visualization: F.L. and A.T.; supervision, C.D.-R. and J.-P.L.; project investigation: A.S., C.D.-R. and J.-P.L.; funding acquisition: A.S. and J.-P.L. All authors have read and agreed to the published version of the manuscript.

Funding: Cassandra Pouget's PhD is supported by a CIFRE grant (Biofilm Pharma).

Institutional Review Board Statement: Not applicable.

Informed Consent Statement: Not applicable.

Data Availability Statement: Data sharing not applicable.

Acknowledgments: We thank Sarah Kabani for her editing assistance. We thank the Nîmes University hospital for its structural, human, and financial support through the award obtained by our team during the internal call for tenders "Thématiques phares". The authors belong to the FHU InCh (Federation Hospitalo Universitaire Infections Chroniques, Aviesan).

Conflicts of Interest: The authors declare no conflict of interest. The funders had no role in the design of the study; in the collection, analyses, or interpretation of data; in the writing of the manuscript; or in the decision to publish the results.

References

1. Armstrong, D.G.; Boulton, A.J.; Bus, S.A. Diabetic foot ulcers and their recurrence. *N. Engl. J. Med.* **2017**, *376*, 2367–2375. [[CrossRef](#)]
2. Lecube, A.; Pachón, G.; Petriz, J.; Hernández, C.; Simó, R. Phagocytic activity is impaired in type 2 diabetes mellitus and increases after metabolic improvement. *PLoS ONE* **2011**, *6*, e23366. [[CrossRef](#)]
3. Tesfaye, S.; Boulton, A.J.; Dyck, P.J.; Freeman, R.; Horowitz, M.; Kempner, P.; Lauria, G.; Malik, R.A.; Spallone, V.; Vinik, A.; et al. Diabetic neuropathies: Update on definitions, diagnostic criteria, estimation of severity, and treatments. *Diabetes Care* **2010**, *33*, 2285–2293. [[CrossRef](#)] [[PubMed](#)]
4. Chawla, R.; Chawla, A.; Jaggi, S. Microvascular and macrovascular complications in diabetes mellitus: Distinct or continuum? *Indian J. Endocrinol. Metab.* **2016**, *20*, 546–551. [[CrossRef](#)]
5. Bakker, K.; Apelqvist, J.; Lipsky, B.A.; Van Netten, J.J.; Schaper, N.C.; International Working Group on the Diabetic Foot (IWGDF). The 2015 IWGDF guidance documents on prevention and management of foot problems in diabetes: Development of an evidence-based global consensus. *Diabetes Metab. Res. Rev.* **2016**, *32*, 2–6. [[CrossRef](#)] [[PubMed](#)]
6. Duniach-Remy, C.; Essebe, C.N.; Sotto, A.; Lavigne, J.-P. *Staphylococcus aureus* toxins and diabetic foot ulcers: Role in pathogenesis and interest in diagnosis. *Toxins* **2016**, *8*, 209. [[CrossRef](#)]
7. Pouget, C.; Duniach-Remy, C.; Pantel, A.; Schuldiner, S.; Sotto, A.; Lavigne, J.-P. Biofilms in diabetic foot ulcers: Significance and clinical relevance. *Microorganisms* **2020**, *8*, 1580. [[CrossRef](#)]
8. Chakraborty, S.P.; Mahapatra, S.K.; Sahu, S.K.; Chattopadhyay, S.; Pramanik, P.; Roy, S. Nitric oxide mediated *Staphylococcus aureus* pathogenesis and protective role of nanoconjugated vancomycin. *Asian Pac. J. Trop. Biomed.* **2011**, *1*, 102–109. [[CrossRef](#)]
9. Josse, J.; Laurent, F.; Diot, A. Staphylococcal adhesion and host cell invasion: Fibronectin-binding and other mechanisms. *Front. Microbiol.* **2017**, *8*, 2433. [[CrossRef](#)] [[PubMed](#)]
10. Falugi, F.; Kim, H.K.; Missiakas, D.M.; Schneewind, O. Role of protein A in the evasion of host adaptive immune responses by *Staphylococcus aureus*. *mBio* **2013**, *4*, e00575-13. [[CrossRef](#)]
11. Bisognano, C.; Vaudaux, P.; Rohner, P.; Lew, D.P.; Hooper, D.C. Induction of fibronectin-binding proteins and increased adhesion of quinolone-resistant *Staphylococcus aureus* by subinhibitory levels of ciprofloxacin. *Antimicrob. Agents Chemother.* **2000**, *44*, 1428–1437. [[CrossRef](#)] [[PubMed](#)]
12. Harraghy, N.; Kormanec, J.; Wolz, C.; Homerova, D.; Goerke, C.; Ohlsen, K.; Qazi, S.; Hill, P.; Herrmann, M. *Sae* is essential for expression of the staphylococcal adhesins Eap and Emp. *Microbiology* **2005**, *151*, 1789–1800. [[CrossRef](#)] [[PubMed](#)]
13. Saeed, K.; Gould, I.; Esposito, S.; Ahmad-Saeed, N.; Ahmed, S.S.; Alp, E.; Bal, A.M.; Bassetti, M.; Bonnet, E.; Chan, M.; et al. Panton–Valentine leukocidin-positive *Staphylococcus aureus*: A position statement from the international society of chemotherapy. *Int. J. Antimicrob. Agents* **2018**, *51*, 16–25. [[CrossRef](#)] [[PubMed](#)]
14. Courjon, J.; Munro, P.; Benito, Y.; Visvikis, O.; Bouchiat, C.; Boyer, L.; Doye, A.; Lepidi, H.; Ghigo, E.; Lavigne, J.-P.; et al. EDIN-B promotes the translocation of *Staphylococcus aureus* to the bloodstream in the course of pneumonia. *Toxins* **2015**, *7*, 4131–4142. [[CrossRef](#)] [[PubMed](#)]
15. Franke, G.C.; Böckenholt, A.; Sugai, M.; Rohde, H.; Aepfelbacher, M. Epidemiology, variable genetic organization and regulation of the EDIN-B toxin in *Staphylococcus aureus* from bacteraemic patients. *Microbiology* **2010**, *156*, 860–872. [[CrossRef](#)]
16. Grumann, D.; Nübel, U.; Bröker, B.M. *Staphylococcus aureus* toxins—Their functions and genetics. *Infect. Genet. Evol.* **2014**, *21*, 583–592. [[CrossRef](#)]
17. Tuscherr, L.; Löffler, B.; Proctor, R.A. Persistence of *Staphylococcus aureus*: Multiple metabolic pathways impact the expression of virulence factors in small-colony variants (SCVs). *Front. Microbiol.* **2020**, *11*, 1028. [[CrossRef](#)]
18. Heravi, F.S.; Zakrzewski, M.; Vickery, K.; Malone, M.; Hu, H. Metatranscriptomic analysis reveals active bacterial communities in diabetic foot infections. *Front. Microbiol.* **2020**, *11*, 1688. [[CrossRef](#)]
19. Richard, J.-L.; Lavigne, J.-P.; Sotto, A. Diabetes and foot infection: More than double trouble. *Diabetes Metab. Res. Rev.* **2012**, *28*, 46–53. [[CrossRef](#)]
20. Dumitrescu, O.; Boisset, S.; Badiou, C.; Bes, M.; Benito, Y.; Reverdy, M.E.; Vandenesch, F.; Etienne, J.; Lina, G. Effect of anti-biotics on *Staphylococcus aureus* producing panton-valentine leukocidin. *Antimicrob. Agents Chemother.* **2007**, *51*, 1515–1519. [[CrossRef](#)]
21. Otto, M.P.; Martin, E.; Badiou, C.; Lebrun, S.; Bes, M.; Vandenesch, F.; Etienne, J.; Lina, G.; Dumitrescu, O. Effects of subinhibitory concentrations of antibiotics on virulence factor expression by community-acquired methicillin-resistant *Staphylococcus aureus*. *J. Antimicrob. Chemother.* **2013**, *68*, 1524–1532. [[CrossRef](#)] [[PubMed](#)]
22. O'Brien, D.J.; Gould, I.M. Does vancomycin have a future in the treatment of skin infections? *Curr. Opin. Infect. Dis.* **2014**, *27*, 146–154. [[CrossRef](#)]
23. Mauriello, C.T.; Hair, P.S.; Rohn, R.D.; Rister, N.S.; Krishna, N.K.; Cunnion, K.M. Hyperglycemia inhibits complement-mediated immunological control of *S. aureus* in a rat model of peritonitis. *J. Diabetes Res.* **2014**, *2014*, 762051. [[CrossRef](#)]
24. Hodille, E.; Rose, W.; Diep, B.A.; Goutelle, S.; Lina, G.; Dumitrescu, O. The role of antibiotics in modulating virulence in *Staphylococcus aureus*. *Clin. Microbiol. Rev.* **2017**, *30*, 887–917. [[CrossRef](#)]
25. Yang, D.; Wijenayaka, A.R.; Solomon, L.B.; Pederson, S.M.; Findlay, D.M.; Kidd, S.P.; Atkins, G.J. Novel insights into *Staphylococcus aureus* deep bone infections: The involvement of osteocytes. *mBio* **2018**, *8*, e00415-18.
26. Bui, L.M.; Turnidge, J.D.; Kidd, S.P. The induction of *Staphylococcus aureus* biofilm formation or small colony variants is a strain-specific response to host-generated chemical stresses. *Microbes Infect.* **2015**, *17*, 77–82. [[CrossRef](#)] [[PubMed](#)]

27. Bui, L.M.G.; Hoffmann, P.; Turnidge, J.D.; Zilm, P.S.; Kidd, S.P. Prolonged growth of a clinical *Staphylococcus aureus* strain selects for a stable small-colony-variant cell type. *Infect. Immun.* **2014**, *83*, 470–481. [[CrossRef](#)]
28. Lee, J.; Zilm, P.S.; Kidd, S.P. Novel Research Models for *Staphylococcus aureus* small colony variants (SCV) development: Co-pathogenesis and Growth Rate. *Front. Microbiol.* **2020**, *11*, 321. [[CrossRef](#)]
29. Sun, Y.; Dowd, S.E.; Smith, E.; Rhoads, D.D.; Wolcott, R.D. In vitro multispecies Lubbock chronic wound biofilm model. *Wound Repair Regen.* **2008**, *16*, 805–813. [[CrossRef](#)]
30. DeLeon, S.; Clinton, A.; Fowler, H.; Everett, J.; Horswill, A.R.; Rumbaugh, K.P. Synergistic interactions of *Pseudomonas aeruginosa* and *Staphylococcus aureus* in an in vitro wound model. *Infect. Immun.* **2014**, *82*, 4718–4728. [[CrossRef](#)] [[PubMed](#)]
31. Sotto, A.; Lina, G.; Richard, J.-L.; Combescure, C.; Bourg, G.; Vidal, L.; Jourdan, N.; Etienne, J.; Lavigne, J.-P. Virulence Potential of *Staphylococcus aureus* strains isolated from diabetic foot ulcers: A new paradigm. *Diabetes Care* **2008**, *31*, 2318–2324. [[CrossRef](#)]
32. Sotto, A.; Richard, J.-L.; Messad, N.; Molinari, N.; Jourdan, N.; Schuldiner, S.; Sultan, A.; Carrière, C.; Canivet, B.; Landraud, L.; et al. Distinguishing colonization from infection with *Staphylococcus aureus* in diabetic foot ulcers with miniaturized oligonucleotide arrays: A French multicenter study. *Diabetes Care* **2012**, *35*, 617–623. [[CrossRef](#)] [[PubMed](#)]
33. Liu, C.; Ponsero, A.J.; Armstrong, D.G.; Lipsky, B.A.; Hurwitz, B.L. The dynamic wound microbiome. *BMC Med.* **2020**, *18*, 1–12. [[CrossRef](#)] [[PubMed](#)]
34. Spichler, A.; Hurwitz, B.L.; Armstrong, D.G.; Lipsky, B.A. Microbiology of diabetic foot infections: From Louis Pasteur to ‘crime scene investigation’. *BMC Med.* **2015**, *13*, 2. [[CrossRef](#)] [[PubMed](#)]
35. Dowd, S.E.; Wolcott, R.D.; Sun, Y.; McKeehan, T.; Smith, E.; Rhoads, D. Polymicrobial nature of chronic diabetic foot ulcer biofilm infections determined using bacterial tag encoded flx amplicon pyrosequencing (bTEFAP). *PLoS ONE* **2008**, *3*, e3326. [[CrossRef](#)] [[PubMed](#)]
36. Pereira, S.G.; Moura, J.; Carvalho, E.; Empadinhas, N. Microbiota of chronic diabetic wounds: Ecology, impact, and potential for innovative treatment strategies. *Front. Microbiol.* **2017**, *8*, 1791. [[CrossRef](#)]
37. Hibbing, M.E.; Fuqua, C.; Parsek, M.R.; Peterson, S.B. Bacterial competition: Surviving and thriving in the microbial jungle. *Nat. Rev. Genet.* **2009**, *8*, 15–25. [[CrossRef](#)] [[PubMed](#)]
38. Kalan, L.R.; Meisel, J.S.; Loesche, M.A.; Horwinski, J.; Soaita, I.; Chen, X.; Uberoi, A.; Gardner, S.E.; Grice, E.A. Strain- and Species-Level variation in the microbiome of diabetic wounds is associated with clinical outcomes and therapeutic efficacy. *Cell Host Microbe* **2019**, *25*, 641–655.e5. [[CrossRef](#)]
39. James, G.A.; Swogger, E.; Wolcott, R.; Pulcini, E.D.; Secor, P.; Sestrich, J.; Costerton, J.W.; Stewart, P.S. Biofilms in chronic wounds. *Wound Repair Regen.* **2008**, *16*, 37–44. [[CrossRef](#)]
40. Malone, M.; Bjarnsholt, T.; McBain, A.; James, G.; Stoodley, P.; Leaper, D.; Tachi, M.; Schultz, G.; Swanson, T.; Wolcott, R. The prevalence of biofilms in chronic wounds: A systematic review and meta-analysis of published data. *J. Wound Care* **2017**, *26*, 20–25. [[CrossRef](#)]
41. Clinton, A.; Carter, T. Chronic wound biofilms: Pathogenesis and potential therapies. *Lab. Med.* **2015**, *46*, 277–284. [[CrossRef](#)]
42. Regassa, L.B.; Couch, J.L.; Betley, M.J. Steady-state staphylococcal enterotoxin type C mRNA is affected by a product of the accessory gene regulator (AGR) and by glucose. *Infect. Immun.* **1991**, *59*, 955–962. [[CrossRef](#)] [[PubMed](#)]
43. Gotz, F. *Staphylococcus* and biofilms. *Mol. Microbiol.* **2002**, *43*, 1367–1378. [[CrossRef](#)] [[PubMed](#)]
44. Waldrop, R.; McLaren, A.; Calara, F.; McLemore, R. Biofilm growth has a threshold response to glucose in vitro. *Clin. Orthop. Relat. Res.* **2014**, *472*, 3305–3310. [[CrossRef](#)] [[PubMed](#)]
45. Bischoff, M.; Wonnenberg, B.; Nippe, N.; Nyffenegger-Jann, N.J.; Voss, M.; Beisswenger, C.; Sunderkötter, C.; Molle, V.; Dinh, Q.T.; Lammert, F.; et al. CcpA affects infectivity of *Staphylococcus aureus* in a hyperglycemic environment. *Front. Cell. Infect. Microbiol.* **2017**, *7*, 172. [[CrossRef](#)] [[PubMed](#)]
46. You, Y.; Xue, T.; Cao, L.; Zhao, L.; Sun, H.; Sun, B. *Staphylococcus aureus* glucose-induced biofilm accessory proteins, GbaAB, influence biofilm formation in a PIA-dependent manner. *Int. J. Med. Microbiol.* **2014**, *304*, 603–612. [[CrossRef](#)] [[PubMed](#)]
47. Cohen, T.S.; Takahashi, V.; Bonnell, J.; Tovchigrechko, A.; Chaerkady, R.; Yu, W.; Jones-Nelson, O.; Lee, Y.; Raja, R.; Hess, S.; et al. *Staphylococcus aureus* drives expansion of low-density neutrophils in diabetic mice. *J. Clin. Investig.* **2019**, *129*, 2133–2144. [[CrossRef](#)] [[PubMed](#)]
48. Shaji, B.V.; Shaji, S.; Haritha, V.H.; Pramod, S.; Anie, Y. Calcium depletion at high glucose concentration promotes vesicle-mediated NET release in response to *Staphylococcus aureus*. *Mol. Immunol.* **2020**, *124*, 211–217. [[CrossRef](#)]
49. Rasigade, J.-P.; Moulay, A.; Lhoste, Y.; Tristan, A.; Bes, M.; Vandenesch, F.; Etienne, J.; Lina, G.; Laurent, F.; Dumitrescu, O. Impact of sub-inhibitory antibiotics on fibronectin-mediated host cell adhesion and invasion by *Staphylococcus aureus*. *BMC Microbiol.* **2011**, *11*, 263. [[CrossRef](#)]
50. Häffner, N.; Bär, J.; Haunreiter, V.D.; Shambat, S.M.; Seidl, K.; Crosby, H.A.; Horswill, A.R.; Zinkernagel, A.S. Intracellular environment and AGR System affect colony size heterogeneity of *Staphylococcus aureus*. *Front. Microbiol.* **2020**, *11*, 1415. [[CrossRef](#)]
51. Gemmell, C.G.; Ford, C.W. Virulence factor expression by Gram-positive cocci exposed to sub-inhibitory concentrations of linezolid. *J. Antimicrob. Chemother.* **2002**, *50*, 665–672. [[CrossRef](#)]
52. Bernardo, K.; Pakulat, N.; Fleer, S.; Schnaith, A.; Utermöhlen, O.; Krut, O.; Müller, S.; Krönke, M. Subinhibitory concentrations of linezolid reduce *Staphylococcus aureus* virulence factor expression. *Antimicrob. Agents Chemother.* **2004**, *48*, 546–555. [[CrossRef](#)] [[PubMed](#)]

53. Pichereau, S.; Pantrangi, M.; Couet, W.; Badiou, C.; Lina, G.; Shukla, S.K.; Rose, W.E. Simulated antibiotic exposures in an in vitro hollow-fiber infection model influence toxin gene expression and production in community-associated methicillin-resistant *Staphylococcus aureus* Strain MW2. *Antimicrob. Agents Chemother.* **2011**, *56*, 140–147. [CrossRef] [PubMed]
54. Boyle-Vavra, S.; Daum, R.S. Community-acquired methicillin-resistant *Staphylococcus aureus*: The role of Pantone–Valentine leukocidin. *Lab. Investig.* **2006**, *87*, 3–9. [CrossRef]
55. Vandenesch, F.; Lina, G.; Henry, T. *Staphylococcus aureus* hemolysins, bi-component leukocidins, and cytolytic peptides: A redundant arsenal of membrane-damaging virulence factors? *Front. Cell. Infect. Microbiol.* **2012**, *2*, 12. [CrossRef] [PubMed]
56. Shallcross, L.J.; Fragaszy, E.; Johnson, A.M.; Hayward, A.C. The role of the Pantone–Valentine leukocidin toxin in staphylococcal disease: A systematic review and meta-analysis. *Lancet Infect. Dis.* **2013**, *13*, 43–54. [CrossRef]
57. Gillet, Y.; Issartel, B.; Vanhems, P.; Fournet, J.-C.; Lina, G.; Bes, M.; Vandenesch, F.; Piémont, Y.; Brousse, N.; Floret, D.; et al. Association between *Staphylococcus aureus* strains carrying gene for Pantone–Valentine leukocidin and highly lethal necrotising pneumonia in young immunocompetent patients. *Lancet* **2002**, *359*, 753–759. [CrossRef]
58. Senneville, E.; Brière, M.; Neut, C.; Messad, N.; Lina, G.; Richard, J.-L.; Sotto, A.; Lavigne, J.-P. First report of the predominance of clonal complex 398 *Staphylococcus aureus* strains in osteomyelitis complicating diabetic foot ulcers: A national French study. *Clin. Microbiol. Infect.* **2014**, *20*, O274–O277. [CrossRef]
59. Boquet, P.; Lemichez, E. Bacterial virulence factors targeting Rho GTPases: Parasitism or symbiosis? *Trends Cell Biol.* **2003**, *13*, 238–246. [CrossRef]
60. Boyer, L.; Doye, A.; Rolando, M.; Flatau, G.; Munro, P.; Gounon, P.; Clément, R.; Pulcini, C.; Popoff, M.R.; Mettouchi, A.; et al. Induction of transient macroapertures in endothelial cells through RhoA inhibition by *Staphylococcus aureus* factors. *J. Cell Biol.* **2006**, *173*, 809–819. [CrossRef]
61. Lemichez, E.; Lecuit, M.; Nassif, X.; Bourdoulous, S. Breaking the wall: Targeting of the endothelium by pathogenic bacteria. *Nat. Rev. Genet.* **2009**, *8*, 93–104. [CrossRef] [PubMed]
62. Rolando, M.; Munro, P.; Stefani, C.; Auberger, P.; Flatau, G.; Lemichez, E. Injection of *Staphylococcus aureus* EDIN by the *Bacillus anthracis* protective antigen machinery induces vascular permeability. *Infect. Immun.* **2009**, *77*, 3596–3601. [CrossRef] [PubMed]
63. Munro, P.; Benchetrit, M.; Nahori, M.-A.; Stefani, C.; Clément, R.; Michiels, J.-F.; Landraud, L.; Dussurget, O.; Lemichez, E. The *Staphylococcus aureus* epidermal cell differentiation inhibitor toxin promotes formation of infection foci in a mouse model of bacteremia. *Infect. Immun.* **2010**, *78*, 3404–3411. [CrossRef] [PubMed]
64. Messad, N.; Landraud, L.; Canivet, B.; Lina, G.; Richard, J.-L.; Sotto, A.; Lavigne, J.-P.; Lemichez, E. Distribution of edin in *Staphylococcus aureus* isolated from diabetic foot ulcers. *Clin. Microbiol. Infect.* **2013**, *19*, 875–880. [CrossRef] [PubMed]
65. The European Committee on Antimicrobial Susceptibility Testing. Breakpoint Tables for Interpretation of MICs and Zone Diameters. Version 10.0. 2020. Available online: http://www.eucast.org/fileadmin/src/media/PDFs/EUCAST_files/Breakpoint_tables/v_10.0_Breakpoint_Tables.pdf (accessed on 8 February 2021).
66. Essebe, C.N.; Visvikis, O.; Fines-Guyon, M.; Vergne, A.; Cattoir, V.; Lecoustumier, A.; Lemichez, E.; Sotto, A.; Lavigne, J.-P.; Dunyach-Remy, C. Decrease of *Staphylococcus aureus* virulence by *Helicobacterium kunzii* in a *Caenorhabditis elegans* model. *Front. Cell. Infect. Microbiol.* **2017**, *7*, 77. [CrossRef]
67. Garsin, D.A.; Sifri, C.D.; Mylonakis, E.; Qin, X.; Singh, K.V.; Murray, B.E.; Calderwood, S.B.; Ausubel, F.M. A simple model host for identifying Gram-positive virulence factors. *Proc. Natl. Acad. Sci. USA* **2001**, *98*, 10892–10897. [CrossRef]
68. Chavant, P.; Gaillard-Martinie, B.; Talon, R.; Hebraud, M.; Bernardi, T. A new device for rapid evaluation of biofilm formation potential by bacteria. *J. Microbiol. Methods* **2007**, *68*, 605–612. [CrossRef]
69. Qiu, J.; Feng, H.; Xiang, H.; Wang, D.; Xia, L.; Jiang, Y.; Song, K.; Lu, J.; Yu, L.; Deng, X. Influence of subinhibitory concentrations of licochalcone A on the secretion of enterotoxins A and B by *Staphylococcus aureus*. *FEMS Microbiol. Lett.* **2010**, *307*, 135–141. [CrossRef]
70. Dumitrescu, O.; Choudhury, P.; Boisset, S.; Badiou, C.; Bes, M.; Benito, Y.; Wolz, C.; Vandenesch, F.; Etienne, J.; Cheung, A.L.; et al. Beta-lactams interfering with PBP1 induce Pantone–Valentine leukocidin expression by triggering sarA and rot global regulators of *Staphylococcus aureus*. *Antimicrob. Agents Chemother.* **2011**, *55*, 3261–3271. [CrossRef]
71. Munro, P.; Clément, R.; Lavigne, J.P.; Pulcini, C.; Lemichez, E.; Landraud, L. High prevalence of edin-C encodign RhoA-targeting toxin in clinical isolates of *Staphylococcus aureus*. *Eur. J. Clin. Microbiol. Infect. Dis.* **2011**, *30*, 965–972. [CrossRef]
72. Atshan, S.S.; Shamsudin, M.N.; Karunanidhi, A.; Van Belkum, A.; Lung, L.T.T.; Sekawi, Z.; Nathan, J.J.; Ling, K.H.; Seng, J.S.C.; Ali, A.M.; et al. Quantitative PCR analysis of genes expressed during biofilm development of methicillin resistant *Staphylococcus aureus* (MRSA). *Infect. Genet. Evol.* **2013**, *18*, 106–112. [CrossRef] [PubMed]
73. Labandeira-Rey, M.; Couzon, F.; Boisset, S.; Brown, E.L.; Bes, M.; Benito, Y.; Barbu, E.M.; Vazquez, V.; Höök, M.; Etienne, J.; et al. *Staphylococcus aureus* Pantone–valentine leukocidin causes necrotizing pneumonia. *Science* **2007**, *315*, 1130–1133. [CrossRef] [PubMed]
74. Garzoni, C.; Francois, P.; Huyghe, A.; Couzinet, S.; Tapparel, C.; Charbonnier, Y.; Renzoni, A.; Lucchini, S.; Lew, D.P.; Vaudaux, P.; et al. A global view of *Staphylococcus aureus* whole genome expression upon internalization in human epithelial cells. *BMC Genom.* **2007**, *8*, 171. [CrossRef] [PubMed]
75. Livak, K.J.; Schmittgen, T.D. Analysis of relative gene expression data using real-time quantitative PCR and the 2(-Delta Delta C(T)) method. *Methods* **2001**, *25*, 402–408. [CrossRef]

Supplementary Materials: Adaptation of *Staphylococcus aureus* in a Medium Mimicking a Diabetic Foot Environment

Cassandra Pouget, Claude-Alexandre Gustave, Christelle Ngba-Essebe, Frédéric Laurent, Emmanuel Lemichez, Anne Tristan, Albert Sotto, Catherine Dunyach-Rémy and Jean-Philippe Lavigne

Table S1. Phenotypical modifications of *S. aureus* cultivated in an in vitro wound-like medium (WLM) mimicking the conditions encountered in chronic wounds and with the addition of high glucose concentration and antibiotics during 24 h.

	NSA739		NSA1077		NSA7475		NSA1385	
	Beta-Hemolysis	SCV	Beta-Hemolysis	SCV	Beta-Hemolysis	SCV	Beta-Hemolysis	SCV
WLM alone	100%	0%	100%	0%	100%	0%	100%	0%
WLM + glucose 10%	100%	0%	100%	0%	100%	0%	100%	0%
WLM + vancomycin	100%	0%	100%	0%	100%	0%	100%	0%
WLM + linezolid	100%	0%	100%	0%	100%	0%	100%	0%
WLM + glucose 10% + vancomycin	100%	0%	100%	0%	100%	0%	100%	0%
WLM + glucose 10% + linezolid	100%	0%	100%	0%	100%	0%	100%	0%

Table S2. Evaluation of feeding behavior by measuring bacterial content of *C. elegans* and pathogen avoidance of *S. aureus* cultivated in an in vitro wound-like medium (WLM) mimicking the conditions encountered in chronic wounds and with the addition of high glucose concentration and antibiotics during 16 weeks.

	NSA739		NSA1077		NSA7475		NSA1385	
	Intestine Survival *	Occupancy Test	Intestine Survival	Occupancy Test	Intestine Survival	Occupancy Test	Intestine Survival	Occupancy Test
Without preculture	5.1 10E5	96 ±3%	6.4 10E5	94 ±5%	4.8 10E5	97 ±3%	5.3 10E5	98 ±2%
WLM alone	4.7 10E5	94 ±5%	5.2 10E5	92 ±4%	4.6 10E5	94 ±5%	5.4 10E5	99 ±2%
WLM + glucose 10%	3.6 10E5	92 ±6%	5.6 10E5	89 ±6%	4.9 10E5	96 ±5%	5.0 10E5	95 ±4%
WLM + vancomycin	5.5 10E5	96 ±2%	5.0 10E5	93 ±3%	4.2 10E5	96 ±4%	5.4 10E5	93 ±5%
WLM + linezolid	6.2 10E5	98 ±2%	4.4 10E5	90 ±5%	4.6 10E5	92 ±6%	4.9 10E5	97 ±2%
WLM + glucose 10% + vancomycin	4.8 10E5	92 ±4%	5.7 10E5	91 ±4%	5.0 10E5	97 ±2%	5.2 10E5	97 ±3%
WLM + glucose 10% + linezolid	3.3 10E5	95 ±3%	5.1 10E5	92 ±6%	4.5 10E5	98 ±2%	5.5 10E5	94 ±4%

Table S3. Effects of a preculture in a WLM and glucose 10% associated or not to sub-MICs of vancomycin (0.5× MIC) and linezolid (0.5× MIC) on *S. aureus* biofilm formation after 24 h of culture. The kinetics of the early phase of biofilm formation were determined on a) NSA739; b) NSA1077; c) NSA7475; d) NSA1385 by the BioFilm ring test® (BioFilm Control, France). The results represent the mean of BFIs for at least three independent replicates.

NSA739 24 h						NSA1077 24 h					
	0 h	2 h	3 h	4 h	5 h		0 h	2 h	3 h	4 h	5 h
Control BHI medium	15.0	14.7	7.5	2.7	1.8	Control BHI medium	14.4	13.2	8.4	3.9	1.9
Glucose 10%	14.9	14.5	7.9	3.1	1.9	Glucose 10%	14.3	13.8	8.6	4.0	2.0
Vancomycin	14.7	14.6	7.2	2.7	1.9	Vancomycin	14.4	13.2	8.2	3.6	1.9
Linezolid	15.1	14.8	7.7	3.0	2.0	Linezolid	14.2	13.5	8.5	3.7	1.8
Glucose 10% + Vancomycin	15.2	14.9	7.8	2.9	1.9	Glucose 10% + Vancomycin	14.3	13.4	8.3	3.5	1.7
Glucose 10% + Linezolid	14.8	14.6	7.1	2.7	1.8	Glucose 10% + Linezolid	14.1	13.1	8.1	3.6	1.8
NSA7475 24 h						NSA1385 24 h					
	0 h	2 h	3 h	4 h	5 h		0 h	2 h	3 h	4 h	5 h
Control BHI medium	15.6	15.1	8.6	3.5	2.3	Control BHI medium	15.1	7.3	2.2	1.7	1.5
Glucose 10%	15.2	14.9	8.3	3.1	2.2	Glucose 10%	15.3	7.5	2.3	1.8	1.4
Vancomycin	15.3	15.0	8.5	3.4	2.1	Vancomycin	15.4	7.4	2.2	1.6	1.6
Linezolid	14.9	14.7	8.4	3.4	2.2	Linezolid	14.8	7.2	2.1	1.7	1.5
Glucose 10% + Vancomycin	15.4	14.9	8.6	3.3	2.2	Glucose 10% + Vancomycin	15.1	7.4	2.4	1.9	1.5
Glucose 10% + Linezolid	14.9	14.6	8.5	3.1	2.1	Glucose 10% + Linezolid	15.3	7.7	2.4	1.7	1.6

Table S4. Relative mRNA expression levels of virulence genes of four *S. aureus* strains cultivated in a WLM added with glucose 10%, vancomycin (0.5× MIC), linezolid (0.5× MIC), glucose 10% + vancomycin (0.5× MIC) and glucose 10% + linezolid (0.5× MIC) after 24 h (H24) and 16 weeks (W16).

		NSA739 H24	NSA739 W16	1077 H24	1077 W16	7475 H24	7475 W16	1385 H24	1385 W16
WLM alone	<i>hla</i>	1.1	-1.88	1.22	-1.92	1.14	-1.78	1.04	-1.25
	<i>sea</i>	1.21	-1.82	1.25	-1.76	1.09	-1.44	1.16	-1.33
	<i>fnbA</i>	-0.26	1.79	1.04	1.84	1.16	1.56	-0.12	1.21
	<i>spa</i>	-0.34	1.84	-0.22	1.59	1.21	1.66	-0.25	1.52
	<i>agr</i>	1.17	-1.8	1.08	-1.83	1.1	-1.59	1.07	-1.39
	<i>edinB</i>	ND	ND	1.45	-1.66	1.02	1.39	ND	ND
	<i>lukFS-PV</i>	ND	ND	1.55	-1.72	ND	ND	ND	ND
WLM + Glucose 10%	<i>hla</i>	1.22	-3.07	1.29	-5.14	1.08	-7.59	1.58	-1.05
	<i>sea</i>	1.27	-2.89	1.25	-1.84	1.03	-2.61	1.14	-1.67
	<i>fnbA</i>	-1.96	4.04	-1.8	3.38	-1.95	3.08	-1.13	1.52
	<i>spa</i>	-2.46	2.39	-7.66	3.44	-2.96	2.47	-1.7	1.77
	<i>agr</i>	1.89	-2.82	1.91	-2.58	1.87	-2.72	1.67	-1.42
	<i>edinB</i>	ND	ND	10.37	-6.1	8.15	-7.41	ND	ND
	<i>lukFS-PV</i>	ND	ND	8.12	-4.02	ND	ND	ND	ND
WLM + Vancomycin	<i>hla</i>	1.6	3.72	1.61	2.25	1.07	2.45	1.19	1.22
	<i>sea</i>	1.93	5.14	1.37	2.04	1.23	3.17	1.14	1.3
	<i>fnbA</i>	-1.19	-9.68	-1.31	-3.31	-1.4	-4.29	-1.01	-1.07
	<i>spa</i>	-1.85	-4.32	-1.1	-2.01	-1.06	-3.71	-1.07	-1.66
	<i>agr</i>	1.97	10.65	1.95	2.07	1.16	2.41	1.19	1.08
	<i>edinB</i>	ND	ND	-1.28	-15.38	-1.4	-9.66	ND	ND
	<i>lukFS-PV</i>	ND	ND	1.88	-1.2	ND	ND	ND	ND
WLM + Linezolid	<i>hla</i>	-2.37	-4.57	-2.15	-3.03	-2.03	-3.31	-1.14	-1.05
	<i>sea</i>	-2.58	-4.37	-2.05	-3.38	-2.06	-2.49	-1.42	-1.21
	<i>fnbA</i>	2.34	3.78	1.93	3.39	1.74	2.1	1.49	1.36
	<i>spa</i>	-1.58	4.25	-3.34	2.44	-3.65	8.99	1.06	1.98
	<i>agr</i>	-1.28	-2.31	-1.56	-2.04	-1.28	-2.85	-1.36	-1.17
	<i>edinB</i>	ND	ND	-2.26	-22.66	-3.22	-14.38	ND	ND
	<i>lukFS-PV</i>	ND	ND	12.51	-12.18	ND	ND	ND	ND
WLM + Glucose + Vancomycin	<i>hla</i>	-1.48	-11.67	-2.1	-8.96	-1.5	-12.52	-1.12	-2.01
	<i>sea</i>	-1.42	-2.21	-1.38	-6.03	-1.89	-6.56	-1.1	-1.67
	<i>fnbA</i>	3.47	5.34	2.9	4.08	2.56	2.93	1	3.78
	<i>spa</i>	2.84	4.61	2.19	5.71	3.33	8.31	1.31	1.99
	<i>agr</i>	-1.97	-4.49	-1.46	-6.37	-1.23	-2.88	-1.27	-1.76
	<i>edinB</i>	ND	ND	3.6	-11.6	2.42	-13.14	ND	ND
	<i>lukFS-PV</i>	ND	ND	4.96	-22.96	ND	ND	ND	ND
WLM + Glucose + Linezolid	<i>hla</i>	-2.13	-8.24	-2.04	-5.09	-1.5	-7.26	-1.1	-2.08
	<i>sea</i>	-2.08	-7.09	-2.11	-2.29	-1.12	-3.17	-1.64	-1.68
	<i>fnbA</i>	2.61	4.6	1.24	2.23	1.13	6.82	1.37	2.84
	<i>spa</i>	-1.85	5.05	-1.99	6.25	-2.5	4.84	-1.19	1.62
	<i>agr</i>	-1.27	-4.78	-2.43	-2.12	-1.5	-2.43	-1.06	-1.9
	<i>edinB</i>	ND	ND	-1.34	-12.2	1.2	-13.07	ND	ND
	<i>lukFS-PV</i>	ND	ND	3.98	-22.32	ND	ND	ND	ND

Table S5. Primers used in the study.

Primer Use and Target Function	Target Region	Primer Name	Oligonucleotide Sequence	Tm (°C)	References
a hemolysin	<i>hla</i>	hla- F	5'- TCCAGTGCAATTGGTAGTCA -3'	55.3	[18]
		hla- R	5'- GGCTCTATGAAAGCAGCAGA-3'	57.3	
Enterotoxin a	<i>sea</i>	sea- F	5'- ATGGTGCTTATTATGGTTATC -3'	52.0	[69]
		sea- R	5'- CGTTTCCAAAGGTACTGTATT -3'	54.0	
PVL ^a	<i>pvl</i>	lukS-F	5'- AATAACGTATGGCAGAAATATGGATGT-3'	58.9	[70]
		lukS-R	5'- CAAATGCGTTGTGTATTCTAGATCCT-3'	60.1	
Edin	<i>edinB</i>	edinB-F	5'- GGTGACGTGAACAAATTATCCGA-3'	58.9	[71]
		edinB-R	5'- ATCTTTCTTTTGTATCAGAAAAGTTTA-3'	54.3	
MSCRAMM	<i>fnbpA</i>	fnbpA- F	5'- AAATTGGGAGCAGCATCAGT -3'	55.3	[72]
		fnbpA- R	5'- GCAGCTGAATTCCCATTTTC -3'	55.3	
Protein A	<i>spa</i>	spa-F	5'- TATGCCTAACTTAAATGCTG -3'	51.1	[73]
		spa- R	5'- TTGGAGCTTGAGAGTCATTA -3'	53.2	
Accessory gene regulator	<i>agrA</i>	agrA-F	5'- CAAAGAGAAAACATGGTTACCATTATTA -3'	58.2	[74]
		agrA-R	5'- CTCAAGCACCTCATAAGGATTATCAG -3'	61.6	
Housekeeping genes	<i>gyrB</i>	gyrB-F	5'- GGTGGCGACTTTGATCTAGC -3'	59.3	[73]
		gyrB-R	5'- TTATACAACGGTGGCTGTGC -3'	57.3	

Travail n°4 : Article Scientifique

A relevant wound-like *in vitro* media to study bacterial cooperation and biofilm in chronic wounds

Cassandra Pouget, Catherine Dunyach-Remy, Thierry Bernardi, Christian Provot, Jason Tasse, Albert Sotto and Jean-Philippe Lavigne

Soumis dans *Frontiers in Microbiology* le 5 Mai 2021

Résumé travail n°4 :

La publication précédente a montré la modulation du potentiel de virulence et de la capacité à former du biofilm des souches de *S. aureus* dans un environnement mimant les infections du pied diabétique. Ces premiers résultats nous ont hautement démontré l'importance de travailler sur des **modèles *in vitro*** proches de ce qui est observé au niveau du lit de la plaie afin de comprendre le comportement des bactéries responsables du processus infectieux. Aussi, nous avons voulu améliorer notre modèle *in vitro* précédemment décrit et se concentrer sur les caractéristiques de l'environnement « **plaies chronique** » en général et non plus uniquement pied diabétique. L'idée était qu'ensuite, nous pourrions compléter ce milieu de base, pour se rapprocher des diverses plaies chroniques existantes telles que les IPD (confer article précédent ; ajout de glucose, d'antibiotiques, condition anaérobie). La première partie de notre travail a alors été de référencer les données de **l'environnement microbiologique, cellulaire et inflammatoire** des plaies chroniques mais aussi les caractéristiques physico-chimiques telles que la température ou encore le pH présent.

Ce nouveau milieu innovant a été appelé **CWM « Chronic Wound-like Media »**, il a été développé pour étudier de manière plus précise le biofilm polymicrobien présent à la surface de la peau des plaies chroniques, facteur majeur du retard de cicatrisation. En effet, les interactions bactériennes qui régissent le biofilm sont des clés pour améliorer la prise en charge des infections chroniques.

Pour valider ce nouveau modèle *in vitro*, des souches cliniques de *S. aureus* et *P. aeruginosa* co-isolées d'infections chroniques ont été cultivées dans ce milieu pendant 24 heures en culture seule ou en association. Nous avons décidé de déterminer dans ledit milieu versus un milieu classique microbiologique (le milieu Brain Heart Infusion - BHI) plusieurs caractéristiques bactériennes via :

- Une étude de la **croissance bactérienne** par une cinétique à 24h
- Une étude phénotypique de la présence de **small colony variants** et de la pigmentation ou β - hémolyse des souches

- Une étude de la formation de **biofilm précoce** au travers de cinétique d'adhésion et de formation de biofilm en BioFilm Ring Test® (1 à 5 h)
- Une étude sur la quantité de **biofilm mature** produit en 24h et 48h en dénombrement
- Une étude de la **virulence** via un modèle *C. elegans*

Après 24h de culture dans le CWM, nous avons observé que seule la croissance de *S. aureus* était affectée par rapport au milieu contrôle, la phase stationnaire étant réduite de 2 log. De manière intéressante la croissance est augmentée quand les souches de *S. aureus* sont co-cultivées avec *P. aeruginosa*. Les études sur la virulence montrent que toutes les souches présentaient une virulence diminuée dans le modèle nématode lorsqu'elles étaient cultivées dans le CWM. Enfin, cette **réduction du potentiel de pathogénicité** est à corrélérer à une augmentation de la capacité de ces mêmes souches à former du biofilm plus rapidement en CWM. En effet, les souches arrivent à former un biofilm complètement mature en seulement 3h versus 5h lorsque cultivées dans un milieu témoin.

Dans cette étude nous avons donc confirmé l'impact de l'environnement sur diverses caractéristiques bactériennes. Nous avons aussi prouvé qu'au sein de la plaie chronique infectée, *S. aureus* et *P. aeruginosa* coopéraient. Finalement, ce modèle fournit un nouvel outil pour l'étude des coopérations bactériennes et de la compréhension du biofilm polymicrobien.



A relevant wound-like in vitro media to study bacterial cooperation and biofilm in chronic wounds

Cassandra POUGET¹, Catherine Dunyach-Remy², Thierry Bernardi³, Christian Provot³, Jason Tasse³, Albert Sotto², Jean-Philippe Lavigne^{2*}

¹INSERM U1047 Virulence bactérienne et maladies infectieuses, France, ²Centre Hospitalier Universitaire de Nîmes, France, ³BioFilm Pharma, France

Submitted to Journal:
Frontiers in Microbiology

Specialty Section:
Microbial Physiology and Metabolism

Article type:
Original Research Article

Manuscript ID:
705479

Received on:
05 May 2021

Journal website link:
www.frontiersin.org

Conflict of interest statement

The authors declare that the research was conducted in the absence of any commercial or financial relationships that could be construed as a potential conflict of interest

Author contribution statement

CP, JPL and AS drafted the manuscript. All authors contributed to manuscript revision, read and approved the submitted version.

Keywords

bacterial cooperation, Biofilm, chronic wound, in vitro medium, nematode killing assay, *Pseudomonas aeruginosa*, *Staphylococcus aureus*, Virulence

Abstract

Word count: 304

Biofilm on the skin surface of chronic wounds is an important factor in the pathology, inhibiting wound healing. The polymicrobial nature of these infected wounds and bacterial interactions inside this pathogenic biofilm are the keys for understanding chronic infection. The aim of our work was to develop an innovative in vitro medium that closely mimics the chronic wound emphasizing the microbiological, cellular and inflammatory environment of chronic wounds but also focusing on the pH found at the wound level. This new medium, called chronic wound medium (CWM), will thus facilitate the study of pathogenic biofilm organization. Clinical *Staphylococcus aureus* and *Pseudomonas aeruginosa* strains co-isolated from diabetic foot infection (DFI) were collected and cultivated in this new medium for 24h in mono- and co-culture. Bacterial growth (growth curves), presence of small colony variant (SCV), biofilm formation (BioFilm Ring Test® assay, biofilm biomass quantification) and virulence (survival curve in a *Caenorhabditis elegans* model) were evaluated. After 24h in the in vitro conditions, we observed that *P. aeruginosa* growth was not affected, compared with a control bacterial medium, whereas for *S. aureus*, the stationary phase was reduced by two logs. Interestingly, *S. aureus* growth increased when co-cultured with *P. aeruginosa* in CWM. In co-culture with *P. aeruginosa*, SCV forms of *S. aureus* were detected. Biofilm studies showed that bacteria, alone and in combination, formed biofilm faster (as soon as 3h) than the bacteria exposed in a control medium (as soon as 5h). The virulence of all strains decreased in the nematode model when cultivated in our new in vitro medium. Taken together, our data confirmed the impact of the chronic wound environment on biofilm formation and bacteria virulence. They indicated that *P. aeruginosa* and *S. aureus* cooperated in co-infected wounds. Therefore, this in vitro model provides a new tool for bacterial cooperation investigation and polymicrobial biofilm formation.

Contribution to the field

This study, presents a new affordable, convenient and reliable in vitro medium called chronic wound medium to study the bacterial interactions in the wound environment and to investigate their role inside the biofilm. The two main pathogens isolated from these wounds (*P. aeruginosa* and *S. aureus*) cooperated in this environment. This new medium gives some new insights in the understanding of the bacterial cooperation in chronic wounds.

Funding statement

This publication is a cooperation between Biofilm Pharma company (France) and our team to develop this new medium. Cassandra Pouget is recipient of a PhD grant from this company (CIFRE Grant). The funder's role participated in the development of the medium.

Ethics statements

Studies involving animal subjects

Generated Statement: No animal studies are presented in this manuscript.

Studies involving human subjects

Generated Statement: No human studies are presented in this manuscript.

Inclusion of identifiable human data

Generated Statement: No potentially identifiable human images or data is presented in this study.

In review

Data availability statement

Generated Statement: The original contributions presented in the study are included in the article/supplementary material, further inquiries can be directed to the corresponding author/s.

In review



A relevant wound-like *in vitro* media to study bacterial cooperation and biofilm in chronic wounds

1 **Cassandra Pouget^{1,2}, Catherine Dunyach-Remy³, Thierry Bernardi², Christian Provot², Jason**
2 **Tasse², Albert Sotto⁴, Jean-Philippe Lavigne^{3*}**

3 ¹ Virulence Bactérienne et Infections Chroniques, INSERM U1047, Université de Montpellier,
4 Nîmes, France

5 ² Biofilm Pharma, Saint Beauzire, France

6 ³ Virulence Bactérienne et Infections Chroniques, INSERM U1047, Université de Montpellier,
7 Department of Microbiology and Hospital Hygiene, CHU Nîmes, Univ Montpellier, Nîmes, France

8 ⁴ Virulence Bactérienne et Infections Chroniques, INSERM U1047, Université de Montpellier,
9 Department of Infectious and Tropical Diseases, CHU Nîmes, Nîmes, France

10

11 *** Correspondence:**

12 Prof. Jean-Philippe Lavigne

13 jean.philippe.lavigne@chu-nimes.fr

14 **Keywords: bacterial cooperation, biofilm, chronic wound, *in vitro* medium, nematode killing**
15 **assay, *Pseudomonas aeruginosa*, *Staphylococcus aureus*, virulence**

16

17 **Abstract**

18 Biofilm on the skin surface of chronic wounds is an important factor in the pathology, inhibiting wound
19 healing. The polymicrobial nature of these infected wounds and bacterial interactions inside this
20 pathogenic biofilm are the keys for understanding chronic infection. The aim of our work was to
21 develop an innovative *in vitro* medium that closely mimics the chronic wound emphasizing the
22 microbiological, cellular and inflammatory environment of chronic wounds but also focusing on the
23 pH found at the wound level. This new medium, called chronic wound medium (CWM), will thus
24 facilitate the study of pathogenic biofilm organization. Clinical *Staphylococcus aureus* and
25 *Pseudomonas aeruginosa* strains co-isolated from diabetic foot infection (DFI) were collected and
26 cultivated in this new medium for 24h in mono- and co-culture. Bacterial growth (growth curves),
27 presence of small colony variant (SCV), biofilm formation (BioFilm Ring Test® assay, biofilm
28 biomass quantification) and virulence (survival curve in a *Caenorhabditis elegans* model) were
29 evaluated. After 24h in the *in vitro* conditions, we observed that *P. aeruginosa* growth was not affected,
30 compared with a control bacterial medium, whereas for *S. aureus*, the stationary phase was reduced by
31 two logs. Interestingly, *S. aureus* growth increased when co-cultured with *P. aeruginosa* in CWM. In
32 co-culture with *P. aeruginosa*, SCV forms of *S. aureus* were detected. Biofilm studies showed that
33 bacteria, alone and in combination, formed biofilm faster (as soon as 3h) than the bacteria exposed in
34 a control medium (as soon as 5h). The virulence of all strains decreased in the nematode model when
35 cultivated in our new *in vitro* medium. Taken together, our data confirmed the impact of the chronic
36 wound environment on biofilm formation and bacteria virulence. They indicated that *P. aeruginosa*
37 and *S. aureus* cooperated in co-infected wounds. Therefore, this *in vitro* model provides a new tool for
38 bacterial cooperation investigation and polymicrobial biofilm formation.

39

40 1. Introduction

41 Chronic wounds are a major public health challenge worldwide. Skin diseases represent an important
42 human issue as well as an economic burden [1]. The incidence of chronic wounds is likely to be
43 underestimated. These pathologies are becoming increasingly frequent due to an aging population and
44 earlier development of chronic illnesses such as diabetes *mellitus*, among others [2]. Recent estimations
45 suggest that more than 7 million people are currently affected in the United States and 4 million people
46 in Europe, and this figure is expected to rise by two percent in the next decade [3]. Chronic wounds
47 are defined by four types of pathologies: diabetic foot ulcers (DFU), vascular ulcers (containing venous
48 and arterial ulcers), and pressure ulcers (PU) [4]. Infections are a common complication of these ulcers
49 delaying healing. They are associated with substantial morbidities, requiring frequent healthcare
50 provider visits, daily wound care, antimicrobial therapy, and surgical procedures with associated high
51 healthcare costs [5]. The difficulty in treating those non-healing wounds is partially caused by the
52 polymicrobial nature of the skin bed [6], in which microorganisms are organized in pathogenic biofilms
53 [7]. In order to better decipher biofilms and to find new anti-biofilm approaches, social traits of bacteria
54 and their interactions inside the matrix of extracellular polymeric substances (EPS) need to be explored.
55 The most frequent, and studied, interaction described in chronic wounds is that between
56 *Staphylococcus aureus* and *Pseudomonas aeruginosa*, due to the high prevalence of both species in
57 these wounds [8]. Some studies, especially in a cystic fibrosis context, have shown that *P. aeruginosa*
58 quickly killed *S. aureus* when grown together *in vitro* [9]. This killing is due to exoproducts of
59 *P. aeruginosa*, such as 4-hydroxy-2-heptylquinoline-N-oxide (HQNO) [10], the Pel and Psl products
60 [11], and pyocyanin [12]. However, more recent data suggested that the interaction between the species
61 could be symbiotic, with, for example, the secretion of *P. aeruginosa* alginate having a protective effect
62 on *S. aureus* [13,14]. So far, very few data are available concerning chronic wounds. The main
63 hypothesis is that both microorganisms are present, but occupy distinct regions of the wound without
64 interacting [15]. Recently, Alves et al. observed interactions between the two species influencing both
65 colonization and pathogenicity in this clinical situation [16]. The only *in vitro* model developed for the
66 study of multispecies biofilms at the wound level was the Lubbock model [17]. DeLeon et al. used it
67 to study interactions between *P. aeruginosa* and *S. aureus* inside the polymicrobial biofilm [18].
68 However, in all these studies, the experiments were performed under conditions that did not consider
69 the “clinical” environment of the chronic wounds. Indeed, to our knowledge, no culture media has been
70 used to study microorganisms closer to *in vivo* conditions considering wound parameters such as pH,
71 temperature, cellular and inflammatory environment, the presence of serum or the wound irrigation.
72 The aim of our work was to develop a new affordable, convenient and reliable *in vitro* medium to study
73 the bacterial interactions in the wound environment encountered in chronic wounds and to investigate
74 their role inside the biofilm.

75

76 2. Materials and Methods

77 2.1 Bacterial strains and culture conditions

78 All bacterial strains used in this study are listed in Table 1.

79 The *in vitro* chronic wound medium (CWM) is composed as follows: 79.5% of Bolton broth, 20% of
80 heat-inactivated human serum, 0.5% of hemolyzed human blood (Table 2). This medium, adapted from
81 Sun et al. [17], was complemented by adding 1.10^6 /mL of human keratinocytes debris (HaCaT cells).
82 Finally, the pH was adjusted to 8.0 by buffering with 10mM HEPES / NaOH. By adding serum and

Bacterial effect of chronic Wound medium

83 blood to the Bolton broth, the CWM mimics the three major constituents of the chronic wound bed:
84 red blood cells, serum and damaged tissues.

85 Bacteria were grown in bacterial culture tubes or in Erlenmeyer culture flasks under shaking at 200
86 rpm, 37°C in brain-heart infusion (BHI, Sigma-Aldrich) broth or in CWM.

87 2.2 Growth curves

88 Samples of the bacterial growing culture were collected at different time points, diluted in 1X
89 phosphate buffered saline ((PBS) Thermo Fisher Scientific, Gibco) and plated on non-selective agar
90 (Luria-Bertani agar, ThermoFisher Scientific) in monoculture or in selective agar when bacteria were
91 grown in co-culture (Mannitol salt agar for *S. aureus*, Oxoid and Cetrimide agar for *P. aeruginosa*,
92 Oxoid) to evaluate the number of CFU/mL. Co-cultures were initiated 1:1 starting with 4.10^4 CFU/mL.
93 Cultures were grown under the same conditions, with the same microbiological culture flask under
94 static and aerobic environment at 37°C for 24-hr. Each experiment was performed in triplicate.

95 2.3 Phenotypical characteristics of the strains

96 To investigate the impact of the co-culture on the strains physiology, the bacteria were plated before
97 and after co-culture in BHI or CWM. 20 µL of the suspension were inoculated onto Tryptic soy blood
98 agar (Sigma-Aldrich), without antibiotics, and incubated 48-72-hr at 37°C. Colonies were described
99 after 48 and 72-hr according to: presence/absence of β-hemolysis (for *S. aureus*), colony morphology,
100 and characteristic pigment production (for *P. aeruginosa*). Both *S. aureus* and *P. aeruginosa* with a
101 distinctive morphology (compatible with small colonies variants (SCV)) were sub-cultured onto
102 Tryptic soy blood agar plates 48-72-hr at 37°C to evaluate the reversibility of the colony morphology.

103 2.4 Kinetics of early biofilm formation

104 The early biofilm formation was assessed using BioFilm Ring Test® (BioFilm Control, Saint Beauzire,
105 France), as previously described [19] and according to the manufacturer's recommendations. This
106 assay allows the observation of the dynamic immobilization of superparamagnetic microbeads
107 embedded in biofilms. *P. aeruginosa* and *S. aureus* strains were sub-cultured on BHI agar (control)
108 and CWM agar at 37°C for 24-hr. Six colonies were inoculated into BHI broth as the control condition
109 or in CWM and homogenized. The bacterial suspension was standardized to an optical density at 600
110 nm of 1.00 ± 0.05 and diluted 1:250 in BHI broth or CWM (without human keratinocytes debris) to
111 obtain a final concentration of 4.10^6 CFU/mL using a defined calibration curve between OD and
112 CFU/mL. This bacterial suspension was complemented with 1% (v/v) magnetic beads (TON004).
113 200µL were then added, in triplicate, into a 96 well microplate (Falcon 96 Flat Bottom Transparent,
114 Corning, USA) for each time point (1, 3 and 5-hrs). The plates were incubated without shaking at 37°C.
115 After incubation, 100µL of liquid contrast (LIC001) solution was added on the top of each well. The
116 microplate was placed on a magnetic block for 5 minutes and scanned using the Biofilm Control plate
117 reader and the BFCE3 software provided by the company. Each experiment was performed twice in
118 triplicate. A negative control was systematically included in each experiment corresponding to the
119 medium and beads without bacterial suspension.

120 Spots were quantified through specialized image algorithms that measure beads aggregation. Biofilm
121 index (BFI) values were calculated for each well, ranging from 0 (no aggregation, i.e. biofilm
122 formation) to 20 (total aggregation, i.e. absence of biofilm formation). A BFI <2 represents the cut-off
123 for fixed biofilm.

124 2.5 Quantification of biofilm biomass

Bacterial effect of chronic wound medium

125 The mature biofilms were evaluated using bacterial quantification [20]. The optical density at 600nm
126 of overnight bacterial suspensions, in BHI broth or CWM, were adjusted to 1.00 ± 0.05 , before a 1:100
127 dilution in BHI broth or CWM. 200 μ L of each suspension were transferred to a microplate (Falcon 96
128 Flat Bottom Transparent, Corning, USA) in triplicate and incubated at 37°C, 5% CO₂ for 24-hr without
129 shaking. Negative control wells contained BHI broth or CWM alone. After incubation, the microplates
130 were washed three times with 200 μ L of 1X PBS. 200 μ L of 1X PBS was finally added into the well
131 before biofilm disruption. The disruption was performed by sonication for 10 min at 40 KHz. Each
132 well was then 10-fold serially diluted and the last dilution was plated on non-selective agar (LB agar)
133 or in selective agar when bacteria were grown in co-culture (Mannitol salt agar for *S. aureus* and
134 Cetrimide agar for *P. aeruginosa*). The agar plate was then incubated overnight at 37°C and CFUs
135 were counted. The experiment was performed twice for each sample. Experiments were performed
136 with either bacteria alone or in co-culture.

2.6 Nematode killing assay

138 The nematode infection assay was performed as described previously [21] using the Fer-15 mutant
139 line, a temperature sensitive fertility defect. Overnight cultures of *S. aureus* and *P. aeruginosa* strains
140 in BHI broth or CWM were incubated at 37°C under shaking. 100 μ L of the bacterial suspension were
141 spotted on nematode growth medium (NGM) agar. A control with the *Escherichia coli* OP50 strain
142 was used for nematodes. This bacterium is the standard feeding strain for Fer-15 since it shows no
143 pathogenic virulence factors. Around 30 L4 stage nematodes were then seeded on each plate and
144 incubated at 25°C. Every day, an independent reader scored the number of alive nematodes under a
145 stereomicroscope (Leica, France). The Lethal time 50% (LT50), which corresponds to time (in days)
146 required to kill 50% of the worms was calculated.

2.7 Statistics

148 t-test was used to compare the *in vitro* bacterial growth of the different strains as well as the comparison
149 of the early kinetics of biofilm formation and biofilm biomass. To compare overall survival curves in
150 nematode killing assays, a Cox regression was used. For pairwise comparison of two survival curves
151 in nematode killing assays, we used a log rank test. Statistical analyses were performed using GraphPad
152 Prism version 7 or R version 3.5.2. Tests used for the p-value determination are mentioned in each
153 figure legend.

154

3. Results**3.1 Modification of *S. aureus* growth in the *in vitro* CWM**

157 CWM is a medium developed to mimic the *in vivo* conditions encountered in chronic wounds. To
158 evaluate its effect on bacteria, we firstly compared the bacterial growth of two of the main
159 microorganisms isolated from chronic wounds in this new medium and in an usual microbiological
160 medium (BHI). Concerning *S. aureus*, we noted that the reference strain Newman presented a
161 significant decrease of the growth curves at early exponential phase in the CWM (Figure 1A) compared
162 to BHI ($p < 0.001$) and a difference of one log once the stationary phase reached ($p < 0.001$). The same
163 profile was observed for the clinical strain SAC1, with a clear delay of the early exponential phase and
164 a significant difference of 0.5 log at stationary phase of bacterial growth in the CWM vs BHI ($p < 0.01$)
165 (Figure 1C).

Bacterial effect of chronic Wound medium

166 For *P. aeruginosa*, no difference was observed in growth curves for the reference strain PAO1 in BHI
167 or CWM medium (Figure 1B). The clinical strain PAC1 had a reduced growth rate of the last part of
168 the exponential phase (after 8hr) and a slight difference of 0.2 log once the stationary phase reached
169 ($p=0.0874$ (not significant (NS)) (Figure 1D).

170 The phenotypic modifications of the bacteria are presented in Supplementary Table S1. Globally,
171 cultures in CWM showed significantly more SCVs and a loss of β -hemolysis by *S. aureus* and of
172 pigmentation by *P. aeruginosa* ($p<0.01$).

173 3.2 Co-culture of *P. aeruginosa* and *S. aureus* in the *in vitro* CWM

174 Due to the frequent co-isolation of *S. aureus* and *P. aeruginosa* in chronic wounds [15], we compared
175 the growth of the co-cultured reference and clinical strains on BHI and CWM. *P. aeruginosa* PAO1 –
176 *S. aureus* Newman were able to grow in co-culture in both media (Figure 2A). Moreover, no difference
177 in bacterial growth was seen when the strains were co-cultured ($p=0.32$ (NS)). Concerning the clinical
178 strains, both species were able to grow in a similar way in the two media ($p=0.21$ (NS)) (Figure 2B).
179 However, a slight decrease of SAC1 growth was observed in CWM ($p = 0.05$ at 8-hrs). Interestingly,
180 the delay of the early exponential phase of SAC1, observed between 0-4-hrs when SAC1 was cultivated
181 alone, was not present in co-culture. Moreover, SAC1 growth was modified in CWM. Indeed, when
182 co-cultured with *P. aeruginosa* PAC1, SAC1 seemed to reach its growth plateau faster at 6hrs versus
183 8hrs) and with higher bacterial load (log 9 vs log 8.7 in monoculture) compared to the growth of SAC1
184 alone (Figures 1C and 2B).

185 As observed with bacteria cultivated alone, the co-culture in CWM significantly increased the
186 morphotypes of SCVs and decreased the β -hemolysis of *S. aureus* and the presence of pigmentation of
187 *P. aeruginosa* ($p<0.01$) (Supplementary Table S2).

188 3.3 Impact of CWM on early biofilm formation

189 To determine the impact of CWM on the bacterial virulence and particularly on biofilm formation, we
190 used the BioFilm Ring Test® on *P. aeruginosa* or *S. aureus* cultivated alone. Firstly, we validated the
191 performance of the BioFilm Ring Test® using the CWM. At 1, 3 and 5-hr, the control conditions
192 showed that the microbeads were perfectly mobile in CWM, similar to results obtained in BHI medium
193 (Supplementary Table S3). This result confirmed that the CMW (without human keratinocytes debris)
194 could be used in this test without modification.

195 Secondly, we evaluated the kinetics of the early biofilm formation of both reference strains. We
196 observed that *S. aureus* Newman and *P. aeruginosa* PAO1 stucked very quickly to form a biofilm in
197 CWM compared to BHI (BFI= 3.7 ± 0.2 vs 19 ± 0.1 and 2 ± 0.2 vs 6.7 ± 0.3 , for *S. aureus* and
198 *P. aeruginosa*, respectively) ($p<0.01$) (Figure 3A). This significant difference was always observed at
199 3hr ($p<0.001$) (Figure 3B). At 5-hr, no difference was seen, showing that both reference strains have
200 strongly adhered.

201 Finally, the study of the *S. aureus* clinical strain showed that SAC1 formed a biofilm in 5-hr in the BHI
202 medium (Figure 3C). This biofilm was constituted significantly faster in CWM than in BHI with a
203 biofilm formed in 3hr (Figure 3B). The kinetics of biofilm formation was significant different between
204 the two media (Figures 3A and 3B) ($p<0.01$), suggesting the influence of CWM on the biofilm
205 induction. The same trend could be noted for *P. aeruginosa* PAC1. This strain developed a biofilm
206 much later, and the biofilm remained incomplete even after 5-hr in BHI (Figure 3C). However, at each
207 measured point, the difference of BFI was significant ($p<0.01$) with, for example, a BFI value of 12 ± 0.4
208 in BHI and 4.8 ± 0.3 in CWM at 5-hr ($p<0.001$).

209 3.4 Mature biofilm biomass is enhanced in the CWM

Bacterial effect of chronic wound medium

210 To corroborate the effect of the CWM on the early biofilm formation, we evaluated the mature biofilm
211 biomass of the different strains. In monoculture, all strains presented a significant higher number of
212 bacteria in the biofilm constituted in CWM than in BHI ($p < 0.01$) (Figure 4). For three of these isolates
213 (Newman, SAC1 and PAO1), this augmentation was particularly significant, with a difference on
214 average of a factor 10 (one log) (Figure 4A) ($p < 0.01$). The difference in number of bacteria counted in
215 biofilm in both media was slightly less significant for the PAC1 strain, but always higher in the CWM
216 vs BHI ($p < 0.1$).

217 In co-culture, the same trend was observed, with a significant increase of the number of bacteria
218 counted in biofilm constituted in CWM than in BHI ($p < 0.01$) (Figure 4B). Interestingly, the
219 combination of *S. aureus* and *P. aeruginosa* in CWM significantly favored the biofilm formation of
220 *S. aureus* at the expense of *P. aeruginosa* (Supplementary Table S4).

221 Those results are correlated with the early biofilm measurements and corroborated that the CWM
222 induced a faster and heavier biofilm.

223 3.5 Bacteria in CWM are less virulent in a nematode killing assay

224 Finally, we evaluated the impact of the CWM on bacterial virulence using a nematode killing model
225 validated to study the host-pathogen interactions [22-24]. In the *C. elegans* model, both *S. aureus*
226 strains killed the nematodes more rapidly than the avirulent *E. coli* OP50 strain, irrespective of the
227 culture medium used ($p < 0.001$) (Figure 5). However, a significant difference of LT50s was noted
228 between Newman and SAC1 in BHI, with an increased nematode lifespan in presence of Newman
229 (LT50 = 6 days ± 0.5 vs 5 days ± 0.5 , respectively; $p < 0.001$). When the *S. aureus* strains were cultivated
230 in CWM, their virulence in the nematode models were significantly decreased compared to strains
231 cultivated in BHI (6-8 ± 0.5 vs 5-6 ± 0.5 , respectively, $p < 0.001$, Figures 5A, 5C).

232 We observed the same trend for *P. aeruginosa* with: i) PAO1 and PAC1 grown in BHI or CWM killed
233 the nematodes more rapidly than the avirulent *E. coli* OP50 strain ($p < 0.001$); ii) the LT50s were shorter
234 for bacteria cultivated in BHI compared to those cultivated in CWM (2-3 days ± 0.5 vs 4-5 ± 0.5 ,
235 respectively; Figures 5B, 5D) ($p < 0.001$).

236

237 4. Discussion

238 Microorganisms behaviour is highly dependent on the environment in which they evolve. Classically,
239 in *in vitro* experiments, bacteria are grown in conventional culture media, a very artificial condition
240 compared to the environment encountered by the bacteria in clinical situations. This condition
241 influences the bacterial virulence, but this effect is currently far from the clinical conditions. The
242 development of new *in vitro* models mimicking *in vivo* conditions remains an important challenge to
243 improve our knowledge on the pathophysiology of the infections and to evaluate new therapeutic
244 solutions.

245 In the chronic wound context, the environment encountered by microorganisms is very different to the
246 general composition of classical microbiological culture media. Interfering factors specific to this
247 clinical situation include the high bacterial diversity, the numerous bacterial interactions, the influence
248 of the patient's immune status with the modifications of the local pH, temperature, and tissue
249 hypoxemia (inducing oxygen deprivation) [7,25-28]. All these elements modulate bacterial virulence
250 and lead the microorganisms to form a complex polymicrobial biofilm community [7]. Previously, Sun
251 et al. [17] developed a chronic wound-like environment (the Lubbock model) adapted to both the
252 growth of bacteria isolated from wounds and biofilm formation, aimed to mimic the microbiological
253 environment of chronic wounds. However, this model did not closely reflect the human wound
254 environment due to the use of animal products such as blood and plasma in concentrations that seemed

Bacterial effect of chronic Wound medium

255 not to be relevant with clinical data obtained in human wounds. Recently, we modified this medium
256 by adding 10% glucose to mimic a DFU environment [24] and observed a clear effect on *S. aureus*
257 virulence, demonstrating the value of developing a more physiological medium. However, we believed
258 that further improvements were necessary. We compared the composition of the medium described by
259 Sun et al. and the clinical observations of chronic wounds. These ulcers are rarely irrigated due, in part,
260 to vascular complication [29,30]. A lower concentration of serum, preferred to plasma [31], and blood
261 in the medium described above were more relevant thus we used 0.5% of hemolyzed human blood and
262 20% of heat-inactivated human serum to be as close as possible to the chronic wound environment.
263 The use of Bolton broth was maintained with a concentration of 79.5%. Bolton broth is a peptone-
264 based medium of animal origin and makes it possible to model the nutrients likely to be present in the
265 early stages following debridement (e.g., damaged and degraded tissue and abundance of extracellular
266 matrix compounds). The Bolton broth, serum and blood thus form the three major constituents found
267 in the wound bed, namely red blood cells, serum and damaged tissues. The Sun *et al.* model used a
268 more acidic pH than those found in chronic wounds (7.2 vs 8.5) [17,32-34]. Indeed, the physiological
269 pH of the skin is acidic (pH: 4-5) [35]. In the wound context, the pH significantly increases to reach
270 around 8-9 [32-34]. This basic pH is one of the main characteristics of a non-healing wound. Usually,
271 the healing process leads, by the local oxygen and nutrient requirements, to an acidification [36,37].
272 The pH then returns to normal upon complete healing. However, in the case of chronic wounds, since
273 there is no healing process, the pH remains around 8-9. We consequently buffered our medium at pH
274 8.0 with 10mM HEPES/NaOH. Finally, to mimic the cellular and inflammatory environment present
275 in the wound [38], we also added 1.10^6 /mL of human keratinocytes debris. Thereby, we proposed a
276 new *in vitro* model more similar to a chronic wound environment.

277 To validate this model, we studied the interaction between *S. aureus* and *P. aeruginosa*, two of the
278 main microorganisms present in chronic wounds [8]. Co-infection by these two strains has been
279 frequently described [15] and shown to cause more severe infections than mono-infection [39,40].
280 However, difficulties in growing them together *in vitro* has delayed the understanding of their
281 interaction. In our study, the CWM gave reproducible and reliable results. *P. aeruginosa* and *S. aureus*
282 were able to grow alone or co-cultivated. Growth was different in CWM than in traditional laboratory
283 growth medium (BHI). In monoculture, the species reached maximum cell density higher in BHI than
284 in the CWM ($p=0.00103$). More importantly, in co-culture, contrarily to what was previously described
285 [9,41], *S. aureus* was not quickly eradicated by *P. aeruginosa* in either BHI or CWM: not only both
286 species were able to coexist in both media, but the co-culture in CWM allowed *S. aureus* to reach a
287 higher cell density. In particular, there was no early lag phase in the growth curve in co-culture as
288 observed in monoculture in CWM (Figure 2). Recent studies have reported that *P. aeruginosa* could
289 have a protective effect for *S. aureus* [13,14]. We confirm this trend, since this initial lag phase did not
290 exist in co-culture. In addition, the plateau reached after 24hr of co-culture corresponds to a higher cell
291 density ($p=0.00261$). This indicates that the CWM influences the behaviour of one or both of the
292 bacteria species.

293
294 As the environment could represent a major source of stress for bacteria, we evaluated the role of CWM
295 on biofilm formation and virulence. Firstly, we examined the early adhesion, the first step of biofilm
296 formation, and the mature biofilm formation by CFU counts of biofilm biomass from mono- and co-
297 cultures. The results obtained showed that adhesion was facilitated in the CWM compared to the BHI
298 (Figure 3). Indeed, all the strains adhered more quickly in the CWM. We also verified whether, beyond
299 the early adhesion step, the CWM facilitates biofilm formation by measuring the biomass present inside
300 the biofilm after 24hr of incubation. The results corroborated the early adhesion evaluation (Figure 4).
301 Globally, this indicates that the CWM medium is compatible with biofilm studies and that this
302 environment induces a rapid and strong biofilm. Interestingly, these results are consistent with the
303 behaviour of the strains described in chronic wounds [7,25], suggesting that this new medium is close

Bacterial effect of chronic wound medium

304 enough to the clinical situation and could mimic the environment encountered by bacteria in these
305 ulcers. Secondly, we investigated the effect of the CWM on bacterial virulence. All *S. aureus* and
306 *P. aeruginosa* strains tested were significantly less virulent in the CMW, compared to BHI (Figure 5).
307 Thus, CMW medium is suitable for virulence tests, supporting our earlier studies showing that the
308 environment present at the chronic wound level influences the strains' virulence [24]. Thus, in this non-
309 rich condition, bacteria are under stress and develop a rapid and dense biofilm and decrease their
310 virulence, hijacking the immune defence system and maintaining the chronicity of the wound. Further
311 studies must be done to evaluate the bacterial cooperation and regulation of biofilm on planktonic and
312 sessile status.

313

314 This medium presents multiple benefits, notably in providing a means to study bacterial virulence and
315 cooperation in a chronic wound environment. It also gives the possibility to modify different
316 parameters. For example, to mimic DFU we could vary the glucose concentration, as glucose is an
317 important factor influencing wound healing [42,43] and bacterial behaviour [24]. Moreover, as
318 antibiotics are classically overused in this clinical situation, we could add different antibiotic
319 concentrations and evaluate their impact on biofilm formation and bacterial virulence. Some authors
320 have already highlighted and criticized the fact that the scientific community does not have a relatively
321 standardized model to reliably study biofilm under *in vivo* conditions [44,45]. Thus, this new medium
322 contributes to this standardization to provide a more reliable model for research on chronic wounds
323 and could help to lead to the discovery of future therapeutic molecules with anti-biofilm strategy.

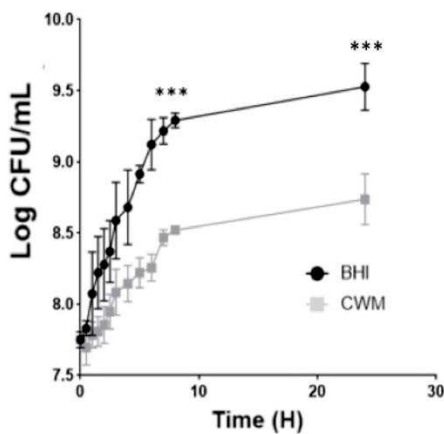
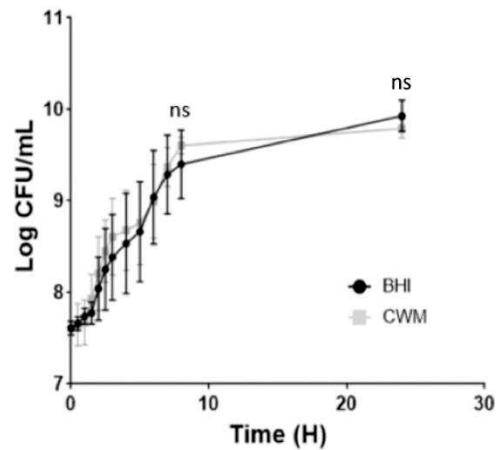
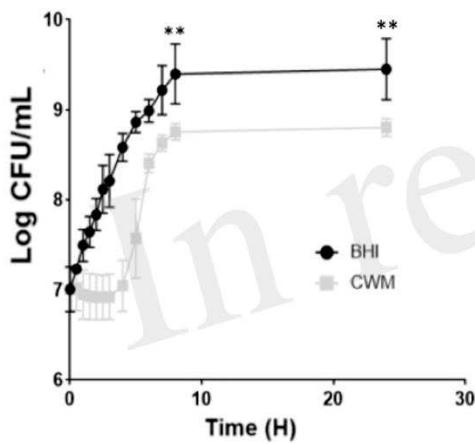
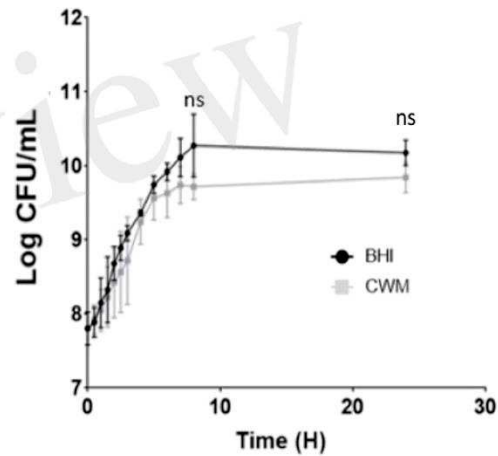
324 In conclusion, we improved the *in vitro* wound-like model described by Sun *et al.* [17] to try to
325 better reflect the chronic wound environment. This study showed that the CWM, an affordable
326 (approximately 100 euros/liter), reproducible and reliable medium, allows the study of multiple
327 bacteria species known to be present in chronic wounds and requiring in-depth study. In this model,
328 we highlighted that the CMW had a strong impact on bacteria behaviour, notably on their growth,
329 interaction, biofilm formation and virulence. Moreover, *S. aureus* and *P. aeruginosa* displayed
330 synergism with an improved growth of *S. aureus* in the presence of *P. aeruginosa*. Taken together,
331 these data suggest that virulent bacteria growing together in wounds have a main common objective to
332 hijack the host immune defence by co-aggregating symbiotically in a pathogenic biofilm [46] that
333 participates considerably in the chronicity of the wound.

334

335 5. Figures

336 **Figure 1.** Growth curves of reference (A, B) and clinical (C, D) strains of *S. aureus* and *P. aeruginosa*
337 in CWM and BHI media. Cultures were sampled at the indicated time points, and the numbers of
338 bacteria were estimated by CFU enumeration of *P. aeruginosa* and *S. aureus* on non-selective medium.
339 Experiments were performed in three biological replicates; data points represent the average of these
340 replicates and error bars represent the standard deviation. Comparisons were performed with t-test.
341 Significance was set to a p-value < 5%. ns, not significant; ***, p<0.001; **, p<0.01.

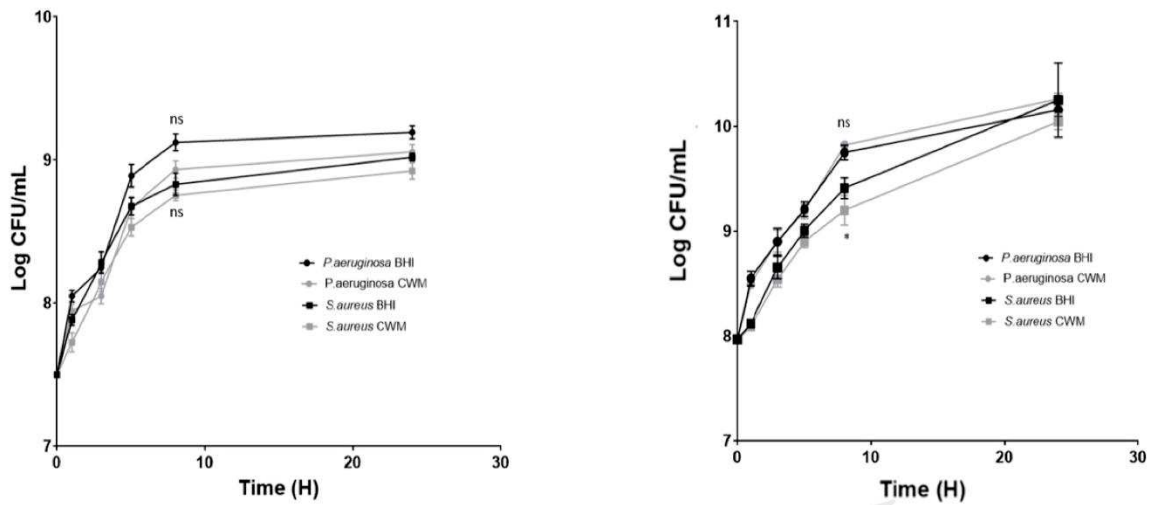
Bacterial effect of chronic Wound medium

(A) *S. aureus* Newman(B) *P. aeruginosa* PAO1(C) *S. aureus* SAC 1(D) *P. aeruginosa* PAC 1

342
343
344
345
346
347
348
349
350

Figure 2. Growth curves of 1:1 co-reference clinical (A) and clinical (B) strains of *S. aureus* and *P. aeruginosa* in CMW and BHI media. Cultures were sampled at the indicated time points, and the numbers of bacteria were estimated by CFU enumeration of *P. aeruginosa* and *S. aureus* on selective medium. Experiments were performed in three biological replicates; data points represent the average of these replicates and error bars represent the standard deviation. Comparisons were performed with t-test. Significance was set to a p-value < 5%. ns, not significant; *, p<0.1.

Bacterial effect of chronic wound medium

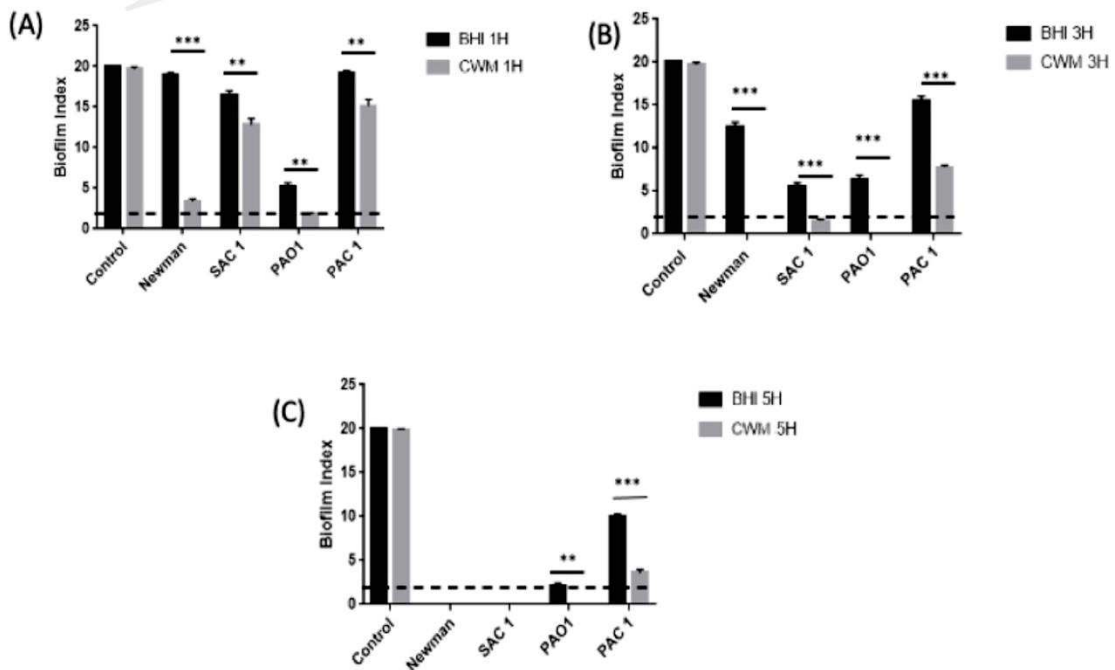


(A) Coculture PAO1/ Newman

(B) Coculture PAC 1/ SAC 1

351
352
353
354
355
356
357

Figure 3. Kinetics of biofilm formation assessed by BioFilm Ring Test® at 1 hour (A), 3 hours (B) and 5 hours (C) for clinical and reference *S. aureus* and *P. aeruginosa* strains. Comparisons were performed with t-test. Error bars represent standard deviation. Significance was set to a p-value < 5%. The dotted horizontal line <2 represents the cut-off for fixed biofilm. Control is well without bacteria.

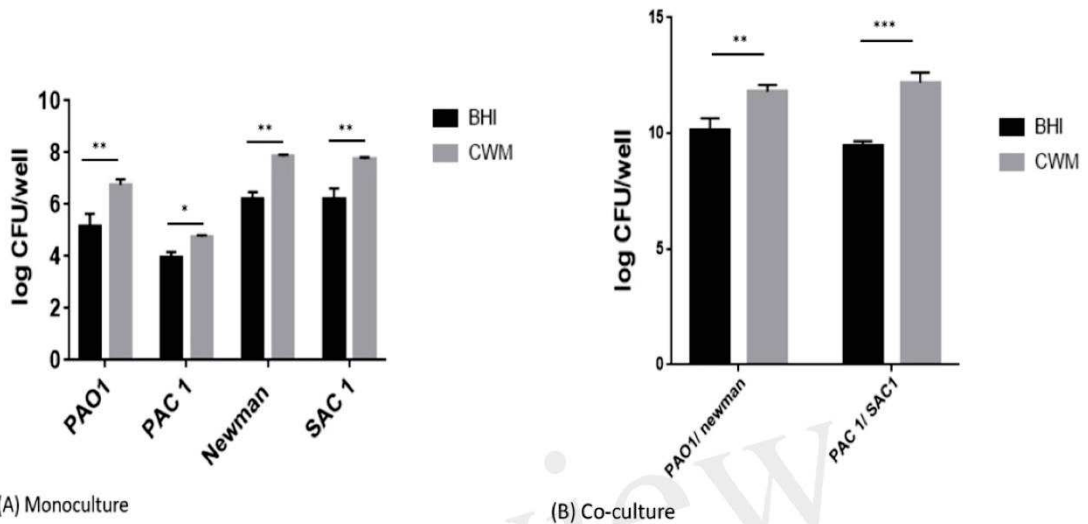


358
359
360

Figure 4. Quantification of biofilm of *S. aureus* and *P. aeruginosa* clinical and reference strains grown in monoculture (A) or 1:1 co-culture (B). Samples were tested in triplicate in two independent experiments.

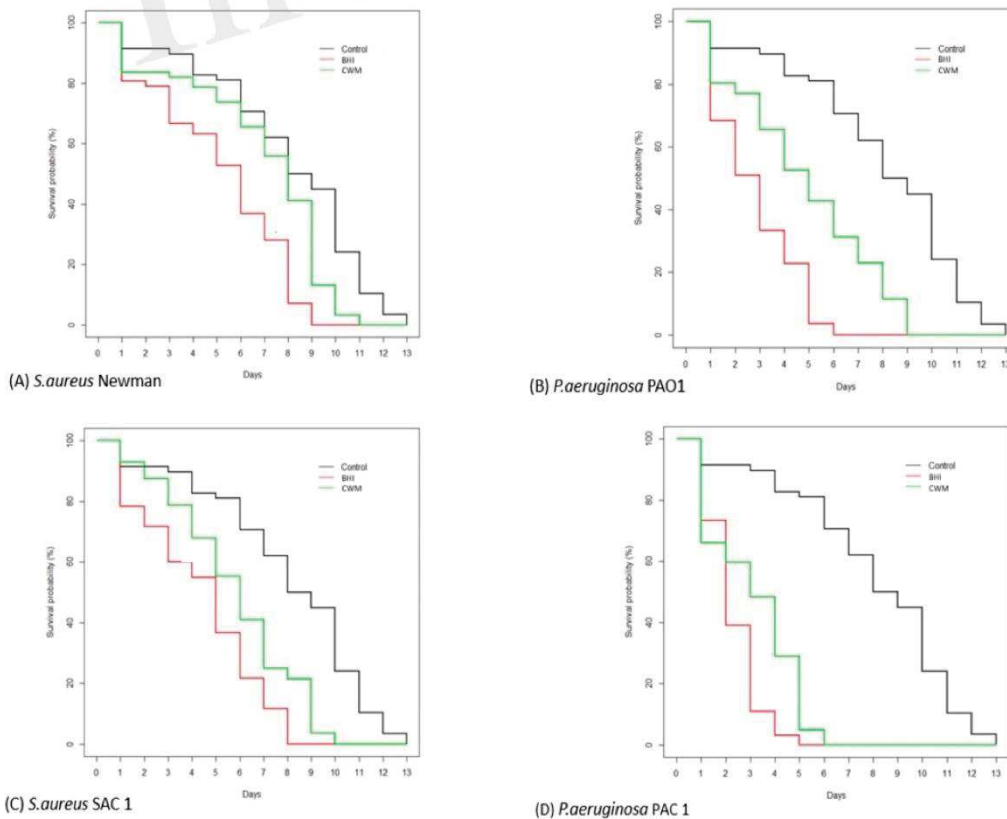
Bacterial effect of chronic Wound medium

361 experiments. Comparisons were performed with t-test. Significance was set to a p-value < 5%. ***,
 362 p<0.001; **, p<0.01; *, p<0.1.



363
 364
 365
 366
 367

Figure 5. Nematode killing assays of mono-infections with reference (A, B) and clinical (C, D) strains of *S. aureus* and *P. aeruginosa* cultured in the different growing media.



368
 369

370 **6. Tables**371 **Table 1.** Strains used in this study.

Strain	Characteristics	References
PAO1	<i>P. aeruginosa</i> reference strain	[47]
Newman	<i>S. aureus</i> reference strain	[48]
SAC1	Clinical strains of <i>S. aureus</i> co-isolated with PAC1 from a diabetic foot ulcer (Grade 3)	In this study
PAC1	Clinical strains of <i>P. aeruginosa</i> co-isolated with SAC1 from a diabetic foot ulcer (Grade 3)	In this study

372

373

374

375

376 **Table 2.** Composition of the chronic wound medium (CWM).

CWM composition
79.5% Bolton broth v/v
20% heat-inactivated human serum v/v
0.5% hemolyzed human blood v/v
1x10 ⁶ /mL debris of human keratinocytes (HaCaT)
NaOH 1M for a fixed pH 8
1% 1M HEPES

377

378 **7. Conflict of Interest**

379 The authors are co-inventors of the CWM (European patent application EP21305337, filed on 18
380 March 2021). Cassandra Pouget is the recipient of a grant from Biofilm Pharma (Bourse CIFRE).

381 **8. Author Contributions**

382 CP, JPL and AS drafted the manuscript. All authors contributed to manuscript revision, read and
383 approved the submitted version.

384 **9. Funding**

385 Cassandra Pouget is the recipient of a PhD's grant from Biofilm Pharma (CIFRE grant).

386 **10. Acknowledgments**

387 PL, CDR, AS and JPL belong to the FHU INCh (Federation Hospitalo Universitaire Infections
388 Chroniques, Aviesan). We thank the Nîmes University hospital for its structural, human and financial
389 support through the award obtained by our team during the internal call for tenders "Thématiques
390 phares". We thank Sarah Kabani for her editing assistance.

391 11. References

- 392 1. Järbrink K, Ni G, Sönnergren H, Schmidtehen A, Pang C, Bajpai R, Car J. The humanistic and
393 economic burden of chronic wounds: a protocol for a systematic review. *Syst Rev* (2017) 6:15.
- 394 2. Sen CK, Gordillo GM, Roy S, Kirsner R, Lambert L, Hunt TK, Gottrup F, Gurtner GC, Longaker
395 MT. Human skin wounds: a major and snowballing threat to public health and the economy.
396 *Wound Repair Regen* (2009) 17:763–771.
- 397 3. Sen CK. Human wounds and its burden: an updated compendium of estimates. *Adv Wound Care*
398 (2019) 8:39-48.
- 399 4. Kirsner R. The Wound Healing Society chronic wound ulcer healing guidelines update of the
400 2006 guidelines--blending old with new. *Wound Repair Regen* (2016) 24:110–111.
- 401 5. Schaper NC, van Netten JJ, Apelqvist J, Bus SA, Hichliffe RJ, Lipsky BA, IWGDF Editorial
402 Board. Practical guidelines on the prevention and management of diabetic foot disease (IWGDF
403 2019 update). *Diab Metab Res Rev* (2020) 36:e3266.
- 404 6. Bowler PG, Duerden BI, Armstrong DG. Wound microbiology and associated approaches to
405 wound management. *Clinical Microbiol Rev* (2001) 14:244–269.
- 406 7. Dowd SE, Wolcott RD, Sun Y, McKeenan T, Smith E, Rhoads D. Polymicrobial nature of
407 chronic diabetic foot ulcer biofilm infections determined using bacterial tag encoded FLX
408 amplicon pyrosequencing (bTEFAP). *PLoS One* (2008) 3:e3326.
- 409 8. Serra R, Grande R, Butrico L, Rossi A, Settimio UF, Caroleo B, Amato B, Gallelli L, de
410 Francis S. Chronic wound infections: the role of *Pseudomonas aeruginosa* and *Staphylococcus*
411 *aureus*. *Expert Rev Anti Infect Ther* (2015) 13:605-613.
- 412 9. Palmer KL, Aye LM, Whiteley M. Nutritional cues control *Pseudomonas aeruginosa*
413 multicellular behavior in cystic fibrosis sputum. *J Bacteriol* (2007) 189:8079–8087.
- 414 10. Hoffman LR, Déziel E, D'Argenio DA, Lepine F, Emerson J, McNamara S, Gibson RL, Ramsey
415 BW, Miller SI. Selection for *Staphylococcus aureus* small-colony variants due to growth in the
416 presence of *Pseudomonas aeruginosa*. *Proc Natl Acad Sci USA* (2006) 103:19890-19895.
- 417 11. Qin Z, Yang L, Qu D, Molin S, Tolker-Nielsen T. *Pseudomonas aeruginosa* extracellular
418 products inhibit staphylococcal growth, and disrupt established biofilms produced by
419 *Staphylococcus epidermidis*. *Microbiology* (2009) 155:2148-2156.
- 420 12. Dietrich LE, Price-Whelan A, Petersen A, Whiteley M, Newman DK. The phenazine pyocyanin
421 is a terminal signalling factor in the quorum sensing network of *Pseudomonas aeruginosa*. *Mol*
422 *Microbiol* (2006) 61: 1308 –1321.
- 423 13. Price CE, Brown DG, Limoli DH, Phelan VV, O'Toole GA. Exogenous alginate protects
424 *Staphylococcus aureus* from killing by *Pseudomonas aeruginosa*. *J Bacteriol* (2020) 202:e00559-
425 19.
- 426 14. Schurr MJ. *Pseudomonas aeruginosa* alginate benefits *Staphylococcus aureus*?. *J Bacteriol*
427 (2020) 202:e00040-20.
- 428 15. Fazli M, Bjarnsholt T, Kirketerp-Møller K, Jørgensen B, Andersen AS, Kroghfelt KA, Givskov M,
429 Tolker-Nielsen T. Nonrandom distribution of *Pseudomonas aeruginosa* and *Staphylococcus*
430 *aureus* in chronic wounds. *J Clin Microbiol* (2009) 47:4084-4089.
- 431 16. Alves PM, Al-Badi E, Withycombe C, Jones PM, Purdy KJ, Maddocks SE. Interaction between
432 *Staphylococcus aureus* and *Pseudomonas aeruginosa* is beneficial for colonisation and
433 pathogenicity in a mixed biofilm. *Pathog Dis* (2018) 76(1).
- 434 17. Sun Y, Dowd SE, Smith E, Rhoads DD, Wolcott RD. In vitro multispecies Lubbock chronic
435 wound biofilm model. *Wound Repair Regen* (2008) 16:805–813.
- 436 18. DeLeon S, Clinton A, Fowler H, Everett J, Horswill AR, Rumbaugh KP. Synergistic interactions
437 of *Pseudomonas aeruginosa* and *Staphylococcus aureus* in an *in vitro* wound model. *Infect*
438 *Immun* (2014) 82:4718-28.

Bacterial effect of chronic wound medium

- 439 19. Chavant P, Gaillard-Martinie B, Talon R, Hébraud M, Bernardi T. A new device for rapid
440 evaluation of biofilm formation potential by bacteria. *J Microbiol Methods* (2007) 68:605–612.
- 441 20. Freitas AI, Vasconcelos C, Vilanova M, Cerca N. Optimization of an automatic counting system
442 for the quantification of *Staphylococcus epidermidis* cells in biofilms. *J Basic Microbiol* (2014)
443 54:750-757.
- 444 21. Lavigne JP, Nicolas-Chanoine MH, Bourg G, Moreau J, Sotto A. Virulent synergistic effect
445 between *Enterococcus faecalis* and *Escherichia coli* assayed by using the *Caenorhabditis elegans*
446 model. *PLoS One* (2008) 3:e3370.
- 447 22. Messad N, Prajsnar TK, Lina G, O'Callaghan D, Foster SJ, Renshaw SA, Skaar EP, Bes M,
448 Dunyach-Remy C, Vandenesch F, Sotto A, Lavigne JP. Existence of a colonizing
449 *Staphylococcus aureus* strain isolated in diabetic foot ulcers. *Diabetes* (2015) 64:2991-2995.
- 450 23. Aballay A, Ausubel FM. *Caenorhabditis elegans* as a host for the study of host-pathogen
451 interactions. *Curr Opin Microbiol* (2002) 5:97-101.
- 452 24. Pouget C, Gustave CA, Ngba-Essebe C, Laurent F, Lemichez E, Tristan A, Sotto A, Dunyach-
453 Remy C, Lavigne JP. Adaptation of *Staphylococcus aureus* in a medium mimicking a diabetic
454 foot environment. *Toxins (Basel)* (2021) 13:230.
- 455 25. Smith BK, Ford RJ, Desjardins EM, Green AE, Hughes MC, Houde VP, Day EA, Marcinko K,
456 Crane JD, Mottillo EP, Perry CGR, Kemp BE, Tarnopolsky MA, Steinberg GR. Salsalate
457 (Salicylate) uncouples mitochondria, improves glucose homeostasis, and reduces liver lipids
458 independent of AMPK- β 1. *Diabetes* (2016) 65:3352-3361.
- 459 26. Rahim K, Saleha S, Zhu X, Huo L, Basit A, Franco OL. Bacterial contribution in chronicity of
460 wounds. *Microb Ecol* (2017) 73:710-721.
- 461 27. Patel S, Srivastava S, Singh MR, Singh D. Mechanistic insight into diabetic wounds:
462 Pathogenesis, molecular targets and treatment strategies to pace wound healing. *Biomed*
463 *Pharmacother* (2019) 112:108615.
- 464 28. Gardner SE, Hillis SL, Heilmann K, Segre JA, Grice EA. The neuropathic diabetic foot ulcer
465 microbiome is associated with clinical factors. *Diabetes* (2013) 62:923-30.
- 466 29. Armstrong DG. An overview of foot infections in diabetes. *Diabetes Technol Ther* (2011)
467 13:951-957.
- 468 30. Pendsey SP. Understanding diabetic foot. *Int J Diabetes Dev Ctries* (2010) 30:75-79.
- 469 31. Bandyopadhyay BI, Fan J, Guan S, Li Y, Chen M, Woodley DT, Li W. A "traffic control" role
470 for TGF β 3: orchestrating dermal and epidermal cell motility during wound healing. *J Cell Biol*
471 (2006) 172:1093-105.
- 472 32. Gethin G. The significance of surface pH in chronic wounds. *Wounds UK* (2007) 3:52-56.
- 473 33. Kumar P, Honnegowda TM. Effect of limited access dressing on surface pH of chronic wounds.
474 *Plast Aesthet Res* (2015) 2:257-260.
- 475 34. Jones EM, Cochrane CA, Percival SL. The Effect of pH on the Extracellular Matrix and
476 Biofilms. *Adv Wound Care (New Rochelle)* (2015) 4:431-439.
- 477 35. Lambers H, Piessens S, Bloem A, Pronk H, Finkel P. Natural skin surface pH is on average
478 below 5, which is beneficial for its resident flora. *Int J Cosmet Sci* (2006) 28:359-370.
- 479 36. Schneider LA, Korber A, Grabbe S, Dissemmond J. Influence of pH on wound-healing: a new
480 perspective for wound-therapy? *Arch Dermatol Res* (2007) 298:413-420.
- 481 37. Svensson E, Wahlström E. Monitoring pH in wounds : The possibilities of textiles in healthcare.
482 (2017). [http://www.diva-](http://www.diva-portal.org/smash/record.jsf?pid=diva2%3A1120581&dswid=mainwindow)
483 [portal.org/smash/record.jsf?pid=diva2%3A1120581&dswid=mainwindow](http://www.diva-portal.org/smash/record.jsf?pid=diva2%3A1120581&dswid=mainwindow) [Accessed March 15,
484 2021].
- 485 38. Boukamp P, Petrussevska RT, Breitkreutz D, Hornung J, Markham A, Fusenig NE. Normal
486 keratinization in a spontaneously immortalized aneuploid human keratinocyte cell line. *J Cell*
487 *Biol* (1988) 106:761-771.

Bacterial effect of chronic Wound medium

- 488 39. Hendricks KJ, Burd TA, Anglen JO, Simpson AW, Christensen GD, Gainor BJ. Synergy between
489 *Staphylococcus aureus* and *Pseudomonas aeruginosa* in a rat model of complex orthopaedic
490 wounds. *J Bone Joint Surg Am* (2001) 83:855-861.
- 491 40. Pastar I, Nusbaum AG, Gil J, Patel SB, Chen J, Valdes J, Stojadinovic O, Plano LR, Tomic-Canic
492 M, Davis SC. Interactions of methicillin resistant *Staphylococcus aureus* USA300 and
493 *Pseudomonas aeruginosa* in polymicrobial wound infection. *PLoS One* (2013) 8:e56846.
- 494 41. Palmer KL, Mashburn LM, Singh PK, Whiteley M. Cystic fibrosis sputum supports growth and
495 cues key aspects of *Pseudomonas aeruginosa* physiology. *J Bacteriol* (2005) 187:5267-5277.
- 496 42. Xiang J, Wang S, He Y, Xu L, Zhang S, Tang Z. Reasonable glycemic control would help wound
497 healing during the treatment of diabetic foot ulcers. *Diabetes Ther* (2019) 10:95–105.
- 498 43. Almaramhy H, Mahabbat NA, Fallatah KY, Al-Ahmadi BA, Al-Alawi HH, Guraya SY. The
499 correlation of fasting blood glucose levels with the severity of diabetic foot ulcers and the
500 outcome of treatment strategies. *BioMed Res* (2018) 29:1961-1967. doi:
501 10.4066/biomedicalresearch.29-18-502
- 502 44. Roberts AEL, Kragh KN, Bjarnsholt T, Diggle SP. The limitations of in vitro experimentation in
503 understanding biofilms and chronic infection. *J Mol Biol* 2015 (427):3646-3661.
- 504 45. Coenye T, Goeres D, Van Bambeke F, Bjarnsholt T. Should standardized susceptibility testing
505 for microbial biofilms be introduced in clinical practice? *Clin Microbiol Infect* (2018) 24:570-
506 572.
- 507 46. Attinger C, Wolcott R. Clinically addressing biofilm in chronic wounds. *Adv Wound Care* (New
508 Rochelle) (2012) 1:127–132.
- 509 47. Holloway BW, Krishnapillai V, Morgan AF. Chromosomal genetics of *Pseudomonas*. *Microbiol*
510 *Rev* (1979) 43:73-102.
- 511 48. Duthie ES, Lorenz LL. Staphylococcal coagulase; mode of action and antigenicity. *J Gen*
512 *Microbiol* (1952) 6:95-107.

PARTIE III.

MISE EN PLACE D'UN SYSTÈME DE FORMATION DE BIOFILM EN FLUX

Travail n°5 : Article Scientifique

New adapted *in vitro* technology to evaluate the biofilm formation and the antibiotic activity using live imaging under flow conditions

Cassandra Pouget, Catherine Dunyach-Remy, Alix Pantel, Sophie Schuldiner, Albert Sotto and Jean-Philippe Lavigne

Accepté dans Diagnostics le 19 Septembre 2021

Résumé travail n°5 :

Après avoir développé un milieu *in vitro* mimant l'environnement plaie chronique, le CWM, nous nous sommes focalisés sur l'utilisation de nouvelles techniques appliquées à notre thématique et notamment celles permettant **l'étude dynamique de biofilm en temps réel**. Classiquement, les approches expérimentales pour étudier les microorganismes ne sont pas adaptées à l'étude de leur mode de vie complexe en biofilm. Au cours des dernières années, les chercheurs ont donc développé différents modèles expérimentaux associant analyse moléculaire et microscopie. L'utilisation des **modèles statiques** de biofilms a permis d'avancer considérablement dans la compréhension de ce mode de vie. La technique des microplaques multi-puits, couplée à l'analyse de mutants de transposition, a permis d'identifier de nombreux gènes impliqués dans la formation des biofilms. Les modèles statiques ont l'avantage d'être simples et faciles à utiliser, ils sont généralement peu coûteux et ne nécessitent, la plupart du temps, pas d'équipement sophistiqué. Ils sont cependant loin de représenter la réalité. L'absence de flux entraînant un épuisement des ressources nutritives et une accumulation des produits métaboliques, l'environnement se modifie mais ce changement n'est pas comparable à celui qui se produit au cours du développement d'un biofilm dans des conditions naturelles. Pour cela, **les modèles dynamiques** sont plus indiqués car ils rendent possible l'apport continu de milieu de culture et l'élimination des déchets, simulant ainsi les conditions *in vivo*. De plus, ils permettent également la simulation des conditions environnementales complexes.

Le système **BioFlux™ 200** de Fluxion permet de réaliser des expériences dans des conditions physiologiques d'écoulement grâce à l'utilisation de microplaques permettant le contrôle précis des forces de cisaillement mais également la visualisation du biofilm polymicrobien en microscopie à contraste de phase ou confocale.

Nous avons donc adapté ce système en flux, le BioFlux™ 200 afin de pouvoir utiliser ce système avec le milieu **CWM** pour mimer les conditions observées dans les plaies chroniques et auxquelles sont soumises les bactéries. Pour cela, deux souches de référence de *S. aureus* et *P. aeruginosa* ont été utilisées en mono et co-culture

dans le BioFlux™ pour suivre une cinétique de formation de biofilm allant de 24 à 72 heures. A l'aide de cette étude nous avons :

- Établi un protocole de **quantification** de biofilm formé
- Établi un protocole de **débridement automatisé** pour mimer la première étape de prise en charge des plaies chroniques
- Établi un protocole pour tester **l'efficacité de différents antibiotiques** (Imipenème, ceftazidime, vancomycine, oxacilline et linézolide) à plusieurs concentrations (1x la concentration minimale inhibitrice, 10x et 100x) sur un biofilm préformé et débridé.

Les résultats ont mis en évidence que, comme dans les études précédemment décrites, les deux espèces qu'elles soient seules ou associées constituaient, de manière **plus rapide**, un biofilm **plus dense** dans le CWM par rapport à un milieu dit contrôle. L'étude de l'effet des antibiotiques sur le biofilm débridé a montré que, même à des concentrations très élevées, certains antibiotiques étaient **incapables de réduire la biomasse** présente dans le biofilm (vancomycine et imipenème).

Cette étude a donc démontré que l'utilisation de milieu de culture mimant un environnement stressant en combinaison avec une technique adaptée à la formation de biofilms proches de ceux observés au niveau des plaies chroniques était un outil intéressant et prometteur pour étendre nos connaissances concernant les coopérations microbiennes mais aussi pour tester le potentiel thérapeutique de nouvelles molécules à valeur ajoutée antibiofilm.

Article

New Adapted In Vitro Technology to Evaluate Biofilm Formation and Antibiotic Activity Using Live Imaging under Flow Conditions

Cassandra Pouget ¹, Catherine Dunyach-Remy ² , Alix Pantel ² , Sophie Schuldiner ³, Albert Sotto ⁴ 
and Jean-Philippe Lavigne ^{2,*} 

¹ Virulence Bactérienne et Infections Chroniques, INSERM U1047, Université de Montpellier, 30908 Nîmes, France; cassandra.pouget@gmail.com

² Virulence Bactérienne et Infections Chroniques, INSERM U1047, Université de Montpellier, Service de Microbiologie et Hygiène Hospitalière, CHU Nîmes, 30029 Nîmes, France; catherine.remy@chu-nimes.fr (C.D.-R.); alix.pantel@chu-nimes.fr (A.P.)

³ Virulence Bactérienne et Infections Chroniques, INSERM U1047, Université de Montpellier, Service des Maladies Métaboliques et Endocriniennes, CHU Nîmes, 30029 Nîmes, France; sophie.schuldiner@chu-nimes.fr

⁴ Virulence Bactérienne et Infections Chroniques, INSERM U1047, Université de Montpellier, Service des Maladies Infectieuses et Tropicales, CHU Nîmes, 30029 Nîmes, France; albert.sotto@chu-nimes.fr

* Correspondence: jean.philippe.lavigne@chu-nimes.fr; Tel.: +33-466-683-202



Citation: Pouget, C.; Dunyach-Remy, C.; Pantel, A.; Schuldiner, S.; Sotto, A.; Lavigne, J.-P. New Adapted In Vitro Technology to Evaluate Biofilm Formation and Antibiotic Activity Using Live Imaging under Flow Conditions. *Diagnosics* **2021**, *11*, 1746. <https://doi.org/10.3390/diagnostics11101746>

Academic Editor: James Bowen Stiehl

Received: 27 July 2021

Accepted: 19 September 2021

Published: 23 September 2021

Publisher's Note: MDPI stays neutral with regard to jurisdictional claims in published maps and institutional affiliations.



Copyright: © 2021 by the authors. Licensee MDPI, Basel, Switzerland. This article is an open access article distributed under the terms and conditions of the Creative Commons Attribution (CC BY) license (<https://creativecommons.org/licenses/by/4.0/>).

Abstract: The polymicrobial nature of biofilms and bacterial interactions inside chronic wounds are keys for the understanding of bacterial cooperation. The aim of this present study was to develop a technique to study and visualize biofilm in live imaging under flow conditions (Bioflux™ 200, Fluxion Biosciences). The Bioflux™ system was adapted using an in vitro chronic wound-like medium (CWM) that mimics the environment encountered in ulcers. Two reference strains of *Staphylococcus aureus* (Newman) and *Pseudomonas aeruginosa* (PAO1) were injected in the Bioflux™ during 24 h to 72 h in mono and coculture (ratio 1:1, bacteria added simultaneously) in the CWM vs. a control medium (BHI). The quantification of biofilm formation at each time was evaluated by inverted microscopy. After 72 h, different antibiotics (ceftazidime, imipenem, linezolid, oxacillin and vancomycin) at 1x MIC, 10x MIC and 100x MIC were administrated to the system after an automatic increase of the flow that mimicked a debridement of the wound surface. Biofilm studies highlighted that the two species, alone or associated, constituted a faster and thicker biofilm in the CWM compared to the BHI medium. The effect of antibiotics on mature or “debrided” biofilm indicated that some of the most clinically used antibiotic such as vancomycin or imipenem were not able to disrupt and reduce the biofilm biomass. The use of a life cell imaging with an in vitro CWM represents a promising tool to study bacterial biofilm and investigate microbial cooperation in a chronic wound context.

Keywords: antibiotics; biofilm; Bioflux™ 200; chronic wounds; flow conditions; live imaging; living cells

1. Introduction

Chronic wounds are a severe and expensive worldwide problem [1]. Wounds are considered chronic when the healing process fails to happen normally and the functional integrity of the skin is not achieved after more than 4 weeks [2]. Infections contribute to nonhealing wounds and are the consequence of microorganisms' multiplication in the wound bed, leading to a prolonged excessive inflammatory response and delays in the re-epithelialization [3]. Chronic wounds include diabetic foot ulcers, pressure or decubitus ulcers and venous or arterial leg ulcers [4]. The cost of treatment, amputation, rehabilitation, and long-term care of these chronic wounds are estimated to be around USD 10.9 billion [1].

A biofilm is a sessile community of bacterial cells enclosed by a self-secreted extracellular polymeric matrix (EPS) present at the wound bed in 60–80% of cases [5,6]. These microbial communities have the potential to colonize and grow on surfaces of medical implants such as catheters or implants but also on tissues themselves [7]. Bacterial biofilms are a serious health problem due to their abilities to tolerate antibiotics, host defence systems and other external stresses contributing to the chronicity of the infection. Indeed, a biofilm EPS provides an additional resistance power of bacteria to tolerate stressful environments and antimicrobial agents, leading to the emergence of multidrug resistant bacteria [8]. Evidence showed that polymicrobial biofilm present in chronic wounds plays a major role in the inability of wounds to heal [9].

The chronic wound bed presents a complex microenvironment that typically includes more than one bacterial species interacting with each other [10]. Antibiotic therapy corresponds to one of the main treatments used to reduce the bacterial burden; however, there is a lack of evidence concerning its complete effectiveness in this clinical situation [11]. Despite this, patients with chronic wounds receive significantly more antibiotic prescriptions than other age- and gender-matched patients [12]. The physicians have to evaluate the role of each microorganism in the persistence of chronic wounds and distinguish between colonizing and infecting bacteria before applying antibiotic treatments [13]. The delicate balance between infection and colonization as well as the presence of sessile bacteria at the wound bed imply that most antibiotics are nonconclusive solutions to optimally treat chronic wound infections. Moreover, according to some publications, antimicrobial susceptibility depends on the environment in which bacteria evolved [14,15]. It is thus important to test the efficiency of antibiotics or new antibiofilm molecules in an environment closely related to the conditions encountered in vivo to clearly evaluate their potential and to avoid the risk of multidrug resistant bacteria emergence. The aim of this work was to describe a new in vitro model to study biofilm formation under flow condition in a medium mimicking chronic wounds environment. This model could be an interesting approach to a better knowledge on biofilm formation and organization but also to evaluate antimicrobial strategies in conditions close to the in vivo wound environment.

2. Materials and Methods

2.1. Bacterial Strains and Culture Conditions

All bacteria and media used in this study are listed in Table 1.

Table 1. Bacterial strains and media used in the study.

Strain	Characteristics	References
PAO1	<i>Pseudomonas aeruginosa</i> reference strain	[16]
Newman	<i>Staphylococcus aureus</i> reference strain	[17]
Media	Characteristics	References
BHI	Brain Heart Infusion, Reference medium for bacterial culture	Sigma-Aldrich
CWM	Chronic wound medium, medium mimicking in vivo conditions encountered in chronic wounds. Composition: 79.5% Bolton broth, 20% decomplemented human serum, 0.5% haemolysed human blood, HaCaT debris	European patent application EP21305337

The composition of the in vitro chronic wound medium (CWM) (corresponding to European patent application EP21305337, filed on 18 March 2021) is presented in Table 1. To summarize, this new in vitro model is composed of a Bolton broth, a peptone-based medium of animal origin that makes it possible to model the nutrients likely to be present in the early stages following the debridement of the wound (e.g., damaged and degraded tissue and abundance of extracellular matrix compounds). Human serum and blood are

also added to form the three major constituents found in the wound level, namely, red blood cells, serum and damaged tissues. Moreover, studying the chemical environment of the wound, we found that the pH is significantly increased to reach around 8. This basic pH is one of the main characteristics of a nonhealing wound caused by a modification due to the local oxygen deprivation and nutrient requirements. We consequently buffered our medium at pH 8.0 with 10 mM HEPES/NaOH. Finally, to mimic the cellular and inflammatory environment present in the wound, we added 1.10^6 /mL of human keratinocytes debris.

Bacteria were grown overnight in bacterial culture tubes under shaking at 200 rpm, in aerobic condition at 37 °C in the brain heart infusion (BHI, Sigma-Aldrich, Saint-Quentin-Fallavier, France) broth or in the CWM.

The antimicrobial susceptibility testing of isolates was performed by a broth microdilution method on the BHI medium according to EUCAST recommendations (https://www.eucast.org/clinical_breakpoints, accessed on 1 January 2021). The same procedure was applied in the CWM to compare the effect of this medium on antibiotics action.

2.2. Biofilm Formation of Monoculture and Mixed-Culture in a Microfluidic System

To investigate biofilm formation, we used the microfluidic system of a BioFlux™ 200 (Fluxion Bioscience Inc., Alameda, CA, USA). The system included an inflow well connected by microchannel to an outflow well (Figure 1). Colonies of the strains were resuspended in 3 mL of BHI or CWM and were incubated at 37 °C with shaking (220 rpm) overnight. A bacterial suspension was then prepared from this overnight culture standardized to an OD₆₀₀ of 0.1 ± 0.05 following two serial 1:200 dilutions. For the mixed culture, after the preparation of those bacterial suspensions, a mixed solution of *S. aureus* and *P. aeruginosa* was made. The primary step of the experiment consisted of priming the channel of the BioFlux™ system with 500 µL of fresh medium in the inflow well with a pressure setting of 1 dyne/cm² for 10 min. The remaining medium present in the well was then withdrawn. Thereafter, the microfluidic channels were inoculated by injecting the bacterial suspension of mono or mixed-culture from the output reservoir for 30 min at 1 dyne/cm². The setup was placed on the heating plate at 37 °C. This step is important to enhance bacterial adhesion in the channel. Finally, the bacterial suspension was transferred in the inflow well for 72 h with pressure and temperature settings of 0.2 dyne/cm² and 37 °C, respectively. Biofilms were obtained with bacteria cultivated either alone or in combination, in the BHI medium and in the CWM.

CFU counts on mixed biofilm (coculture of *S. aureus* Newman and *P. aeruginosa* PAO1) after 24 h, 48 h and 72 h inside the Bioflux™ 200 system in both the BHI and CWM media were performed by flow reversion in order to control the presence of each species. After dilutions, the bacteria were plated on nonselective (Luria–Bertani agar) and selective agar (cetrimide agar for *P. aeruginosa* and mannitol salt agar for *S. aureus*) plates. Three independent experiments were performed.

2.3. Gene Expression of *P. aeruginosa* Exopolysaccharides and Alginate Biosynthesis by Real-Time (RT)-PCR

Sessile bacteria were recovered from the microfluidic channel to the output well by an increase of the flow. We applied a pressure of 20 dynes/cm² for 30 min. Bacteria were then pelleted by centrifugation and resuspended in 1 mL of PBS 1X. We analysed the mRNA (transcription) levels of the exopolysaccharides *pel*, *psl* and of the regulator of alginate biosynthesis *algD*. Total cellular RNA was extracted using the Rneasy® Mini kit (Qiagen, Courtaboeuf, France) and treated with RNase-free DNase (Qiagen) for 30 min at 37 °C, after which a second step of purification was performed. RT-PCR was carried out in a LightCycler® using the one-step LightCycler® RNA Master SYBR Green I kit (Roche Applied Science, Meylan, France) according to the manufacturer's protocol. The specificity of the generated products was tested by melting point analysis. Amplifications were performed in triplicate from three different RNA preparations. Cycle threshold (Ct) values of

the target genes were compared with the Ct values of the housekeeping *rpoD* gene, chosen as an endogenous reference for normalizing the transcription levels of the target gene. The condition where bacteria were cultivated in a BHI medium was used as the control and the normalized relative expressions of the studied genes in the CWM were determined for each strain according to the equation $2^{-\Delta\Delta Ct}$, where $\Delta\Delta Ct = (Ct_{\text{gene}} - C_{\text{rpoD}})$ in the CWM and $(Ct_{\text{gene}} - C_{\text{rpoD}})$ in the BHI medium. Primers used were listed in Table 2.

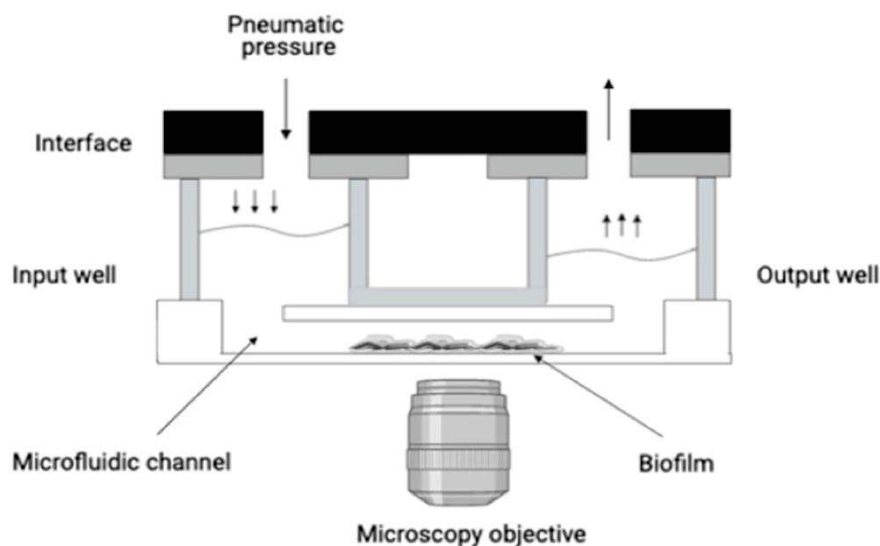


Figure 1. Schematization of the BioFlux™ 200 organization. This system delivers controlled shear flow for simulating physiological and environmental conditions. It allows the connection by microchannel of an inflow well to an outflow well. Biofilm formation will occur in the microfluidic channel under shear flow condition. A microscope can be placed underneath the microfluidic channel, allowing a live observation of the biofilm formation.

Table 2. Primers used in the study.

Primers Used and Target Function	Target Region	Primer Name	Oligonucleotide Sequence	Reference
GDP-mannose 6-dehydrogenase	<i>algD</i>	algD-F algD-R	5'-CGTCAACGTCAACGTCGTG-3' 5'-AACAGCAGCTTGCCCTTGTA-3'	[18]
Exopolysaccharides	<i>pel</i>	pel-F pel-R	5'-AGCAAGAAAGGAATCGCCG-3' 5'-GACCGACAGATAGGCGAAGG-3'	[19]
Exopolysaccharides	<i>psl</i>	psl-F psl-R	5'-CTGCCCTCACCTTTCGCC-3' 5'-GGAAGGATCAGCTGCG-3'	[19]
Housekeeping gene	<i>rpoD</i>	rpoD-F rpoD-R	5'-CGATCGGTGACGACGAAGAT-3' 5'-GTTTCATGTCGATGCCGAAGC-3'	[18]

2.4. Automatized Debridement and Antibiotic Treatment in the Microfluidic System

In order to mimic a clinical debridement, which represents the first step of clinical management of a chronic wound, we developed a technique to remove part of the pre-formed biofilm. After 72 h of biofilm formation, a shear flow of 5 dynes/cm² was applied from the input well to the output well for 10 min. The flow was then reversed from the output well for 10 min. This process of flow reversion was performed twice for debrided monomicrobial biofilm and 4 times for the debridement of a mixed polymicrobial biofilm. The aim of this flow inversion was to significantly reduce the biofilm constituted in the microfluidic channel.

After an analysis of clinical studies [2,20–22] concerning the debridement efficiency of the wound bed, we determined that the biofilm was never completely removed. There was always a percentage of remaining biofilm that facilitated its reformation. Clinical data estimated the effectiveness of debridement whether mechanical, surgical, enzymatic or other to be around 85% [23]. Thus, using flow inversion on the BioFlux™ system, we tried to recreate this phenomenon of remaining preformed biofilm. Therefore, we fixed a maximum of 13 to 15% of remaining biofilm in the channel to mimic the in vivo conditions. The aim of this mechanical debridement was to further study the effect of antimicrobial molecules on preformed debrided biofilm. After the automatized debridement, a dynamic flow (0.2 dyne/cm² at 37 °C) of antibiotics was applied to evaluate their actions on the remaining preformed biofilm for 24 h. All antibiotics and the concentrations used in this study are listed in Table 3.

Table 3. Antibiotics used and minimum inhibitory concentration determined in the study.

Antibiotics	Strains	Concentrations Used in the Preformed Biofilm	EUCAST MIC Breakpoints (mg/L)	MIC in the BHI Medium (mg/L)	MIC in the CWM (mg/L)
Vancomycin (Mylan)	<i>S. aureus</i> Newman	1, 10, 100x MIC	2	1	1
Oxacillin (Astellas)		1, 10, 100x MIC	ND ¹	0.5	1
Linezolid (Fresenius Kabi)		1, 10, 100x MIC	4	1	1
Imipenem	<i>P. aeruginosa</i> PAO1	1, 10, 100x MIC	4	1	2
Ceftazidime (PanPharma)		1, 10, 100x MIC	8	1	1

¹ ND, not defined.

To confirm the effect of antibiotics, a determination of dead bacteria among the disrupted biofilm was performed as previously published [24]. Briefly, bacteria released from the biofilm were collected in the output well after 24 h of antibiotics exposure in the BioFlux™ 200 in both the BHI medium and the CWM. The total number of bacteria present in the suspension was calculated by measuring the optical density at 600 nm and concentrations were obtained following our standard curve. After dilutions, bacteria were plated on nonselective (Luria–Bertani agar for monocultures) or selective agar plates (cetrimide agar for *P. aeruginosa* and mannitol salt agar for *S. aureus* for coculture). CFU counts were then performed giving the number of living bacteria present in the output well. The number of dead bacteria was calculated by the difference between the total number of bacteria and the number of living bacteria. Finally, the percentage of dead bacteria corresponded to the ratio: number of dead bacteria/total number of bacteria. Three independent experiments were performed.

2.5. Visualisation and Quantification of Biofilm

After 24 h, 48 h and 72 h of incubation, biofilm formation was recorded using a fluorescence inverted microscope DM IRB (Leica Biosystems, Nanterre, France) coupled with a CoolSNAP FX camera (Roper Scientific, Lisses, France). A video was recorded in real time at a rate of 60 frames per seconds. MetaVue™ software (Molecular Devices, Sunnyvale, CA, USA) was used for imaging. ImageJ® was utilized to colour black and white images, to include scale bars and to calculate biofilm percentage. The 16-bit grayscale images were adjusted with the threshold function to fit the bacterial structure and were analysed using the “Analyze Particles” function. The percentage of biofilm was evaluated before and after automatized debridement and after 24 h of antibiotics treatment following the same protocol as previously described [25,26].

2.6. Statistical Analysis

Statistical analyses were performed using GraphPad Prism version 7 or R version 3.5.2. Tests used for the p value determination are mentioned in each figure legend.

3. Results

3.1. Evaluation of Biofilm Formation in the Bioflux™ System

To evaluate the potential of biofilm formation under BioFlux™ flowthrough conditions of two of the main species isolated from chronic wounds, we determined the percentage of biofilm formation of *S. aureus* Newman, *P. aeruginosa* PAO1 and a mixed culture in the control BHI medium and the new CWM (better adapted to mimic the environment encountered in wounds) developed in our unit.

The two reference strains were able to form biofilm and to remain attached under shear force (Figures 2 and 3).

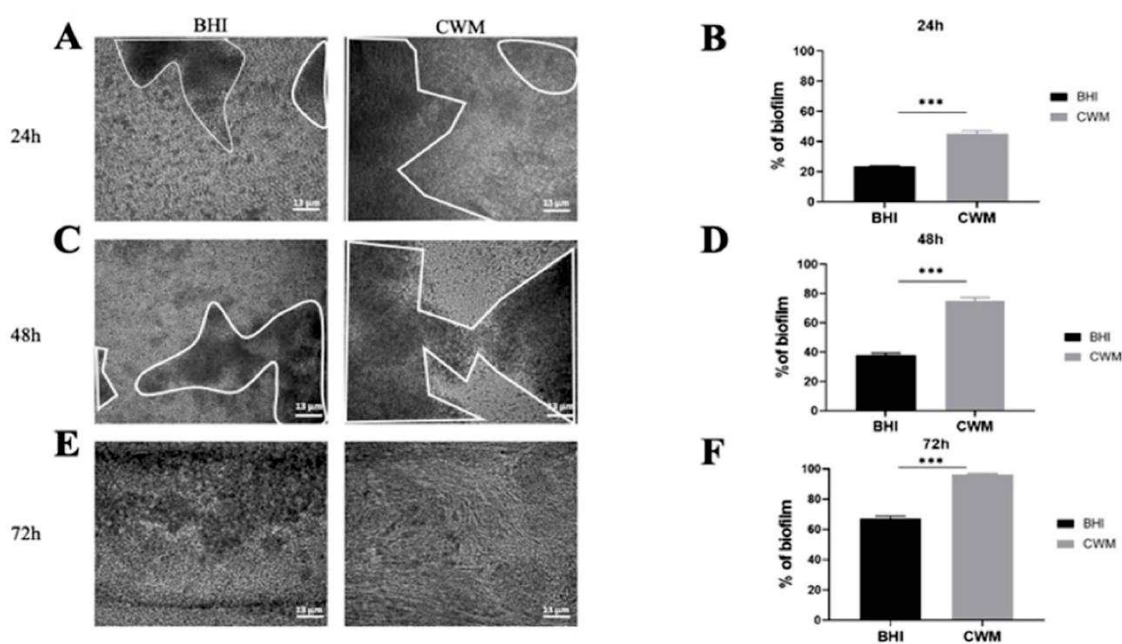


Figure 2. Kinetics of the biofilm formation of *Staphylococcus aureus* Newman in the BioFlux™ system. (A,C,E) correspond to representative images taken at different times ((A) 24 h; (C) 48 h and (E) 72 h) of biofilm formation in the CWM and BHI media. The images are the result of one of the three experimental triplicates. Biofilm is visualized by the black part in between the white lines. Percentages of biofilm formation are presented at 24 h (B), 48 h (D) and 72 h (F) postincubation in both media after three independent experiments. They were determined by the ImageJ software application. Results are presented as the mean \pm standard deviation. Statistics were performed using a t -test on GraphPad Prism version 7. Ns, $p > 0.05$; *** $p < 0.001$.

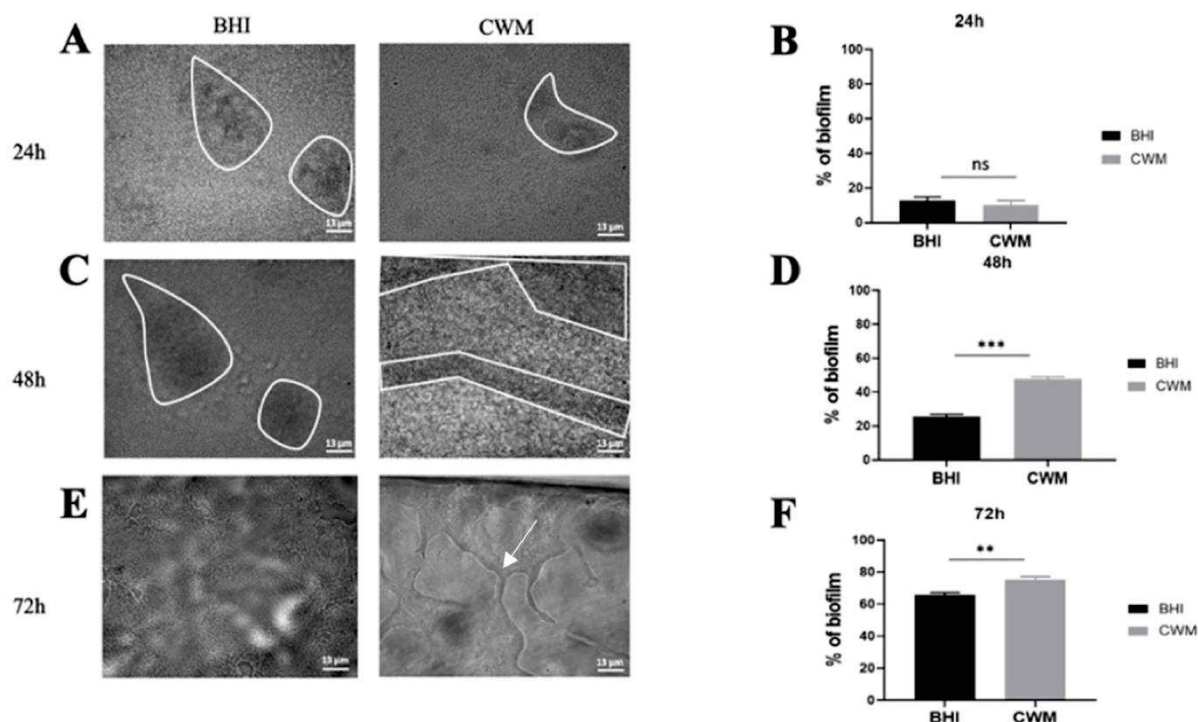


Figure 3. Kinetics of biofilm formation of *Pseudomonas aeruginosa* PAO1 in the BioFlux™ system. (A,C,E) correspond to representative images taken at different times ((A) 24 h; (C) 48 h and (E) 72 h) of biofilm formation in the CWM and BHI media. The images are the result of one of the three experimental triplicates. Biofilm is visualized by the black part in between the white lines. Percentages of biofilm formation are presented at 24 h (B), 48 h (D) and 72 h (F) postincubation in both media after three independent experiments. They were determined by the ImageJ software application. The white arrow indicates the presence of the exopolysaccharides structures formed by *P. aeruginosa* during biofilm formation. Results are presented as the mean \pm standard deviation. Statistics were performed using a *t*-test on GraphPad Prism version 7. Ns, $p > 0.05$; ** $p < 0.01$; *** $p < 0.001$.

The *S. aureus* Newman strain formed a biofilm at each time point (Figure 2). Interestingly, at 24 h the percentage of constituted biofilms ranged from $22.0\% \pm 0.2$ when the strain was cultivated in the BHI medium to $46.5\% \pm 0.4$ in the CWM ($p < 0.001$) (Figure 2B). This significant difference was increased at 48 h post inoculation with $36.0\% \pm 0.2$ of bacteria in the biofilm within the BHI medium vs. $77.2\% \pm 0.5$ within the CWM ($p < 0.001$) (Figure 2D). Finally, after 72 h, the percentage of formed biofilm in CWM was almost complete ($98.3\% \pm 0.1$), whereas it was still incomplete in the BHI medium ($63.1\% \pm 0.3$) ($p < 0.001$) (Figure 2F). The significant difference in the biofilm formation of *S. aureus* in the CWM compared to the BHI medium are visualized in Figure 2A,C,E.

P. aeruginosa biofilm formation inside the Bioflux™ system is shown in Figure 3. Contrary to *S. aureus*, no difference in the percentage of biofilm formation has been observed after 24 h post inoculation in the CWM ($14.1\% \pm 0.4$) vs. BHI medium ($16.0\% \pm 0.3$) ($p =$ Not Significant (NS)) (Figure 3B). However, significantly higher percentages of biofilm constituted in the CWM compared to the BHI medium were noted at 48 h ($49.4\% \pm 0.1$ and $22.0\% \pm 0.1$, respectively) (Figure 3D) and at 72 h ($75.7\% \pm 0.2$ and $63.1\% \pm 0.1$, respectively) ($p < 0.001$) (Figure 3F). The coloured pixels in the images (Figure 3A,C,E) confirmed the presence of a more intense biofilm in the CWM after 48 h. Interestingly, the presence of particular structures has been observed at 72 h in the CWM (Figure 3E). To understand those particular structures (arrow in Figure 3E) observed after 72 h of monoculture of *P. aeruginosa* cultured in the CWM in the Bioflux™ system, the gene expressions of the exopolysaccharides, *pel* and *psl*, as well as the regulator of alginate biosynthesis, *algD*, were analysed by qRT-PCR. Those three extracellular polysaccharides have been implicated

in biofilm development. The results are shown in Figure 4. A significant difference in the expression of the exopolysaccharides-encoding genes, *pel* ($p < 0.01$) and *psl* ($p < 0.01$), was observed after 72 h of culture. Moreover, the expression of a key regulator of the alginate production, *algD*, was also significantly increased in the CWM compared to the BHI ($p < 0.001$).

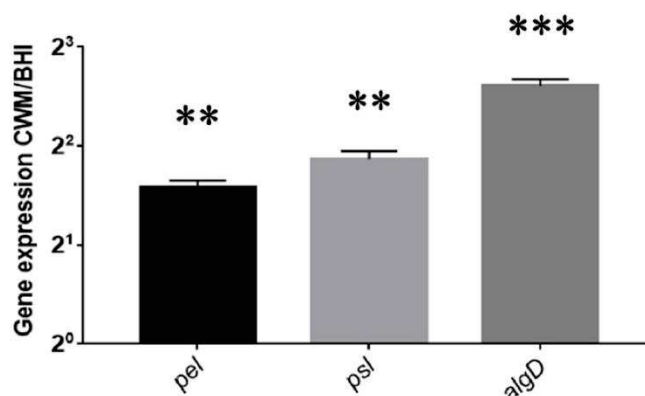


Figure 4. Expression of *Pseudomonas aeruginosa* PAO1 *pel*, *psl* and *algD* genes after recovering sessile cells in the BioFlux™ system after 72 h of culture. The normalized relative expressions of the studied genes in the CWM were determined for each strain according to the equation $2^{-\Delta\Delta Ct}$, where $\Delta\Delta Ct = (Ct_{gene} - Ct_{rpoD})$ in the CWM - $(Ct_{gene} - Ct_{rpoD})$ in the BHI medium. Results are presented as the mean \pm standard deviation of three different experiments. Statistics were performed using a *t*-test on GraphPad Prism version 7. ** $p < 0.01$; *** $p < 0.001$.

Finally, inside a mixed biofilm composed of *S. aureus* and *P. aeruginosa*, the two species formed a faster and denser biofilm in the CWM compared to the BHI medium at any time point (Figure 5). Indeed, a significant difference in the percentage of biofilm formation was noted at 24 h ($36.0\% \pm 0.3$ in the CWM vs. $17.4\% \pm 0.2$ in the BHI medium) (Figure 5B), at 48 h ($78.0\% \pm 0.2$ and $41.0\% \pm 0.1$, respectively) (Figure 5D) and at 72 h ($93.3\% \pm 0.2$ and $72.0\% \pm 0.4$, respectively) (Figure 5F). It is also interesting to note that *S. aureus* formed a biofilm more rapidly than *P. aeruginosa* PAO1 at 24 h ($p < 0.001$) and at 48 h ($p < 0.01$) in the CWM. Moreover, in coculture, *P. aeruginosa* PAO1 established a more important biofilm in coculture compared to monoculture in the CWM ($p < 0.001$) and the BHI medium ($p < 0.1$). To confirm that the mixed biofilm was equally composed by *S. aureus* and *P. aeruginosa*, CFU counts were performed inside the BioFlux™ 200. No statistical difference in the proportion of bacteria isolated in the BHI medium and the CWM at the same times was observed (Table S1).

3.2. Antibiotics Activity on Preformed Biofilm Is Dependent on the Culture Media

To mimic the management of chronic wounds, we adapted an automatized debridement of the biofilm inside the BioFlux™ system and administrated different antibiotics on preformed biofilms by *S. aureus* Newman, *P. aeruginosa* PAO1 and mixed culture in the BHI medium and the CWM.

The MIC values for each antibiotic against the studied strains are shown in Table 2.

After the constitution of a biofilm with *S. aureus* Newman, no effect on the reduction of this preformed biofilm was observed using 1x MIC of vancomycin regardless of the medium used ($14.7\% \pm 0.3$ in the BHI medium and $15.0\% \pm 0.1$ in the CWM) ($p = NS$) (Figure 6A). At 10x and 100x MIC of vancomycin, a significant reduction of the preformed biofilm was shown in the BHI medium ($11.9\% \pm 0.2$) ($p < 0.1$), whereas no effect was noted when the biofilm was constituted in the CWM ($14.8\% \pm 0.1$) ($p = NS$) (Figure 6A). No difference in the percentage of dead bacteria was noted on disrupted biofilm regardless of the concentration of vancomycin used (Table S2). Using oxacillin, a significant reduction in the percentage of preformed biofilm was observed at 1x MIC in the BHI medium

($10.8\% \pm 0.2$) ($p < 0.1$) (Figure 5B). Interestingly, an important reduction of the biofilm was detected using 10 and 100x MIC of oxacillin in both media (in the BHI medium: $7.4\% \pm 0.3$ and $4.7\% \pm 0.4$, respectively; in the CWM: $8.9\% \pm 0.3$ and $8.2\% \pm 0.3$, respectively) ($p < 0.01$) (Figure 6B). This observation was correlated with a significant increase in the percentage of dead bacteria detected in the two media ($p < 0.01$) (Table S2). The same observation was noted using linezolid. A reduction of the preformed biofilm at 1x MIC was only shown in the BHI medium ($9.8\% \pm 0.3$) ($p < 0.1$), whereas the decreased percentage of biofilm was more important at 10 and 100x MIC, regardless of the medium used (in the BHI medium: $7.2\% \pm 0.2$ and $6.7\% \pm 0.3$, respectively; in the CWM: $10.6\% \pm 0.3$ and $8.5\% \pm 0.2$, respectively) ($p < 0.01$) (Figure 6C). We could note that regardless of the antibiotic used and their concentrations, their action on preformed biofilm was significantly reduced in the CWM compared to the BHI medium ($p < 0.01$).

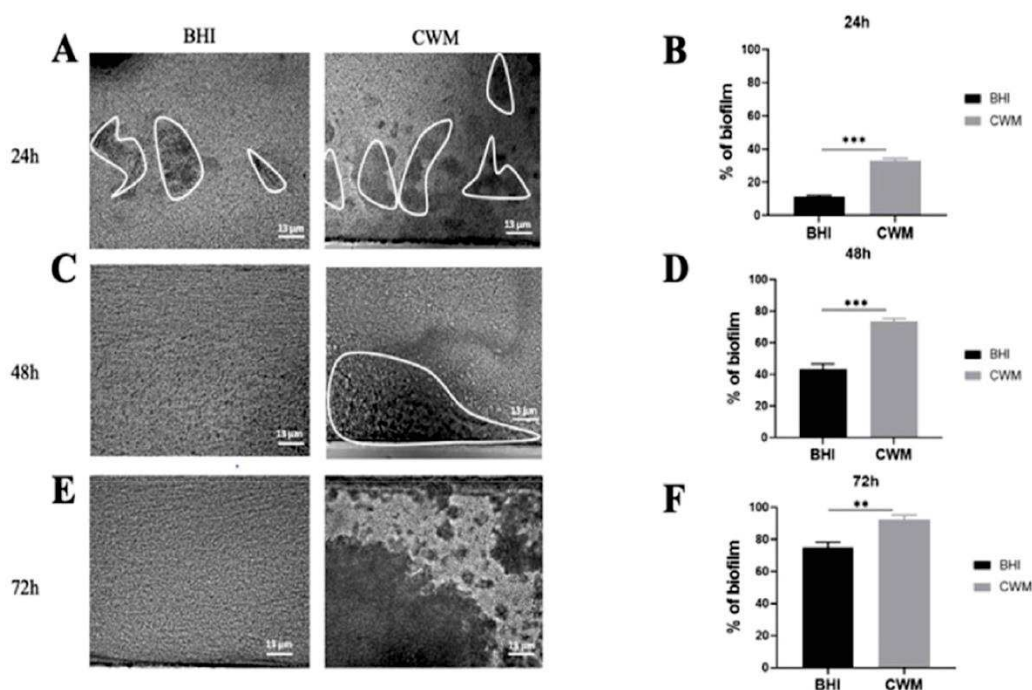


Figure 5. Kinetics of biofilm formation of coculture of *Staphylococcus aureus* Newman and *Pseudomonas aeruginosa* PAO1 in the BioFlux™ system. The ratio of coculture used was 1:1. The two species were added into the system simultaneously. (A,C,E) correspond to representative images taken at different times ((A) 24 h; (C) 48 h and (E) 72 h) of biofilm formation in the CWM and BHI media. The images are the result of one of the three experimental triplicates. Biofilm is visualized by the black part in between the white lines. Percentages of biofilm formation are presented at 24 h (B), 48 h (D) and 72 h (F) postincubation in both media after three independent experiments. They were determined by the ImageJ software application. Results are presented as the mean \pm standard deviation. Statistics were performed using a *t*-test on GraphPad Prism version 7. Ns, $p > 0.05$; ** $p < 0.01$; *** $p < 0.001$.

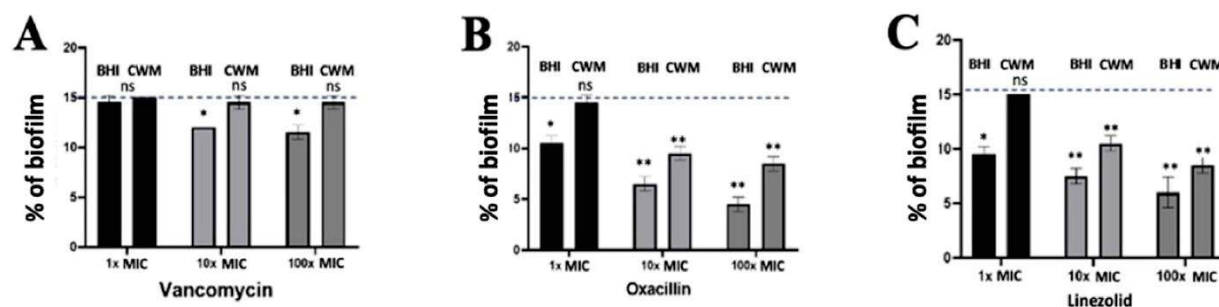


Figure 6. Percentage of biofilm reduction on preformed *Staphylococcus aureus* Newman biofilm in the BioFlux™ system using vancomycin (A), oxacillin (B) and linezolid (C) at different concentrations (1x, 10x and 100x MIC) and in the CWM and BHI media. An automatized debridement was fixed at 15% of biofilm left in the microfluidic channel. Samples were tested in three independent experiments. Results are presented as the mean \pm standard deviation. Statistics were performed using a *t*-test on GraphPad Prism version 7. Ns, $p > 0.05$; * $p < 0.1$; ** $p < 0.01$.

Using *P. aeruginosa* PAO1, no effect could be noted on the reduction of the preformed biofilm when 1x MIC of imipenem was administrated regardless of the medium used ($15.0\% \pm 0.1$ in the BHI medium and $14.9\% \pm 0.2$ in the CWM) ($p = \text{NS}$) (Figure 7A). When the antibiotic concentration was increased (10x MIC and 100x MIC), a significant reduction of the biofilm could be observed with similar results in both media (in the BHI medium: $13.4\% \pm 0.2$ and $12.3\% \pm 0.2$, respectively; in the CWM: $13.7\% \pm 0.4$ and $13\% \pm 0.3$, respectively) ($p < 0.01$) (Figure 7A). Interestingly, 1x MIC of ceftazidime had a significant impact on the preformed biofilm ($12.4\% \pm 0.2$ in the BHI medium and $12.9\% \pm 0.4$ in the CWM) ($p < 0.1$). This trend was increased at 10x MIC ($7.6\% \pm 0.2$ in the BHI medium and $7.7\% \pm 0.3$ in the CWM) and 100x MIC ($5.6\% \pm 0.3$ in the BHI medium and $6.4\% \pm 0.4$ in the CWM) regardless of the medium used ($p < 0.01$) (Figure 7B). We could note that both media had no influence on the antimicrobial action of ceftazidime and imipenem against *P. aeruginosa*. The percentage of dead bacteria showed significant results at 10x and 100x MIC of ceftazidime ($p < 0.01$) (Table S2).

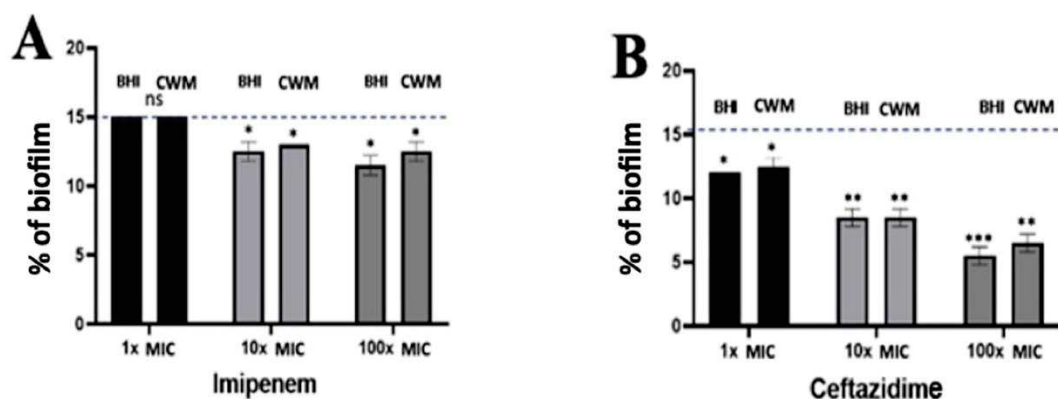


Figure 7. Percentage of biofilm reduction on preformed *Pseudomonas aeruginosa* PAO1 biofilm in the BioFlux™ system using imipenem (A), and ceftazidime (B) at different concentrations (1x, 10x and 100x MIC) and in the CWM and BHI media. An automatized debridement was fixed at 15% of biofilm left in the microfluidic channel. Samples were tested in three independent experiments. Results are presented as the mean \pm standard deviation. Statistics were performed using a *t*-test on GraphPad Prism version 7. Ns, $p > 0.05$; * $p < 0.1$; ** $p < 0.01$; *** $p < 0.001$. Antibiotics efficiency on preformed *Pseudomonas aeruginosa* PAO1 biofilm.

Finally, when an optimized combination of antibiotics (10x MIC of ceftazidime + 10x MIC of oxacillin and 10x MIC of ceftazidime + 10x MIC of linezolid) was used on a preformed biofilm constituted by *S. aureus* Newman and *P. aeruginosa* PAO1, a significant

reduction of the preformed mixed biofilm was observed in both media when the association of ceftazidime and oxacillin ($6.7\% \pm 0.2$ in the BHI medium and $7.1\% \pm 0.3$ in the CWM) and of ceftazidime and linezolid ($5.6\% \pm 0.1$ in the BHI medium and $6.2\% \pm 0.7$ in the CWM) were used ($p < 0.01$) (Figure 8). The efficiency of the combination of antibiotics was significantly increased in comparison to the antibiotic used alone on a single species at the same concentration ($p < 0.01$). This observation was correlated with a significant increase in the percentage of dead bacteria detected when we used these combinations ($p < 0.01$) (Table S2). As observed with *P. aeruginosa* alone, the two media had no influence on the antimicrobial action of the combination of antibiotics.

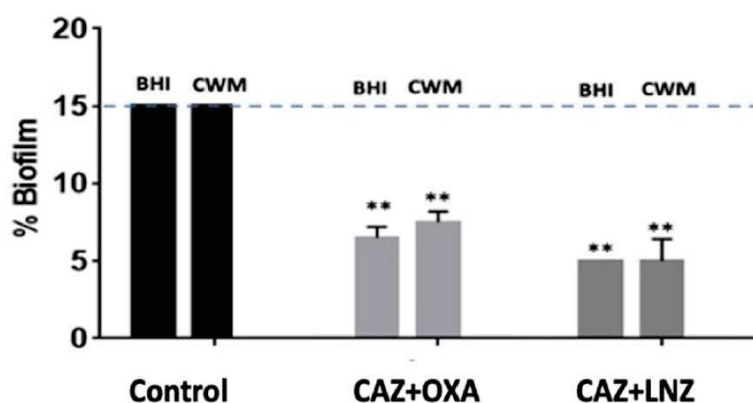


Figure 8. Percentage of biofilm reduction on preformed *Staphylococcus aureus* Newman and *Pseudomonas aeruginosa* PAO1 mixed biofilm in the BioFlux™ system using 10x MIC of ceftazidime (CAZ) + oxacillin (OXA) and 10x MIC of ceftazidime (CAZ) + linezolid (LNZ) in the CWM and BHI media. An automatized debridement was fixed at 15% of biofilm left in the microfluidic channel. Samples were tested in three independent experiments. Results are presented as the mean \pm standard deviation. Statistics were performed using a *t*-test on GraphPad Prism version 7. Ns, $p > 0.05$; ** $p < 0.01$.

4. Discussion

Biofilm formation is a crucial step in the pathophysiology of chronic wounds [6]. Its study is of concern and requires the development of new tools [27]. Classically, biofilms are investigated using in vitro experiments in static conditions (e.g., crystal violet method, resazurin, plates count, or microscopy). These traditional microbiological techniques have provided great knowledge about bacterial biofilm potential. However, they present several limitations, such as difficulties in culturing some bacteria, the study of polymicrobial biofilm, the heterogeneity of bacterial populations inside a biofilm or difficulties in recreating some physical or biological conditions [28]. Microfluidics technologies are new and emerging technologies that complement current biological assays. Their evaluation is important to estimate their potential. In this study, we showed that the BioFlux™ system was a particularly adapted and interesting strategy to study dynamic biofilm formation in mono or mixed culture, to mimic the debridement (a crucial step in the eviction of the biofilm, notably in wounds) and to characterize the effect of antimicrobial agents against a preformed and debrided mono or polymicrobial biofilm. Moreover, it has been clearly established that the behaviour of microorganisms was highly dependent on the environment in which they evolved [6]. The environment encountered by bacteria in clinical situations influences bacterial virulence and its potential for biofilm formation. The development of a new in vitro medium mimicking in vivo conditions remains an important challenge to evaluate the bacterial behaviour in a specific environment and the effect of therapeutic solutions. Therefore, our group has adapted the “Chronic Wound-like Medium” with the aim to be closer to physiological environments encountered in wounds.

Inside the BioFlux™ system, we observed that if the two studied species formed a robust biofilm after 72 h as expected, species cultivated in the CWM had a significant higher

ability to facilitate microbial adhesion and its subsequent biofilm formation compared to the traditional microbiological medium (BHI) ($p < 0.001$). The *S. aureus* Newman strain was particularly influenced by the CWM and formed a faster and denser biofilm compared to *P. aeruginosa* PAO1. Differences in the biofilm formation of the species might underline that the culture medium had an important impact on the bacterial behaviour as previously observed [29]. This reinforces the need to cultivate bacteria in an environment that closely mimics the in vivo conditions. Bacterial culture media have different compositions that can influence bacterial phenotype such as fitness, early adhesion, biofilm formation or genes expression [30]. To corroborate these constataions, we observed a different behaviour of a same species in the two studied media in our study. Alginate is an exopolysaccharide synthesized to respond to environmental conditions. It is produced by *P. aeruginosa* as the most abundant extracellular matrix polysaccharide and regulated virulence, biofilm formation and resistance to different antibiotics [31]. It has been previously shown that the reference strain of *P. aeruginosa* PAO1 was a non-mucoid strain, which does not exhibit any alginate production in the conventional culture media [32]. However, in our study, we observed the presence and production of structures harbouring the characteristics of exopolysaccharides as alginate, when this strain was cultivated for 72 h in the CWM (Figure 3E) contrary to the BHI medium. After extended cultivation (72 h in our study), we observed that *P. aeruginosa* PAO1 strain up-regulated expression of the gene involved in biosynthesis of the alginate but also of exopolysaccharides-encoding genes (*pel* and *psl*). Those three components are keys for creating a strong scaffold involved in maintaining biofilm integrity. Those data suggested that in the CWM mimicking stressful conditions, bacteria could produce a stronger and denser biofilm compared to a classical microbiological culture medium. It also proves that this new in vitro medium promotes a strong and noticeable scaffold of exopolysaccharide. *algG* is involved in the alginate biosynthetic operon that is required for the incorporation of L-gulonate residues into alginate. So far, observations corroborated the fact that the strains had different behaviour depending on the media used for culture. We could also note that a medium mimicking wound conditions improved biofilm formation by influencing the secretion of proteins involved in the biofilm process (e.g., alginate). The surfaces used to study biofilm formation also represent an important parameter that influences microbial adhesion. In static models, polystyrene is the main component of the adherent surfaces used controversially for dynamic assays where glass is predominant. Surface-dependent attachment is especially more pronounced in in vitro assays where no human matrix proteins such as fibrinogen or fibronectin, which normally serve as anchors for attachment, are present [33]. The microfluidic model used in this study allows precoating on the glass support of the shear model damaged human cells, such as keratinocytes or melanocytes, to mimic the cellular environment present at the wound bed, which serves as adhesion support [34].

The investigation of biofilms must also include the action of antimicrobial agents. Biofilms are involved in more than 80% of chronic wounds infections [35]. The penetration of antibiotics is usually reduced in biofilm due, among others, to the EPS matrix [7]. Thus, the antimicrobial effect of antibiotics is compromised within these environments. Biofilms of *P. aeruginosa* and *S. aureus* are particularly relevant in chronic wounds, since they are most of the time isolated together at the wound bed and their interactions create an additional difficulty to eradicate the biofilm [36]. Two types of in vitro biofilm models are currently used to predict antimicrobial efficiency against biofilm: closed and open systems. Closed systems are characterised by limited nutrients and accumulation of metabolic waste which can create a bias in biofilm quantification [37]. Open systems better reproduce the conditions encountered in vivo, as there is a permanent control of nutrient delivery, flow, and temperature [38]. The BioFlux™ system is a microfluidic open system in which multiple biofilms can be run at the same time [39] and where protocols adaptation to mimic in vivo biofilm formation or biofilm management is possible (e.g., automatized debridement for chronic wounds). In this study, we evaluated different antibiotics commonly used against *S. aureus* and *P. aeruginosa* infections. They serve as a model, acting at different levels in

bacteria and presenting variable activities against biofilm formation. In the BioFlux™ system, we were able to test antibiotics alone or in combination, at different concentrations and in different media on mono or polymicrobial biofilms. The multiplicity of studies available with this technology is reinforced by the possibility to obtain image intensity results, which can be translated to a remaining biofilm percentage evaluating the efficiency of antibiotics on a preformed biofilm. Thus, we highlighted a variety of antibiotics action in our study. Oxacillin, linezolid and ceftazidime were particularly active alone or in combination against a preformed biofilm whereas vancomycin and imipenem had clearly few activities. Even at 100x MIC, vancomycin was unable to reduce the *S. aureus* preformed biofilm. This difference could be explained by the ability of linezolid or β -lactams to penetrate deeper into the biofilms and to be able to directly come into contact with the bacteria. Interestingly, although the two antibiotics (imipenem and ceftazidime) used against *P. aeruginosa* were not influenced by the culture medium tested, a significant difference could be observed with the antibiotics used against *S. aureus*. These antibiotics presented a lower ability to decrease the monomicrobial preformed biofilm cultured in the CWM compared to the BHI medium. This observation is of concern and could explain the difficulties to treat common microbial-biofilm-associated infections where bacteria are installed in this chronic situation even if the antibiotic seems active against the bacteria following the antibiogram results. Regarding the recent literature data on *P. aeruginosa* biofilm and the efficacy of antibiotics, several studies have highlighted an inefficiency of the imipenem at sub-MIC and MIC concentrations to reduce bacteriological biomass within the biofilm. Authors have shown that the use of imipenem even favoured the maturation and increase of bacterial biomass in biofilm from clinical isolates of cystic fibrosis [40,41]. Only Musafer et al. [42] demonstrated an action of imipenem on three clinical strains isolated in a context of cystic fibrosis. However, those conclusions were drawn with a static in vitro model of biofilm formation. Concerning the ceftazidime effect, some studies concur with the conclusions presented in this article. Otani et al. [43] noted the effectiveness of ceftazidime to reduce the PAO1 biofilm even at sub-MIC concentrations. The efficacy of ceftazidime was also demonstrated in an in vivo model of ureteral stent infection in combination with another antibiotic (azithromycin) [44]. This antibiotic therefore has a very valuable antibiofilm potential but could be modulated. Indeed, it was reported by several studies that despite the important antibiofilm potential of ceftazidime, the long-term use of the antibiotic can cause an increase in resistance in the planktonic and sessile population [45,46]. For *S. aureus* strains, the literature on the effect of vancomycin as a potential antibiofilm is consistent with what this study highlighted. Vancomycin at MIC concentration are not capable of generating a reduction in bacterial density within the biofilm [47]. At sub-MIC concentrations, vancomycin use increased the formation of mature biofilm [48]. Some studies highlighted an effect on sessile bacteria; however, the concentrations used were particularly high (90–120x MIC) or the administration time was too long to be clinically useful [49,50]. There are few data on the use of oxacillin on biofilm during the early stage of formation or on preformed mature biofilm. Mirani et al. [51] demonstrated an influence of this antibiotic on *S. aureus* reference strains. The mechanism could be due to the modulation of the *icaA* and *agr* expression, two major regulator genes of biofilm formation. The efficacy of oxacillin on mature biofilm was confirmed by Manner et al. [52]. Finally, regarding linezolid, publications reported that this antibiotic used alone was ineffective to reduce the biofilm of *S. aureus* [53] notably in osteoarticular infections [54]. Only Gander et al. [55] observed an effect of 1x MIC on the early stage of biofilm formation but with a classic microbiological medium and in static conditions. Those data thus reinforce the need to use more reliable and standardized media and models to evaluate the antimicrobial agents and their potential effects and risks. This also validates the interest in the BioFlux™ system in these investigations.

5. Conclusions

S. aureus and *P. aeruginosa* biofilms are implicated in several infections. In chronic wounds, pathological biofilm is frequent and difficult to treat. Thus, new therapeutic strategies are needed and the inhibition of preformed biofilms is a great challenge for the treatment of these infections. Therefore, *in vitro* biofilm models should be improved in clinical microbiology to predict the efficiency of antimicrobial treatments on sessile cells. The combination of a new chronic wound medium and the BioFlux™ microfluidic system represents a powerful tool to study biofilm formation and to screen the potential antibiofilm actions of candidate molecules under conditions mimicking those encountered *in vivo*.

Supplementary Materials: The following are available online at <https://www.mdpi.com/article/10.3390/diagnostics11101746/s1>, Table S1: Percentage of *S. aureus* Newman and *P. aeruginosa* PAO1 present inside the mixed biofilm formed in the Bioflux™ 200 system after 24 h, 48 h and 72 h in both the BHI medium and the CWM and obtained by flow reversion. Results are expressed as the mean ± standard deviation of three independent experiments. Statistics were performed using a t-test on GraphPad Prism version 7. Ns, non-significant. Table S2: Percentage of dead bacteria of *Staphylococcus aureus* Newman (A) and *Pseudomonas aeruginosa* PAO1 (B) alone or combined in a mixed biofilm (C) in the BioFlux™ 200 system after exposition to antibiotics in the different media. Samples were tested in three independent experiments. Results are presented as the mean ± standard deviation. Statistics were performed using a t-test on GraphPad Prism version 7. Ns, non-significant.

Author Contributions: Conceptualization, J.-P.L. and A.S.; methodology, J.-P.L., C.P. and C.D.-R.; software, C.P.; formal analysis, C.P., C.D.-R. and A.P.; data curation, C.P., C.D.-R. and A.P.; writing—original draft preparation, C.P. and J.-P.L.; writing—review and editing, C.D.-R., A.P., S.S. and A.S.; visualization, S.S. and A.S.; supervision, J.-P.L.; project administration, A.S. and J.-P.L.; funding acquisition, A.S. and J.-P.L. All authors have read and agreed to the published version of the manuscript.

Funding: This research was funded by CHU Nîmes, Thématique Phare. CP is supported by a PhD grant from Biofilm Pharma (Bourse CIFRE). The funders had no role in study design, data collection and analysis, decision to publish, or preparation of the manuscript.

Institutional Review Board Statement: Not applicable.

Informed Consent Statement: Not applicable.

Data Availability Statement: Data supporting reported results can be found on the BioFlux software in our Unit at Bioflux experiments—PAO1 and Newman—Kinetics and ATB effect.

Acknowledgments: A.P., C.D.-R., A.S. and J.-P.L. belong to the FHU INCh (Federation Hospitalo Universitaire Infections Chroniques, Aviesan). We thank the Nîmes University hospital for its structural, human and financial support through the award obtained by our team during the internal call for tenders “Thématiques phares”. We thank Sarah Kabani for her editing assistance. This study was presented orally at the 31st ECCMID (N°1469).

Conflicts of Interest: The authors declare no conflict of interest.

References

1. Sen, C.K. Human wounds and its burden: An updated compendium of estimates. *Adv. Wound Care* **2019**, *8*, 39–48. [CrossRef]
2. Frykberg, R.G.; Banks, J. Challenges in the treatment of chronic wounds. *Adv. Wound Care* **2015**, *4*, 560–582. [CrossRef]
3. Bowler, P.G.; Duerden, B.I.; Armstrong, D.G. Wound microbiology and associated approaches to wound management. *Clin. Microbiol. Rev.* **2001**, *14*, 244–269. [CrossRef]
4. Nunan, R.; Harding, K.G.; Martin, P. Clinical challenges of chronic wounds: Searching for an optimal animal model to recapitulate their complexity. *Dis. Model Mech.* **2014**, *7*, 1205–1213. [CrossRef]
5. James, G.A.; Swogger, E.; Wolcott, R.; Pulcini, E.D.; Secor, P.; Sestrich, J.; Costerton, J.W.; Stewart, P. Biofilms in chronic wounds. *Wound Repair Regen.* **2008**, *16*, 37–44. [CrossRef]
6. Pouget, C.; Dunyach-Remy, C.; Pantel, A.; Schuldiner, S.; Sotto, A.; Lavigne, J.-P. Biofilms in Diabetic Foot Ulcers: Significance and Clinical Relevance. *Microorganisms* **2020**, *8*, 1580. [CrossRef]
7. Sharma, D.; Misba, L.; Khan, A.U. Antibiotics versus biofilm: An emerging battleground in microbial communities. *Antimicrob. Resist. Infect. Control.* **2019**, *8*, 76. [CrossRef]

8. Yin, W.; Wang, Y.; Liu, L.; He, J. Biofilms: The microbial “protective clothing” in extreme environments. *Int. J. Mol. Sci.* **2019**, *20*, 3423. [CrossRef]
9. Zhao, G.; Usui, M.L.; Lippman, S.I.; James, G.A.; Stewart, P.; Fleckman, P.; Olerud, J.E. Biofilms and inflammation in chronic wounds. *Adv. Wound Care* **2013**, *2*, 389–399. [CrossRef]
10. Demidova-Rice, T.N.; Hamblin, M.R.; Herman, I.M. Acute and impaired wound healing: Pathophysiology and current methods for drug delivery, part 1: Normal and chronic wounds: Biology, causes, and approaches to care. *Adv. Skin Wound Care* **2012**, *25*, 304–314. [CrossRef]
11. Howell-Jones, R.S.; Wilson, M.J.; Hill, K.E.; Howard, A.J.; Price, P.E.; Thomas, D. A review of the microbiology, antibiotic usage and resistance in chronic skin wounds. *J. Antimicrob. Chemother.* **2005**, *55*, 143–149. [CrossRef] [PubMed]
12. Tzaneva, V.; Mladenova, I.; Todorova, G.; Petkov, D. Antibiotic treatment and resistance in chronic wounds of vascular origin. *Clujul Med.* **2016**, *89*, 365–370. [CrossRef] [PubMed]
13. Smith, R.; Russo, J.; Fiegel, J.; Brogden, N. Antibiotic delivery strategies to treat skin infections when innate antimicrobial defense fails. *Antibiotics* **2020**, *9*, 56. [CrossRef] [PubMed]
14. World Health Organization. *Standardization of Methods for Conducting Microbic Sensitivity Tests*; Second Report of the Expert Committee on Antibiotics; WHO Technical Report Series, No. 210; WHO: Geneva, Switzerland, 1961. Available online: <https://apps.who.int/iris/handle/10665/40480> (accessed on 30 June 2021).
15. Sawyer, I.; Berry, M.; Ford, J. Effect of medium composition, agitation and the presence of EDTA on the antimicrobial activity of cryptolepine. *Lett. Appl. Microbiol.* **1997**, *25*, 207–211. [CrossRef]
16. Holloway, B.W.; Krishnapillai, V.; Morgan, A.F. Chromosomal genetics of *Pseudomonas*. *Microbiol. Rev.* **1979**, *43*, 73–102. [CrossRef]
17. Duthie, E.S.; Lorenz, L.L. Staphylococcal coagulase: Mode of action and antigenicity. *Microbiology* **1952**, *6*, 95–107. [CrossRef]
18. Seder, N.; Abu Bakar, M.H.; Abu Rayyan, W.S. Transcriptome Analysis of *Pseudomonas aeruginosa* biofilm following the exposure to Malaysian stingless bee honey. *Adv. Appl. Bioinform. Chem.* **2021**, *14*, 1–11. [CrossRef]
19. Colvin, K.M.; Gordon, V.; Murakami, K.; Borlee, B.R.; Wozniak, D.J.; Wong, G.C.L.; Parsek, M.R. The pel polysaccharide can serve a structural and protective role in the biofilm matrix of *Pseudomonas aeruginosa*. *PLoS Pathog.* **2011**, *7*, e1001264. [CrossRef]
20. Schultz, G.; Bjarnsholt, T.; James, G.A.; Leaper, D.J.; McBain, A.; Malone, M.; Stoodley, P.; Swanson, T.; Tachi, M.; Wolcott, R.D.; et al. Consensus guidelines for the identification and treatment of biofilms in chronic nonhealing wounds. *Wound Repair Regen.* **2017**, *25*, 744–757. [CrossRef]
21. Blake, F.A.S.; Abromeit, N.; Bubenheim, M.; Li, L.; Schmelzle, R. The biosurgical wound debridement: Experimental investigation of efficiency and practicability. *Wound Repair Regen.* **2007**, *15*, 756–761. [CrossRef]
22. Steed, D.L. Debridement. *Am. J. Surg.* **2004**, *187*, S71–S74. [CrossRef]
23. Mori, Y.; Rn, G.N.; Kitamura, A.; Minematsu, T.; Kinoshita, M.; Suga, H.; Kurita, M.; Hayashi, C.; Kawasaki, A.; Sanada, H. Effectiveness of biofilm-based wound care system on wound healing in chronic wounds. *Wound Repair Regen.* **2019**, *27*, 540–547. [CrossRef]
24. Hernández, S.B.; Cota, I.; Ducret, A.; Aussel, L.; Casadesús, J. Adaptation and preadaptation of *Salmonella enterica* to bile. *PLoS Genet.* **2012**, *8*, e1002459. [CrossRef]
25. Naudin, B.; Heins, A.; Pinhal, S.; Dé, E.; Nicol, M. BioFlux™ 200 microfluidic system to study a. *Baumannii* Biofilm Formation in a Dynamic Mode of Growth. *Methods Mol. Biol.* **2019**, 167–176. [CrossRef]
26. Tremblay, Y.; Voegelé, P.; Jacques, M.; Harel, J. High-throughput microfluidic method to study biofilm formation and host-pathogen interactions in pathogenic *Escherichia coli*. *Appl. Environ. Microbiol.* **2015**, *81*, 2827–2840. [CrossRef]
27. Silva, N.B.S.; Marques, L.A.; Röder, D.D.B. Diagnosis of biofilm infections: Current methods used, challenges and perspectives for the future. *J. Appl. Microbiol.* **2021**, in press. [CrossRef]
28. Pérez-Rodríguez, S.; García-Aznar, J.M.; Gonzalo-Asensio, J. Microfluidic devices for studying bacterial taxis, drug testing and biofilm formation. *Microb. Biotechnol.* **2021**, *0*, 1–20. [CrossRef]
29. López, D.; Vlamakis, H.; Kolter, R. Biofilms. *Cold Spring Harb. Perspect. Biol.* **2010**, *2*, a000398. [CrossRef]
30. Kostakioti, M.; Hadjifrangiskou, M.; Hultgren, S.J. Bacterial biofilms: Development, dispersal, and therapeutic strategies in the dawn of the postantibiotic era. *Cold Spring Harb. Perspect. Med.* **2013**, *3*, a010306. [CrossRef]
31. Rasamiravaka, T.; Labtani, Q.; Duez, P.; El Jaziri, M. The formation of biofilms by *Pseudomonas aeruginosa*: A review of the natural and synthetic compounds interfering with control mechanisms. *BioMed. Res. Int.* **2015**, *2015*, 759348. [CrossRef]
32. Hentzer, M.; Teitzel, G.M.; Balzer, G.J.; Heydorn, A.; Molin, S.; Givskov, M.; Parsek, M.R. Alginate overproduction affects *Pseudomonas aeruginosa* biofilm structure and function. *J. Bacteriol.* **2001**, *183*, 5395–5401. [CrossRef] [PubMed]
33. Otto, M. Staphylococcal biofilms. *Curr. Top Microbiol. Immunol.* **2008**, *322*, 207–228. [PubMed]
34. Rodrigues, M.; Kosaric, N.; Bonham, C.A.; Gurtner, G.C. Wound healing: A cellular perspective. *Physiol. Rev.* **2019**, *99*, 665–706. [CrossRef]
35. Jamal, M.; Ahmad, W.; Andleeb, S.; Jalil, F.; Imran, M.; Nawaz, M.A.; Hussain, T.; Ali, M.M.; Rafiq, M.; Kamil, M.A. Bacterial biofilm and associated infections. *J. Chin. Med. Assoc.* **2018**, *81*, 7–11. [CrossRef]
36. Omar, A.; Wright, J.B.; Schultz, G.; Burrell, R.; Nadworny, P. Microbial biofilms and chronic wounds. *Microorganisms* **2017**, *5*, 9. [CrossRef]

37. Wilson, C.; Lukowicz, R.; Merchant, S.; Valquier-Flynn, H.; Caballero, J.; Sandoval, J.; Okuom, M.; Huber, C.; Brooks, T.D.; Wilson, E.; et al. Quantitative and qualitative assessment methods for biofilm growth: A mini-review. *Res. Rev. J. Eng. Technol.* **2017**, *6*.
38. Diez-Aguilar, M.; Morosini, M.I.; Köksal, E.; Oliver, A.; Ekkelenkamp, M.; Cantón, R. Use of Calgary and microfluidic bioflux systems to test the activity of fosfomicin and tobramycin alone and in combination against cystic fibrosis *Pseudomonas aeruginosa* biofilms. *Antimicrob. Agents Chemother.* **2018**, *62*, e01650-17. [[CrossRef](#)]
39. Lebeaux, D.; Chauhan, A.; Rendueles, O.; Beloin, C. From in vitro to in vivo models of bacterial biofilm-related infections. *Pathogens* **2013**, *2*, 288–356. [[CrossRef](#)]
40. Bagge, N.; Schuster, M.; Hentzer, M.; Ciofu, O.; Givskov, M.; Greenberg, E.P.; Høiby, N. *Pseudomonas aeruginosa* biofilms exposed to imipenem exhibit changes in global gene expression and beta-lactamase and alginate production. *Antimicrob. Agents Chemother.* **2004**, *48*, 1175–1187. [[CrossRef](#)]
41. Karaman, M.; Firinci, F.; Arıkan Ayyıldız, Z.; Bahar, I.H. Effects of imipenem, tobramycin and curcumin on biofilm formation of *Pseudomonas aeruginosa* strains. *Mikrobiyol Bull.* **2013**, *47*, 192–194. [[CrossRef](#)]
42. Musafir, H.; Kuchma, S.L.; Naimie, A.A.; Schwartzman, J.D.; Al-Mathkhury, H.; O'Toole, G.A. Investigating the link between imipenem resistance and biofilm formation by *Pseudomonas aeruginosa*. *Microb. Ecol.* **2014**, *68*, 111–120. [[CrossRef](#)] [[PubMed](#)]
43. Otani, S.; Hiramatsu, K.; Hashinaga, K.; Komiya, K.; Umeki, K.; Kishi, K.; Kadota, J.-I. Sub-minimum inhibitory concentrations of ceftazidime inhibit *Pseudomonas aeruginosa* biofilm formation. *J. Infect. Chemother.* **2018**, *24*, 428–433. [[CrossRef](#)] [[PubMed](#)]
44. Wang, X.; Cai, Y.; Xing, H.; Wu, W.; Wang, G.; Li, L.; Chen, J. Increased therapeutic efficacy of combination of azithromycin and ceftazidime on *Pseudomonas aeruginosa* biofilm in an animal model of ureteral stent infection. *BMC Microbiol.* **2016**, *16*, 124. [[CrossRef](#)]
45. Bagge, N.; Ciofu, O.; Skovgaard, L.T.; Høiby, N. Rapid development in vitro and in vivo of resistance to ceftazidime in bio-film-growing *Pseudomonas aeruginosa* due to chromosomal beta-lactamase. *APMIS* **2000**, *108*, 589–600. [[CrossRef](#)] [[PubMed](#)]
46. Bowler, L.L.; Zhanel, G.G.; Ball, T.B.; Saward, L.L. Mature *Pseudomonas aeruginosa* biofilms prevail compared to young biofilms in the presence of ceftazidime. *Antimicrob. Agents Chemother.* **2012**, *56*, 4976–4979. [[CrossRef](#)]
47. Hsu, C.-Y.; Lin, M.-H.; Chen, C.-C.; Chien, S.-C.; Cheng, Y.-H.; Su, I.-N.; Shu, J.-C. Vancomycin promotes the bacterial autolysis, release of extracellular DNA, and biofilm formation in vancomycin-non-susceptible *Staphylococcus aureus*. *FEMS Immunol. Med. Microbiol.* **2011**, *63*, 236–247. [[CrossRef](#)]
48. He, X.; Yuan, F.; Lu, F.; Yin, Y.; Cao, J. Vancomycin-induced biofilm formation by methicillin-resistant *Staphylococcus aureus* is associated with the secretion of membrane vesicles. *Microb. Pathog.* **2017**, *110*, 225–231. [[CrossRef](#)]
49. Rose, W.E.; Poppens, P.T. Impact of biofilm on the in vitro activity of vancomycin alone and in combination with tigecycline and rifampicin against *Staphylococcus aureus*. *J. Antimicrob. Chemother.* **2008**, *63*, 485–488. [[CrossRef](#)]
50. Post, V.; Wahl, P.; Richards, R.G.; Moriarty, T.F. Vancomycin displays time-dependent eradication of mature *Staphylococcus aureus* biofilms. *J. Orthop. Res.* **2017**, *35*, 381–388. [[CrossRef](#)]
51. Mirani, Z.A.; Aziz, M.; Khan, M.N.; Lal, I.; Hassan, N.U.; Khan, S.I. Biofilm formation and dispersal of *Staphylococcus aureus* under the influence of oxacillin. *Microb. Pathog.* **2013**, *61–62*, 66–72. [[CrossRef](#)]
52. Manner, S.; Goeres, D.; Skogman, M.; Vuorela, P.; Fallarero, A. Prevention of *Staphylococcus aureus* biofilm formation by anti-biotics in 96-microtiter well plates and drip flow reactors: Critical factors influencing outcomes. *Sci. Rep.* **2017**, *7*, 43854. [[CrossRef](#)] [[PubMed](#)]
53. Parra-Ruiz, J.; Molina, A.B.; Peña-Monje, A.; Hernández-Quero, J. Activity of linezolid and high-dose daptomycin, alone or in combination, in an in vitro model of *Staphylococcus aureus* biofilm. *J. Antimicrob. Chemother.* **2012**, *67*, 2682–2685. [[CrossRef](#)] [[PubMed](#)]
54. Abad, L.; Tafani, V.; Tasse, J.; Josse, J.; Chidiac, C.; Lustig, S.; Ferry, T.; Diot, A.; Laurent, F.; Valour, F. Evaluation of the ability of linezolid and tedizolid to eradicate intraosteoblastic and biofilm-embedded *Staphylococcus aureus* in the bone and joint infection setting. *J. Antimicrob. Chemother.* **2018**, *74*, 625–632. [[CrossRef](#)]
55. Gander, S.; Hayward, K.; Finch, R. An investigation of the antimicrobial effects of linezolid on bacterial biofilms utilizing an in vitro pharmacokinetic model. *J. Antimicrob. Chemother.* **2002**, *49*, 301–308. [[CrossRef](#)] [[PubMed](#)]

Travail n°6 : Article Scientifique

Comparison of bacterial phenotype after biofilm lifecycle and evaluation of polymicrobial biofilm organization and antibiotics effect in a chronic wound environment

Cassandra Pouget, Catherine Dunyach-Remy, Alix Pantel, Albert Sotto and
Jean-Philippe Lavigne

Draft au 20 Novembre 2021

Résumé travail n°6 :

Suite aux premiers résultats obtenus dans l'article scientifique précédent, nous avons souhaité confirmer les données préliminaires établies sur les souches de référence en utilisant, cette fois-ci, des souches cliniques isolées de plaies chroniques chez des patients. Ces souches ont l'avantage de correspondre davantage à la réalité clinique. Également, nous voulions améliorer le modèle *in vitro* décrit notamment pour l'étude des **coopérations bactériennes** au sein du biofilm polymicrobien.

Pour cela, nous avons étudié le comportement de **souches cliniques** de *S. aureus* et *P. aeruginosa* isolées chez des patients présentant des plaies chroniques. Nous avons, à l'aide de notre modèle précédemment décrit :

- Étudié la **cinétique** de formation de biofilm des souches en mono et co-culture
- Adapté nos microplaques du Bioflux™ 200 à l'aide de fond amovible afin de visualiser et quantifier le biofilm mature
- Établi un protocole de **microscopie confocale** afin de visualiser l'organisation de biofilm mature polymicrobien incluant la transformation des souches cliniques étudiées à l'aide de plasmides conférant une **fluorescence** (GFP pour *S. aureus* et *mCherry* pour *P. aeruginosa*)
- Testé **l'efficacité de différents antibiotiques** (Ceftazidime, imipénème, vancomycine, oxacilline, linézolide, dalbavancine et daptomycine) à 10x la concentration minimale inhibitrice sur le biofilm préformé et débridé (biofilm mono-espèce et mixte)
- Établi un protocole afin d'isoler **les bactéries** sessiles et les bactéries planctoniques libérées du biofilm
- **Comparé le comportement** des bactéries planctoniques initiales, des bactéries sessiles et des planctoniques libérées du biofilm sur plusieurs caractéristiques bactériennes (croissance, formation de biofilm précoce, expression de gènes impliqués dans la régulation et la formation du biofilm)

Les résultats de l'étude ont confirmé que toutes les espèces bactériennes formaient un biofilm **plus rapidement** dans le CWM comparé à un milieu classique microbiologique. L'utilisation des antibiotiques sur un biofilm débridé a indiqué que l'imipenème et la vancomycine étaient incapables de réduire la biomasse du biofilm contrairement au **linézolide**, à la **ceftazidime** et à la **dalbavancine**. L'expression génique de *lasI*, *rhII*, *pqsH*, *pel* et *psl* pour *P. aeruginosa* et *fnbpA* et *icaA* pour *S. aureus* était **augmentée chez les bactéries sessiles** par rapport à l'expression mesurée chez les bactéries planctoniques initiales et libérées. L'expression d'un des facteurs de virulence de *S. aureus* (*hla*) était, quant à elle, diminuée chez les bactéries présentes dans le biofilm. Les bactéries sessiles et libérées du biofilm ont démontré également une facilité à adhérer et **réformer du biofilm** plus rapidement mais une capacité de **croissance réduite** (différence de 2 log UFC/ml en comparaison avec les bactéries planctoniques initiales). Enfin, nos observations en microscopie confocale du biofilm polymicrobien ont prouvé que *P. aeruginosa* et *S. aureus* étaient **organisés de manière non aléatoire** au sein du biofilm polymicrobien. En effet, *Pseudomonas aeruginosa* était localisé plus en profondeur dans le biofilm contrairement à *S. aureus*.

Ce travail de recherche a permis de mettre en évidence que la technique du Bioflux™ 200 couplée à notre milieu de culture, le CWM, était un outil performant afin d'étudier la coopération bactérienne au sein des biofilms polymicrobiens mais également afin d'estimer le potentiel de nouvelles cibles thérapeutiques utilisables contre le biofilm observé au niveau des plaies chroniques.

Comparison of bacterial phenotype after biofilm lifecycle and evaluation of polymicrobial biofilm organization and antibiotics effect in a chronic wound environment

Cassandra Pouget¹, Catherine Dunyach-Remy², Alix Pantel², Sophie Shuldiner³, Albert Sotto⁴, Jean-Philippe Lavigne^{2*}

¹Virulence Bactérienne et Infections Chroniques, INSERM U1047, Université de Montpellier, Nîmes, France

²Virulence Bactérienne et Infections Chroniques, INSERM U1047, Université de Montpellier, Service de Microbiologie et Hygiène hospitalière, CHU Nîmes, Nîmes, France

³Virulence Bactérienne et Infections Chroniques, INSERM U1047, Université de Montpellier, Service des Maladies Métaboliques et Endocriniennes, CHU Nîmes, France

⁴Virulence Bactérienne et Infections Chroniques, INSERM U1047, Université de Montpellier, Service des Maladies Infectieuses et Tropicales, CHU Nîmes, France

*** Correspondence:**

Prof. Jean-Philippe Lavigne

jean.philippe.lavigne@chu-nimes.fr

Keywords: antibiotics, biofilm, chronic wounds, Bioflux™ 200, live imaging, flow conditions, clinical strains.

Abstract

Biofilm on the skin surface of chronic wounds (CW) is an important step which makes wound healing difficult to resolve. The polymicrobial nature inside this pathogenic biofilm is key for understanding the chronic infection. Few models exist to study bacterial interactions inside CW. The aim of our study was to evaluate a technique of biofilm formation under flow condition (Bioflux™ 200) using an *in vitro* chronic wound-like medium (CWM) that mimics CW environment. We determined the biofilm organization and the effect of antibiotics on biofilm.

Two clinical *S. aureus* and *P. aeruginosa* strains co-isolated from diabetic foot infections (DFI) were collected. Fluorescent strains of bacteria were developed. Strains were incubated in the Bioflux™ during 24h-72h in mono and co-culture (ratio1:1, bacteria added simultaneously) in the CWM vs a control medium (BHI). Quantification of biofilm formation and bacterial distribution were evaluated by confocal microscopy.

After 72h, different antibiotics (Imipenem, ceftazidime, vancomycin, oxacillin, linezolid, daptomycin, dalbavancin; 10xMIC) were evaluated after a flow increase mimicking a wound debridement. Bacterial growth, early adhesion (Biofilm Ring Test[®]) and qRT-PCR on biofilm-encoding genes (*spaA*, *fnbpA*, *agrA*, *hla* for *S. aureus*; *lasI*, *rhII*, *pel*, *psl* for *P. aeruginosa*) were evaluated before (planktonic initial) and after (sessile and planktonic released from the biofilm) incubation in biofilm.

Our study showed that all species constituted a faster biofilm in the WLM. Biofilm organization is a non-random structure where bacteria are found together. Antibiotics on debrided biofilm indicated that imipenem and vancomycin were not able to reduce biofilm biomass contrary to linezolid, dalbavancin and ceftazidime. The genes expressions of biofilm markers (*lasI*, *rhII* and *fnbpA*, *spaA*) were overexpressed in sessile bacteria compared to bacteria released from the biofilm. Gene expression of a virulence factor (*hla* for *S. aureus*) was decreased in sessile cells. Biofilm-released bacteria presented a reduce growth plateau (difference: 2 log UFC/mL) but were able to adhere faster compared to initial cells.

Our data confirmed the impact of CW environment on biofilm formation and the limitation of antibiotics. They indicated that *P. aeruginosa* and *S. aureus* were non-randomly organized inside polymicrobial biofilm. The Bioflux[™] is valuable to investigate bacterial cooperation, polymicrobial biofilm and evaluate new therapeutic targets against biofilm

1. Introduction

Chronic wounds are a growing medical problem that cause high rates of morbidity and mortality, costing the healthcare industry worldwide millions of dollars annually. Wounds are considered chronic when the healing process fails to proceed normally and that the anatomic function and integrity of the skin is not achieved in approximately 6 weeks (Clinton, 2015). Chronic wounds include diabetic foot ulcers, pressure or decubitus ulcers, venous leg ulcers, and nonhealing surgical-site infections. Chronic wound healing is partly hampered by the presence of bacterial infections growing as biofilms on a complex wound exudate (Dowd, 2008; James, 2008; Metcalf, 2015;

Peters, 2012; Nguyen 2016; Pastar 2013). Microorganisms residing in biofilms exhibit phenotypes distinct from planktonic cells, making treatment as a major challenge. Indeed, bacteria in biofilms can tolerate antimicrobial agent at some concentration rate 10,000 times higher than the same bacteria grown planktonically (Anderl, 2000; Zuroff, 2010). The penetration of antibiotics is generally reduced in the biofilm due, among others, to the extrapolymeric matrix (Sharma, 2019). Two types of *in vitro* biofilm models are currently used to predict antimicrobial efficacy against biofilm: closed and open systems. Closed systems are characterized by a limited supply of nutrients and an accumulation of wastes (Wilson, 2017). Open systems better reproduce the conditions encountered *in vivo* by a permanent control of nutrient supply, flow and temperature (Diez-Aguilar, 2017). The BioFlux™ 200 system is an open microfluidic system supporting high throughput testing (Lebeaux, 2014) and where adaptation of protocols to mimic the formation and management of biofilms *in vivo* is possible.

Chronic wounds are typically colonized by consortia of microbial species (Dowd, 2008; James, 2008; Wolcott, 2009). Those polymicrobial infections have been proved to present an elevated mortality rates relative to monocultures infections (Pulimood, 2002) and *in vivo* rabbit models demonstrated that mixte biofilm prevented wound healing compared to their respective monocultures (Pastar, 2013 et Seth, 2012). A major challenge of biofilm community is to understand the complex interactions which occur between the bacterial species. Interactions between different bacterial but also between bacterial microenvironmental factors are known to affect the outcome of wound infections. For example, it has been observed that co-infection with *P. aeruginosa* and *S. aureus* is associated with higher inflammatory responses, increased antimicrobial tolerance and contributes to the chronicity of the wounds (Hotterbeekx, 2017; Nguyen, 2016; Hoffman 2006). It appears that the spatial organization formed by these bacteria influences their behaviour and are a key factor for the understanding of bacterial interactions inside polymicrobial biofilm. In wounds biopsies, it has been described that *P. aeruginosa* and *S. aureus* occupy different niches in the wound microenvironment, with *P. aeruginosa* aggregates located deeper in the wound, as compared to the more superficially located *S. aureus* (Fazli, 2009). The deep *P. aeruginosa* aggregates produce virulence factors that destroy infiltrating neutrophils, which also results in a constant cycle of recruitment of immune mediators and persistent inflammatory state. This indicates that this niche is likely beneficial for

maintaining a stable, persistent infection state (Alves, 2018). In an *inter-kingdom* wound infection model, *C. albicans* and *Citrobacter freundii* were shown to assemble (Kalan, 2016) into structured, three-dimensional biofilms, where *C. albicans* provided a scaffold for *C. freundii* to attach and proliferate. Those studies show the importance of considering all the species present in biofilms but also that their organization can give us answers on the interactions they build to cooperate in order to make the infection thrive.

An important step in the management of bacterial biofilm is based on the control of the dissemination. Indeed, more and more studies are interested in the description of characteristics of bacteria released from the biofilm to improve understanding of the biofilm life cycle. Kaplan and Fine have recently shown that *A. actinomycetemcomitans* biofilm colonies are capable of releasing single cells or small clusters of cells into liquid medium and that these released cells can attach to the surface of the culture vessel and form new biofilm colonies faster, enabling the biofilm to spread (Kaplan, 2002). The ability of cells released from the biofilm to have different characteristics from the original planktonic cells or sessile bacteria was confirmed in *P. aeruginosa* and in *Klebsiella pneumoniae* (Rollet 2009 et Guilhen 2019).

In view of those recent discoveries, from this study we describe the biofilm formation and antibiotic efficiency on preformed biofilm of several clinical strains of *P. aeruginosa* and *S. aureus*. We also investigated the spatial organization of *P. aeruginosa* and *S. aureus* inside a mixed biofilm. Finally, we determine the differences of behaviour of bacteria depending of their mode of growth. All the experiments lead in this study were done using a culture medium and a biofilm formation model mimicking the micro-environment found at the wound bed.

2. Materials and Methods

2.1 Bacterial strains and culture conditions

Bacteria and media used in this study are listed in **Table 1**.

Bacteria were grown overnight in bacterial culture tubes under shaking at 200 rpm, in aerobic condition at 37°C in brain heart infusion (BHI, Sigma-Aldrich, Saint-Quentin-

Fallavier, France) broth or in CWM (European patent application EP21305337) previously described (Pouget, 2021).

Antimicrobial susceptibility testing of isolates was performed by broth microdilution method on BHI according to EUCAST recommendations (https://www.eucast.org/clinical_breakpoints). The same procedure was applied in the CWM to compare the effect of this medium on antibiotics action.

Bacteria were transformed to be fluorescents using a plasmid with GFP for *S. aureus* and *mCherry* for *P. aeruginosa* strains. For maintenance of plasmids, antibiotic concentrations used was 10 µg/ml of tetracycline in *S. aureus* and 100 µg/ml of gentamycin in *P. aeruginosa*.

2.2 Biofilm formation of mono and mixed-culture in microfluidic conditions

Biofilm formation in flow conditions was performed using the microfluidic system BioFlux™ 200 (Fluxion Bioscience Inc., Alameda, CA, USA). Bacteria tested were plated on selective agar (Mannitol salt for *S. aureus* and Cetrimide for *P. aeruginosa*). Colonies of the strains were resuspended in 3 mL of BHI or CWM and were incubated at 37°C with shaking (220 rpm) overnight. A bacterial suspension was then prepared from this overnight culture standardized to an OD₆₀₀ of 0.1 ±0.05 following a serials 200th dilutions (Naudin, 2019). The first step of the experiment consisted of priming the channel with 500µL of medium without bacteria in the inflow well with a pressure setting of 1 dyne/cm² for 10 minutes. The remained medium present in the well was then withdrawn. Thereafter, the microfluidic channels were inoculated by injecting the bacterial suspension from the output reservoir for 30 minutes at 1 dyne/cm². The setup was placed on the heating plate at 37°C. Finally, the bacterial suspension was added in the inflow well for 72-hr with pressure and temperature settings of 0.2 dyne/cm² and 37°C. Biofilms were obtained with bacteria cultivated either alone or in mixed culture in BHI and in the CWM.

2.3 Recovery of sessile and free-bacteria from mature biofilm

In order to recover bacteria at the end of their biofilm life cycle, the outflow well was discarded at 24-hr and 48-hr to avoid the collection of non-adherent bacteria. The output well was then recovered at 72-hr to collect planktonic bacteria released from the biofilm. To collect sessile bacteria, we used an increase of the flow as previously

described (Pouget, 2021). Briefly, 500 μ l of culture medium was added in the input well and a flow rate of 20 dynes/cm² was applied for 20 minutes, alternating the direction every 5 minutes. Bacteria are then centrifuged and the bacterial pellet is stored at -20 ° C. A cell viability test was carried out for each sample using the LIVE/DEAD™ BacLight™ Bacterial Viability Kit (ThermoFisher Scientific, France).

2.4Automatized debridement and antibiotic treatment in the microfluidic system

To mimic the first step of clinical management of a chronic wound, we developed an automatized debridement the aim of which is to remove part of the pre-formed biofilm (Pouget, 2021). After 72-hrs of biofilm formation, a shear flow of 5 dynes/cm² was applied from the inflow well to the outflow well for 10 minutes. The flow was then reinversed between the inflow and the outflow wells for 10 minutes. This process of flow reversion was performed twice for monomicrobial biofilm and 4-times for mixed polymicrobial biofilm. The aim of this flow inversion was to significantly reduce the biofilm constituted in the microfluidic channel to a maximum of 15% of remaining biofilm in the channel to mimic the *in vivo* conditions. Indeed, clinical studies determined that the biofilm is never completely removed after a wound debridement. There is always a percentage of remaining biofilm that makes its reformation facilitated. Clinical data estimate the effectiveness of debridement whether mechanical, surgical, enzymatic or other around 85% (Mori, 2019). After this automatized debridement, a dynamic flow (0.2 dyne/cm² at 37°C for 24-hrs) of antibiotics was applied to evaluate their actions on the remaining pre-formed biofilm. All antibiotics and the concentrations used in this study are listed in **Table 2**.

2.5Visualisation and quantification of biofilm

After 24-hr, 48-hr and 72-hr of incubation, biofilm formation was recorded using a fluorescence inverted microscope DM IRB (Leica Biosystems, Nanterre, France) coupled with a CoolSNAP FX camera (Roper Scientific, Lisses, France). MetaVue™ software (Molecular Devices, Sunnyvale, CA, USA) was used for imaging. ImageJ® was utilized to color black and white images, to overlay fluorescent images, to include scale bars and calculate biofilm percentage. The 16-bit grayscale images were adjusted with the threshold function to fit the bacterial structure and were analyzed

using the “Analyze Particles” function. The percentage of biofilm was evaluated before and after automatized debridement and after 24-hr of antibiotics treatment

2.6 Organization of polymicrobial biofilm using confocal microscopy

Planktonic *S. aureus* and *P. aeruginosa* cells expressing GFP or *mCherry* were grown and imaged by CLSM as followed. Overnight cultures were diluted to an OD₆₀₀ of 0.1 followed by a 400th serial dilution into fresh medium (CWM). Mixed solution of *S. aureus* expressing GFP and *P. aeruginosa* expressing *mCherry* at the same concentration were done. A microscopy slide was added on the microfluidic channel of the BioFlux system to be able to remove mature biofilm formed in the channel. We let biofilm formed for 72-hr. Then, the microscopy slide is carefully removed and washed twice in 1X PBS before fixing cells with 3 % PFA. The slide is then covered with a coverslip, and imaged with an inverted Olympus Fluoview FV10i confocal laser scanning microscope fitted with a Plan-Apochromat 63×/1.40 numerical aperture oil differential interference contrast (DIC) objective set to a 1.0× digital zoom. In addition to the acquisition of DIC images, a 488-nm argon laser was used to excite any GFP present in the cells; a 588-nm argon laser was used to excite *mCherry* fluorescence and the emissions were collected with a 600- to 650-nm band pass filter. Images collected from biofilms were rendered with the Imaris 7.0.0 software suite (Bitplane, Saint Paul, MN).

2.7 Growth curves

Sessile cells, planktonic initial and release from biofilm were inoculated into 3 mL of CWM and grown for 3 hours with shaking. Cultures were then diluted into fresh media so that the initial OD was detectable above the OD of media alone (1:1–1:20 dilution rate). Cells (200 µL) were then inoculated into a 96-well flat-bottom microplate (Costar). Cultures were grown at 37 °C in an automatic microplate reader (Tecan Infinite F200), shaking at 200 rpm. OD₆₀₀ readings were taken every hour with continuous shaking between readings. Each experiment was performed three times.

2.8 Kinetics of early biofilm formation

The early biofilm formation was assessed using Biofilm Ring Test[®] (BioFilm Control, Saint Beauzire, France) as previously described (Chavant, 2007) and according to the manufacturer’s recommendations. *P. aeruginosa* and *S. aureus* (sessile and planktonic initial and released) strains were cultured on liquid medium (CWM) at 37°C

for 6-hr. The bacterial suspension was standardized to an optical density at 600 nm of 1.00 ± 0.05 and diluted at 1:250 in CWM to obtain a final concentration of 4.10^6 CFU/mL. This bacterial suspension was complemented with 1% (v/v) magnetic beads (TON004). 200 μ L were then added, in triplicate, into a 96 well microplate for each time point (1, 3 and 5 hours). The plates were incubated without shaking at 37°C. After incubation, 100 μ L of liquid contrast (LIC001) solution was added on the top of each well. The microplate was placed on a magnetic block for 5 minute and scanned using the scanner and the BFCE3 software. Each experiment was performed two times using triplicates. Spots are quantified through specialized image algorithms that measures beads aggregation. Biofilm index (BFI) values are calculated for each well, and range from 0 (no aggregation, i.e. biofilm formation) to 20 (total aggregation, i.e. absence of biofilm formation)

2.9 Quantification of biofilm biomass

The mature biofilms were evaluated using bacterial quantification of biofilm biomass. The optical density at 600nm after 6-hr of incubation of bacterial suspensions, in CWM, were adjusted to 1.00 ± 0.05 , before a 1:100 dilution in CWM. 200 μ L of each suspension were transferred to a microplate (Falcon 96 Flat Bottom Transparent, Corning, USA) in triplicates and incubated at 37°C, 5% CO₂ for 24h without shaking. Negative controls wells contained CWM alone. After incubation, the microplates were washed three times with 200 μ L of 1X PBS. 200 μ L of 1X PBS was finally added into the well before biofilm disruption. The disruption was performed by sonication for 10 min at 40 KHz. Each well was then serially diluted and the last dilution was plated on non-selective agar (LB agar). The agar plate was then incubated overnight at 37°C and CFUs were counted. The experiment was performed twice for each sample.

2.10 Gene expression of key regulators of biofilm formation

Analysis of the mRNA (transcription) levels of *spaA*, *fnbpA*, *hla*, *agrA* for *S. aureus* and *lasI*, *rhII*, *pel*, *psl* for *P. aeruginosa* genes were performed following the method previously described by Doumith *et al* (Doumith, 2009). Briefly, total cellular RNA was extracted using the Rneasy® Mini kit (Qiagen, Courtaboeuf, France) and treated with RNase-free DNase (Qiagen) for 30 min at 37°C, after which a second step of purification was performed. RT-PCR was carried out in a LightCycler® using the one-step LightCycler® RNA Master SYBR Green I kit (Roche Applied Science, Meylan,

France) according to the manufacturer's protocol. The specificity of the generated products was tested by melting-point analysis. Amplifications were performed in triplicate from three different RNA preparations. Cycle threshold (Ct) values of the target genes were compared with the Ct values of the house-keeping *rpoD* gene for *P. aeruginosa* and *gyrB* gene for *S. aureus*. Those genes were chosen as endogenous reference for normalizing the transcription levels of the target gene. The condition where planktonic initial bacteria were cultivated in CWM was used as control and the normalized relative expressions of the studied genes in sessile and planktonic cells released from the biofilm in CWM were determined for each strain according to the equation $2^{-\Delta\Delta Ct}$, where $\Delta\Delta Ct = (Ct_{\text{gene}} - Ct_{\text{housekeeping gene}})_{\text{initial planktonic bacteria CWM}} - (Ct_{\text{gene}} - Ct_{\text{housekeeping gene}})_{\text{sessile or released cells in CWM}}$. Primers used in this study are listed in Table 3.

2.11 Statistics

Statistical analyses were performed using GraphPad Prism version 7 or R version 3.5.2. Tests used for the p-value determination are mentioned in each figure legend.

3. Results

3.1 Biofilm formation is enhanced in CWM

To evaluate the potential of biofilm formation of two of the main species isolated from chronic wounds, we determined the percentage of biofilm formed in our Bioflux™ 200 open system of *S. aureus* and *P. aeruginosa* reference and clinical strains. We test the bacteria either alone (**Figure 1A and 1B**) or associated in a co-culture where bacteria were added simultaneously and at a ratio 1:1 (**Figure 1C**). Experiments were done in a control BHI medium and the CWM (more adapted to mimic the environment encountered in wounds) developed in our unit. All the strains were able to form biofilm and to remain attached under shear force (**Figures 1**).

The *S. aureus* Newman strain formed biofilm at each time (**Figure 1A**). Interestingly, at 24-hr the percentage of constituted biofilms ranged from 22.0% ±0.2 when the strain was cultivated in BHI to 43.5% ±0.4 in CWM (p<0.01) (**Figure 1A**). This significant difference was increased at 48-hr post incubation in the Bioflux™ system with 43.0%

± 0.2 of bacteria in biofilm within the BHI medium vs $72.4\% \pm 0.5$ within the CWM ($p < 0.01$) (**Figure 1A**). Finally, after 72-hr, the percentage of formed biofilm in CMW was almost complete ($97.3\% \pm 0.1$) whereas it was still incomplete in BHI ($68.1\% \pm 0.3$) ($p < 0.01$) (**Figure 1A**). The significant difference in the biofilm formation of *S. aureus* in the CMW compared to BHI was confirmed with the clinical strains. Percentage of biofilm formed in BHI after 24-hr was $24.1\% \pm 0.5$ and $27.3\% \pm 0.3$ for SAC 2 and SAC 4 respectively but $39.2\% \pm 0.6$ for SAC 2 and $38.4\% \pm 0.7$ for SAC 4 in CWM ($p < 0.1$) (**Figure 1A**). Same observation for 48-hr and 72-hr, the percentage of biofilm formed was always significantly higher ($p < 0.01$) in CWM than in BHI ($41.1\% \pm 0.4$ versus $77.4\% \pm 0.3$ for SAC 2 and $43.1\% \pm 0.3$ versus $77.7\% \pm 0.2$ for SAC 4 at 48-hr; percentage at 72-hr were $79.5\% \pm 0.5$ in BHI and $95.7\% \pm 0.5$ in CWM for SAC 2; $81.0\% \pm 0.4$ in BHI and $97.9\% \pm 0.8$ in CWM for SAC 4) (**Figure 1A**).

P. aeruginosa biofilm formation inside the Bioflux™ system was shown in **Figure 1B**. Contrary to *S. aureus*, no difference in the percentage of biofilm formation has been observed after 24-hr post inoculation in the CWM ($13.1\% \pm 0.4$) vs BHI medium ($12.0\% \pm 0.3$) ($p = \text{Not Significant (ns)}$) (**Figure 1B**). However, significant higher percentages of biofilm constituted in CWM compared to BHI were noted at 48-hr ($52.4\% \pm 0.1$ vs $38.0\% \pm 0.1$, respectively) (**Figure 1B**) ($p < 0,1$) and at 72-hr ($99.7\% \pm 0.2$ vs $70.1\% \pm 0.1$, respectively) ($p < 0.01$) (**Figure 1B**). For PAC 2, the first clinical strain of *P. aeruginosa*, percentage of biofilm formed in BHI after 24-hr was $14.1\% \pm 0.5$ in BHI and $17.3\% \pm 0.3$ in CWM ($p < 0.1$). This tendency was confirmed after 48-hr were the strain formed $58.2\% \pm 0.6$ of biofilm in CWM to $42.4\% \pm 0.4$ in CWM ($p < 0.01$). At 72h, those deviations were confirmed since we measured $97.7\% \pm 0.2$ of biofilm formed in CWM vs $72.1\% \pm 0.6$ in BHI ($p < 0.01$) (**Figure 1B**). For PAC 4, after 24-hr the percentage of biofilm formed in the microfluidic channel was $15.1\% \pm 0.2$ in CWM versus $12.1\% \pm 0.3$ in BHI ($p < 0,1$); $61.7\% \pm 0.2$ in CWM versus $41.7\% \pm 0.5$ in BHI ($p < 0,01$). Finally, the percentage at 72-hr were $98.5\% \pm 0.1$ in CWM and $75.2\% \pm 0.5$ in BHI ($p < 0,01$) (**Figure 1B**).

Finally, inside a mixed biofilm composed by *S. aureus* and *P. aeruginosa* reference strains, the two species formed faster and denser biofilm in CWM compared to BHI at any time ($p < 0,01$) (**Figure 1C**). Indeed, a significant difference in the percentage of biofilm formation was noted at 24-hr ($45.0\% \pm 0.3$ in CMW vs $27.4\% \pm 0.2$ in BHI), at 48-hr ($85.0\% \pm 0.2$ vs $70.0\% \pm 0.1$, respectively) and at 72-hr ($99.3\% \pm 0.2$ and $72.0\% \pm 0.4$, respectively) (**Figure 1C**). It is interesting to note that the same conclusions were

observed with clinical couple of *S. aureus* Newman and *P. aeruginosa* SAC 2/PAC 2 and SAC 4/ PAC 4 ($p < 0,01$) (Figure 1C).

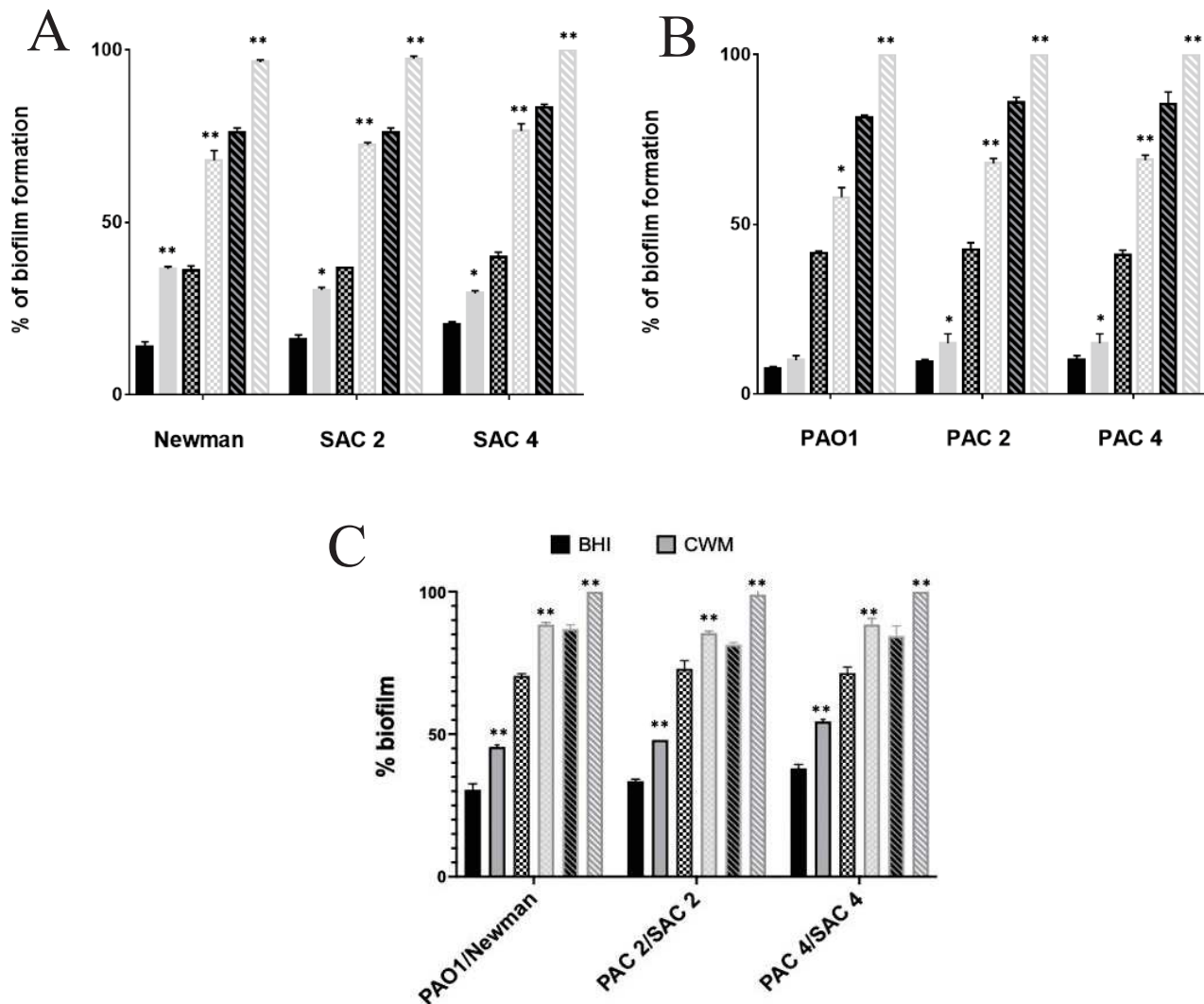


Figure 1. Kinetics of biofilm formation of *Staphylococcus aureus* Newman and clinical strains SAC 2 and SAC 4 (A); *Pseudomonas aeruginosa* PAO1 and clinical strains PAC 2 and PAC 4 (B) and co-culture (C) in BHI (black) and CWM (grey) media in the BioFlux™ system. Percentages of biofilm formation were calculated at 24-hr, 48-hr (squared) and 72-hr (hatched) post-incubation in both media after three independent experiments. Percentage have been determined by the software ImageJ. Results are presented as the mean \pm standard deviation. Statistics were performed using a t-test on GraphPad Prism version 7 to compared the % of biofilm formed in BHI and CWM for each time point. ns, $p > 0.05$; * $p < 0.1$; ** $p < 0.01$; *** $p < 0.001$.

3.2 Antibiotic efficiency is dependent of the culture media in which bacteria evolved

To mimic the management of chronic wounds, we adapted an automatized debridement of the biofilm inside the Bioflux™ system and administrated different antibiotics on pre-formed biofilms of *S. aureus* reference and clinical strains (**Figure 2A**), *P. aeruginosa* reference and clinical strains (**Figure 2B**) and mixed culture (**Figure 2C**) in BHI and CWM.

The MIC values for each antibiotic against the studied strains are shown in **Table 2**. After formation of a biofilm with *S. aureus* strains, no effect on the reduction of this pre-formed biofilm was observed using 10x MIC of vancomycin whatever the media used and the strain (12.7% ±0.3 in BHI and 14.8% ±0.1 in CWM for Newman; 11.6% ±0.3 in BHI and 14.6% ±0.2 in CWM for SAC 2; 13.2% ±0.6 in BHI and 14.0% ±0.2 in CWM for SAC 4) (p=NS) (**Figure 2A**). At 10x MIC, oxacillin effect in terms of reduction of biofilm percentage for Newman (only in BHI; 9,8% ±0.6 (p<0.1) versus 12,4% ±0.3 in CWM) and SAC 4 (11.1% ±0.2 in BHI and 11,8% ±0.5 in CWM) (p<0.1). No effect was highlighted with SAC 2 (p=NS) (**Figure 2A**). Interestingly, an important reduction of the biofilm was detected using 10x MIC of linezolid in both media. *S. aureus* Newman showed a reduction of 8.4 % ±0.3 in BHI and 10.2 % ±0.2 in CWM (p<0,01). This tendency was confirmed with clinical strains where biofilm reduction was significant with the use of linezolid on SAC 4 (8.7% ±0.3 (p<0.01) in BHI and 11.1 % ±0.2 in CWM (p<0.1) and SAC 2 but only when culture in BHI (7.8% ±0.1) (p<0.01) whereas in CWM the effect was not significant (11.6% ±0.2) (p=NS) (**Figure 2A**). Dalbavancin used at a concentration of 10x MIC show no significant decrease of biofilm percentage in the majority of our tests. Newman culture in BHI show a significant reduction (9.9 % ±0.4) (p<0.1) that was not confirmed in CWM (13.5 % ±0.6) (p=NS). SAC 4 show the exact same pattern with a significant reduction only when the strain was culture in BHI (8.1 % ±0.3) (p<0.1) whereas 12.7 % ±0.4 in CWM (p=NS). Dalbavancin was completely inefficient on SAC 2 pre-formed biofilm (13.6 % ±0.3 in BHI and 14.7 % ±0.5 in CWM) (p=NS) (**Figure 2A**). Finally, daptomycin at 10x MIC, proved a significant reduction of pre-formed biofilm in BHI (6.4% ±0.2 for Newman; 6.7 % ±0.3 for SAC 2 and 6.5 % ±0.4 for SAC 4) (p<0.01). This effect was confirmed in CWM (7.5% ±0.1 for Newman (p<0.01); 10.9% ±0.3 for SAC 2 (p<0.1) and 8.6% ±0.1 for SAC 4 (p<0.01) (**Figure 2A**).

Using *P. aeruginosa* strain, no effect could be noted on the reduction of a pre-formed biofilm when 10x MIC of imipenem was administrated whatever the media used (12.8% \pm 0.4 for PAO1; 12.6 % \pm 0.3 for PAC 2; 12. 8% \pm 0.6 for PAC 4 in BHI and 12.6% \pm 0.4 for PAO1; 13.3% \pm 0.4 for PAC 2; 14.7% \pm 0.5 for PAC 4 in CWM) (p=NS) (**Figure 2B**). Interestingly, 10x MIC of ceftazidime had a significant impact on the pre-formed biofilm whatever the media used (9.7% \pm 0.3 for PAO1; 7.5% \pm 0.4 for PAC 2; 7.0% \pm 0.5 for PAC 4 in BHI (p<0.01) and 10.3% \pm 0.6 for PAO1 (p<0.1); 8.6% \pm 0.3 for PAC 2; 8.4% \pm 0.4 for PAC 4 in CWM) (**Figure 2B**).

Finally, when an optimized combination of antibiotics (10x MIC of ceftazidime + 10x MIC of linezolid and 10x MIC of ceftazidime + 10x MIC of daptomycin) was used on a pre-formed biofilm constituted by association of *S. aureus* Newman and *P. aeruginosa* PAO1, a significant reduction of the pre-formed mixed biofilm was observed in both media when the association of ceftazidime and linezolid (7.4% \pm 0.2 in BHI (p<0.01) and 8.7% \pm 0.3 in CWM (p<0.1)) and of ceftazidime and daptomycin (5.6% \pm 0.2 in BHI (p<0.01) and 10.2% \pm 0.4 in CWM (p<0.1)) were used (**Figure 3C**). The efficiency of the association of antibiotics was significantly highlighted by the mixte clinical biofilm. The association of ceftazidime and linezolid reduce percentage of biofilm to 7.2 % \pm 0.2 and 7.9 % \pm 0.3 in BHI (p<0.01) and CWM (p<0.1) for SAC 2/ PAC 2 and to 7.5 % \pm 0.3 and 8.4 % \pm 0.2 in BHI and CWM for SAC 4/ PAC 4 (p<0.1) (**Figure 3C**). The association of ceftazidime and daptomycin also show a significant decrease of percentage of biofilm to 5.6 % \pm 0.1 and 9.9 % \pm 0.3 in BHI (p<0.01) and CWM (p<0.1) for SAC 2/ PAC 2 and to 7.1 % \pm 0.2 and 9.4 % \pm 0.2 in BHI (p<0.01) and CWM (p<0.1) for SAC 4/ PAC 4 (**Figure 3C**).

We observe that the media used have an influence on the antimicrobial action of the antibiotics either on mono-specie biofilm or mixte biofilm of *S. aureus* and *P. aeruginosa*.

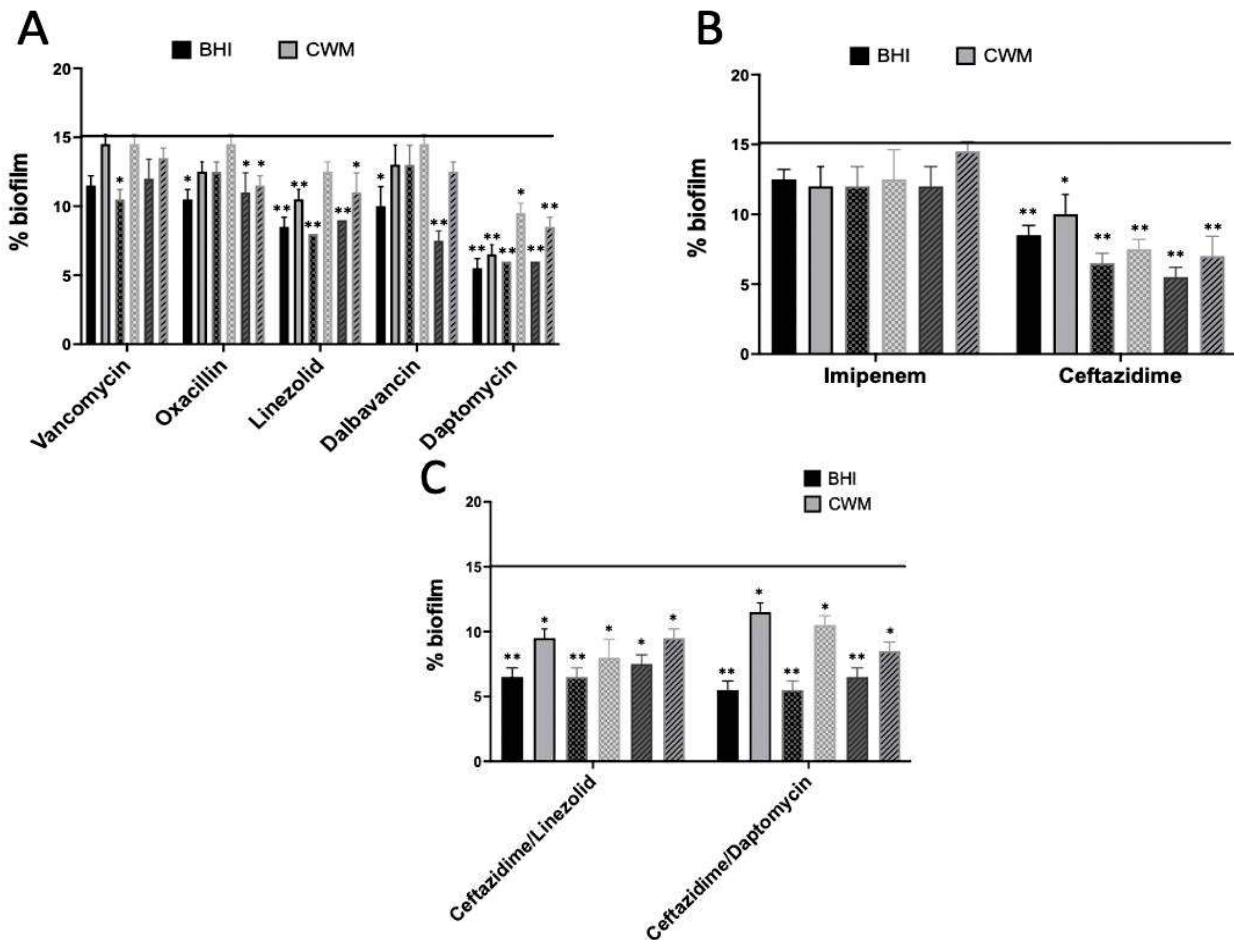


Figure 2. Percentage of biofilm reduction on pre-formed *Staphylococcus aureus* (A), *Pseudomonas aeruginosa* (B) and mixed biofilm (C) using 10x MIC of vancomycin, oxacillin, linezolid, dalbavancin, daptomycin, imipenem and ceftazidime in the CWM and BHI media. Reference strains are represented by the rectangle full of colour, the two clinical strains are represented in squared and in hatched. An automatized debridement was fixed at 15% of biofilm left in the microfluidic channel before applied antibiotic treatment during 24h. The percentage of biofilm after the automatized debridement and before antibiotics treatment is represented by the black line. Samples were tested in three independent experiments. Results are presented as the mean \pm standard deviation. Statistics were per-formed using a t-test on GraphPad Prism version 7 to compare the efficiency of antibiotics on pre-formed and debrided biofilm. ns, $p > 0.05$; * $p < 0.1$; ** $p < 0.01$; *** $p < 0.001$.

3.3 *Pseudomonas aeruginosa* and *Staphylococcus aureus* are not randomly associated in biofilm

Initially, we identified *P. aeruginosa* and *S. aureus* in swab material from chronic wounds by culturomique and MADI-TOF analyze. On the basis of those identities, we selected wounds containing both *P. aeruginosa* and *S. aureus*. In order to study the spatial distribution of *P. aeruginosa* and *S. aureus* we decided to make those clinical strains fluorescent. We modified *S. aureus* with a plasmid giving green fluorescence (pHOM-GFP) and *P. aeruginosa* with a plasmid giving red fluorescence (pBPF-*mCherry*). Those strains were cultivated for 72-hr in the Bioflux™ 200 in the CWM before fixing the cells for a microscopy acquisition. *We subsequently acquired images* at three different regions on each section of the formed biofilm by confocal laser scanning microscopy (CLSM).

The bacteria were predominantly present as large aggregates (**Figure 3**). We located the center of bacterial aggregates identified on each image (**Figure 3 - bottom image**) by using the calculator tool of Imaris software and measured its distance to the surface. This analysis showed that the *S. aureus* aggregates were located close to the wound surface, whereas the *P. aeruginosa* aggregates were located deeper in the wound bed (arrow). *S. aureus* strains were located at a distance of 10 to 15 µm to the “wound” surface, whereas *P. aeruginosa* aggregates were primarily located at a distance of 25 to 28 µm to the surface (**Figure 3**). Images show that the range of the distribution of *P. aeruginosa* and *S. aureus* was limited, indeed colocalization of the two bacterial species was rare.

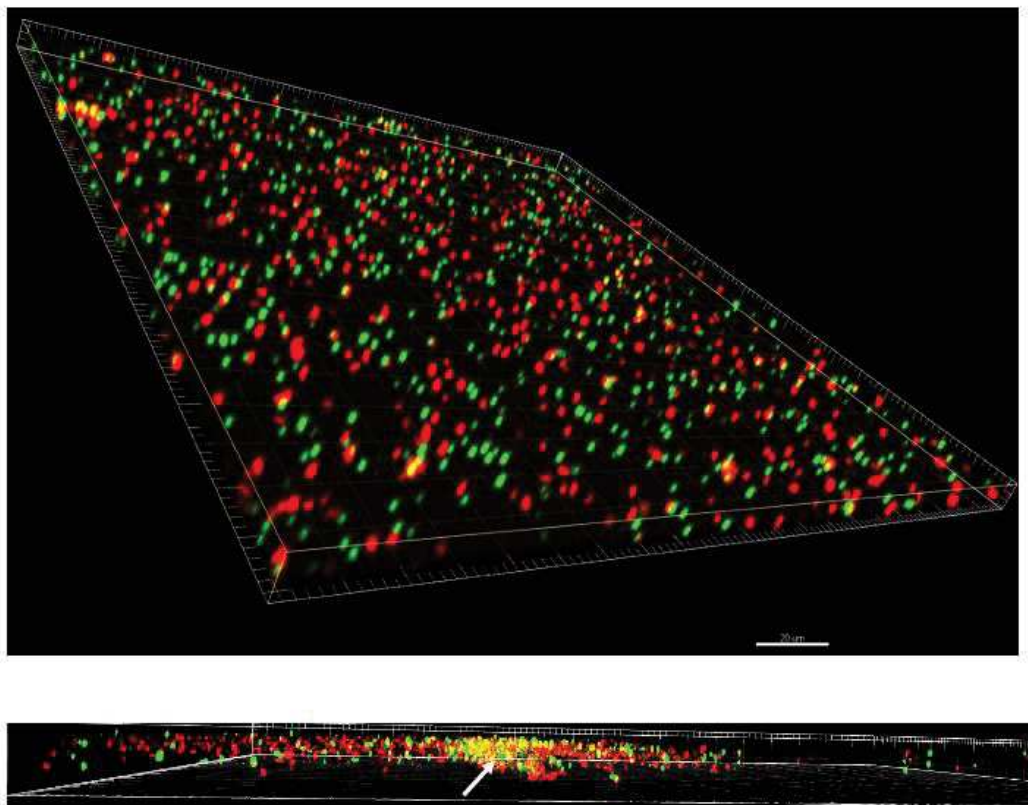


Figure 3. *Staphylococcus aureus* SAC 2-GFP cells (green) were cocultured with *Pseudomonas aeruginosa* PAC 2-mCherry (red) cells at a ratio 1:1. Cells were fixed after 3 days of coculture and visualised by confocal microscopy. White arrows point out *S. aureus* strain on top of *P. aeruginosa* strains. Scale bar = 20 μm .

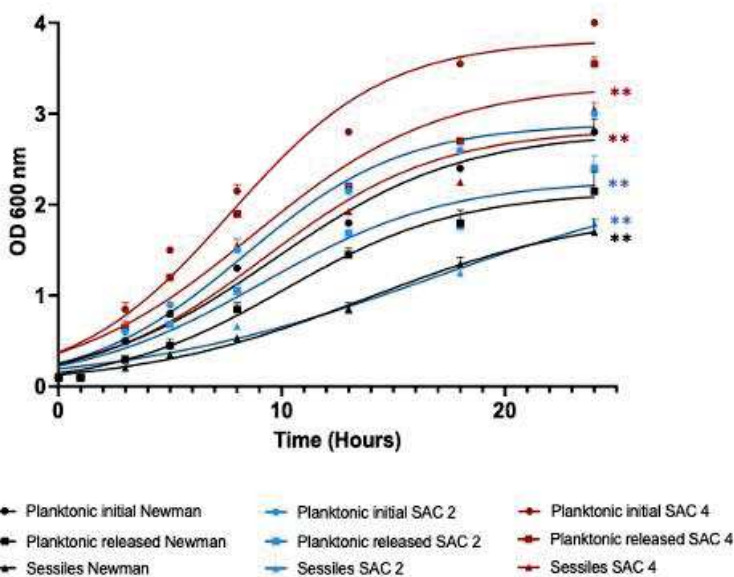
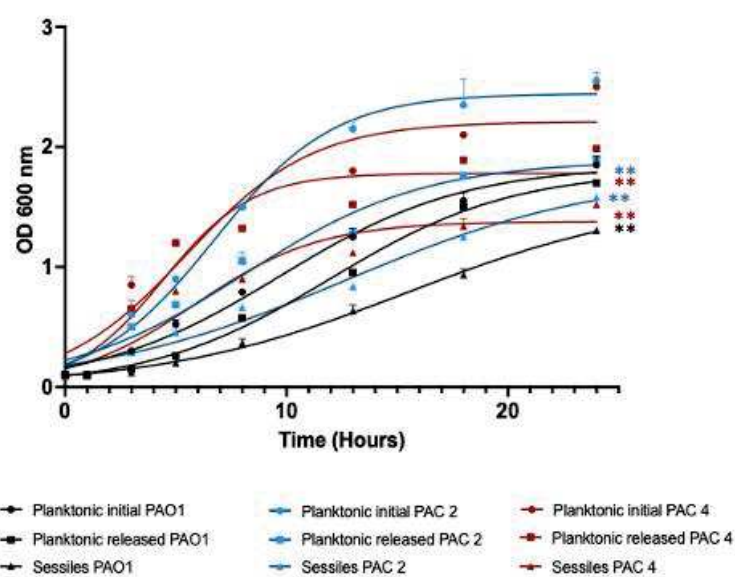
3.4 Planktonic released from the biofilm cells harbors a different behavior that sessile and initial bacteria

In order to characterize the cells released from the biofilm, we test several bacterial parameters and compare initial planktonic cells to sessile cells and planktonic released from the biofilm cultured in CWM.

Bacterial Growth

First, we showed that all bacteria regardless of their biofilm lifestyle were able to grow in the CWM. Concerning *S. aureus* reference strain Newman, we noticed that the planktonic released cells presented no statistical difference compared to initial cells. Sessile cells, contrarily, presented a significant decrease of the growth particularly at the end of exponential phase with one log difference ($p < 0.01$) (**Figure 4A**). As it concerns the first clinical strain of *S. aureus*, planktonic released and sessile cells presented difference on the growth curve. Planktonic released have an intermediate behaviour. We noticed a difference of 0.6 log at the end of the exponential phase compare to initial bacteria ($p < 0.01$). Sessile cells have a difference of 1.3 log ($p < 0.01$). We also remark that the profile of the curve for sessile cells seemed flatter than their counterpart bacteria (**Figure 4A**). The same profile was observed for the clinical strain SAC 4, with a clear difference of growth. Sessile cells presented a significant difference of 1 log at stationary phase of bacterial growth ($p < 0.01$), this difference was measured by 0.5 log for bacteria released from the biofilm compare to initial bacteria ($p < 0.01$) (**Figure 4A**).

For *P. aeruginosa*, no difference was observed in growth curves for the reference strain PAO1 planktonic released versus planktonic initial. We noticed however a reduced growth (0.8 log) for sessile cells compared to initial ones ($p < 0.01$) (**Figure 4B**). The clinical strain PAC 2 had a reduced growth rate for planktonic released (difference of

A

B


0.7 log) ($p < 0.01$) and sessile cells (1.2 log) ($p < 0.01$) at the stationary phase compared to initial bacteria (**Figure 4B**). For PAC 4, planktonic released presented also an intermediate behaviour with a growth rate less important than initial cells (reduced growth of 0.4 log at the stationary phase) ($p < 0.01$) but more important than sessile cells (difference of 1 log with planktonic initial bacteria at the end of the exponential phase) ($p < 0.01$) (**Figure 4B**).

Figure 4. Growth curves of *S. aureus* reference and clinical strains (A) and *P. aeruginosa* reference and clinical strains (B) cultured in CWM. Planktonic initial cells are represented in round, sessile cells in triangle and planktonic released from the biofilm in square. Cultures were sampled at the indicated time points, measure of the OD₆₀₀ were performed. Experiments were performed in three biological replicates. Results are presented as the mean \pm standard deviation of three different experiments. Statistics were performed using a t-test on GraphPad Prism version 7 to compare planktonic released and sessile cells compare to initial bacteria. ns, $p > 0.05$; * $p < 0.1$; ** $p < 0.01$; *** $p < 0.001$

Biofilm formation

To determine the impact of bacteria lifecycle on biofilm formation and particularly on the first step of adhesion, we used the BioFilm Ring Test® on *P. aeruginosa* reference and clinical strains and *S. aureus* reference and clinical strains cultivated in CWM. We performed the BioFilm Ring Test® after 3-hr of incubation in the CWM at 37°C.

We observed that *S. aureus* Newman sessile cells have the ability to adhere more importantly than planktonic released ($p < 0.1$) and planktonic initial ($p < 0.01$) (BFI= 8.7 ± 0.2 vs 7.45 ± 0.4 vs 6.4 ± 0.3) (**Figure 5A**). This intermediate behavior of the planktonic released cell was confirmed with clinical *S. aureus* strains. SAC 2 planktonic released cells showed a BFI of 13.3 ± 0.4 versus 14.9 ± 0.3 for planktonic initial ($p < 0.1$). Sessile cells were able to adhere significantly more (10.2 ± 0.2) compare to initial ones ($p < 0.01$) (**Figure 5A**). Those differences of behavior were increased in the case of SAC 4 where BFI of planktonic initial were measure to 16.7 ± 0.2 ; planktonic released from the biofilm 14.8 ± 0.1 ($p < 0.001$) and sessile cells 10.1 ± 0.2 ($p < 0.001$) (**Figure 5A**). The same trend could be noted for *P. aeruginosa* PAO1, PAC 2 and PAC 4. Those strain developed a biofilm much easier when bacteria have already been in biofilm compare to initial cells which BFI were measured at 14.4 ± 0.1 for PAO1; 15.5 ± 0.3 for

PAC 2 and finally 15 ± 0.2 for PAC 4 (**Figure 5B**). BFI values for planktonic released were 7.4 ± 0.1 ($p < 0.01$); 13.1 ± 0.2 ($p < 0.001$) and 11.8 ± 0.1 ($p < 0.001$) for PAO1; PAC 2 and PAC 4 respectively (**Figure 5B**). Adhesion was significantly increased in the case of the sessile cells (4.2 ± 0.3 for PAO1 ($p < 0.001$); 7.4 ± 0.2 for PAC 2 ($p < 0.001$) and 7.3 ± 0.3 for PAC 4 ($p < 0.001$)) (**Figure 5B**).

To corroborate the effect of the biofilm on the capacity of cell to adhere and form biofilm we evaluated the mature biofilm biomass of the different strains in monoculture in the CWM. *S. aureus* strains presented a significant higher number of bacteria in the biofilm when sessile bacteria were used (8.1 ± 0.6 for Newman, 8.3 ± 0.3 for SAC 2 and 8.5 ± 0.3 for SAC 4) ($p < 0.001$) compare to planktonic initial bacteria (4.2 ± 0.5 ; 4.6 ± 0.4 and 3.7 ± 0.3 for Newman, SAC 2 and SAC 4 respectively) (**Figure 5C**). Once again, planktonic released seem to have an intermediate behaviour since biofilm biomasse was significantly higher compare to initial bacteria (6 ± 0.4 for Newman ($p < 0.01$); 5.7 ± 0.2 for SAC 2 ($p < 0.01$) and 6.2 ± 0.4 for SAC 4 ($p < 0.01$)) but less important than sessile cells (**Figure 5C**).

For PAO1 and the clinical strains of *P. aeruginosa*, the intermediate behaviour of planktonic released cells to form biofilm was confirmed. Released cells were able to formed a denser biofilm than initial cells (8.1 ± 0.1 versus 6.2 ± 0.2 for PAO1 ($p < 0.01$); 8.4 ± 0.3 versus 6.5 ± 0.3 for PAC 2 ($p < 0.01$); 8.1 ± 0.3 versus 5.9 ± 0.2 for PAC 4 ($p < 0.01$)) (**Figure 5D**). From all the bacteria mode analyze, sessile cells were once again the mode of growth allowing the reformation of biofilm faster and denser (10.2 ± 0.2 for PAO1 ($p < 0.001$ comparison with planktonic initial cells), 10.3 ± 0.1 for PAC 2 ($p < 0.001$) and 9.7 ± 0.4 for PAC 4 ($p < 0.001$)) (**Figure 5D**).

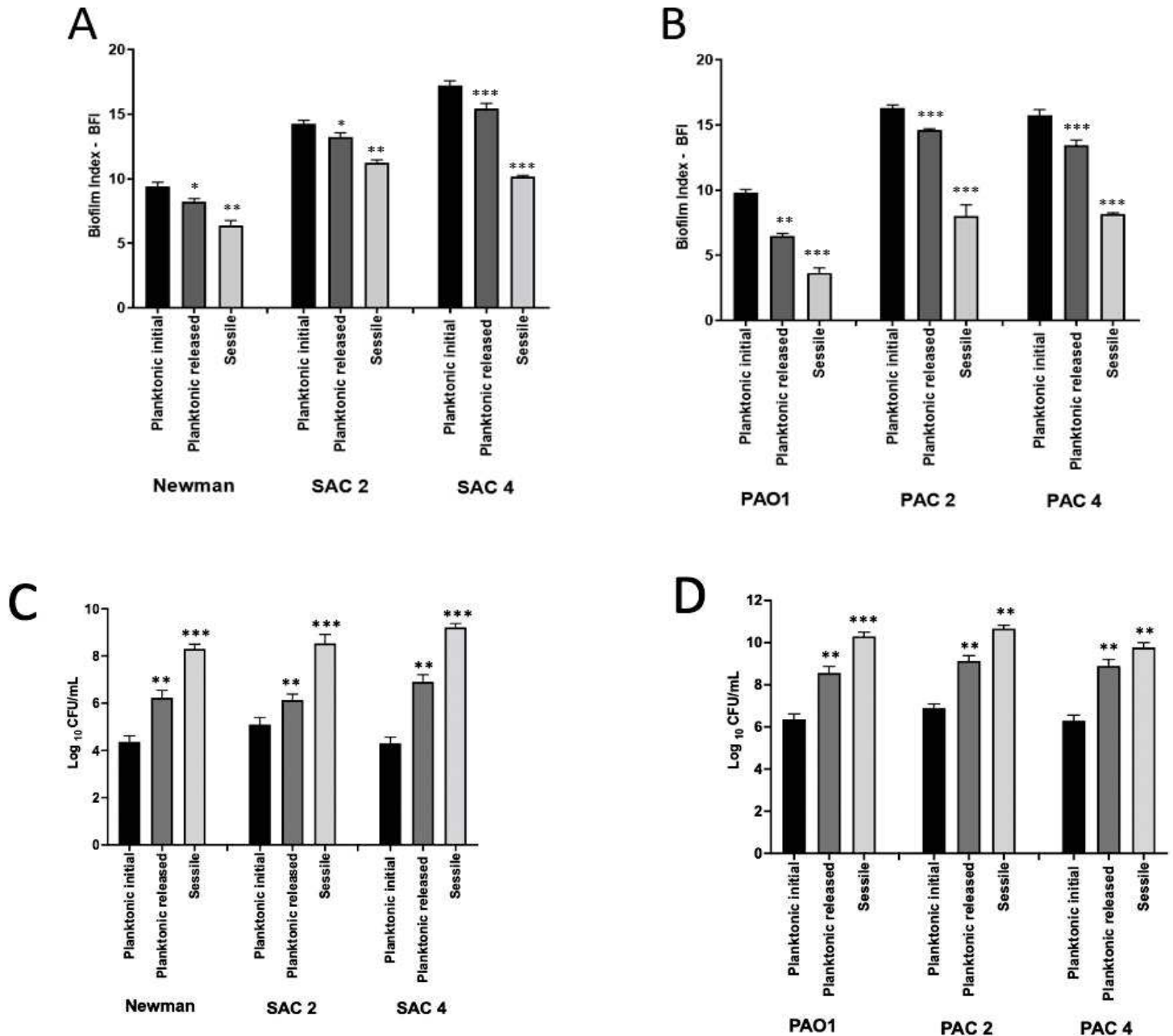


Figure 5. Quantification of biofilm formation of *S. aureus* and *P. aeruginosa* reference and clinical strains in CWM. Early biofilm step is represented by the Biofilm ring test assay after 3h of incubation in the medium (A and B), mature biofilm biomass quantification after 24h of incubation was also measured (C and D). Planktonic initial cells are represented in dark, sessile cells in light grey and planktonic released from the biofilm in dark grey. Samples were tested in triplicate in two independent experiments. Results are presented as the mean \pm standard deviation of three different experiments. Statistics were performed using a t-test on GraphPad Prism version 7 to

compare planktonic released and sessile cells compare to initial bacteria. ns, $p > 0.05$; * $p < 0.1$; ** $p < 0.01$; *** $p < 0.001$.

Gene expression

To assess and confirm the effect of lifecycle on biofilm formation we test the gene expression of some key regulators of biofilm formation. We measured the gene expression of *fnbpA*, *hla*, *spaA* and *agrA* on *S. aureus* reference and clinical strains cultivated in CWM. For *P. aeruginosa* strains, we chose to analyse the expression of *rhII*, *lasI*, *pel* and *psl*.

The gene expression of the positive regulator of biofilm formation of *S. aureus* *fnbpA* and *spaA* show the same pattern for all the strains tested. The gene expression of *fnbpA* and *spaA* is increased in planktonic released cell compare to initial bacteria ($2^{1.9 \pm 0.3}$ for Newman ($p < 0.1$); $2^{1.8 \pm 0.2}$ for SAC 2 ($p < 0.1$) and $2^{1.5 \pm 0.1}$ for SAC 4 ($p < 0.1$) for *fnbpA* expression and $2^{1.4 \pm 0.2}$ for Newman ($p < 0.1$); $2^{1.8 \pm 0.3}$ for SAC 2 ($p < 0.1$) and $2^{1.9 \pm 0.2}$ for SAC 4 ($p < 0.1$) for *spaA* expression) (**Figure 6A**). This increase is more important with sessile cells ($2^{2.5 \pm 0.1}$ for Newman ($p < 0.01$); $2^{2.4 \pm 0.1}$ for SAC 2 ($p < 0.01$) and $2^{2.3 \pm 0.2}$ for SAC 4 ($p < 0.01$) for *fnbpA* expression and $2^{2.15 \pm 0.2}$ for Newman ($p < 0.01$); $2^{2.4 \pm 0.2}$ for SAC 2 ($p < 0.01$) and $2^{2.4 \pm 0.1}$ for SAC 4 ($p < 0.01$) for *spaA* expression) (**Figure 6A**).

This tendency was completely inverted for the expression of *agrA*, a negative regulator of biofilm formation, and *hla*, a virulence marker. For *hla*, the expression was decreased in planktonic released cells ($2^{-1.12 \pm 0.1}$ for Newman ($p < 0.1$); $2^{-2.3 \pm 0.2}$ for SAC 2 ($p < 0.01$) and $2^{-1.2 \pm 0.2}$ for SAC 4 ($p < 0.1$). This tendency is significantly more important in sessile cells ($2^{-2.4 \pm 0.2}$ for Newman ($p < 0.01$); $2^{-2.6 \pm 0.1}$ for SAC 2 ($p < 0.01$) and $2^{-2.4 \pm 0.3}$ for SAC 4 ($p < 0.01$) (**Figure 6B**). Finally, the expression of *agrA* highlighted also that sessile cells have the expression the more decreased after released cells compare to planktonic initial cells expression ($2^{-1.7 \pm 0.1}$ for Newman ($p < 0.1$); $2^{-1.6 \pm 0.1}$ for SAC 2 ($p < 0.1$) and $2^{-1.5 \pm 0.3}$ for SAC 4 ($p < 0.1$) for planktonic released and $2^{-2.2 \pm 0.2}$ for Newman ($p < 0.01$); $2^{-2.5 \pm 0.3}$ for SAC 2 ($p < 0.01$) and $2^{-2.7 \pm 0.2}$ for SAC 4 ($p < 0.01$) for sessile cells (**Figure 6B**).

P. aeruginosa expression of exo-polysaccharides *pel* and *psl*, two extracellular polysaccharides implicated in biofilm development have been analysed by qRT-PCR. These results are shown in **Figure 6C**. A significant difference in the expression of the

exopolysaccharides *pel* and *psl* was observed after recovering of planktonic released cells ($2^{1.6\pm 0.2}$ for PAO1; $2^{1.8\pm 0.2}$ for PAC 2 and $2^{1.45\pm 0.1}$ for PAC 4 for *pel* and $2^{1.3\pm 0.1}$ for PAO1; $2^{1.2\pm 0.4}$ for PAC 2 and $2^{1.28\pm 0.4}$ for PAC 4 for *psl*) ($p < 0.1$) but also in sessile cells where the difference was significantly more important ($2^{2.4\pm 0.1}$ for PAO1; $2^{2.6\pm 0.4}$ for PAC 2 and $2^{2.5\pm 0.3}$ for PAC 4 for *pel* and $2^{2.03\pm 0.2}$ for PAO1; $2^{2.15\pm 0.3}$ for PAC 2 and $2^2\pm 0.2$ for PAC 4 for *psl*) ($p < 0.01$) (**Figure 6C**).

As it concerns the expression of key regulators of quorum sensing in *P. aeruginosa*, *rhlI* expression after recovery of sessile bacteria was significantly higher compared to initial bacteria ($2^{1.6\pm 0.3}$ for PAO1; $2^{2.2\pm 0.3}$ for PAC 2 and $2^{2.3\pm 0.2}$ for PAC 4) ($p < 0.1$). This observation was also true for planktonic released cells even if the expression was not increase as much as what we measured in sessile cells ($2^{1.1\pm 0.2}$ for PAO1; $2^{1.3\pm 0.3}$ for PAC 2 and $2^{1.15\pm 0.2}$ for PAC 4) ($p < 0,01$) (**Figure 6D**). Expression of *lasI* showed also a similar patter with an intermediate expression in the biofilm released cells ($2^{1.9\pm 0.1}$ for PAO1 ($p < 0.01$); $2^{1.3\pm 0.2}$ for PAC 2 ($p < 0.1$) and $2^{1.7\pm 0.3}$ for PAC 4 ($p < 0.1$)). Once again, the expression of our regulator was significantly more increased when bacteria were in a mode of growth sessile ($2^{2.23\pm 0.2}$ for PAO1; $2^{2.25\pm 0.3}$ for PAC 2 and $2^{1.19\pm 0.4}$ for PAC 4) ($p < 0.01$) (**Figure 6D**).

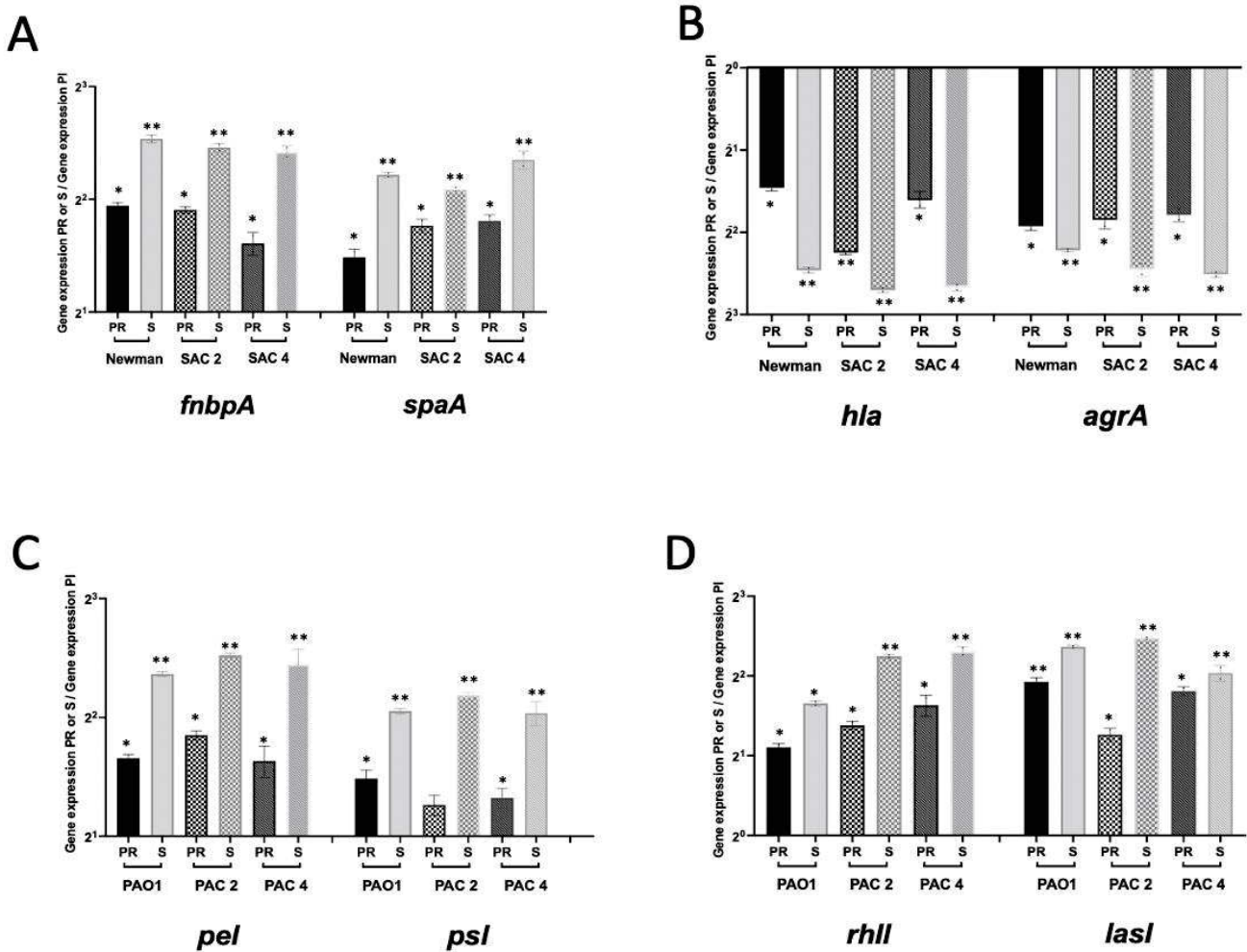


Figure 6. Gene expression of *Staphylococcus aureus* Newman, SAC 2 and SAC 4 *fnbpA*, *agrA*, *spaA*, *hla* (A, B) and *Pseudomonas aeruginosa* PAO1, PAC 2 and PAC 4 *lasI*, *rhII*, *pel*, and *psl* (C, D) after recovering sessile and released from the biofilm cells in the BioFlux™ system after 72h of culture in CWM. Planktonic released cells are represented in dark, sessile cells in light grey. Reference strains are represented by the rectangle full of colour, the two clinical strains are represented in squared and in hatched. Samples were tested in triplicate in two independent experiments. Results are presented as the mean \pm standard deviation of three different experiments. Statistics were performed using a t-test on GraphPad Prism version 7. ns, $p > 0.05$; * $p < 0.1$; ** $p < 0.01$; *** $p < 0.001$. PR: Planktonic released; PI: Planktonic initial; S: Sessile cells.

4. Discussion

Biofilm formation is a crucial step in the pathophysiology of chronic wounds (Pouget, 2020). Its study is of concern and need the development of new tools (Silva, 2021), in particular for the determination of the action and efficacy of antimicrobial agents. Biofilms are involved in more than 80% of chronic wound infections (Jamal, 2018). The penetration of antibiotics is generally reduced in the biofilm due, among other things, to EPS (Sharma, 2019). The study of the efficacy of antimicrobials on a biofilm mixture of *P. aeruginosa* and *S. aureus* is particularly interesting, because these bacteria are most of the time co-isolated at the level of the wound bed and their interactions confer an additional difficulty in the eradication of the biofilm (Omar, 2017). We therefore developed a protocol to test the efficiency of some antibiotics after an automatized debridement mimicking the first step of chronic wound management (Pouget, 2021). Oxacillin, vancomycin and dalbavancin were particularly inefficient at a concentration of 10x MIC against a pre-formed biofilm of *S. aureus*. Only daptomycin and linezolid had clearly activities. This difference could be explained by the ability to linezolid or β -lactams to penetrate deeper into the biofilms and to be able to directly contact with bacteria. The literature data on the effect of vancomycin as a potential antibiofilm is consistent with what this study highlighted. Vancomycin at MIC concentration are not capable of generating a reduction in bacterial density within the biofilm (He, 2017). Regarding linezolid, Gander et al. (Gander, 2002) have observed an effect of 1x MIC on early step of biofilm formation. Finally, daptomycin have already been reported effective on clinical isolate of *S. aureus* (Siala, 2014). Interestingly, the two antibiotics used against *P. aeruginosa* showed different effect. Only ceftazidime at 10x MIC were able to disrupt pre-formed biofilm. Regarding the recent literature data on *P. aeruginosa* biofilm and the efficacy of antibiotics, several studies have highlighted an inefficiency of the imipenem at sub-MIC and MIC concentrations to reduce bacteriological biomass within the biofilm. Authors have shown that the use of imipenem even favoured the maturation and increase of bacterial biomass in biofilm from clinical isolates of cystic fibrosis (Bagge, 2004; Karaman, 2013). Association of several demonstrated active antibiotics on mixte biofilm of *S. aureus* and *P. aeruginosa* showed a significative reduced percentage of biofilm formed in the microfluidic channel. As far as we know, no studies have investigated the effect of the association

of antibiotics on mono-species or polymicrobial biofilm formed by *S. aureus* and *P. aeruginosa*. This study could, therefore, be used as reference for comparison of other association of antibiotics against biofilm.

After studying mono-species biofilms, research gradually turned to investigate the complexity and interactions in multispecies biofilms (Zengler, 2012; Burmolle, 2014). Observations highlighted that bacteria residing in mixed biofilms organize themselves in a particular spatial way in response to interspecies interactions (Burmolle, 2014; Momeni, 2013; Dowd, 2008). Metabolic interactions, leading to bacterial cooperation or competition, are ubiquitous in polymicrobial biofilms and play an important role in maintaining diversity and stability of the microbial communities (Moller, 1998; Embree, 2014; Zelezniak, 2015). In general, in structured environments such as biofilm, coexistence of bacterial species is favoured through beneficial interactions such as co-metabolism and coordinated interactions (Hanse, 2007; Pande, 2015) as proved by Harrison on bacterial virulence (Harrison, 2006). However, in recent years a number of studies demonstrate that those interactions are not always in favour of the infection (Ngba Essebe, 2017; Hoffman, 2006; Price, 2019; Schurr, 2020). Investigate the mechanisms of cooperation and inhibitions which govern the bacterial mixte biofilms of chronic wounds go through the study of spatial organization of species. To achieve this, we modified our clinical strains of *S. aureus* and *P. aeruginosa* to incorporate a fluorescence vector plasmid. Then, we developed a protocol to visualize in confocal microscopy the organization of the different bacterial species in the mature biofilm formed in chronic wound conditions. Results demonstrate that within the polymicrobial biofilm, *S. aureus* and *P. aeruginosa* are not randomly organized. Thanks to confocal microscopy and fluorescence, we observe that *P. aeruginosa* is found deeper in the wound bed than *S. aureus*. This observation has already been described *in vitro* by studying mixed Pseudomonas/Staphylococcus biofilms in chronic wounds from biopsies (Fazli, 2009). The ability of *P. aeruginosa* to migrate deeper in the wound can be explain by via its type IV pili and the flagellum (Barken, 2009; Klausen, 2003; Madsen, 1996) may explain the presence of these bacteria in the deeper regions of chronic wounds. Further studies are necessary to confirm and understand why those bacteria are not found at the same level in chronic wounds and that it brings in terms of cooperation.

During biofilm formation, it is shown that sessile cells acquire different physiological characteristics than planktonic initial cells. The modifications concern the production of EPS, the bacterial growth, the expression of some genes regulating cell adhesion and biofilm regulation, or the resistance to antimicrobial agents and antibiotics (Davies, 2003). Among important stages in the development of biofilm, cell detachment (Sauer, 2002) is a key element in allowing the colonization of new surfaces (Kaplan, 2003; Hunt, 2004). However, little work has been done to elucidate characteristics of the cells released from the biofilm. Some studies have focused on mechanisms using a molecular approach, but very little research has been done to study the physiology of those particular cells (Boles, 2004; Bester, 2005; Ymele-Leki, 2007).

The technique and protocols developed in this work to collect sessile and biofilm-released cells and cultivate them under stressful conditions could constitute a new reproducible tool to study the characteristics of bacterial biofilms. Regarding the growth kinetics, the sessile and detached cells appear to be in a different physiological state from the original cells. The differences observed at the end of the exponential phase in sessile and released bacteria suggest that they need a period of adaptation to return to planktonic growth. These results confirm that sessile and planktonic bacteria exhibit different characters (Costerton, 1987). They agree with published results showing that limiting the diffusion of oxygen and nutrients in biofilms alters bacterial growth rates (Xu, 1998, Rollet, 2009). They also indicate that released cells are less able to revert to the planktonic mode. The ability to re-adhere to surfaces and re-form a biofilm also proved that sessile and released bacteria were able to exhibit a faster adhesion compare to initial bacteria. These adhesion data are confirmed by other publications in *P. aeruginosa* (Rollet, 2009) and in *Klebsiella pneumoniae* (Guilhen, 2019). These results could be explained by changes in the physicochemical properties of the cells resulting on an easier adhesion to various supports. For example, studies have shown differences in hydrophobia (Berlanga, 2017) or in affinity for non-polar solvents (Pelletier, 1997; Bellon-Fontaine, 1996). Finally, concerning the gene expression measured in the various populations of bacteria, two hypotheses are currently being considered. The first maintains that the bacteria released have characteristics very similar to sessile bacteria temporarily until they gradually regain a planktonic phenotype (Gilbert, 1993; Bester, 2005). The second hypothesis highlighted released from the biofilm cells as a real isolated population (Guilhen, 2016).

In chronic wounds, pathological biofilm formed by *S. aureus* and *P. aeruginosa* is frequent and difficult to treat. Indeed, new therapeutic strategies are needed and proved efficiency on pre-formed biofilms *in vitro* is a great first step in the discovery of future management of these infections. The combination of a chronic wound medium and the BioFlux™ microfluidic system represents a powerful tool to study the biofilm formation and to screen the potential anti-biofilm actions of candidate molecules under conditions mimicking those encountered *in vivo*. Improving current management techniques for chronic wounds also involves enhancing knowledge of the organization of polymicrobial biofilms as well as the control of its dissemination. The development of the techniques presented below seems a good way to improve the state of the art of biofilms found at the wound bed of chronic wounds.

Tables.

Strain	Characteristics	Reference
PAO1	Reference strain	Holloway et al, 1979
Newman	Reference strain	Duthie et al, 1952
PAO1- <i>mCherry</i>	PAO1 reference strain with pBPF- <i>mCherry</i> plasmid	Belon et al, 2015
Newman-GFP	Newman reference strain with pHOM-GFP plasmid	Provided by V. Molle
SAC 2	<i>Staphylococcus aureus</i> clinical strain isolated on a DFI	This study
SAC 4	<i>Staphylococcus aureus</i> clinical strain isolated on a DFI	This study
SAC 2-GFP	<i>S. aureus</i> clinical strain with pHOM-GFP plasmid	This study
SAC 4-GFP	<i>S. aureus</i> clinical strain with pHOM-GFP plasmid	This study
PAC 2	<i>Pseudomonas aeruginosa</i> clinical strain isolated on a DFI	This study
PAC 4	<i>Pseudomonas aeruginosa</i> clinical strain isolated on a DFI	This study

PAC 2- <i>mCherry</i>	<i>P. aeruginosa</i> clinical strain with pBPF- <i>mCherry</i> plasmid	This study
PAC 4- <i>mCherry</i>	<i>P. aeruginosa</i> clinical strain with pBPF- <i>mCherry</i> plasmid	This study
Media	Characteristics	Reference
BHI	Brain Heart Infusion, reference medium for bacterial culture	Sigma-Aldrich
CWM	Chronic Wound Medium, medium mimicking <i>in vivo</i> conditions encounter in chronic wounds	European patent application EP21305337

Table 1. Bacterial strains and media used in this study.

Antibiotics	Strains	Concentrations used	EUCAST MIC breakpoints (mg/L)	MIC in BHI (mg/L)	MIC in CWM (mg/L)
Vancomycin (Mylan)	<i>S. aureus</i> Newman	10 xMIC	2	1	1
	SAC 2	10 xMIC	2	2	2
	SAC 4	10 xMIC	2	2	4
Oxacillin (Astellas)	<i>S. aureus</i> Newman	10 xMIC	ND	0.5	1
	SAC 2	10 xMIC	ND	1	2
	SAC 4	10 xMIC	ND	0.5	2
Linezolid (Fresenius Kabi)	<i>S. aureus</i> Newman	10 xMIC	4	1	1
	SAC 2	10 xMIC	4	1	1
	SAC 4	10 xMIC	4	1	2
Daptomycin (Cubicin)	<i>S. aureus</i> Newman	10 xMIC	1	0.5	0.5
	SAC 2	10 xMIC	1	1	2
	SAC 4	10 xMIC	1	1	1
Dalbavancine (IHMA)	<i>S. aureus</i> Newman	10 xMIC	0.125	0.125	0.250
	SAC 2	10 xMIC	0.125	0.5	1
	SAC 4	10 xMIC	0.125	0.5	1
Imipenem (Arrow Generique)	<i>P. aeruginosa</i> PAO1	10 xMIC	4	1	2
	PAC 2	10 xMIC	4	2	2
	PAC 4	10 xMIC	4	2	4

Ceftazidime (PanPharma)	<i>P. aeruginosa</i> PAO1	10 xMIC	8	1	1
	PAC 2	10 xMIC	8	2	4
	PAC 4	10 xMIC	8	2	4

*ND, not defined

Table 2. Antibiotics used and Minimal Inhibitory Concentration determined in this study.

Primers used and target function	Target region	Primer name	Oligonucleotide sequence	Reference
Acyl homoserine lactone	<i>lasI</i>	lasI-F lasI-R	5' – GCCCCTACATGCTGAAGAACA – 3' 5'- GTCCAGAGTTGATGGCGAAA – 3'	Aghamollaei, 2015
Acyl homoserine lactone	<i>rhII</i>	rhII-F rhII-R	5'- AGCTTCTCGATGAAGACCTGATG -3' 5'- TGCTCTCTGAATCGCTGGAA - 3'	Mukherjee, 2017
Exopolysaccharides	<i>pel</i>	pel-F pel-R	5' – AGCAAGAAAGGAATCGCCG – 3' 5' – GACCGACAGATAGGCGAAGG – 3'	Colvin 2011
Exopolysaccharides	<i>psl</i>	psl-F psl-R	5'- CTGCCCTCACCTTTTCGCC – 3' 5'- GGAAGGATCAGCTGCG – 3'	Colvin 2011
Housekeeping gene <i>P. aeruginosa</i>	<i>rpoD</i>	rpoD-F rpoD-R	5'- CGATCGGTGACGACGAAGAT- 3' 5'- GTTCATGTGATGCCGAAGC- 3'	Seder 2021
α hemolysin	<i>hla</i>	hla-F hla-R	5'- TCCAGTGCAATTGGTAGTCA - 3' 5'- GGCTCTATGAAAGCAGCAGA - 3'	Otto, 2013
Protein A	<i>spa</i>	spa-F spa-R	5'-TATGCCTAACTTAAATGCTG - 3' 5'- TTGGAGCTTGAGAGTCATTA- 3'	Otto, 2013
Accessory gene regulator	<i>agrA</i>	agrA-F agrA-R	5'- CAAAGAGAAAACATGGTTACCATTATTAA -3' 5'- CTCAAGCACCTCATAAGGATTATCAG -3'	Garzoni, 2007
MSCRAM	<i>fnbpA</i>	fnbpA-F fnbpA-R	5'- AAATTGGGAGCAGCATCAGT - 3' 5'- GCAGCTGAATTCCCATTTC - 3'	Pfaffl, 2001
Gyrase B	<i>gyrB</i>	gyrB-F gyrB-R	5'- AGTAACGGATAACGGACGTGGTA - 3' 5'- CCAACACCATGTAAACCACCAGAT - 3'	Ngba essebe, 2017

Table 3. Primers used in this study

Author Contribution

Conceptualization, J.P.L. and A.S.; methodology, J.P.L., C.P., and C.D.R.; software, C.P.; formal analysis, C.P., C.D.R. and A.P.; data curation, C.P., C.D.R. and A.P.; writing—original draft preparation, C.P. and J.P.L.; writing—review and editing,

C.D.R., A.P., S.S. and A.S.; visualization, S.S., and A.S.; supervision, J.P.L.; project administration, A.S. and J.P.L.; funding acquisition, A.S. and J.P.L. All authors have read and agreed to the published version of the manuscript

Funding

This research was funded by CHU Nîmes, grant number Thématique Phare. CP is supported by a PhD grant from ANRT (Bourse CIFRE). The funders had no role in study design, data collection and analysis, decision to publish, or preparation of the manuscript.

Acknowledgments

AP, CDR, AS and JPL belong to the FHU INCh (Federation Hospitalo Universitaire Infections Chroniques, Aviesan). We thank the Nîmes University hospital for its structural, human and financial support through the award obtained by our team during the internal call for tenders « Thématiques phares ». We thank Sarah Kabani for her editing assistance. We thank Virginie Molle for providing plasmid pHOM-GFP.

Conflict of Interest

The authors declare that the research was conducted in the absence of any commercial or financial relationships that could be construed as a potential conflict of interest.

References

Aghamollaei H, Moghaddam MM, Kooshki H, Heiat M, Mirnejad R, Barzi NS. Detection of *Pseudomonas aeruginosa* by a triplex polymerase chain reaction assay based on *lasI/R* and *gyrB* genes. *J Infect Public Health*. 2015 Jul-Aug;8(4):314-22.

Alves P, Eida Al-Badi, Cathryn Withycombe, Paul M Jones, Kevin J Purdy, Sarah E Maddocks, Interaction between *Staphylococcus aureus* and *Pseudomonas aeruginosa* is beneficial for colonisation and pathogenicity in a mixed biofilm, *Pathogens and Disease*, Volume 76, Issue 1, February 2018

Anderl JN, Franklin MJ, Stewart PS. Role of antibiotic penetration limitation in *Klebsiella pneumoniae* biofilm resistance to ampicillin and ciprofloxacin. *Antimicrob Agents Chemother*. 2000;44(7):1818–24.

Bagge, N., Schuster, M., Hentzer, M., Ciofu, O., Givskov, M., Greenberg, E.P., et al. *Pseudomonas aeruginosa* biofilms exposed to imipenem exhibit changes in global

gene expression and beta-lactamase and alginate production. *Antimicrob Agents Chemother* 2004, 48, 1175-87.

Barken, K. B., S. J. Pamp, L. Yang, M. Gjermansen, J. J. Bertrand, M. Klausen, M. Givskov, C. B. Whitchurch, J. N. Engel, and T. Tolker-Nielsen. 2008. Roles of type IV pili, flagellum-mediated motility and extracellular DNA in the formation of mature structures in *Pseudomonas aeruginosa* biofilms. *Environ. Microbiol.* 10:2331-2343

Bellon-Fontaine MN Rault J Van Oss CJ (1996) Microbial adhesion to solvents: a novel method to determine the electron-donor/electron-acceptor or Lewis acid-base properties of microbial cells. *Colloid Surface B* 7: 47–53

Belon C, Soscia C, Bernut A, Laubier A, Bleves S, Blanc-Potard AB. A Macrophage Subversion Factor Is Shared by Intracellular and Extracellular Pathogens. *PLoS Pathog.* 2015 Jun 16;11(6):e1004969.

Berlanga, M., Gomez-Perez, L. & Guerrero, R. Biofilm formation and antibiotic susceptibility in dispersed cells versus planktonic cells from clinical, industry and environmental origins. *Antonie Van. Leeuwenhoek* 110, 1691–1704 (2017).

Bester E, Wolfaardt G, Joubert L, Garny K, Saftic S. Planktonic-cell yield of a pseudomonad biofilm. *Appl Environ Microbiol.* 2005 Dec;71(12):7792-8.

Boles BR, Thoendel M, Singh PK. Self-generated diversity produces "insurance effects" in biofilm communities. *Proc Natl Acad Sci U S A.* 2004 Nov 23;101(47):16630-5.

Burmølle, M., Ren, D., Bjarnsholt, T., and Sørensen, S. J. (2014). Interactions in multispecies biofilms: do they actually matter? *Trends Microbiol.* 22, 84–91. doi: 10.1016/j.tim.2013.12.004

Cécile Rollet, Laurent Gal, Jean Guzzo, Biofilm-detached cells, a transition from a sessile to a planktonic phenotype: a comparative study of adhesion and physiological characteristics in *Pseudomonas aeruginosa*, *FEMS Microbiology Letters*, Volume 290, Issue 2, January 2009, Pages 135–142

Chavant P, Gaillard-Martinie B, Talon R, Hébraud M, Bernardi T. A new device for rapid evaluation of biofilm formation potential by bacteria. *J Microbiol Methods.* 2007;68(3):605– 612.

Clinton A, Carter T. Chronic Wound Biofilms: Pathogenesis and Potential Therapies. *Lab Med.* 2015 Fall;46(4):277-84.

Colvin KM, Gordon VD, Murakami K, Borlee BR, Wozniak DJ, Wong GC, Parsek MR. The pel polysaccharide can serve a structural and protective role in the biofilm matrix of *Pseudomonas aeruginosa*. *PLoS Pathog.* 2011 Jan 27;7(1):e1001264.

Costerton JW, Cheng KJ, Geesey GG, Ladd TI, Nickel JC, Dasgupta M, Marrie TJ. Bacterial biofilms in nature and disease. *Annu Rev Microbiol.* 1987;41:435-64.

Davies D. Understanding biofilm resistance to antibacterial agents. *Nat Rev Drug Discov.* 2003 Feb;2(2):114-22.

Díez-Aguilar, M., Morosini, M.I., Köksal, E., Oliver, A., Ekkelenkamp, M., Cantón, R. Use of Calgary and Microfluidic BioFlux Systems To Test the Activity of Fosfomycin

and Tobramycin Alone and in Combination against Cystic Fibrosis *Pseudomonas aeruginosa* Biofilms. *Antimicrob Agents Chemother* 2017, 62, e01650-17.

Dowd SE, Wolcott RD, Sun Y, McKeehan T, Smith E, Rhoads D. Polymicrobial nature of chronic diabetic foot ulcer biofilm infections determined using bacterial tag encoded FLX amplicon pyrosequencing (bTEFAP). *PLoS One*. 2008;3(10):e3326.

Duthie, E.S., Lorenz, L.L. Staphylococcal coagulase; mode of action and antigenicity. *J Gen Microbiol* 1952, 6, 95-107.

Embree, M., Nagarajan, H., Movahedi, N., Chitsaz, H., and Zengler, K. (2014). Single-cell genome and metatranscriptome sequencing reveal metabolic interactions of an alkane-degrading methanogenic community. *ISME J*. 8, 757–767. doi: 10.1038/ismej.2013.187

Fazli M., Bjarnsholt T., Kirketerp-Møller K., Jørgensen B., Andersen A.S., Krogfelt K.A., Givskov M., Tolker-Nielsen T. Nonrandom distribution of *Pseudomonas aeruginosa* and *Staphylococcus aureus* in chronic wounds. *J Clin Microbiol*. 2009;47:4084–4089

Gander, S., Hayward, K., Finch, R. An investigation of the antimicrobial effects of linezolid on bacterial biofilms utilizing an *in vitro* pharmacokinetic model. *J Antimicrob Chemother* 2002, 49, 301–308.

Garzoni C, Francois P, Huyghe A, Couzinet S, Tapparel C, Charbonnier Y, Renzoni A, Lucchini S, Lew DP, Vaudaux P, Kelley WL, Schrenzel J. A global view of *Staphylococcus aureus* whole genome expression upon internalization in human epithelial cells. *BMC Genomics*. 2007 Jun 14;8:171.

Gilbert P Evans DJ Brown MRW (1993) Formation and dispersal of bacterial biofilms *in vivo* and *in situ*. *J Appl Bacteriol Symp* 74: (suppl): 67S–78S

Guilhen, C. et al. Transcriptional profiling of *Klebsiella pneumoniae* defines signatures for planktonic, sessile and biofilm-dispersed cells. *BMC Genomics* 17, 237 (2016).

Guilhen, C., Miquel, S., Charbonnel, N. et al. Colonization and immune modulation properties of *Klebsiella pneumoniae* biofilm-dispersed cells. *npj Biofilms Microbiomes* 5, 25 (2019)

Hansen, S. K., Rainey, P. B., Haagensen, J. A. J., and Molin, S. (2007). Evolution of species interactions in a biofilm community. *Nature* 445, 533–536. doi: 10.1038/nature05514

Harrison, F., Browning, L. E., Vos, M., and Buckling, A. (2006). Cooperation and virulence in acute *Pseudomonas aeruginosa* infections. *BMC Biol*. 4:21. doi: 10.1186/1741-7007-4-21

He, X., Yuan, F., Lu, F., Yin, Y., Cao, J. Vancomycin-induced biofilm formation by methicillin-resistant *Staphylococcus aureus* is associated with the secretion of membrane vesicles. *Microb Pathog* 2017, 110, 225-231.

Hoffman L.R., Deziel E., D'Argenio D.A., Lépine F., Emerson J., McNamara S., Gibson R.L., Ramsey B.W., Miller S.I. Selection for *Staphylococcus aureus* small-colony variants due to growth in the presence of *Pseudomonas aeruginosa*. *Proc Natl Acad Sci USA*. 2006;103:19890–19895

Holloway, B.W., Krishnapillai, V., Morgan, A.F. Chromosomal genetics of *Pseudomonas*. *Microbiol Rev* **1979**, *43*, 73-102.

Hotterbeekx A., Kumar-Singh S., Goossens H., Malhotra-Kumar S. In vivo and in vitro interactions between *Pseudomonas aeruginosa* and *Staphylococcus* spp. *Front Cell Infect. Microbiol.* 2017;*7*:106

Hunt SM, Werner EM, Huang B, Hamilton MA, Stewart PS. Hypothesis for the role of nutrient starvation in biofilm detachment. *Appl Environ Microbiol.* 2004 Dec;*70*(12):7418-25.

Jamal, M., Ahmad, W., Andleeb, S., Jalil, F., Imran, M., Nawaz, M.A., et al. Bacterial biofilm and associated infections. *J Chin Med Assoc* 2018, *81*, 7-11

James GA, Swogger E, Wolcott R, Secor P, Sestrich J, Costerton JW, Stewart PS. Biofilms in chronic wounds. *Wound Repair Regen.* 2008;*16*(1):37–44.

Kalan L, Loesche M, Hodkinson BP, Heilmann K, Ruthel G, Gardner SE, Grice EA. Redefining the Chronic-Wound Microbiome: Fungal Communities Are Prevalent, Dynamic, and Associated with Delayed Healing. *mBio.* 2016 Sep 6;*7*(5):e01058-16.

Kaplan JB, Fine DH. Biofilm dispersal of *Neisseria subflava* and other phylogenetically diverse oral bacteria. *Appl Environ Microbiol.* 2002 Oct;*68*(10):4943-50.

Kaplan JB, Meyenhofer MF, Fine DH. Biofilm growth and detachment of *Actinobacillus actinomycetemcomitans*. *J Bacteriol.* 2003 Feb;*185*(4):1399-404.

Karaman, M., Fırıncı, F., Arıkan Ayyıldız, Z., Bahar, I.H. [Effects of Imipenem, Tobramycin and Curcumin on Biofilm Formation of *Pseudomonas aeruginosa* Strains]. *Mikrobiyol Bul* 2013, *47*, 192-4.

Klausen, M., A. Heydorn, P. Ragas, L. Lambertsen, A. Aaes-Jørgensen, S. Molin, and T. Tolker-Nielsen. 2003. Biofilm formation by *Pseudomonas aeruginosa* wild type, flagella and type IV pili mutants. *Mol. Microbiol.* 48:1511-1524
Lebeaux D, Ghigo JM, Beloin C. Biofilm-related infections: bridging the gap between clinical management and fundamental aspects of recalcitrance toward antibiotics. *Microbiol Mol Biol Rev.* 2014;*78*(3):510-543.

Madsen, S. M., H. Westh, L. Danielsen, and V. T. Rosdahl. 1996. Bacterial colonization and healing of venous leg ulcers. *APMIS* 104:895-899

Metcalf DG, Bowler PG. Biofilm delays wound healing: a review of the evidence. *Burns Trauma.* 2015;*1*(1):5.

Michel Doumith, Matthew J. Ellington, David M. Livermore, Neil Woodford, Molecular mechanisms disrupting porin expression in ertapenem-resistant *Klebsiella* and *Enterobacter* spp. clinical isolates from the UK, *Journal of Antimicrobial Chemotherapy*, Volume 63, Issue 4, April 2009, Pages 659–667

Møller, S., Sternberg, C., Andersen, J. B., Christensen, B. B., Ramos, J. L., Givskov, M., et al. (1998). In situ gene expression in mixed-culture biofilms: evidence of metabolic interactions between community members. *Appl. Environ. Microbiol.* 64, 721–732.

- Momeni, B., Brileya, K. A., Fields, M. W., and Shou, W. (2013). Strong inter-population cooperation leads to partner intermixing in microbial communities. *Elife* 2013:e00230. doi: 10.7554/eLife.00230
- Mori Y, Nakagami G, Kitamura A, Minematsu T, Kinoshita M, Suga H, Kurita M, Hayashi C, Kawasaki A, Sanada H. Effectiveness of biofilm-based wound care system on wound healing in chronic wounds. *Wound Repair Regen.* 2019 Sep;27(5):540-547.
- Mukherjee S, Moustafa D, Smith CD, Goldberg JB, Bassler BL. The RhIR quorum-sensing receptor controls *Pseudomonas aeruginosa* pathogenesis and biofilm development independently of its canonical homoserine lactone autoinducer. *PLoS Pathog.* 2017 Jul 17;13(7):e1006504.
- Naudin B, Heins A, Pinhal S, Dé E, Nicol M. BioFlux™ 200 Microfluidic System to Study *A. baumannii* Biofilm Formation in a Dynamic Mode of Growth. *Methods Mol Biol.* 2019;1946:167-176.
- Ngba Essebe C, Visvikis O, Fines-Guyon M, Vergne A, Cattoir V, Lecoustumier A, Lemichez E, Sotto A, Lavigne JP, Dunyach-Remy C. Decrease of *Staphylococcus aureus* Virulence by *Helcococcus kunzii* in a *Caenorhabditis elegans* Model. *Front Cell Infect Microbiol.* 2017 Mar 16;7:77
- Nguyen AT, Oglesby-Sherrouse AG. Interactions between *Pseudomonas aeruginosa* and *Staphylococcus aureus* during co-cultivations and polymicrobial infections. *Appl Microbiol Biotechnol.* 2016;100:6141–8.
- Omar, A., Wright, J.B., Schultz, G., Burrell, R., Nadworny, P. Microbial Biofilms and Chronic Wounds. *Microorganisms* 2017, 5, 9.
- Otto, M.P.; Martin, E.; Badiou, C.; Lebrun, S.; Bes, M.; Vandenesch, F.; Etienne, J.; Lina, G.; Dumitrescu, O. Effects of subinhibitory concentrations of antibiotics on virulence factor expression by community-acquired methicillin-resistant *Staphylococcus aureus*. *J. Antimicrob. Chemother.* **2013**, *68*, 1524–1532.
- Pande, S., Kaftan, F., Lang, S., Svatos, A., Germerodt, S., and Kost, C. (2015). Privatization of cooperative benefits stabilizes mutualistic cross-feeding interactions in spatially structured environments. *ISME J.* 10, 1413–1423. doi: 10.1038/ismej.2015.212
- Pastar I, Nusbaum AG, Gil J, Patel SB, Chen J, Valdes J, Stojadinovic O, Plano LR, Tomic-Canic M, Davis SC. Interactions of methicillin resistant *Staphylococcus aureus* USA300 and *Pseudomonas aeruginosa* in polymicrobial wound infection. *PLoS One.* 2013;8(2):e56846.
- Pelletier C, Bouley C, Cayuela C, Bouttier S, Bourlioux P, Bellon-Fontaine MN. Cell surface characteristics of *Lactobacillus casei* subsp. *casei*, *Lactobacillus paracasei* subsp. *paracasei*, and *Lactobacillus rhamnosus* strains. *Appl Environ Microbiol.* 1997 May;63(5):1725-31.
- Peters BM, Jabra-Rizk MA, Graeme A, Costerton JW, Shirtliff ME. Polymicrobial interactions: impact on pathogenesis and human disease. *Clin Microbiol Rev.* 2012;25(1):193–213.

Pfaffl, M.W., Hageleit, M. Validities of mRNA quantification using recombinant RNA and recombinant DNA external calibration curves in real-time RT-PCR. *Biotechnology Letters* **23**, 275–282 (2001).

Pouget C, Dunyach-Remy C, Pantel A, Schuldiner S, Sotto A, Lavigne JP. Biofilms in Diabetic Foot Ulcers: Significance and Clinical Relevance. *Microorganisms*. 2020 Oct 14;8(10):1580.

Price CE, Brown DG, Limoli DH, Phelan VV, O'Toole GA. Exogenous Alginate Protects *Staphylococcus aureus* from Killing by *Pseudomonas aeruginosa*. *J Bacteriol*. 2020 Mar 26;202(8):e00559-19.

Pulimood S, Ganesan L, Alangaden G, Chandrasekar P. Polymicrobial candidemia. *Diagn Microbiol Infect Dis*. 2002;44(4):353–7.

Sauer K, Camper AK, Ehrlich GD, Costerton JW, Davies DG. *Pseudomonas aeruginosa* displays multiple phenotypes during development as a biofilm. *J Bacteriol*. 2002 Feb;184(4):1140-54.

Schurr M.J. *Pseudomonas aeruginosa* alginate benefits *Staphylococcus aureus*? *J Bacteriol*. 2020;202

Seder N, Abu Bakar MH, Abu Rayyan WS. Transcriptome Analysis of *Pseudomonas aeruginosa* Biofilm Following the Exposure to Malaysian Stingless Bee Honey. *Adv Appl Bioinform Chem*. 2021;14:1-11. Published 2021 Jan 14. doi:10.2147/AABC.S292143

Seth AK, Geringer MR, Hong SJ, Leung KP, Galiano RD, Mustoe TA. Comparative analysis of single-species and polybacterial wound biofilms using a quantitative, in vivo, rabbit ear model. *PLoS One*. 2012;7(8):e42897.

Sharma, D., Misba, L., Khan, A.U. Antibiotics versus biofilm: an emerging battleground in microbial communities. *Antimicrob Resist Infect Control* 2019, **8**, 76.

Siala W, Mingeot-Leclercq MP, Tulkens PM, Hallin M, Denis O, Van Bambeke F. Comparison of the antibiotic activities of Daptomycin, Vancomycin, and the investigational Fluoroquinolone Delafloxacin against biofilms from *Staphylococcus aureus* clinical isolates. *Antimicrob Agents Chemother*. 2014 Nov;58(11):6385-97.

Silva, N.B.S., Marques, L.A., Röder, D.D.B. Diagnosis of biofilm infections : current methods used, challenges and perspectives for the future. *J Appl Microbiol* 2021 (in press).

Wilson, C., Lukowicz, R., Merchant, S., Valquier-Flynn, H., Caballero, J., Sandoval, J., et al. Quantitative and Qualitative Assessment Methods for Biofilm Growth: A Mini-review. *Res Rev J Eng Technol* 2017, **6**.

Wolcott R, Gontcharova V, Sun Y, Zischakau A, Dowd S. Bacterial diversity in surgical site infections: not just aerobic cocci any more. *J Wound Care*. 2009;18(8):317–23.

Xu KD, Stewart PS, Xia F, Huang CT, McFeters GA. Spatial physiological heterogeneity in *Pseudomonas aeruginosa* biofilm is determined by oxygen availability. *Appl Environ Microbiol*. 1998 Oct;64(10):4035-9

Ymele-Leki P, Ross JM. Erosion from *Staphylococcus aureus* biofilms grown under physiologically relevant fluid shear forces yields bacterial cells with reduced avidity to collagen. *Appl Environ Microbiol.* 2007 Mar;73(6):1834-41

Zelezniak, A., Andrejev, S., Ponomarova, O., Mende, D. R., Bork, P., and Patil, K. R. (2015). Correction for Zelezniak et al., metabolic dependencies drive species co-occurrence in diverse microbial communities. *Proc. Natl. Acad. Sci. U.S.A.* 112, 6449–6454. doi: 10.1073/pnas.1522642113

Zengler, K., and Palsson, B. O. (2012). A road map for the development of community systems (CoSy) biology. *Nat. Rev. Microbiol.* 10, 366–372. doi: 10.1038/nrmicro2763

Zuroff TR, Bernstein H, Lloyd-Randolfi J, Jimenez-Taracido L, Stewart PS, Carlson RP. Robustness analysis of culturing perturbations on *Escherichia coli* colony biofilm beta-lactam and aminoglycoside antibiotic tolerance. *BMC Microbiol.* 2010;10(1):185.

DISCUSSION & PERSPECTIVES

Les plaies chroniques sont un problème de santé publique. La difficulté de prise en charge des infections sous-jacentes corrélée à la présence d'un biofilm polymicrobien au niveau du lit de la plaie, augmente le risque d'amputations des membres inférieurs.

Dans le but d'améliorer la compréhension du rôle de ce biofilm multi-espèce, d'améliorer la prise en charge des plaies chroniques et de développer de nouvelles stratégies thérapeutiques nous avons axé ce travail de thèse autour de 2 questions :

1. Est-ce que les **facteurs environnementaux** rencontrés par les bactéries au niveau des plaies chroniques influencent le comportement (virulence, fitness, morphologie, adhésion, expression génique) de souches de *S. aureus* et *P. aeruginosa* isolées des plaies de patients ?
2. Est-il possible de mettre au point un nouveau modèle *in vitro* permettant l'étude de la formation d'un biofilm polymicrobien dans des conditions proche de l'*in vivo* afin de suivre l'**organisation** des différentes espèces bactériennes mais aussi d'évaluer le **pouvoir antibiofilm** de potentielles molécules thérapeutiques ?

Le milieu plaie : un modèle *in vitro* innovant

L'équipe INSERM U1047 (axe plaies chroniques) travaille depuis longtemps sur l'évolution de la virulence de souches de *S. aureus* isolées de plaies du pied diabétique. Ils ont notamment mis en évidence la présence d'un phage ROSA-like chez une souche clinique de *S. aureus* affectant son potentiel de virulence. Ces travaux ont nourri des interrogations autour de l'influence des facteurs environnementaux sur le comportement des souches bactériennes.

En effet, au sein des UPD, les bactéries sont soumises à des conditions environnementales particulières du fait de la physiopathologie diabétique (artériopathie, neuropathie, déséquilibre glycémique...). Ces conditions ont un impact sur le comportement des bactéries. Le but de notre premier travail était alors d'évaluer

l'effet des conditions stranges observées au sein des plaies du pied chez le patient diabétique sur le potentiel de virulence de *S. aureus*. Nous avons initialement testé 3 conditions particulières liées au UPD : l'**hyperglycémie** (ajout de glucose), l'**ischémie** (anaérobiose) et enfin la **présence d'antibiotiques** à des concentrations subinhibitrices dans le milieu environnant.

Cette étude de l'adaptation de souches de *S. aureus* cliniques aux facteurs de stress environnant rencontrés dans le pied diabétique a été effectuée dans un modèle *in vitro* adapté pour mimer les conditions de chronicité des UPD. Ce modèle adapté depuis le « Lubbock model » décrit par Sun et *al.*¹⁷³ a pu être validé par l'apparition de small colony variants (SCVs) après une exposition prolongée de *S. aureus* à ce milieu. Ces petites colonies métaboliquement inactives sont caractéristiques de *S. aureus* en situation d'infections persistantes. D'autre part, l'étude a permis la comparaison du potentiel de virulence des souches après une exposition courte (24h) et une **exposition prolongée de 16 semaines**, correspondant à une situation chronique.

Les études transcriptomiques ont mis en évidence qu'après 16 semaines de culture en conditions stressantes, l'expression de gènes de virulence codant pour la toxine de Panton et Valentine et EdinB étaient fortement diminuée. Le système de régulation *LukF/LukS-PV* présentait une diminution de 3 « fold change » sous vancomycine, 7 dans un milieu hyperglucosé, 8 fois en anaérobiose, et de 2 fois sous linézolide. Les « fold changes » d'*edinB* et *edinC* étaient également diminués entre 10 et 30 fois sous vancomycine, linézolide et en milieu hyperglucosé et de 15 fois en anaérobiose. En ce qui concerne les autres toxines, l'expression des gènes codant pour les hémolysines alpha et beta étaient diminuées pour toutes les souches quelle que soit la condition testée. L'ensemble de ces résultats suggère que les principaux gènes de virulence de *S. aureus* sont sous-exprimés après une exposition prolongée à des concentrations subinhibitrices d'antibiotiques, en condition d'anaérobiose et en hyperglycémie. Il est également intéressant de noter qu'après 16 semaines de culture en excès de glucose, l'expression des gènes d'adhésion *fnbpA* et *eap* était augmentée. Nos résultats semblent donc indiquer que l'ajout d'antibiotiques (vancomycine et linézolide) **diminuent de façon significative la virulence des souches** de *S. aureus*. Le

linézolide s'est avéré être plus efficace que la vancomycine, résultat fidèle aux conclusions proposées par d'autres études qui présentent le linézolide comme étant plus efficace cliniquement que la vancomycine ¹⁷⁴⁻¹⁷⁶. **La formation de biofilm** après une exposition longue au glucose et à la vancomycine s'est avérée être augmentée chez toutes les souches de *S. aureus*. Le glucose semble stimuler l'opéron *gbaAB* qui régule la formation du biofilm en activant l'expression de *ica* chez *S. aureus*. GbaA est modulé par l'interaction avec des composés inducteurs et facilite l'adaptation de *S. aureus* au stress en induisant la formation de biofilm ¹⁷⁷.

Ces résultats nous confirment que la virulence de *S. aureus* est impactée par les différentes conditions stressantes rencontrées au niveau des infections du pied diabétique, en particulier pour les gènes codant pour les toxines PVL et Edin. Les souches sont toutefois capables de survivre soit par l'activation d'autres facteurs de virulence (toxines Sea, Hla), soit par un changement phénotypique en small colony variant et un comportement dirigé vers la formation de biofilm.

Encouragés par nos résultats préliminaires sur le modèle mis en place pour les UPD, nous avons donc conclu que toutes les plaies chroniques constituaient des environnements particuliers qui, pour être étudiées, nécessitaient l'obtention de **modèles *in vitro* fiables et représentatifs**. Le but de notre travail a alors été de référencer le plus exhaustivement possible l'environnement (qu'il soit microbiologique, physico-chimique, inflammatoire ou encore cellulaire) rencontré dans les plaies chroniques en général et non plus dans les infections des plaies chez le patient diabétique. L'idée était de développer **un modèle de base robuste** pour ensuite pouvoir l'adapter à des plaies particulières (UPD, escarres, brûlures...).

Au cours de nos recherches, nous avons découvert des études démontrant l'effet du milieu de culture sur la sensibilité à différents antibiotiques de souches cliniques de *S. aureus* issues de plaies ¹⁷³. Comparativement à la sensibilité établie en milieu Mueller-Hinton, la croissance de souches de *S. aureus* dans du milieu de culture Lacks modifié (milieu MLM ; simulant l'environnement du nasopharynx) accroît la sensibilité des souches d'un facteur 4 à 256 pour l'azithromycine, l'érythromycine, la streptomycine, le ceftriaxone et la cefalotine. Au contraire, la résistance de ces souches à la daptomycine et la rifampicine est augmentée en milieu MLM d'un facteur 4 à 16. Dans le cas de la daptomycine et la rifampicine, les souches étant considérées

comme sensibles en milieu MH, ces 2 antibiotiques auraient donc pu être prescrits, alors qu'ils sont considérés comme inefficaces dans la condition MLM. Il apparaît donc clairement que le milieu de culture a un effet sur la capacité des microorganismes à s'adapter à leur environnement et que les milieux utilisés en routine sur de nombreux microorganismes ne permettent pas d'obtenir des résultats fiables quant au comportement des dits microorganismes dans leur environnement naturel.

Outre les caractéristiques intrinsèques à la plaie, il était important de baser notre modèle sur des données également microbiologiques. Une des caractéristiques essentielles des plaies chroniques est le fait qu'elles soient plurimicrobiennes, théâtre d'interactions entre espèces bactériennes via le biofilm. Le modèle « plaies chroniques » devait alors permettre une **co-culture** de microorganismes les plus couramment isolés des plaies chroniques tout en permettant de prendre en compte des facteurs environnementaux et en favorisant le mode de croissance **sessile** des bactéries. Une des interactions bactériennes les plus référencées concernant les plaies chroniques est la coopération entre *S. aureus* et *P. aeruginosa*¹²⁶. Ainsi, nous nous sommes concentrés sur la co-culture et l'association entre ces deux bactéries.

Il existait à notre connaissance 3 modèles ayant été développés pour étudier les biofilms multi-espèces observés dans les plaies chroniques. Ces modèles s'intéressaient en particulier à la formation de biofilm par 3 microorganismes isolés dans les plaies chroniques, à savoir *S. aureus*, *P. aeruginosa* et *Enterococcus faecalis*. Il s'agit notamment du **milieu Lubbock** basé sur le milieu de culture Bolton¹⁷³ comprenant 50% de plasma défibriné de bovin ainsi que 5% d'hématies de cheval hémolysées. Ce milieu a été utilisé afin de montrer d'éventuelles interactions synergiques entre *S. aureus* et *P. aeruginosa*¹²⁶. Les auteurs ont montré que la co-culture de *S. aureus* avec *P. aeruginosa* dans du milieu Lubbock est possible. Ladite co-culture dans du milieu Lubbock permet aussi la sélection d'une sous population de *S. aureus* résistant à la gentamicine.

Toutefois, le milieu Lubbock ne tient pas compte d'un certain nombre de facteurs environnementaux. Les milieux connus ont été établis à partir de constituants très différents de ceux décrits dans les plaies humaines, par exemple du plasma de bovin et du sang de cheval ont été utilisés associés à un pH de l'ordre de 7,2 – 7,4. De plus, les milieux connus ne **reproduisent pas les conditions physiologiques** et

environnementales des plaies chroniques, les bactéries étant en contact avec du sérum¹⁷³ et non du plasma. Cette différence impacte le processus de cicatrisation et également le comportement des bactéries : croissance, sensibilité aux antimicrobiens, sous forme planctonique ou biofilm.

Un second milieu **IVWM** (« **In Vitro Wound Milieu** ») a été proposé par Kadam et al.¹⁷⁷ pour étudier spécifiquement les biofilms de plaies chroniques. Ce milieu IVWM est constitué de sérum de veau foetal (70%), d'acide lactique (11-12mM), de lactoferrine (20-30µg/mL), de fibrinogène (200-400µg/mL), de fibronectine (30-60µg/mL), de collagène (10-12µg/mL), et est ajusté à pH 5,25. Ce pH acide étant celui d'une peau saine, et non celui d'une plaie non cicatrisée, plus alcalin. Les auteurs ont comparé la croissance d'une souche de *S. aureus* AH133, d'origine non précisée et d'une souche de référence *P. aeruginosa* (PAO1) non clinique, seule ou en co-culture. La croissance en milieu IVWM des souches *S. aureus* et *P. aeruginosa* était moins rapide qu'en milieu Lysogeny Broth, en particulier celle de *S. aureus*. En co-culture, autant en Lysogeny Broth qu'en IVWM, la croissance de *S. aureus* a été fortement diminuée. La mesure de la sensibilité aux antibiotiques, en particulier la tobramycine pour *P. aeruginosa* et la vancomycine pour *S. aureus* a été réalisée sur des bactéries dans des biofilms établis et non sur des bactéries en état planctonique. Ce milieu a ainsi été décrit pour mesurer la croissance bactérienne de *S. aureus* et *P. aeruginosa* en culture simple ou co-culture ainsi que pour mesurer une sensibilité de bactéries sessiles vis-à-vis d'un antibiotique (1 antibiotique testé sur les 2 souches).

Dans ce contexte, nous avons développé notre propre modèle *in vitro* appelé CWM pour « **Chronic Wound-like Medium** » afin de résoudre les inconvénients et obstacles de l'art antérieur.

Ce milieu permet :

- La culture des microorganismes les plus souvent isolés des plaies chroniques (*S. aureus*, *P. aeruginosa*, *S. epidermidis*, *E. coli*, *H. kunzii*...).
- La **co-culture** des différentes espèces citées pendant une exposition de longue durée, au moins 6 semaines.
- De **mimer l'environnement d'une plaie**, d'une part par les constituants, et d'autre part par le pH. Le milieu comprend du milieu

Bolton, source de peptone (79,5%), du sérum humain décomplémenté (20%), du sang humain hémolysé (0,5%), des débris cellulaires (kératinocytes), des sels minéraux et un pH tamponné à 8. Les peptones, le sérum et le sang miment les 3 constituants essentiels retrouvés au niveau des plaies chroniques à savoir des tissus endommagés, des globules rouges et du sérum humain comprenant cytokines, protéines matricielles ...

- Le mode de croissance des bactéries sous forme planctonique mais également **sessile**.
- De tester l'efficacité de composés antimicrobiens existants mais également l'efficacité de nouvelles molécules quelles que soient les conditions de culture et/ou les microorganismes.

Le CWM fait l'objet d'un **brevet européen** déposé dont le numéro de dépôt est le suivant : EP21305337.

Afin de valider le CWM, nous avons comparé la croissance seule ou en association de souches de référence et de souches cliniques de *S. aureus* et *P. aeruginosa* dans le CWM et dans un milieu classique, le BHI. Le CWM a montré des **résultats reproductibles et fiables**. *Pseudomonas aeruginosa* et *S. aureus* ont pu être cultivés seuls ou en culture mixte. En monoculture, *S. aureus* a atteint une densité cellulaire maximale plus élevée en BHI que dans le CWM. Plus important encore, dans la culture mixte, contrairement à ce qui a été décrit précédemment dans la littérature ^{124,128,129}, *S. aureus* n'a pas été rapidement éradiqué par *P. aeruginosa* : non seulement les deux espèces ont pu **coexister** dans les deux milieux, mais la co-culture dans le « milieu plaie chronique » a permis à *S. aureus* d'atteindre une densité cellulaire plus élevée. Ces résultats sont en accord avec des études récentes qui ont signalé que *P. aeruginosa* pourrait avoir un effet protecteur sur *S. aureus* ^{133, 134}. Nous confirmons effectivement cette tendance, puisque la phase initiale de décalage observée pour la croissance de *S. aureus* en CWM n'existait pas dans la culture mixte. De plus, le plateau atteint après 24h de co-culture correspond à une densité cellulaire plus élevée. Nous avons également évalué le rôle du « milieu plaie chronique » sur la capacité à former du biofilm des bactéries. Nous nous sommes intéressés à l'adhésion, première étape de la formation de biofilm, ainsi qu'à la

quantification de la biomasse de biofilm mono ou multi-espèces. Les résultats obtenus ont montré que **l'adhésion était facilitée** dans le « milieu plaie chronique » par rapport au BHI. En effet, toutes les souches adhéraient plus rapidement dans le CWM. Nous avons également vérifié si, au-delà de l'étape d'adhésion précoce, le « milieu plaie chronique » facilitait la formation de biofilm en mesurant la biomasse du biofilm après 24 heures d'incubation. Les résultats corroborent l'évaluation précoce de l'adhésion indiquant que notre nouveau modèle *in vitro* est compatible avec les études de biofilm et que cet environnement favorise un biofilm rapide et dense. De manière intéressante, ces résultats sont cohérents avec le comportement des souches décrites dans les plaies chroniques ^{135, 178} suggérant que ce nouveau milieu pourrait bien mimer l'environnement rencontré par les bactéries dans les lésions chroniques. Enfin, nous avons étudié l'effet du CWM sur la virulence bactérienne. Toutes les souches de *S. aureus* et de *P. aeruginosa* testées présentaient **une virulence moindre** dans le CWM que dans le BHI. Ainsi, le nouveau modèle vient étayer nos études antérieures montrant que l'environnement présent au niveau des plaies influence la virulence des souches. Certains auteurs ont déjà souligné et critiqué le fait que la communauté scientifique ne dispose pas d'un modèle standardisé pour étudier de façon fiable et reproductible le biofilm dans des conditions *in vivo* ^{179, 180}. Ce nouveau milieu peut ainsi contribuer à fournir un modèle de base plus robuste pour étudier les plaies chroniques.

Ce modèle *in vitro* nous a été utile afin d'étudier la virulence, la croissance, le phénotype, et la formation en biofilm des souches de *S. aureus* et *P. aeruginosa*. Néanmoins, en ce qui concerne la formation, la régulation et l'efficacité de molécules thérapeutiques sur le biofilm bactérien, il nous semblait intéressant de ne pas s'arrêter au stade du CWM mais de développer d'autres techniques permettant de se rapprocher des conditions naturelles dans lesquelles se forme le biofilm présent sur la peau des plaies chroniques.

Coopération bactérienne et mesure de l'efficacité de molécules sur biofilm formé : le Bioflux™ 200, un sérieux atout

L'un des objectifs centraux de cette thèse était de pouvoir renforcer l'état de l'art sur les modèles *in vitro* disponibles permettant l'investigation des plaies chroniques en se focalisant tout particulièrement sur l'étude des biofilms polymicrobiens. C'est ainsi

que, dans la logique du développement du « Chronic wound-like medium », nous souhaitons utiliser une **nouvelle technique reproductible, standardisée et permettant le criblage à haut débit** de potentielles molécules thérapeutiques tout en simulant les **conditions dans lesquelles se forme ce biofilm chez les patients**.

En réalisant un tour de la littérature, nous avons observé que la majorité des techniques qui visent à étudier le biofilm, qu'il soit en cours de formation ou mature, présentent des inconvénients majeurs. En effet, ces méthodes utilisent des conditions statiques de formation du biofilm ¹⁸¹. Les plus répandues sont les méthodes en microplaque 96 puits associant une mesure de la biomasse via l'utilisation du Cristal Violet ou la méthode du Calgary Biofilm Device ^{138, 182}. Même si ces techniques répondent aux critères de standardisation et de criblage à haut débit, les résultats, ajouté aux conditions statiques, manquent de reproductibilité en raison des nombreuses étapes de rinçages nécessaires. Ces techniques microbiologiques traditionnelles ont permis l'approfondissement des connaissances sur le biofilm bactérien. Cependant, les difficultés à recréer certaines conditions physiques ou biologiques, telles que l'absence de renouvellement de nutriments, d'oxygène ou des forces de cisaillements auxquelles sont soumises les bactéries *in vivo*, ont conduit les scientifiques à développer de nouvelles méthodes ¹⁸³. Ces techniques ont permis l'investigation de biofilm polymicrobien et de cultiver une hétérogénéité de populations bactériennes. Pour pallier ces problèmes, des **modèles en microfluidique** ont vu le jour permettant une étude des biofilms standardisée, reproductible, à haut débit et de plusieurs espèces bactériennes à la fois. Ces modèles prennent également en compte le renouvellement du milieu de culture et des nutriments ainsi que les forces de cisaillement qui régissent l'élaboration de cette communauté microbienne organisée. La « flow cell » et ces dérivés automatisés tel le Bioflux™ 200 sont les fers de lance de l'application microfluidique ^{184, 185}.

Au cours de ce travail, l'unité INSERM U1047 a pu acquérir le système Bioflux™ 200, ce qui a permis de combiner ce modèle d'étude à notre milieu *in vitro* afin d'étudier la formation du biofilm mono et polymicrobien des souches de référence et cliniques de *S. aureus* et *P. aeruginosa* en temps réel. Nous avons élaboré, en concordance avec des données publiées, une méthode permettant de suivre l'évolution du pourcentage de biofilm formé dans le canal de microfluidique en fonction du temps

ainsi que du milieu utilisé (CWM ou BHI). Les résultats de ces expériences ont montré que les espèces étudiées formaient un biofilm robuste après 72 heures de culture dans le Bioflux™ 200. La formation de ce biofilm était d'autant plus facilitée dans le CWM qu'en BHI, la souche de référence de *S. aureus* Newman a été particulièrement influencée par le CWM et a formé un biofilm plus dense et de façon plus rapide que la souche de *P. aeruginosa* PAO1. Ces différences observées renforcent l'idée que le milieu de culture a eu un impact important sur le comportement bactérien ¹⁸⁶. De manière intéressante, lorsque les bactéries sont cultivées dans un environnement qui imite étroitement les conditions *in vivo*, leur comportement change ¹⁸⁷. A l'aide de ces expériences nous avons pu particulièrement constater le comportement différent de la souche PAO1 dans les deux milieux étudiés. Nous avons observé la présence et la production de **structures caractéristiques** des exopolysaccharides de *P. aeruginosa* tels que l'alginate lorsque cette souche était cultivée 72 heures dans le CWM. Ces structures n'étaient pas visibles dans les conditions de culture en BHI. L'alginate est un exopolysaccharide synthétisé en réponse aux conditions environnementales. Il est produit par *P. aeruginosa* en tant que polysaccharide de la matrice extracellulaire et joue un rôle dans la virulence, la formation de biofilm et la résistance à différents antibiotiques ¹⁸⁸. Il a été précédemment montré que la souche de référence de *P. aeruginosa* PAO1 était une souche non mucoïde qui ne présente aucune production d'alginate dans les milieux de culture conventionnels ¹⁸⁹. Pour confirmer notre hypothèse, nous avons donc mis au point un protocole pour récupérer les bactéries sessiles mais également les bactéries planctoniques libérées du biofilm à partir de notre Bioflux™ 200. Nous avons par la suite, analysé les cellules sessiles par qRT-PCR afin d'évaluer l'expression génique de régulateurs de la biosynthèse de plusieurs exopolysaccharides chez *P. aeruginosa*. Après une culture prolongée de 72 heures dans le CWM, nous démontrons ainsi pour la première fois que la souche PAO1 est capable de surexprimer des gènes impliqués dans la biosynthèse de **l'alginate** mais aussi des **exopolysaccharides Pel et Psl**. Ces trois composants sont essentiels pour créer un échafaudage solide impliqué dans le maintien de l'intégrité du biofilm chez *P. aeruginosa* ⁸⁷. Ces données ont ainsi démontré que la combinaison du CWM et du Bioflux™ 200, permettait la création d'un outil innovant et prometteur pour l'investigation des biofilms de plaies chroniques.

Une partie importante de l'étude des biofilms des plaies chroniques porte aussi sur l'action et **l'efficacité des agents antimicrobiens**. Les biofilms sont impliqués dans plus de 80% des infections chroniques des plaies ³⁴. La pénétration des antibiotiques est généralement réduite dans le biofilm en raison, entre autres, de l'EPS ¹⁹⁰. L'étude de l'efficacité des antimicrobiens sur un biofilm mixte de *P. aeruginosa* et *S. aureus* est particulièrement intéressante, car ces bactéries sont la plupart du temps co-isolées au niveau du lit de la plaie et leur interaction confère une difficulté supplémentaire à l'éradication du biofilm ¹⁹¹. Deux types de modèles de biofilm *in vitro* sont actuellement utilisés pour prédire l'efficacité antimicrobienne contre le biofilm : les systèmes fermés et ouverts. Les systèmes fermés sont caractérisés par un apport limité de nutriments et une accumulation de déchets métaboliques ¹⁹². Les systèmes ouverts reproduisent mieux les conditions rencontrées *in vivo*, car il existe un contrôle permanent de l'apport des nutriments, du débit et de la température ¹⁹³. Le système **BioFlux™ 200** est un système ouvert microfluidique qui après adaptation du protocole initial, permettrait la mise en place de tests à haut débit ¹⁸⁵ imitant la formation et la prise en charge des biofilms *in vivo*. Dans cette optique, nous avons élaboré un protocole sur le BioFlux™ 200 permettant de **mimer mécaniquement un débridement** et de retirer une partie du biofilm préformé. Le débridement représente la première étape de la prise en charge clinique d'une plaie chronique. Après avoir formé un biofilm mature dans le Bioflux™ 200 pendant 72 heures, un débridement automatique est réalisé par un processus de réversion du flux au travers du canal microfluidique. Cette étape permet de réduire significativement le biofilm constitué. Après analyse d'études cliniques ^{3, 194, 195} concernant l'efficacité du débridement du lit de la plaie chez le patient, nous avons établi que le biofilm n'est jamais complètement éliminé peu importe la nature du débridement utilisé. Il y a toujours un pourcentage de biofilm restant qui facilite la rechute et la rematuration rapide d'un biofilm. Les données cliniques estiment l'efficacité du débridement qu'il soit mécanique, chirurgical, enzymatique ou autre, autour de 85%. Nous avons donc fixé un maximum de **13 à 15% de biofilm** restant dans le canal microfluidique après inversion du flux pour mimer les conditions *in vivo*. Le but de ce débridement mécanique était d'étudier **l'effet des molécules** antimicrobiennes dans un contexte similaire à la clinique, c'est-à-dire sur un biofilm débridé.

Nous avons donc évalué l'efficacité de différents antibiotiques (plusieurs concentrations testées) habituellement prescrits contre les infections à *S. aureus* et *P. aeruginosa* isolées depuis des plaies chroniques. Cette étude a permis de mettre en évidence que :

- L'oxacilline, le linézolide et la ceftazidime étaient efficaces contre un biofilm préformé et débridé.
- La vancomycine et l'imipénème étaient, quant à eux inefficaces, même à des concentrations élevées (100x CMI).
- Fait intéressant, si l'action des deux antibiotiques (imipénème et ceftazidime) utilisés contre *P. aeruginosa* ne semble pas être influencés par le milieu de culture testé, une différence significative est observée avec les antibiotiques utilisés contre *S. aureus*. En effet, la vancomycine, le linézolide et l'oxacilline présentent une capacité limitée à diminuer le biofilm monomicrobien lorsque les bactéries sont cultivées dans un milieu stressant tel le CWM. Cette observation est intéressante et pourrait expliquer les difficultés rencontrées dans l'évaluation de l'efficacité de nouvelle thérapeutique anti-biofilm qui peuvent présenter une activité modérée *in vivo* alors que les résultats *in vitro* en milieu de culture classique étaient encourageants.
- Ces résultats semblent en accords avec des data récemment publiées. Plusieurs études ont mis en évidence une **inefficacité de l'imipénème** aux concentrations sub-inhibitrices et CMI pour réduire la biomasse bactériologique dans le biofilm. Les auteurs ont montré que l'utilisation de l'imipénème favorisait même la maturation et l'augmentation de la biomasse bactérienne dans les biofilms à partir d'isolats cliniques de mucoviscidose ^{196, 197}. En ce qui concerne l'effet de la ceftazidime, certaines études sont corrélées avec les conclusions présentées dans ces recherches. Otani et al. ¹⁹⁸ ont noté **l'efficacité de la ceftazidime** pour réduire le biofilm de PAO1, même à des concentrations sous-CMI. L'efficacité de la ceftazidime a également été démontrée dans un modèle *in vivo* de stent urétéral en association avec l'azythromycine ¹⁹⁹. Cet

antibiotique semble donc présenter un potentiel antibiofilm. Toutefois, l'utilisation à long terme de la ceftazidime pourrait entraîner une augmentation de résistance dans la population planctonique mais également sessile^{200, 201}. En ce qui concerne *S. aureus*, l'effet de la vancomycine en tant que potentiel antibiofilm a déjà été décrit. La vancomycine à une concentration de 1x la CMI n'est pas capable de réduire la densité bactérienne dans le biofilm²⁰². À des concentrations sub-inhibitrices, la vancomycine augmenterait même la formation de biofilm mature²⁰³. Certaines études ont mis en évidence un effet de la vancomycine sur les bactéries sessiles. Cependant, les concentrations utilisées étaient particulièrement élevées (120x MIC) et prolongées dans le temps. Peu de données sur l'utilisation de l'oxacilline sur le biofilm sont publiées à ce jour. Mirani et *al.*²⁰⁴ ont démontré une influence de cet antibiotique sur les souches de référence de *S. aureus*. Le mécanisme pourrait être dû à la modulation de l'expression de *icaA* et du régulateur *agr*, deux gènes majeurs de la formation du biofilm. **L'efficacité de l'oxacilline** sur le biofilm mature a été confirmée par Manner et *al.*²⁰⁵. Enfin, en ce qui concerne le linézolide, des publications ont rapporté que cet antibiotique utilisé seul était inefficace pour réduire le biofilm de *S. aureus*²⁰⁶ notamment dans les infections ostéoarticulaires²⁰⁷. Seuls Gander et *al.*²⁰⁸ ont observé un effet de 1x la CMI sur un biofilm en cours de formation. Ces données renforcent donc la nécessité d'utiliser des milieux de culture mais également des techniques plus fiables et mimant la clinique pour évaluer l'efficacité des agents antimicrobiens et leurs risques potentiels.

Au cours de la formation de biofilm, il est maintenant démontré que les cellules sessiles acquièrent des caractéristiques physiologiques différentes de celles des cellules planctoniques. Les modifications concernent, entre autres, la production d'EPS, la croissance bactérienne, l'expression de certains gènes, en particulier ceux régulant l'adhésion cellulaire et la formation de biofilm, ou encore la résistance aux agents désinfectants et aux antibiotiques²⁰⁹. Parmi les étapes importantes du

développement du biofilm, le **détachement cellulaire** ^{52, 210} est un élément central pour permettre la colonisation de nouvelles surfaces ^{211,212}. Néanmoins, peu de travaux ont été menés pour élucider cette étape clef du détachement. Certaines études se sont focalisées sur des mécanismes utilisant une approche moléculaire, mais très peu de recherches ont été menées pour étudier **la physiologie des cellules libérées** depuis le biofilm ²¹³⁻²¹⁵. La majorité des études sur les biofilms se sont concentrées sur les mécanismes d'adhésion bactérienne et les changements de comportement survenant lors du passage de l'état planctonique à l'état de biofilm ⁹⁶. Toutefois, il nous semblait fondamental de mener une étude aussi bien sur les cellules planctoniques initiales et sessiles que sur les cellules détachées et libérées du biofilm pour élucider le risque potentiel de recontamination et optimiser les procédures de prise en charge thérapeutique. Nous avons cherché à étudier les caractéristiques phénotypiques des cellules détachées du biofilm et les comparer avec leurs homologues sessiles et planctoniques initiales.

Nous avons, donc dans un premier temps, adapté un protocole pour pouvoir isoler, à partir des expériences réalisées dans le Bioflux TM 200, les bactéries sessiles mais également les bactéries libérées du biofilm. Nous avons par la suite comparé ces 3 populations bactériennes en décrivant des caractéristiques phénotypiques, de croissance, d'adhésion et d'expression de certains gènes impliqués dans la formation du biofilm.

Les résultats de cette étude ont mis en avant que :

- Les bactéries libérées du biofilm de *S. aureus* et *P. aeruginosa* présentaient des **croissances intermédiaires** par rapport aux cellules planctoniques initiales et aux bactéries sessiles. Les plateaux de croissance étaient plus importants que ceux des bactéries sessiles mais significativement moins importants que celui retrouvé lorsque la bactérie n'est pas passée par un cycle de vie en biofilm.
- Ces différences de croissance étaient d'autant plus importantes quand les bactéries étaient cultivées en milieu stressant et mimant l'environnement plaie chronique que dans un milieu classique.

- Ce comportement « intermédiaire » a été confirmé en analysant les capacités d'adhésion et de formation de biofilm des diverses bactéries. Peu importe l'espèce étudiée, les bactéries sessiles sont capables de **ré adhérer** très rapidement à une surface. Cette capacité à adhérer très rapidement est également présente chez les bactéries libérées du biofilm. Encore une fois, ces différences notables sont accentuées par le milieu dans lequel les bactéries sont cultivées.
- L'expression de gènes importants dans la régulation du biofilm bactérien tel que *fnbpA* ou *agrA* pour les souches de *S. aureus* était aussi impactée par les différentes populations. *fnbpA* était **surexprimé** chez les bactéries sessiles, à l'inverse d'*agrA*, qui lui était surexprimé dans la population initiale. A noter, le profil d'expression dit « intermédiaire » de ces gènes chez les bactéries libérées du biofilm.

Pour les souches de *P. aeruginosa* nous avons mis en avant que tous les gènes impliqués dans la synthèse des exopolysaccharides ; *pel*, *psl* et *algR*, mais également les gènes régulant le QS ; *rhlI*, *lasI* et *pqsH*, étaient exprimés de manière significativement **plus importante** dans les cellules sessiles par rapport aux cellules planctoniques initiales et libérées du biofilm. La différence d'expression entre cellules initiales et détachées était également notable.

Les bactéries sessiles présentent un phénotype distinct de celui de leurs homologues planctoniques. La technique et les protocoles développés dans ce travail afin de collecter les cellules sessiles et libérées du biofilm et de les cultiver en conditions stressantes pourraient constituer un nouvel outil reproductible pour étudier les caractéristiques des biofilms bactériens. En ce qui concerne la cinétique de croissance, les cellules sessiles et détachées semblent être dans un état physiologique différent de celui des cellules originelles. Les phases de latence observées chez les bactéries sessiles et libérées du biofilm suggèrent qu'elles ont besoin d'une **période d'adaptation** pour revenir à la croissance planctonique. Ces résultats confirment que les bactéries sessiles et planctoniques présentent des caractères différents ²¹⁶. Ils sont en accord avec les résultats publiés ^{217, 218} montrant

que la limitation de la diffusion de l'oxygène et des nutriments dans les biofilms altère les taux de croissance bactérienne. Ils indiquent également que les cellules détachées sont moins aptes à revenir au mode planctonique. La capacité à ré-adhérer à des surfaces et reformer un biofilm a aussi prouvé que les bactéries sessiles et libérées étaient capables de présenter une adhésion plus rapide, autour de 2 heures avant les bactéries initiales. Ces données d'adhésion sont confirmées par d'autres publications chez *P. aeruginosa*²¹⁸ ou chez *Klebsiella pneumoniae*²¹⁹. Ces résultats pourraient être expliqués par les **changements des propriétés physico-chimiques** des cellules issues du biofilm qui leur confèreraient une adhésion facilitée aux différents supports. Des études ont démontré des différences d'hydrophobie²²⁰ ou d'affinité pour les solvants apolaires^{221, 222}. Enfin, concernant l'expression génique mesurée chez les diverses populations, deux hypothèses sont à l'heure actuelle envisagées. La première soutient que les bactéries libérées possèdent des caractéristiques très proches des bactéries sessiles **temporairement** jusqu'à retrouver progressivement un phénotype planctonique^{223, 224}. La seconde hypothèse met en avant les cellules libérées du biofilm comme réelle population isolée²²⁵.

Nos résultats démontrent donc que les cellules détachées du biofilm sont distinctes des cellules cultivées initialement et des cellules sessiles. Les changements de comportement survenus lors de l'attachement bactérien semblent conservés après la dispersion. Ces conclusions montrent que les cellules détachées du biofilm représentent également un risque élevé de recolonisation du lit de la plaie chez le patient. Il serait maintenant intéressant de comparer la virulence ainsi que la sensibilité aux agents infectieux des trois populations.

Après avoir étudié la formation de biofilms de souches bactériennes isolées, la recherche s'est progressivement tournée vers l'étude de la **complexité et des interactions dans les biofilms multi-espèces**^{226, 227}. Les observations convergent vers la découverte que les bactéries résidant dans les biofilms mixtes s'organisent de manière particulière dans l'espace en réponse aux interactions inter-espèces^{135,227, 228}. Les interactions métaboliques, conduisant à la coopération ou la compétition, sont omniprésentes dans les biofilms polymicrobiens et jouent un rôle important dans le maintien de la diversité et de la stabilité des communautés microbiennes^{229- 231}. En général, dans les environnements structurés tel que le biofilm, une coexistence des

espèces bactériennes est privilégiée grâce à des interactions bénéfiques telles que le co-métabolisme et les interactions coordonnées^{232, 233} comme l'a prouvé Harrison en ce qui concerne la virulence bactérienne²³⁴. Toutefois, ces dernières années nombres d'études ont permis de mettre en évidence que ces liens étroits ne sont pas toujours en faveur de l'infection^{132, 133, 134, 235}. Investiguer les mécanismes de coopération et d'inhibition qui régissent les biofilms bactériens des plaies chroniques passe en partie par la compréhension de **l'organisation spatiale** des espèces.

Nous avons donc initié, en se basant sur notre technique permettant la combinaison du BiofluxTM 200 et du milieu « plaie chronique », une étude permettant **la visualisation en 3 dimensions** des espèces bactériennes à l'intérieur d'un biofilm mature mixte composé de *S. aureus* et *P. aeruginosa*. Pour réaliser ceci, nous avons premièrement modifié nos souches cliniques de *S. aureus* et *P. aeruginosa* afin d'y intégrer un plasmide vecteur de **fluorescence**. Ensuite, nous avons élaboré un protocole permettant d'utiliser des plaques à fond amovible pour visualiser en microscopie confocale l'organisation des différentes espèces bactériennes dans le biofilm mature.

Nos résultats sont encourageants et semblent démontrer qu'au sein du biofilm polymicrobien, *S. aureus* et *P. aeruginosa* ne sont pas organisés de manière aléatoire. Grâce à la microscopie confocale et à la fluorescence, nous observons que ***P. aeruginosa* est situé plus en profondeur** que *S. aureus*. En effet, lorsque les bactéries sont localisées à un même endroit, *S. aureus* est positionnée au-dessus de *P. aeruginosa* qui forme la première couche d'adhésion contre le support. Cette observation avait déjà pu être matérialisée *in vitro* en étudiant des biofilms mixtes Pseudomonas/Staphylocoque de plaies chroniques²³⁶. La capacité de *P. aeruginosa* à migrer via ses pili de type IV et le flagelle dans les biofilms²³⁷⁻²³⁸ peut expliquer la présence de ces bactéries dans les régions plus profondes des plaies chroniques.

Nous souhaitons en perspective améliorer cette technique de visualisation en 3 dimensions mais également pourvoir étudier, via l'outil de microscopie confocale, d'autres paramètres. A l'heure actuelle nous sommes en train d'analyser l'effet sur chaque espèce bactérienne du débridement automatique que nous avons développé mais également de l'utilisation des antibiotiques. Cet outil semble réellement

prometteur pour comprendre les interactions entre espèces bactériennes mais aussi pour interpréter l'efficacité de nouvelles approches thérapeutiques.

Conclusion & Perspectives

Les travaux de recherche menés lors de cette thèse sont le reflet d'un partenariat abouti entre la société Biofilm Pharma, l'unité Inserm U1047 « Virulence bactérienne et infections chroniques » et le Centre Hospitalo-Universitaire de Nîmes. La force de cette collaboration a été le moteur du développement d'un nouveau milieu de culture mimant l'environnement rencontré au sein des plaies chroniques. Ce milieu a permis d'étudier le lien entre facteurs environnants et capacité des souches de *S. aureus* et *P. aeruginosa* à former du biofilm mais également à moduler l'expression de gènes impliqués dans la régulation et la formation dudit biofilm, à croître ou encore à être virulentes. Nous avons également confirmé l'importance des coopérations bactériennes en évaluant l'effet de l'association de *S. aureus* et *P. aeruginosa* sur divers paramètres tels que la virulence, la croissance, l'adhésion précoce, la formation de biofilm. Enfin nous avons pu décrire une méthode de quantification et de visualisation du biofilm polymicrobien permettant également de tester sur un biofilm préformé et débridé l'efficacité antibiofilm de nouvelles molécules thérapeutiques.

Ces recherches posent donc les bases de modèles *in vitro* innovants permettant d'améliorer nos connaissances sur la physiopathologie des plaies chroniques qui pourraient, *in fine*, faire progresser la prise en charge des patients. Toutefois, il est possible d'aller plus loin dans l'utilisation des modèles.

Dans notre étude, les tests ont été réalisés sur seulement 3 couples cliniques de *S. aureus* et *P. aeruginosa* et deux souches de références. Il semble donc, en premier lieu, important de confirmer les data obtenues en augmentant **le nombre de couples cliniques** et en prenant également en compte **le grade d'infection** des plaies chroniques sur lesquelles sont isolées les souches.

Une des optimisations pertinentes est de pouvoir adapter le CWM de base créée lors de cette thèse à certaines plaies chroniques particulières. Aussi, dans le cadre des infections du pied chez le patient diabétique, des études ont mis en avant la présence de glucose ou d'antibiotiques dans l'environnement des plaies. La

composition du CWM peut donc être complétée avec les composants précédemment cités pour mimer ces infections spécifiques.

Des **études transcriptomiques** plus complètes telles que le RNAseq devraient être réalisées sur les souches cultivées seules et/ou association dans le milieu contrôle versus le CWM pour visualiser l'effet du milieu « plaie chronique » mais également celui de la coopération des deux bactéries sur leurs génomes respectifs. De plus, la colonisation des plaies chroniques par le couple *S. aureus* / *P. aeruginosa* est fréquente mais il existe également **d'autres coopérations bactériennes** mises en évidence par des études métagénomiques. Il serait, par conséquent, intéressant de tester d'autres interactions bactériennes telles que *S. aureus* / *S. epidermidis* ; *S. aureus* / *E. coli* etc...

Enfin, le nombre de molécules décrites ayant une valeur ajoutée antibiofilm ne cesse d'augmenter. De nombreux projets cherchent, au travers du criblage à haut débit, à développer de nouvelles molécules permettant la prévention de la formation ou la dispersion du biofilm bactérien. Dans ce contexte, il sera certainement important de tester l'efficacité de ces nouvelles molécules « antibiofilm » dans des conditions de formation de biofilm similaires à ce que l'on retrouve au niveau du lit de la plaie chez le patient. Il est donc important de posséder de nouvelles techniques reproductibles permettant de rendre compte aussi bien de l'activité préventive que curative de ce potentiel arsenal thérapeutique. Le CWM couplé aux protocoles développés et optimisés au cours de cette thèse et appliqués au Bioflux™ 200, représente un ensemble technologique pouvant répondre aux besoins futurs dans la détermination de nouvelles ressources contre les biofilms polymicrobiens. Des études menées au sein de notre laboratoire se concentrent actuellement sur l'évaluation d'autres **antibiotiques** (utilisés seuls ou en association) couramment prescrits en clinique, ainsi que sur l'évaluation de certains **antiseptiques** qui pourraient être utilisés dans la prévention et la dispersion du biofilm mature. Enfin, le partenaire industriel BioFilm Pharma, dont un des volets de recherche consiste à développer de **nouvelles molécules dit « hit » à valeur ajoutée antibiofilm**, devrait prochainement tester, à l'aide des modèles développés durant cette thèse, plusieurs « hits » thérapeutiques prometteurs.

RÉFÉRENCES BIBLIOGRAPHIQUES

1. Gonzalez AC, Costa TF, Andrade ZA, Medrado AR. Wound healing - A literature review. *An Bras Dermatol*. 2016;91(5):614-620
2. Velnar T, Bailey T, Smrkolj V. The wound healing process: an overview of the cellular and molecular mechanisms. *The Journal of International Medical Research*. 2009; 37:1528-1542
3. Frykberg RG, Banks J. Challenges in the Treatment of Chronic Wounds. *Adv Wound Care (New Rochelle)*. 2015;4(9):560-582
4. Agrawal K, Chauhan N. Pressure ulcers: Back to the basics. *Indian J Plast Surg*. 2012;45(2):244-254
5. Agale SV. Chronic Leg Ulcers: Epidemiology, Aetiopathogenesis and Management. *Ulcers*, vol. 2013 ID 413604, 9 pages
6. Jeffcoate WJ, Harding KG. Diabetic foot ulcers. *Lancet*. 2003 May 3;361(9368):1545-51
7. Järbrink K, Ni G, Sönnergren H, et al. Prevalence and incidence of chronic wounds and related complications: a protocol for a systematic review. *Syst Rev*. 2016;5(1):152
8. P. G. Bowler, B. I. Duerden, D. G. Armstrong. Wound Microbiology and Associated Approaches to Wound Management. *Clinical Microbiology Reviews* Apr 2001, 14 (2) 244-269
9. Edwards, Ruth; Harding, Keith G Bacteria and wound healing, *Current Opinion in Infectious Diseases*: April 2004 - Volume 17 - Issue 2 - p 91-96
10. Assurance Maladie, chiffre 2018. <https://WWW.ameli.fr>
11. Sen CK, Gordillo GM, Roy S, et al. Human skin wounds: a major and snowballing threat to public health and the economy. *Wound Repair Regen*. 2009;17(6):763-771
12. Cutting KF. Wound exudate: composition and functions. *Br J Community Nurs*. 2003;8(9 Suppl):suppl 4-9
13. Hunt TK, Hopf HW. WOUND HEALING AND WOUND INFECTION: What Surgeons and Anesthesiologists Can Do. *Surg Clin North Am*. 1 juin 1997;77(3):587- 606.

14. Ikeda T, Tayefeh F, Sessler DI, Kurz A, Plattner O, Petschnigg B, et al. Local Radiant Heating Increases Subcutaneous Oxygen Tension. *Am J Surg*. 1 janv 1998;175(1):33- 7.
15. Gethin GT, Cowman S, Conroy RM. The impact of Manuka honey dressings on the surface pH of chronic wounds. *Int Wound J*. 2008 Jun;5(2):185-94. Retraction in: *Int Wound J*. 2014 Jun;11(3):342.
16. Percival S, Mccarty S & Woods E. The effects of pH on wound healing, biofilms, and antimicrobial efficacy. *Wound repair and regeneration: official publication of the Wound Healing Society and the European Tissue Repair Society*. 22
17. American Diabetes Association. Diagnosis and classification of diabetes mellitus. *Diabetes Care*. 2009;32 Suppl 1(Suppl 1):S62-S67
18. Atlas 2019 de l'international Diabetes Federation. Diabetesatlas.org
19. Centre européen d'étude du diabète. <http://ceed-diabetes.org>
20. Deshpande AD, Harris-Hayes M, Schootman M. Epidemiology of diabetes and diabetes-related complications. *Phys Ther*. 2008;88(11):1254-1264
21. American Diabetes Association. Standards of medical care for patients with diabetes mellitus. *Diabetes Care*. 2003 Jan;26 Suppl 1:S33-50
22. Chawla A, Chawla R, Jaggi S. Microvascular and macrovascular complications in diabetes mellitus: Distinct or continuum?. *Indian J Endocrinol Metab*. 2016;20(4):546-551
23. Eneroth M, Larsson J, Apelqvist J. Deep foot infections in patients with diabetes and foot ulcer: an entity with different characteristics, treatments, and prognosis. *J Diabetes Complications*. 1999 Sep-Dec;13(5-6):254-63
24. Pendsey SP. Understanding diabetic foot. *Int J Diabetes Dev Ctries*. 2010;30(2):75-79
25. Yazdanpanah L, Nasiri M, Adarvishi S. Literature review on the management of diabetic foot ulcer. *World J Diabetes*. 2015;6(1):37-53
26. Uçkay I, Gariani K, Pataky Z, Lipsky BA. Diabetic foot infections: state-of-the-art. *Diabetes Obes Metab*. 2014 Apr;16(4):305-16
27. Armstrong DG, Fisher TK, Lepow B, et al. Pathophysiology and Principles of Management of the Diabetic Foot. *Mechanisms of Vascular Disease: A Reference Book for Vascular Specialists*. Adelaide (AU): University of Adelaide Press; 2011. 26
28. Vinik A, Casellini C, Nevoret ML. Diabetic Neuropathies. *Endotext*. 2018

29. Cade WT. Diabetes-related microvascular and macrovascular diseases in the physical therapy setting. *Phys Ther.* 2008;88(11):1322-1335
30. Turina M, Fry DE, Polk HC Jr. Acute hyperglycemia and the innate immune system: clinical, cellular, and molecular aspects. *Crit Care Med.* 2005 Jul;33(7):1624-33.
31. Al-Rubeaan K, Al Derwish M, Ouizi S, et al. Diabetic foot complications and their risk factors from a large retrospective cohort study. *PLoS One.* 2015;10(5):e0124446.
32. Richard JL, Sotto A, Lavigne JP. New insights in diabetic foot infection. *World J Diabetes.* 2011;2(2):24-32.
33. James, G.A., Swogger, E., Wolcott, R., Pulcini, E.d., Secor, P., Sestrich, J., Costerton, J.W. and Stewart, P.S. (2008), Biofilms in chronic wounds. *Wound Repair and Regeneration*, 16: 37-44.
34. Jamal, M., Ahmad, W., Andleeb, S., Jalil, F., Imran, M., Nawaz, M.A., et al. Bacterial biofilm and associated infections. *J Chin Med Assoc* **2018**, 81, 7-11
35. Metcalf DG, Bowler PG. Biofilm delays wound healing: A review of the evidence. *Burns Trauma.* 2013 Jun 18;1(1):5-12.
36. Grice EA, Segre JA. The skin microbiome. *Nat Rev Microbiol.* 2011;9(4):244-253.
37. Kalan LR, Meisel JS, Loesche MA, et al. Strain- and Species-Level Variation in the Microbiome of Diabetic Wounds Is Associated with Clinical Outcomes and Therapeutic Efficacy. *Cell Host Microbe.* 2019;25(5):641-655.e5
38. Citron DM, Goldstein EJ, Merriam CV, Lipsky BA, Abramson MA. Bacteriology of moderate-to-severe diabetic foot infections and in vitro activity of antimicrobial agents. *J Clin Microbiol.* 2007;45(9):2819-2828.
39. Dunyach-Remy C, Ngba Essebe C, Sotto A, Lavigne JP. *Staphylococcus aureus* Toxins and Diabetic Foot Ulcers: Role in Pathogenesis and Interest in Diagnosis. *Toxins (Basel).* 2016;8(7):209.
40. Radzieta, M., Sadeghpour-Heravi, F., Peters, T.J. *et al.* A multiomics approach to identify host-microbe alterations associated with infection severity in diabetic foot infections: a pilot study. *npj Biofilms Microbiomes* 7, 29 (2021)
41. Sadeghpour Heravi F, Zakrzewski M, Vickery K, G Armstrong D, Hu H. Bacterial Diversity of Diabetic Foot Ulcers: Current Status and Future Prospectives. *J Clin Med.* 2019;8(11):1935. d
42. Bassetti M, Vena A, Croxatto A, Righi E, Guery B. How to manage *Pseudomonas aeruginosa* infections. *Drugs Context.* 2018;7:212527.

43. Jneid J, Lavigne JP, La Scola B, Cassir N. The diabetic foot microbiota : A review. *Hum Mibrobiome J.* 2017. Volume 5-6:1-6.
44. Choi, Y., Banerjee, A., McNish, S. *et al.* Co-occurrence of Anaerobes in Human Chronic Wounds. *Microb Ecol* **77**, 808–820 (2019).
45. Guo S, Dipietro LA. Factors affecting wound healing. *J Dent Res.* 2010 Mar;89(3):219-29.
46. Costerton JW, Geesey GG, Cheng KJ. How bacteria stick. *Sci. Am.* 1978;238(1):86–95
47. Westall F, de Wit MJ, Dann J, Van der Gaast S, de Ronde CEJ, Gerneke D. Early Archean fossil bacteria and biofilms in hydrothermally-influenced sediments from the Barberton greenstone belt, South Africa. *Precambrian Res.* 2001;106(1–2):93–116
48. Porter JR. Antony van Leeuwenhoek: tercentenary of his discovery of bacteria. *Bacteriol Rev.* 1976;40(2):260–269
49. J W Costerton, R T Irvin, Cheng and KJ. The Bacterial Glycocalyx in Nature and Disease. *Annu Rev Microbiol.* 1981;35(1):299–324
50. Potera C. Forging a link between biofilms and disease. *Science* 1999;283(5409):1837, 1839
51. Arciola CR, Campoccia D, Ehrlich GD, Montanaro L. Biofilm-Based Implant Infections in Orthopaedics. *Advances in Experimental Medicine and Biology.* Springer International Publishing; 2015:29–46. 107
52. Donlan RM. Biofilms: microbial life on surfaces. *Emerg. Infect Dis.* 2002;8(9):881–890
53. Trautner BW, Darouiche RO. Role of biofilm in catheter-associated urinary tract infection. *Am J Infect Control* 2004;32(3):177–183
54. Costerton JW. Cystic fibrosis pathogenesis and the role of biofilms in persistent infection. *Trends Microbiol.* 2001;9(2):50–52
55. Hall-Stoodley L, Costerton JW, Stoodley P. Bacterial biofilms: from the Natural environment to infectious diseases. *Nat Rev Microbiol.* 2004;2(2):95–108
56. Hojo K, Nagaoka S, Ohshima T, Maeda N. Bacterial Interactions in Dental Biofilm Development. *J Dent Res.* 2009;88(11):982–990
57. Lebeaux D, Ghigo JM, Beloin C. Biofilm-related infections: bridging the gap between clinical management and fundamental aspects of recalcitrance toward antibiotics. *Microbiol Mol Biol Rev.* 2014;78(3):510-543.

58. Pouget C, Dunyach-Remy C, Pantel A, Schuldiner S, Sotto A, Lavigne JP. Biofilms in Diabetic Foot Ulcers: Significance and Clinical Relevance. *Microorganisms*. 2020 Oct 14;8(10):1580.
59. Rijnaarts HH, Nord W, Bouwer A, Lyklema J, Zehnder AJ. Reversibility and Mechanism of Bacterial Adhesion. *Colloids Surf B Biointerface*. 1995;4:5–22
60. Gross M, Cramton SE, Götz F, Peschel A. Key role of teichoic acid net charge in *Staphylococcus aureus* colonization of artificial surfaces. *Infect Immun*. 2001;69(5):3423– 3426
61. Whitchurch CB, Tolker-Nielsen T, Ragas PC, Mattick JS. Extracellular DNA Required for Bacterial Biofilm Formation. *Science*. 2002;295(5559):1487–1487
62. Foster TJ, Geoghegan JA, Ganesh VK, Höök M. Adhesion, invasion and evasion: the many functions of the surface proteins of *Staphylococcus aureus*. *Nat Rev Microbiol*. 2014;12(1):49–62
63. Mcdevitt D, Nanavaty T, House-Pompeo K, Bell E, Turner N, Mcintire L, Foster T, Höök M. Characterization of the Interaction Between the *Staphylococcus Aureus* Clumping Factor (ClfA) and Fibrinogen. *Eur J Biochem*. 1997;247(1):416–424
64. Greene C, McDevitt D, Francois P, Vaudaux P e., Lew D p., Poster T j. Adhesion properties of mutants of *Staphylococcus aureus* defective in fibronectin-binding proteins and studies on the expression of fnb genes. *Mol Microbiol*. 1995;17(6):1143–1152
65. Hudson MC, Ramp WK, Frankenburg KP. *Staphylococcus aureus* adhesion to bone matrix and bone-associated biomaterials. *FEMS Microbiol Lett*. 1999 ;173(2):279–284
66. Colvin KM, Irie Y, Tart CS, et al. The Pel and Psl polysaccharides provide *Pseudomonas aeruginosa* structural redundancy within the biofilm matrix. *Environ Microbiol*. 2012;14(8):1913-1928
67. Carniello V, Peterson BW, van der Mei HC, Busscher HJ. Physico-chemistry from initial bacterial adhesion to surface-programmed biofilm growth. *Adv Colloid Interface Sci*. 2018 Nov;261:1-14
68. Czaczyk K, Myszka K. Biosynthesis of Extracellular Polymeric Substances and Its Role in Microbial Biofilm Formation. *Polish J of Environ Stud*. Vol 16, No. 6 (2007), 799-806
69. Limoli DH, Jones CJ, Wozniak DJ. Bacterial Extracellular Polysaccharides in Biofilm Formation and Function. *Microbiol Spectr*. 2015;3(3):10. 2014
70. Hibbing M.E., Fuqua C., Parsek M.R., Peterson S.B. Bacterial competition: Surviving and thriving in the microbial jungle. *Nat. Rev. Microbiol*. 2010;8:15–25

71. Rutherford S.T., Bassler B.L. Bacterial quorum sensing: Its role in virulence and possibilities for its control. *Cold Spring Harb Perspect Med.* 2012;2:a012427
72. Papenfort K, Bassler BL. Quorum sensing signal-response systems in Gram-negative bacteria. *Nat Rev Microbiol.* 2016;14(9):576-588
73. Kimihiro Abe, Nobuhiko Nomura, Satoru Suzuki, Biofilms: hot spots of horizontal gene transfer (HGT) in aquatic environments, with a focus on a new HGT mechanism, *FEMS Microbiology Ecology*, Volume 96, Issue 5, May 2020
74. Rumbaugh, K.P., Sauer, K. Biofilm dispersion. *Nat Rev Microbiol* 18, 571–586 (2020)
75. McDougald D, Rice SA, Barraud N, Steinberg PD, Kjelleberg S. Should we stay or should we go: mechanisms and ecological consequences for biofilm dispersal. *Nat Rev Microbiol.* 2012;10(1):39–50
76. Kaplan JB. Biofilm dispersal: mechanisms, clinical implications, and potential therapeutic uses. *J Dent Res.* 2010;89(3):205-218
77. Peschel A, Otto M. Phenol-soluble modulins and staphylococcal infection. *Nat Rev Microbiol.* 2013;11(10):667–673
78. Basu Roy A, Sauer K. Diguanylate cyclase NicD-based signalling mechanism of nutrient-induced dispersion by *Pseudomonas aeruginosa*. *Mol Microbiol.* 2014 Nov;94(4):771-93
79. Morgan R, Kohn S, Hwang SH, Hassett DJ, Sauer K. BdlA, a chemotaxis regulator essential for biofilm dispersion in *Pseudomonas aeruginosa*. *J Bacteriol.* 2006 Nov;188(21):7335-43
80. Petrova OE, Cherny KE, Sauer K. The diguanylate cyclase GcbA facilitates *Pseudomonas aeruginosa* biofilm dispersion by activating BdlA. *J Bacteriol.* 2015 Jan 1;197(1):174-87
81. McSwain BS, Irvine RL, Hausner M, Wilderer PA. Composition and distribution of extracellular polymeric substances in aerobic flocs and granular sludge. *Appl Environ Microbiol.* 2005;71(2):1051-1057
82. Vu B, Chen M, Crawford RJ, Ivanova EP. Bacterial extracellular polysaccharides involved in biofilm formation. *Molecules.* 2009;14(7):2535-2554
83. Chang WS, van de Mortel M, Nielsen L, Nino de Guzman G, Li X, Halverson LJ. Alginate production by *Pseudomonas putida* creates a hydrated microenvironment and contributes to biofilm architecture and stress tolerance under water-limiting conditions. *J Bacteriol.* 2007 Nov;189(22):8290-9

84. Lee KY, Mooney DJ. Alginate: properties and biomedical applications. *Prog Polym Sci.* 2012;37(1):106-126
85. Wu W, Badrane H, Arora S, Baker HV, Jin S. MucA-mediated coordination of type III secretion and alginate synthesis in *Pseudomonas aeruginosa*. *J Bacteriol.* 2004;186(22):7575-7585
86. Ma L, Lu H, Sprinkle A, Parsek MR, Wozniak DJ. *Pseudomonas aeruginosa* Psl is a galactose- and mannose-rich exopolysaccharide. *J Bacteriol.* 2007 Nov;189(22):8353-6
87. Ryder C, Byrd M, Wozniak DJ. Role of polysaccharides in *Pseudomonas aeruginosa* biofilm development. *Curr Opin Microbiol.* 2007;10(6):644-648
88. Franklin MJ, Nivens DE, Weadge JT, Howell PL. Biosynthesis of the *Pseudomonas aeruginosa* Extracellular Polysaccharides, Alginate, Pel, and Psl. *Front Microbiol.*
89. Rohde H, Frankenberger S, Zähringer U, Mack D. Structure, function and contribution of polysaccharide intercellular adhesin (PIA) to *Staphylococcus epidermidis* biofilm formation and pathogenesis of biomaterial-associated infections. *Eur J Cell Biol.* 2010 Jan;89(1):103-11
90. Ghadban, A. & Albertin Luca. 2013. Synthesis of glycopolymer architectures by reversible-deactivation radical polymerization. *Polymers.* 5, 431 - 526.
91. Fluckiger U, Ulrich M, Steinhuber A, Döring G, Mack D, Landmann R, Goerke C, Wolz C. Biofilm formation, icaADBC transcription, and polysaccharide intercellular adhesin synthesis by staphylococci in a device-related infection model. *Infect Immun.* 2005;73(3):1811–1819
92. Chavakis T, Wiechmann K, Preissner KT, Herrmann M. *Staphylococcus aureus* interactions with the endothelium: the role of bacterial “secretable expanded repertoire adhesive molecules” (SERAM) in disturbing host defense systems. *Thromb Haemost.* 2005;94(2):278– 285
93. Paharik AE, Horswill AR. The Staphylococcal Biofilm: Adhesins, Regulation, and Host Response. *Microbiol Spectr.* 2016;4(2):10.1128
94. Huseby MJ, Kruse AC, Digre J, Kohler PL, Vocke JA, Mann EE, Bayles KW, Bohach GA, Schlievert PM, Ohlendorf DH, Earhart CA. Beta toxin catalyzes formation of nucleoprotein matrix in staphylococcal biofilms. *Proc Natl Acad Sci.* 2010;107(32):14407–14412
95. Caiazza NC, O’Toole GA. Alpha-Toxin Is Required for Biofilm Formation by *Staphylococcus aureus*. *J Bacteriol.* 2003;185(10):3214–3217
96. O’Toole GA, Gibbs KA, Hager PW, Phibbs PV Jr, Kolter R. The global carbon metabolism regulator Crc is a component of a signal transduction pathway

- required for biofilm development by *Pseudomonas aeruginosa*. *J Bacteriol*. 2000;182(2):425-431
97. Chatterjee A, Cui Y, Yang H, Collmer A, Alfano JR, Chatterjee AK. GacA, the response regulator of a two-component system, acts as a master regulator in *Pseudomonas syringae* pv. tomato DC3000 by controlling regulatory RNA, transcriptional activators, and alternate sigma factors. *Mol Plant Microbe Interact*. 2003 Dec;16(12):1106-17
98. Hall S, McDermott C, Anoopkumar-Dukie S, et al. Cellular Effects of Pyocyanin, a Secreted Virulence Factor of *Pseudomonas aeruginosa*. *Toxins (Basel)*. 2016;8(8):236
99. Clarke SR, Wiltshire MD, Foster SJ. IsdA of *Staphylococcus aureus* is a broad spectrum, ironregulated adhesin. *Mol Microbiol*. 2004;51(5):1509–1519
100. Merino N, Toledo-Arana A, Vergara-Irigaray M, Valle J, Solano C, Calvo E, Lopez JA, Foster TJ, Penadés JR, Lasa I. Protein A-Mediated Multicellular Behavior in *Staphylococcus aureus*. *J Bacteriol*. 2009;191(3):832–843
101. Roche FM, Meehan M, Foster TJ. The *Staphylococcus aureus* surface protein SasG and its homologues promote bacterial adherence to human desquamated nasal epithelial cells. *Microbiol Read Engl*. 2003;149(Pt 10):2759–2767
102. O'Toole GA, Kolter R. Flagellar and twitching motility are necessary for *Pseudomonas aeruginosa* biofilm development. *Mol Microbiol*. 1998 Oct;30(2):295-304
103. Koczan JM, Lenneman BR, McGrath MJ, Sundin GW. Cell surface attachment structures contribute to biofilm formation and xylem colonization by *Erwinia amylovora*. *Appl Environ Microbiol*. 2011;77(19):7031-7039
104. Nguyen HTT, Nguyen TH, Otto M. The staphylococcal exopolysaccharide PIA - Biosynthesis and role in biofilm formation, colonization, and infection. *Comput Struct Biotechnol J*. 2020;18:3324-3334. Published 2020 Nov 4.
105. Yarwood JM, Bartels DJ, Volper EM, Greenberg EP. Quorum sensing in *Staphylococcus aureus* biofilms. *J Bacteriol*. 2004 Mar;186(6):1838-50
106. Boles BR, Horswill AR. Agr-mediated dispersal of *Staphylococcus aureus* biofilms. *PLoS Pathog*. 2008 Apr 25;4(4):e1000052.
107. Queck SY, Jameson-Lee M, Villaruz AE, Bach TH, Khan BA, Sturdevant DE, Ricklefs SM, Li M, Otto M. RNAIII-independent target gene control by the agr quorum-sensing system: insight into the evolution of virulence regulation in *Staphylococcus aureus*. *Mol Cell*. 2008 Oct 10;32(1):150-8.

108. Trottonda MP, Manna AC, Cheung AL, Lasa I, Penadés JR. SarA positively controls bap-dependent biofilm formation in *Staphylococcus aureus*. *J Bacteriol.* 2005 Aug;187(16):5790-8.
109. Ballal A, Manna AC. Regulation of superoxide dismutase (sod) genes by SarA in *Staphylococcus aureus*. *J Bacteriol.* 2009 May;191(10):3301-10.
110. Izano EA, Amarante MA, Kher WB, Kaplan JB. Differential roles of poly-N-acetylglucosamine surface polysaccharide and extracellular DNA in *Staphylococcus aureus* and *Staphylococcus epidermidis* biofilms. *Appl Environ Microbiol.* 2008;74(2):470–476
111. Thomas VC, Hancock LE. Suicide and fratricide in bacterial biofilms. *Int J Artif Organs.* 2009;32(9):537–544
112. Houston P, Rowe SE, Pozzi C, Waters EM, O’Gara JP. Essential role for the major autolysin in the fibronectin-binding protein-mediated *Staphylococcus aureus* biofilm phenotype. *Infect Immun.* 2011;79(3):1153–1165
113. Zhao J, Yu X, Zhu M, et al. Structural and Molecular Mechanism of CdpR Involved in Quorum-Sensing and Bacterial Virulence in *Pseudomonas aeruginosa*. *PLoS Biol.* 2016;14(4):e1002449
114. Nagler, M., Insam, H., Pietramellara, G. *et al.* Extracellular DNA in natural environments: features, relevance and applications. *Appl Microbiol Biotechnol* 102, 6343–6356 (2018)
115. Lei J, Sun L, Huang S, et al. The antimicrobial peptides and their potential clinical applications. *Am J Transl Res.* 2019;11(7):3919-3931
116. Schwartz K, Ganesan M, Payne DE, Solomon MJ, Boles BR. Extracellular DNA facilitates the formation of functional amyloids in *Staphylococcus aureus* biofilms. *Mol Microbiol.* 2016;99(1):123–134
117. Ibáñez de Aldecoa AL, Zafra O, González-Pastor JE. Mechanisms and Regulation of Extracellular DNA Release and Its Biological Roles in Microbial Communities. *Front Microbiol.* 2017;8:1390
118. Thurlow LR, Hanke ML, Fritz T, Angle A, Aldrich A, Williams SH, Engbretsen IL, Bayles KW, Horswill AR, Kielian T. *Staphylococcus aureus* Biofilms Prevent Macrophage Phagocytosis and Attenuate Inflammation In Vivo. *J Immunol.* 2011;186(11):6585–6596
119. Neut D, Tijdens-Creusen EJ, Bulstra SK, Van der Mei HC, Busscher HJ. Biofilms in chronic diabetic foot ulcers--a study of 2 cases. *Acta Orthop.* 2011;82(3):383-385

120. Machado, D., Maistrenko, O.M., Andrejev, S. *et al.* Polarization of microbial communities between competitive and cooperative metabolism. *Nat Ecol Evol* 5, 195–203 (2021)
121. Serra R, Grande R, Butrico L, Rossi A, Settimio UF, Caroleo B, Amato B, Gallelli L, de Franciscis S. Chronic wound infections: the role of *Pseudomonas aeruginosa* and *Staphylococcus aureus*. *Expert Rev Anti Infect Ther.* 2015 May;13(5):605-13
122. Yung DBY, Sircombe KJ, Pletzer D. Friends or enemies? The complicated relationship between *Pseudomonas aeruginosa* and *Staphylococcus aureus*. *Mol Microbiol.* 2021 Feb 12
123. Harrison, F., Paul, J., Massey, R. *et al.* Interspecific competition and siderophore-mediated cooperation in *Pseudomonas aeruginosa*. *ISME J* 2, 49–55 (2008)
124. Patrícia M Alves, Eida Al-Badi, Cathryn Withycombe, Paul M Jones, Kevin J Purdy, Sarah E Maddocks, Interaction between *Staphylococcus aureus* and *Pseudomonas aeruginosa* is beneficial for colonisation and pathogenicity in a mixed biofilm, *Pathogens and Disease*, Volume 76, Issue 1, February 2018
125. Orazi G, Jean-Pierre F, O'Toole GA. *Pseudomonas aeruginosa* PA14 Enhances the Efficacy of Norfloxacin against *Staphylococcus aureus* Newman Biofilms. *J Bacteriol.* 2020 Aug 25;202(18):e00159-20
126. DeLeon S, Clinton A, Fowler H, Everett J, Horswill AR, Rumbaugh KP. Synergistic interactions of *Pseudomonas aeruginosa* and *Staphylococcus aureus* in an *in vitro* wound model. *Infect Immun.* 2014;82(11):4718-4728
127. Justin R Lenhard, Nicholas M Smith, Christine D Quach, Tuan Q Nguyen, Linh H Doan, Jeanette Chau, Bacterial brothers in arms: cooperation of *Staphylococcus aureus* and *Pseudomonas aeruginosa* during antimicrobial exposure, *Journal of Antimicrobial Chemotherapy*, Volume 74, Issue 9, September 2019, Pages 2657–2665
128. Hotterbeekx A., Kumar-Singh S., Goossens H., Malhotra-Kumar S. *In vivo* and *in vitro* interactions between *Pseudomonas aeruginosa* and *Staphylococcus spp.* *Front Cell Infect. Microbiol.* 2017;7:106
129. Nguyen A.T., Oglesby-Sherrouse A.G. Interactions between *Pseudomonas aeruginosa* and *Staphylococcus aureus* during co-cultivations and polymicrobial infections. *Appl Microbiol Biotechnol.* 2016;100:6141–6148
130. Hoffman L.R., Deziel E., D'Argenio D.A., Lépine F., Emerson J., McNamara S., Gibson R.L., Ramsey B.W., Miller S.I. Selection for *Staphylococcus aureus* small-colony variants due to growth in the presence of *Pseudomonas aeruginosa*. *Proc Natl Acad Sci USA.* 2006;103:19890–19895

131. Fazli M., Bjarnsholt T., Kirketerp-Møller K., Jørgensen B., Andersen A.S., Kroghfelt K.A., Givskov M., Tolker-Nielsen T. Nonrandom distribution of *Pseudomonas aeruginosa* and *Staphylococcus aureus* in chronic wounds. *J Clin Microbiol.* 2009;47:4084–4089
132. Chan K.G., Liu Y.C., Chang C.Y. Inhibiting N-acyl-homoserine lactone synthesis and quenching *Pseudomonas* quinolone quorum sensing to attenuate virulence. *Front Microbiol.* 2015;6:1173
133. Schurr M.J. *Pseudomonas aeruginosa* alginate benefits *Staphylococcus aureus*? *J Bacteriol.* 2020;202
134. Price C.E., Brown D.G., Limoli D.H., Phelan V.V., O'Toole G.A. Exogenous alginate protects *Staphylococcus aureus* from killing by *Pseudomonas aeruginosa*. *J Bacteriol.* 2020;202
135. Dowd SE, Wolcott RD, Sun Y, McKeenan T, Smith E, Rhoads D. Polymicrobial nature of chronic diabetic foot ulcer biofilm infections determined using bacterial tag encoded FLX amplicon pyrosequencing (bTEFAP). *PLoS One.* 2008 Oct 3;3(10):e3326
136. Wolcott R, Costerton JW, Raoult D, Cutler SJ. The polymicrobial nature of biofilm infection. *Clin Microbiol Infect.* 2013 Feb;19(2):107-12
137. Mathur T, Singhal S, Khan S, Upadhyay DJ, Fatma T, Rattan A. Detection of biofilm formation among the clinical isolates of Staphylococci: an evaluation of three different screening methods. *Indian J Med Microbiol.* 2006 Jan;24(1):25-9.
138. Stepanovic S, Vukovic D, Dakic I, Savic B, Svabic-Vlahovic M. A modified microtiter-plate test for quantification of staphylococcal biofilm formation. *J Microbiol Methods.* 2000 Apr;40(2):175-9.
139. Djordjevic D, Wiedmann M, McLandsborough LA. Microtiter Plate Assay for Assessment of *Listeria monocytogenes* Biofilm Formation. *Appl Environ Microbiol.* 2002;68(6):2950–2958
140. Bjerkan G, Witsø E, Bergh K. Sonication is superior to scraping for retrieval of bacteria in biofilm on titanium and steel surfaces in vitro. *Acta Orthop.* 2009;80(2):245-250.
141. Konrat K, Schwebke I, Laue M, et al. The Bead Assay for Biofilms: A Quick, Easy and Robust Method for Testing Disinfectants. *PLoS One.* 2016;11(6):e0157663. Published 2016 Jun 17.
142. Bellifa S. (2014). Evaluation de la formation du biofilm des souches de *Klebsiella pneumoniae* isolées de dispositifs médicaux au CHU Tlemcen. Thèse de doctorat .Université abou bekr belkaid, Tlemcen

143. Ceri H, Olson ME, Stremick C, Read RR, Morck D, Buret A. The Calgary Biofilm Device: New Technology for Rapid Determination of Antibiotic Susceptibilities of Bacterial Biofilms. *J Clin Microbiol.* 1999;37(6):1771–1776
144. Chavant P, Gaillard-Martinie B, Talon R, Hébraud M, Bernardi T. A new device for rapid evaluation of biofilm formation potential by bacteria. *J Microbiol Methods.* 2007;68(3):605– 612
145. Lee HJ, Ho MR, Bhuwan M, Hsu CY, Huang MS, Peng HL, Chang HY. Enhancing ATP-based bacteria and biofilm detection by enzymatic pyrophosphate regeneration. *Anal Biochem.* 2010 Apr 15;399(2):168-73.
146. Chew SC, Kundukad B, Seviour T, Maarel JRC van der, Yang L, Rice SA, Doyle P, Kjelleberg S. Dynamic Remodeling of Microbial Biofilms by Functionally Distinct Exopolysaccharides. *mBio.* 2014;5(4):e01536-14
147. Coenye T, Nelis HJ. *In vitro* and *in vivo* model systems to study microbial biofilm formation. *J Microbiol Methods.* 2010 Nov;83(2):89-105.
148. Benoit MR, Conant CG, Ionescu-Zanetti C, Schwartz M, Matin A. New Device for HighThroughput Viability Screening of Flow Biofilms. *Appl Environ Microbiol.* 2010;76(13):4136– 4142
149. Davis SC, Ricotti C, Cazzaniga A, Welsh E, Eaglstein WH, Mertz PM. Microscopic and physiologic evidence for biofilm-associated wound colonization in vivo. *Wound Repair Regen.* 2008;16(1):23–29
150. Akiyama H, Hamada T, Huh W-K, Yamasaki O, Oono T, Fujimoto W, Iwatsuki K. Confocal laser scanning microscopic observation of glycocalyx production by *Staphylococcus aureus* in skin lesions of bullous impetigo, atopic dermatitis and pemphigus foliaceus. *Br J Dermatol.* 2003;148(3):526– 532
151. Stiefel P, Schmidt-Emrich S, Maniura-Weber K, Ren Q. Critical aspects of using bacterial cell viability assays with the fluorophores SYTO9 and propidium iodide. *BMC Microbiol.* 2015;15:36
152. Chaw KC, Manimaran M, Tay FEH. Role of Silver Ions in Destabilization of Intermolecular Adhesion Forces Measured by Atomic Force Microscopy in *Staphylococcus epidermidis* Biofilms. *Antimicrob Agents Chemother.* 2005;49(12):4853–4859
153. Begun J, Gaiani JM, Rohde H, Mack D, Calderwood SB, Ausubel FM, Sifri CD. Staphylococcal Biofilm Exopolysaccharide Protects against *Caenorhabditis elegans* Immune Defenses. *PLOS Pathog.* 2007;3(4):e57
154. Cafora, M., Deflorian, G., Forti, F. *et al.* Phage therapy against *Pseudomonas aeruginosa* infections in a cystic fibrosis zebrafish model. *Sci Rep.* 9, 1527 (2019)

155. Halim AS, Khoo TL, Saad AZ. Wound bed preparation from a clinical perspective. *Indian J Plast Surg.* 2012;45(2):193-202. doi:10.4103/0970-0358.101277
156. Manna B, Nahirniak P, Morrison CA. Wound Debridement. 2021 Sep 6. In: StatPearls [Internet]. Treasure Island (FL): StatPearls Publishing; 2021 Jan-. PMID: 29939659.
157. Stephen-Haynes J, Thompson G. The different methods of wound debridement. *Br J Community Nurs.* 2007 Jun;12(6):S6, S8-10, S12-14, S16. PMID: 17577156.
158. Schultz GS, Chin GA, Moldawer L, et al. Principles of Wound Healing. *Mechanisms of Vascular Disease: A Reference Book for Vascular Specialists;* 2011. 23.
159. Sood A, Granick MS, Tomaselli NL. Wound Dressings and Comparative Effectiveness Data. *Adv Wound Care (New Rochelle).* 2014;3(8):511-529. doi:10.1089/wound.2012.0401
160. Bollero D, Driver V, Glat P et al. The Role of Negative Pressure Wound Therapy in the Spectrum of Wound Healing. *Ostomy Wound Management.* 2010;56(5 Suppl):1–18.
161. Lipsky B, Dryden M, Gottrup F, Nathwani D, Seaton RA, Stryja J. Antimicrobial stewardship in wound care: a Position Paper from the British Society for Antimicrobial Chemotherapy and European Wound Management Association, *Journal of Antimicrobial Chemotherapy*, Volume 71, Issue 11, November 2016, Pages 3026–3035,
162. Ventola CL. The antibiotic resistance crisis: part 1: causes and threats. *P T.* 2015;40(4):277-283.
163. Agyepong, N., Govinden, U., Owusu-Ofori, A. et al. Multidrug-resistant gram-negative bacterial infections in a teaching hospital in Ghana. *Antimicrob Resist Infect Control* 7, 37 (2018).
164. Delerue T, Ramamurthi KS. How bacteria block their own biofilms. *J Biol Chem.* 2021 Mar 4;296:100392
165. Neu HC. The crisis in antibiotic resistance. *Science.* 1992 Aug 21;257(5073):1064-73.
166. Olson ME, Ceri H, Morck DW, Buret AG, Read RR. Biofilm bacteria: formation and comparative susceptibility to antibiotics. *Can J Vet Res.* 2002;66(2):86-92.
167. Stephanie Fulaz, Stefania Vitale, Laura Quinn, Eoin Casey, Nanoparticle–Biofilm Interactions: The Role of the EPS Matrix, *Trends in Microbiology*, Volume 27, Issue 11, 2019, Pages 915-926

168. Wan N, Wang H, Ng CK, et al. Bacterial Metabolism During Biofilm Growth Investigated by ¹³C Tracing. *Front Microbiol.* 2018;9:2657. Published 2018 Nov 20. doi:10.3389/fmicb.2018.02657
169. Madsen JS, Burmølle M, Hansen LH, Sørensen SJ. The interconnection between biofilm formation and horizontal gene transfer. *FEMS Immunol Med Microbiol.* 2012 Jul;65(2):183-95.
170. Singh S, Singh SK, Chowdhury I, Singh R. Understanding the Mechanism of Bacterial Biofilms Resistance to Antimicrobial Agents. *Open Microbiol J.* 2017 Apr 28;11:53-62.
171. Guillemot D. Antibiotic use in humans and bacterial resistance. *Curr Opin Microbiol.* 1999 Oct;2(5):494-8.
172. Høiby N, Bjarnsholt T, Givskov M, Molin S, Ciofu O. Antibiotic resistance of bacterial biofilms. *Int J Antimicrob Agents.* 2010 Apr;35(4):322-32
173. Sun Y, Dowd SE, Smith E, Rhoads DD, Wolcott RD. In vitro multispecies Lubbock chronic wound biofilm model. *Wound Repair Regen* (2008) 16:805–813.
174. Watkins, R. R., Lemonovich, T. L. & File, T. M. An evidence-based review of linezolid for the treatment of methicillin-resistant *Staphylococcus aureus* (MRSA): place in therapy. *Core Evid.* 7, 131-143 (2012).
175. Peppard, W. J. & Weigelt, J. A. Role of linezolid in the treatment of complicated skin and soft tissue infections. *Expert Rev. Anti Infect. Ther.* 4, 357-366 (2006).
176. O'Brien, D. J. & Gould, 1. M. Does vancomycin have a future in the treatment of skin infections? *Curr. Opin. Infect. Dis.* 27, 146-154 (2014).
177. Kadam S, Madhusoodhanan V, Bhide D, Ugale R, Tikhole U, Kaushik KS. Milieu matters : An wound milieu to recapitulate key features of, and probe new insights into, polymicrobial biofilms.
178. Smith BK, Ford RJ, Desjardins EM, Green AE, Hughes MC, Houde VP, Day EA, Marcinko K, Crane JD, Mottillo EP, Perry CGR, Kemp BE, Tarnopolsky MA, Steinberg GR. Salsalate (Salicylate) uncouples mitochondria, improves glucose homeostasis, and reduces liver lipids independent of AMPK-β1. *Diabetes* (2016) 65:3352-3361.
179. Roberts AEL, Kragh KN, Bjarnsholt T, Diggle SP. The limitations of in vitro experimentation in understanding biofilms and chronic infection. *J Mol Biol* 2015 (427):3646-3661.

180. Coenye T, Goeres D, Van Bambeke F, Bjarnsholt T. Should standardized susceptibility testing for microbial biofilms be introduced in clinical practice? *Clin Microbiol Infect* (2018) 24:570-572.
181. Santos DMSD, Pires JG, Braga AS, Salomão PMA, Magalhães AC. Comparison between static and semi-dynamic models for microcosm biofilm formation on dentin. *J Appl Oral Sci.* 2019 Jan 7;27:e20180163
182. Harrison JJ, Stremick CA, Turner RJ, Allan ND, Olson ME, Ceri H. Microtiter susceptibility testing of microbes growing on peg lids: a miniaturized biofilm model for high-throughput screening. *Nat. Protoc.* 2010;5(7):1236–1254.
183. Pérez-Rodríguez, S., García-Aznar, J.M., Gonzalo-Asensio, J. Microfluidic devices for studying bacterial taxis, drug testing and biofilm formation. *Microb Biotechnol* 2021 (in press).
184. Sternberg C, Tolker-Nielsen T. Growing and analyzing biofilms in flow cells. *Curr Protoc Microbiol.* 2006 Jan;Chapter 1:Unit 1B.2.
185. Naudin B, Heins A, Pinhal S, Dé E, Nicol M. BioFlux™ 200 Microfluidic System to Study *A. baumannii* Biofilm Formation in a Dynamic Mode of Growth. *Methods Mol Biol.* 2019;1946:167-176.
186. López, D., Vlamakis, H., Kolter, R. Biofilms. *Cold Spring Harb Perspect Biol* 2010, 2, a000398.
187. Kostakioti, M., Hadjifrangiskou, M., Hultgren, S.J. Bacterial biofilms: development, dispersal, and therapeutic strategies in the dawn of the postantibiotic era. *Cold Spring Harb Perspect Med* 2013, 3, a010306.
188. Rasamiravaka, T., Labtani, Q., Duez, P., El Jaziri, M. The formation of biofilms by *Pseudomonas aeruginosa*: a review of the natural and synthetic compounds interfering with control mechanisms. *Biomed Res Int* 2015, 2015, 759348.
189. Hentzer, M., Teitzel, G.M., Balzer, G.J., Heydorn, A., Molin, S., Givskov, M., et al. Alginate overproduction affects *Pseudomonas aeruginosa* biofilm structure and function. *J Bacteriol* 2001, 183, 5395-5401.
190. Sharma, D., Misba, L., Khan, A.U. Antibiotics versus biofilm: an emerging battleground in microbial communities. *Antimicrob Resist Infect Control* 2019, 8, 76.
191. Omar, A., Wright, J.B., Schultz, G., Burrell, R., Nadworny, P. Microbial Biofilms and Chronic Wounds. *Microorganisms* 2017, 5, 9.
192. Wilson, C., Lukowicz, R., Merchant, S., Valquier-Flynn, H., Caballero, J., Sandoval, J., et al. Quantitative and Qualitative Assessment Methods for Biofilm Growth: A Mini-review. *Res Rev J Eng Technol* 2017, 6

193. Díez-Aguilar, M., Morosini, M.I., Köksal, E., Oliver, A., Ekkelenkamp, M., Cantón, R. Use of Calgary and Microfluidic BioFlux Systems To Test the Activity of Fosfomycin and Tobramycin Alone and in Combination against Cystic Fibrosis *Pseudomonas aeruginosa* Biofilms. *Antimicrob Agents Chemother* 2017, 62, e01650-17.
194. Schultz, G., Bjarnsholt, T., James, G.A., Leaper, D.J., McBain, A.J., Malone, M., et al. Consensus guidelines for the identification and treatment of biofilms in chronic nonhealing wounds. *Wound Repair Regen* 2017, 25, 744-757.
195. Steed, D.L. Debridement. *Am J Surg* 2004, 187, 71S-74S.
196. Bagge, N., Schuster, M., Hentzer, M., Ciofu, O., Givskov, M., Greenberg, E.P., et al. *Pseudomonas aeruginosa* biofilms exposed to imipenem exhibit changes in global gene expression and beta-lactamase and alginate production. *Antimicrob Agents Chemother* 2004, 48, 1175-87.
197. Karaman, M., Firinci, F., Arıkan Ayyıldız, Z., Bahar, I.H. [Effects of Imipenem, Tobramycin and Curcumin on Biofilm Formation of *Pseudomonas aeruginosa* Strains]. *Mikrobiyol Bul* 2013, 47, 192-4.
198. Otani, S., Hiramatsu, K., Hashinaga, K., Komiya, K., Umeki, K., Kishi, K., et al. Sub-minimum inhibitory concentrations of ceftazidime inhibit *Pseudomonas aeruginosa* biofilm formation. *J Infect Chemother* 2018, 24, 428-433.
199. Wang, X., Cai, Y., Xing, H., Wu, W., Wang, G., Li, L., et al. Increased therapeutic efficacy of combination of azithromycin and ceftazidime on *Pseudomonas aeruginosa* biofilm in an animal model of ureteral stent infection. *BMC Microbiol* 2016, 16, 124.
200. Bagge, N., Ciofu, O., Skovgaard, L.T., Høiby, N. Rapid development in vitro and in vivo of resistance to ceftazidime in biofilm-growing *Pseudomonas aeruginosa* due to chromosomal beta-lactamase. *APMIS* 2000, 108, 589-600.
201. Bowler, L.L., Zhanel, G.G., Ball, T.B., Saward, L.L. Mature *Pseudomonas aeruginosa* biofilms prevail compared to young biofilms in the presence of ceftazidime. *Antimicrob Agents Chemother* 2012, 56, 4976-9.
202. Hsu, C.Y., Lin, M.H., Chen, C.C., Chien, S.C., Cheng, Y.H., Su, I.N., et al. Vancomycin promotes the bacterial autolysis, release of extracellular DNA, and biofilm formation in vancomycin-non-susceptible *Staphylococcus aureus*. *FEMS Immunol Med Microbiol* 2011, 63, 236-47.
203. He, X., Yuan, F., Lu, F., Yin, Y., Cao, J. Vancomycin-induced biofilm formation by methicillin-resistant *Staphylococcus aureus* is associated with the secretion of membrane vesicles. *Microb Pathog* 2017, 110, 225-231.

204. Mirani, Z.A., Aziz, M., Khan, M.N., Lal, I., Hassan, N.U., Khan, S.I. Biofilm formation and dispersal of *Staphylococcus aureus* under the influence of oxacillin. *Microb Pathog* 2013, 61-62, 66-72.
205. Manner, S., Goeres, D., Skogman, M., Vuorela, P., Fallarero, A. Prevention of *Staphylococcus aureus* biofilm formation by antibiotics in 96-Microtiter Well Plates and Drip Flow Reactors: critical factors influencing outcomes. *Sci Rep* 2017, 7, 43854.
206. Parra-Ruiz, J., Bravo-Molina, A., Peña-Monje, A., Hernández-Quero, J. Activity of linezolid and high-dose daptomycin, alone or in combination, in an *in vitro* model of *Staphylococcus aureus* biofilm. *J Antimicrob Chemother* 2012, 67, 2682–2685.
207. Abad, L., Tafani, V., Tasse, J., Josse, J., Chidiac, C., Lustig, S., et al. Evaluation of the ability of linezolid and tedizolid to eradicate intraosteoblastic and biofilm-embedded *Staphylococcus aureus* in the bone and joint infection setting. *J Antimicrob Chemother* 2019, 74, 625-632.
208. Gander, S., Hayward, K., Finch, R. An investigation of the antimicrobial effects of linezolid on bacterial biofilms utilizing an *in vitro* pharmacokinetic model. *J Antimicrob Chemother* 2002, 49, 301–308.
209. Davies D. Understanding biofilm resistance to antibacterial agents. *Nat Rev Drug Discov.* 2003 Feb;2(2):114-22.
210. Sauer K, Camper AK, Ehrlich GD, Costerton JW, Davies DG. *Pseudomonas aeruginosa* displays multiple phenotypes during development as a biofilm. *J Bacteriol.* 2002 Feb;184(4):1140-54.
211. Kaplan JB, Meyenhofer MF, Fine DH. Biofilm growth and detachment of *Actinobacillus actinomycetemcomitans*. *J Bacteriol.* 2003 Feb;185(4):1399-404.
212. Hunt SM, Werner EM, Huang B, Hamilton MA, Stewart PS. Hypothesis for the role of nutrient starvation in biofilm detachment. *Appl Environ Microbiol.* 2004 Dec;70(12):7418-25.
213. Boles BR, Thoendel M, Singh PK. Self-generated diversity produces "insurance effects" in biofilm communities. *Proc Natl Acad Sci U S A.* 2004 Nov 23;101(47):16630-5.
214. Bester E, Wolfaardt G, Joubert L, Garny K, Saftic S. Planktonic-cell yield of a *pseudomonas* biofilm. *Appl Environ Microbiol.* 2005 Dec;71(12):7792-8.
215. Ymele-Leki P, Ross JM. Erosion from *Staphylococcus aureus* biofilms grown under physiologically relevant fluid shear forces yields bacterial cells

- with reduced avidity to collagen. *Appl Environ Microbiol.* 2007 Mar;73(6):1834-41
216. Costerton JW, Cheng KJ, Geesey GG, Ladd TI, Nickel JC, Dasgupta M, Marrie TJ. Bacterial biofilms in nature and disease. *Annu Rev Microbiol.* 1987;41:435-64.
217. Xu KD, Stewart PS, Xia F, Huang CT, McFeters GA. Spatial physiological heterogeneity in *Pseudomonas aeruginosa* biofilm is determined by oxygen availability. *Appl Environ Microbiol.* 1998 Oct;64(10):4035-9
218. Cécile Rollet, Laurent Gal, Jean Guzzo, Biofilm-detached cells, a transition from a sessile to a planktonic phenotype: a comparative study of adhesion and physiological characteristics in *Pseudomonas aeruginosa*, *FEMS Microbiology Letters*, Volume 290, Issue 2, January 2009, Pages 135–142
219. Guilhen, C., Miquel, S., Charbonnel, N. *et al.* Colonization and immune modulation properties of *Klebsiella pneumoniae* biofilm-dispersed cells. *npj Biofilms Microbiomes* 5, 25 (2019)
220. Berlanga, M., Gomez-Perez, L. & Guerrero, R. Biofilm formation and antibiotic susceptibility in dispersed cells versus planktonic cells from clinical, industry and environmental origins. *Antonie Van. Leeuwenhoek* 110, 1691–1704 (2017).
221. Pelletier C, Bouley C, Cayuela C, Bouttier S, Bourlioux P, Bellon-Fontaine MN. Cell surface characteristics of *Lactobacillus casei subsp. casei*, *Lactobacillus paracasei subsp. paracasei*, and *Lactobacillus rhamnosus* strains. *Appl Environ Microbiol.* 1997 May;63(5):1725-31.
222. Bellon-Fontaine MN Rault J Van Oss CJ (1996) Microbial adhesion to solvents: a novel method to determine the electron-donor/electron-acceptor or Lewis acid-base properties of microbial cells. *Colloid Surface B* 7: 47–53
223. Gilbert P Evans DJ Brown MRW (1993) Formation and dispersal of bacterial biofilms *in vivo* and *in situ*. *J Appl Bacteriol Symp* 74: (suppl): 67S–78S
224. Bester E, Wolfaardt G, Joubert L, Garny K, Saftic S. Planktonic-cell yield of a pseudomonas biofilm. *Appl Environ Microbiol.* 2005 Dec;71(12):7792-8.
225. Guilhen, C. *et al.* Transcriptional profiling of *Klebsiella pneumoniae* defines signatures for planktonic, sessile and biofilm-dispersed cells. *BMC Genomics* 17, 237 (2016).
226. Zengler, K., and Palsson, B. O. (2012). A road map for the development of community systems (CoSy) biology. *Nat. Rev. Microbiol.* 10, 366–372. doi: 10.1038/nrmicro2763

227. Burmølle, M., Ren, D., Bjarnsholt, T., and Sørensen, S. J. (2014). Interactions in multispecies biofilms: do they actually matter? *Trends Microbiol.* 22, 84–91. doi: 10.1016/j.tim.2013.12.004
228. Momeni, B., Brileya, K. A., Fields, M. W., and Shou, W. (2013). Strong inter-population cooperation leads to partner intermixing in microbial communities. *Elife* 2013:e00230. doi: 10.7554/eLife.00230
229. Møller, S., Sternberg, C., Andersen, J. B., Christensen, B. B., Ramos, J. L., Givskov, M., et al. (1998). In situ gene expression in mixed-culture biofilms: evidence of metabolic interactions between community members. *Appl. Environ. Microbiol.* 64, 721–732.
230. Embree, M., Nagarajan, H., Movahedi, N., Chitsaz, H., and Zengler, K. (2014). Single-cell genome and metatranscriptome sequencing reveal metabolic interactions of an alkane-degrading methanogenic community. *ISME J.* 8, 757–767. doi: 10.1038/ismej.2013.187
231. Zelezniak, A., Andrejev, S., Ponomarova, O., Mende, D. R., Bork, P., and Patil, K. R. (2015). Correction for Zelezniak et al., metabolic dependencies drive species co-occurrence in diverse microbial communities. *Proc. Natl. Acad. Sci. U.S.A.* 112, 6449–6454. doi: 10.1073/pnas.1522642113
232. Hansen, S. K., Rainey, P. B., Haagensen, J. A. J., and Molin, S. (2007). Evolution of species interactions in a biofilm community. *Nature* 445, 533–536. doi: 10.1038/nature05514
233. Pande, S., Kaftan, F., Lang, S., Svatos, A., Germerodt, S., and Kost, C. (2015). Privatization of cooperative benefits stabilizes mutualistic cross-feeding interactions in spatially structured environments. *ISME J.* 10, 1413–1423. doi: 10.1038/ismej.2015.212
234. Harrison, F., Browning, L. E., Vos, M., and Buckling, A. (2006). Cooperation and virulence in acute *Pseudomonas aeruginosa* infections. *BMC Biol.* 4:21. doi: 10.1186/1741-7007-4-21
235. Ngba Essebe C, Visvikis O, Fines-Guyon M, Vergne A, Cattoir V, Lecoustumier A, Lemichez E, Sotto A, Lavigne JP, Dunyach-Remy C. Decrease of *Staphylococcus aureus* Virulence by *Helcococcus kunzii* in a *Caenorhabditis elegans* Model. *Front Cell Infect Microbiol.* 2017 Mar 16;7:77
236. Fazli M, Bjarnsholt T, Kirketerp-Møller K, Jørgensen B, Andersen AS, Krogfelt KA, Givskov M, Tolker-Nielsen T. Nonrandom distribution of *Pseudomonas aeruginosa* and *Staphylococcus aureus* in chronic wounds. *J Clin Microbiol.* 2009 Dec;47(12):4084-9
237. Barken, K. B., S. J. Pamp, L. Yang, M. Gjermansen, J. J. Bertrand, M. Klausen, M. Givskov, C. B. Whitchurch, J. N. Engel, and T. Tolker-Nielsen. 2008. Roles of type IV pili, flagellum-mediated motility and

extracellular DNA in the formation of mature structures in *Pseudomonas aeruginosa* biofilms. Environ. Microbiol. 10:2331-2343

238. Klausen, M., A. Heydorn, P. Ragas, L. Lambertsen, A. Aaes-Jørgensen, S. Molin, and T. Tolker-Nielsen. 2003. Biofilm formation by *Pseudomonas aeruginosa* wild type, flagella and type IV pili mutants. Mol. Microbiol. 48:1511-1524

ANNEXES

Annexe 1: Brevet de propriété intellectuelle du Milieu Plaie



Europäisches
Patentamt

European
Patent Office

Office européen
des brevets

Accusé de réception

Par la présente, nous accusons réception de votre requête en délivrance d'un brevet européen, comme suit:

Numéro de soumission	1000501613	
Numéro de demande	EP21305337.4	
N° de dépôt à utiliser pour la déclaration de priorité	EP21305337	
Date de réception	18 mars 2021	
Votre référence	BNT229481EP00	
Demandeur	BIOFILM PHARMA	
Pays	FR	
Titre	MILIEU MIMETIQUE DE CULTURE MICROBIOLOGIQUE ET UTILISATIONS DE CELUI-CI	
Documents produits	package-data.xml application-body.xml SPECEPO-1.pdf BNT229481EP00 Texte et figures depot.pdf (71 p.)	ep-request.xml ep-request.pdf (5 p.) f1002-1.pdf (2 p.)
Effectué par	CN=Eric Enderlin 37842	
Méthode de soumission	En ligne	
Date et heure de réception	18 mars 2021, 22:36:41 (CET)	
Digest	4E:37:6D:1F:F9:9D:8C:EB:7B:D0:1A:46:BB:3D:71:C8:C8:2F:A3:FB	

/INPI, section dépôt/

Annexe 2 : Publication associée en 5^{ème} auteur – Infection and Immunity

BACTERIAL INFECTIONS



Success of *Escherichia coli* O25b:H4 Sequence Type 131 Clade C Associated with a Decrease in Virulence

Marion Duprilot,^{a,b} Alexandra Baron,^a François Blanquart,^{a,c} Sara Dion,^a Cassandra Pouget,^d Philippe Lettéron,^e Saskia-Camille Flament-Simon,^f Olivier Clermont,^a  Erick Denamur,^{a,g}  Marie-Hélène Nicolas-Chanoine^a

^aUniversité de Paris, INSERM, IAME, Paris, France

^bAP-HP, Laboratoire de Microbiologie, Hôpital Beaujon, Clichy, France

^cCentre for Interdisciplinary Research in Biology (CIRB), Collège de France, CNRS, INSERM, PSL Research University, Paris, France

^dVBMI, INSERM U1047, Université de Montpellier, Nîmes, France

^eUniversité de Paris, UMR 1149, INSERM-ERL, CNRS 8252, Paris, France

^fLaboratorio de Referencia de *Escherichia coli* (LREC), Departamento de Microbiología e Parasitología, Facultad de Veterinaria, Universidade de Santiago de Compostela (USC), Lugo, Spain

^gAP-HP, Laboratoire de Génétique Moléculaire, Hôpital Bichat, Paris, France

Marion Duprilot and Alexandra Baron contributed equally to this work. The order of the authors was determined by the greatest contribution of each of them in relation to the number of years required to carry out this work.

ABSTRACT *Escherichia coli* O25b:H4 sequence type 131 (ST131), which is resistant to fluoroquinolones and which is a producer of CTX-M-15, is globally one of the major extraintestinal pathogenic *E. coli* (ExPEC) lineages. Phylogenetic analyses showed that multidrug-resistant ST131 strains belong to clade C, which recently emerged from clade B by stepwise evolution. It has been hypothesized that features other than multidrug resistance could contribute to this dissemination since other major global ExPEC lineages (ST73 and ST95) are mostly antibiotic susceptible. To test this hypothesis, we compared early biofilm production, presence of ExPEC virulence factors (VFs), and *in vivo* virulence in a mouse sepsis model in 19 and 20 epidemiologically relevant strains of clades B and C, respectively. Clade B strains were significantly earlier biofilm producers ($P < 0.001$), carriers of more VFs ($P = 4e-07$), and faster killers of mice ($P = 2e-10$) than clade C strains. Gene inactivation experiments showed that the *H30-fimB* and *ibeART* genes were associated with *in vivo* virulence. Competition assays in sepsis, gut colonization, and urinary tract infection models between the most anciently diverged strain (B1 subclade), one C1 subclade strain, and a B4 subclade recombining strain harboring some clade C-specific genetic events showed that the B1 strain always outcompeted the C1 strain, whereas the B4 strain outcompeted the C1 strain, depending on the mouse niches. All these findings strongly suggest that clade C evolution includes a progressive loss of virulence involving multiple genes, possibly enhancing overall strain fitness by avoiding severe infections, even if it comes at the cost of a lower colonization ability.

KEYWORDS *Escherichia coli*, ST131, fimbriae, *ibeART* operon, *in vivo* virulence, niche adaptation

In the last 2 decades, multidrug-resistant (MDR) *Escherichia coli* O25b:H4 sequence type 131 (ST131) has emerged worldwide among human extraintestinal pathogenic *E. coli* (ExPEC) strains (1, 2). This *E. coli* lineage is composed of two clades, called clades B and C, defined on the basis of the *fimH* alleles H22 and H30 (3, 4). A time-calibrated phylogeny showed that clade C emerged from clade B and that sequential mutational events shaped the evolution of O25b:H4 ST131 from the 1950s, resulting in the diversification of clade B into different subclades (subclades B1 to B5 and then the

Citation Duprilot M, Baron A, Blanquart F, Dion S, Pouget C, Lettéron P, Flament-Simon S-C, Clermont O, Denamur E, Nicolas-Chanoine M-H. 2020. Success of *Escherichia coli* O25b:H4 sequence type 131 clade C associated with a decrease in virulence. *Infect Immun* 88:e00576-20. <https://doi.org/10.1128/IAI.00576-20>.

Editor Andreas J. Bäuml, University of California, Davis

Copyright © 2020 Duprilot et al. This is an open-access article distributed under the terms of the Creative Commons Attribution 4.0 International license.

Address correspondence to Marie-Hélène Nicolas-Chanoine, marie-helene.nicolas-chanoine@inserm.fr.

Received 14 September 2020

Accepted 14 September 2020

Accepted manuscript posted online 28 September 2020

Published 16 November 2020

intermediate subclade, B0) and the appearance of clade C (5). The diversification of clade C into different subclades was characterized by the acquisition of the *fimH30* allele in about 1980, resulting in the C0 subclade, followed by the acquisition of the *gyrA1AB* and *parC1aAB* alleles, encoding fluoroquinolone resistance, in about 1987, resulting in the C1 and C2 subclades (5). All C2 subclade strains and a fraction of the C1 subclade strains forming the C1-M27 cluster (6) are additionally resistant to extended-spectrum cephalosporins (ESC) due to the production of extended-spectrum β -lactamases (ESBL) of the CTX-M type, CTX-M-15 and CTX-M-27, respectively.

Existing epidemiological studies have examined the prevalence of ST131 among *E. coli* isolates that are resistant to fluoroquinolones and/or that are producers of ESBL (7). Few studies have assessed the relative frequencies of ST131 clade B and clade C (8–11), and none of them have assessed the relative frequencies of the B and C subclades.

The evolutionary success of MDR ST131 clade C is still largely unexplained. Multidrug resistance may explain this success, as resistance to fluoroquinolones and ESC was shown to not impact the growth fitness of clade C strains (12, 13). However, *E. coli* lineages susceptible to antibiotics, such as ST73 and ST95, are as successful as ST131 clade C (in terms of their frequency in bacteremia and urinary tract infections), suggesting that factors other than antibiotic resistance can participate in the success of a lineage (9). Thus, by combining population genomics and modeling approaches, McNally et al. (14) showed that, compared to other dominant *E. coli* lineages and also to ST131 clade B, MDR ST131 clade C has accumulated a significantly elevated allelic diversity particularly enriched for genes involved in anaerobic metabolisms and other loci encoding factors contributing to human colonization by ExPEC. Given the low frequency of occurrence of this allelic diversity, the authors suggested adaptation to separate ecological niches among ST131 clades. For their part, Billard-Pomares et al. (15) showed that since 2000 the arginine deiminase operon has been increasing in prevalence in isolates producing ESBL, especially CTX-M, largely due to its presence in ST131 clade C. This operon was deleterious for the ESBL-producing strain tested in a mouse gut colonization model but contributed to its virulence in a mouse model of urinary tract infection (15). Therefore, this suggests the potential for ST131 clade C to adapt to different human niches.

In the present study, we chose to mostly perform phenotypic comparisons between clade B and clade C strains to get further insights into factors that have favored clade C dissemination. To this end, we established a collection of 39 *E. coli* O25b:H4 ST131 strains composed of strains representing the O25b:H4 ST131 clade and subclade diversity. The characterization of the 39 strains with regard to early biofilm formation and the capability to kill mice in a sepsis model, as well as competitions between selected clade B and clade C strains in various mouse models, allowed us to highlight the difference in the virulence potential of clade B and clade C strains.

RESULTS

Epidemiology of the O25b:H4 ST131 B and C subclades in extraintestinal infections over time. Recently, Kallonen et al. depicted 197 O25b:H4 ST131 isolates (161 belonging to clade C and 36 belonging to clade B) among 1,509 bacteremia *E. coli* isolates systematically collected between 2001 and 2012 in England (9). To have an overview of the epidemiology of the O25b:H4 ST131 B and C subclades, we used the whole-genome sequence of the English O25b:H4 ST131 isolates and reference strains of the different O25b:H4 ST131 B and C subclades (5) to build a phylogenetic tree from nonrecombinant single nucleotide polymorphisms (SNPs) of core genomes and clarify to which B and C subclades the 197 English O25b:H4 ST131 isolates belonged (see Fig. S1 in the supplemental material). We then assessed their relative frequencies (Fig. 1A and B) and investigated the trends in their frequency over the period from 2001 to 2012 (Fig. 1C). Among clade B strains, only the B5 subclade strains exhibited a notable increase (logistic regression for B5 strain presence as a function of time, 0.24 per year [95% confidence interval {CI}, -0.005 to 0.5 per year]). Both the C1 and C2 subclade

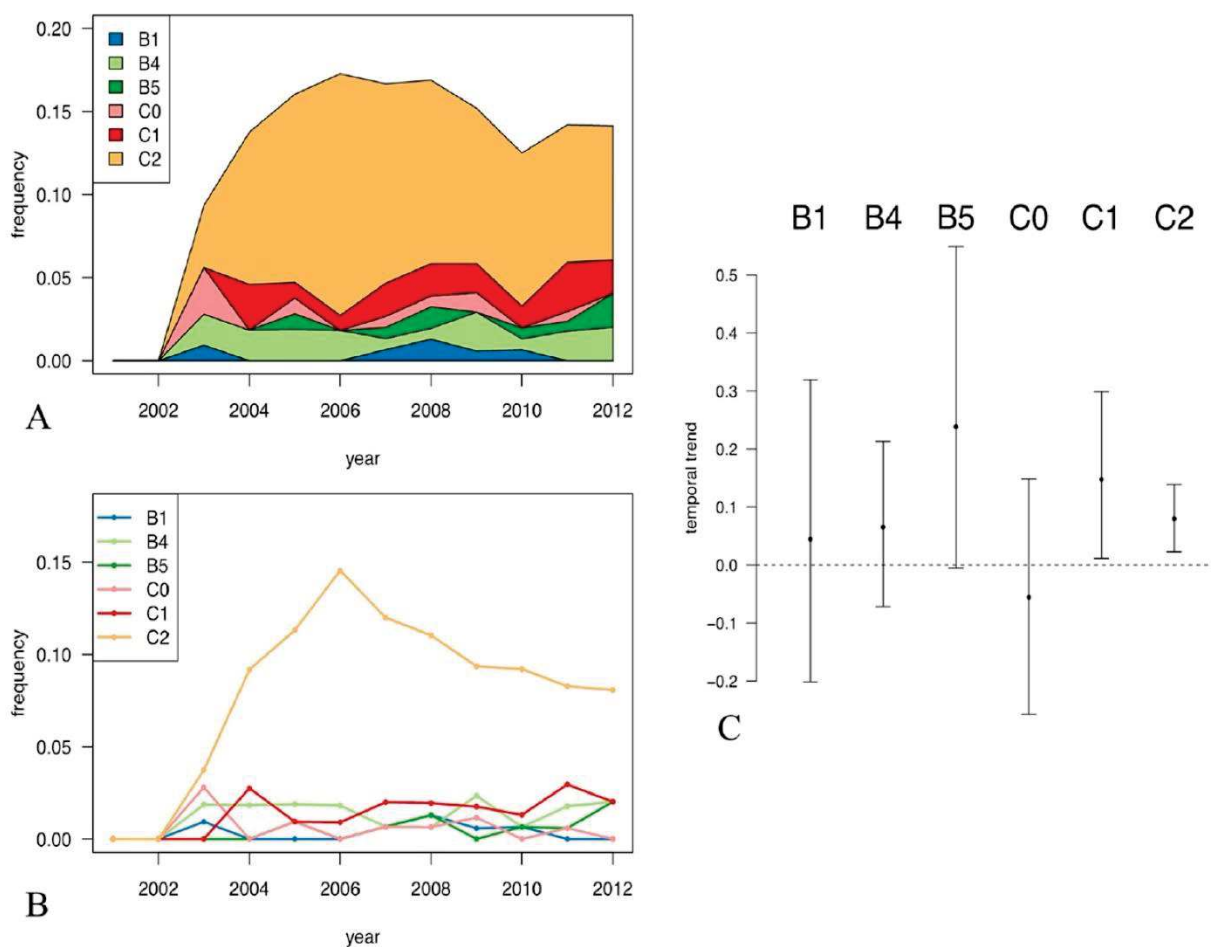


FIG 1 Dynamics of subclades in 197 O25b:H4 ST131 *Escherichia coli* strains isolated from cases of bacteremia over a 11-year sampling period (data are from Kallonen et al. [9]). (A) Cumulative frequencies of O25b ST131 subclades as a function of time, from the most ancestral B1 subclade at the bottom to the derived C2 subclade on the top. (B) Frequency of ST131 subclades as a function of time. Subclades are represented by colors. (C) Inferred linear trends of ST131 subclade frequencies (among all *E. coli* strains [$n = 1,509$]) as a function of time from 2001 to 2012. Among the clade B strains, only the subclade B5 strains exhibited a notable increase (logistic regression for subclade B5 strain presence as a function of time, 0.24 per year [95% CI, -0.005 to 0.55 per year]). Both the C1 and C2 subclade strains significantly increased (0.15 per year [95% CI, 0.01 to 0.30 per year] for C1, 0.08 per year [95% CI, 0.02 to 0.14 per year] for C2).

strains significantly increased (0.15 per year [95% CI, 0.01 to 0.30 per year] for C1, 0.08 per year [95% CI, 0.02 to 0.14 per year] for C2).

Molecular characteristics of the 39 studied O25b:H4 ST131 strains. As illustrated in Fig. 1 and by studies that had used the *fimH* typing method to characterize O25b:H4 ST131 collections (16, 17), clade B/*fimH22* strains are much less frequent than clade C/*fimH30* strains. Therefore, to establish an O25b ST131 collection comprising as many clade B strains as clade C strains, we obtained *fimH22* strains either previously published or belonging to the coauthors' personal collections (Table S1). Thus, we were able to get 18 *fimH22* strains, to which were added 21 *fimH30* strains, which generally came from the same collections as the *fimH22* strains (Table S1). The 39 strains were human strains isolated in Spain and France between 1993 and 2012 mostly from the blood of adult patients and the feces of healthy adults and children (Table S1). Through the phylogenetic tree constructed from nonrecombinant SNPs of core genome genes (Fig. S1), we found that the 39 strains were composed of 19 clade B strains distributed into the different B subclades, except for the B0 and B2 subclades (two subclades also absent among the 36 English O25b:H4 ST131 clade B isolates), and 20 clade C strains distributed into the three C subclades (subclades C0, C1, and C2). Among the 19 clade B strains, 17 displayed the *fimH22* allele; 1 displayed a *fimH22*-like allele; and 1, B4

subclade strain CES131C, displayed the *fimH30* allele that had been described to be specific to clade C strains (Table 1). For this reason, the CES131C strain is called "Recombinant" in the rest of this report.

All strains but one (strain 208) harbored an IncF plasmid with an FII, FIA, and FIB replicon allele composition corresponding to the one previously described for clade B and C0/C1 and C2 subclade strains (13), except for one C1 subclade strain (CES9C) that lacked the FIB replicon observed in C2 subclade strains (Table 1). Four clade B strains (two of the B1 subclade, one of the B3 subclade, and one of the B5 subclade) harbored a RepF1C replicon that belonged to the RepFIIA family (18), and one B3 subclade strain harbored two replicons of the RepFIIA family (Table 1).

As shown in Table 1, the 39 strains comprised 30 strains, 10 of which were clade B, displaying diverse antibiotic resistance-encoding genes with a gradual accumulation from clade B to clade C.

***In vitro* phenotypes of the 39 studied O25b:H4 ST131 strains.** We first assessed four *in vitro* phenotypes of the 39 collected strains: the maximum growth rate (MGR), the kinetics of early biofilm formation, and the expression of both type 1 and curli fimbriae.

For the MGR measured in a complex medium (lysogeny broth [LB]) under planktonic and shaking conditions (Fig. 2), there was no significant difference regardless of the comparisons made: clade B versus clade C ($P = 0.08$) (Fig. 2A), clinical versus fecal strains ($P = 0.07$) (Fig. 2B), nalidixic acid-resistant versus nalidixic acid-susceptible clade B strains ($P = 0.9$) (Fig. 2C), and nalidixic acid-/ciprofloxacin-resistant versus nalidixic acid-/ciprofloxacin-susceptible clade C strains ($P = 0.9$) (Fig. 2D).

We investigated the kinetics of early biofilm formation because previous results had shown that among a large collection of *E. coli* clinical isolates composed of 99 sequence type (ST) lineages, the O25b:H4 ST131 lineage belongs to the few lineages able to form a biofilm early in the experiment (19). We showed here that clade B strains were more frequently early biofilm producers than clade C strains ($P < 0.001$). More specifically, we found three significantly different phenotypes of early biofilm production ($P < 0.0001$) among the 39 studied strains (Fig. 3A; Table 1): early and persistent producers (biofilm index [BFI] ≤ 10 at 2, 3, and 5 h), delayed producers (BFI > 10 at 2 and 3 h but BFI ≤ 10 at 5 h), and never producers (BFI > 10 at 2, 3, and 5 h). As BFI values after 2 and 3 h of incubation classified a given strain into the same early biofilm formation phenotype (Fig. 3A), only BFI values obtained after 2 and 5 h of incubation were considered for further analyses. The 19 clade B strains were either early producers ($n = 8$), delayed producers ($n = 8$), or never producers ($n = 3$), whereas the 20 clade C strains were either delayed producers ($n = 8$) or never producers ($n = 12$) (Fig. 3A; Table 1). Within clade B, there was a significant difference between the seven B5 subclade strains (early producers, $n = 5$; delayed producers, $n = 2$) and the seven B4 subclade strains (delayed producers, $n = 4$; never producers, $n = 3$) ($P = 0.02$). Inversely, there was no significant difference between the three clade C subclades regarding the early biofilm formation phenotypes.

As the ability to form a biofilm is linked to type 1 and curli fimbria expression (20), we studied the expression of these types of fimbriae in the 39 strains at different times and under different growth conditions. After 2 and 5 h of shaking growth, the early biofilm producers more frequently expressed type 1 fimbriae than the delayed ($P < 0.01$) and never ($P \leq 0.0001$) producers, and clade B strains more frequently expressed type 1 fimbriae than clade C strains ($P \leq 0.0001$) (Table 2). All these significant differences were still observed after 24 h of growth under shaking conditions, but no significant difference was observed under static conditions (Table 2). Curli fimbria expression (Table 3), as assessed by the Congo red morphotype, was significantly associated with the early biofilm formation phenotype ($P < 0.0001$). Significantly more clade B strains (47%) than clade C strains (15%) were positive by the Congo red assay ($P < 0.001$).

TABLE 1 Genotypic and phenotypic characteristics of the 39 O25b:H4 ST131 *Escherichia coli* strains^a

Strain	fimH operon type	β-Lactamase		Allele		Gene(s) encoding resistance to:		Plasmid Inc system	pMLST	Col-like plasmid	VF score	Biofilm phenotype
		Non-ESBL	ESBL	gyrA	parC	Aminoglycosides	Other antibiotics					
B11J12	H22	B1	D3	gyrA1A	parC1	aac(3)-Iva, aph(4)-Ia		F1C, FIB	F89A--B62	156	16	+
S250	H22	B1	D3	gyrA1a	parC1			F1C, FIB	F89A--B62		14	++
CES106C2	H22	B3	D4	gyrA1a	parC2		su12, tet(A)	F1C, FIB, I1	F18A--B1, I1--ST3	pVC	16	++
H2381	H22	B3	D4	gyrA1A	parC2		tet(A)	F1I, FIB, X1	F2A--B1	MG828	18	++
H3345	H22	B3	D4	gyrA1A	parC2			F1I, FIB, FIC	F18A--B1	pVC	19	+
H1659	H22	B4	D3	gyrA1a	parC1			F1I, FIB	F29A--B10	156	16	+
B7J19	H22	B4	D3	gyrA1a	parC1			F1I, FIB	F29A--B10	156	16	+
B12C27	H22	B4	D3	gyrA1a	parC1			F1I, FIB	F29A--B10	156, MG828	16	+
B5E11	H22	B4	D3	gyrA1a	parC1			F1I, FIB	F29A--B10	156	16	+
011-005	H22	B4	D3	gyrA1a	parC1			F1I, FIB	F29A--B10	156	15	+
001-001	H22-like	B4	ND	gyrA1a	parC1			F1I, FIB	F29A--B10	156	15	+
CES131C	H30	B4	ND	gyrA1a	parC1		aac(3)-Ild, aadA2	F1I, FIB	F2A--B10	BS512	15	+
H219B	H22	B5	D1	gyrA1a	parC1		strA, strB, aadA5	F1I, FIB	F24A--B1		19	++
H1447	H22	B5	D1	gyrA1A	parC1		mph(B), sul12, tet(A), dfrA1	F1C, FB1, Q1	F18A--B8		17	++
H1698	H22	B5	D2	gyrA1a	parC1		tet(A)	F1I, FIB, X1	F2A--B1		22	+
196	H22	B5	D1	gyrA1a	parC1		mph(A), sul1, dfrA1	F1I, FIB	F24A--B6		16	++
208	H22	B5	D1	gyrA1a	parC1		strA, strB, aadA5	X1		156	12	++
H2262	H22	B5	D2	gyrA1a	parC1		aadB, aacA4, aadA2	F1I, FIB, N, HI2	F2A--B1, N-ST9, HI2-ST1	MG828	21	++
005-019	H22	B5	D1	gyrA1a	parC1		aadA1	F1I, FIB	F24A--B6		16	++
H1088	H30	C0	C2	gyrA1a	parC1a+A199G		mph(A), sul1, dfrA1	F1I, FIA, FIB	F36A1:B20	156, BS512, IMG531	14	+
B1G9	H30	C0	C2	gyrA1a	parC1a		mph(A), sul1, dfrA1	F1I, FIA, FIB	F22A1:B20	MG828	15	+
H2214	H30	C0	C2	gyrA1a	parC1a		aadA5	F1I, FIA, FIB	F36A1:B20	MG828	14	+
B1A5	H30	C1	C3	gyrA1AB	parC1aAB		aac(3)-Ild	F1I, FIA, FIB	F1:A2:B20	IMG531	12	+
B1H12	H30	C1	C3	gyrA1AB	parC1aAB		aadA5, strA, strB	F1I, FIA, FIB	F1:A2:B20	156, IMG531	12	+
B2B2	H30	C1	C2	gyrA1AB	parC1aAB		aadA5	F1I, FIA, FIB	F10:A2:B20	156, IMG531	14	+
02	H30	C1	C3	gyrA1AB	parC1aAB		mph(A), sul1-sul2, tet(A), dfrA17	F1I, FIA, FIB, N	F1:A2:B20, N--UST	KPH56	12	+
39	H30	C1	C2	gyrA1AB	parC1aAB		strA, strB, aadA5	F1I, FIA, FIB	F1:A2:B20	BS512, KPH56	14	+
183	H30	C1	C3	gyrA1AB	parC1aAB		strA, strB, aadA5	F1I, FIA, FIB, I1, X1	F1:A2:B20, I1-ST196	BS512, IMG531	13	+
187	H30	C1	C3	gyrA1AB	parC1aAB		strA, strB, aadA5	F1I, FIA, FIB, I1, X4	F1:A2:B20, I1--UST	BS512	12	+
CES103C	H30	C1	C3	gyrA1AB	parC1aAB		aac(3)-Ild	F1I, FIA, FIB	F1:A2:B20	BS512	12	+
CES9C	H30	C1	C2	gyrA1AB	parC1aAB		aac(3)-Ild	F1I, FIA	F1:A2:B--	IMG531	14	+
CES164C	H30	C1	C2	gyrA1AB	parC1aAB		aac(3)-Ild	F1I, FIA, FIB	F1:A2:B20	BS512	13	+
H3084B	H30	C1	C2	gyrA1AB	parC1aAB		aac(3)-Ild	F1I, FIA, FIB	F1:A2:B20	BS512	11	+
C5	H30	C1-M27	C2	gyrA1AB	parC1aAB		strA, strB, aadA5	F1I, FIA, FIB, I1, N	F1:A2:B20, I1--UST, N-ST9	BS512, IMG531	14	+
TN03	H30	C2	C2	gyrA1AB	parC1aAB		aac(3)-Ila, aac(6')/Ib-cr	F1I, FIA, FIB, I1	F1:A2:B20, I1--ST193	BS512, IMG531	14	+
B5B6	H30	C2	C2	gyrA1AB	parC1aAB		aac(3)-Ila, aac(6')/Ib-cr	F1I, FIA	F2A1:B--	BS512	14	+
B1211	H30	C2	ND	gyrA1AB	parC1aAB		aac(6')/Ib-cr, aadA5	F1I, FIA	F2A1:B--	IMG531	14	+
C23	H30	C2	ND	gyrA1AB	parC1aAB		aac(6')/Ib-cr, aadA5	F1I, FIA	F2A1:B--	BS512, IMG531	15	+
C3	H30	C2	ND	gyrA1AB	parC1aAB		aac(6')/Ib-cr, aadA5	F1I, FIA	F2A1:B--	BS512	15	+

^aInc, incompatibility; ND, not described so far; ++, early biofilm producer; +, delayed biofilm producer; --, never a biofilm producer.

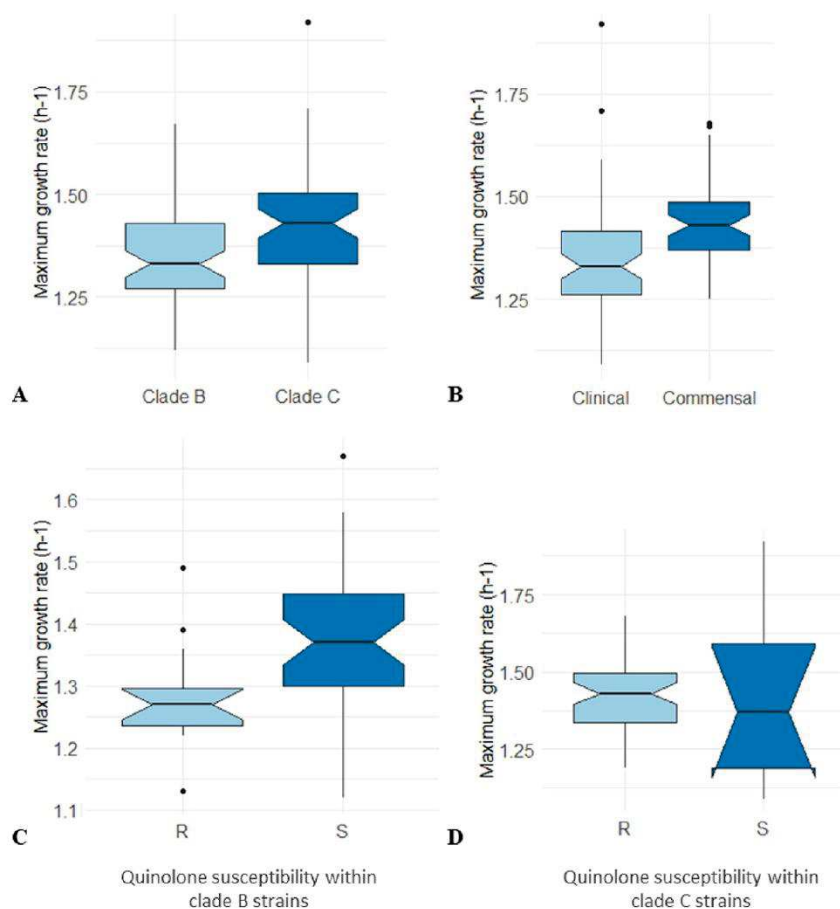


FIG 2 Maximum growth rate (MGR) in LB of the 39 O25b:H4 ST131 *Escherichia coli* strains studied. MGR was calculated from three independent LB culture assays and is expressed in hours⁻¹. Box plots indicate the MGR distribution across strains, and horizontal black bars indicate median values. The upper and lower ends of the box correspond to the upper and the lower quartiles, respectively. Error bars represent the standard error of the mean from three experiments. Outliers are represented by dots. (A) MGR of clade B and clade C strains. (B) MGR of clinical and commensal (fecal) strains. (C) MGR of nalidixic acid-resistant (R) and -susceptible (S) strains within clade B. (D) MGR of nalidixic acid-resistant (R) and -susceptible (S) strains within clade C. No significant difference was observed in each comparison (Wilcoxon test).

In sum, the MGR in a complex medium did not differ significantly between clade B and clade C strains, whereas clade B strains had a higher capability than clade C strains to form a biofilm early and express type 1 and curli fimbriae earlier.

Potential role of the *fimB* and the *ibeA* genes in the different phenotypes of early biofilm formation and type 1 fimbria expression identified among the 39 O25b:H4 ST131 strains studied. To decipher the molecular supports for the different early biofilm formation and type 1 fimbria expression phenotypes observed among the 39 strains, we analyzed the *fim* operon across the 39 studied strains, knowing that (i) the ISEc55 insertion sequence, which encodes a cofactor of type 1 fimbria synthesis regulation, has been described within the clade C *fimB* gene (21) and (ii) Recombinant displayed the *fimH30* allele previously thought to be a specific trait of clade C strains. Between the *fim* operon of the *fimH22* clade B strains and that of Recombinant, there were from 5 to 50 SNPs per gene, depending on the gene (Fig. 4). Inversely, between the *fim* operon of Recombinant and that of clade C strains, there was a perfect match, except for two SNPs and the absence of ISEc55 within the *fimB* gene of Recombinant (Fig. 4). We also found a partial deletion of the *fim* operon in two *fimH22* clade B strains, the B4 subclade strain 001-001 and the B5 subclade strain H1447 (data not shown).

To assess the role of the *fimB* gene in early biofilm formation and type 1 fimbria expression, we constructed Δ *fimB* mutants from the B1 subclade strain S250, which

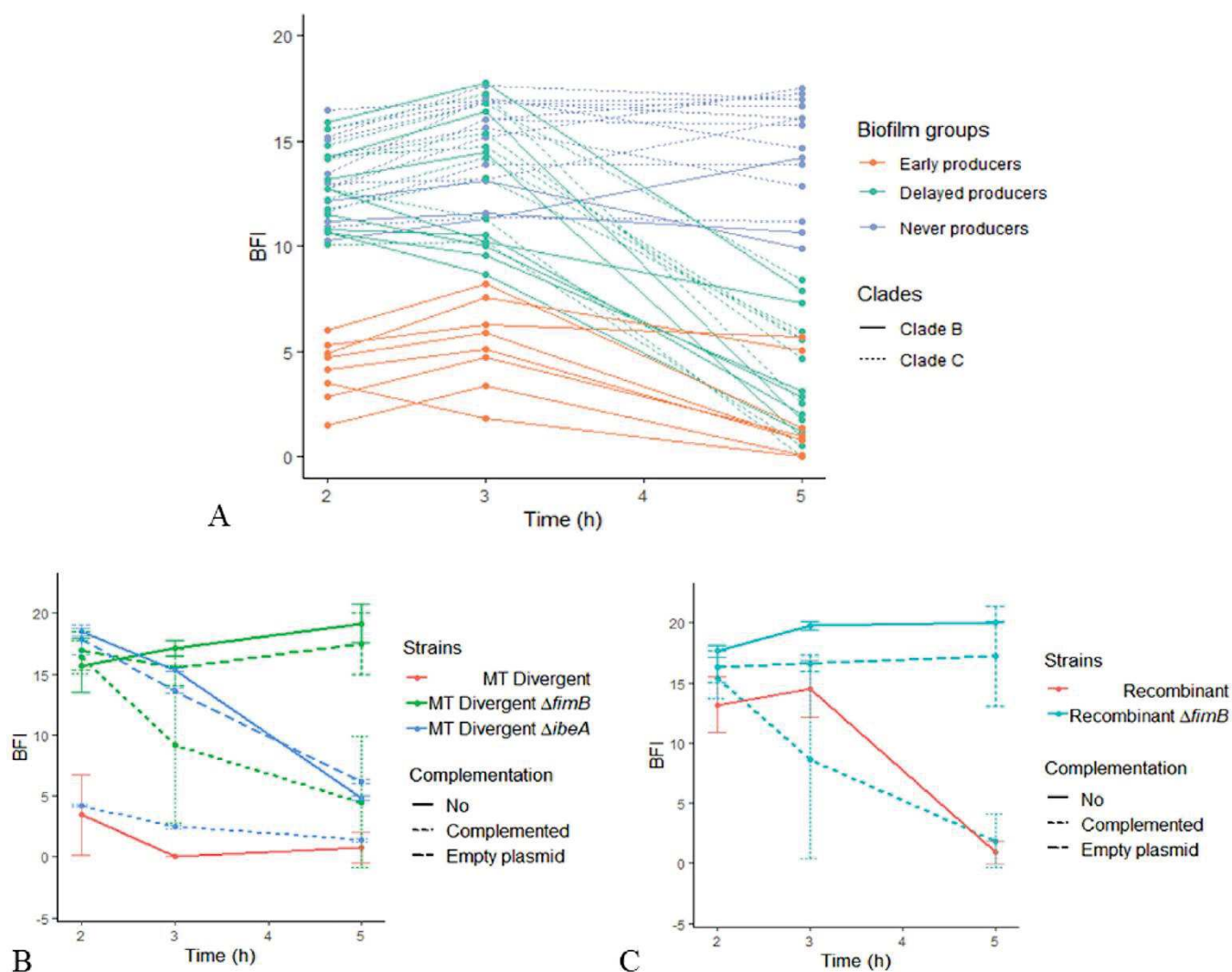


FIG 3 Early biofilm kinetics of the 39 O25b:H4 ST131 *Escherichia coli* strains and mutants studied. The BioFilm ring test was used to measure early biofilm formation, i.e., after 2, 3, and 5 h of static incubation. Biofilm index (BFI) values are inversely proportional to the biofilm formation capacity, with a BFI value of ≤ 10 meaning biofilm formation and a BFI value of > 10 meaning no biofilm formation. (A) Biofilm kinetics for the 39 O25b ST131 strains. Clade B strains were more frequently early biofilm producers than clade C strains ($P < 0.0001$). (B) Biofilm kinetics for (i) MT Divergent and its Δ *fimB*:FRT and Δ *ibeA*:FRT mutants, which became never and delayed biofilm producers, respectively, in the 5-h assay period; (ii) MT Divergent Δ *fimB*:FRT and Δ *ibeA*:FRT mutants complemented with the wild-type *fimB* gene (Δ *fimB*C) and the wild-type *ibeA* gene (*ibeA*C), both of which were harbored by plasmid pSC-A, in which the early biofilm formation phenotype of the parental strain was partially and totally restored, respectively; and (iii) MT Divergent Δ *fimB*:FRT and MT Divergent Δ *ibeA*:FRT mutants complemented with the empty plasmid pSC-A (Δ *fimB*p and Δ *ibeA*p, respectively). (C) Biofilm kinetics of Recombinant, its Δ *fimB*:FRT mutant, and the Recombinant Δ *fimB*:FRT mutant complemented with the wild-type *fimB* gene harbored by plasmid pSC-A (Δ *fimB*C) or transfected with the empty plasmid pSC-A (Δ *fimB*p). The Δ *fimB*:FRT mutant lost the capacity to produce a biofilm early, whereas when it was complemented with the wild-type *fimB* gene, it produced a biofilm earlier than the parental strain.

displayed an early (from 2 h) phenotype for the two traits (Tables 1 and 4), and Recombinant, which displayed a delayed (at 5 h) phenotype for the two traits (Tables 1 and 4). Both the S250 Δ *fimB* and Recombinant Δ *fimB* mutants lost their ability to form a biofilm (Fig. 3B and C) and to express type 1 fimbriae during the 5-h time period (Table 4). Complementation with the wild-type S250 *fimB* gene rendered the complemented strain a producer of a biofilm from 3 h, but at a level lower than that observed in strain S250 (Fig. 3B), and restored the expression of type 1 fimbriae observed in strain S250 (Table 4). Complementation with the wild-type recombinant *fimB* gene rendered the complemented strain a producer of a biofilm from 3 h, meaning that it was an earlier producer than Recombinant (Fig. 3C), and permitted the expression of type 1 fimbriae during the 5-h period of the experiment instead of only at 3 h, as observed in Recombinant (Table 4). Type 1 fimbria expression was also assessed after 24 h of

TABLE 2 Yeast agglutination test applied to the 39 O25b:H4 *Escherichia coli* strains under different growth conditions and at different time points according to biofilm production phenotype and clade type^a

Group	No. (%) of strains positive by yeast agglutination test			
	Early test, shaking culture		Standard test, 24 h ^a	
	2 h	5 h	Shaking culture	Static culture
Biofilm ++ (n = 8)	8 (100) ^{b,c}	8 (100) ^{b,c}	8 (100) ^{b,c}	8 (100)
Biofilm +- (n = 16)	5 (31) ^{b,c}	5 (31) ^{b,c,d}	4 (25) ^{b,c}	11 (69)
Biofilm - (n = 15)	2 (13) ^c	0 ^{c,d}	0 ^c	11 (73)
Clade B (n = 19)	15 (79) ^c	13 (68) ^c	12 (63) ^c	17 (90)
Clade C (n = 20)	0 ^c	0 ^c	0 ^c	13 (65)

^aThe standard test was performed as described by Totsika et al. (21). Early tests were always negative in static cultures (data not shown). ++, early biofilm producer; +-, delayed biofilm producer; -, never biofilm producer. *P* values were determined by Fisher's exact test.

^b*P* < 0.01.

^c*P* < 0.0001.

^d*P* < 0.05.

incubation (Table 4). This experiment showed that the S250 Δ *fimB* mutant did not express type 1 fimbriae at 24 h under either shaking or static conditions, whereas the Recombinant Δ *fimB* mutant and the tested clade C strain (CES164C) did, but only under static conditions (Table 4).

We then investigated the *ibeA* gene, knowing that (i) it was previously suggested that the brain endothelial cell invasion and adhesion determinants encoded by the *ibeA* gene and the *ibeT* gene, respectively, would have a role in modulating the expression of type 1 fimbriae (22) and (ii) the *ibeA* gene is absent in clade C strains (Table 5). We found that the *gimA* locus, including the *ibeAT* genes, encompassed with the *ibeR* gene in the *gimA4* operon, was present in all clade B strains except for strain 001-001 (data not shown) and Recombinant, in which it was completely deleted, as in clade C strains (Fig. 4). Additionally, we found that the inactivation of the *ibeA* gene of strain S250 rendered the S250 Δ *ibeA* mutant a delayed producer of a biofilm, whereas its complementation with the wild-type *ibeA* gene restored the early biofilm phenotype observed in the parental strain (Fig. 3B). Inversely, *ibeA* inactivation in strain S250, as well as that of the *ibeART* operon, had no impact on the expression of type 1 fimbriae (Table 4).

In sum, the targeted-gene analysis performed *in vitro*, i.e., in a simple environment, showed the involvement of both H22/H30 FimB and IbeA in early biofilm formation and only that of H22/H30 FimB in the early expression of type 1 fimbriae.

***In vivo* virulence and ExPEC VF gene content of the 39 studied O25b:H4 ST131 strains.** By using a well-calibrated mouse sepsis model (23), we assessed, *in vivo*, a more complex phenotype i.e., the intrinsic extraintestinal virulence, of the 39 strains studied. We found that clade B strains were significantly more virulent than clade C strains (*P* = 2e-10) (Fig. 5). Among the clade B strains (Fig. 6A), no significant difference was

TABLE 3 Colony color and morphotype on Congo red agar plates of the 39 O25b:H4 ST131 *Escherichia coli* strains according to biofilm production phenotype and clade type^a

Group	No. (%) of strains with a positive Congo red test	
	Congo red staining	rdar morphotype
Biofilm ++ (n = 8)	8 (100) ^b	8 (100) ^b
Biofilm +- (n = 16)	1 (6) ^b	1 (6) ^b
Biofilm - (n = 15)	4 (27) ^b	3 (20) ^b
Clade B (n = 19)	9 (47) ^c	9 (47) ^c
Clade C (n = 20)	3 (15) ^c	2 (10) ^c

^a++, early biofilm producer; +-, delayed biofilm producer; -, never biofilm producer; rdar, red, dry, and rough colonies. *P* values were determined by Fisher's exact test.

^b*P* < 0.0001 for the early biofilm producer group versus both the delayed biofilm producer and never biofilm producer groups.

^c*P* < 0.001 for clade B versus clade C.

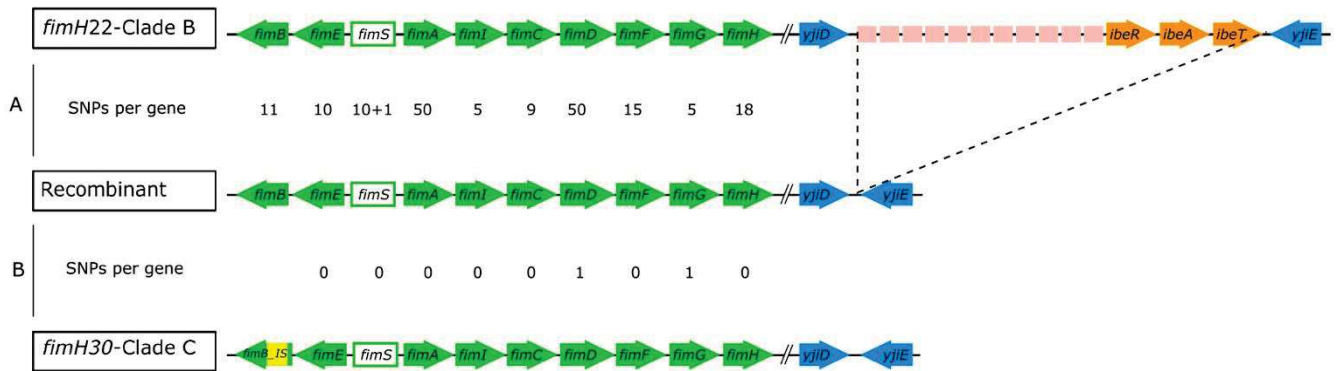


FIG 4 Schematic representation of the *fim* operon and the *gimA* locus in O25b:H4 ST131 *fimH22*-clade B strains, Recombinant, and clade C strains. The genes of the *fim* operon are depicted by green arrows, except for the *fimS* gene, which is an invertible element; those of the *gimA4* operon, including the *ibeART* operon, which are indicated by other arrows; and those of the three other operons of the *gimA* locus, which are indicated by pink rectangles. The dashed lines indicate the deletion of the *gimA* locus in both Recombinant and the clade C strains. Yellow indicates the *ISEc55* insertion within the *fimB* gene of all clade C strains. (A) Comparison between *fimH22*-clade B strains based on the *fim* operon of a B1 subclade strain (strain S250) and Recombinant (B4 subclade). (B) Comparison between Recombinant and clade C strains based on the operon of a C1 subclade strain (CES164C). SNPs, single nucleotide polymorphisms; +1, the presence of a gap.

observed between the strains of each subclade except for B3 subclade strains, which killed mice significantly faster than those of B4 subclade ($P = 0.02$). Among the clade C strains (Fig. 6B), the C0 subclade strains were significantly more virulent than those of the C1 subclade ($P = 5e-09$) and C2 subclade ($P = 6e-05$), while there was no significant difference between those of the C1 and C2 subclades.

Considering the described association between virulence assessed in mouse sepsis models and the number of genes encoding ExPEC virulence factors (VFs) (24, 25), we analyzed the distribution of the ExPEC VF-encoding genes in the 39 strains. The average number of VF-encoding genes was higher in clade B strains (16.2 ± 2.4) than in clade C strains (13.3 ± 1.3) ($P = 4e-07$) (Table 5). The *hlyF*, *cdtB*, *iroN*, *kpsMIII*, *cvaC*, *iss*, and *ibeA* genes were significantly more frequent among clade B strains than among clade C strains, whereas the opposite was found for the *sat* gene (Table 5). Within clade B, there was no significant difference between the mean number of VF genes of the

TABLE 4 Yeast agglutination test applied to B1 subclade strain S250 (MT Divergent) and its mutants, B4 subclade strain CES131 (Recombinant) and its mutant, and C1 subclade strain CES164 (Emergent)

Strain	Yeast agglutination test result ^a			
	Shaking growth			
	Early test ^b			Static growth, standard test at 24 h
At 2 h	At 5 h	Standard test at 24 h		
S250	++++	++++	+++	++++
S250 Δ <i>fimB</i> :: <i>kan</i>	-	-	-	-
S250 Δ <i>fimB</i> ::FRT/pSC-AS250 <i>fimB</i>	++++	++++	+++	+++
S250 Δ <i>fimB</i> :: FRT/pSC-A	-	-	-	-
S250 Δ <i>ibeA</i> :: <i>kan</i>	++++	++++	+++	++++
S250 Δ <i>fimB</i> ::FRT Δ <i>ibeA</i> :: <i>kan</i>	-	-	-	-
S250 Δ <i>ibeART</i> :: <i>kan</i>	++++	++++	+++	++++
S250 Δ <i>fimB</i> ::FRT Δ <i>ibeART</i> :: <i>kan</i>	-	-	-	-
CES131C	-	+	-	++++
CES131C Δ <i>fimB</i> :: <i>kan</i>	-	-	-	+++
CES131C Δ <i>fimB</i> ::FRT/pSC-ACES131C <i>fimB</i>	++	+++	+++	++++
CES131C Δ <i>fimB</i> ::FRT/pSC-A	-	+	-	+++
CES164C	-	-	-	+++
Positive control (<i>E. coli</i> UT189)	+++	+++	+++	+++
Negative control (<i>E. coli</i> UBA83972)	-	-	-	-

^aThe yeast agglutination test was positive when agglutination appeared within 3 min. +++++, fast appearance of agglutination with thick aggregations; +++, fast appearance of agglutination with fine aggregations; ++, slow appearance of agglutination with thick aggregations; +, slow appearance of agglutination with fine aggregations; -, no agglutination.

^bThe early test was always negative under static growth conditions (data not shown).

TABLE 5 Main virulence factor-encoding genes in the 39 O25b:H4 ST131 *Escherichia coli* strains, by clade

Gene	No. (%) of strains			P value ^a for clade B vs clade C
	Total (n = 39)	Clade B (n = 19)	Clade C (n = 20)	
Adhesin				
<i>yfcV</i>	39 (100)	19	20	
<i>fimH</i>	39 (100)	19	20	
<i>papAH</i>	2 (5)	2	0	
<i>papC</i>	2 (5)	2	0	
<i>papEF</i>	3 (8)	2	1	
<i>sfa</i> and <i>foc</i>	1 (3)	0	1	
<i>afa</i> and <i>dra</i>	8 (21)	6	2	
Toxin				
<i>hlyA</i>	0	0	0	
<i>hlyF</i>	10 (26)	10	0	0.0002
<i>cnf1</i>	0	0	0	
<i>cdtB</i>	7 (18)	7	0	0.003
<i>sat</i>	25 (64)	7	18	0.0008
<i>vat</i>	0	0	0	
<i>tsh</i>	1 (3)	1	0	
Iron uptake				
<i>iroN</i>	10 (26)	10	0	0.0002
<i>fyuA</i>	39 (100)	19	20	
<i>iutA</i>	32 (82)	14	19	
<i>iucD</i>	32 (82)	14	19	
<i>irp2</i>	39 (100)	19	20	
<i>chuA</i>	39 (100)	19	20	
Capsule				
<i>kpsMIII</i>	33 (85)	19	14	0.02
<i>kpsMIII</i>	0	0	0	
<i>K1</i>	3 (8)	3	0	
<i>K2</i>	0	0	0	
<i>K5</i>	30 (77)	16	14	
Miscellaneous				
<i>iss</i> type 1	11 (28)	11	0	0.00005
<i>traT</i>	36 (92)	17	19	
<i>cvaC</i>	5 (13)	5	0	0.02
<i>ibeA</i>	17 (44)	17	0	3×10^{-9}
<i>usp</i>	39 (100)	19	20	
<i>ompT</i>	39 (100)	19	20	
<i>malX</i>	39 (100)	19	20	
Mean \pm SD VF ^b	14.9 \pm 2.5	16.6 \pm 2.4	13.3 \pm 1.3	0.000004

^aP values (shown when they were <0.05) were obtained by Fisher's exact test for the gene distribution comparison between clades and by the Wilcoxon rank-sum test for the VF mean comparison.

^bVF, virulence factor-encoding gene.

strains of the different B subclades, except for those belonging to the B3 subclade, which displayed a higher mean number of VF genes than those belonging to the B4 subclade ($P < 0.05$) (data not shown). Within clade C, there was no significant difference either between the C1 and C2 subclade strains or between those of the C0 and C2 subclades, but there was a significant difference between those of C0 and C1 subclades, with the C0 subclade strains having a higher mean number of VF genes ($P = 0.03$) (data not shown). Among the four main VF-based virotypes (virotypes A, B, C and D) previously described for O25b:H4 ST131 (26), we found that virotypes D and C were significantly associated with clade B and clade C strains, respectively ($P < 0.00001$), and that two B4 subclade strains (including Recombinant), one C1 subclade strain, and three C2 subclade strains displayed previously undescribed virotypes (Table 1).

In sum, clade B strains displayed a higher *in vivo* virulence than clade C strains in a mouse sepsis model in relation to a greater number of VFs.

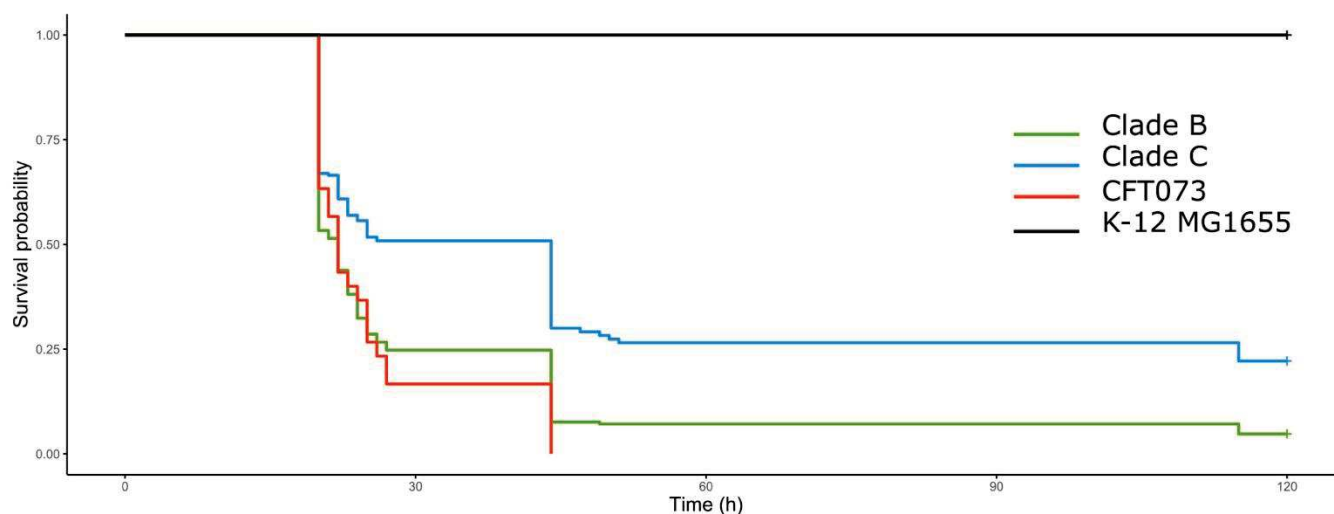


FIG 5 Kaplan-Meier survival curves of mice with sepsis due to the 39 O25b:H4 ST131 *Escherichia coli* strains studied, by clade. Clade B and C strains and controls (positive control, strain CFT073; negative control, strain K-12 MG1655) are represented by different colored lines. Clade B strains (210 mice) killed mice significantly faster than clade C strains (230 mice) ($P = 2e-10$).

Selection of strains for further *in vivo* experiments. To go deeper into the differences observed in the *in vitro* and *in vivo* virulence phenotypes between clades B and C, we selected three strains that allowed us to test (i) gene inactivation and (ii) other relevant *in vivo* mouse model complex phenotypes. Thus, within clade B, we selected strain S250, belonging to the B1 subclade, whose fitness had already been assessed in *Caenorhabditis elegans* and zebrafish models (27) and *in vitro* (28) and which corresponded, in our collection, to one of the two most anciently diverged strains. We called this strain “MT Divergent,” where MT stands for “the most.” Among the C1 and C2 subclade strains that did not show significant differences with regard to early biofilm formation, the mean number of VF genes, and mouse lethality, we selected C1 subclade strain CES164C, which we called “Emergent.” We also retained Recombinant. Table 6 presents the major characteristics displayed by these three strains. To assess *in vivo* the potential role of the *fimB* gene and the *ibeART* operon, we retained the $\Delta fimB::kan$, $\Delta ibeART::kan$, and $\Delta fimB::FLP$ recombination target (FRT) $\Delta ibeART::kan$ mutants of MT Divergent and the $\Delta fimB::kan$ mutant of Recombinant.

Competition assays in mouse models of sepsis, intestinal colonization, and urinary tract infection (UTI). Before performing competition assays between MT Divergent, Emergent, and Recombinant and between parental strains and mutants in the mouse sepsis model, we checked their virulence phenotype in this model in a mono-infection (Fig. S3). MT Divergent killed mice faster than Emergent ($P = 0.04$) but not than Recombinant ($P = 0.8$), whereas Recombinant and Emergent did not kill mice differently ($P = 0.06$) (Fig. S3A). There was no significant difference either between MT Divergent and its $\Delta fimB::kan$, $\Delta ibeART::kan$, and $\Delta fimB::FRT \Delta ibeART::kan$ mutants or between Recombinant and its $\Delta fimB::kan$ mutant (Fig. S3B).

In competition assays performed in the mouse sepsis model, MT Divergent outcompeted both Recombinant ($P = 0.002$) and Emergent ($P = 0.002$) and Recombinant outcompeted Emergent ($P = 0.002$) (Fig. 7). MT Divergent did not outcompete its $\Delta fimB::kan$ mutant, whereas Recombinant outcompeted its $\Delta fimB::kan$ mutant ($P = 0.004$) (Fig. 7). Inversely, MT Divergent outcompeted its $\Delta ibeART::kan$ ($P = 0.01$) and $\Delta fimB::FRT \Delta ibeART::kan$ ($P = 0.002$) mutants (Fig. 7). Neither the kanamycin resistance cassette $\Delta fimB$ ($P = 0.3$) nor the kanamycin resistance cassette $\Delta ibeART$ ($P = 0.06$) had a cost to *in vivo* virulence in this mouse model (Fig. 7).

Competitions between the three strains as well as between the parental strains and their mutants were also performed in a mouse intestinal colonization model because intestinal colonization is the first step of infection and extraintestinal virulence is a

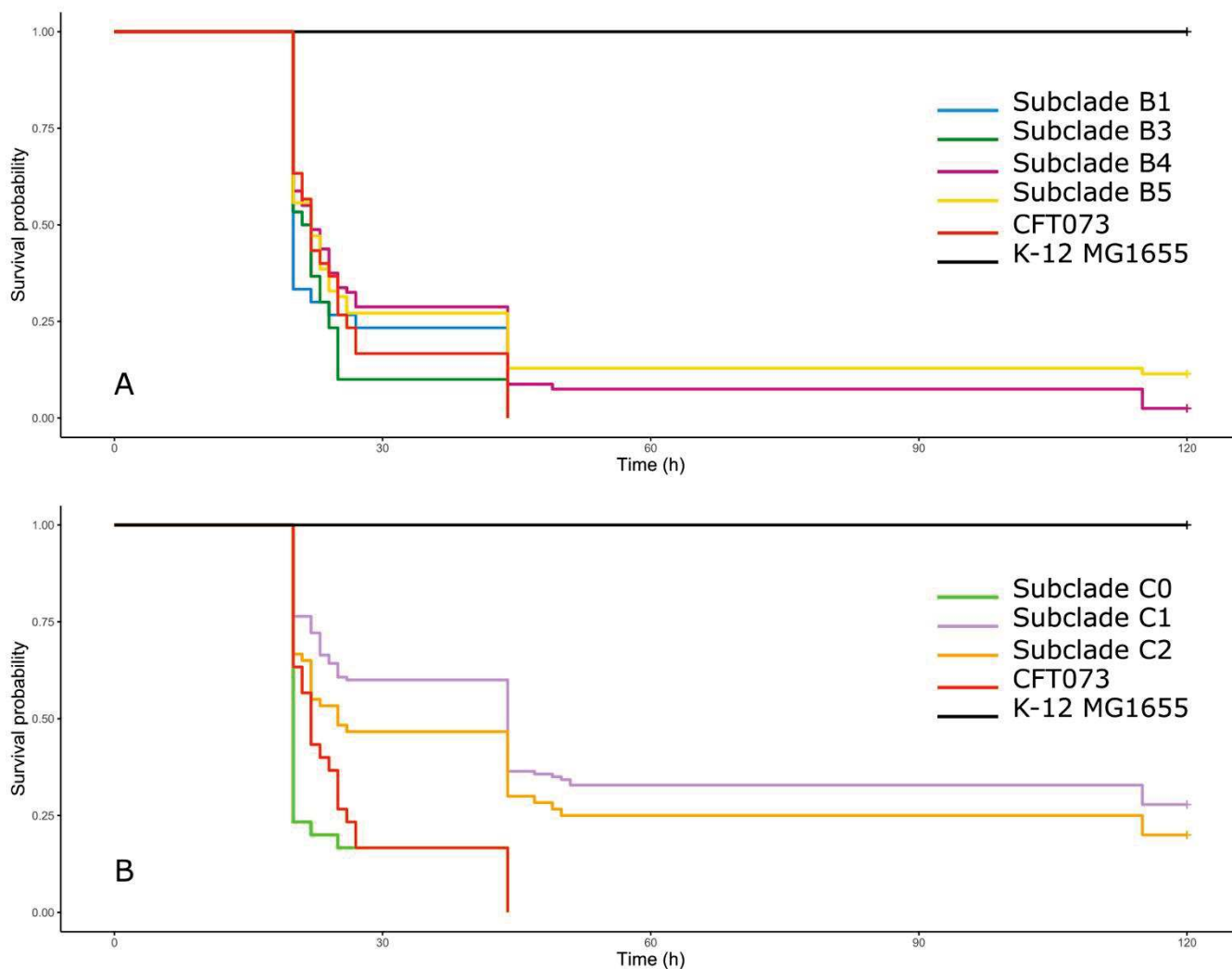


FIG 6 Kaplan-Meier survival curves of mice with sepsis due to the 39 O25b:H4 ST131 *Escherichia coli* strains studied, by subclade. B subclade strains (A), C subclade strains (B), and controls (positive control, strain CFT073; negative control, strain K-12 MG1655) are represented by different colored lines. No significant difference was observed between B1 subclade strains (30 mice) and those of the B3 subclade (30 mice), B4 subclade (80 mice), and B5 subclade (70 mice), whereas B3 subclade strains killed mice significantly faster than those of the B4 subclade ($P = 0.02$). Among the clade C strains, C0 subclade strains (30 mice) killed mice significantly faster than those of the C1 subclade (140 mice) ($P = 5e-09$) and C2 subclade (60 mice) ($P = 6e-05$), while there was no significant difference between the C1 and C2 subclade strains.

coincidental by-product of commensalism in B2 phylogenetic group *E. coli* strains (29). Given that this model requires competitive strains with an equal level of susceptibility to streptomycin and that both MT Divergent and Emergent were susceptible to streptomycin, we used a kanamycin resistance cassette to inactivate the plasmid-mediated *aadA2* gene, encoding streptomycin resistance, in Recombinant. This cassette showed no fitness cost through a competition assay between Recombinant and Recombinant $\Delta aadA2::kan$ under planktonic conditions in LB (data not shown). In this mouse model, we found that MT Divergent outcompeted Emergent ($P = 0.02$) at day 4 and day 7, whereas there was no significant difference at any time point between MT Divergent and Recombinant or between Recombinant and Emergent (Fig. 8). There was also no significant difference between the mutants and their parental strains, i.e., the $\Delta fimB::kan$, $\Delta ibeART::kan$, and $\Delta fimB::FRT \Delta ibeART::kan$ mutants for MT Divergent and the $\Delta fimB::kan$ mutant for Recombinant (Fig. 8).

Finally, we put MT Divergent, Recombinant, and Emergent in competition in the mouse UTI model, knowing that clade C strains have frequently been identified among uropathogenic *E. coli* (UPEC) strains (7). We found that MT Divergent outcompeted

TABLE 6 Comparative characteristics of the three O25b:H4 *Escherichia coli* strains selected for competition assays^a

Strain	MGR (h ⁻¹)	Colicin/phage production	Biofilm formation phenotype	Time (h) of type 1 fimbria expression	Congo red assay phenotype	Antibiotic resistance-encoding genes	No. of VF-encoding genes ^b	No. of ExPEC VF-encoding genes	<i>fim</i> operon type	<i>gimA</i> locus
MT Divergent (B1 subclade S250)	1.35 ± 0.06	No	Early	2 ^c	rdar		53	14	H22	+
Emergent (C1 subclade CES164C)	1.48 ± 0.06	No	Never	24 ^d	Red staining	<i>bla_{TEM}</i> , <i>gyrA1AB</i> , <i>parC1aAB</i>	52	13	H30	-
Recombinant (B4 subclade CES131C)	1.47 ± 0.09	No	Delayed	5 ^d	White staining	<i>bla_{TEM}</i> , <i>aac(3)-IId</i> , <i>aadA2</i> , <i>mph(A)</i> , <i>sulI</i> , <i>tet(A)</i> , <i>dfpA12</i>	63	15	H30	-

^aVF, virulence factor; rdar, red, dry, and rough; +, present.

^bSee Fig. S2 in the supplemental material for details.

^cWith shaking growth.

^dWith static growth.

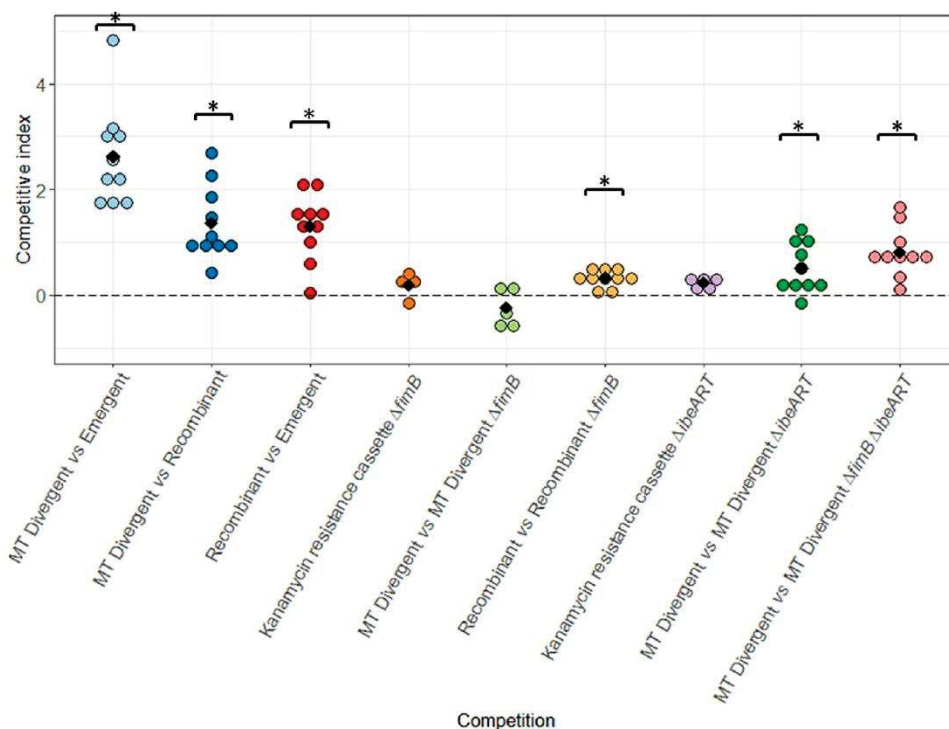


FIG 7 Competitions between MT Divergent, Recombinant, and Emergent and between MT Divergent and its mutants and Recombinant and its mutant in the mouse sepsis model. Competitions were determined by the spleen bacterial load. The competitive index (CI) is expressed in log. A CI above 0 means that the isolate cited first in the legend outcompetes the one cited second, and a CI below 0 means that the isolate cited second outcompetes the one cited first. Each dot represents one mouse, and different colors were attributed to the different competitions. Black diamonds depict the mean values of CI. MT Divergent outcompeted Emergent ($P = 0.002$) and Recombinant ($P = 0.002$), and Recombinant outcompeted Emergent ($P = 0.002$). Before performing competitions between the parental strains and their mutant(s), we checked that the kanamycin resistance cassette introduced in the targeted gene did not have any cost: kanamycin resistance cassette Δ *fimB* (competition between MT Divergent Δ *fimB*:FRT versus MT Divergent Δ *fimB*::*kan* and Recombinant Δ *fimB*:FRT versus Recombinant Δ *fimB*::*kan*, $P = 0.2$) and kanamycin resistance cassette Δ *ibeART* (competition between MT Divergent Δ *ibeART*:FRT versus MT Divergent Δ *ibeART*::*kan*: and MT Divergent Δ *fim*:FRT Δ *ibeART*:FRT versus MT Divergent Δ *fimB*:FRT Δ *ibeART*::*kan*, $P = 0.062$). *, significant difference generated by the Wilcoxon signed-rank test. MT Divergent did not outcompete MT Divergent Δ *fimB*::*kan* ($P = 0.3$), whereas Recombinant outcompeted Recombinant Δ *fimB*::*kan* ($P = 0.004$). MT Divergent outcompeted both MT Divergent Δ *ibeART*::*kan* ($P = 0.001$) and MT Divergent Δ *fimB*:FRT Δ *ibeART*::*kan* ($P = 0.002$).

Emergent in the bladder ($P = 0.004$) and the kidneys ($P = 0.004$) and that Recombinant outcompeted Emergent in the bladder ($P = 0.008$) but not in the kidneys ($P = 0.13$), whereas there was no significant difference between MT Divergent and Recombinant either in the bladder ($P = 0.08$) or in the kidneys ($P = 0.05$) (Fig. 9). In sum, MT Divergent outcompeted Emergent regardless of the mouse model used.

DISCUSSION

To find out the factors other than multidrug resistance that could have favored the dissemination of *E. coli* O25b:H4 ST131 clade C, we used an original approach based on phenotypic comparisons of clade B and clade C strains. To this end, we established an O25b:H4 ST131 collection composed of clade B ($n = 19$) and clade C ($n = 20$) strains belonging to the various B and C subclades. However, in this collection, we found a B4 subclade strain with a *fimH30* allele (called "Recombinant"), a peculiar feature previously found in another B4 subclade strain (5). Here, we clarified that Recombinant shared with clade C not only the same *fim* operon (however, it lacked the ISEc55 sequence always found in the clade C *fimB* gene) but also a deletion of the *gimA* locus, including the *ibeART* operon. This suggests that identical genetic events had occurred in clades B and C but, apparently, with a lower adaptive success in the genetic background of clade B than in that of clade C.

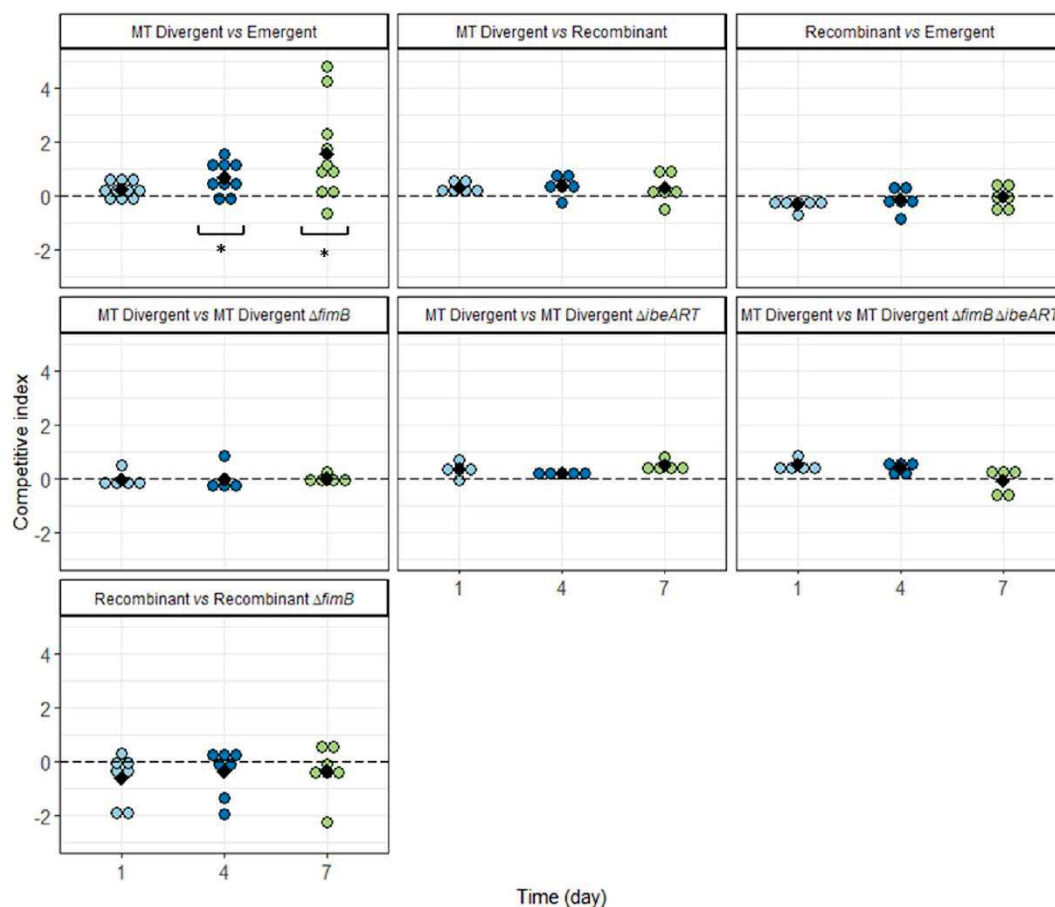


FIG 8 Competitions between MT Divergent, Recombinant, and Emergent and between MT Divergent and its mutants and Recombinant and its mutant in the mouse gut colonization model. Competitions were determined by the fecal bacterial load. The competitive index (CI) is expressed in log. A CI above 0 means that the isolate cited first in the legend outcompetes the one cited second, and a CI below 0 means that the isolate cited second outcompetes the one cited first. Each dot represents one mouse, with the different colors indicating the time period, as follows: light blue, day 1 postinoculation; dark blue, day 4 postinoculation; green, day 7 postinoculation. Black diamonds depict the mean values of CI. All mutants harbored the *kan* gene of the kanamycin resistance cassette. *, significant difference generated by the Wilcoxon signed-rank test and corrected for multiple comparisons by the Benjamini-Hochberg procedure. MT Divergent outcompeted Emergent at both day 4 ($P = 0.01$) and day 7 ($P = 0.001$), whereas the other competitions were not significant (P values, between 1 and 0.09, according to the two strain types in the competition and the competition day).

In all but one (MGR in LB) phenotypic experiment applied to the 39 strains, we found that clade B had a significantly higher virulence and competitive ability than clade C, and the level of these features for Recombinant was intermediate between those of *fimH22*-clade B and clade C strains. This indicated that, despite the same ability to grow under optimal conditions *in vitro*, the strains behaved differently in more complex environments more closely related to the normal niches of *E. coli* ST131.

We confirmed that the early biofilm production phenotype, which is a property displayed by <10% of ExPEC strains belonging to few *E. coli* lineages (19), was always displayed by clade B strains and never by clade C strains (19, 28). By using the MT Divergent $\Delta H22$ -*fimB* and Recombinant $\Delta H30$ -*fimB* mutants, we showed that biofilm formation and type 1 fimbriae expression during the first 5 h of incubation require a functional *fimB* gene. We also showed that the Recombinant $H30$ - Δ *fimB* mutant required, like Emergent, at least 24 h of growth under static conditions to express type 1 fimbriae, whereas the MT Divergent $\Delta H22$ -*fimB* mutant was unable to express these fimbriae at 24 h under both shaking and static conditions. All these findings strongly suggest that the presence of the *ISEc55* sequence in the *fimB* gene of clade C strains contributes to their incapacity to form a biofilm early and express type 1 fimbriae

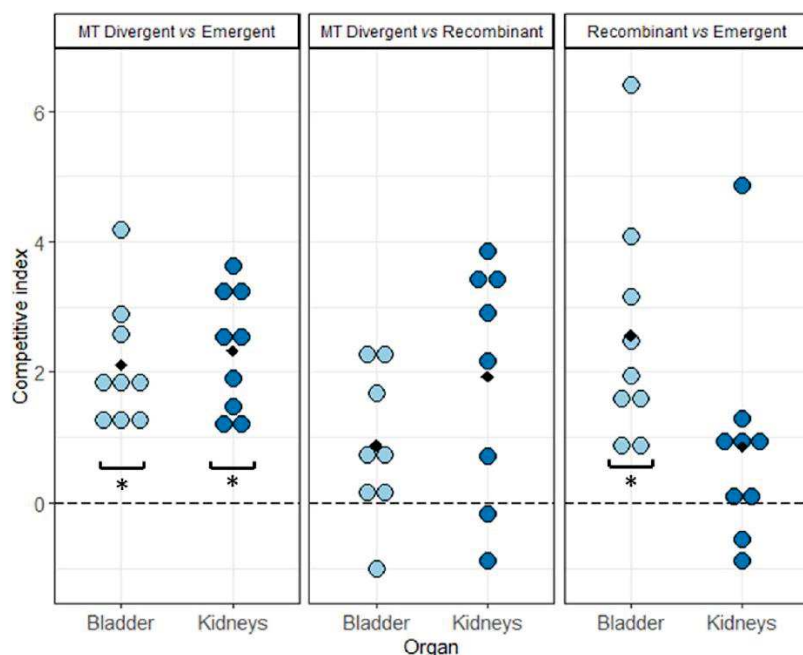


FIG 9 Competitions between MT Divergent, Recombinant, and Emergent in the mouse urinary tract infection model. Competitions were determined by the bladder and kidney bacterial loads. Each dot represents one mouse, with the different colors indicating the organs tested; light blue for urine and dark blues for the kidneys. The competitive index (CI) is expressed in log. A CI above 0 means that the isolate cited first in the legend outcompetes the one cited second, and a CI below 0 means that the isolate cited second outcompetes the one cited first. Black diamonds depict the mean values of CI. *, significant difference generated by the Wilcoxon signed-rank test. MT Divergent outcompeted Emergent in the bladder ($P = 0.004$) and the kidneys ($P = 0.004$), whereas it did not outcompete Recombinant either in the bladder ($P = 0.08$) or in the kidneys ($P = 0.05$). Recombinant outcompeted Emergent in the bladder ($P = 0.004$) but not in the kidneys ($P = 0.13$).

before 24 h of incubation and that, in addition to the genetic differences between the two *fim* operon types, there could be differences in their regulation. Our results for type 1 fimbria expression by Emergent and other clade C strains are concordant with those found by Totsika et al. with clade C strain EC958 and other O25b:H4 ST131 strains harboring the ISEc55 sequence in the *fimB* gene (21). Using a mouse UTI model, these authors showed that strain EC958 colonized the bladder when type 1 fimbria expression was strong and persisted in urine when it was weak (21). On the other hand, Gunther et al., also through competition assays in a mouse UTI model between a wild-type CFT073 strain and mutants expressing their type 1 fimbriae only weakly or strongly, concluded that type 1 fimbria phase variation contributes significantly to virulence early (24 h postinoculation) in the 76-h course of the mouse UTI and profoundly influences colonization of the bladder (30). Our competition assays, performed in the same mouse UTI model as that used in the cited studies, showed that MT Divergent outcompeted Emergent in the bladder and the kidneys. These *in vivo* results, combined with those that we obtained *in vitro*, strongly suggest that the early expression of type 1 fimbriae allows clade B to quickly cause bladder colonization and pyelonephritis, while clade C requires more time to have a functional temporal on/off regulation of type 1 fimbria expression in a link to bladder colonization and urine persistence, respectively, as described for multiple UPEC strains by Schwan and Ding (31). In short, the loss of early expression of type 1 fimbriae by clade C strains makes them classical phylogroup B2 UPEC strains with, however, a peculiar trait, i.e., antibiotic and even multiantibiotic resistance (32).

The other major significant phenotypic differences between clade B and clade C consisted of a higher VF score and faster killing of mice by clade B than by clade C. This result is in accordance with the results of previous studies that showed the association

between virulence, as assessed in mouse sepsis models, and the number of VFs (24, 25). Within clade B, B3 subclade strains had both higher VF scores and a higher *in vivo* virulence than B4 subclade strains, whereas within clade C, C0 subclade strains had higher VF scores and a higher *in vivo* virulence than either C1 or C2 subclade strains, but this difference was not found between C1 and C2 subclade strains. Making comparisons between our results and those previously obtained with the same mouse sepsis model is difficult because the previous studies used only surrogates of clade B and clade C strains (strains with susceptibility to fluoroquinolones, *fimH30* versus non-*fimH30* alleles, and virotypes) (33–35). Using well-characterized strains, as we did, permitted the various levels of *in vivo* virulence between and within the clades and subclades of O25b:H4 ST131 to be deciphered.

We performed a genome-wide association study (GWAS) using Scoary software (36), which assesses the association between the presence/absence of genes and *in vivo* virulence in the mouse sepsis assay, but did not obtain any significant hit over the 17,951 tested genes (data not shown). This failure could have been due to the small number of strains tested; the limited genetic variability of the strains, all of which belonged to a single *E. coli* lineage (37); or an *in vivo* virulence resulting from VF cooperation in an additive manner to achieve extraintestinal virulence (25). However, targeted-gene analyses performed in competition assays in the mouse sepsis model showed that the *H30-fimB* gene was associated with the *in vivo* virulence of Recombinant and the *ibeART* operon was associated with that of MT Divergent. These results, together with those showing that MT Divergent outcompeted both Recombinant and Emergent and that Recombinant outcompeted Emergent in the mouse sepsis model, strongly suggest that the absence of the *ibeART* operon in Recombinant and clade C and the nonfunctionality of the *H30-fimB* gene in clade C may have contributed to the gradually lower levels of *in vivo* virulence displayed by Recombinant and Emergent in the mouse sepsis model.

As competition assays provide more evidence than assays with single strains of the difference in fitness of only a few percentage points, indicating stronger differences, we used only competition assays to study more thoroughly three representative strains (i.e., MT Divergent, Recombinant, and Emergent) in a mouse model of sepsis, gut colonization, and UTI. In all competition assays, Emergent was outcompeted by MT Divergent regardless of the mouse ecological niches, whereas it was outcompeted by Recombinant, depending on the niches: it was outcompeted in the blood and partially outcompeted in the urinary tract (in the bladder but not in the kidneys) but was not outcompeted in the gut. Such features may suggest an adaptation to ecological niches within the ST131 lineage, as assessed by McNally et al. (14).

In conclusion, by measuring several simple and more complex phenotypes, we highlighted the lower level of virulence of clade C strains than of clade B strains, what had previously been suggested in the zebrafish model (27).

It may appear to be surprising that the clade most disseminated worldwide, i.e., ST131 clade C, displays attenuated virulence. We propose two explanations for its widespread dissemination. First, the resistance to fluoroquinolones displayed by clade C may come at a direct cost (38). This cost would not be revealed in the MGR under planktonic conditions but would manifest *in vivo*, as suggested here in various mouse models. In spite of this cost, antibiotic resistance allowed clade C to spread. Second, the lower virulence may actually confer an additional evolutionary advantage to clade C. According to the trade-off theory (39), host exploitation by a pathogen evolves to an optimal level under a balance between the benefits in terms of transmission and the costs in terms of host mortality (40). Thus, lower virulence could confer improved fitness overall by avoiding severe infections (41, 42), even if it comes at the cost of a lower colonization ability.

Whether the phenotypic clade B and clade C differences represent a cost, in spite of which clade C is successful, or an additional adaptation remains an open question that requires further work, especially as the *in vivo* behavior of fluoroquinolone-susceptible Recombinant favors the additional adaptation hypothesis.

MATERIALS AND METHODS

More technical details for each section of Materials and Methods are available in Text S1 in the supplemental material.

Bacterial strains. The 39 O25b:H4 ST131 *E. coli* strains studied comprised 18 *fimH22* and 21 *fimH30* strains obtained between 1993 and 2012 from different geographic origins and sources (Table S1). The *E. coli* CFT073 and *E. coli* K-12 MG1655 strains were used as positive and negative controls, respectively, in the mouse sepsis model, and the *E. coli* UT189 and *E. coli* UBA83972 strains were used as positive and negative controls, respectively, in the yeast agglutination assays.

Genome sequencing and analysis. Whole-genome sequencing (WGS) of the 39 studied strains was performed (Table S2). All genomes were analyzed for plasmid content and typing (with the Plasmid Finder tool, which showed an identity of >95%, and plasmid multilocus sequence typing [pMLST] [43]). The Abricate tool (44) was used to detect (i) genes encoding antibiotic resistance with the ResFinder program (45) and (ii) genes encoding VF with a custom virulence database composed of VirulenceFinder (46), the virulence factor database (VFDB) (47), and the classical ExPEC VF-encoding genes (19). Virotypes were determined as previously described (26). All contigs were submitted to the MicroScope platform (48) for further gene investigations, such as the investigation of the *gyrA* and *parC* genes. When necessary, the presence or absence of some genes was controlled by PCR.

To assess the different B and C subclades among the 39 collected strains as well as among the 218 bacteremia O25b ST131 *E. coli* strains collected by Kallonen et al. in England between 2001 and 2012 (9), we complemented the genomes of these 257 strains with those of 21 strains representing the genetic diversity of the B and C subclades (5) and constructed a phylogenetic tree from nonrecombinant SNPs of the core genome genes using the maximum likelihood method. To infer the linear trend of the isolates of Kallonen et al. (9) from 2001 to 2012, we fitted a logistic model to the presence/absence of each subclone as a function of time (in years).

Gene deletion and complementation. Replacement by a kanamycin resistance cassette was used to inactivate genes following a strategy adapted from that of Datsenko and Wanner (49). When necessary, the kanamycin resistance-encoding gene of the cassette was eliminated, as previously described (49). $\Delta fimbB::FRT$ and $\Delta libeA::FRT$ mutants were complemented with the parental wild-type gene cloned into pSC-A-amp/kan by using a StrataClone PCR cloning kit (Agilent Technologies, Massy, France). The primers and plasmids used are listed in Tables S3 and S4.

Kinetics of early biofilm formation. The primary step (5 h of incubation) of biofilm formation was measured using the BioFilm ring test (BioFilm Control, Saint-Beauzire, France) according to the manufacturer's recommendations and as previously described (19, 28). The BFI, which had values ranging from 20 (the absence of biofilm formation) to 0 (high level of biofilm formation), is inversely proportional to the biofilm formation ability. A BFI value of 10 was chosen as the biofilm production cutoff (a BFI of ≤ 10 indicates biofilm formation, a BFI of > 10 indicates no biofilm formation).

Expression of type 1 fimbriae. Expression of type 1 fimbriae was assessed by using the yeast (*Saccharomyces cerevisiae*) cell agglutination assay, as previously described (21), and, after adaptations to highlight the early expression of type 1 fimbriae, by using 10 μ l of a pellet obtained after centrifugation (3,000 \times g, 10 min) of 3 ml of LB culture after 2- and 5-h incubations. This test was positive when aggregations appeared within 3 min.

Curli expression and cellulose production. Congo red assays were used to assess curli fimbria expression and cellulose production, as previously described (50). Assay positivity resulted in the red, dry, and rough (rdar) colony morphotype.

Colicin and/or phage production. Colicin and/or phage production in the strains tested was detected as previously described (51) in competition assays.

Maximum growth rate. The maximum growth rate (MGR) assay was performed as previously described (52) in LB by using an automatic spectrophotometer (Tecan Infinite F200 Pro) that measures the optical density at 600 nm in each well every 5 min over a period of 24 h. The experiment was repeated three times. Growth curves were then analyzed, and the MGR was calculated and expressed in hours^{-1} .

Mouse models. (i) Monoinfection assay in the sepsis model. The individual ability of the 39 strains and mutants to cause mouse sepsis was assessed as previously described (53). From 10 to 20 mice were used for each assay. Kaplan-Meier curves of mouse survival were performed.

(ii) Competition assays in sepsis, intestinal colonization, and UTI models. In competition assays, the relative ability of the two strains tested together (i) to cause sepsis was determined from the spleen bacterial load (53), (ii) their relative ability to colonize the intestine mouse was determined from the fecal bacterial load at days 1, 4, and 7 postinoculation (52), and (iii) their relative ability to cause an ascending unobstructed UTI was determined from the bladder and kidney bacterial load (54). From 5 to 10 mice were used for each competition assay. Competitive indexes (CI) were obtained using the following formula: $[(\log \text{ number of CFU of isolate1} / \log \text{ number of CFU of isolate2}) \text{ at } T_x] / [(\log \text{ number of CFU of isolate1} / \log \text{ number of CFU of isolate2}) \text{ at } T_0]$, with isolate1 being the first strain cited in the figure legends, isolate2 being the second one cited in the figure legends, T_x being time x , and T_0 being time zero.

Statistical analysis. The Wilcoxon rank-sum test was used to compare the average number of VF-encoding genes per clade, and Fisher's exact test was used to test the distribution of each VF-encoding gene between the clades. The individual fitness measurement was estimated by used of a mixed model with the random effect on the strain to take into account the triplicate determination. For biofilm data, a two-way repeated-measures analysis of variance, followed by Tukey's range test, when there were three groups, was performed. The association between groups (biofilm phenotypes, yeast

agglutination test, Congo red assay, and virotype assay) was assessed by Fisher's exact test. For *in vivo* competitions, a nonparametric Wilcoxon test on paired data was conducted on CI values, and *P* values were corrected for multiple comparisons by the Benjamini-Hochberg procedure (55), when necessary. Mouse survival differences were determined by the log-rank test. A significance level of <0.05 was used for all tests. All statistical analyses were carried out with R software (56).

Ethics statement. Murine protocols of sepsis, intestinal colonization, and pyelonephritis (protocol numbers APAFIS#4948- and APAFIS#4951-2016020515004032 v2, 2016021216251548 v4, and APAFIS#4950-2016021211417682 v4, respectively) were approved by the French Ministry of Research and by the Ethical Committee for Animal Experiments, CEEA-121, Comité d'éthique Paris-Nord.

Data availability. The raw sequences of the 39 isolates were deposited in GenBank under BioProject accession numbers PRJNA320043 and PRJNA566165.

SUPPLEMENTAL MATERIAL

Supplemental material is available online only.

SUPPLEMENTAL FILE 1, PDF file, 0.2 MB.

SUPPLEMENTAL FILE 2, PDF file, 0.1 MB.

SUPPLEMENTAL FILE 3, PDF file, 0.1 MB.

SUPPLEMENTAL FILE 4, PDF file, 0.2 MB.

SUPPLEMENTAL FILE 5, PDF file, 0.2 MB.

ACKNOWLEDGMENTS

We thank Christophe Beloin for his advice about biofilm exploration. We thank Méric Massot, Marie Vigan, and Cedric Laouénan for their help with statistical analyses. We also thank Olivier Tenaillon and Antoine Bridier-Nahmias for genomic analysis assistance. Finally, we thank Johann Beghain, Mélanie Magnan, Françoise Chau, and Zineb Azzaoui for their technical assistance in this work.

This study was supported by a grant from the project JPI-EC-AMR 2016 with the French Agence Nationale de la Recherche (ANR) as the sponsor (grant number ANR-16-JPEC-0002-04) to M.-H.N.-C. and by the Fondation pour la Recherche Médicale (Equipe FRM 2016, grant number DEQ20161136698) to E.D. S.-C.F.-S. acknowledges the FPU program for her grant (grant FPU15/02644) from the Secretaría General de Universidades, Spanish Ministerio de Educación, Cultura y Deporte.

REFERENCES

- Price LB, Johnston JR, Aziz M, Clabots C, Johnston B, Tchesnokova V, Nordstrom L, Billig M, Chattopadhyay S, Stegger M, Andersen PS, Pearson T, Riddell K, Rogers P, Scholes D, Kahl B, Keim P, Sokurenko EV. 2013. The epidemic of extended-spectrum- β -lactamase-producing *Escherichia coli* ST131 is driven by a single highly pathogenic subclone, H30-Rx. *mBio* 4:e00377-13. <https://doi.org/10.1128/mBio.00377-13>.
- Johnson JR, Tchesnokova V, Johnston B, Clabots C, Roberts PL, Billig M, Riddell K, Rogers P, Qin X, Butler-Wu S, Price LB, Aziz M, Nicolas-Chanoine M-H, Debroy C, Robicsek A, Hansen G, Urban C, Platell J, Trott DJ, Zhanel G, Weissman SJ, Cookson BT, Fang FC, Limaye AP, Scholes D, Chattopadhyay S, Hooper DC, Sokurenko EV. 2013. Abrupt emergence of a single dominant multidrug-resistant strain of *Escherichia coli*. *J Infect Dis* 207:919–928. <https://doi.org/10.1093/infdis/jjs933>.
- Olesen B, Frimodt-Møller J, Leihof RF, Struve C, Johnston B, Hansen DS, Scheutz F, Krogfelt KA, Kuskowski MA, Clabots C, Johnson JR. 2014. Temporal trends in antimicrobial resistance, and virulence-associated traits within the *Escherichia coli* sequence type 131 clonal group and its H30 and H30-Rx subclones, 1968 to 2012. *Antimicrob Agents Chemother* 58:6886–6895. <https://doi.org/10.1128/AAC.03679-14>.
- Petty NK, Ben Zakour NL, Stanton-Cook M, Skippington E, Totsika M, Forde BM, Phan M-D, Gomes Moriel D, Peters KM, Davies M, Rogers BA, Dougan G, Rodríguez-Baño J, Pascual A, Pitout JDD, Upton M, Paterson DL, Walsh TR, Schembri MA, Beatson SA. 2014. Global dissemination of a multidrug resistant *Escherichia coli* clone. *Proc Natl Acad Sci U S A* 111:5694–5699. <https://doi.org/10.1073/pnas.1322678111>.
- Ben Zakour NL, Alsheikh-Hussain AS, Ashcroft MM, Khanh Nhu NT, Roberts LW, Stanton-Cook M, Schembri MA, Beatson SA. 2016. Sequential acquisition of virulence and fluoroquinolone resistance has shaped the evolution of *Escherichia coli* ST131. *mBio* 7:e00347-16. <https://doi.org/10.1128/mBio.00347-16>.
- Matsumura Y, Pitout JDD, Gomi R, Matsuda T, Noguchi T, Yamamoto M, Peirano G, DeVinney R, Bradford PA, Motyl MR, Tanaka M, Nagao M, Takakura S, Ichiyama S. 2016. Global *Escherichia coli* sequence type 131 clade with *bla*_{CTX-M-27} gene. *Emerg Infect Dis* 22:1900–1907. <https://doi.org/10.3201/eid2211.160519>.
- Nicolas-Chanoine M-H, Bertrand X, Madec J-Y. 2014. *Escherichia coli* ST131, an intriguing clonal group. *Clin Microbiol Rev* 27:543–574. <https://doi.org/10.1128/CMR.00125-13>.
- Morales-Barroso I, López-Cerero L, Molina J, Bellido M, Navarro MD, Serrano L, González-Galán V, Praena J, Pascual A, Rodríguez-Baño J. 2017. Bacteraemia due to non-ESBL-producing *Escherichia coli* O25b:H4 sequence type 131: insights into risk factors, clinical features and outcomes. *Int J Antimicrob Agents* 49:498–502. <https://doi.org/10.1016/j.ijantimicag.2016.12.013>.
- Kallonen T, Brodrick HJ, Harris SR, Corander J, Brown NM, Martin V, Peacock SJ, Parkhill J. 2017. Systematic longitudinal survey of invasive *Escherichia coli* in England demonstrates a stable population structure only transiently disturbed by the emergence of ST131. *Genome Res* 27:1437–1449. <https://doi.org/10.1101/gr.216606.116>.
- Blanco J, Mora A, Mamani R, López C, Blanco M, Dahbi G, Herrera A, Blanco JE, Alonso MP, García-Garrote F, Chaves F, Orellana MÁ, Martínez-Martínez L, Calvo J, Prats G, Larrosa MN, González-López JJ, López-Cerero L, Rodríguez-Baño J, Pascual A. 2011. National survey of *Escherichia coli* causing extraintestinal infections reveals the spread of drug-resistant clonal groups O25b:H4-B2-ST131, O15:H1-D-ST393 and CGA-D-ST69 with high virulence gene content in Spain. *J Antimicrob Chemother* 66:2011–2021. <https://doi.org/10.1093/jac/dkr235>.
- Ludden C, Decano AG, Jamrozny D, Pickard D, Morris D, Parkhill J, Peacock SJ, Cormican M, Downing T. 2020. Genomic surveillance of *Escherichia coli* ST131 identifies local expansion and serial replacement of subclones. *Microb Genom* 6:e000352. <https://doi.org/10.1099/mgen.0.000352>.

12. Huseby DL, Pietsch F, Brandis G, Garoff L, Tegehall A, Hughes D. 2017. Mutation supply and relative fitness shape the genotypes of ciprofloxacin-resistant *Escherichia coli*. *Mol Biol Evol* 34:1029–1039. <https://doi.org/10.1093/molbev/msx052>.
13. Johnson TJ, Danzeisen JL, Youmans B, Case K, Llop K, Munoz-Aguayo J, Flores-Figueroa C, Aziz M, Stoessner N, Sokurenko E, Price LB, Johnson JR. 2016. Separate F-type plasmids have shaped the evolution of the H30 subclone of *Escherichia coli* sequence type 131. *mSphere* 1:e00121-16. <https://doi.org/10.1128/mSphere.00121-16>.
14. McNally A, Kallonen T, Connor C, Abudahab K, Aanensen DM, Horner C, Peacock SJ, Parkhill J, Croucher NJ, Corander J. 2019. Diversification of colonization factors in a multidrug-resistant *Escherichia coli* lineage evolving under negative frequency-dependent selection. *mBio* 10:e00644-19. <https://doi.org/10.1128/mBio.00644-19>.
15. Billard-Pomares T, Clermont O, Castellanos M, Magdoud F, Royer G, Condamine B, Fouteau S, Barbe V, Roche D, Cruveiller S, Médigue C, Pognard D, Glodt J, Dion S, Rigal O, Picard B, Denamur E, Branger C. 2019. The arginine deiminase operon is responsible for a fitness trade-off in extended-spectrum- β -lactamase-producing strains of *Escherichia coli*. *Antimicrob Agents Chemother* 63:e00635-19. <https://doi.org/10.1128/AAC.00635-19>.
16. Leflon-Guibout V, Blanco J, Amaqdouf K, Mora A, Guize L, Nicolas-Chanoine M-H. 2008. Absence of CTX-M enzymes but high prevalence of clones, including clone ST131, among fecal *Escherichia coli* isolates from healthy subjects living in the area of Paris, France. *J Clin Microbiol* 46:3900–3905. <https://doi.org/10.1128/JCM.00734-08>.
17. Clermont O, Couffignal C, Blanco J, Menétré F, Picard B, Denamur E, COLIVILLE and COLIBAFI Groups. 2017. Two levels of specialization in bacteriophage *Escherichia coli* strains revealed by their comparison with commensal strains. *Epidemiol Infect* 145:872–882. <https://doi.org/10.1017/S0950268816003010>.
18. Saadi S, Maas WK, Hill DF, Bergquist PL. 1987. Nucleotide sequence analysis of RepFIC, a basic replicon present in IncFI plasmids P307 and F, and its relation to the RepA replicon of IncFII plasmids. *J Bacteriol* 169:1836–1846. <https://doi.org/10.1128/jb.169.5.1836-1846.1987>.
19. Flament-Simon S-C, Duprilot M, Mayer N, García V, Alonso MP, Blanco J, Nicolas-Chanoine M-H. 2019. Association between kinetics of early biofilm formation and clonal lineage in *Escherichia coli*. *Front Microbiol* 10:1183. <https://doi.org/10.3389/fmicb.2019.01183>.
20. Fronzes R, Remaut H, Waksman G. 2008. Architectures and biogenesis of non-flagellar protein appendages in Gram-negative bacteria. *EMBO J* 27:2271–2280. <https://doi.org/10.1038/emboj.2008.155>.
21. Totsika M, Beatson SA, Sarkar S, Phan M-D, Petty NK, Bachmann N, Szubert M, Sidjabat HE, Paterson DL, Upton M, Schembri MA. 2011. Insights into a multidrug resistant *Escherichia coli* pathogen of the globally disseminated ST131 lineage: genome analysis and virulence mechanisms. *PLoS One* 6:e26578. <https://doi.org/10.1371/journal.pone.0026578>.
22. Cortes MAM, Gibon J, Chanteloup NK, Moulin-Schouleur M, Gilot P, Germon P. 2008. Inactivation of *ibeA* and *ibeT* results in decreased expression of type 1 fimbriae in extraintestinal pathogenic *Escherichia coli* strain BEN2908. *Infect Immun* 76:4129–4136. <https://doi.org/10.1128/IAI.00334-08>.
23. Johnson JR, Clermont O, Menard M, Kuskowski MA, Picard B, Denamur E. 2006. Experimental mouse lethality of *Escherichia coli* isolates, in relation to accessory traits, phylogenetic group, and ecological source. *J Infect Dis* 194:1141–1150. <https://doi.org/10.1086/507305>.
24. Picard B, Garcia JS, Gouriou S, Duriez P, Brahimi N, Bingen E, Elion J, Denamur E. 1999. The link between phylogeny and virulence in *Escherichia coli* extraintestinal infection. *Infect Immun* 67:546–553. <https://doi.org/10.1128/IAI.67.2.546-553.1999>.
25. Tourret J, Diard M, Garry L, Matic I, Denamur E. 2010. Effects of single and multiple pathogenicity island deletions on uropathogenic *Escherichia coli* strain 536 intrinsic extra-intestinal virulence. *Int J Med Microbiol* 300:435–439. <https://doi.org/10.1016/j.ijmm.2010.04.013>.
26. Dahbi G, Mora A, Mamani R, López C, Alonso MP, Marzoa J, Blanco M, Herrera A, Viso S, García-Garrote F, Tchesnokova V, Billig M, de la Cruz F, de Toro M, González-López JJ, Prats G, Chaves F, Martínez-Martínez L, López-Cerezo L, Denamur E, Blanco J. 2014. Molecular epidemiology and virulence of *Escherichia coli* O16:H5-ST131: comparison with H30 and H30-Rx subclones of O25b:H4-ST131. *Int J Med Microbiol* 304:1247–1257. <https://doi.org/10.1016/j.ijmm.2014.10.002>.
27. Lavigne J-P, Vergunst AC, Goret L, Sotto A, Combescure C, Blanco J, O'Callaghan D, Nicolas-Chanoine M-H. 2012. Virulence potential and genomic mapping of the worldwide clone *Escherichia coli* ST131. *PLoS One* 7:e34294. <https://doi.org/10.1371/journal.pone.0034294>.
28. Nicolas-Chanoine M-H, Petitjean M, Mora A, Mayer N, Lavigne J-P, Boulet O, Leflon-Guibout V, Blanco J, Hocquet D. 2017. The ST131 *Escherichia coli* H22 subclone from human intestinal microbiota: comparison of genomic and phenotypic traits with those of the globally successful H30 subclone. *BMC Microbiol* 17:71. <https://doi.org/10.1186/s12866-017-0984-8>.
29. Le Gall T, Clermont O, Gouriou S, Picard B, Nassif X, Denamur E, Tenaillon O. 2007. Extraintestinal virulence is a coincidental by-product of commensalism in B2 phylogenetic group *Escherichia coli* strains. *Mol Biol Evol* 24:2373–2384. <https://doi.org/10.1093/molbev/msm172>.
30. Gunther NW, Snyder JA, Lockett V, Blomfield J, Johnson DE, Mobley HLT. 2002. Assessment of virulence of uropathogenic *Escherichia coli* type 1 fimbrial mutants in which the invertible element is phase-locked on or off. *Infect Immun* 70:3344–3354. <https://doi.org/10.1128/IAI.70.7.3344-3354.2002>.
31. Schwan WR, Ding H. 2017. Temporal regulation of *fim* genes in uropathogenic *Escherichia coli* during infection of the murine urinary tract. *J Pathog* 2017:8694356. <https://doi.org/10.1155/2017/8694356>.
32. Bricse S, Diancourt L, Laouénan C, Vigan M, Caro V, Arlet G, Drioux L, Leflon-Guibout V, Menétré F, Jarlier V, Nicolas-Chanoine M-H, Coli β Study Group. 2012. Phylogenetic distribution of CTX-M- and non-extended-spectrum- β -lactamase-producing *Escherichia coli* isolates: group B2 isolates, except clone ST131, rarely produce CTX-M enzymes. *J Clin Microbiol* 50:2974–2981. <https://doi.org/10.1128/JCM.00919-12>.
33. Johnson JR, Porter SB, Zhanel G, Kuskowski MA, Denamur E. 2012. Virulence of *Escherichia coli* clinical isolates in a murine sepsis model in relation to sequence type ST131 status, fluoroquinolone resistance, and virulence genotype. *Infect Immun* 80:1554–1562. <https://doi.org/10.1128/IAI.06388-11>.
34. Mora A, Dahbi G, López C, Mamani R, Marzoa J, Dion S, Picard B, Blanco M, Alonso MP, Denamur E, Blanco J. 2014. Virulence patterns in a murine sepsis model of ST131 *Escherichia coli* clinical isolates belonging to serotypes O25b:H4 and O16:H5 are associated to specific virotypes. *PLoS One* 9:e87025. <https://doi.org/10.1371/journal.pone.0087025>.
35. Merino I, Porter SB, Johnston B, Clabots C, Thuras P, Ruiz-Garbajosa P, Cantón R, Johnson JR. 2020. Molecularly defined extraintestinal pathogenic *Escherichia coli* status predicts virulence in a murine sepsis model better than does virotype, individual virulence genes, or clonal subset among *E. coli* ST131 isolates. *Virulence* 11:327–336. <https://doi.org/10.1080/21505594.2020.1747799>.
36. Brynildsrud O, Bohlin J, Scheffer L, Eldholm V. 2016. Rapid scoring of genes in microbial pan-genome-wide association studies with Scoary. *Genome Biol* 17:238. <https://doi.org/10.1186/s13059-016-1108-8>.
37. Galardini M, Clermont O, Baron A, Busby B, Dion S, Schubert S, Beltrao P, Denamur E. 2020. Major role of iron uptake systems in the intrinsic extra-intestinal virulence of the genus *Escherichia* revealed by a genome-wide association study. *bioRxiv* 712034. <https://doi.org/10.1101/712034>.
38. Basra P, Alsaadi A, Bernal-Astrain G, O'Sullivan ML, Hazlett B, Clarke LM, Schoenrock A, Pitre S, Wong A. 2018. Fitness tradeoffs of antibiotic resistance in extraintestinal pathogenic *Escherichia coli*. *Genome Biol Evol* 10:667–679. <https://doi.org/10.1093/gbe/evy030>.
39. Anderson RM, May RM. 1982. Coevolution of hosts and parasites. *Parasitology* 85(Pt 2):411–426. <https://doi.org/10.1017/s0031182000055360>.
40. Diard M, Hardt W-D. 2017. Evolution of bacterial virulence. *FEMS Microbiol Rev* 41:679–697. <https://doi.org/10.1093/femsre/flux023>.
41. Liu CM, Stegger M, Aziz M, Johnson TJ, Waits K, Nordstrom L, Gauld L, Weaver B, Rolland D, Statham S, Horwinski J, Sariya S, Davis GS, Sokurenko E, Keim P, Johnson JR, Price LB. 2018. *Escherichia coli* ST131-H22 as a foodborne uropathogen. *mBio* 9:e00470-18. <https://doi.org/10.1128/mBio.00470-18>.
42. Salvador E, Wagenlehner F, Köhler C-D, Mellmann A, Hacker J, Svanborg C, Dobrindt U. 2012. Comparison of asymptomatic bacteriuria *Escherichia coli* isolates from healthy individuals versus those from hospital patients shows that long-term bladder colonization selects for attenuated virulence phenotypes. *Infect Immun* 80:668–678. <https://doi.org/10.1128/IAI.06191-11>.
43. Carattoli A, Zankari E, García-Fernández A, Voldby Larsen M, Lund O, Villa L, Møller Aarestrup F, Hasman H. 2014. *In silico* detection and typing of plasmids using PlasmidFinder and plasmid multilocus sequence typing. *Antimicrob Agents Chemother* 58:3895–3903. <https://doi.org/10.1128/AAC.02412-14>.

44. Seemann T. 2018. Abricate. <https://github.com/tseemann/abricate>.
45. Zankari E, Hasman H, Cosentino S, Vestergaard M, Rasmussen S, Lund O, Aarestrup FM, Larsen MV. 2012. Identification of acquired antimicrobial resistance genes. *J Antimicrob Chemother* 67:2640–2644. <https://doi.org/10.1093/jac/dks261>.
46. Joensen KG, Scheutz F, Lund O, Hasman H, Kaas RS, Nielsen EM, Aarestrup FM. 2014. Real-time whole-genome sequencing for routine typing, surveillance, and outbreak detection of verotoxigenic *Escherichia coli*. *J Clin Microbiol* 52:1501–1510. <https://doi.org/10.1128/JCM.03617-13>.
47. Chen L, Zheng D, Liu B, Yang J, Jin Q. 2016. VFDB 2016: hierarchical and refined dataset for big data analysis—10 years on. *Nucleic Acids Res* 44:D694–D697. <https://doi.org/10.1093/nar/gkv1239>.
48. Vallenet D, Engelen S, Mornico D, Cruveiller S, Fleury L, Lajus A, Rouy Z, Roche D, Salvignol G, Scarpelli C, Médigue C. 2009. MicroScope: a platform for microbial genome annotation and comparative genomics. *Database (Oxford)* 2009:bap021. <https://doi.org/10.1093/database/bap021>.
49. Datsenko KA, Wanner BL. 2000. One-step inactivation of chromosomal genes in *Escherichia coli* K-12 using PCR products. *Proc Natl Acad Sci U S A* 97:6640–6645. <https://doi.org/10.1073/pnas.120163297>.
50. Dudin O, Geiselman J, Ogasawara H, Ishihama A, Lacour S. 2014. Repression of flagellar genes in exponential phase by CsgD and CpxR, two crucial modulators of *Escherichia coli* biofilm formation. *J Bacteriol* 196:707–715. <https://doi.org/10.1128/JB.00938-13>.
51. Smati M, Clermont O, Bleibtreu A, Fourreau F, David A, Daubié A-S, Hignard C, Loison O, Picard B, Denamur E. 2015. Quantitative analysis of commensal *Escherichia coli* populations reveals host-specific enterotypes at the intra-species level. *Microbiologyopen* 4:604–615. <https://doi.org/10.1002/mbo3.266>.
52. Vimont S, Boyd A, Bleibtreu A, Bens M, Goujon J-M, Garry L, Clermont O, Denamur E, Arlet G, Vandewalle A. 2012. The CTX-M-15-producing *Escherichia coli* clone O25b:H4-ST131 has high intestine colonization and urinary tract infection abilities. *PLoS One* 7:e46547. <https://doi.org/10.1371/journal.pone.0046547>.
53. Smati M, Magistro G, Adiba S, Wieser A, Picard B, Schubert S, Denamur E. 2017. Strain-specific impact of the high-pathogenicity island on virulence in extra-intestinal pathogenic *Escherichia coli*. *Int J Med Microbiol* 307:44–56. <https://doi.org/10.1016/j.ijmm.2016.11.004>.
54. Labat F, Pradillon O, Garry L, Peuchmaur M, Fantin B, Denamur E. 2005. Mutator phenotype confers advantage in *Escherichia coli* chronic urinary tract infection pathogenesis. *FEMS Immunol Med Microbiol* 44:317–321. <https://doi.org/10.1016/j.femsim.2005.01.003>.
55. Holm S. 1979. A simple sequentially rejective multiple test procedure. *Scand J Stat* 6:65–70.
56. R Development Core Team. 2014. R: a language and environment for statistical computing. R Foundation for Statistical Computing, Vienna, Austria. <http://www.R-project.org>.

Annexe 3 : Publication associée en 3^{ème} auteur – Acceptée dans Toxins le 21 Septembre 2021



Review

Staphylococcus aureus Toxins: An Update on Their Pathogenic Properties and Potential Treatments

Nour Ahmad-Mansour¹, Paul Loubet², Cassandra Pouget³, Catherine Dunyach-Remy⁴, Albert Sotto², Jean-Philippe Lavigne⁴ and Virginie Molle^{1,*}

- ¹ Laboratory of Pathogen Host Interactions, CNRS UMR5235, Université de Montpellier, 34000 Montpellier, France; nour.mansour@umontpellier.fr
² Virulence Bactérienne et Infections Chroniques, INSERM U1047, Department of Infectious and Tropical Diseases, Université de Montpellier, 30908 Nîmes, France; paul.loubet@chu-nîmes.fr (P.L.); albert.sotto@chu-nîmes.fr (A.S.)
³ Virulence Bactérienne et Infections Chroniques, INSERM U1047, Université de Montpellier, 30908 Nîmes, France; cassandra.pouget@gmail.com
⁴ Virulence Bactérienne et Infections Chroniques, INSERM U1047, Department of Microbiology and Hospital Hygiene, Université de Montpellier, 30908 Nîmes, France; catherine.remy@chu-nîmes.fr (C.D.-R.); jean.philippe.lavigne@chu-nîmes.fr (J.-P.L.)
 * Correspondence: virginie.molle@umontpellier.fr; Tel.: +33-4671-44725

Abstract: *Staphylococcus aureus* is a clinically important pathogen that causes a wide range of human infections, from minor skin infections to severe tissue infection and sepsis. *S. aureus* has a high level of antibiotic resistance and is a common cause of infections in hospitals and the community. The rising prevalence of community-acquired methicillin-resistant *S. aureus* (CA-MRSA), combined with the important severity of *S. aureus* infections in general, has resulted in the frequent use of anti-staphylococcal antibiotics, leading to increasing resistance rates. Antibiotic-resistant *S. aureus* continues to be a major health concern, necessitating the development of novel therapeutic strategies. *S. aureus* uses a wide range of virulence factors, such as toxins, to develop an infection in the host. Recently, anti-virulence treatments that directly or indirectly neutralize *S. aureus* toxins have showed promise. In this review, we provide an update on toxin pathogenic characteristics, as well as anti-toxin therapeutical strategies.

Keywords: *Staphylococcus aureus*; pathogenicity; toxins; anti-toxin strategies; virulence

Key Contribution: This review described the main toxins produced by *Staphylococcus aureus* and discussed anti-toxin strategies to fight these bacteria.



Citation: Ahmad-Mansour, N.; Loubet, P.; Pouget, C.; Dunyach-Remy, C.; Sotto, A.; Lavigne, J.-P.; Molle, V. *Staphylococcus aureus* Toxins: An Update on Their Pathogenic Properties and Potential Treatments. *Toxins* **2021**, *13*, 677. <https://doi.org/10.3390/toxins13100677>

Received: 16 June 2021

Accepted: 21 September 2021

Published: 23 September 2021

Publisher's Note: MDPI stays neutral with regard to jurisdictional claims in published maps and institutional affiliations.



Copyright: © 2021 by the authors. Licensee MDPI, Basel, Switzerland. This article is an open access article distributed under the terms and conditions of the Creative Commons Attribution (CC BY) license (<https://creativecommons.org/licenses/by/4.0/>).

1. Introduction

Staphylococcus aureus continues to be one of the most involved bacteria in human diseases. This bacteria is found in the normal skin microbiota of both animals and humans, with a carriage rate between 20 and 30% in the healthy human population [1,2]. Abscesses, lung infections, bacteremia, endocarditis, and osteomyelitis are all caused by *S. aureus* infections in humans [3]. With the appearance of methicillin-resistant *S. aureus* (MRSA) strains, the pathogenicity of *S. aureus* has become a problem in both health institutions and community settings. MRSA is on the rise since its discovery in the early 1960s, although there has been some stabilization or decline in European countries [4]. However, MRSA remains an important opportunistic pathogen in Europe and the most frequently identified worldwide [5]. MRSA is prevalent in several hospitals, especially those in Europe, Asia, and the United States. The prevalence of CA-MRSA strains from community-acquired (CA) infections among previously healthy individuals with few or no traditional healthcare-associated (HA) risk factors for MRSA increased in the late 1990s.

S. aureus infections rely on the production of surface proteins that initiate bacterial adherence to host tissues, the secretion of extracellular toxins and enzymes that destroy host cells and tissues, the avoidance or inactivation of the host immune system, and the growth and expansion of bacteria in host cells and tissue [6]. Coagulase, hyaluronidase, deoxyribonuclease, and lipase are some of the enzymes that *S. aureus* can synthesize to enhance its pathogenicity and disseminate within the host [7]. Moreover, enterotoxins, toxic shock syndrome toxin 1 (TSST-1), exfoliative toxins (ETs), hemolysins, epidermal cell differentiation inhibitors (EDINs), and Panton–Valentine leukocidin (PVL) have all been identified as extracellular protein toxins that enhance pathogenicity [8]. Interestingly, some of these toxins were detected in MRSA infections more frequently than non-MRSA cases [9–11].

Hospitalizations related to staphylococcal infections are frequent, increasing mortality and health costs [12,13]. Moreover, *S. aureus*' capacity to produce antibiotic-neutralizing enzymes has exacerbated the issues associated with antimicrobial therapy, resulting in numerous resistances to these drugs [14]. Antibiotic resistance enzymes play a significant role in bacterial resistance to antibiotic pressure regarding diversity, evolution, and spread. Antibiotic-producing bacteria need strategies to counteract the chemicals' deadly effects, by the production of degradative enzymes [14,15]. However, the selection pressure caused by the widespread use of antibiotics in humans and animals propagated resistant bacterial clones.

Antibiotic resistance develops quickly in *S. aureus*, and the rise of multidrug-resistant forms is a major problem. It has been reported that the annual mortality toll from antibiotic-resistant diseases has surpassed 10 million and that by 2050, it will outnumber cancer deaths [16]. The morbidity and mortality consequences reinforce the need to urgently discover new effective solutions due to the inefficiency of traditional antibiotics. Therefore, alternative treatments represent a promising field of investigation due to the lack of new antibiotic classes. Different strategies have been conducted, notably based on drug design with synthetic analogs, that could inhibit virulence factors. However, these studies have not yet generated promising results due to toxicity and/or low bioavailability. New options are now under study with a focus on biological molecules or compounds to interfere with toxins or toxin-regulator genes, constituting a new generation of promising anti-staphylococcal treatments [17–21].

This review outlines key properties related to the pathogenic roles of numerous *S. aureus* toxins (Table 1), as well as up to date anti-toxin treatments (Table 2).

2. Toxins Involved in the Pathogenicity of *S. aureus*

2.1. Staphylococcal Pore-Forming Toxins (PFTs)

PFTs are a type of bacterial virulence factor found in a wide range of human diseases, including *S. aureus*, which uses a variety of pore-forming cytotoxins (i.e., hemolysins, leukotoxins, and phenol-soluble modulins) to create pores in the host cell membrane causing cell lysis or to disrupt host cell actin cytoskeleton creating breaches in endothelial cells (EDIN exotoxin).

2.1.1. Hemolysins

S. aureus encodes α -, β -, γ -, and δ -hemolysins, which are regulated by the accessory gene regulator (Agr) and, principally, lyse erythrocytes by creating pores in host cell membranes or dissolving cell wall components [22]. The best-studied virulence factor of *S. aureus* is α -hemolysin, encoded by the *hla* gene, causing damage to a large variety of host cells, such as epithelial cells, endothelial cells, erythrocytes, monocytes, and keratinocytes, as well as causing cell membrane damage and apoptosis [22]. It is the prototype for the small β -barrel class pore-forming cytotoxins that is secreted as a 33 kDa water-soluble monomer that forms a prepore by assembling into one homoheptamer. Then, this prepore matures as a β -barrel transmembrane aqueous channel [23]. Finally, the binding of α -hemolysin to its host receptor ADAM10 stimulates ADAM10's metalloprotease activity, allowing it to cleave endothelial cadherin, compromising endothelial barrier function [24]. Cellular reactions, including the release of potent lipid mediators originating from the

arachidonate cascade, are then activated by the transport of ions such as Ca^{2+} through the pore, resulting in the target cells apoptosis [25].

The large majority of *S. aureus* strains (95%) possess the *hla* gene, irrespective of their resistance to methicillin, without showing a specific repartition in *S. aureus* clones nor a higher prevalence in certain regions of the world [26]. The role of the α -hemolysin toxin in the development of severe infections, such as pneumonia, osteomyelitis, and bacteremia, has been established in studies employing different experimental models infected with the *S. aureus* USA300 strain [27,28]. Interestingly, even though most recent *S. aureus* strains encode *hla*, data suggest that greater *hla* expression promotes pathogenicity. For instance, in a rat model of pneumonia, the epidemic strain USA300, which supplanted USA400 to become the dominant community-acquired methicillin-resistant *S. aureus* (CA MRSA) strain in the United States during the early 2000s, was reported to be significantly more virulent and fatal than USA400 and was strongly correlated with a substantial increase in *hla* expression [27,29].

Therefore, based on its crucial role in virulence, the α -hemolysin toxin is an ideal target for the development of anti-toxin treatments against *S. aureus*.

2.1.2. Pantan-Valentine Leukocidin (PVL)

Leukotoxins target white blood cells, such as neutrophils, monocytes, or macrophages [30]. Pantan-Valentine leukocidin (PVL), LukDE, and LukAB (sometimes known as LukGH) are all members of the bi-component Luk toxin family, with PVL presenting a 100-fold higher leukocytotoxic activity than the others. This Luk toxin family includes 32–35 kDa leukotoxins, which are encoded on the core genome or phage and oligomerize to form a pore structure [31]. Leukotoxins' leukocytotoxic activity is based on receptor interaction. CCR5 on immune cells is the receptor for LukDE, whereas C5aR, C5L2, and CD11b are the receptors for PVL and LukAB [32–34]. PVL is a toxin that is made of two parts: LukS-PV and LukF-PV. These two components are excreted before assembling into a pore-forming heptamer on neutrophil membranes, resulting in their lysis [35].

PVL is primarily linked to skin and soft tissue disease, with other types of invasive disease, such as pneumonia, musculoskeletal disease, and bacteremia, being far less common. Infection with a PVL-positive strain does not appear to predict a poor clinical outcome for staphylococcal pneumonia, musculoskeletal disease, or bacteremia in adults, but patients with PVL-positive skin and soft tissue disease seem to be more likely to require surgical intervention [36]. PVL is linked to skin and soft tissue infections in both MRSA and MSSA strains, irrespective of the strain type [36–38].

Therefore, new treatments are required because the likelihood of infection with PVL-positive *S. aureus* strains is rising, and some of these strains are MRSA that already have limited treatment options.

2.1.3. Phenol-Soluble Modulins (PSMs)

PSMs are one of the most important and aggressive virulence factors in *S. aureus* involved in a variety of staphylococcal pathogenesis, such as red and white blood cell lysis, inflammatory response induction, and antimicrobial activities [39–41]. Moreover, while PSMs are reported to be the most cytolytic and immunological modulating factors, they all play a function in epithelial surface spreading and have also been associated with the structuring and detachment of biofilms [42,43]. *S. aureus* produces a variety of PSMs, each with unique cytolytic and antibacterial characteristics [41]. These toxins are a class of small peptides with an amphipathic α -helical structure and surfactant-like characteristics [41]. PSMs are categorized into two subfamilies: (i) PSM α peptides that are 20–26 amino acids long and contain PSM α 1–PSM α 4 and the δ -toxin and (ii) PSM β peptides that are 43–44 amino acids in length and contain PSM β 1 and PSM β 2 [39]. The PSM α and β peptides are encoded in the *psm α* and *psm β* operon, while the δ -toxin gene is within the sequence of RNAlII, the effector molecule of the Agr (accessory gene regulator) quorum-sensing pathway [44,45]. PSMs attach to the formyl peptide receptor 2 (FPR2), which attracts innate

immune cells, such as neutrophils, macrophages, and dendritic cells [46,47]. As a result, holes formed in the host cell membrane cause osmotic instability and cell lysis. PSM α peptides have shown their great capacity to lyse human leukocytes and erythrocytes, with PSM α 3 having the most important activity. The δ -toxin, on the other hand, has a mild cytolytic activity, while the PSM β peptides are non-cytolytic [40].

PSMs are mainly present in highly virulent *S. aureus*, notably CA-MRSA. In vitro, these strains show a greater expression of PSMs, particularly cytolytic PSM α peptides, than that of hospital-acquired MRSA (HA-MRSA) strains [48]. In animal infection models, the PSM α peptides generated by the CA-MRSA USA300 and USA400 have a significant impact on the ability of virulent *S. aureus* to generate cutaneous infection and bacteremia [49–51].

Therefore, targeting PSMs for anti-staphylococcal treatment and drug development would be beneficial since eliminating all PSMs' cytolytic and pro-inflammatory activities would lower their potency against host cells and possibly their overall contribution to *S. aureus* disease progression.

2.1.4. Epidermal Cell Differentiation Inhibitor (EDIN) Exotoxins

To date, three forms of EDIN toxins have been identified: EDIN-A, EDIN-B, and EDIN-C [52,53]. EDINs enter host cells and induce macroapertures, which are large and temporary transcellular tunnels within endothelial cells, thus compromising the integrity of the endothelium barrier, and then target and inhibit the small host protein RhoA [54,55]. This small GTPase is a critical regulator of the actin cytoskeleton in the host cell [56]. The inhibition of RhoA has been shown in several cell biology studies to have a negative effect on the cohesiveness of the epithelial and endothelium barrier, thus favoring bacterial spread [54,57]. In addition, RhoA inhibition suppresses complement-mediated phagocytosis [58]. Overall, a significant number of research exploring the effects of RhoA inhibition indicate that EDINs secreted factors play an important role in *S. aureus* colonization and bacterial host tissue invasion [59,60].

Numerous pathogenic strains of *S. aureus*, especially those from the European MRSA lineage (ST80-MRSA-IV) [53], express EDIN or EDIN-like exotoxins [61–63]. The prevalence of these genes in *S. aureus* is poorly described. Though, in diabetic foot ulcers, *S. aureus* isolates were positive for *edin* (A and B) genes in 14 (7.2%) out of 195 patients [53]. A prevalence of 14 % of EDIN-encoding genes (primarily *edinC*) was found in 256 *S. aureus* isolates from diverse clinical sites of infection in Nice (France) [64]. Interestingly, the association between PVL and EDIN among MRSA has been observed with a prevalence varying between 12 and 100% [65].

EDIN exotoxins are thus important virulence factors in promoting bacterial colonization and host tissue invasion, such as in diabetic foot infections, bacteremia, and pneumonia [53,66,67].

2.2. Exfoliative Toxins (ETs)

Staphylococcal exfoliative toxins (ETs) are responsible for staphylococcal scalded skin syndrome (SSSS), also known as Ritter's disease, and characterized by dehydration, the loss of superficial skin layers, and secondary infections [68]. Large areas of the body are affected by SSSS, and the lesions are frequently sterile. Bullous impetigo is a skin disease caused by the same exfoliative toxin that causes SSSS, generated by the same underlying infection, and most commonly affects the face, hands, trunk, and buttocks. Pustules and blisters grow near the original site of infection in bullous impetigo but not elsewhere on the body as in SSSS. Because the blisters and pustules originate so close to the epidermis' surface, they never grow larger than a few millimeters before perforating and expanding at the border, where oozing and yellow crusting develop, and the infection might disseminate to the surrounding skin when patients rub the rash [69]. Therefore, the only difference between the two disorders is the level of skin damage. Bullous impetigo usually affects young children and infants, although redness and rashes do not develop as they would in SSSS because older children and adults possess neutralizing antibodies that inactivate the

toxin [69]. SSSS also primarily affects newborns and infants, although it can also impact adults with renal insufficiency or immunological deficiencies [68]

ETA, ETB, ETC, and ETD are the most common ETs, while ETA and ETB have received most of the attention due to their link to SSSS [68]. ETs are encoded on various genetic elements, and their expression is controlled by the accessory gene regulator (Agr) [31,70]. ETs exhibit glutamate-specific serine protease activity and target desmoglein 1 (Dsg1; desmosomal intercellular adhesion molecule), a keratinocyte cell–cell adhesion protein [71]. ETs bind to Dsg1, destroying desmosomal cell attachments and causing epidermal dissociation of the human epidermis [72]. The rupture of epidermal layers allows bacteria to penetrate the skin and induce blistering disorders, such as bullous impetigo and SSSS [73].

The prevalence of ETA in methicillin-resistant (MRSA) and methicillin-susceptible (MSSA) strains does not differ considerably. According to recent studies, 4% of MSSA strains possess the *eta* or *etb* gene, while about 10% of MRSA strains are *eta* positive [74,75]. Resistant strains, however, may pose a problem in the future. For instance, in Japan, issues with treating *etb*-positive CA-MRSA infections that causes SSSS in healthy persons have already been described [76,77].

2.3. Superantigens (SAGs)

S. aureus superantigens (SAGs) are the most effective T-cell mitogens. The mechanism of action of SAGs varies from those of traditional peptide antigens. Antigen-presenting cells (APCs) ingest and process conventional antigens [78]. T-cells are able to identify an MHC class II-restricted antigenic peptide exposed on APC surfaces utilizing hypervariable regions of T-cell receptor (TCR) α - and β -chains [78]. However, SAGs can directly link TCR β -domains by exploiting conserved MHC class II structures displayed on APCs, then triggering T-cell activation and proliferation without the use of antigen processing [79]. This causes pro-inflammatory cytokines, including IL-2, IFN- γ , and TNF- α , to become overactive and release causing a multitude of side effects and symptoms, including the possibility of multi-system organ failure that is specific to each superantigen [79].

SAGs include staphylococcal enterotoxins (SEs) that have emetic effects after oral administration and the toxic shock syndrome toxin 1 (TSST-1) that does not have emetic properties [80].

2.3.1. Staphylococcal Enterotoxins (SEs)

SEs are 20–30 kDa released toxins that disrupt intestinal activity and induce staphylococcal food poisoning (SFP), which is characterized by nausea, vomiting, abdominal pain, and diarrhea without indications of toxic effects, such as fever or hypotension [81–83]. Based on antigenic heterogeneity, more than 20 SEs (SEA—SEIV) have been discovered [81,84,85]. Although the receptors involved in the emetic response to SEs have not been discovered, clinical signs of SFP have been linked to inflammatory mediators, such as leukotriene B4 and prostaglandin E2, both of which are produced in response to SEs [86,87]. The stomach and upper small intestine present the most significant mucosa lesions, which are associated with neutrophil infiltrates in the epithelium and lamina propria, whereas the jejunum exhibits broken brush boundaries and enlarged crypts [88].

In some CA-MRSA infections, lethal sepsis, infective endocarditis, and kidney infections are critically dependent on a high level of staphylococcal enterotoxin C (SEC) [89]. While staphylococcal enterotoxin B (SEB) is associated with food poisoning, it has been studied for potential utilization as an inhaled biological weapon [88].

2.3.2. Toxic Shock Syndrome Toxin 1 (TSST-1)

Unlike SEs, TSST-1 (22-kD) does not trigger emesis but stimulates the release of substantial amounts of pro-inflammatory cytokines from the host T-cells and macrophages [90]. This cytokine outburst causes toxic shock syndrome (TSS) symptoms, such as high fever, rash, desquamation, hypotension, and hypovolemic shock, which can progress to multiorgan failure [91].

Given the growing development of MRSA infections associated with TSST-1 expression, it is therefore becoming more difficult to treat and may ultimately lead to death.

Table 1. Toxins secreted by *S. aureus*.

Toxin	Biological Properties and Function	Associated Disease	References
α -hemolysin	<ul style="list-style-type: none"> - Pore-forming activity - Lysis of erythrocytes, leukocytes, epithelial cells, and fibroblasts - Pro-inflammatory properties 	<ul style="list-style-type: none"> - Pneumonia - Sepsis 	[23,24,92,93]
Panton–Valentine Leukocidin (PVL)	<ul style="list-style-type: none"> - Pore-forming activity - Lysis of neutrophils, monocytes, macrophages - Pro-inflammatory properties 	<ul style="list-style-type: none"> - Pneumonia - Bacteremia - Necrotizing fasciitis - Skin and soft tissue infections 	[30,31,94]
Phenol-Soluble Modulins (PSMs)	<ul style="list-style-type: none"> - Pore-forming activity - Lysis of erythrocytes, neutrophils, monocytes, bacterial protoplasts, spheroplasts - Pro-inflammatory properties - Promote biofilm formation 	<ul style="list-style-type: none"> - Bacteremia - Skin infection 	[40,82,95,96]
Epidermal Cell Differentiation Inhibitor (EDIN)	<ul style="list-style-type: none"> - Transcellular tunnel activity - Breaches in endothelial cells 	<ul style="list-style-type: none"> - Pneumonia - Bacteremia - Diabetic foot ulcer 	[53,54,66]
Exfoliative Toxins (ETs)	<ul style="list-style-type: none"> - Serine protease activity - Disruption of the cell–cell adhesions and junctions of the epidermis cells 	<ul style="list-style-type: none"> - Staphylococcal scalded skin syndrome (SSSS) 	[68,97]
Staphylococcal Enterotoxins (SEs)	<ul style="list-style-type: none"> - Superantigen activity - Pro-inflammatory activity 	<ul style="list-style-type: none"> - Staphylococcal food poisoning - Toxic shock syndrome 	[19,81,85]
Toxic Shock Syndrome Toxin 1 (TSST-1)	<ul style="list-style-type: none"> - Superantigen activity - Pro-inflammatory activity 	<ul style="list-style-type: none"> - Toxic shock syndrome 	[82,90,91]

3. Anti-Toxin Treatments

The growth and spread of antibiotic resistance among *S. aureus* strains emphasize the imperative need for the development of alternative treatments that do not exert selective pressure in order to avoid evolution toward multi-resistance, such as that experienced with antibiotics. Interestingly, toxin-targeting therapy has already been effective against a variety of pathogenic bacteria, including *S. aureus* [17]. The therapeutic treatments that neutralize or interfere with the expression of staphylococcal toxins are detailed in this section.

3.1. Antibodies

Antibodies are one of the most important anti-virulence strategies for neutralizing toxins. Unlike active immunization, which would necessitate multiple boosters and a lengthy time to produce optimal immune responses, passive immunization would give prompt treatment for infected patients, thereby reducing the severity of *S. aureus* infections.

For instance, attempts to neutralize the α -hemolysin toxin during the course of human infection are underway and are based on substantial evidence for its participation in pathogenesis in murine models, as well as its putative importance in human disease. MEDI4893 (suvratoxumab), an α -hemolysin-neutralizing monoclonal antibody (mAb) formerly called LC10, is among the best-studied anti-virulence treatments against *S. aureus* infections [21]. As described above, α -hemolysin interacts with the metallopro-

tease ADAM10, which promotes oligomerization and pore formation [98]. By binding to a highly conserved area of the α -hemolysin toxin, MEDI4893 inhibits its interaction with ADAM10 as well as its self-oligomerization, thus neutralizing its action [98–100]. The treatment of rabbits with MEDI4893 resulted in a considerable reduction in clinical outcomes, according to Le et al. [101]. Similarly, Ortines et al. found that *S. aureus*-infected mice previously passively immunized with MEDI4893 showed fewer wounds and decreased bacterial counts than those of untreated controls in non-diabetic and diabetic mice [102]. Surewaard et al. recently revealed that α -hemolysin causes rapid platelet aggregation and liver injury, resulting in multi-organ failure during *S. aureus* sepsis, but these consequences could be avoided in mice treated with MEDI4893 [103]. MEDI4893 has passed Phase 2 clinical studies for the prevention of *S. aureus* pneumonia in high-risk critical care unit patients in 2020, and more recently, MEDI4893 showed efficacy and safety in preventing *S. aureus* ventilator-associated pneumonia [104,105]. In addition, AR-301 and ASN100 are two other neutralizing antibodies that have entered clinical trials. AR-301 is an α -hemolysin-targeting monoclonal antibody that has recently entered Phase 3 tests as an adjuvant therapy for *S. aureus* pneumonia [106], and ASN100 is a combination of two monoclonal antibodies that neutralize six cytolytic toxins corresponding to α -hemolysin, PVL, LukAB, γ -hemolysin AB (HlgAB), γ -hemolysin CB (HlgCB), and leukocidin ED (LukED) [107]. Unfortunately, while ASN100 passed the Phase 1 clinical safety testing by reducing tissue damage in a rabbit model of *S. aureus* pneumonia, the Phase 2 trial was stopped due to inefficiency [107]. Although these trials involving MEDI4893 [108], AR-301 [106], and the multivalent antitoxin ASN100 [107] were not statistically significant, passive immunization was found to have some protective potential. For example, AR-301 shortened the time spent on mechanical ventilation, whilst MEDI4893 decreased hospital and intensive care unit stay, as well as antibiotic treatment duration, while remaining safe and well tolerated [106–108]. Foletti et al. identified antibodies against α -hemolysin from a human donor-derived single-chain variable fragment (scFv) phage library [99]. LTM14, a notable clone in this family, was transformed to a complete IgG and showed an unusually high affinity for α -hemolysin. LTM14 offered protection against *S. aureus* cutaneous and bacteremia mice models of infection and also demonstrated therapeutic potential in a pneumonia model [99]. In addition, when combined with the antibiotic linezolid, LTM14 showed improved efficacy. This is essential because, in a therapeutic situation, passive immune treatment will almost certainly be delivered in conjunction with the most suitable antibiotic [99].

While some studies have found an epidemiological link between PVL and CA-MRSA, the presence of large levels of neutralizing antibodies did not provide resistance to PVL-positive MRSA skin and soft tissue infections [109–111]. Despite this, PVL is still one of the most important targets for anti-toxin drug research. PVL-specific antibodies are present in available commercial human intravenous polyclonal immunoglobulin preparations (IVIg), which decrease the cytopathic effects of PVL in a dose-dependent manner, most likely through interfering with PVL–neutrophil interactions [112]. In 2015, Mairpady Shambat et al. showed that IVIg abolished PVL and α -hemolysin-mediated cytotoxicity in epithelial cells in a human lung tissue model [113]. Moreover, antibiotic therapy combined with IVIg anti-toxin treatment significantly improved the situation of patients with acute necrotizing pneumonia caused by PVL-positive *S. aureus* strains, demonstrating the effectiveness of IVIg in limiting disease progression, particularly in highly lethal *S. aureus* infections linked to PVL production [114]. Moreover, in vitro humanized antibodies developed by Leventie et al. are able to disrupt PVL binding to polymorphonuclear leukocytes and impede the development of new pores [115]. A reduction in inflammatory reactions and tissue damage was also found in this non-infectious rabbit model of endophthalmitis, with the tetravalent anti-PVL antibody [115].

In various in vivo models, antibodies targeting superantigens were shown to neutralize these toxins and have been linked to protection [116]. The staphylococcal enterotoxin B (SEB) is one of the most studied enterotoxins, and its designation as a bioweapon makes it an interesting target to produce anti-toxin-neutralizing antibodies. Drozdowski et al. generated and selected human monoclonal antibodies (HuMAbs) specific for SEB from

human B-cell hybridomas [117]. In vitro, these antibodies exhibited biological activity against SEB, and, HuMAb-154, which had the highest anti-SEB affinity, demonstrated both preventive and therapeutic action in a mouse model of SEB-induced mortality [117]. In addition, in numerous mouse models, including sepsis and cutaneous and deep tissue abscesses, another monoclonal antibody against SEB, named 20B1, was demonstrated to be protective against MRSA infection [118].

Therefore, all these therapy examples highlight the usefulness of antibodies as anti-virulence treatments able to neutralize staphylococcal toxins.

3.2. Nanoparticles

Aside from the use of anti-toxin antibodies in anti-virulence therapies, researchers have also shown the effectiveness of manufactured nanoparticles that imitate cell membranes, such as liposomes, in sequestering bacterial toxins in vitro and in vivo [119]. For example, Henry et al. demonstrated the ability of artificial liposomes to trap bacterial toxins in vitro while maintaining the integrity of mammalian cells [120]. They also discovered that administering artificial liposomes to mice during in vivo studies helped them recover from septicemia induced by *S. aureus*, as well as protect them against pneumonia [120]. Because customized liposomes are made entirely of naturally occurring lipids, they are not bactericidal and could be employed alone or in combination with antibiotics to treat bacterial infections and reduce toxin-induced tissue damage [120]. Interestingly, Wolfmeier et al. employed sphingomyelin liposomes, with or without cholesterol, to neutralize secreted PSMs and other virulence factors in vitro during human blood or epithelial cell staphylococcal infections, as well as in a murine dermonecrosis model [121]. Sphingomyelin liposomes blocked cell lysis by PSMs, particularly PSM3, whereas cholesterol-containing sphingomyelin liposomes preferentially trapped α -hemolysin [121]. A combination of both liposome types was recently evaluated in a Phase I clinical trial against severe pneumococcal pneumonia, although its utility in *S. aureus* pneumonia remains unknown. Furthermore, targeting both PSMs and α -hemolysin at the same time remains a possibility, as PSMs have been demonstrated to regulate α -hemolysin expression both in vitro and in vivo [23].

Recently, in response to *S. aureus* infection, exosomes (called “defensosomes”) with increased ADAM10 receptors were discovered to be produced from host cells in a TLR-dependent mode, resulting in α -hemolysin retention and a reduction in disease mortality [122]. Then, therapeutic poly (lactic-co-glycolic acid) (PLGA)-based nanoparticles covered with natural human erythrocyte membranes performed a comparable decoy effect to fight infection and reduce the activity of α -hemolysin [123].

Moreover, similar to other anti-virulence strategies, the nanoparticle-based neutralization and administration not only help to avoid severe bacterial infections but can also participate in reducing the development of antibiotic resistance [124].

3.3. RNAIII-Inhibiting Peptides

In addition to the direct neutralization strategy outlined in the previous sections, targeting *S. aureus* toxins can be carried out indirectly by affecting the regulatory processes that govern virulence genes' expression. This approach is based on the utilization of small molecules, such as peptides, to target global regulators, such as the accessory gene regulator Agr in *S. aureus*. Agr regulates the quorum-sensing pathway that controls whether *S. aureus* develops a biofilm or remains planktonic, as well as toxin gene synthesis [44,125,126]. The P3 promoter of the *S. aureus* quorum-sensing Agr system transcribes RNAIII, a stable regulatory RNA that regulates the expression of a large variety of virulence factors [127]. Therefore, inhibiting RNAIII represents a promising strategy for reducing toxin expression as well as other virulence factors. When evaluated in cellulitis in in vivo models, RNAIII-inhibiting peptides (RIP) were found to block agr RNA transcripts and impede staphylococcal adhesion to mammalian cells, resulting in a decrease in *S. aureus* pathogenicity [128–130]. In an MRSA sepsis model, two new RIP derivatives were recently discovered to substantially extend mouse survival and reduce pathological damage without impacting

bacterial viability [131]. Interestingly, in an *S. aureus*-induced sepsis mouse model, and in association with clinically prescribed antibiotics, RIP increased the healing of wounds and reduced mortality in comparison to antibiotics alone, thus confirming the potential of combined therapies [132,133]. Moreover, PSMs have been specifically targeted using a variety of methods to neutralize their pathogenic effect. In a mouse pneumonia model, targeting PSMs indirectly by inhibiting the Agr system with an RNAPIII-inhibiting peptide resulted in a lower bacterial load and mortality [134].

3.4. Antimicrobial Peptides (AMPs)

Antimicrobial peptides (AMPs) have been known for several decades and are part of the innate immunity of practically all living organisms, ranging from bacteria, insects, and plants to vertebrates [135]. As of August 2021, the antimicrobial peptide database (<https://aps.unmc.edu/> (accessed on 23 August 2021)) contains 3273 antimicrobial peptides from six kingdoms (369 bacteriocins/peptide antibiotics from bacteria, 5 from archaea, 8 from protists, 22 from fungi, 361 from plants, and 2424 from animals, including some synthetic peptide records). AMPs have a wide spectrum of antibacterial, antifungal, antiparasitic, and antiviral properties [135]. AMPs not only possess a large spectrum of antibacterial activity but can also display anti-toxin activities [136,137]. Cathelicidins and defensins are the two major categories of AMPs in humans. Human defensins are amphipathic cationic peptides that are divided into two types: α - and β -defensins, and, to date, four α -defensins have been identified from polymorphonuclear neutrophils (PMNs) [138]. Human neutrophil peptides (HNP1–HNP4) are part of the phagolysosome's microbicidal machinery that can be detected in the extracellular environment after degranulation [139]. PVL is thought to have a role in CA-MRSA pathogenesis by attracting and lysing PMNs at the infection site, which induces tissue damage caused by the release of cytotoxic granule constituents [140]. Interestingly, Cardot-Martin et al. found that HNP3 defensins, but not HNP-1 or -2, substantially protect neutrophils from PVL-induced lysis by interacting with LukS-PV and LukF-PV, which disables PVL's pore creation function and reduces PVL cytotoxic effects [141].

3.5. Natural Compounds

Natural product-based compounds that present anti-toxin properties correspond to a promising therapeutical approach to treat *S. aureus* infections [18]. A modified cyclodextrin compound, named IB201, is used to treat pneumonia. Cyclodextrins are cyclic oligosaccharides that are made from starch or starch derivatives. Because of its spatial resemblance to α -hemolysin, this compound was identified based on the prediction that it would prevent α -hemolysin action with a high affinity [142]. Moreover, in mice *S. aureus* pneumonia models, aloe-emodin, an active component from aloe vera, and apigenin, an active compound from parsley, both exhibited sufficient protection [143,144]. Other compounds, such as morin hydrate (also known as 2',3,4',5,7-pentahydroxyflavone), which is a flavonoid present in *Maclura pomifera* (Osage orange), in *Maclura tinctoria* (old fustic), and in the leaves of *Psidium guajava* (common guava), was discovered to disrupt the self-assembly of the transmembrane pore of α -hemolysin in a mouse model of pneumonia and then to decrease its hemolytic activity [145].

Oroxin A (ORA), oroxin B (ORB), and oroxylin A 7-O-glucuronide (OLG), three oroxylin glycosides, are natural flavonoids found in strawberries, grapes, onions, apples, Bignoniaceae plants, and other vegetables and fruits. These substances possess structural similarities and bind to hemolysin's stem domain, preventing it from transitioning from monomer to oligomer in vitro and inhibiting its hemolytic action [146,147].

Friedman et al. showed that the pure olive chemical 4-hydroxytyrosol and the commercialized olive powder Hidrox-12, containing 6% of 4-hydroxytyrosol and 6% of additional phenolic compounds, were able to suppress the biological action of the superantigen enterotoxin A (SEA) [148]. However, this effect still remains to be validated in animal models.

Solonamide B, a cyclodepsipeptide from the halotolerant bacterium *Photobacterium halotolerans*, was one of the first natural inhibitors of the Agr signaling pathway to be reported [149]. Solonamide B and its derivatives prevent the quorum-sensing peptide AIP from interacting with AgrC. Interestingly, in CA-MRSA strains, such as USA300, solonamide B strongly reduced the activity of α -hemolysin and the transcription of *psma*-encoding PSMs resulting in an 80% reduction in toxicity of supernatants toward human neutrophils and rabbit erythrocytes [150–152].

Isorhamnetin, chrysin, and puerarin have been shown to inhibit RNAPIII transcription and, hence, α -hemolysin expression, providing protection against MRSA and MSSA-induced pneumonia [153–155]. Isorhamnetin (also known as 3'-methoxy-3,4',5,7-tetrahydroxyflavone) is an O-methylated flavanol found in apples, blackberries, cherries, and pears, as well as in medicinal plants and herbs [155]. Honey, propolis, the passion flowers *Passiflora caerulea* and *Passiflora incarnata*, and *Oroxylum indicum* all contain chrysin (5,7-dihydroxyflavone) [156]. Puerarin is the main bioactive compound obtained from the root plant *Pueraria lobata Ohwi*, also called Gegen in traditional Chinese medicine [157].

Naringenin, a flavanone found primarily in grapefruit, but also in a range of fruits and herbs, has been shown to drastically lower the amounts of *agrA* and *hla* transcripts in *S. aureus* culture as well as to inhibit hemolysin synthesis and protect mice from *S. aureus*-induced pneumonia [158,159].

In vitro, *Castanea sativa* leaf extract 224C-F2 [160] and *Schinus terebinthifolia* berry extract 430D-F5 [161] were found to inhibit *agr* expression, thus resulting in decreased hemolysin synthesis and hemolytic activity. A pretreatment with 224C-F2 diminished infection-induced ulcer sizes and substantially lowered morbidity in an in vivo model of MRSA infection [160]. In addition, pretreatment with a single dose of 430D-F5 massively reduced skin ulcer formation and mortality in a mouse model of MRSA skin infection [161].

Ambuic acid is a fungal product that targets AgrB activity and has been shown to prevent hemolysin and RNAPIII production in MRSA infections [162]. A single preventive administration of ambuic acid totally prevented skin ulcer formation in a murine mouse model [162]. Another fungal product, named omega-hydroxyemodin (OHM) and produced by *Penicillium restrictum*, decreases Agr activity by disrupting AgrA binding to its promoter. Importantly, OHM particularly inhibited the Agr pathway activation in a mouse model of MRSA cutaneous infection without affecting the host [163,164].

Even though some of the molecular mechanisms of these natural compounds have yet to be determined, they provide possible novel scaffolds for the development of successful anti-virulence therapeutics toward *S. aureus* infection.

3.6. Vaccines

Despite numerous attempts, there is currently no vaccination against *S. aureus*. As mentioned in the first section, *S. aureus* secretes a broad range of toxins during colonization and infection of the host, which poses a challenge for vaccine development.

There have been several studies to investigate the efficacy of α -hemolysin as a vaccine agent. Indeed, H35L, a mutant isoform of α -hemolysin, was discovered to have minimal hemolytic action [165]. In a mouse pneumonia model, this inactivated toxin (toxoid) was studied in two separate models and found to be efficacious through both active vaccination and the development of protective rabbit anti α -hemolysin antibodies; despite this fact, no human trials have been conducted to date [166].

IBT-VO2 is a multivalent vaccine currently under investigation. α -hemolysin, PVL LukS, LukF, LukAB, enterotoxins A and B, and toxic shock syndrome toxin 1 toxoids are all included in this heptavalent vaccine [167]. The multi-subunit vaccine generates an antibody response that is cross-reactive with 12 to 15 *S. aureus* toxins and gives protection in different mice and rabbit infection models due to structural similarities [167]. Recently, IBT-VO2 entered a Phase I clinical study after completing the encouraging pre-clinical phase, and as a result, received additional funding to help it progress.

Previous studies in animal models suggested that PVL subunits could be useful vaccines, but these attempts have yet to be converted into human trials [168,169]. However, for the creation of the StaphVax vaccine, recombinant PVL subunits were exploited (Nabi Biopharmaceuticals, Alpharetta, GA), but this vaccine failed in Phase 3 clinical testing [170]. However, some of the vaccine antigens, including PVL, were recycled into a new vaccine called PentaStaph, which was acquired by GlaxoSmithKline Biologicals (GSK) [171,172].

In mice, an inactive isoform of the staphylococcal enterotoxin B (SEB) was cloned into an *Lactococcus lactis* strain and tested as an oral vaccine. The vaccination was able to generate a significant antibody response, thus resulting in improved survival of infected mice [173]. Another vaccine against this SEB toxin, named STEBVax, was also generated and corresponds to a recombinant isoform that impedes the toxin from interacting with the major histocompatibility complex (MHC) class II [174]. If effective, this vaccine could be useful as a polyvalent *S. aureus* vaccine in general.

In another study, the injection of TSST-1-specific antibodies to treat toxic shock syndrome has been found to reduce mortality in a septic mouse model of infection [175]. Moreover, a modified TSST-1 antigen was also exploited to create an attenuated TSST-1 vaccine able to prevent infection during sepsis in mice [175]. Subsequently, a recombinant TSST-1 variant vaccine was created and tested in a Phase I clinical study, which was quite well tolerated, and a Phase II trial was engaged [176,177].

Even though numerous vaccine candidates have demonstrated protective efficacy in preclinical or early clinical investigations as detailed above, no vaccine has been authorized to date for human use.

3.7. Others

Eukaryotes, archaea, and bacteria create extracellular vesicles (EVs), which are lipid bilayers that form lumen-containing spheres with diameters ranging from 20 to 500 nm. EVs contain a variety of proteins, polysaccharides, nucleic acids, and lipids. EVs from Gram-positive bacteria carry physiologically active toxins, display cytotoxicity, and stimulate proinflammatory mediators, thus having a significant role in host–pathogen interactions [178]. Unfortunately, the toxicity of staphylococcal EVs limited their use as a vaccine platform. However, in a recent study, Wang et al. engineered EVs with unique features in the *S. aureus* USA300 strain, representative of the dominant CA-MRSA clone in the United States [179]. The originality of this study was to consider that *S. aureus* EVs could be used as a vaccine platform if their cytotoxicity was reduced. Therefore, EVs over producing Hla- and LukE-modified toxins that possess the capacity to be immunogenic without being toxic were engineered in order to stimulate the production of toxin-neutralizing antibodies. Immunization with engineered EVs showed considerable protection in an *S. aureus* lethal sepsis model [179]. Though the efficiency of these vesicles as a novel vaccine platform against different *S. aureus* strains and in additional infection models has yet to be determined, they do represent an attractive promise.

Moreover, novel approaches have been developed to combat enterotoxins. In an *in vitro* T-cell experiment, Mattis et al. developed a yeast display technology to create a soluble T-cell receptor variable domain variation capable of neutralizing both SEC and SEB enterotoxins. In different rabbit models, including endocarditis and necrotizing pneumonia, this variation was proven to be effective in reducing the infection [180].

Table 2. Summary of the anti-toxin treatments strategies.

Treatment	Name	Target	References
Antibodies	MEDI4893 (suvratoxumab)	α -hemolysin	[98–100]
	AR-301	α -hemolysin	[106]
	ASN100	α -hemolysin, Panton–Valentine leukocidin (PVL), LukAB, γ -hemolysin AB (HlgAB), γ -hemolysin CB (HlgCB), leukocidin ED (LukED)	[107]
	LTM14	α -hemolysin	[99]
	IVIg	α -hemolysin, PVL	[112–114]
	HuMAb-154	Staphylococcal enterotoxin B (SEB)	[117]
	20B1	Staphylococcal enterotoxin B (SEB)	[118]
Nanoparticles	Sphingomyelin liposomes	Phenol-soluble modulins (PSMs)	[121]
	Cholesterol-containing sphingomyelin liposomes	α -hemolysin	[121]
	Poly (lactic-co-glycolic acid) (PLGA)-based nanoparticles covered with natural human erythrocyte membranes	α -hemolysin	[123]
RNAIII-inhibiting peptides	RNAIII-inhibiting peptides (RIP)	<i>agr</i> RNA transcripts	[128–130]
Antimicrobial peptides	HNP3	PVL	[141]
Natural compounds	Cyclodextrin IB201	α -hemolysin	[142]
	Aloe-emodin	α -hemolysin	[144]
	Apigenin	α -hemolysin	[143]
	Morin hydrate (2',3,4',5,7-pentahydroxyflavone)	α -hemolysin	[145]
	Oroxylin glycosides (oroxin A (ORA), oroxin B (ORB), and oroxylin A 7-O-glucuronide (OLG))	α -hemolysin	[146,147]
	4-hydroxytyrosol Hidrox-12	Staphylococcal enterotoxin A (SEA)	[148]
	Solonamide B	Quorum-sensing peptide (AIP)	[149–152]
	Isorhamnetin (3'-methoxy-3,4',5,7-tetrahydroxyflavone)	α -hemolysin	[155]
	Chrysin (5, 7-dihydroxyflavone)	α -hemolysin	[156]
	Puerarin	α -hemolysin	[157]
	Naringenin	<i>agrA</i> and <i>hla</i> expression	[158,159]
	224C-F2 (<i>Castanea sativa</i> leaf) 430D-F5 (<i>Schinus terebinthifolia</i> berry)	<i>agr</i> expression	[161]
	Ambuic acid	AgrB activity, RNAIII expression	[162]
Omega-hydroxyemodin (OHM)	AgrA	[163,164]	
Vaccines	H35L	α -hemolysin	[165,166]
	IBT-VO2	α -hemolysin, PVL, enterotoxins A and B, toxic shock syndrome toxin 1 (TSST-1)	[167]
	StaphVax	PVL	[170]
	STEBVax	SEB	[174]
	Attenuated TSST-1 vaccine	TSST-1	[175–177]
Others	Extracellular vesicles (EVs)	α -hemolysin, Luke	[181]
	Yeast display technology to create a soluble T-cell receptor	SEC, SEB	[180]

4. Conclusions and Future Directions

The problem of antibiotic resistance has prompted scientists around the world to explore alternatives for effective treatments. Because antimicrobial resistance is a complex phenomenon, the solution to this problem comprises a variety of techniques aimed at reducing the factors that contribute to the establishment of resistance and spread. These strategies require the development of novel therapeutic drugs that work on principles distinct from those currently available for antibiotics. Bacterial toxins, as detailed in this review, are directly involved in disease outcomes. Anti-toxin therapies have been proposed as a promising alternative in this regard, with the intention of reducing pathogen virulence without exposing pathogens to selective pressure.

Anti-toxin therapies target diseases that are the most dangerous to patients, such as hospital-acquired bacterial pneumonia and ventilator-associated bacterial pneumonia, osteomyelitis, sepsis, and endocarditis, and have the capacity to enhance chances of survival. One of the benefits of these anti-toxin treatments is their use in conjunction with antibiotics to help fight the most dangerous infections. Furthermore, anti-toxin therapies contribute to significantly reduce the bacterial load, most likely by interfering with the bacterial strategies used to multiply involving secreted toxins [182]. Moreover, anti-toxin treatments do not place selective pressure on bacterial growth since they neutralize the pathogen rather than killing it, which could provide a long-term solution to the resistance issue. However, the potential of anti-toxin treatments to counter drug resistance without putting severe selective pressure on the bacterial population needs more investigation.

Even though efforts to develop innovative anti-toxin compounds have had varying levels of success, the potential leads need pharmacology and toxicology evidence. For extensive mechanistic study, additional studies should concentrate on a few very promising candidates. The anti-toxin treatments potential negative effects must also be considered. Because of the toxins' extensive combination and cross-reactivity, efforts to interfere at the host–toxin level necessitate robust anti-toxin efficacy. Therefore, staphylococcal toxin biology requires more research to decipher the specific toxin roles, the differences in expression or genetic existence of toxins all over strain lineages, and the importance of specific toxins along various clinical strains. Another drawback of anti-toxin compounds is their possible limited spectrum efficacy, as these treatment candidates only specifically target virulence-mediated pathways in certain *S. aureus* strains, thereby limiting their general clinical use.

Moreover, it is clear that evaluating the effectiveness of anti-toxin compounds is delayed by the lack of therapy models, which may more precisely mimic the clinical condition in humans. Thus, developing such models represents an essential future direction. Human clinical trials will always be required to prove the success of a treatment. However, even though animal models remain necessary to decipher fundamental host–pathogen interactions and even though many potentially promising *S. aureus* anti-toxin therapeutics exist, most have failed in human trials or have not been tested. Therefore, the development of humanized mice with engrafted human immune cells for instance could help improve the translatability of animal investigations to human trials in the future [183–185]. This strategy will improve animal models, thus helping in deciding which treatments should proceed to clinical trials.

It is also necessary to specify which criteria will be used to assess the anti-virulence therapy's efficacy, as well as which types of infections the treatment is most suited for. For instance, a defective Agr–quorum sensing system appears to be favorable for the pathogen in *S. aureus* chronic infections or bacteremia [186]. Furthermore, it was recently demonstrated that a dysfunctional Agr system could facilitate antibiotic resistance to gentamicin and ciprofloxacin [187]. Moreover, phenol-soluble modulins are known to be implicated in the regulation of *S. aureus* persister cell populations [188]. Then, as the Agr system oversees PSMs' production, a malfunctioning system is likely to suppress PSM expression, favoring the formation of persister cells resistant to antibiotics.

To summarize, a tremendous amount of work has investigated *S. aureus* toxins, expanding our understanding of their mode of action and involvement in pathogenesis, and several promising therapies have resulted from various treatment strategies. However, improved therapeutical models need to be developed to validate most of these anti-toxin treatments.

Author Contributions: Conceptualization J.-P.L. and V.M.; investigation, N.A.-M. and V.M.; resources, P.L., C.P. and C.D.-R.; writing—original draft preparation, N.A.-M., J.-P.L. and V.M.; writing—review and editing, P.L., C.P., C.D.-R. and A.S.; visualization, N.A.-M., P.L., C.P., C.D.-R. and A.S.; supervision, J.-P.L. and V.M.; project administration, J.-P.L. and V.M.; funding acquisition, J.-P.L. and V.M. All authors have read and agreed to the published version of the manuscript.

Funding: This research was funded by the Fondation de Coopération Scientifique, Méditerranée-Infection (Marseille IHU grant).

Institutional Review Board Statement: Not applicable.

Informed Consent Statement: Not applicable.

Acknowledgments: We thank the Nîmes University hospital for its structural, human, and financial support through the award obtained by our team during the internal call for tenders “Thématiques phares”. The authors belong to the FHU InCh (Federation Hospitalo Universitaire Infections Chroniques, Aviesan).

Conflicts of Interest: The authors declare no conflict of interest.

References

1. Wertheim, H.F.; Melles, D.C.; Vos, M.C.; van Leeuwen, W.; van Belkum, A.; Verbrugh, H.A.; Nouwen, J.L. The Role of Nasal Carriage in *Staphylococcus aureus*. *Lancet Infect. Dis.* **2005**, *5*, 751–762. [CrossRef]
2. Hanselman, B.A.; Kruth, S.A.; Rousseau, J.; Weese, J.S. Coagulase Positive Staphylococcal Colonization of Humans and Their Household Pets. *Can. Vet. J.* **2009**, *50*, 954–958. [PubMed]
3. Tong, S.Y.C.; Davis, J.S.; Eichenberger, E.; Holland, T.L.; Fowler, V.G. *Staphylococcus aureus* Infections: Epidemiology, Pathophysiology, Clinical Manifestations, and Management. *Clin. Microbiol. Rev.* **2015**, *28*, 603–661. [CrossRef]
4. Antimicrobial Resistance in the EU/EEA (EARS-Net)—Annual Epidemiological Report for 2019. Available online: <https://www.ecdc.europa.eu/en/publications-data/surveillance-antimicrobial-resistance-europe-2019> (accessed on 23 August 2021).
5. Borg, M.A.; Camilleri, L. What Is Driving the Epidemiology of Methicillin-Resistant *Staphylococcus aureus* Infections in Europe? *Microb. Drug Resist.* **2020**, *27*, 889–894. [CrossRef] [PubMed]
6. Lowy, F.D. *Staphylococcus aureus* Infections. *N. Engl. J. Med.* **1998**, *339*, 520–532. [CrossRef] [PubMed]
7. Tam, K.; Torres, V.J. *Staphylococcus aureus* Secreted Toxins and Extracellular Enzymes. *Microbiol. Spectr.* **2019**, *7*, 16. [CrossRef]
8. Oliveira, D.; Borges, A.; Simões, M. *Staphylococcus aureus* Toxins and Their Molecular Activity in Infectious Diseases. *Toxins* **2018**, *10*, 252. [CrossRef] [PubMed]
9. Shimaoka, M.; Yoh, M.; Takarada, Y.; Yamamoto, K.; Honda, T. Detection of the Gene for Toxic Shock Syndrome Toxin 1 in *Staphylococcus aureus* by Enzyme-Labelled Oligonucleotide Probes. *J. Med. Microbiol.* **1996**, *44*, 215–218. [CrossRef] [PubMed]
10. Liu, M.; Liu, J.; Guo, Y.; Zhang, Z. Characterization of Virulence Factors and Genetic Background of *Staphylococcus aureus* Isolated from Peking University People’s Hospital between 2005 and 2009. *Curr. Microbiol.* **2010**, *61*, 435–443. [CrossRef]
11. Ezeamagu, C.; Imanatue, I.; Dosunmu, M.; Odeseye, A.; Baysah, G.; Aina, D.; Odutayo, F.; Mensah-Agyei, G. Detection of Methicillin Resistant and Toxin-Associated Genes in *Staphylococcus aureus*. *Beni-Suef Univ. J. Basic Appl. Sci.* **2018**, *7*, 92–97. [CrossRef]
12. Suaya, J.A.; Mera, R.M.; Cassidy, A.; O’Hara, P.; Amrine-Madsen, H.; Burstin, S.; Miller, L.G. Incidence and Cost of Hospitalizations Associated with *Staphylococcus aureus* Skin and Soft Tissue Infections in the United States from 2001 through 2009. *BMC Infect. Dis.* **2014**, *14*, 296. [CrossRef] [PubMed]
13. Zhen, X.; Lundborg, C.S.; Zhang, M.; Sun, X.; Li, Y.; Hu, X.; Gu, S.; Gu, Y.; Wei, J.; Dong, H. Clinical and Economic Impact of Methicillin-Resistant *Staphylococcus aureus*: A Multicentre Study in China. *Sci. Rep.* **2020**, *10*, 3900. [CrossRef] [PubMed]
14. Egorov, A.M.; Ulyashova, M.M.; Rubtsova, M.Y. Bacterial Enzymes and Antibiotic Resistance. *Acta Naturae* **2018**, *10*, 33–48. [CrossRef]
15. Varela, M.F.; Stephen, J.; Lekshmi, M.; Ojha, M.; Wenzel, N.; Sanford, L.M.; Hernandez, A.J.; Parvathi, A.; Kumar, S.H. Bacterial Resistance to Antimicrobial Agents. *Antibiotics* **2021**, *10*, 593. [CrossRef] [PubMed]
16. Tackling Drug-Resistant Infections Globally: Final Report and Recommendations—The Review on Antimicrobial Resistance. Available online: https://amr-review.org/sites/default/files/160525_Final%20paper_with%20cover.pdf (accessed on 23 August 2021).
17. Fleitas Martínez, O.; Cardoso, M.H.; Ribeiro, S.M.; Franco, O.L. Recent Advances in Anti-Virulence Therapeutic Strategies with a Focus on Dismantling Bacterial Membrane Microdomains, Toxin Neutralization, Quorum-Sensing Interference and Biofilm Inhibition. *Front. Cell. Infect. Microbiol.* **2019**, *9*, 74. [CrossRef]

18. Kim, M.-K. *Staphylococcus aureus* Toxins: From Their Pathogenic Roles to Anti-Virulence Therapy Using Natural Products. *Biotechnol. Bioprocess Eng.* **2019**, *24*, 424–435. [[CrossRef](#)]
19. Bennett, M.R.; Thomsen, I.P. Epidemiological and Clinical Evidence for the Role of Toxins in *Staphylococcus aureus* Human Disease. *Toxins* **2020**, *12*, 408. [[CrossRef](#)] [[PubMed](#)]
20. Vlaeminck, J.; Raafat, D.; Surmann, K.; Timbermont, L.; Normann, N.; Sellman, B.; van Wamel, W.J.B.; Malhotra-Kumar, S. Exploring Virulence Factors and Alternative Therapies against *Staphylococcus aureus* Pneumonia. *Toxins* **2020**, *12*, 721. [[CrossRef](#)]
21. Ford, C.A.; Hurford, I.M.; Cassat, J.E. Antivirulence Strategies for the Treatment of *Staphylococcus aureus* Infections: A Mini Review. *Front. Microbiol.* **2021**, *11*, 3568. [[CrossRef](#)]
22. Divyakolu, S.; Chikkala, R.; Ratnakar, K.S.; Sritharan, V. Hemolysins of *Staphylococcus aureus*—An Update on Their Biology, Role in Pathogenesis and as Targets for Anti-Virulence Therapy. *Adv. Infect. Dis.* **2019**, *9*, 80–104. [[CrossRef](#)]
23. Berube, B.J.; Wardenburg, J.B. *Staphylococcus aureus* α -Toxin: Nearly a Century of Intrigue. *Toxins* **2013**, *5*, 1140–1166. [[CrossRef](#)]
24. Hernandez, S.L.; Nelson, M.; Sampedro, G.R.; Bagrodia, N.; Defnet, A.M.; Lec, B.; Emolo, J.; Kirschner, R.; Wu, L.; Biermann, H.; et al. *Staphylococcus aureus* Alpha Toxin Activates Notch in Vascular Cells. *Angiogenesis* **2019**, *22*, 197–209. [[CrossRef](#)]
25. Bhakdi, S.; Tranum-Jensen, J. Alpha-Toxin of *Staphylococcus aureus*. *Microbiol. Rev.* **1991**, *55*, 733–751. [[CrossRef](#)]
26. Pereira-Franchi, E.P.L.; Barreira, M.R.N.; de Costa, N.d.S.L.M.; Riboli, D.F.M.; Abraão, L.M.; Martins, K.B.; Victória, C.; da Cunha, M.d.L.R.d.S. Molecular Epidemiology of Methicillin-Resistant *Staphylococcus aureus* in the Brazilian Primary Health Care System. *Trop. Med. Int. Health* **2019**, *24*, 339–347. [[CrossRef](#)] [[PubMed](#)]
27. Bubeck Wardenburg, J.; Palazzolo-Ballance, A.M.; Otto, M.; Schneewind, O.; DeLeo, F.R. Panton-Valentine Leukocidin Is Not a Virulence Determinant in Murine Models of Community-Associated Methicillin-Resistant *Staphylococcus aureus* Disease. *J. Infect. Dis.* **2008**, *198*, 1166–1170. [[CrossRef](#)] [[PubMed](#)]
28. Crémieux, A.-C.; Saleh-Mghir, A.; Danel, C.; Couzon, F.; Dumitrescu, O.; Lilin, T.; Perronne, C.; Etienne, J.; Lina, G.; Vandenesch, F. α -Hemolysin, Not Panton-Valentine Leukocidin, Impacts Rabbit Mortality from Severe Sepsis with Methicillin-Resistant *Staphylococcus aureus* Osteomyelitis. *J. Infect. Dis.* **2014**, *209*, 1773–1780. [[CrossRef](#)]
29. Montgomery, C.P.; Boyle-Vavra, S.; Adem, P.V.; Lee, J.C.; Husain, A.N.; Clasen, J.; Daum, R.S. Comparison of Virulence in Community-Associated Methicillin-Resistant *Staphylococcus aureus* Pulsotypes USA300 and USA400 in a Rat Model of Pneumonia. *J. Infect. Dis.* **2008**, *198*, 561–570. [[CrossRef](#)] [[PubMed](#)]
30. Spaan, A.N.; van Strijp, J.A.G.; Torres, V.J. Leukocidins: Staphylococcal Bi-Component Pore-Forming Toxins Find Their Receptors. *Nat. Rev. Microbiol.* **2017**, *15*, 435–447. [[CrossRef](#)] [[PubMed](#)]
31. Grumann, D.; Nübel, U.; Bröker, B.M. *Staphylococcus aureus* Toxins—Their Functions and Genetics. *Infect. Genet. Evol.* **2014**, *21*, 583–592. [[CrossRef](#)]
32. Alonzo, F.; Kozhaya, L.; Rawlings, S.A.; Reyes-Robles, T.; DuMont, A.L.; Myszka, D.G.; Landau, N.R.; Unutmaz, D.; Torres, V.J. CCR5 Is a Receptor for *Staphylococcus aureus* Leukotoxin ED. *Nature* **2013**, *493*, 51–55. [[CrossRef](#)]
33. Spaan, A.N.; Henry, T.; van Rooijen, W.J.M.; Perret, M.; Badiou, C.; Aerts, P.C.; Kemmink, J.; de Haas, C.J.C.; van Kessel, K.P.M.; Vandenesch, F.; et al. The Staphylococcal Toxin Panton-Valentine Leukocidin Targets Human C5a Receptors. *Cell Host Microbe* **2013**, *13*, 584–594. [[CrossRef](#)] [[PubMed](#)]
34. DuMont, A.L.; Yoong, P.; Day, C.J.; Alonzo, F.; McDonald, W.H.; Jennings, M.P.; Torres, V.J. *Staphylococcus aureus* LukAB Cytotoxin Kills Human Neutrophils by Targeting the CD11b Subunit of the Integrin Mac-1. *Proc. Natl. Acad. Sci. USA* **2013**, *110*, 10794–10799. [[CrossRef](#)] [[PubMed](#)]
35. Kaneko, J.; Kamio, Y. Bacterial Two-Component and Hetero-Heptameric Pore-Forming Cytolytic Toxins: Structures, Pore-Forming Mechanism, and Organization of the Genes. *Biosci. Biotechnol. Biochem.* **2004**, *68*, 981–1003. [[CrossRef](#)]
36. Shallcross, L.J.; Fragaszy, E.; Johnson, A.M.; Hayward, A.C. The Role of the Panton-Valentine Leucocidin Toxin in Staphylococcal Disease: A Systematic Review and Meta-Analysis. *Lancet Infect. Dis.* **2013**, *13*, 43–54. [[CrossRef](#)]
37. Otter, J.A.; French, G.L. Molecular Epidemiology of Community-Associated Methicillin-Resistant *Staphylococcus aureus* in Europe. *Lancet Infect. Dis.* **2010**, *10*, 227–239. [[CrossRef](#)]
38. Mesrati, I.; Saïdani, M.; Ennigrou, S.; Zouari, B.; Ben Redjeb, S. Clinical Isolates of Pantone-Valentine Leucocidin- and Gamma-Haemolysin-Producing *Staphylococcus aureus*: Prevalence and Association with Clinical Infections. *J. Hosp. Infect.* **2010**, *75*, 265–268. [[CrossRef](#)] [[PubMed](#)]
39. Otto, M. Phenol-Soluble Modulins. *Int. J. Med. Microbiol.* **2014**, *304*, 164–169. [[CrossRef](#)] [[PubMed](#)]
40. Peschel, A.; Otto, M. Phenol-Soluble Modulins and Staphylococcal Infection. *Nat. Rev. Microbiol.* **2013**, *11*, 667–673. [[CrossRef](#)] [[PubMed](#)]
41. Cheung, G.Y.C.; Joo, H.-S.; Chatterjee, S.S.; Otto, M. Phenol-Soluble Modulins—Critical Determinants of Staphylococcal Virulence. *FEMS Microbiol. Rev.* **2014**, *38*, 698–719. [[CrossRef](#)] [[PubMed](#)]
42. Baldry, M.; Bojer, M.S.; Najarzadeh, Z.; Vestergaard, M.; Meyer, R.L.; Otzen, D.E.; Ingmer, H. Phenol-Soluble Modulins Modulate Persister Cell Formation in *Staphylococcus aureus*. *Front. Microbiol.* **2020**, *11*, 573253. [[CrossRef](#)] [[PubMed](#)]
43. Zaman, M.; Andreasen, M. Cross-Talk between Individual Phenol-Soluble Modulins in *Staphylococcus aureus* Biofilm Enables Rapid and Efficient Amyloid Formation. *eLife* **2020**, *9*, e59776. [[CrossRef](#)]
44. Queck, S.Y.; Jameson-Lee, M.; Villaruz, A.E.; Bach, T.-H.L.; Khan, B.A.; Sturdevant, D.E.; Ricklefs, S.M.; Li, M.; Otto, M. RNAIII-Independent Target Gene Control by the Agr Quorum-Sensing System: Insight into the Evolution of Virulence Regulation in *Staphylococcus aureus*. *Mol. Cell* **2008**, *32*, 150–158. [[CrossRef](#)]

45. Zapf, R.L.; Wiemels, R.E.; Keogh, R.A.; Holzschu, D.L.; Howell, K.M.; Trzeciak, E.; Caillet, A.R.; King, K.A.; Selhorst, S.A.; Naldrett, M.J.; et al. The Small RNA Teg41 Regulates Expression of the Alpha Phenol-Soluble Modulins and Is Required for Virulence in *Staphylococcus aureus*. *MBio* **2019**, *10*, e02484-18. [[CrossRef](#)] [[PubMed](#)]
46. Kretschmer, D.; Gleske, A.-K.; Rautenberg, M.; Wang, R.; Köberle, M.; Bohn, E.; Schöneberg, T.; Rabiet, M.-J.; Boulay, F.; Klebanoff, S.J.; et al. Human Formyl Peptide Receptor 2 Senses Highly Pathogenic *Staphylococcus aureus*. *Cell Host Microbe* **2010**, *7*, 463–473. [[CrossRef](#)]
47. Schreiner, J.; Kretschmer, D.; Klenk, J.; Otto, M.; Bühring, H.-J.; Stevanovic, S.; Wang, J.M.; Beer-Hammer, S.; Peschel, A.; Autenrieth, S.E. *Staphylococcus aureus* Phenol-Soluble Modulins Peptides Modulate Dendritic Cell Functions and Increase In Vitro Priming of Regulatory T Cells. *J. Immunol.* **2013**, *190*, 3417–3426. [[CrossRef](#)]
48. Wang, R.; Braughton, K.R.; Kretschmer, D.; Bach, T.-H.L.; Queck, S.Y.; Li, M.; Kennedy, A.D.; Dorward, D.W.; Klebanoff, S.J.; Peschel, A.; et al. Identification of Novel Cytolytic Peptides as Key Virulence Determinants for Community-Associated MRSA. *Nat. Med.* **2007**, *13*, 1510–1514. [[CrossRef](#)] [[PubMed](#)]
49. Gonzalez, D.J.; Vuong, L.; Gonzalez, I.S.; Keller, N.; McGrosso, D.; Hwang, J.H.; Hung, J.; Zinkernagel, A.; Dixon, J.E.; Dorrestein, P.C.; et al. Phenol Soluble Modulins (PSM) Variants of Community-Associated Methicillin-Resistant *Staphylococcus aureus* (MRSA) Captured Using Mass Spectrometry-Based Molecular Networking. *Mol. Cell. Proteom.* **2014**, *13*, 1262–1272. [[CrossRef](#)] [[PubMed](#)]
50. Davido, B.; Saleh-Mghir, A.; Laurent, F.; Danel, C.; Couzon, F.; Gatin, L.; Vandenesch, F.; Rasigade, J.-P.; Crémieux, A.-C. Phenol-Soluble Modulins Contribute to Early Sepsis Dissemination Not Late Local Usa300-Osteomyelitis Severity in Rabbits. *PLoS ONE* **2016**, *11*, e0157133. [[CrossRef](#)]
51. Richardson, J.R.; Armbruster, N.S.; Günter, M.; Biljecki, M.; Klenk, J.; Heumos, S.; Autenrieth, S.E. PSM Peptides from Community-Associated Methicillin-Resistant *Staphylococcus aureus* Impair the Adaptive Immune Response via Modulation of Dendritic Cell Subsets in Vivo. *Front. Immunol.* **2019**, *10*, 995. [[CrossRef](#)]
52. Czech, A.; Yamaguchi, T.; Bader, L.; Linder, S.; Kaminski, K.; Sugai, M.; Aepfelbacher, M. Prevalence of Rho-Inactivating Epidermal Cell Differentiation Inhibitor Toxins in Clinical *Staphylococcus aureus* Isolates. *J. Infect. Dis.* **2001**, *184*, 785–788. [[CrossRef](#)]
53. Messad, N.; Landraud, L.; Canivet, B.; Lina, G.; Richard, J.-L.; Sotto, A.; Lavigne, J.-P.; Lemichez, E. Distribution of Edin in *Staphylococcus aureus* Isolated from Diabetic Foot Ulcers. *Clin. Microbiol. Infect.* **2013**, *19*, 875–880. [[CrossRef](#)] [[PubMed](#)]
54. Boyer, L.; Doye, A.; Rolando, M.; Flatau, G.; Munro, P.; Gounon, P.; Clément, R.; Pulcini, C.; Popoff, M.R.; Mettouchi, A.; et al. Induction of Transient Macroapertures in Endothelial Cells through RhoA Inhibition by *Staphylococcus aureus* Factors. *J. Cell Biol.* **2006**, *173*, 809–819. [[CrossRef](#)] [[PubMed](#)]
55. Aktories, K.; Lang, A.E.; Schwan, C.; Mannherz, H.G. Actin as Target for Modification by Bacterial Protein Toxins. *FEBS J.* **2011**, *278*, 4526–4543. [[CrossRef](#)]
56. Jaffe, A.B.; Hall, A. Rho GTPases: Biochemistry and Biology. *Annu. Rev. Cell Dev. Biol.* **2005**, *21*, 247–269. [[CrossRef](#)] [[PubMed](#)]
57. Nusrat, A.; Giry, M.; Turner, J.R.; Colgan, S.P.; Parkos, C.A.; Carnes, D.; Lemichez, E.; Boquet, P.; Madara, J.L. Rho Protein Regulates Tight Junctions and Perijunctional Actin Organization in Polarized Epithelia. *Proc. Natl. Acad. Sci. USA* **1995**, *92*, 10629–10633. [[CrossRef](#)]
58. Caron, E.; Hall, A. Identification of Two Distinct Mechanisms of Phagocytosis Controlled by Different Rho GTPases. *Science* **1998**, *282*, 1717–1721. [[CrossRef](#)] [[PubMed](#)]
59. Lemichez, E.; Lecuit, M.; Nassif, X.; Bourdoulous, S. Breaking the Wall: Targeting of the Endothelium by Pathogenic Bacteria. *Nat. Rev. Microbiol.* **2010**, *8*, 93–104. [[CrossRef](#)]
60. Edwards, A.M.; Massey, R.C. How Does *Staphylococcus aureus* Escape the Bloodstream? *Trends Microbiol.* **2011**, *19*, 184–190. [[CrossRef](#)]
61. Sugai, M.; Enomoto, T.; Hashimoto, K.; Matsumoto, K.; Matsuo, Y.; Ohgai, H.; Hong, Y.-M.; Inoue, S.; Yoshikawa, K.; Suginaka, H. A Novel Epidermal Cell Differentiation Inhibitor (EDIN): Purification and Characterization from *Staphylococcus aureus*. *Biochem. Biophys. Res. Commun.* **1990**, *173*, 92–98. [[CrossRef](#)]
62. Yamaguchi, T.; Hayashi, T.; Takami, H.; Ohnishi, M.; Murata, T.; Nakayama, K.; Asakawa, K.; Ohara, M.; Komatsuzawa, H.; Sugai, M. Complete Nucleotide Sequence of a *Staphylococcus aureus* Exfoliative Toxin B Plasmid and Identification of a Novel ADP-Ribosyltransferase, EDIN-C. *Infect. Immun.* **2001**, *69*, 7760–7771. [[CrossRef](#)] [[PubMed](#)]
63. Yamaguchi, T.; Nishifuji, K.; Sasaki, M.; Fudaba, Y.; Aepfelbacher, M.; Takata, T.; Ohara, M.; Komatsuzawa, H.; Amagai, M.; Sugai, M. Identification of the *Staphylococcus aureus* Etd Pathogenicity Island Which Encodes a Novel Exfoliative Toxin, ETD, and EDIN-B. *Infect. Immun.* **2002**, *70*, 5835–5845. [[CrossRef](#)] [[PubMed](#)]
64. Munro, P.; Benchetrit, M.; Nahori, M.-A.; Stefani, C.; Clément, R.; Michiels, J.-F.; Landraud, L.; Dussurget, O.; Lemichez, E. The *Staphylococcus aureus* Epidermal Cell Differentiation Inhibitor Toxin Promotes Formation of Infection Foci in a Mouse Model of Bacteremia. *Infect. Immun.* **2010**, *78*, 3404–3411. [[CrossRef](#)] [[PubMed](#)]
65. Antri, K.; Rouzic, N.; Boubekri, I.; Dauwalder, O.; Beloufa, A.; Ziane, H.; Djennane, F.; Neggazi, M.; Benhabyles, B.; Bes, M.; et al. High prevalence of community and hospital acquired infections of methicillin-resistant *Staphylococcus aureus* containing Panton-Valentine leukocidin gene in Algiers. *Pathol. Biol.* **2010**, *58*, e15–e20. [[CrossRef](#)] [[PubMed](#)]

66. Courjon, J.; Munro, P.; Benito, Y.; Visvikis, O.; Bouchiat, C.; Boyer, L.; Doye, A.; Lepidi, H.; Ghigo, E.; Lavigne, J.-P.; et al. EDIN-B Promotes the Translocation of *Staphylococcus aureus* to the Bloodstream in the Course of Pneumonia. *Toxins* **2015**, *7*, 4131–4142. [[CrossRef](#)]
67. Pérez-Montarelo, D.; Viedma, E.; Larrosa, N.; Gómez-González, C.; Ruiz de Gopegui, E.; Muñoz-Gallego, I.; San Juan, R.; Fernández-Hidalgo, N.; Almirante, B.; Chaves, F. Molecular Epidemiology of *Staphylococcus aureus* Bacteremia: Association of Molecular Factors With the Source of Infection. *Front. Microbiol.* **2018**, *9*, 2210. [[CrossRef](#)] [[PubMed](#)]
68. Bukowski, M.; Wladyka, B.; Dubin, G. Exfoliative Toxins of *Staphylococcus aureus*. *Toxins* **2010**, *2*, 1148–1165. [[CrossRef](#)]
69. Stanley, J.R.; Amagai, M. Pemphigus, Bullous Impetigo, and the Staphylococcal Scalded-Skin Syndrome. *N. Engl. J. Med.* **2006**, *355*, 1800–1810. [[CrossRef](#)] [[PubMed](#)]
70. Kato, F.; Kadomoto, N.; Iwamoto, Y.; Bunai, K.; Komatsuzawa, H.; Sugai, M. Regulatory Mechanism for Exfoliative Toxin Production in *Staphylococcus aureus*. *Infect. Immun.* **2011**, *79*, 1660–1670. [[CrossRef](#)] [[PubMed](#)]
71. Eyre, R.W.; Stanley, J.R. Human Autoantibodies against a Desmosomal Protein Complex with a Calcium-Sensitive Epitope Are Characteristic of Pemphigus Foliaceus Patients. *J. Exp. Med.* **1987**, *165*, 1719–1724. [[CrossRef](#)]
72. Hanakawa, Y.; Schechter, N.M.; Lin, C.; Garza, L.; Li, H.; Yamaguchi, T.; Fudaba, Y.; Nishifuji, K.; Sugai, M.; Amagai, M.; et al. Molecular Mechanisms of Blister Formation in Bullous Impetigo and Staphylococcal Scalded Skin Syndrome. *J. Clin. Investig.* **2002**, *110*, 53–60. [[CrossRef](#)] [[PubMed](#)]
73. Nishifuji, K.; Sugai, M.; Amagai, M. Staphylococcal Exfoliative Toxins: “Molecular Scissors” of Bacteria That Attack the Cutaneous Defense Barrier in Mammals. *J. Dermatol. Sci.* **2008**, *49*, 21–31. [[CrossRef](#)] [[PubMed](#)]
74. Sila, J.; Sauer, P.; Kolar, M. Comparison of the Prevalence of Genes Coding for Enterotoxins, Exfoliatins, Panton-Valentine Leukocidin and Tsst-1 between Methicillin-Resistant and Methicillin-Susceptible Isolates of *Staphylococcus aureus* at the University Hospital in Olomouc. *Biomed. Pap. Med. Fac. Univ. Palacky Olomouc Czechoslov.* **2009**, *153*, 215–218. [[CrossRef](#)] [[PubMed](#)]
75. Mégevand, C.; Gervais, A.; Heining, U.; Berger, C.; Aebi, C.; Vaudaux, B.; Kind, C.; Gnehm, H.-P.; Hitzler, M.; Renzi, G.; et al. Molecular Epidemiology of the Nasal Colonization by Methicillin-Susceptible *Staphylococcus aureus* in Swiss Children. *Clin. Microbiol. Infect.* **2010**, *16*, 1414–1420. [[CrossRef](#)]
76. Yamaguchi, T.; Yokota, Y.; Terajima, J.; Hayashi, T.; Aepfelbacher, M.; Ohara, M.; Komatsuzawa, H.; Watanabe, H.; Sugai, M. Clonal Association of *Staphylococcus aureus* Causing Bullous Impetigo and the Emergence of New Methicillin-Resistant Clonal Groups in Kansai District in Japan. *J. Infect. Dis.* **2002**, *185*, 1511–1516. [[CrossRef](#)]
77. Noguchi, N.; Nakaminami, H.; Nishijima, S.; Kurokawa, I.; So, H.; Sasatsu, M. Antimicrobial Agent of Susceptibilities and Antiseptic Resistance Gene Distribution among Methicillin-Resistant *Staphylococcus aureus* Isolates from Patients with Impetigo and Staphylococcal Scalded Skin Syndrome. *J. Clin. Microbiol.* **2006**, *44*, 2119–2125. [[CrossRef](#)]
78. Wiczorek, M.; Abualrous, E.T.; Sticht, J.; Álvaro-Benito, M.; Stolzenberg, S.; Noé, F.; Freund, C. Major Histocompatibility Complex (MHC) Class I and MHC Class II Proteins: Conformational Plasticity in Antigen Presentation. *Front. Immunol.* **2017**, *8*, 292. [[CrossRef](#)]
79. Fraser, J.D.; Proft, T. The Bacterial Superantigen and Superantigen-like Proteins. *Immunol. Rev.* **2008**, *225*, 226–243. [[CrossRef](#)]
80. Lina, G.; Bohach, G.A.; Nair, S.P.; Hiramatsu, K.; Jouvin-Marche, E.; Mariuzza, R. Standard Nomenclature for the Superantigens Expressed by *Staphylococcus*. *J. Infect. Dis.* **2004**, *189*, 2334–2336. [[CrossRef](#)] [[PubMed](#)]
81. Hennekinne, J.-A.; De Buyser, M.-L.; Dragacci, S. *Staphylococcus aureus* and Its Food Poisoning Toxins: Characterization and Outbreak Investigation. *FEMS Microbiol. Rev.* **2012**, *36*, 815–836. [[CrossRef](#)] [[PubMed](#)]
82. Otto, M. *Staphylococcus aureus* Toxins. *Curr. Opin. Microbiol.* **2014**, *17*, 32–37. [[CrossRef](#)]
83. Hu, D.-L.; Li, S.; Fang, R.; Ono, H.K. Update on Molecular Diversity and Multipathogenicity of Staphylococcal Superantigen Toxins. *Anim. Dis.* **2021**, *1*, 7. [[CrossRef](#)]
84. Kong, C.; Neoh, H.; Nathan, S. Targeting *Staphylococcus aureus* Toxins: A Potential Form of Anti-Virulence Therapy. *Toxins* **2016**, *8*, 72. [[CrossRef](#)]
85. Fisher, E.L.; Otto, M.; Cheung, G.Y.C. Basis of Virulence in Enterotoxin-Mediated Staphylococcal Food Poisoning. *Front. Microbiol.* **2018**, *9*, 436. [[CrossRef](#)] [[PubMed](#)]
86. Uchiyama, T.; Araake, M.; Yan, X.J.; Miyanaga, Y.; Igarashi, H. Involvement of HLA Class II Molecules in Acquisition of Staphylococcal Enterotoxin A-Binding Activity and Accessory Cell Activity in Activation of Human T Cells by Related Toxins in Vascular Endothelial Cells. *Clin. Exp. Immunol.* **1992**, *87*, 322–328. [[CrossRef](#)]
87. Pezato, R.; Świerczyńska-Krępa, M.; Niżankowska-Mogilnicka, E.; Derycke, L.; Bachert, C.; Pérez-Novo, C.A. Role of Imbalance of Eicosanoid Pathways and Staphylococcal Superantigens in Chronic Rhinosinusitis. *Allergy* **2012**, *67*, 1347–1356. [[CrossRef](#)] [[PubMed](#)]
88. Pinchuk, I.V.; Beswick, E.J.; Reyes, V.E. Staphylococcal Enterotoxins. *Toxins* **2010**, *2*, 2177–2197. [[CrossRef](#)] [[PubMed](#)]
89. Salgado-Pabón, W.; Breshears, L.; Spaulding, A.R.; Merriman, J.A.; Stach, C.S.; Horswill, A.R.; Peterson, M.L.; Schlievert, P.M. Superantigens Are Critical for *Staphylococcus aureus* Infective Endocarditis, Sepsis, and Acute Kidney Injury. *MBio* **2013**, *4*, e00494-13. [[CrossRef](#)] [[PubMed](#)]
90. Stach, C.S.; Herrera, A.; Schlievert, P.M. Staphylococcal Superantigens Interact with Multiple Host Receptors to Cause Serious Diseases. *Immunol. Res.* **2014**, *59*, 177–181. [[CrossRef](#)] [[PubMed](#)]
91. McCormick, J.K.; Yarwood, J.M.; Schlievert, P.M. Toxic Shock Syndrome and Bacterial Superantigens: An Update. *Annu. Rev. Microbiol.* **2001**, *55*, 77–104. [[CrossRef](#)]

92. Adhikari, R.P.; Ajao, A.O.; Aman, M.J.; Karauzum, H.; Sarwar, J.; Lydecker, A.D.; Johnson, J.K.; Nguyen, C.; Chen, W.H.; Roghmann, M.-C. Lower Antibody Levels to *Staphylococcus aureus* Exotoxins Are Associated With Sepsis in Hospitalized Adults With Invasive *S. aureus* Infections. *J. Infect. Dis.* **2012**, *206*, 915–923. [[CrossRef](#)] [[PubMed](#)]
93. Sharma-Kuinkel, B.K.; Tkaczyk, C.; Bonnell, J.; Yu, L.; Tovchigrechko, A.; Tabor, D.E.; Park, L.P.; Ruffin, F.; Esser, M.T.; Sellman, B.R.; et al. Associations of Pathogen-Specific and Host-Specific Characteristics with Disease Outcome in Patients with *Staphylococcus aureus* Bacteremic Pneumonia. *Clin. Transl. Immunol.* **2019**, *8*, e01070. [[CrossRef](#)] [[PubMed](#)]
94. Gillet, Y.; Issartel, B.; Vanhems, P.; Fournet, J.-C.; Lina, G.; Bes, M.; Vandenesch, F.; Piémont, Y.; Brousse, N.; Floret, D.; et al. Association between *Staphylococcus aureus* Strains Carrying Gene for Panton-Valentine Leukocidin and Highly Lethal Necrotising Pneumonia in Young Immunocompetent Patients. *Lancet* **2002**, *359*, 753–759. [[CrossRef](#)]
95. Verdon, J.; Girardin, N.; Lacombe, C.; Berjeaud, J.-M.; Héchard, Y. Delta-Hemolysin, an Update on a Membrane-Interacting Peptide. *Peptides* **2009**, *30*, 817–823. [[CrossRef](#)]
96. Surewaard, B.G.J.; de Haas, C.J.C.; Vervoort, E.; Rigby, K.M.; DeLeo, F.R.; Otto, M.; van Strijp, J.A.G.; Nijland, R. Staphylococcal Alpha-Phenol Soluble Modulins Contribute to Neutrophil Lysis after Phagocytosis. *Cell. Microbiol.* **2013**, *15*, 1427–1437. [[CrossRef](#)] [[PubMed](#)]
97. Mishra, A.K.; Yadav, P.; Mishra, A. A Systemic Review on Staphylococcal Scalded Skin Syndrome (SSSS): A Rare and Critical Disease of Neonates. *Open Microbiol. J.* **2016**, *10*, 150. [[CrossRef](#)]
98. Wilke, G.A.; Bubeck Wardenburg, J. Role of a Disintegrin and Metalloprotease 10 in *Staphylococcus aureus* Alpha-Hemolysin-Mediated Cellular Injury. *Proc. Natl. Acad. Sci. USA* **2010**, *107*, 13473–13478. [[CrossRef](#)]
99. Foletti, D.; Strop, P.; Shaughnessy, L.; Hasa-Moreno, A.; Casas, M.G.; Russell, M.; Bee, C.; Wu, S.; Pham, A.; Zeng, Z.; et al. Mechanism of Action and in Vivo Efficacy of a Human-Derived Antibody against *Staphylococcus aureus* α -Hemolysin. *J. Mol. Biol.* **2013**, *425*, 1641–1654. [[CrossRef](#)]
100. Oganessian, V.; Peng, L.; Damschroder, M.M.; Cheng, L.; Sadowska, A.; Tkaczyk, C.; Sellman, B.R.; Wu, H.; Dall’Acqua, W.F. Mechanisms of Neutralization of a Human Anti- α -Toxin Antibody. *J. Biol. Chem.* **2014**, *289*, 29874–29880. [[CrossRef](#)]
101. Le, V.T.M.; Tkaczyk, C.; Chau, S.; Rao, R.L.; Dip, E.C.; Pereira-Franchi, E.P.; Cheng, L.; Lee, S.; Koelkebeck, H.; Hilliard, J.J.; et al. Critical Role of Alpha-Toxin and Protective Effects of Its Neutralization by a Human Antibody in Acute Bacterial Skin and Skin Structure Infections. *Antimicrob. Agents Chemother.* **2016**, *60*, 5640–5648. [[CrossRef](#)]
102. Ortines, R.V.; Liu, H.; Cheng, L.I.; Cohen, T.S.; Lawlor, H.; Gami, A.; Wang, Y.; Dillen, C.A.; Archer, N.K.; Miller, R.J.; et al. Neutralizing Alpha-Toxin Accelerates Healing of *Staphylococcus aureus*-Infected Wounds in Nondiabetic and Diabetic Mice. *Antimicrob. Agents Chemother.* **2018**, *62*, e02288-17. [[CrossRef](#)]
103. Surewaard, B.G.J.; Thanabalasuriar, A.; Zeng, Z.; Tkaczyk, C.; Cohen, T.S.; Bardoel, B.W.; Jorch, S.K.; Deppermann, C.; Bubeck Wardenburg, J.; Davis, R.P.; et al. α -Toxin Induces Platelet Aggregation and Liver Injury during *Staphylococcus aureus* Sepsis. *Cell Host Microbe* **2018**, *24*, 271–284.e3. [[CrossRef](#)] [[PubMed](#)]
104. Yu, X.-Q.; Robbie, G.J.; Wu, Y.; Esser, M.T.; Jensen, K.; Schwartz, H.I.; Bellamy, T.; Hernandez-Illas, M.; Jafri, H.S. Safety, Tolerability, and Pharmacokinetics of MEDI4893, an Investigational, Extended-Half-Life, Anti-*Staphylococcus aureus* Alpha-Toxin Human Monoclonal Antibody, in Healthy Adults. *Antimicrob. Agents Chemother.* **2017**, *61*, e01020-16. [[CrossRef](#)]
105. François, B.; Jafri, H.S.; Chastre, J.; Sánchez-García, M.; Eggimann, P.; Dequin, P.-F.; Huberlant, V.; Viña Soria, L.; Boulain, T.; Bretonnière, C.; et al. Efficacy and Safety of Suvratoxumab for Prevention of *Staphylococcus aureus* Ventilator-Associated Pneumonia (SAATELLITE): A Multicentre, Randomised, Double-Blind, Placebo-Controlled, Parallel-Group, Phase 2 Pilot Trial. *Lancet Infect. Dis.* **2021**, *21*, 1313–1323. [[CrossRef](#)]
106. François, B.; Mercier, E.; Gonzalez, C.; Asehnoune, K.; Nseir, S.; Fiancette, M.; Desachy, A.; Plantefève, G.; Meziani, F.; de Lame, P.-A.; et al. Safety and Tolerability of a Single Administration of AR-301, a Human Monoclonal Antibody, in ICU Patients with Severe Pneumonia Caused by *Staphylococcus aureus*: First-in-Human Trial. *Intensive Care Med.* **2018**, *44*, 1787–1796. [[CrossRef](#)]
107. Magyarics, Z.; Leslie, F.; Bartko, J.; Rouha, H.; Luperchio, S.; Schörghofer, C.; Schwameis, M.; Derhaschnig, U.; Lagler, H.; Stiebellehner, L.; et al. Randomized, Double-Blind, Placebo-Controlled, Single-Ascending-Dose Study of the Penetration of a Monoclonal Antibody Combination (ASN100) Targeting *Staphylococcus aureus* Cytotoxins in the Lung Epithelial Lining Fluid of Healthy Volunteers. *Antimicrob. Agents Chemother.* **2019**, *63*, e00350-19. [[CrossRef](#)]
108. Ruzin, A.; Yu, L.; Barraud, O.; François, B.; Sánchez Garcia, M.; Eggimann, P.; Dequin, P.-F.; Laterre, P.-F.; Huberlant, V.; Viña, L.; et al. 2160. Performance of the Cepheid Rapid PCR Test for Patient Screening and Association with Efficacy of Suvratoxumab, A Novel Anti-*Staphylococcus aureus* Monoclonal Antibody, During the Phase 2 SAATELLITE Study. *Open Forum Infect. Dis.* **2019**, *6*, S733. [[CrossRef](#)]
109. Vandenesch, F.; Naimi, T.; Enright, M.C.; Lina, G.; Nimmo, G.R.; Heffernan, H.; Liassine, N.; Bes, M.; Greenland, T.; Reverdy, M.-E.; et al. Community-Acquired Methicillin-Resistant *Staphylococcus aureus* Carrying Panton-Valentine Leukocidin Genes: Worldwide Emergence. *Emerg. Infect. Dis.* **2003**, *9*, 978–984. [[CrossRef](#)] [[PubMed](#)]
110. Diep, B.A.; Otto, M. The Role of Virulence Determinants in Community-Associated MRSA Pathogenesis. *Trends Microbiol.* **2008**, *16*, 361–369. [[CrossRef](#)] [[PubMed](#)]
111. Hermos, C.R.; Yoong, P.; Pier, G.B. High Levels of Antibody to Panton-Valentine Leukocidin Are Not Associated with Resistance to *Staphylococcus aureus*-Associated Skin and Soft-Tissue Infection. *Clin. Infect. Dis.* **2010**, *51*, 1138–1146. [[CrossRef](#)]

112. Gauduchon, V.; Cozon, G.; Vandenesch, F.; Genestier, A.-L.; Eyssade, N.; Peyrol, S.; Etienne, J.; Lina, G. Neutralization of *Staphylococcus aureus* Panton Valentine Leukocidin by Intravenous Immunoglobulin In Vitro. *J. Infect. Dis.* **2004**, *189*, 346–353. [[CrossRef](#)] [[PubMed](#)]
113. Mairpady Shambat, S.; Chen, P.; Nguyen Hoang, A.T.; Bergsten, H.; Vandenesch, F.; Siemens, N.; Lina, G.; Monk, I.R.; Foster, T.J.; Arakere, G.; et al. Modelling Staphylococcal Pneumonia in a Human 3D Lung Tissue Model System Delineates Toxin-Mediated Pathology. *Dis. Model. Mech.* **2015**, *8*, 1413–1425. [[CrossRef](#)] [[PubMed](#)]
114. Rouzic, N.; Janvier, F.; Libert, N.; Javouhey, E.; Lina, G.; Nizou, J.-Y.; Pasquier, P.; Stamm, D.; Brinquin, L.; Pelletier, C.; et al. Prompt and Successful Toxin-Targeting Treatment of Three Patients with Necrotizing Pneumonia Due to *Staphylococcus aureus* Strains Carrying the Panton-Valentine Leukocidin Genes. *J. Clin. Microbiol.* **2010**, *48*, 1952–1955. [[CrossRef](#)] [[PubMed](#)]
115. Laventie, B.-J.; Rademaker, H.J.; Saleh, M.; de Boer, E.; Janssens, R.; Bourcier, T.; Subilia, A.; Marcellin, L.; van Haperen, R.; Lebbink, J.H.G.; et al. Heavy Chain-Only Antibodies and Tetravalent Bispecific Antibody Neutralizing *Staphylococcus aureus* Leukotoxins. *Proc. Natl. Acad. Sci. USA* **2011**, *108*, 16404–16409. [[CrossRef](#)]
116. Aman, M.J. Superantigens of a Superbug: Major Culprits of *Staphylococcus aureus* Disease? *Virulence* **2017**, *8*, 607–610. [[CrossRef](#)] [[PubMed](#)]
117. Drozdowski, B.; Zhou, Y.; Kline, B.; Spidel, J.; Chan, Y.Y.; Albone, E.; Turchin, H.; Chao, Q.; Henry, M.; Balogach, J.; et al. Generation and Characterization of High Affinity Human Monoclonal Antibodies That Neutralize Staphylococcal Enterotoxin B. *J. Immune Based Ther. Vaccines* **2010**, *8*, 9. [[CrossRef](#)] [[PubMed](#)]
118. Varshney, A.K.; Wang, X.; Scharff, M.D.; MacIntyre, J.; Zollner, R.S.; Kovalenko, O.V.; Martinez, L.R.; Byrne, F.R.; Fries, B.C. Staphylococcal Enterotoxin B-Specific Monoclonal Antibody 20B1 Successfully Treats Diverse *Staphylococcus aureus* Infections. *J. Infect. Dis.* **2013**, *208*, 2058–2066. [[CrossRef](#)]
119. Fang, R.H.; Luk, B.T.; Hu, C.-M.J.; Zhang, L. Engineered Nanoparticles Mimicking Cell Membranes for Toxin Neutralization. *Adv. Drug Deliv. Rev.* **2015**, *90*, 69–80. [[CrossRef](#)]
120. Henry, B.D.; Neill, D.R.; Becker, K.A.; Gore, S.; Bricio-Moreno, L.; Ziobro, R.; Edwards, M.J.; Mühlemann, K.; Steinmann, J.; Kleuser, B.; et al. Engineered Liposomes Sequester Bacterial Exotoxins and Protect from Severe Invasive Infections in Mice. *Nat. Biotechnol.* **2015**, *33*, 81–88. [[CrossRef](#)]
121. Wolfmeier, H.; Mansour, S.C.; Liu, L.T.; Pletzer, D.; Draeger, A.; Babiychuk, E.B.; Hancock, R.E.W. Liposomal Therapy Attenuates Dermonecrosis Induced by Community-Associated Methicillin-Resistant *Staphylococcus aureus* by Targeting α -Type Phenol-Soluble Modulins and α -Hemolysin. *EBioMedicine* **2018**, *33*, 211–217. [[CrossRef](#)]
122. Keller, M.D.; Ching, K.L.; Liang, F.-X.; Dhabaria, A.; Tam, K.; Ueberheide, B.M.; Unutmaz, D.; Torres, V.J.; Cadwell, K. Decoy Exosomes Provide Protection against Bacterial Toxins. *Nature* **2020**, *579*, 260–264. [[CrossRef](#)]
123. Chen, Y.; Chen, M.; Zhang, Y.; Lee, J.H.; Escajadillo, T.; Gong, H.; Fang, R.H.; Gao, W.; Nizet, V.; Zhang, L. Broad-Spectrum Neutralization of Pore-Forming Toxins with Human Erythrocyte Membrane-Coated Nanosponges. *Adv. Healthc. Mater.* **2018**, *7*, e1701366. [[CrossRef](#)] [[PubMed](#)]
124. Wei, X.; Gao, J.; Wang, F.; Ying, M.; Angsantikul, P.; Kroll, A.V.; Zhou, J.; Gao, W.; Lu, W.; Fang, R.H.; et al. In Situ Capture of Bacterial Toxins for Antivirulence Vaccination. *Adv. Mater.* **2017**, *29*, 1701644. [[CrossRef](#)] [[PubMed](#)]
125. Yarwood, J.M.; Bartels, D.J.; Volper, E.M.; Greenberg, E.P. Quorum Sensing in *Staphylococcus aureus* Biofilms. *J. Bacteriol.* **2004**, *186*, 1838–1850. [[CrossRef](#)] [[PubMed](#)]
126. Cheung, G.Y.C.; Wang, R.; Khan, B.A.; Sturdevant, D.E.; Otto, M. Role of the Accessory Gene Regulator Agr in Community-Associated Methicillin-Resistant *Staphylococcus aureus* Pathogenesis. *Infect. Immun.* **2011**, *79*, 1927–1935. [[CrossRef](#)] [[PubMed](#)]
127. Novick, R.P.; Ross, H.F.; Projan, S.J.; Kornblum, J.; Kreiswirth, B.; Moghazeh, S. Synthesis of Staphylococcal Virulence Factors Is Controlled by a Regulatory RNA Molecule. *EMBO J.* **1993**, *12*, 3967–3975. [[CrossRef](#)] [[PubMed](#)]
128. Balaban, N.; Collins, L.V.; Cullor, J.S.; Hume, E.B.; Medina-Acosta, E.; Vieira da Motta, O.; O’Callaghan, R.; Rossitto, P.V.; Shirtliff, M.E.; Serafim da Silveira, L.; et al. Prevention of Diseases Caused by *Staphylococcus aureus* Using the Peptide RIP. *Peptides* **2000**, *21*, 1301–1311. [[CrossRef](#)]
129. Gov, Y.; Bitler, A.; Dell’Acqua, G.; Torres, J.V.; Balaban, N. RNAIII Inhibiting Peptide (RIP), a Global Inhibitor of *Staphylococcus aureus* Pathogenesis: Structure and Function Analysis. *Peptides* **2001**, *22*, 1609–1620. [[CrossRef](#)]
130. Vieira-da-Motta, O.; Damasceno Ribeiro, P.; Dias da Silva, W.; Medina-Acosta, E. RNAIII Inhibiting Peptide (RIP) Inhibits Agr-Regulated Toxin Production. *Peptides* **2001**, *22*, 1621–1627. [[CrossRef](#)]
131. Ma, B.; Zhou, Y.; Li, M.; Yu, Q.; Xue, X.; Li, Z.; Da, F.; Hou, Z.; Luo, X. RIP-V Improves Murine Survival in a Sepsis Model by down-Regulating RNAIII Expression and α -Hemolysin Release of Methicillin-Resistant *Staphylococcus aureus*. *Pharmazie* **2015**, *70*, 81–87.
132. Giacometti, A.; Cirioni, O.; Ghiselli, R.; Dell’Acqua, G.; Orlando, F.; D’Amato, G.; Mocchegiani, F.; Silvestri, C.; Del Prete, M.S.; Rocchi, M.; et al. RNAIII-Inhibiting Peptide Improves Efficacy of Clinically Used Antibiotics in a Murine Model of Staphylococcal Sepsis. *Peptides* **2005**, *26*, 169–175. [[CrossRef](#)]
133. Simonetti, O.; Cirioni, O.; Ghiselli, R.; Goteri, G.; Scalise, A.; Orlando, F.; Silvestri, C.; Riva, A.; Saba, V.; Madanahally, K.D.; et al. RNAIII-Inhibiting Peptide Enhances Healing of Wounds Infected with Methicillin-Resistant *Staphylococcus aureus*. *Antimicrob. Agents Chemother.* **2008**, *52*, 2205–2211. [[CrossRef](#)] [[PubMed](#)]
134. Zhou, Y.; Niu, C.; Ma, B.; Xue, X.; Li, Z.; Chen, Z.; Li, F.; Zhou, S.; Luo, X.; Hou, Z. Inhibiting PSM α -Induced Neutrophil Necroptosis Protects Mice with MRSA Pneumonia by Blocking the Agr System. *Cell Death Dis.* **2018**, *9*, 362. [[CrossRef](#)] [[PubMed](#)]

135. Huan, Y.; Kong, Q.; Mou, H.; Yi, H. Antimicrobial Peptides: Classification, Design, Application and Research Progress in Multiple Fields. *Front. Microbiol.* **2020**, *11*, 2559. [[CrossRef](#)] [[PubMed](#)]
136. Kudryashova, E.; Seveau, S.M.; Kudryashov, D.S. Targeting and Inactivation of Bacterial Toxins by Human Defensins. *Biol. Chem.* **2017**, *398*, 1069–1085. [[CrossRef](#)] [[PubMed](#)]
137. Patrulea, V.; Borchard, G.; Jordan, O. An Update on Antimicrobial Peptides (AMPs) and Their Delivery Strategies for Wound Infections. *Pharmaceutics* **2020**, *12*, 840. [[CrossRef](#)]
138. Lehrer, R.I.; Lu, W. α -Defensins in Human Innate Immunity. *Immunol. Rev.* **2012**, *245*, 84–112. [[CrossRef](#)] [[PubMed](#)]
139. Lillard, J.W.; Boyaka, P.N.; Chertov, O.; Oppenheim, J.J.; McGhee, J.R. Mechanisms for Induction of Acquired Host Immunity by Neutrophil Peptide Defensins. *Proc. Natl. Acad. Sci. USA* **1999**, *96*, 651–656. [[CrossRef](#)]
140. Diep, B.A.; Chan, L.; Tattevin, P.; Kajikawa, O.; Martin, T.R.; Basuino, L.; Mai, T.T.; Marbach, H.; Braughton, K.R.; Whitney, A.R.; et al. Polymorphonuclear Leukocytes Mediate *Staphylococcus aureus* Panton-Valentine Leukocidin-Induced Lung Inflammation and Injury. *Proc. Natl. Acad. Sci. USA* **2010**, *107*, 5587–5592. [[CrossRef](#)] [[PubMed](#)]
141. Cardot-Martin, E.; Casalegno, J.S.; Badiou, C.; Dauwalder, O.; Keller, D.; Prévost, G.; Rieg, S.; Kern, W.V.; Cuerq, C.; Etienne, J.; et al. α -Defensins Partially Protect Human Neutrophils against Panton-Valentine Leukocidin Produced by *Staphylococcus aureus*. *Let. Appl. Microbiol.* **2015**, *61*, 158–164. [[CrossRef](#)]
142. Karginov, V.A.; Nestorovich, E.M.; Schmidtman, F.; Robinson, T.M.; Yohannes, A.; Fahmi, N.E.; Bezrukov, S.M.; Hecht, S.M. Inhibition of *S. aureus* α -Hemolysin and *B. anthracis* Lethal Toxin by β -Cyclodextrin Derivatives. *Bioorg. Med. Chem.* **2007**, *15*, 5424–5431. [[CrossRef](#)]
143. Dong, J.; Qiu, J.; Wang, J.; Li, H.; Dai, X.; Zhang, Y.; Wang, X.; Tan, W.; Niu, X.; Deng, X.; et al. Apigenin Alleviates the Symptoms of *Staphylococcus aureus* Pneumonia by Inhibiting the Production of Alpha-Hemolysin. *FEMS Microbiol. Lett.* **2013**, *338*, 124–131. [[CrossRef](#)] [[PubMed](#)]
144. Jiang, L.; Yi, T.; Shen, Z.; Teng, Z.; Wang, J. Aloe-Emodin Attenuates *Staphylococcus aureus* Pathogenicity by Interfering with the Oligomerization of α -Toxin. *Front. Cell. Infect. Microbiol.* **2019**, *9*, 157. [[CrossRef](#)] [[PubMed](#)]
145. Wang, J.; Zhou, X.; Liu, S.; Li, G.; Shi, L.; Dong, J.; Li, W.; Deng, X.; Niu, X. Morin Hydrate Attenuates *Staphylococcus aureus* Virulence by Inhibiting the Self-Assembly of α -Hemolysin. *J. Appl. Microbiol.* **2015**, *118*, 753–763. [[CrossRef](#)]
146. Dong, J.; Qiu, J.; Zhang, Y.; Lu, C.; Dai, X.; Wang, J.; Li, H.; Wang, X.; Tan, W.; Luo, M.; et al. Oroxylin A Inhibits Hemolysis via Hindering the Self-Assembly of α -Hemolysin Heptameric Transmembrane Pore. *PLoS Comput. Biol.* **2013**, *9*, e1002869. [[CrossRef](#)]
147. Qiu, J.; Wang, D.; Zhang, Y.; Dong, J.; Wang, J.; Niu, X. Molecular Modeling Reveals the Novel Inhibition Mechanism and Binding Mode of Three Natural Compounds to Staphylococcal α -Hemolysin. *PLoS ONE* **2013**, *8*, e80197. [[CrossRef](#)]
148. Friedman, M.; Rasooly, R.; Do, P.M.; Henika, P.R. The Olive Compound 4-Hydroxytyrosol Inactivates *Staphylococcus aureus* Bacteria and Staphylococcal Enterotoxin A (SEA). *J. Food Sci.* **2011**, *76*, M558–M563. [[CrossRef](#)] [[PubMed](#)]
149. Mansson, M.; Nielsen, A.; Kjærulff, L.; Gotfredsen, C.H.; Wietz, M.; Ingmer, H.; Gram, L.; Larsen, T.O. Inhibition of Virulence Gene Expression in *Staphylococcus aureus* by Novel Depsipeptides from a Marine Photobacterium. *Mar. Drugs* **2011**, *9*, 2537–2552. [[CrossRef](#)]
150. Nielsen, A.; Månsson, M.; Bojer, M.S.; Gram, L.; Larsen, T.O.; Novick, R.P.; Frees, D.; Frøkiær, H.; Ingmer, H. Solonamide B Inhibits Quorum Sensing and Reduces *Staphylococcus aureus* Mediated Killing of Human Neutrophils. *PLoS ONE* **2014**, *9*, e84992. [[CrossRef](#)]
151. Baldry, M.; Kitiir, B.; Frøkiær, H.; Christensen, S.B.; Taverne, N.; Meijerink, M.; Franzyk, H.; Olsen, C.A.; Wells, J.M.; Ingmer, H. The Agr Inhibitors Solonamide B and Analogues Alter Immune Responses to *Staphylococcus aureus* but Do Not Exhibit Adverse Effects on Immune Cell Functions. *PLoS ONE* **2016**, *11*, e0145618. [[CrossRef](#)] [[PubMed](#)]
152. Baldry, M.; Nakamura, Y.; Nakagawa, S.; Frees, D.; Matsue, H.; Núñez, G.; Ingmer, H. Application of an Agr-Specific Antivirulence Compound as Therapy for *Staphylococcus aureus*-Induced Inflammatory Skin Disease. *J. Infect. Dis.* **2018**, *218*, 1009–1013. [[CrossRef](#)]
153. Wang, J.; Qiu, J.; Dong, J.; Li, H.; Luo, M.; Dai, X.; Zhang, Y.; Leng, B.; Niu, X.; Zhao, S.; et al. Chrysin Protects Mice from *Staphylococcus aureus* Pneumonia. *J. Appl. Microbiol.* **2011**, *111*, 1551–1558. [[CrossRef](#)]
154. Tang, F.; Li, W.-H.; Zhou, X.; Liu, Y.-H.; Li, Z.; Tang, Y.-S.; Kou, X.; Wang, S.-D.; Bao, M.; Qu, L.-D.; et al. Puerarin Protects against *Staphylococcus aureus*-Induced Injury of Human Alveolar Epithelial A549 Cells via Downregulating Alpha-Hemolysin Secretion. *Microb. Drug Resist.* **2014**, *20*, 357–363. [[CrossRef](#)] [[PubMed](#)]
155. Jiang, L.; Li, H.; Wang, L.; Song, Z.; Shi, L.; Li, W.; Deng, X.; Wang, J. Isorhamnetin Attenuates *Staphylococcus aureus*-Induced Lung Cell Injury by Inhibiting Alpha-Hemolysin Expression. *J. Microbiol. Biotechnol.* **2016**, *26*, 596–602. [[CrossRef](#)]
156. Nabavi, S.F.; Braid, N.; Habtemariam, S.; Orhan, I.E.; Daglia, M.; Manayi, A.; Gortzi, O.; Nabavi, S.M. Neuroprotective Effects of Chrysin: From Chemistry to Medicine. *Neurochem. Int.* **2015**, *90*, 224–231. [[CrossRef](#)]
157. Zhou, Y.-X.; Zhang, H.; Peng, C. Puerarin: A Review of Pharmacological Effects. *Phytother. Res. PTR* **2014**, *28*, 961–975. [[CrossRef](#)] [[PubMed](#)]
158. Zhang, Y.; Wang, J.-F.; Dong, J.; Wei, J.-Y.; Wang, Y.-N.; Dai, X.-H.; Wang, X.; Luo, M.-J.; Tan, W.; Deng, X.-M.; et al. Inhibition of α -Toxin Production by Subinhibitory Concentrations of Naringenin Controls *Staphylococcus aureus* Pneumonia. *Fitoterapia* **2013**, *86*, 92–99. [[CrossRef](#)] [[PubMed](#)]
159. Salehi, B.; Fokou, P.V.T.; Sharifi-Rad, M.; Zucca, P.; Pezzani, R.; Martins, N.; Sharifi-Rad, J. The Therapeutic Potential of Naringenin: A Review of Clinical Trials. *Pharmaceutics* **2019**, *12*, 11. [[CrossRef](#)]

160. Quave, C.L.; Plano, L.R.W.; Bennett, B.C. Quorum Sensing Inhibitors of *Staphylococcus aureus* from Italian Medicinal Plants. *Planta Med.* **2011**, *77*, 188–195. [CrossRef]
161. Muhs, A.; Lyles, J.T.; Parlet, C.P.; Nelson, K.; Kavanaugh, J.S.; Horswill, A.R.; Quave, C.L. Virulence Inhibitors from Brazilian Peppertree Block Quorum Sensing and Abate Dermonecrosis in Skin Infection Models. *Sci. Rep.* **2017**, *7*, 42275. [CrossRef] [PubMed]
162. Todd, D.A.; Parlet, C.P.; Crosby, H.A.; Malone, C.L.; Heilmann, K.P.; Horswill, A.R.; Cech, N.B. Signal Biosynthesis Inhibition with Ambuic Acid as a Strategy To Target Antibiotic-Resistant Infections. *Antimicrob. Agents Chemother.* **2017**, *61*, e00263-17. [CrossRef]
163. Geisinger, E.; Muir, T.W.; Novick, R.P. Agr Receptor Mutants Reveal Distinct Modes of Inhibition by Staphylococcal Autoinducing Peptides. *Proc. Natl. Acad. Sci. USA* **2009**, *106*, 1216–1221. [CrossRef]
164. Malachowa, N.; Kobayashi, S.D.; Braughton, K.R.; DeLeo, F.R. Mouse Model of *Staphylococcus aureus* Skin Infection. In *Mouse Models of Innate Immunity*; Humana Press: Totowa, NJ, USA, 2013; Volume 1031, pp. 109–116. [CrossRef]
165. Menzies, B.E.; Kernodle, D.S. Site-Directed Mutagenesis of the Alpha-Toxin Gene of *Staphylococcus aureus*: Role of Histidines in Toxin Activity in Vitro and in a Murine Model. *Infect. Immun.* **1994**, *62*, 1843–1847. [CrossRef]
166. Bubeck-Wardenburg, J.; Schneewind, O. Vaccine Protection against *Staphylococcus aureus* Pneumonia. *J. Exp. Med.* **2008**, *205*, 287–294. [CrossRef]
167. Karauzum, H.; Venkatasubramaniam, A.; Adhikari, R.P.; Kort, T.; Holtsberg, F.W.; Mukherjee, I.; Mednikov, M.; Ortines, R.; Nguyen, N.T.Q.; Doan, T.M.N.; et al. IBT-V02: A Multicomponent Toxoid Vaccine Protects Against Primary and Secondary Skin Infections Caused by *Staphylococcus aureus*. *Front. Immunol.* **2021**, *12*, 624310. [CrossRef]
168. Brown, E.L.; Dumitrescu, O.; Thomas, D.; Badiou, C.; Koers, E.M.; Choudhury, P.; Vazquez, V.; Etienne, J.; Lina, G.; Vandenesch, F.; et al. The Panton-Valentine Leukocidin Vaccine Protects Mice against Lung and Skin Infections Caused by *Staphylococcus aureus* USA300. *Clin. Microbiol. Infect.* **2009**, *15*, 156–164. [CrossRef]
169. Karauzum, H.; Adhikari, R.P.; Sarwar, J.; Devi, V.S.; Abaandou, L.; Haudenschild, C.; Mahmoudieh, M.; Boroun, A.R.; Vu, H.; Nguyen, T.; et al. Structurally Designed Attenuated Subunit Vaccines for *S. aureus* LukS-PV and LukF-PV Confer Protection in a Mouse Bacteremia Model. *PLoS ONE* **2013**, *8*, e65384. [CrossRef]
170. Landrum, M.L.; Lalani, T.; Niknian, M.; Maguire, J.D.; Hospenthal, D.R.; Fattom, A.; Taylor, K.; Fraser, J.; Wilkins, K.; Ellis, M.W.; et al. Safety and Immunogenicity of a Recombinant *Staphylococcus aureus* α -Toxoid and a Recombinant Panton-Valentine Leukocidin Subunit, in Healthy Adults. *Hum. Vaccines Immunother.* **2017**, *13*, 791–801. [CrossRef] [PubMed]
171. Jones, T. StaphVAX (Nabi). *Curr. Opin. Investig. Drugs Lond. Engl.* **2002**, *3*, 48–50.
172. *Staphylococcus aureus* Vaccine Conjugate–Nabi: Nabi-StaphVAX, StaphVAX. *Drugs RD* **2003**, *4*, 383–385. [CrossRef]
173. Asensi, G.F.; de Sales, N.F.F.; Dutra, F.F.; Feijó, D.F.; Bozza, M.T.; Ulrich, R.G.; Miyoshi, A.; de Moraes, K.; Azevedo, V.A.d.C.; Silva, J.T.; et al. Oral Immunization with *Lactococcus lactis* Secreting Attenuated Recombinant Staphylococcal Enterotoxin B Induces a Protective Immune Response in a Murine Model. *Microb. Cell Fact.* **2013**, *12*, 32. [CrossRef] [PubMed]
174. Chen, W.H.; Pasetti, M.F.; Adhikari, R.P.; Baughman, H.; Douglas, R.; El-Khorazaty, J.; Greenberg, N.; Holtsberg, F.W.; Liao, G.C.; Reymann, M.K.; et al. Safety and Immunogenicity of a Parenterally Administered, Structure-Based Rationally Modified Recombinant Staphylococcal Enterotoxin B Protein Vaccine, STEBVax. *Clin. Vaccine Immunol.* **2016**, *23*, 918–925. [CrossRef]
175. Hu, D.-L.; Omoe, K.; Sasaki, S.; Sashinami, H.; Sakuraba, H.; Yokomizo, Y.; Shinagawa, K.; Nakane, A. Vaccination with Nontoxic Mutant Toxic Shock Syndrome Toxin 1 Protects against *Staphylococcus aureus* Infection. *J. Infect. Dis.* **2003**, *188*, 743–752. [CrossRef] [PubMed]
176. Schwameis, M.; Roppenser, B.; Firbas, C.; Gruener, C.S.; Model, N.; Stich, N.; Roetzer, A.; Buchtele, N.; Jilma, B.; Eibl, M.M. Safety, Tolerability, and Immunogenicity of a Recombinant Toxic Shock Syndrome Toxin (RTSST)-1 Variant Vaccine: A Randomised, Double-Blind, Adjuvant-Controlled, Dose Escalation First-in-Man Trial. *Lancet Infect. Dis.* **2016**, *16*, 1036–1044. [CrossRef]
177. Roetzer, A.; Jilma, B.; Eibl, M.M. Vaccine against Toxic Shock Syndrome in a First-in-Man Clinical Trial. *Expert Rev. Vaccines* **2017**, *16*, 81–83. [CrossRef] [PubMed]
178. Brown, L.; Wolf, J.M.; Prados-Rosales, R.; Casadevall, A. Through the Wall: Extracellular Vesicles in Gram-Positive Bacteria, Mycobacteria and Fungi. *Nat. Rev. Microbiol.* **2015**, *13*, 620–630. [CrossRef]
179. Wang, X.; Koffi, P.F.; English, O.F.; Lee, J.C. *Staphylococcus aureus* Extracellular Vesicles: A Story of Toxicity and the Stress of 2020. *Toxins* **2021**, *13*, 75. [CrossRef] [PubMed]
180. Mattis, D.M.; Spaulding, A.R.; Chuang-Smith, O.N.; Sundberg, E.J.; Schlievert, P.M.; Kranz, D.M. Engineering a Soluble High-Affinity Receptor Domain That Neutralizes Staphylococcal Enterotoxin C in Rabbit Models of Disease. *Protein Eng. Des. Sel. PEDS* **2013**, *26*, 133–142. [CrossRef]
181. Wang, X.; Thompson, C.D.; Weidenmaier, C.; Lee, J.C. Release of *Staphylococcus aureus* Extracellular Vesicles and Their Application as a Vaccine Platform. *Nat. Commun.* **2018**, *9*, 1379. [CrossRef]
182. da Silveira, S.A.; Perez, A. Improving the Fate of Severely Infected Patients: The Promise of Anti-Toxin Treatments and Superiority Trials. *Expert Rev. Anti Infect. Ther.* **2017**, *15*, 973–975. [CrossRef]
183. Parker, D. Humanized Mouse Models of *Staphylococcus aureus* Infection. *Front. Immunol.* **2017**, *8*, 512. [CrossRef]
184. Allen, T.M.; Brehm, M.A.; Bridges, S.; Ferguson, S.; Kumar, P.; Mirochnitchenko, O.; Palucka, K.; Pelanda, R.; Sanders-Beer, B.; Shultz, L.D.; et al. Humanized Immune System Mouse Models: Progress, Challenges and Opportunities. *Nat. Immunol.* **2019**, *20*, 770–774. [CrossRef] [PubMed]

185. Mrochen, D.M.; Fernandes de Oliveira, L.M.; Raafat, D.; Holtfreter, S. *Staphylococcus aureus* Host Tropism and Its Implications for Murine Infection Models. *Int. J. Mol. Sci.* **2020**, *21*, 7061. [[CrossRef](#)] [[PubMed](#)]
186. Khan, B.A.; Yeh, A.J.; Cheung, G.Y.; Otto, M. Investigational Therapies Targeting Quorum-Sensing for the Treatment of *Staphylococcus aureus* Infections. *Expert Opin. Investig. Drugs* **2015**, *24*, 689–704. [[CrossRef](#)] [[PubMed](#)]
187. Kumar, K.; Chen, J.; Drlica, K.; Shopsin, B. Tuning of the Lethal Response to Multiple Stressors with a Single-Site Mutation during Clinical Infection by *Staphylococcus aureus*. *MBio* **2017**, *8*, e01476-17. [[CrossRef](#)] [[PubMed](#)]
188. Bojer, M.S.; Lindemose, S.; Vestergaard, M.; Ingmer, H. Quorum Sensing-Regulated Phenol-Soluble Modulins Limit Persister Cell Populations in *Staphylococcus aureus*. *Front. Microbiol.* **2018**, *9*, 255. [[CrossRef](#)] [[PubMed](#)]

Annexe 4: Publication associée – 3ème auteur – Acceptée dans Frontiers
in Microbiology le 22 Septembre 2021



ORIGINAL RESEARCH
published: 15 October 2021
doi: 10.3389/fmicb.2021.750489



Biofilm Formation in Methicillin-Resistant *Staphylococcus aureus* Isolated in Cystic Fibrosis Patients Is Strain-Dependent and Differentially Influenced by Antibiotics

Agathe Boudet^{1†}, Pauline Sorlin^{2†}, Cassandra Pouget³, Raphaël Chiron⁴, Jean-Philippe Lavigne¹, Catherine Dunyach-Remy¹ and Héléne Marchandin^{2*}

OPEN ACCESS

Edited by:

Giovanni Di Bonaventura,
University of Studies G. d'Annunzio
Chieti and Pescara, Italy

Reviewed by:

Barbara C. Kahl,
University of Münster, Germany
Rosa Del Campo,
Ramón y Cajal Institute for Health
Research, Spain
Louise Frances Roddam,
University of Tasmania, Australia

*Correspondence:

Héléne Marchandin
helene.marchandin@umontpellier.fr

[†]These authors have contributed
equally to this work

Specialty section:

This article was submitted to
Infectious Agents and Disease,
a section of the journal
Frontiers in Microbiology

Received: 30 July 2021

Accepted: 22 September 2021

Published: 15 October 2021

Citation:

Boudet A, Sorlin P, Pouget C,
Chiron R, Lavigne J-P,
Dunyach-Remy C and
Marchandin H (2021) Biofilm
Formation in Methicillin-Resistant
Staphylococcus aureus Isolated in
Cystic Fibrosis Patients Is
Strain-Dependent and Differentially
Influenced by Antibiotics.
Front. Microbiol. 12:750489.
doi: 10.3389/fmicb.2021.750489

¹VBIC, INSERM U1047, Université de Montpellier, Service de Microbiologie et Hygiène Hospitalière, CHU Nîmes, Nîmes, France, ²HydroSciences Montpellier, Université de Montpellier, CNRS, IRD, Département de Microbiologie, CHU de Nîmes, Montpellier, France, ³VBIC, INSERM U1047, Université de Montpellier, Nîmes, France, ⁴HydroSciences Montpellier, Université de Montpellier, CNRS, IRD, Centre de Ressources et de Compétences de la Mucoviscidose, CHU de Montpellier, Montpellier, France

Cystic fibrosis (CF) is a genetic disease with lung abnormalities making patients particularly predisposed to pulmonary infections. *Staphylococcus aureus* is the most frequently identified pathogen, and multidrug-resistant strains (MRSA, methicillin-resistant *S. aureus*) have been associated with more severe lung dysfunction leading to eradication recommendations. Diverse bacterial traits and adaptive skills, including biofilm formation, may, however, make antimicrobial therapy challenging. In this context, we compared the ability of a collection of genotyped MRSA isolates from CF patients to form biofilm with and without antibiotics (ceftaroline, ceftobiprole, linezolid, trimethoprim, and rifampicin). Our study used standardized approaches not previously applied to CF MRSA, the BioFilm Ring test® (BRT®), the Antibiofilmogram®, and the BioFlux™ 200 system which were adapted for use with the artificial sputum medium (ASM) mimicking conditions more relevant to the CF lung. We included 63 strains of 10 multilocus sequence types (STs) isolated from 35 CF patients, 16 of whom had chronic colonization. The BRT® showed that 27% of the strains isolated in 37% of the patients were strong biofilm producers. The Antibiofilmogram® performed on these strains showed that broad-spectrum cephalosporins had the lowest minimum biofilm inhibitory concentrations (bMIC) on a majority of strains. A focus on four chronically colonized patients with inclusion of successively isolated strains showed that ceftaroline, ceftobiprole, and/or linezolid bMICs may remain below the resistance thresholds over time. Studying the dynamics of biofilm formation by strains isolated 3 years apart in one of these patients using BioFlux™ 200 showed that inhibition of biofilm formation was observed for up to 36 h of exposure to bMIC and ceftaroline and ceftobiprole had a significantly greater effect than linezolid. This study has brought new insights into the behavior of CF MRSA which has been little studied for its ability to form biofilm. Biofilm formation is a common characteristic of prevalent MRSA clones in CF.

Early biofilm formation was strain-dependent, even within a sample, and not only observed during chronic colonization. Ceftaroline and ceftobiprole showed a remarkable activity with a long-lasting inhibitory effect on biofilm formation and a conserved activity on certain strains adapted to the CF lung environment after years of colonization.

Keywords: cystic fibrosis, methicillin-resistance *Staphylococcus aureus* (MRSA), biofilm, antibiofilm activity, ceftaroline, ceftobiprole, linezolid

INTRODUCTION

Cystic fibrosis (CF) is a recessive genetic disease linked to a mutation in the cystic fibrosis transmembrane conductance regulator (*cfr*) gene encoding for an ion channel whose dysfunction causes thickening of the respiratory mucus in CF patients (Rowe et al., 2005). The resulting dehydrated, sticky mucus provides an ideal environment for bacterial colonization, and CF patients are therefore particularly exposed to pulmonary infections from an early age. Among the prevalent opportunistic pathogens in CF worldwide, *Staphylococcus aureus* is generally the most commonly identified microorganism (Registre français de la mucoviscidose - Bilan des données, 2019; The Cystic Fibrosis Foundation Patient Registry, 2019; Zolin et al., 2020). *S. aureus* is acquired early on in the life of CF patients, and from the age of 5 years, *S. aureus* will colonize or infect approximately 70% of children. Infections may be persistent in certain patients, and in 2018 in Europe, the prevalence of chronic *S. aureus* in CF patients was 35.68% (34.34% in children; 37.12% in adults; Zolin et al., 2020). Multidrug-resistant *S. aureus* strains, known as methicillin-resistant *S. aureus* (MRSA), are of particular concern. A degree of variation in MRSA prevalence is observed between countries for the CF population with a lower prevalence observed in Europe (e.g., 5.9% in France in 2019; Registre français de la mucoviscidose - Bilan des données, 2019) compared with the United States where the widespread distribution of community-acquired MRSA clones like the USA300 clone (Glikman et al., 2008; Goss and Muhlebach, 2011) is associated with a 25% rate of CF patients with at least one MRSA isolate in 2019 (The Cystic Fibrosis Foundation Patient Registry, 2019). In Europe, the epidemiology of circulating MRSA clones in the CF population remains largely unexplored. MRSA eradication in CF patients is currently recommended as compared with methicillin-susceptible *S. aureus* (MSSA), MRSA persists longer in the airways of these patients, resulting in more serious pulmonary dysfunction and lung damage with a greater decline in mean forced expiratory volume in 1 s (FEV1) and in greater use of antibiotics (Ren et al., 2007; Dasenbrook et al., 2008; Vanderhelst et al., 2012). However, MRSA eradication is challenging, not only due to the antimicrobial multidrug resistance patterns of the strains but also to the diverse bacterial adaptation pathways developed in the CF lung environment, including biofilm formation which represents an important barrier to eradication treatment and host defenses, thus contributing to bacterial persistence

in the CF lung (Goerke and Wolz, 2010; Hirschhausen et al., 2013). Identifying antimicrobial treatments that may limit biofilm formation has become a matter of concern in the management of numerous infections, particularly those involving *S. aureus* which is a well-known pathogen causing diverse biofilm-associated infections other than those encountered in CF, such as medical device-associated and catheter-related infections, and bone infections (Miquel et al., 2016), and over the years, studies have aimed to evaluate the antibiofilm activity of various antimicrobial agents (antibiotics as well as antimicrobial peptides and natural substances). These studies underline the limitations of *in vitro* studies of bacterial biofilms, particularly the poor reproducibility of certain methods and the influence of cultivation conditions. Considering these limitations, a variety of protocols and methods for *in vitro* drug activity testing against staphylococcal biofilms has been successively introduced with the aim of standardizing protocols and improving inter-laboratory reproducibility, including microfluidics systems which more closely approximate natural biofilms (Benoit et al., 2010; Guzmán-Soto et al., 2021).

In this context, the main objective of our study was to evaluate the effects of antibiotics on the biofilm formation of MRSA isolates from CF patients. Our study focused on trimethoprim, rifampicin, and linezolid which are some of the drugs that may be used to deal with MRSA infections in CF patients (Fusco et al., 2015; Zobell et al., 2015; Akil and Muhlebach, 2018). Two broad-spectrum cephalosporins (more recently approved for the treatment of bacterial pneumonia due to MRSA), ceftaroline and ceftobiprole, were also evaluated. Our study was based on standardized approaches not previously applied to CF MRSA isolates, that is, the BioFilm Ring test[®] (Chavant et al., 2007; Ren et al., 2007) and the microfluidics system BioFlux[™] 200 (Benoit et al., 2010) which were adapted for use with the artificial sputum medium (ASM), a mucin-containing synthetic growth medium (Sriramulu et al., 2005; Dinesh, 2010) to test MRSA biofilm formation, and antibiotic efficacy against biofilm formation in conditions more relevant to the CF lung. The BRT[®] is used to quickly evaluate bacterial adhesion and early biofilm formation. The BRT[®] has also been proposed as a tool for evaluating the capacity of antibiotics to inhibit biofilm formation through an approach called the Antibiofilmogram[®] (Tasse et al., 2016), also used in our study. Finally, we used the BioFlux[™] 200 continuous flow system to study biofilm formation in dynamic conditions. Strains studied were clinical isolates genotyped by multi locus sequence typing (MLST)

and, for selected strains, by whole-genome sequencing (WGS). Due to the highly complex patterns of bacterial colonization in CF patients' airways, we also included strains that were co-isolated from within a sample or successively isolated from chronically colonized patients with the aim of bringing new insights into the behavior of strains adapted to the CF lung during persistent colonization.

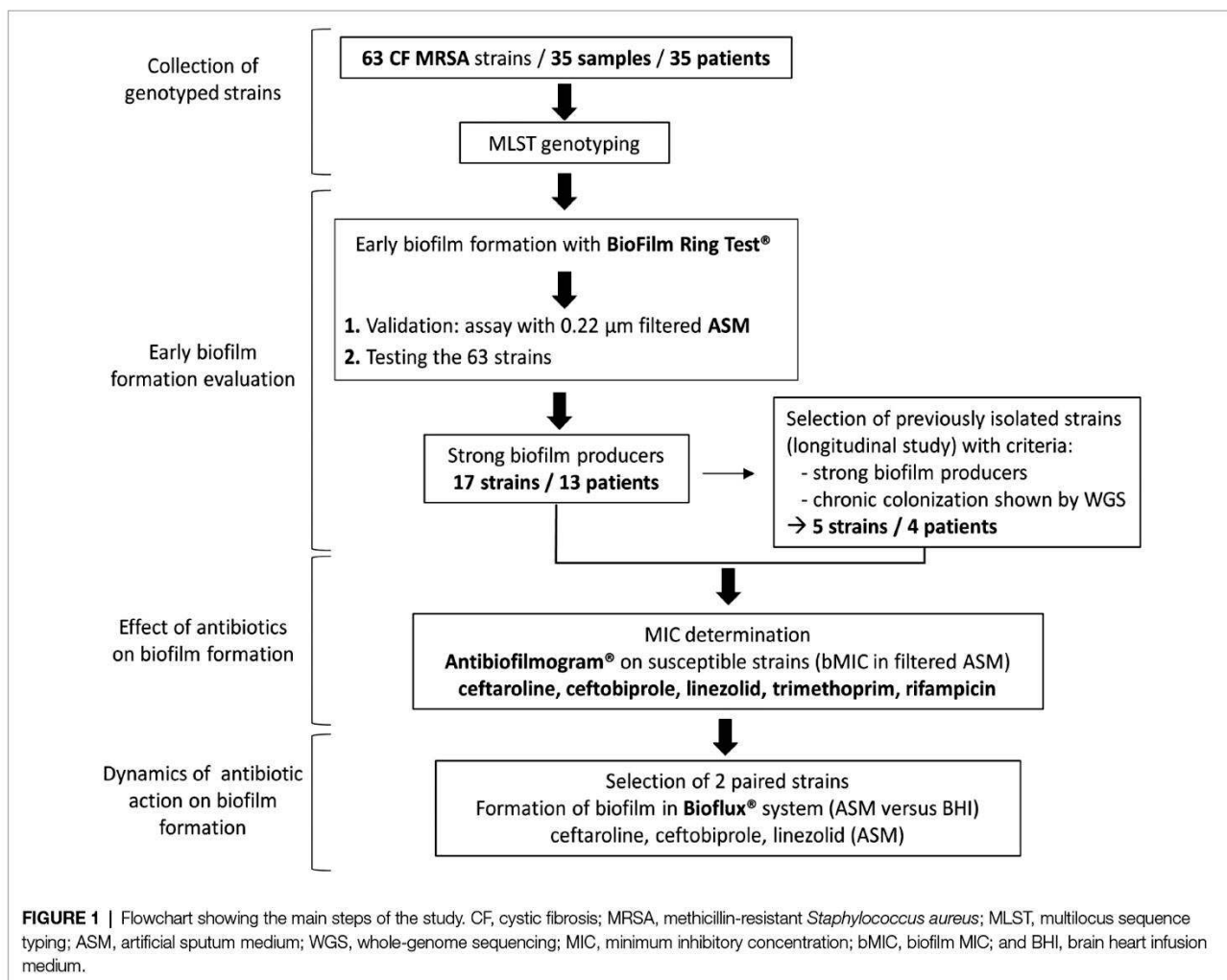
To the best of our knowledge, studies like this have never been performed before and our study therefore provides original results on comparative biofilm formation with and without antibiotics for a collection of clinically and genetically documented MRSA from CF patients.

MATERIALS AND METHODS

Patients, Strains, and Study Design

Methicillin-resistant *S. aureus* strains included in this study were isolated from routinely sampled sputum specimens in patients attending the CF center at Montpellier University

Hospital, France, and analyzed as part of their standard follow-up. Strains were recovered in 35 patients representing all patients with MRSA isolation in our center over a 9-year period. Strains had been stored at -80°C . These strains were studied for their ability to form biofilm in the presence or absence of antibiotics according to the steps presented in the flow diagram in **Figure 1**. Briefly, we first identified strains that were strong biofilm producers among a collection of clinically documented and genetically characterized CF MRSA using the BRT[®] and the ASM. Strong biofilm producers were then included in the evaluation of antibiotic efficacy against biofilm formation using the Antibiofilmogram[®] method. Selected isolates were then used to conduct: (i) a longitudinal analysis of the evolution of antibiotic efficacy on biofilm formation over time in chronically colonized patients (selection of clonal strains successively isolated in four patients) and (ii) a study of the dynamics of biofilm formation under flow in the absence and presence of antibiotics (selection of two paired strains successively isolated in a chronically colonized patient).



Multilocus Sequence Typing

All strains were cultured on Trypticase Soy Agar with 5% Sheep Blood (bioMérieux, Marcy l'Étoile, France), and one colony was subcultured on the same agar medium for further analysis. DNA extraction was performed as previously described (Predari et al., 1991). The amplification of the seven housekeeping genes included in the MLST scheme for *S. aureus* was performed as previously described (Enright et al., 2000; Crisóstomo et al., 2001). Sequencing was done on a 3500xL Genetic Analyser (Thermo Fisher Scientific Waltham, Massachusetts, United States), and sequence analysis was performed using SeqScape Software v3.0™ from the same company. The sequence type (ST) was determined for each strain *via* the PubMLST database (Jolley et al., 2018)¹ or after whole-genome sequencing (wgMLST).

Whole-Genome Sequence Analysis

Whole-genome sequencing analysis was performed for the 11 CF MRSA isolates (five “early” isolated strains and six “late” isolated strains in four chronically colonized patients) selected for the longitudinal analysis of the evolution of antibiotic efficacy on biofilm formation over time to prove that the MRSA persistence in these patients was truly a chronic colonization by a clonal strain. For six of these strains, WGSs were available from previous work (Boudet et al., 2021); for the five remaining strains, WGSs were obtained by an Illumina MiSeq platform (Illumina Inc., San Diego, CA, United States) and analyzed as previously described (Boudet et al., 2021). Regarding analysis of single nucleotide polymorphisms (SNPs), SNPs were called using Snippy (Seemann, 2015) and SNPs numbers were interpreted according to the criteria of Ankrum and Hall (2017) which define strains with ≤ 71 SNPs as the “same” strains, strains with 72–123 SNPs as “very closely related” strains, strains with 124–156 SNPs as “closely related” strains, and strains with ≥ 157 SNPs as “distantly related” strains.

DDBJ/ENA/GenBank accession numbers for the 11 WGS are JAGPWS000000000, JAGPWY000000000 and JAGPWZ000000000 (strains 5.1, 5.2, and 5.3 in Patient 5); JAGPWI000000000, JAGPWQ000000000 and JAGPWR000000000 (strains 6.1, 6.3, and 6.4 in Patient 6); JAHXBM000000000, JAHXBL000000000, and JAHXBK000000000 (strains 17.2, 17.3, and 17.6 in Patient 17); JAHXBJ000000000 and JAHXBI000000000 (strains 18.1 and 18.2 in Patient 18).

Culture Media and Growth Rates

After initial culture of frozen strains on Trypticase Soy Agar with 5% Sheep Blood (bioMérieux, Marcy l'Étoile, France), we used different media according to the test performed. Mueller-Hinton broth was used as the broth microdilution reference method to determine minimum inhibitory concentrations (MIC) of antibiotics. The ASM, a medium mimicking the sputum found in the respiratory tract of CF patients (Sriramulu et al., 2005; Dinesh, 2010), was used to

evaluate biofilm formation and antibiotic efficacy against biofilm formation in conditions more relevant to the CF lung using the different approaches of this study and developed below: the Biofilm ring Test® (BRT®), the Antibiofilmogram®, and the continuous flow system BioFlux™ 200. However, the brain heart infusion (BHI) medium is recommended by the BRT® manufacturer and was therefore used with ASM for comparative purposes. As the opacity of the ASM did not provide a compatible image with the BRT® reading software, 0.22 μm -filtered ASM was compared to BHI medium on selected isolates with the BRT®. BHI medium was also compared with ASM in the assays conducted on the BioFlux™ system. According to the medium used for the assay, strains were pre-cultured for 24 h in the same medium, BHI broth, or ASM. Due to the use of these three culture conditions, growth properties of selected strains in BHI broth, ASM, and 0.22 μm -filtered ASM were compared. Overnight cultures at 37°C were inoculated into the same fresh medium [identical dilution factor for all three conditions to obtain a suspension of optical density (OD) at 600 nm (OD₆₀₀) of 0.1], and incubation was carried out at 37°C with agitation for 24 h. Cell growth was monitored over 24 h through colony-forming unit (CFU) counts with eight data points: 0, 0.5, 1, 2, 3, 4, 6, and 24 h. For CFU counts, cultures were diluted serially in the medium and plated on Trypticase Soy Agar with 5% Sheep Blood plates which were incubated for 24 h at 37°C. All assays were performed in duplicate.

Bacterial Adhesion and Biofilm Formation Assessment Using Biofilm Ring Test®

The BRT® based on the measurement of the mobility of superparamagnetic microbeads subjected to a magnetic field was used to study the early stages of biofilm formation according to the manufacturer's recommendations (Chavant et al., 2007). Briefly, standardized bacterial cultures were incubated at 37°C in 96-well microtiter plates in the presence of magnetic beads. At set time-points, the plates were placed on a magnetic block and put in the reader. The images of each well before and after magnetic attraction were analyzed with the BioFilm Control software (BFC Elements® 3), which gives a biofilm formation index (BFI). The adhesion ability of each strain was expressed as this BFI that is inversely proportional to the attached cell number. A high BFI value indicates high bead mobility under magnetic action that corresponds to the absence of biofilm formation (a spot is visible due to bead accumulation above the mini-magnet), while lower values reflect partial to complete immobilization of beads due to the bacteria embedded in a biofilm (no visible spot for complete bead immobilization). Two incubation times were defined: 1.5 and 4 h. Three replicate wells were performed per strain and per incubation time in three (BHI/filtered ASM comparison) or two independent experiments (tests in filtered ASM only). A negative control was systematically included in each experiment corresponding to the medium and beads without bacterial suspension. BFI values were calculated for each well, ranging from 0 (total bead

¹<https://pubmlst.org/saureus/>

immobilization, i.e., strongly adherent cells/strong biofilm formation) to 20 (no bead aggregation, i.e., non-adherent cells/no biofilm formation in the experiment conditions).

Susceptibility Testing

Minimum inhibitory concentrations of ceftaroline, ceftobiprole, linezolid, rifampicin, and trimethoprim were determined for all CF MRSA strains using the microdilution method in Mueller-Hinton broth. According to the interpretative criteria of the European Committee on Antimicrobial Susceptibility Testing (EUCAST), strains were classified as susceptible (including “susceptible” and “susceptible, increased exposure” categories) or resistant (European Committee on Antimicrobial Susceptibility Testing, 2021). Serial 2-fold dilutions of antibiotics were as follows: 0.125–16 mg/L for ceftaroline, 0.25–32 for ceftobiprole, 0.5–64 mg/L for linezolid, 0.015–2 mg/L for rifampicin, and 0.25–32 for trimethoprim. The reference strain *S. aureus* ATCC 29213 was used to monitor test performance.

The minimum biofilm inhibitory concentrations (bMIC) were determined using the Antibiofilmogram® test (BioFilm Control; Tasse et al., 2016). A schematic representation of the Antibiofilmogram® principle is available in Olivares et al. (2020). The test was performed using 0.22 µm-filtered ASM for initial bacterial growth and suspension preparation. The microplates containing bacteria, magnetic beads, and antibiotics (20 µl of antibiotic solutions) were incubated at 37°C for 4 h before visual reading. The bMIC was determined for each antibiotic as the lowest concentration at which a spot corresponding to free beads attracted to the center of each well during magnetization, similar to negative control (0.22 µm-filtered ASM and magnetic beads), was visible. A well without antibiotics filled with the bacterial suspension in 0.22 µm-filtered ASM and magnetic beads was used as the positive control (absence of spot due to bead immobilization in biofilm). All assays were performed in duplicate.

Biofilm Formation Assessment Using the BioFlux™ 200 System

The kinetics of biofilm formation and quantification in the absence and presence of antibiotics (ceftaroline, ceftobiprole, and linezolid) were assessed with the BioFlux™ 200 microfluidic system as previously described (Naudin et al., 2019) with two different media, BHI medium and ASM. In this system, biofilm formation is studied under dynamic and controlled flow conditions and is followed by light microscopy in microfluidic wells (Benoit et al., 2010). The system consists of a 48-well plate with a microchannel connection between 24 pairs of two types of wells, an input well and an output well. Bacteria were grown overnight in each media. Bacterial suspensions with an OD₆₀₀ of 0.1 +/- 0.05 after two 200th serial dilutions from the overnight culture were prepared in both media. To quantify biofilm formation, we prepared BioFlux system by adding 500 µl of medium into the input well with a pressure of 1 dyne/cm² for 10 min. At the end of the 10 min, the medium remaining in the input well was removed. Bacterial suspensions were then added in the input well for 36 h of incubation at

37°C in BHI medium and ASM with a pressure of 0.2 dyne/cm². The bacterial suspension was either added alone or in the antibiotic solution, i.e., last dilution performed in the antibiotic solution to give final concentrations of bacteria of 10³ CFU/ml and antibiotic corresponding to the bMIC determined by the Antibiofilmogram® either in BHI broth or in filtered ASM. Biofilms were grown in monoculture, and the quantification of biofilm formation was done at 5, 12, 24, and 36 h post-inoculation in the absence of antibiotics and at 5, 12, and 36 h post-inoculation in the presence of antibiotics. Experiments were performed in duplicate. Biofilms were visualized with a Leica DM IRB inverted fluorescence microscope coupled with a CoolSNAP FX black and white camera (Roper Scientific, Trenton NJ, United States). ImageJ® software was utilized to calculate biofilm percentage. The 16-bit grayscale images were adjusted with the threshold function to fit the bacterial structure and were analyzed using the “Analyze Particles” function to calculate biofilm percentage in the microfluidic channel.

Statistics

Results are presented as the mean ± standard deviation. Statistical analyses were made using a t test in version 7 of GraphPad Prism (comparison of biofilm formed according to the condition, either medium or incubation time, in the BioFlux™ analyses) or using a Mann-Whitney U test in version 3.5.2 of R software (comparison of BFI values in BHI medium and filtered ASM). A value of $p \leq 0.05$ was considered to reflect significance.

RESULTS

Patients and MRSA Collection Characteristics

The 35 CF patients (54.3% of female) had a mean age of 22.1 years at inclusion in the study (range: 2–52 years). Sixteen of them fulfilled the criteria for chronic colonization (>50% of respiratory samples collected during the last 12 months positive for MRSA with at least four samples collected during that period; Zolin et al., 2020). The 63 strains had been isolated between 2007 and 2016 from 35 sputum samples in these patients (2–4 colonial morphotypes visually distinct observed during the routine bacteriological analysis of sputum samples recovered from 18 samples in 18 patients were included; **Supplementary Table**). MLST genotyping showed that the 63 strains belonged to 10 STs (**Figure 2A**). MRSA of ST5 (50.8% of strains and 48.6% of patients) and ST8 (30.2% of strains and 31.4% of patients) were the most frequent representing 81% of the strains (51 strains/63) and being identified in 80% of the patients (28 patients/35). Two patients had co-colonizations with strains from different STs within the same clonal complex (CC) identified in one sample [ST5 and ST4782 (CC5) in Patient 14, ST8 and ST5829 (CC8) in Patient 33]. In these cases, both genotypes identified differed by one (strains in Patient 14) or five mutations (strains in Patient 33) in one of the seven genes of the MLST scheme (*aroE* gene and *gmk* gene, respectively).

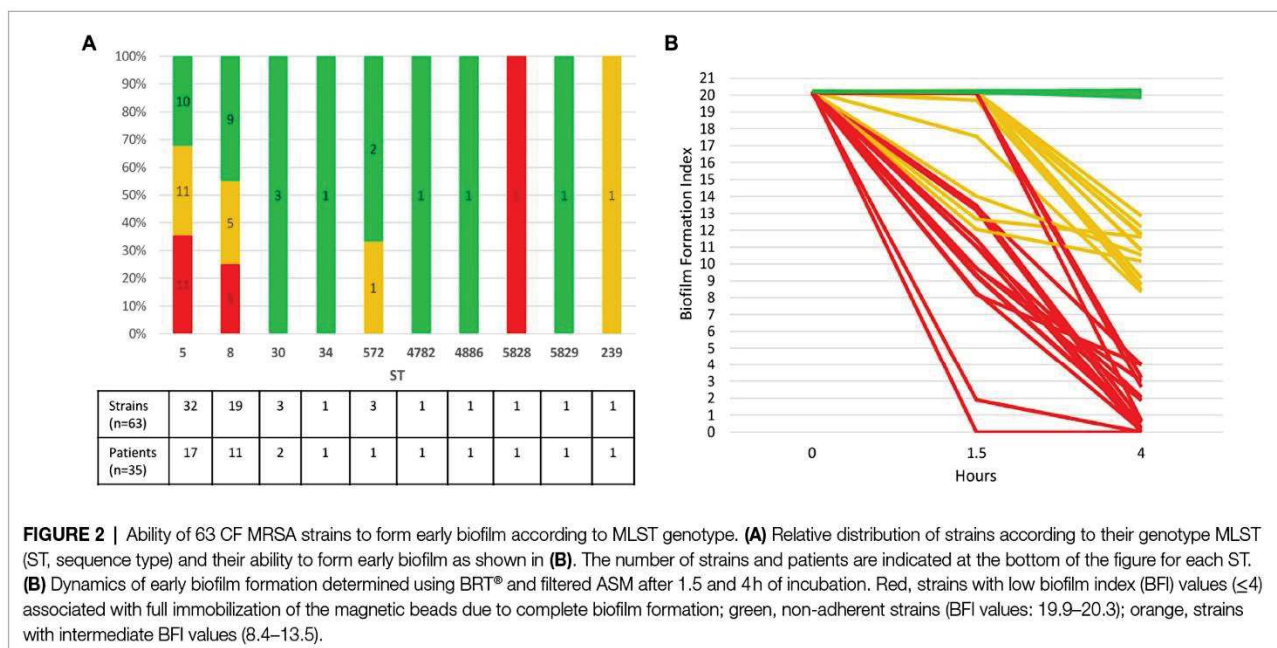


FIGURE 2 | Ability of 63 CF MRSA strains to form early biofilm according to MLST genotype. **(A)** Relative distribution of strains according to their genotype MLST (ST, sequence type) and their ability to form early biofilm as shown in **(B)**. The number of strains and patients are indicated at the bottom of the figure for each ST. **(B)** Dynamics of early biofilm formation determined using BRT[®] and filtered ASM after 1.5 and 4 h of incubation. Red, strains with low biofilm index (BFI) values (≤ 4) associated with full immobilization of the magnetic beads due to complete biofilm formation; green, non-adherent strains (BFI values: 19.9–20.3); orange, strains with intermediate BFI values (8.4–13.5).

Use of Artificial Sputum Medium to Test Bacterial Adhesion Using the Biofilm Ring Test[®]

Brain heart infusion medium is recommended by the BRT[®] manufacturer. However, the ASM containing mucin, amino acids, and free DNA was formulated to mimic the sputum of CF patients and its use is thought to be more representative of the lung conditions during CF. We therefore aimed to evaluate the use of ASM in the Biofilm Ring Test[®], either to characterize the adhesion pattern and ability to form biofilm of clinical CF MRSA (BFI determination) or to perform an Antibiofilmogram[®] (bMIC determination). ASM is a turbid medium which yields invalid results in the BRT[®] but using ASM filtered through a 0.22 μM filter system made it possible for the system to calculate the BFI. To go further with the use of filtered ASM, we compared the growth ability in BHI, ASM, and filtered ASM of three selected strains that were further categorized as strong biofilm producers: strains 5.3 and 6.4 that were also used for the comparison of the BRT[®] use in BHI medium and ASM, and strain 17.6 that was later studied using the BioFlux[™] 200 system. Similar growth rates were observed in the three media for these three strains (**Supplementary Figure 1**). We then compared both media for BRT[®] use by comparing BFI values measured after 4 h of incubation in BHI medium and filtered ASM for strains 5.3 and 6.4 (**Supplementary Figure 2**). Differences in adhesion patterns were observed depending on the medium used, with lower BFI values observed in filtered ASM compared with BHI medium and a significantly more pronounced adherence behavior in ASM compared with BHI medium for strain 5.3 (value of $p < 0.001$ by Mann-Whitney U test). On the whole, these observations led us to consider the use of filtered ASM for further experiments using the BRT[®].

Evaluation of Early Biofilm Formation Using Biofilm Ring Test[®] in Filtered ASM

Biofilm formation index values evaluating the CF MRSA adhesion ability were distributed in three clearly separated groups after an incubation time of 4 h: BFI values ≤ 4 , BFI values comprised between 8.37 and 13.52, and BFI values ranging from 19.87 to 20.31 (**Supplementary Table; Supplementary Figure 3**). We found that 27% of strains (17/63) isolated in samples from 37.1% of the patients (13/35) formed a strong biofilm after 4 h of incubation in filtered ASM (BFI < 4), including two strains of ST5 (strains 17.6 and 30.1) which were strongly adherent after 1.5 h of incubation (**Figure 2B**). Nearly all the strains (94.1%, 16/17) that were early biofilm producers belonged to ST5 and ST8. It is worth noting that intra-sample heterogeneity in the ability to form biofilm was observed, strong biofilm-producing strains being co-isolated with strains displaying distinct ability to form biofilm in samples from five patients (38.5%, 5/13). A striking example was observed for Patient 25 for whom strong biofilm producers and non-adherent strains coexisted in a sample (**Supplementary Table**). Half of chronically colonized patients (8/16) were colonized by such strains with a strong capacity for biofilm production (**Supplementary Table**). Non-adherent strains represented 44.4% of the strains and were isolated in 18 patients (BFI: 19.87–20.31, as observed for the negative control that contained filtered ASM and beads only). Finally, 28.6% of the strains, isolated from 13 patients, with intermediate BFI values (8.37–13.52), were likely slower biofilm formers, and characterization of their adhesion kinetics would have required a longer incubation time (**Supplementary Table; Supplementary Figure 3**).

No obvious relation was observed between the ability to form early biofilm of the MRSA strains and the co-colonizers, particularly *Pseudomonas aeruginosa*. Out of the 63 strains/35

patients of the study, 40 MRSA strains were isolated in 21 patients with chronic colonization by *P. aeruginosa*. These strains were distributed in the three groups of strains defined according to their ability to form early biofilm (13 strains showed $BFI \leq 4$, 17 strains were non-adherent and 10 had intermediate BFI values).

Antimicrobial Susceptibility of the 17 Strongly Adherent Strains

Determination of the MICs of the five antibiotics under consideration in this study showed that 11 strains (64.7%) were resistant to rifampicin, and three strains (17.6%) were resistant to linezolid, while the 17 strains were susceptible to trimethoprim, ceftobiprole, and ceftaroline (Table 1). bMICs were then determined using the Antibiofilmogram® approach in filtered ASM. Highly distinct patterns of bMICs were observed according to the antimicrobial agent (Table 1). No strains displayed bMIC for trimethoprim below the EUCAST threshold for resistance at 4 mg/L (bMIC range: 8–>32 mg/L) showing that this antibiotic was totally inefficient on biofilm formation initiation. The lowest bMICs were observed for ceftaroline and ceftobiprole with efficacy in preventing biofilm formation observed for 76.5 and 70.6% of strains, respectively (bMICs below the respective resistance breakpoint of 1 and 2 mg/L) compared with linezolid (64.7% of strains with bMICs ≤ 4 mg/L) and rifampicin (17.6% of strains with bMICs ≤ 0.5 mg/L). Individual results for each of the 17 strains under evaluation are presented in Table 2. The capacity of rifampicin and linezolid to prevent biofilm installation was also evaluated for the sole strains that were susceptible in planktonic cultures; linezolid was able to inhibit biofilm formation of 78.6% of the susceptible strains (three out of 14) and rifampicin prevented biofilm installation of 50% of the susceptible strains (three out of six; Table 2).

For three strains (strains 1.1, 5.3, and 20.1), bMICs of all the five antibiotics were above the corresponding resistance breakpoint and these strains were excluded from further analysis conducted to compare the efficacy of the various antimicrobial agents on biofilm formation by CF MRSA. Analysis was, thus, restricted to susceptible strains (planktonic cultures) that

displayed at least one bMIC below the threshold for resistance ($n = 14$; Table 2). Under these conditions, bMICs for ceftaroline were below the resistance threshold for 13 strains, bMICs for ceftobiprole were below the resistance threshold for 12 strains, and bMICs for linezolid were below the resistance threshold for 11 strains. A limited effect was observed for rifampicin with three strains out of 14, isolated from three patients, showing low bMIC values < 0.015 mg/L. However for two patients, these strains were associated either with a resistant strain (Patient 28) or with a strain for which the formation of biofilm was not inhibited by rifampicin (Patient 25) thereby making the drug of low interest considering its global effect on biofilm formation inhibition. More generally, intra-sample heterogeneity with coexistence of adaptive variants displaying distinct bMICs was observed for three out of the four patients for whom the analysis of multiple strains from a sample was performed (Patients 5, 25, and 28; Table 2).

Study of Clonally-Related, Longitudinally-Isolated Strains in Four Patients

For chronically colonized patients, we searched for strains that had been isolated before the strains studied above, which met the following criteria: (i) strongly adherent strains/strains forming early biofilm as determined by the BRT® in filtered ASM ($BFI \leq 4$), and (ii) WGS-based analysis confirming the chronic colonization based on the identification of less than 123 SNPs between the sequences of the “early” and the “late” isolated strains (signing either a “same” strain or “very closely related” strains according to the criteria of Ankrum and Hall, 2017). A total of five earlier-isolated strains from four patients matching these criteria were selected and compared with six strains isolated during patient follow-up. The characteristics of patients and selected strains are presented in Figure 3A. MICs were determined, and an Antibiofilmogram® was performed on these strains (as described above), and bMICs are presented in Figure 3B. MIC and bMIC values for the five antibiotics were all below the EUCAST threshold for susceptibility for the five strains isolated earlier. For later-isolated strains that remained susceptible to antimicrobial agents in planktonic culture, we showed that ceftaroline and ceftobiprole (Patients 5 and 6) or linezolid (Patients 17 and 18)

TABLE 1 | Overall susceptibility results for the 17 CF MRSA strains that were classified as strongly adherent/strong biofilm producers according to the Biofilm Ring Test® assay.

Antimicrobial agent	Minimal inhibitory concentration (MIC in mg/L)				Minimal biofilm inhibitory concentration (bMIC in mg/L)			
	Range	MIC ₅₀	MIC ₉₀	Resistant (% , n)	Range	bMIC ₅₀	bMIC ₉₀	Above the threshold for resistance (% , n)
Ceftaroline	<0.125–0.25	0.125	0.25	0	<0.125–4	0.25	4	23.5 (4)
Ceftobiprole	<0.25	<0.25	<0.25	0	<0.25–16	2	8	29.4 (5)
Linezolid	<0.5–32	1	16	17.6 (3)	<0.5–>64	2	>64	35.3 (6)
Rifampicin	<0.015–2	2	2	64.7 (11)	<0.015–>2	>2	>2	82.4 (14)
Trimethoprim	<0.25–2	0.5	2	0	8–>32	>32	>32	100 (17)

European Committee on Antimicrobial Susceptibility Testing (EUCAST) breakpoints for resistance were as follows: ceftaroline, 1 mg/L; ceftobiprole, 2 mg/L; linezolid, 4 mg/L; trimethoprim, 4 mg/L, and rifampicin, 0.5 mg/L.

TABLE 2 | Detailed susceptibility results for the 17 CF MRSA strains that were classified as strongly adherent/strong biofilm producers according to the Biofilm Ring Test® assay.

Patient	Strain	ST	BFI	Ceftaroline		Ceftobiprole		Linezolid		Rifampicin		Trimethoprim	
				MIC	bMIC	MIC	bMIC	MIC	bMIC	MIC	bMIC	MIC	bMIC
1	1.1	8	4	<0.125	2	<0.25	16	<0.5	16	2	>2	1	>32
5	5.2	5	0.12	<0.125	<0.125	<0.25	<0.25	32	>64	2	>2	0.5	>32
	5.3	5	0.75	<0.125	4	<0.25	8	16	32	2	>2	1	>32
6	6.3	5	0.58	<0.125	0.25	<0.25	2	1	16	2	>2	1	>32
	6.4	5	0.25	0.25	<0.25	<0.25	<0.25	16	>64	2	1	1	>32
7	7.2	5	0.71	0.25	0.25	<0.25	2	<0.5	2	0.5	>2	0.5	8
17	17.6	5	0	<0.125	4	<0.25	4	<0.5	2	2	>2	0.5	>32
18	18.2	8	3.03	<0.125	0.5	<0.25	2	1	1	2	>2	1	8
20	20.1	5828	0.66	<0.125	4	<0.25	4	1	64	2	>2	2	>32
25	25.5	5	4	0.25	0.25	<0.25	<0.25	2	2	<0.015	<0.015	2	32
	25.6	5	3.22	<0.125	0.25	<0.25	8	4	4	<0.015	>2	0.5	>32
26	26.1	8	2.08	<0.125	<0.125	<0.25	2	<0.5	2	<0.015	0.015	<0.25	>32
28	28.3	5	0	<0.125	1	<0.25	2	<0.5	<0.5	2	>2	<0.25	>32
	28.4	5	0.25	<0.125	<0.125	<0.25	<0.25	<0.5	1	<0.015	<0.015	<0.25	8
30	30.1	5	0	<0.125	<0.125	<0.25	<0.25	<0.5	1	<0.015	>2	1	32
31	31.2	8	2.68	<0.125	<0.125	<0.25	0.5	<0.5	1	2	>2	0.5	>32
32	32.1	8	1.89	<0.125	<0.125	<0.25	<0.25	1	1	2	>2	0.5	>32

Minimum inhibitory concentrations (MIC) and biofilm MIC (bMIC) in mg/L. MICs were determined according to the reference dilution method. bMICs were determined in filtered ASM. Gray cells indicate MIC and bMIC values above the EUCAST breakpoints for resistance (indicated in footnotes of Table 1). ST, sequence type. BFI, biofilm formation index.

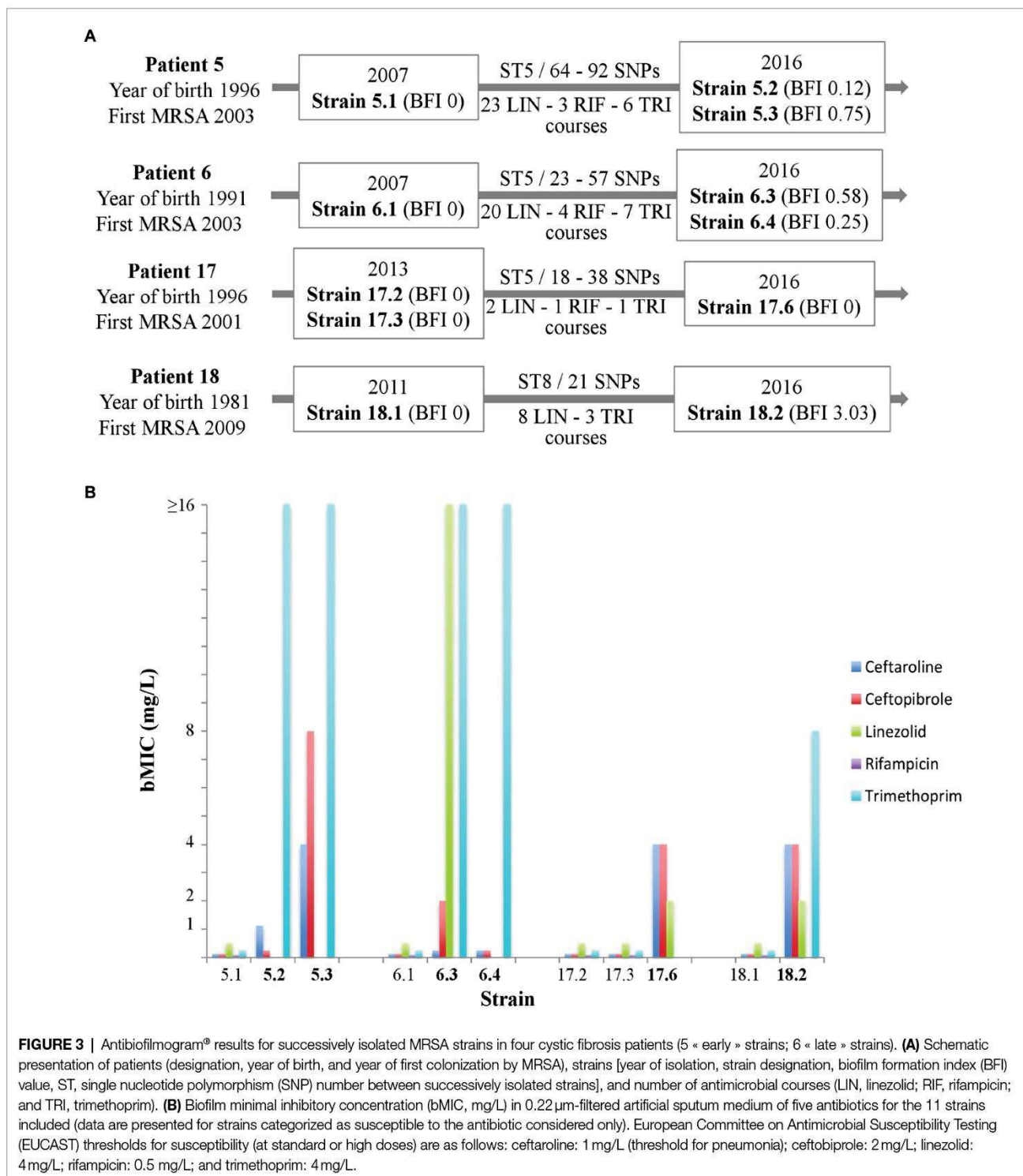
retained their ability to prevent biofilm formation (bMICs below the corresponding EUCAST thresholds for resistance) over time. We related these observations to the antimicrobial courses received by the patients (Figure 3). The more important antibiotic selective pressure was noted for linezolid and Patients 5 and 6. Three out of the four strains isolated in these patients were resistant to linezolid in planktonic cultures (resistance, investigated in a previous study; Boudet et al., 2021) was related to a G2576T substitution present in a variable number of 23S rRNA gene copies, while susceptible strain 6.3 displayed a high bMIC of 16mg/L. For strains isolated in Patients 17 and 18 (who had received fewer linezolid courses during their follow-up), increased bMICs were observed over time, but bMICs were still below the resistance threshold (Figure 3). Although a low number of rifampicin and trimethoprim courses (possibly associated) were noted in the four patients, both antibiotics were no more active on later-collected strains, showing MICs or bMICs above the corresponding resistance thresholds. None of the patients had received ceftaroline or ceftobiprole.

Dynamics of Biofilm Formation Under Flow in the Presence and Absence of Antibiotics

To complete the characterization of biofilm formation of CF MRSA in the presence or absence of antibiotics, a study was performed in dynamic conditions using the BioFlux™ 200 microfluidic system. We selected strain 17.6, one of the two strains that were strongly adherent after 1.5h of incubation in the BRT® and the paired 17.2 strain isolated 3years before in Patient 17. For these paired strains, we first compared their dynamics of biofilm formation over time according to the medium used (BHI or ASM). The formation of biofilm increased regularly over time for each condition of the assay (“early” strain in BHI

medium, “early” strain in ASM, “late” strain in BHI medium, “late” strain in ASM) with a systematically higher percentage of biofilm formed in ASM compared with BHI medium and for “late” strain compared with “early” strain (Figure 4). Although both strains were shown to have high adhesion ability using the BRT®, these results revealed that strains 17.2 and 17.6 each had distinct dynamics of biofilm formation, with a slower biofilm formation for the earlier-isolated strain 17.2 (Figure 4).

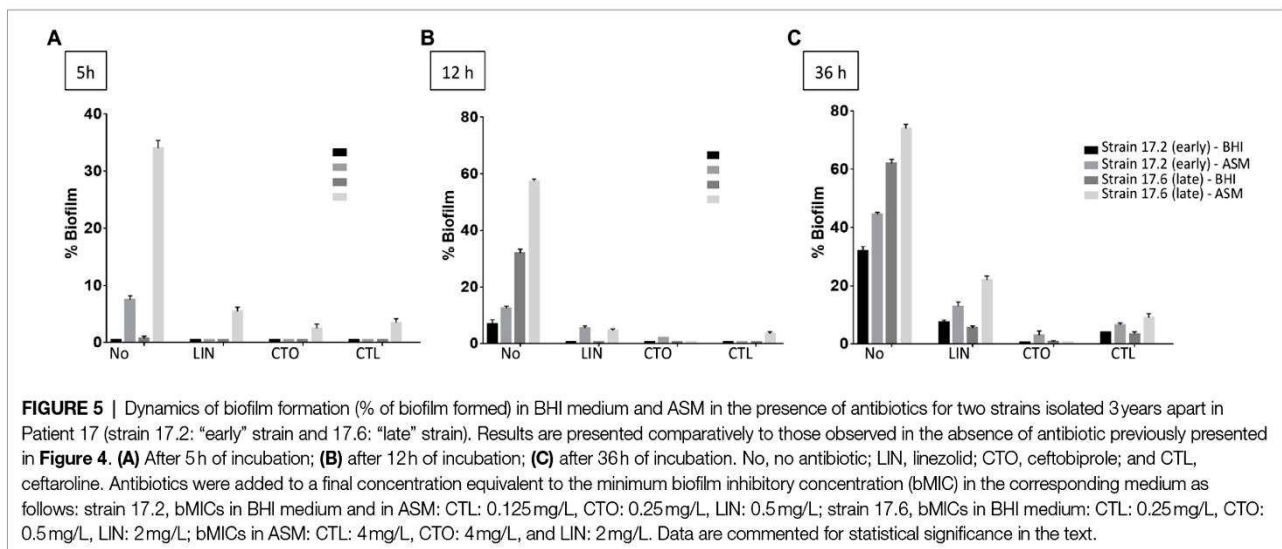
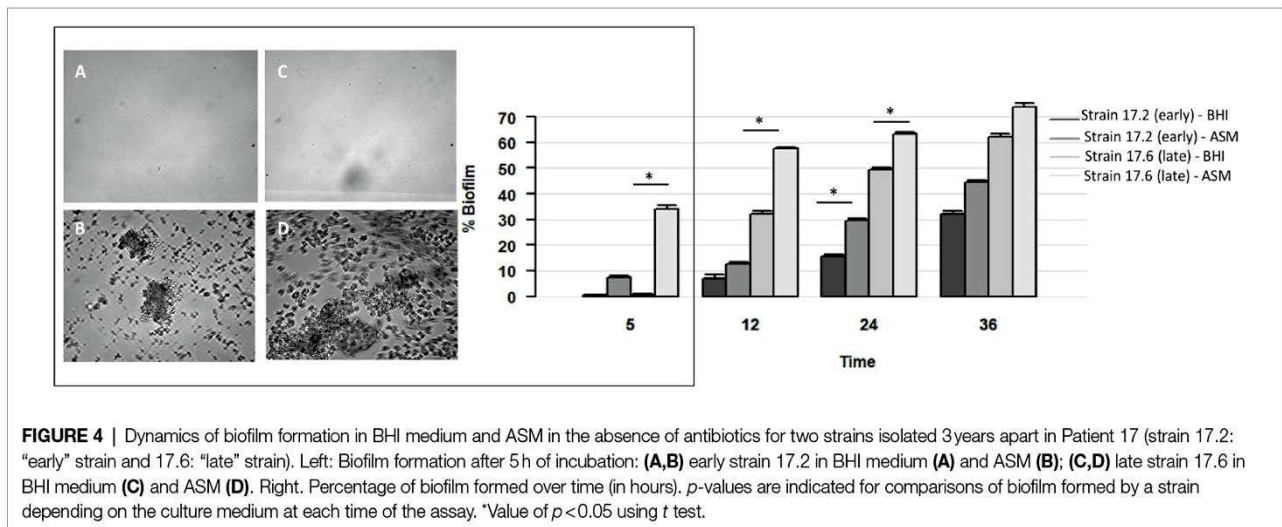
Further testing with antibiotics was limited to three times of measure (5, 12, and 36h) and to the three antimicrobial agents with the lowest bMICs, that is, ceftaroline, ceftobiprole, and linezolid. With the BioFlux™ device, the percentage of biofilm formed in the presence of one of the three drugs tested was drastically lower than that observed for the control without antibiotics showing that all three antibiotics had the ability to limit biofilm formation and that this effect was long-lasting as it was observed up to 36h of exposure to the bMIC of the corresponding antimicrobial agent in both media (Figure 5). Differences in biofilm formation in ASM were compared for statistical significance by a t test. A significantly higher inhibition of biofilm formed by the earlier isolated strain 17.2 was observed from 12h of incubation and up to 36h of incubation for ceftaroline and ceftobiprole compared with linezolid (values of $p < 0.05$ at 12h; values of $p < 0.01$ at 36h). Differences observed between ceftaroline and ceftobiprole were also statistically significant (value of $p < 0.05$ at 36h), ceftaroline being more active in biofilm formation inhibition than ceftobiprole after 12h, whereas ceftobiprole was more active in biofilm formation inhibition than ceftaroline after 36h. Inhibition of the biofilm formation by the “late” strain 17.6 in ASM was more pronounced with ceftobiprole than with linezolid (values of $p < 0.01$ at 12 and 36h) or ceftaroline (values of $p < 0.01$ at 36h). Ceftaroline was also more active than linezolid after 36h (value of $p < 0.01$).



DISCUSSION

Cystic fibrosis is a chronic disease in which bacterial colonizations/infections of the airways are usual. Due to local specific conditions in the CF lung, diverse selective pressure is applied to colonizing microorganisms (interactions with the host immune response, high levels of antibiotic use, oxygen

deprivation in mucus, altered antimicrobial peptide production, etc.) which, in turn, develop several traits to adapt to the surrounding environment and survive in the CF lung (Hauser et al., 2011). Among these traits, biofilm growth has been observed with several opportunistic pathogens in certain human diseases including CF, conferring protection against antimicrobial treatments and therefore contributing to bacterial persistence



(Donlan and Costerton, 2002). While the role of biofilm and the dynamics of its formation have been extensively studied for *P. aeruginosa* (Høiby et al., 2010), there have been few studies on MRSA in CF patients. However, biofilm formation is an important virulence trait of *S. aureus* which has been frequently observed (67% of the strains) in a recent study on CF pediatric patients (Kodori et al., 2021). Biofilm formation was also significantly more often observed for strains isolated from CF patients compared with those recovered from non-CF patients (Aktas et al., 2013). In MRSA, biofilm represents an additional obstacle to eradication in addition to multidrug resistance making these strains the most problematic ones and a great matter of concern due to their involvement in negative clinical evolution (Ren et al., 2007; Dasenbrook et al., 2008; Vanderhelst et al., 2012). One recent study found that 85.6% of MRSA isolates were biofilm producers compared with 54.2% of MSSA, suggesting that MRSA isolates are better able to form biofilm during CF (Kadkhoda et al., 2020). Biofilm formation was also observed in 14 of 15 CF MRSA pulsotypes

in the study by Molina et al. (2008), supporting the fact that biofilm formation is a common characteristic of CF MRSA. In the specific and distinct conditions of our study – BRT® used with a 4-h incubation for selection of strong producers of early biofilm rather than the microtiter test used in previous studies, we found a rate of strong biofilm-forming MRSA of 27% of the strains and these strains had been isolated in samples from 37% of the studied patients.

Previous studies have related the propensity of specific clones of *S. aureus* for forming biofilm (Vanhommerig et al., 2014; Tasse et al., 2018) as well as *Escherichia coli* (Flament-Simon et al., 2019). For CF MRSA, due to the lack of studies including genetically characterized strains, it remains to be explored whether some lineages are more prone to forming biofilm. More generally, there is a lack of knowledge of MRSA clones circulating in the CF population in Europe (Vu-Thien et al., 2010; Cocchi et al., 2011) although no comparisons can be drawn with non-European data, particularly American data, due to the highly distinct epidemiology between these continents

(Glikman et al., 2008). Congruent with the studies of Vu-Thien et al. (2010) in France and Cocchi et al. (2011) in Italy, we observed that ST5 and ST8 were the most frequent STs identified in our study with 81% of the strains isolated in 80% of the patients belonging to these MLST genotypes. We observed that clonal lineages differed in terms of their biofilm-forming capacities as the majority of strong biofilm-producing strains belonged to ST5 and ST8, a trait that may contribute to the large representation of both genotypes in CF. However, due to the important representation of both STs in the overall population, ST5 and ST8 were major MLST genotypes observed in the three groups of BFI values in our study. They are also major MRSA lineages in the global population. Previous studies showed that some MRSA lineages like the predominant clone of community-acquired (CA)-MRSA in the United States, the USA300 clone in the clonal complex 8, have enhanced biofilm-forming capacity (Vanhommerig et al., 2014). Strains included in our study did not harbor the Panton-Valentine leukocidin-encoding gene characteristic of some CA-MRSA clones (unpublished) but were not characterized further in our study, thus preventing any conclusions about the implication of specific biofilm-forming lineages of ST5 or ST8 in CF.

Although antimicrobial treatments are considered as effective according to the results of *in vitro* assays, microorganisms may still persist in the CF airways for years, partly due to their ability to be protected within the polymer matrix produced during biofilm formation. In this context, the efficacy of antimicrobial therapy is reduced within the biofilm and approaches targeting bacterial biofilms in cystic fibrosis airways are required (Martin et al., 2021). However, as recently stated by Guzmán-Soto et al. (2021), “for the successful development of antibiofilm treatments and therapies, understanding biofilm development and being able to mimic such processes is vital.” Several natural or synthetic compounds have shown to be active on biofilm formed by *S. aureus* (Miquel et al., 2016). However, most studies on *S. aureus* focused on the effects of antibiotics on established biofilm in the context of biofilm-associated infections other than CF, mainly medical device-associated infections. The antibiofilm activity of antibiotics on *S. aureus* isolated from CF patients has been scarcely investigated. Considering the 5 antibiotics included in this work, a PubMed search conducted on July 19, 2021, with « ceftaroline » or « ceftobiprole » or « linezolid » or « rifampicin » or « trimethoprim » and « *Staphylococcus aureus* » and « cystic fibrosis » and « biofilm » found five non-redundant publications supporting the need for data acquisition on the subject of antibiotics' antibiofilm activity against CF *S. aureus* isolates (Molina et al., 2008; Aktas et al., 2013; Iglesias et al., 2019; Gilpin et al., 2021; Harrington et al., 2021). This is reinforced by the observations that most of these antimicrobial agents have been found to display an antibiofilm activity on *S. aureus* isolated in other settings. For example, ceftaroline was effective against biofilm established by MRSA *in vitro* and *in vivo* models of catheter-associated biofilm formation suggesting that ceftaroline could be considered for the treatment of biofilm-associated MRSA infections (Meeker et al., 2016). In CF, ceftaroline was

recently shown to represent an effective antimicrobial option for the management of acute pulmonary exacerbations involving MRSA in pediatric CF patients (Branstetter et al., 2020) and, on the other hand, has been shown to have an antibiofilm effect on biofilm-producing MRSA in other chronic infections (Mottola et al., 2016). Ceftobiprole has also previously demonstrated promising activity against biofilm from methicillin-resistant staphylococci (Abbanat et al., 2014). However, previous studies mainly included limited numbers of strains, either reference strains that may not reflect the behavior of CF strains or strains with no associated clinical data. In our study, we report the first data on the effect of antibiotics, including fifth-generation cephalosporins, on biofilm formation *via* a collection of clinically documented and genotypically characterized CF MRSA and seek to mimic CF sputum by using ASM in the different *in vitro* assays.

Due to the strong influence of environmental conditions on bacterial biofilm formation, the use of ASM formulated to mimic the sputum of CF patients appears promising for *in vitro* studies on CF isolates (Sriramulu et al., 2005; Dinesh, 2010). However, this technique remains little used in published studies and has mostly been used in studies on *P. aeruginosa* (Sriramulu et al., 2005; Kirchner et al., 2012; Rozenbaum et al., 2019; Iglesias and Van Bambeke, 2020). For *S. aureus*, it was previously used in a single study to determine the influence of the medium on the antibiofilm activity of antibiotics including two of those under consideration in this study (linezolid and rifampicin). ASM, containing amino acids, mucin, and free DNA, was shown to provide the most protective matrix (Rozenbaum et al., 2019) and all the antibiotics previously tested were drastically less potent and less effective in ASM than in comparators with respect to viability, metabolic activity, and biomass (Iglesias and Van Bambeke, 2020; Frisch et al., 2021). Here, through the comparative study of biofilm formation dynamics in ASM and BHI medium, we show that the use of ASM should be encouraged for further studies on biofilm formation by CF MRSA clinical isolates as an enhanced and accelerated biofilm formation was observed in ASM. However, we also found that ASM was not adaptable to all devices probably due to some of its characteristics like turbidity and viscoelasticity (Iglesias et al., 2019) and we had to consider filtered ASM for use in the BRT[®] despite the impact of the ASM filtration and the components which may be affected by this step remain unknown. Of note, ASM did not contain glucose despite glucose is present, at various levels according to the studies, in the sputum of CF patients (Van Sambeek et al., 2015; Nielsen et al., 2020) and glucose was shown to promote *S. aureus* biofilm formation (Lade et al., 2019). The supplementation of ASM with glucose may thus represent an interesting perspective for future work unless the best glucose concentration to be used can be defined considering the inter-individual (but also intra-individual) variability highlighted in previous studies of sputum samples from CF patients (Van Sambeek et al., 2015; Nielsen et al., 2020).

The inhibition of early biofilm formation observed in ASM in this study for linezolid and, more markedly, for ceftobiprole and ceftaroline represents an important finding because the first

two stages of biofilm development, that is, adsorption and adhesion, are key determinants in the next stages leading to biofilm development during initial colonization by MRSA and also during the biofilm life cycle at the dispersal stage. These observations warrant complementary studies on established biofilm and on antibiotic combinations as previously studied in other settings such as endocarditis, diabetic foot infections, and medical device-associated infections for associations including ceftaroline (Barber et al., 2015; Mottola et al., 2016; Thieme et al., 2018), as they may contribute to the required optimization of antibiotic regimens against biofilm (Lebeaux et al., 2014).

Bacterial populations colonizing CF patients are known to be highly complex and dynamic, encompassing a variety of variants whose equilibrium varies according to the changing conditions of the surrounding environment. This population diversification is an increasingly well-known host adaptation strategy which has been widely studied in Gram-negative bacilli during chronic colonization of CF patients' lungs (Winstanley et al., 2016; Menetrey et al., 2021). For *S. aureus*, diversified populations have been more rarely documented in CF (Goerke et al., 2007; Vu-Thien et al., 2010; Hirschhausen et al., 2013; Ankrum and Hall, 2017; Boudet et al., 2021; Wieneke et al., 2021). Regarding biofilm formation, we observed that patients may be colonized by clonally related strains corresponding to adaptive variants displaying distinct abilities to form biofilm, as previously described (Savage et al., 2013; Wieneke et al., 2021). Such diversification of MRSA populations and intra-sample heterogeneity of biofilm formation ability may contribute to compromising the antibiotic management of CF airway infections. Other adaptive phenotypic modifications observed for CF *S. aureus* have included the increase in antimicrobial resistance and the biofilm development observed in certain studies (Hirschhausen et al., 2013). In our study, strains adapted to the CF lung environment after years of colonization may still display low bMICs for ceftaroline, an observation that requires further investigation on a larger panel of MRSA strains isolated in chronically colonized patients. Adaptive modifications like mucoidy and nuclease activity were recently shown to be more frequently observed in case of *P. aeruginosa* co-colonization highlighting the importance of cross-talk and interactions between bacterial pathogens in shaping the adaptation of *S. aureus* to the CF lung environment (Wieneke et al., 2021). In our study, no obvious association was observed between chronic colonization by *P. aeruginosa* and the ability of MRSA to form early biofilm. Finally, future studies are still needed to investigate the behavior of CF MRSA within multispecies biofilm as well as the effect of exposure of these multispecies biofilms to different antibiotics (Vandeplassche et al., 2020).

CONCLUSION

We hereby report the first data on early biofilm formation by MRSA clinical isolates from CF patients using original and standardized approaches which had never been previously applied to such isolates and whose use should be encouraged. Indeed, the BRT[®] is well-designed to investigate the early and capital stages of biofilm formation contrarily to the most frequently used

microtiter plate dye-staining (crystal violet) assays and presents the other advantages of being a rapid, high-throughput, easy-to-handle, and highly reproducible method. The BioFlux is meanwhile a fully integrated and easy-to-use system allowing the study of the dynamic formation of the biofilm and the small volumes required make this system highly applicable for screening of biofilm inhibitory agents (for a critical review of methods usable to study biofilm formation, see Azeredo et al., 2017).

As previously observed for other CF pathogens like *P. aeruginosa* or in other settings like medical device-associated infections, antibiotic susceptibility was reduced in biofilm, thereby complicating anti-MRSA treatments and representing a risk of treatment failure in CF patients. The Antibiofilmogram[®] is a promising tool for guiding the choice of the most effective drugs against biofilm formation by MRSA in CF airways. In our study, the two broad-spectrum anti-MRSA cephalosporins ceftaroline and ceftobiprole displayed a notable ability to limit biofilm formation of CF MRSA. Hitherto little used for CF patients, the characteristics of both antimicrobial agents, together with recent studies showing that ceftaroline represents an additional treatment option for treating MRSA-associated acute pulmonary exacerbations (Branstetter et al., 2020), should promote their larger use in the management of CF patients infected by MRSA.

DATA AVAILABILITY STATEMENT

The datasets presented in this study can be found in online repositories. The names of the repository/repositories and accession number(s) can be found in the article/Supplementary Material.

ETHICS STATEMENT

The studies involving human participants were reviewed and approved by the Institutional Review Board at Nimes University hospital (Interface Recherche Bioéthique IRB n 21.03.01, March 04, 2021). Written informed consent from the participants' legal guardian/next of kin was not required to participate in this study in accordance with the national legislation and the institutional requirements.

AUTHOR'S NOTE

This work was partly presented at the 44th European Cystic Fibrosis Conference (digital), 9–12 June 2021.

AUTHOR CONTRIBUTIONS

HM: conceptualization. AB, PS, and CP: methodology. AB, PS, CP, CD-R, and HM: formal analysis. AB, PS, and RC: investigation. AB, PS, CP, and RC: data curation. AB, PS, and HM: writing – original draft preparation. CP, CD-R, RC, and J-PL: writing – review and editing. AB, CD-R, and HM: supervision. CD-R, J-PL,

and HM: funding acquisition. All authors contributed to the article and approved the submitted version.

FUNDING

This research was funded by the University Hospital of Nîmes (NimAO 2018.02 grant).

ACKNOWLEDGMENTS

The authors gratefully acknowledge Teresa Sawyers, English medical writer at Nîmes University Hospital, for editing this

paper, and Bastien Baud and Vincenette Lopez for their help with clinical and therapeutic data collection. We thank Nîmes University Hospital for its structural, human, and financial support through the award obtained by our team during the internal call for tenders “Thématiques phares.” All authors belong to the FHU InCh (Fédération Hospitalo-Universitaire Infections Chroniques, Aviesan).

SUPPLEMENTARY MATERIAL

The Supplementary Material for this article can be found online at: <https://www.frontiersin.org/articles/10.3389/fmicb.2021.750489/full#supplementary-material>

REFERENCES

- Abbanat, D., Shang, W., Amsler, K., Santoro, C., Baum, E., Crespo-Carbone, S., et al. (2014). Evaluation of the in vitro activities of ceftobiprole and comparators in staphylococcal colony or microtitre plate biofilm assays. *Int. J. Antimicrob. Agents* 43, 32–39. doi: 10.1016/j.ijantimicag.2013.09.013
- Akil, N., and Muhlebach, M. S. (2018). Biology and management of methicillin resistant *Staphylococcus aureus* in cystic fibrosis. *Pediatr. Pulmonol.* 53, S64–S74. doi: 10.1002/ppul.24139
- Aktas, N. C., Erturan, Z., Karatuna, O., and Yagci, A. K. (2013). Pantovaleutine leukocidin and biofilm production of *Staphylococcus aureus* isolated from respiratory tract. *J. Infect. Dev. Ctries.* 7, 888–891. doi: 10.3855/jidc.4135
- Ankrum, A., and Hall, B. G. (2017). Population dynamics of *Staphylococcus aureus* in cystic fibrosis patients to determine transmission events by use of whole-genome sequencing. *J. Clin. Microbiol.* 55, 2143–2152. doi: 10.1128/JCM.00164-17
- Azeredo, J., Azevedo, N. F., Briandet, R., Cerca, N., Coenye, T., Costa, A. R., et al. (2017). Critical review on biofilm methods. *Crit. Rev. Microbiol.* 43, 313–351. doi: 10.1080/1040841X.2016.1208146
- Barber, K. E., Smith, J. R., Ireland, C. E., Boles, B. R., Rose, W. E., and Rybak, M. J. (2015). Evaluation of ceftaroline alone and in combination against biofilm-producing methicillin-resistant *Staphylococcus aureus* with reduced susceptibility to daptomycin and vancomycin in an in vitro pharmacokinetic/pharmacodynamic model. *Antimicrob. Agents Chemother.* 59, 4497–4503. doi: 10.1128/AAC.00386-15
- Benoit, M. R., Conant, C. G., Ionescu-Zanetti, C., Schwartz, M., and Matin, A. (2010). New device for high-throughput viability screening of flow biofilms. *Appl. Environ. Microbiol.* 76, 4136–4142. doi: 10.1128/AEM.03065-09
- Boudet, A., Jay, A., Dunyach-Remy, C., Chiron, R., Lavigne, J.-P., and Marchandin, H. (2021). In-host emergence of linezolid resistance in a complex pattern of toxic shock syndrome toxin-1-positive methicillin-resistant *Staphylococcus aureus* colonization in siblings with cystic fibrosis. *Toxins* 13:317. doi: 10.3390/toxins13050317
- Branstetter, J., Searcy, H., Benner, K., Yarbrough, A., Crowder, C., and Troxler, B. (2020). Ceftaroline vs vancomycin for the treatment of acute pulmonary exacerbations in pediatric patients with cystic fibrosis. *Pediatr. Pulmonol.* 55, 3337–3342. doi: 10.1002/ppul.25029
- Chavant, P., Gaillard-Martinie, B., Talon, R., Hebraud, M., and Bernardi, T. (2007). A new device for rapid evaluation of biofilm formation potential by bacteria. *J. Microbiol. Methods* 68, 605–612. doi: 10.1016/j.mimet.2006.11.010
- Cocchi, P., Cariani, L., Favari, F., Lambiase, A., Fiscarelli, E., Gioffrè, F. V., et al. (2011). Molecular epidemiology of methicillin-resistant *Staphylococcus aureus* in Italian cystic fibrosis patients: a national overview. *J. Cyst. Fibros.* 10, 407–411. doi: 10.1016/j.jcf.2011.06.005
- Crisóstomo, M. I., Westh, H., Tomasz, A., Chung, M., Oliveira, D. C., and De Lencastre, H. (2001). The evolution of methicillin resistance in *Staphylococcus aureus*: similarity of genetic backgrounds in historically early methicillin-susceptible and resistant isolates and contemporary epidemic clones. *Proc. Natl. Acad. Sci. U. S. A.* 98, 9865–9870. doi: 10.1073/pnas.161272898
- Dasenbrook, E. C., Merlo, C. A., Diener-West, M., Lechtzin, N., and Boyle, M. P. (2008). Persistent methicillin-resistant *Staphylococcus aureus* and rate of FEV₁ decline in cystic fibrosis. *Am. J. Respir. Crit. Care Med.* 178, 814–821. doi: 10.1164/rccm.200802-327OC
- Dinesh, S. D. (2010). Artificial sputum medium. *Protoc. Exch.* doi: 10.1038/protex.2010.212
- Donlan, R. M., and Costerton, J. W. (2002). Biofilms: survival mechanisms of clinically relevant microorganisms. *Clin. Microbiol. Rev.* 15, 167–193. doi: 10.1128/CMR.15.2.167-193.2002
- Enright, M. C., Day, N. P. J., Davies, C. E., Peacock, S. J., and Spratt, B. G. (2000). Multilocus sequence typing for characterization of methicillin-resistant and methicillin-susceptible clones of *Staphylococcus aureus*. *J. Clin. Microbiol.* 38, 1008–1015. doi: 10.1128/JCM.38.3.1008-1015.2000
- European Committee on Antimicrobial Susceptibility Testing (2021). Breakpoint tables for interpretation of MICs and zone diameters. Version 11.0. Available at: https://www.eucast.org/fileadmin/src/media/PDFs/EUCAST_files/Breakpoint_tables/v_11.0_Breakpoint_Tables.pdf (Accessed February 8, 2021).
- Flament-Simon, S.-K., Duprilot, M., Mayer, N., Garcia, V., Alonso, M. P., Blanco, J., et al. (2019). Association between kinetics of early biofilm formation and clonal lineage in *Escherichia coli*. *Front. Microbiol.* 10:1183. doi: 10.3389/fmicb.2019.01183
- Frisch, S., Boese, A., Huck, B., Horstmann, J. C., Ho, D. K., Schwarzkopf, K., et al. (2021). A pulmonary mucus surrogate for investigating antibiotic permeation and activity against *Pseudomonas aeruginosa* biofilms. *J. Antimicrob. Chemother.* 76, 1472–1479. doi: 10.1093/jac/dkab068
- Fusco, N. M., Toussaint, K. A., and Prescott, W. A. Jr. (2015). Antibiotic management of methicillin-resistant *Staphylococcus aureus*-associated acute pulmonary exacerbations in cystic fibrosis. *Ann. Pharmacother.* 49, 458–468. doi: 10.1177/1060028014567526
- Gilpin, D., Hoffman, L. R., Ceppe, A., and Muhlebach, M. S. (2021). Phenotypic characteristics of incident and chronic MRSA isolates in cystic fibrosis. *J. Cyst. Fibros.* 20, 692–698. doi: 10.1016/j.jcf.2021.05.015
- Glikman, D., Siegel, J. D., David, M. Z., Okoro, N. M., Boyle-Vavra, S., Dowell, M. L., et al. (2008). Complex molecular epidemiology of methicillin-resistant *Staphylococcus aureus* isolates from children with cystic fibrosis in the era of epidemic community-associated methicillin-resistant *S. aureus*. *Chest* 133, 1381–1387. doi: 10.1378/chest.07-2437
- Goerke, C., Gressinger, M., Endler, K., Breitkopf, C., Wardecki, K., Stern, M., et al. (2007). High phenotypic diversity in infecting but not in colonizing *Staphylococcus aureus* populations. *Environ. Microbiol.* 9, 3134–3142. doi: 10.1111/j.1462-2920.2007.01423.x
- Goerke, C., and Wolz, C. (2010). Adaptation of *Staphylococcus aureus* to the cystic fibrosis lung. *Int. J. Med. Microbiol.* 300, 520–525. doi: 10.1016/j.ijmm.2010.08.003
- Goss, C. H., and Muhlebach, M. S. (2011). Review: *Staphylococcus aureus* and MRSA in cystic fibrosis. *J. Cyst. Fibros.* 10, 298–306. doi: 10.1016/j.jcf.2011.06.002
- Guzmán-Soto, I., McTiernan, C., Gonzalez-Gomez, M., Ross, A., Gupta, K., Suuronen, E. J., et al. (2021). Mimicking biofilm formation and development: recent progress in vitro and in vivo biofilm models. *iScience* 24:102443. doi: 10.1016/j.isci.2021.102443

- Harrington, N. E., Sweeney, E., Alav, I., Allen, F., Moat, J., and Harrison, F. (2021). Antibiotic efficacy testing in an ex vivo model of *Pseudomonas aeruginosa* and *Staphylococcus aureus* biofilms in the cystic fibrosis lung. *J. Vis. Exp.* doi: 10.3791/62187
- Hauser, A. R., Jain, M., Bar-Meir, M., and McColley, S. A. (2011). Clinical significance of microbial infection and adaptation in cystic fibrosis. *Clin. Microbiol. Rev.* 24, 29–70. doi: 10.1128/CMR.00036-10
- Hirschhausen, N., Block, D., Bianconi, I., Bragonzi, A., Birtel, J., Lee, J. C., et al. (2013). Extended *Staphylococcus aureus* persistence in cystic fibrosis is associated with bacterial adaptation. *Int. J. Med. Microbiol.* 303, 685–692. doi: 10.1016/j.ijmm.2013.09.012
- Høiby, N., Ciofu, O., and Bjarnsholt, T. (2010). *Pseudomonas aeruginosa* biofilms in cystic fibrosis. *Future Microbiol.* 5, 1663–1674. doi: 10.2217/fmb.10.125
- Iglesias, Y. D., and Van Bambeke, F. (2020). Activity of antibiotics against *Pseudomonas aeruginosa* in an in vitro model of biofilms in the context of cystic fibrosis: influence of the culture medium. *Antimicrob. Agents Chemother.* 64, e02204–e02219. doi: 10.1128/AAC.02204-19
- Iglesias, Y. D., Wilms, T., Vanbever, R., and Van Bambeke, F. (2019). Activity of antibiotics against *Staphylococcus aureus* in an in vitro model of biofilms in the context of cystic fibrosis: influence of the culture medium. *Antimicrob. Agents Chemother.* 63, e00602–e00619. doi: 10.1128/AAC.00602-19
- Jolley, K. A., Bray, J. E., and Maiden, M. C. J. (2018). Open-access bacterial population genomics: BIGSdb software, the PubMLST.org website and their applications. *Wellcome Open Res.* 3:124. doi: 10.12688/wellcomeopenres.14826.1
- Kadkhoda, H., Ghalavand, Z., Nikmanesh, B., Kodori, M., Hourri, H., Maleki, D. T., et al. (2020). Characterization of biofilm formation and virulence factors of *Staphylococcus aureus* isolates from paediatric patients in Tehran, Iran. *Iran J. Basic Med. Sci.* 23, 691–698. doi: 10.22038/ijbms.2020.36299.8644
- Kirchner, S., Fothergill, J. L., Wright, E. A., James, C. E., Mowat, E., and Winstanley, C. (2012). Use of artificial sputum medium to test antibiotic efficacy against *Pseudomonas aeruginosa* in conditions more relevant to the cystic fibrosis lung. *J. Vis. Exp.* 64:e3857. doi: 10.3791/3857
- Kodori, M., Nikmanesh, B., Hakimi, H., and Ghalavand, Z. (2021). Antibiotic susceptibility and biofilm formation of bacterial isolates derived from pediatric patients with cystic fibrosis from Tehran, Iran. *Arch. Razi. Inst.* 76, 397–406. doi: 10.22092/ari.2020.128554.1416
- Lade, H., Park, J. H., Chung, S. H., Kim, I. H., Kim, J. M., Joo, H. S., et al. (2019). Biofilm formation by *Staphylococcus aureus* clinical isolates is differentially affected by glucose and sodium chloride supplemented culture media. *J. Clin. Med.* 8:1853. doi: 10.3390/jcm8111853
- Lebeaux, D., Ghigo, J. M., and Beloin, C. (2014). Biofilm-related infections: bridging the gap between clinical management and fundamental aspects of recalcitrance toward antibiotics. *Microbiol. Mol. Biol. Rev.* 78, 510–543. doi: 10.1128/MMBR.00013-14
- Martin, I., Waters, V., and Grasmann, H. (2021). Approaches to targeting bacterial biofilms in cystic fibrosis airways. *Int. J. Mol. Sci.* 22:2155. doi: 10.3390/ijms22042155
- Meeker, D. G., Beenken, K. E., Mills, W. B., Loughran, A. J., Spencer, H. J., Lynn, W. B., et al. (2016). Evaluation of antibiotics active against methicillin-resistant *Staphylococcus aureus* based on activity in an established biofilm. *Antimicrob. Agents Chemother.* 60, 5688–5694. doi: 10.1128/AAC.01251-16
- Menetrey, Q., Sorlin, P., Jumas-Bilak, E., Chiron, R., Dupont, C., and Marchandin, H. (2021). *Achromobacter xylosoxidans* and *Stenotrophomonas maltophilia*: emerging pathogens well-armed for life in the cystic fibrosis patients' lung. *Gene* 12:610. doi: 10.3390/genes12050610
- Miquel, S., Lagrèfeuille, R., Souweine, B., and Forestier, C. (2016). Anti-biofilm activity as a health issue. *Front. Microbiol.* 7:592. doi: 10.3389/fmicb.2016.00592
- Molina, A., Del Campo, R., Máz, L., Morosini, M. I., Lamas, A., Baquero, F., et al. (2008). High prevalence in cystic fibrosis patients of multiresistant hospital-acquired methicillin-resistant *Staphylococcus aureus* ST228-SCCmecI capable of biofilm formation. *J. Antimicrob. Chemother.* 62, 961–967. doi: 10.1093/jac/dkn302
- Mottola, C., Matias, C. S., Mendes, J. J., Melo-Cristino, J., Tavares, L., Cavaco-Silva, P., et al. (2016). Susceptibility patterns of *Staphylococcus aureus* biofilms in diabetic foot infections. *BMC Microbiol.* 16:119. doi: 10.1186/s12866-016-0737-0
- Naudin, B., Heins, A., Pinhal, S., Dé, E., and Nicol, M. (2019). BioFlux™ 200 microfluidic system to study *A. baumannii* biofilm formation in a dynamic mode of growth. *Methods Mol. Biol.* 1946, 167–176. doi: 10.1007/978-1-4939-9118-1_16
- Nielsen, B. U., Kolpen, M., Jensen, P. Ø., Katzenstein, T., Pressler, T., Ritz, C., et al. (2020). Neutrophil count in sputum is associated with increased sputum glucose and sputum L-lactate in cystic fibrosis. *PLoS One* 15:e0238524. doi: 10.1371/journal.pone.0238524
- Olivares, E., Badel-Berchoux, S., Provot, C., Prévost, G., Bernardi, T., and Jehl, F. (2020). Clinical impact of antibiotics for the treatment of *Pseudomonas aeruginosa* biofilm infections. *Front. Microbiol.* 10:2894. doi: 10.3389/fmicb.2019.02894
- Predari, S. C., Ligozzi, M., and Fontana, R. (1991). Genotypic identification of methicillin-resistant coagulase-negative staphylococci by polymerase chain reaction. *Antimicrob. Agents Chemother.* 35, 2568–2573. doi: 10.1128/AAC.35.12.2568
- Registre français de la mucoviscidose - Bilan des données (2019). Vaincre la Mucoviscidose Paris, 2020. Available at: https://www.vaincrelamuco.org/sites/default/files/registre_2019_vf.pdf (Accessed July 24, 2021).
- Ren, C. L., Morgan, W. J., Konstan, M. W., Schechter, M. S., Wagener, J. S., and Fisher, K. A., et al. (2007). Presence of methicillin resistant *Staphylococcus aureus* in respiratory cultures from cystic fibrosis patients is associated with lower lung function. *Pediatr. Pulmonol.* 42, 513–518. doi: 10.1002/ppul.20604
- Rowe, S. M., Miller, S., and Sorscher, E. J. (2005). Cystic fibrosis. *N. Engl. J. Med.* 352, 1992–2001. doi: 10.1056/NEJMra043184
- Rozenbaum, R. T., van der Mei, H. C., Woudstra, W., de Jong, E. D., Busscher, H. J., and Sharma, P. K. (2019). Role of viscoelasticity in bacterial killing by antimicrobials in differently grown *Pseudomonas aeruginosa* biofilms. *Antimicrob. Agents Chemother.* 63, e01972–e02018. doi: 10.1128/AAC.01972-18
- Savage, V. J., Chopra, I., and O'Neill, A. J. (2013). Population diversification in *Staphylococcus aureus* biofilms may promote dissemination and persistence. *PLoS One* 8:e62513. doi: 10.1371/journal.pone.0062513
- Seemann, T. (2015). Snippy: Fast bacterial variant calling from NGS reads. Available at: <https://github.com/tseemann/snippy> (Accessed July 2, 2021).
- Sriramulu, D. D., Lünsdorf, H., Lam, J. S., and Römling, U. (2005). Microcolony formation: a novel biofilm model of *Pseudomonas aeruginosa* for the cystic fibrosis lung. *J. Med. Microbiol.* 54, 667–676. doi: 10.1099/jmm.0.45969-0
- Tasse, J., Croisier, D., Badel-Berchoux, S., Chavanet, P., Bernardi, T., Provot, C., et al. (2016). Preliminary results of a new antibiotic susceptibility test against biofilm installation in device-associated infections: the Antibiofilmogram®. *Pathog. Dis.* 74:ftw057. doi: 10.1093/femspd/ftw057
- Tasse, J., Trouillet-Assant, S., Josse, J., Martins-Simões, P., Valour, F., Langlois-Jacques, C., et al. (2018). Association between biofilm formation phenotype and clonal lineage in *Staphylococcus aureus* strains from bone and joint infections. *PLoS One* 13:e0200064. doi: 10.1371/journal.pone.0200064
- The Cystic Fibrosis Foundation Patient Registry (2019). Annual data report 2020. Available at: <https://www.cff.org/Research/Researcher-Resources/Patient-Registry/2019-Patient-Registry-Annual-Data-Report.pdf> (Accessed July 24, 2021).
- Thieme, L., Klingler-Strobel, M., Hartung, A., Stein, C., Makarewicz, O., and Pletz, M. W. (2018). In vitro synergism and anti-biofilm activity of ampicillin, gentamicin, ceftaroline and ceftriaxone against *Enterococcus faecalis*. *J. Antimicrob. Chemother.* 73, 1553–1561. doi: 10.1093/jac/dky051
- Vandeplassche, E., Sass, A., Ostyn, L., Burmølle, M., Kragh, K. N., Bjarnsholt, T., et al. (2020). Antibiotic susceptibility of cystic fibrosis lung microbiome members in a multispecies biofilm. *Biofilm* 2:100031. doi: 10.1016/j.biofilm.2020.100031
- Vanderhelst, E., De Meirleir, L., Verbanck, S., Piérard, D., Vincken, W., and Malfroot, A. (2012). Prevalence and impact on FEV₁ decline of chronic methicillin-resistant *Staphylococcus aureus* (MRSA) colonization in patients with cystic fibrosis: a single-center, case control study of 165 patients. *J. Cyst. Fibros.* 11, 2–7. doi: 10.1016/j.jcf.2011.08.006
- Vanhommerig, E., Moons, P., Pirici, D., Lammens, C., Hernalsteens, J.-P., De Greve, H., et al. (2014). Comparison of biofilm formation between major clonal lineages of methicillin resistant *Staphylococcus aureus*. *PLoS One* 9:e104561. doi: 10.1371/journal.pone.0104561
- Van Sambeek, L., Cowley, E. S., Newman, D. K., and Kato, R. (2015). Sputum glucose and glycemic control in cystic fibrosis-related diabetes: a cross-sectional study. *PLoS One* 10:e0119938. doi: 10.1371/journal.pone.0119938
- Vu-Thien, H., Hormigos, K., Corbineau, G., Fauroux, B., Corvol, H., Moissenet, D., et al. (2010). Longitudinal survey of *Staphylococcus aureus* in cystic fibrosis

- patients using a multiple-locus variable number of tandem-repeats analysis method. *BMC Microbiol.* 10:24. doi: 10.1186/1471-2180-10-24
- Wieneke, M. K., Dach, F., Neumann, C., Görlich, D., Kaese, L., Thifßen, T., et al. (2021). Association of diverse *Staphylococcus aureus* populations with *Pseudomonas aeruginosa* coinfection and inflammation in cystic fibrosis airway infection. *mSphere* 6:e0035821. doi: 10.1128/mSphere.00358-21
- Winstanley, C., O'Brien, S., and Brockhurst, M. A. (2016). *Pseudomonas aeruginosa* evolutionary adaptation and diversification in cystic fibrosis chronic lung infections. *Trends Microbiol.* 24, 327–337. doi: 10.1016/j.tim.2016.01.008
- Zobell, J. T., Epps, K. L., Young, D. C., Montague, M., Olson, J., Ampofo, K., et al. (2015). Utilization of antibiotics for methicillin-resistant *Staphylococcus aureus* infection in cystic fibrosis. *Pediatr. Pulmonol.* 50, 552–559. doi: 10.1002/ppul.23132
- Zolin, A., Orenti, A., Naehrlich, L., Jung, A., and van Rens, J. (2020). ECFSPR annual report 2018. Available online: https://www.ecfs.eu/sites/default/files/general-content-files/working-groups/ecfs-patient-registry/ECFSPR_Report_2018_v1.4.pdf (Accessed July 24, 2021).
- Conflict of Interest:** The authors declare that this research was conducted in the absence of any commercial or financial relationships that could be construed as potential conflicts of interest.
- Publisher's Note:** All claims expressed in this article are solely those of the authors and do not necessarily represent those of their affiliated organizations, or those of the publisher, the editors and the reviewers. Any product that may be evaluated in this article, or claim that may be made by its manufacturer, is not guaranteed or endorsed by the publisher.
- Copyright © 2021 Boudet, Sorlin, Pouget, Chiron, Lavigne, Dunyach-Remy and Marchandin. This is an open-access article distributed under the terms of the Creative Commons Attribution License (CC BY). The use, distribution or reproduction in other forums is permitted, provided the original author(s) and the copyright owner(s) are credited and that the original publication in this journal is cited, in accordance with accepted academic practice. No use, distribution or reproduction is permitted which does not comply with these terms.

Annexe 5: Liste des communications durant la thèse

Congrès	Type de présentation	Sujet
MicrobiOccitanie 2019 Montpellier	Présentation orale 20 minutes	Bacterial translocation and rheumatoid arthritis
Eccmid 2020 Paris	Présentation orale 5 minutes	A relevant wound-like in vitro media for the study of biofilm in DFI Annulé COVID
Eccmid 2020 Paris	Présentation orale 15 minutes	Genomic adaptation of <i>S.</i> <i>aureus</i> in diabetic foot environment Annulé COVID
Eccmid 2021 En ligne	Présentation orale 10 minutes	Evaluation of Bioflux 200 system to characterize polymicrobial biofilm organization and antibiotics effect in a chronic wound environment